

**THE DEFINITION OF SERUM FREE PARAPETERS  
FOR HUMAN ADULT STEM CELLS**

Thesis submitted in accordance with the requirements of the University of  
Liverpool for the degree of Doctor in Philosophy

By

**Nicholas Bryan**

May 2009

## The Definition of Serum Free Parameters for Human Adult Stem Cells

### ABSTRACT

The expansion of primary human cells of a grade such that could be used directly in conjunction with a clinical application is a paradigm which has hindered any rapid and influential progressions in the field of tissue engineering and regenerative medicine. One of the major hindrances in achieving this objective is the general requirement for the use of animal derived serum throughout routine cell culture applications. Animal serum used in this context is a double edged sword; providing a melee of proteins, cytokines and other growth factors that the cells require for adhesion, expansion and general maintenance of integrity whilst also potentially introducing animal derived zoonotic pathogens to the cell culture matrix and additionally removing any definition. Purely from an experimental perspective the intimate components of serum vary dependent on a number of factors including donor species, gender, lineage and diet which introduce undefined variability into the cell culture milieu, a factor which is of particular importance when dealing with cells with a variable phenotype or plasticity including mesenchymal stem cells.

Adult stem cells are a primary cell of particular interest to the field of regenerative medicine. These cells provide a pluripotent cell source; a blank canvas from which potentially can be generated any number of defined terminal lineages of autologous adult cells whilst overcoming the ethical and practical constraints associated with embryonic stem cells. Adult stem cells can be derived from an ever increasing number of tissues and while bone marrow is widely regarded as the most commonly exploited sink of these cells, dental pulp also has large potential; providing an easily accessible source of early stem cells developmentally derived from the neural crest.

Post culture delivery of the clinical grade cells also poses a problem, with the necessity to provide a stable environment in which the cells can expand and carry out their functions, correctly forming a tissue whilst initiating a minimal host immune response which ultimately will result in destruction of the new tissue and potential suffering to the patient.

Serum substitutes were therefore synthesised de novo from raw components which when combined were capable of maintaining the phenotype of a number of primary human cells of tissue engineering relevance including primary human fibroblasts, osteoblasts and smooth muscle cells in an environment entirely devoid of whole serum. Furthermore, the chemically defined cell culture media illustrated its potential to maintain the undifferentiated phenotype of bone marrow and crucially dental pulp derived stem cells. Additional defined exogenous

modifications to the chemically defined medium were demonstrated to differentiate bone marrow derived stem cells down 'tri-lineage' fates of chondrogenic, osteogenic and adipogenic pathways and additionally further media were synthesised which were capable of differentiating dental pulp derived stem cells into the previous lineages and also neural and hepatic cells.

A suitable means of delivery for cells of a clinical grade was derived by means of exploitation of an autologous hydrogel generated from platelet poor plasma extracted from a patient's own whole blood. This system resulted in a hydrogel which was capable of supporting cellular expansion and phenotype of a number of primary human cells when used as an *in vitro* culture matrix and interestingly also supported the microvascular endothelial differentiation of dental pulp derived stem cells. *In vivo* using immunosuppressed animal models the hydrogel supported the formation of sub-cutaneous neo-tissue from human dermal fibroblast cells which was extensively characterised. The human cells maintained their phenotype within the hydrogel and integrated intimately and reliably with the surrounding host tissues whilst instigating a minimal host immune response. The hydrogel also demonstrated itself as a suitable candidate material to support the expansion of primary human osteoblast cells when delivered intramuscularly.

Therefore presented in this study is a complete solution for the progression of primary human cells of a clinical grade from bench to bedside designed for use in clinical engineering and regenerative medical strategies. Media of potentially pharmacopeia grade was synthesised completely devoid of whole serum which supported the expansion and differentiation of primary human cells. These cells could then be transplanted in an autologous manner using the patient specific platelet poor plasma hydrogel system, presenting a complete cell culture and delivery system, directly translatable as a solution to a number of clinical scenarios.

## **The Definition of Serum Free Parameters for Human Adult Stem Cells**

### **ACKNOWLEDGEMENTS**

Firstly, I would like to thank my supervisors John Hunt and Nick Rhodes. I am particularly grateful to John who without his expertise, guidance and reassurance particularly that 'a negative result is still a result' this project would not have been possible. I would also like to thank STEPS; a systems approach to tissue engineering processes and products for funding this research. Not only did STEPS provide financial support but also the opportunity to meet and work with a fantastic group of people containing some of the leading members of the tissue engineering field, whom hopefully, in time will become close colleagues. I would also like to thank the Tissue Engineering and Regenerative Medicine Society (TERMIS) and the European Society for Biomaterials (ESB) for giving me the opportunity to present my data at their highly regarded meetings at several points throughout my studies.

My gratitude also go out to all who have worked and become close friends on the 4<sup>th</sup> floor of the Edwards building throughout my project for putting up with me and my associated mess. Particularly I would like to thank Jude Curran for molecular biology help and consistently reminding me that I've still got a lot to learn. Sandra Fawcett for histological assistance, Mick Loughran for support with ICPMS, Kirstie Andrew for statistical assistance, Vic Kearns for keeping my feet firmly on the ground via the medium of squash. Also, Katie Nickson and Shirley Rawlings who I'm sure must bored of my company during my extended thesis procrastination lunch breaks by now. Some other names too, Keith, John, Gary, Ahmed, Matt for being there for a completely non cellular chat at the times when science got the better of me.

Penultimately, my thanks go out to Jo. Who despite writing her own thesis at the same time as me has had to endure my tantrums throughout my



writing particularly and is living proof that something beneficial can come from research skills development courses. And finally my parents, whose financial 'investment' has made my entire academic career possible and by now after 6 years must be thinking their money pit of a son is never going to disappear. And furthermore despite the extent that a thesis engulfs your life, despite my grumblings, whose Tuesday evening home cooked meals, reminded me that life need not stop for research. Although PCR is considerably more fruitful if it does!

# The Definition of Serum Free Parameters for Human Adult Stem Cells

<b>Contents</b>	<b>i</b>
<b>Abbreviations</b>	<b>iv</b>
<b>Definition of Aims</b>	<b>v</b>
<b>Chapter 1 Introduction</b>	<b>1</b>
1.i Tissue Engineering – an Introduction	1
1.ii A Candidate Cell for Tissue Engineering – Lineage Committed or Pluripotent?	2
1.iii Mesenchymal stem cells; Analysis and examination of phenotype	6
1.iv The origins of the Mesenchymal stem cell	7
1.v Dental Pulp Derived Stem Cells	11
1.vi Cell Culture – A Brief History	12
1.vii Adult Stem Cell Growth <i>ex vivo</i>	13
1.viii Serum Exploitation in Cell Culture – the Need for an Alternative	13
1.ix Alternatives to Serum	15
1.x Stem Cell Differentiation in Vitro	20
<b>Chapter 2 Materials &amp; Methods</b>	<b>29</b>
2.i Immunohistochemistry	29
2.ii Fluorescence in-situ hybridisation	33
2.iii RNA Isolation	34
2.iv DNA Isolation from Crude Tissue	35
2.v Reverse Transcription / cDNA Generation	36
2.vi Real-Time Polymerase Chain Reaction (qRT-PCR)	36
2.vi Oil Red O Staining Protocol for Visualisation of Lipid Droplets	40
2.vii Alcian Blue Staining Protocol for Visualisation of Glycosaminoglycans	40
2.viii Von Kossa Staining Protocol for Visualisation of Calcification	41
2.ix Methylene Blue Staining for Observation of Cell Morphology	42
2.x Cell Culture	42
2.xi Protein Extraction	43
2.xii Enzyme-Linked Immunosorbent Assay (ELISA) – Human Serum Albumin	43
2.xiii Enzyme-Linked Immunosorbent Assay (ELISA) – Human Transferrin	45
2.xiv Alamar Blue Assay	46
2.xv Flow-Cytometry	47
2.xvi Plasma Isolation	52
2. xvii <i>In Vitro</i> Hydrogel Synthesis	52
2.xvii Cell Culture – Hydrogel Substrate	53
2.xviii Cell Tracking Dyes	55
2.xix In vivo cell growth and defect site delivery model	56

2.xx Cryo-Scanning Electron Microscopy (CryoSEM)	57
2.xxi Histopathology and Antigen Preservation	58
2.xxii Immunohistochemistry – Resin Embedded Samples	60
2.xxiii Haematoxylin and Eosin Staining for Observation of Tissue Structures	61
2.xxiv Primer Design	61
2.xxv Statistics	65
2.xxvi Dynamic Contact Angle	65
<b>Chapter 3 Media Derivation</b>	<b>66</b>
3.i Introduction	67
3.ii Definition of basal media – Lineage committed cells	71
3.iii Expansion of Primary Human Cells in Conjunction with Defined Serum Free Parameters – Dermal Fibroblast Cells	77
3.iv Expansion of Primary Human Cells in Conjunction with Defined Serum Free Parameters – Osteoblasts	80
3.v Expansion of Primary Human Cells in Conjunction with Defined Serum Free Parameters – Arterial Smooth Muscle Cells	81
3.vi Expansion of Primary Pluripotent Human Cells in Conjunction with Defined Serum Free Parameters – Bone Marrow Derived Mesenchymal Stem Cells	92
3.vii Expansion of Primary Pluripotent Human Cells in Conjunction with Defined Serum Free Parameters – Dental Pulp Derived Mesenchymal Stem Cells	114
3.viii Defined Chondrogenic Differentiation of Dental Pulp Derived Stem Cells	120
3.ix Defined Osteogenic Differentiation of Dental Pulp Derived Stem Cells	130
3.x Defined Adipogenic Differentiation of Dental Pulp Derived Stem Cells	138
3.xi Defined Neural Differentiation of Dental Pulp Derived Stem Cells	144
3.xii Defined Hepatic Differentiation of Dental Pulp Derived Stem Cells	156
3.xiii Metabolic Activity of Dental Pulp Derived Stem Cells in Conjunction with Serum Free Differentiation Media Formulations	161
3.xiv Summary	164
<b>Chapter 4 Hydrogel Derivation and Characterisation</b>	<b>166</b>
4.i. Introduction	166
4.ii. Dynamic Contact Angle	169
4.iii Hypoxic Cell Maintenance Model	174
4.iv Gel Surface Validation	176
4.v Cell growth and migration <i>in vitro</i> , embedded within gel	191
4.vi Optimisation of suitable cell phenotype for ectopic soft tissue formation model	194
4.vii Tissue Formation Model	198

4.viii Summary	229
<b>Chapter 5 Discussion</b>	<b>232</b>
5.i Transferrin Degradation Studies	232
5.ii Lineage committed cells – Dermal Fibroblasts	233
5.iii Lineage committed cells – Osteoblasts	235
5.iv Lineage committed cells – Arterial Smooth Muscle Cells	236
5.v Lineage uncommitted cells – Bone Marrow Derived Mesenchymal Stem Cells	239
5.vi Hydrogel Characterisation	259
5.vii <i>In Vitro</i> Cell Culture in Conjunction with Platelet Poor Plasma Derived Hydrogel	262
5.viii <i>In Vivo</i> Cell Culture in Conjunction With Platelet Poor Plasma Derived Hydrogel	268
<b>Chapter 6 Conclusions</b>	<b>280</b>
6.i. Derivation of Defined Media	280
6.ii Synthesis of Autologous Hydrogel	285
<b>Chapter 7 References</b>	<b>288</b>

## **Appendix 1**

Bryan N., Rhodes N.P. & Hunt J.A (2009) Derivation and Performance of an Entirely Autologous Injectable Hydrogel Delivery System for Cell-Based Therapies. *Biomaterials*. 30. 180-188

## **Appendix 2**

Table & Figure Legends

## The Definition of Serum Free Parameters for Human Adult Stem Cells

### ABBREVIATIONS

ABCG2 – ATP binding cassette, subfamily G, member 2  
AFP – Alpha-fetoprotein  
ANOVA – Analysis of variance  
APTES - 3-aminopropyl triethoxysilane  
BMP – Bone morphogenic protein  
BMSC – Bone marrow stem cell  
BSA – Bovine serum albumin  
CBFA1 – Core binding factor alpha 1  
CD – Cluster of differentiation  
CK18 – Cytokeratin 18  
DCA – Dynamic contact angle  
DPSC – Dental pulp stem cell  
EDTA - Ethylenediaminetetraacetic acid  
EGF – Endothelial growth factor  
ELISA – Enzyme linked immunosorbent assay  
FCS – Fetal calf serum  
FGF – Fibroblast growth factor  
FISH – Fluorescence *in situ* hybridisation  
GFAP – Glial fibrillary acidic protein  
HAC – Human articular chondrocyte  
HDF – Human dermal fibroblast  
H&E – Haematoxylin and eosin  
HGF – Hepatocyte growth factor  
HLA – Human leukocyte antigen  
HOB – Human osteoblast  
HSC – Haematopoietic stem cell  
MEM – Minimal essential medium  
MHC – Major histocompatibility complex  
MSC – Mesenchymal stem cell  
NGF – Neural growth factor  
NOD/SCID – Non-obese/severe combined immuno-deficiency  
OCT4 – Octamer 4  
PBS – Phosphate buffered saline  
PCR – Polymerase chain reaction  
PDGF – Platelet derived growth factor  
PPAR – Peroxisome proliferator-activated receptor  
REST – RE1-silencing transcription factor  
SEM – Scanning electron microscopy  
SMA – Smooth muscle actin  
SMC – Smooth muscle cell  
SOX - Sry-related HMG box  
TCP – Tissue culture plastic  
TGF – Transforming growth factor  
VEGFR – Vascular endothelial growth factor receptor

## **The Definition of Serum Free Parameters for Human Adult Stem Cells**

### **DEFINITION OF AIMS**

#### **DERIVATION OF DEFINED MEDIA FOR THE PHENOTYPE MAINTENANCE AND DIRECTED DIFFERENTIATION OF PRIMARY HUMAN PLURIPOTENT CELLS**

- Derivation of a defined basal media formulation which in conjunction with fetal calf serum at identical concentrations to those employed using commercially available basal media is capable of maintaining the expansion of primary human cells.
- Replacement of serum using minimal additions of exogenous components in conjunction with the defined basal media formulation such that a completely chemically defined media can be presented, entirely devoid of serum which is capable of maintaining the expansion of a range of primary human cells.
- Assessment of the extent to which the chemically defined serum free basal media formulation maintains the phenotype of several primary human cells of tissue engineering relevance.
- Elucidation of the capability of the defined basal media formulation to maintain undifferentiated plastic phenotype of primary human bone marrow derived stem cells.
- Validation of controlled exogenous additions to the basal media formulation to stimulate 'tri-lineage' differentiation of bone marrow derived mesenchymal stem cells and subsequent characterisation of differentiated cells.
- Elucidation of the capability of the defined basal media formulation to maintain the early undifferentiated plastic phenotype of stem cells derived from a more accessible source than bone marrow, those obtained from dental pulp.
- Validation of controlled exogenous additions to the basal media formulation to explore the potential of a hypothesised transgermal

differentiation potential of primary human dental pulp derived stem cells into classical tri-lineage fates and additional neural and never previously described hepatic lineages.

### **DEVELOPMENT AND VALIDATION OF A DEFINED STRATEGY FOR THE SITE DIRECTED DELIVERY OF CLINICAL GRADE PRIMARY HUMAN CELLS**

- Development of a potentially autologous means for the delivery of primary human cells of clinical grade to a defect site by a minimally invasive manner.
- Characterisation of the capacity of human platelet poor plasma to form a stable hydrogel; an ideal matrix for soft tissue augmentation, when citrated at the point of extraction and subsequently re-calcified using basal cell culture media as a calcium source to initiate the residing blood coagulation cascade.
- Elucidation of the potential of this platelet poor plasma derived hydrogel as a substrate for culture of cells *in vitro* using several areas of the gel, with particular interest in the culture of human chondrocyte cells a critically relevant cell in regenerative medical applications which favour culture in hypoxic environment and the potential for this to be conferred using a hydrogel substrate.
- Investigation of the potential of the platelet poor plasma derived hydrogel as a medium for minimally invasive cell delivery and subsequent neo-tissue generation by injection using primary human cells in conjunction with an immunosuppressed animal model.
- Characterisation of the resultant tissues using several methods to identify the origins of the cells contained within the ectopic tissues. Additionally characterisation of the extent of host acceptance of the implant by means of observation of the interaction of host anatomical structures with the neo-tissue masses.

- Characterisation of the extent to which the initial cell seeding number is responsible for the final size of the neo-tissues and additional extensive characterisation of the extent of the immune response raised by the host animal as a result of the implanted hydrogel derived tissue.
- Validation of the hydrogel to form hard tissue using an intramuscular delivery strategy in conjunction with primary human osteoblast cells and characterisation of the resultant tissues.



# DERIVATION OF DEFINED MEDIA FOR THE PHENOTYPE MAINTENANCE AND DIRECTED DIFFERENTIATION OF PRIMARY HUMAN PLURIPOTENT CELLS

## Chapter 1. Introduction

### 1.i Tissue Engineering – an Introduction

Tissue engineering can be defined as ‘an interdisciplinary field that applies the principles of engineering and life sciences toward the development of biological substitutes that restore, maintain, or improve the function of a tissue or a whole organ’ [1]. As a discipline, tissue engineering is regarded with much anticipation, having a vast potential to revolutionize the outlook for injury and degenerative diseases. The focus of tissue engineering lies in the repair, replacement or regeneration of a damaged tissue utilising a patients own cells in conjunction with a choice from a palette of candidate biocompatible materials of suitable physiomechanical properties as a cellular substrate to provide an autologous means to restore the function of a defined damaged or defective tissue [77]. This artificially assisted ‘self repair’ approach has lead to the emergence of the field of regenerative medicine, a cumulation of current therapeutic understanding in combination with biomechanics. This approach does not seek to reproduce all the complexities involved in development, but rather seeks to promote an environment which permits the native capacity of cells to integrate, differentiate, and develop new tissues [273]. Tissue engineering also has massive commercial implications; in 2001, it was reported that first-generation organ replacement therapies could prolong or improve the lives of over 20 million patients worldwide. In the United States, an estimated one person in five reaching 65 years of age will receive temporary or permanent organ replacement therapy during their remaining life span. Worldwide, organ replacement therapies consume 8% of medical spending or approximately \$350 billion per year, an extremely valuable market, open for exploitation by suitable devices [272].

1.ii A Candidate Cell for Tissue Engineering – Lineage Committed or Pluripotent?

A large number of cell phenotypes have the capability to be involved in biotherapeutic treatments, dependent on the specific cell type native to the tissue destined for repair. Whilst lineage committed cells such as osteoblasts [2], smooth muscle cells [3], chondrocytes [75] and urothelial cells [4] have proven roles in tissue engineering for tissue specific applications, the cell with the greatest expectation in the development and advancement of tissue engineering is undoubtedly the stem cell [5, 76, 78]. Stem cells are a class of 'pluripotent' cells, meaning *in vivo* their terminal lineage commitment is undecided; they have the ability to differentiate into multiple terminal lineages within an organism, assisting in the repair of the tissue in which they reside, while additionally, having the capacity to self renew in an undifferentiated state in an apparently immortalized manner due to transcription of the enzyme telomerase. This is a crucial protein in the prevention of DNA damage during genomic replication, whose absence, in a lineage committed cell, plays a role in cell aging and controlled cell death [79-80].

Stem cell 'niches' are located in various adult tissues in eukaryotic organisms. During embryogenesis the stem cells within the inner cell mass of the embryonic blastocyst are ultimately the precursor to every other cell type in a developed infant, highlighting their unparalleled potential for controlled differentiation and tissue generation *de novo* in the laboratory [6, 81, 82]. Currently, whilst intense ethical constraints forbid the harvesting of human embryos for stem cell isolation for use in regenerative medicine, alternative sources of pluripotent cells have needed to be sought. Although investigations into the refinement of protocols which allow the harvest of embryonic stem cells without blastocyst sacrifice are being pursued, this area of pluripotent cell research is still very much in its infancy and any potential rapid progression in understanding hindered by legislation and red tape [7,83]. The tight moral boundaries surrounding the clinical use of embryo-derived stem cells in biomedical research has

encouraged considerably more concentrated research on adult stem cells, now regarded as a less conflicting alternative as a source of plastic cells in future regenerative therapies [8, 84]. Adult stem cells are located within a diverse host of adult tissues, and are responsible for the regeneration of cells that are lost or damaged beyond self repair within a tissue or organ by terminal differentiation into a lineage matching that of the damaged cell. A direct role for adult stem cells has been identified in the repair of tissues as diverse as brain and myocardium [85-89].

A stem cell population sourced routinely from adult tissues is referred to collectively as mesenchymal stem cells due to the observation that the tissues in which they reside are derived from the mesodermal germ layer during embryogenesis. The adjective 'mesenchymal' is fraught with ambiguity since 'mesenchyme' describes tissue of mesodermal origin, the middle embryological germ layer, giving rise to the musculoskeletal, blood, vascular and urinogenital systems, and to connective tissue (including dermis). Thus, developmentally speaking, the term 'mesenchymal' should include both blood and connective tissue cells. Generally, however, solely solid tissue-forming stem cells are referred to as mesenchymal. The subset of stem cells which are responsible for the development, maintenance, and regeneration of blood-forming tissues are referred to as haematopoietic stem cells [94]. Early investigations into the plasticity of mesenchymal stem cells hypothesized that these cells only possessed the capacity to differentiate into cells native to the tissue from which they were derived. However, this theory has now been disregarded, with many groups regularly demonstrating extensive plasticity, irrespective of the tissue from which they were isolated. The number of tissues from which these cells can be harvested is rapidly increasing as mesenchymal stem cell research gains greater momentum. Thus far, the list of candidate tissues is diverse and includes post natal tissues as varied as adipose tissue [10], peripheral blood [11, 99], dental pulp [90], ocular conjunctiva [93], tonsils [98], pancreas [117] and renal tissue [113] in addition to the widely publicized bone marrow [9]. Stem cell sources have also been established from both pre and neonatal tissues in an attempt to

attain a population of cells as developmentally 'early' as possible; hypothesized to have increased plasticity compared to adult stem cells. These tissues also have the benefit over postnatal tissues that they are a by-product of childbirth and thus can be obtained simply from both a physical and ethical perspective. These tissues include placenta [95], umbilical cord blood [96] and amniotic fluid [97]. As mentioned previously, mesenchymal stem cells have demonstrated the potential to provide a renewable, autologous source of cells for use in regenerative medical therapies. However, although histocompatibly identical to cells which remain in the donor, immunosuppression is often still required, despite the cell type. Considering this, allogeneic or stem cells with a matched donor HLA type have shown similar potential in transplantation, with similar immunosuppression and prognosis to autologous stem cells in a range of diseases [100-101, 103-104]. Furthermore, recent studies have highlighted cord blood stem cells as a candidate cell for transplantation, based on the hypothesis that early fetal cells will not be cleared by the recipients' immune system, in a similar manner that they are not cleared from the mothers peripheral circulation during gestation [102]. Interestingly, investigations have also noted the capacity of mesenchymal stem cells to inhibit T-cell proliferation, through a largely unknown pathway possibly involving IFN $\gamma$ , perhaps emphasizing a role in self protection from autoimmunity in conjunction with implantation [141]. Therefore, in addition to overcoming the ethical boundaries associated with the harvest of embryonic stem cells in research, mesenchymal stem cells provide a potential source of plastic cells for direct exploitation in biomedical applications, having similar immunogenic implications in autologous and even allogeneic forms.

As knowledge of mesenchymal stem cells increases at a molecular level, discussions have arisen concerning adult stem cell plasticity compared to those of embryonic origin. That is, are mesenchymal stem cells capable of differentiation into the same number of tissue types as stem cells derived from the blastocyst, or is their lineage more committed, limiting their differentiation to a restricted number of specific predefined cellular

subsets? This line of reasoning has led to MSCs being termed 'multipotent' meaning that differentiation down their final lineage is slightly more committed, being restricted to a smaller, defined range of tissues than their pluripotent embryonic counterparts [12- 13]. Initial hypotheses surrounding the plasticity of adult stem cells suggested that their terminal lineage would be restricted to a cell type specifically located in the tissue from which they were initially isolated. The increasing momentum of mesenchymal stem cell research has since caused this theory to be disregarded. To date, mesenchymal stem cells have been differentiated down an impressive and regularly increasing list of terminal defined lineages. Adipocyte [14], chondrocyte [15] and osteoblasts [16] are the classical 'tri-lineage' mesenchymal stem cell terminal phenotypes, now widely accepted as a confirmatory test of the 'stem' potential of a cell, typifying three simple mesodermal terminal lineages down which all mesenchymal stem cells can be driven *in vitro*. Bone marrow-derived stem cells demonstrate one of the greatest promises for regenerative medical applications having been artificially driven down the greatest number of lineages of any stem cell of non-hematopoietic origin *ex vivo*, including complex 'trans-germal' functional cell types such as neuronal [17, 108-109, 115] cardiomyocyte [18, 118], hepatocyte [91, 105-107], urothelial [114], smooth muscle [122] and pancreatic islet cells [92]. Now that the potential for exploitation of mesenchymal stem cells as a tool for tissue engineering applications is well established, the question of how to optimize *in vitro* conditions to maintain and expand them following isolation and purification is open for investigation.

In order for mesenchymal stem cells to live up to their expectations in regenerative medicine, culture parameters need to be established to clearly define the following: 1. How can these cells be maintained in their undifferentiated 'wild type' state in culture? And 2, how can the culture environment in which they are maintained *ex vivo* be altered such that their fate is guided down a defined terminal lineage? If both of these points are combined it raises the question, by what means can we identify a mesenchymal stem cell in its undifferentiated state? And what methods

can we use to acknowledge that the cell has reached its final lineage determined fate?

*1.iii Mesenchymal stem cells; Analysis and examination of phenotype*

If mesenchymal stem cells are to be exploited in surgery, it is imperative that their exact phenotype and state of differentiation is known at the point of isolation and ultimately, implantation. Mesenchymal stem cells have the unfortunate property of differentiating spontaneously in culture [19, 116, 117]. In light of this fact, close attention needs to be paid to the monitoring of their phenotype throughout expansion. Stem cell phenotype is classically defined at the proteomic level using a subset of cellular antigen molecules shown to associate with cells of a 'stem' phenotype. One can define an undifferentiated mesenchymal stem cell using a subset of proteins from the following group extracellular antigens: +CD29, +CD44, +CD90, +CD271 (NGFR), +CD105, +CD54, +CD13, +CD106, +CD73, +CD166, +SSEA-4 and +frizzled-9 [20-24, 119-121, 123-124, 136, 138]. In addition to surface antigens, intracellular proteins specific to mesenchymal stem cells can be examined in a similar manner to extracellular proteins, with candidate molecules including STRO-1 [125-127], nucleostemin [128-130], Oct-4 (which although proven to be a crucial mediator of pluripotency in embryonic stem cells, its comparative role in mesenchymal stem cells is debated [25, 133-134]), the small conserved protein domains SH2 and SH3 [131-132], nanog [135, 137], REX-1 and GATA-4 [139-140]. One can also examine the phenotype and state of differentiation of the cell by examining the aforementioned proteins at the level of gene expression patterns within the cell. Expression of specific genes that allow the cell to maintain its 'stemness' will decrease during differentiation, and just as stem cell specific proteins can be visualized using immunofluorescent techniques, the expression of pluripotency-associated specific genes can be visualized using micro array, southern blot or polymerase chain reaction based assays and their modulation can

be characterized as the stem cell loses plasticity during differentiation [26, 140, 142-143].

*1.iv The origins of the Mesenchymal stem cell*

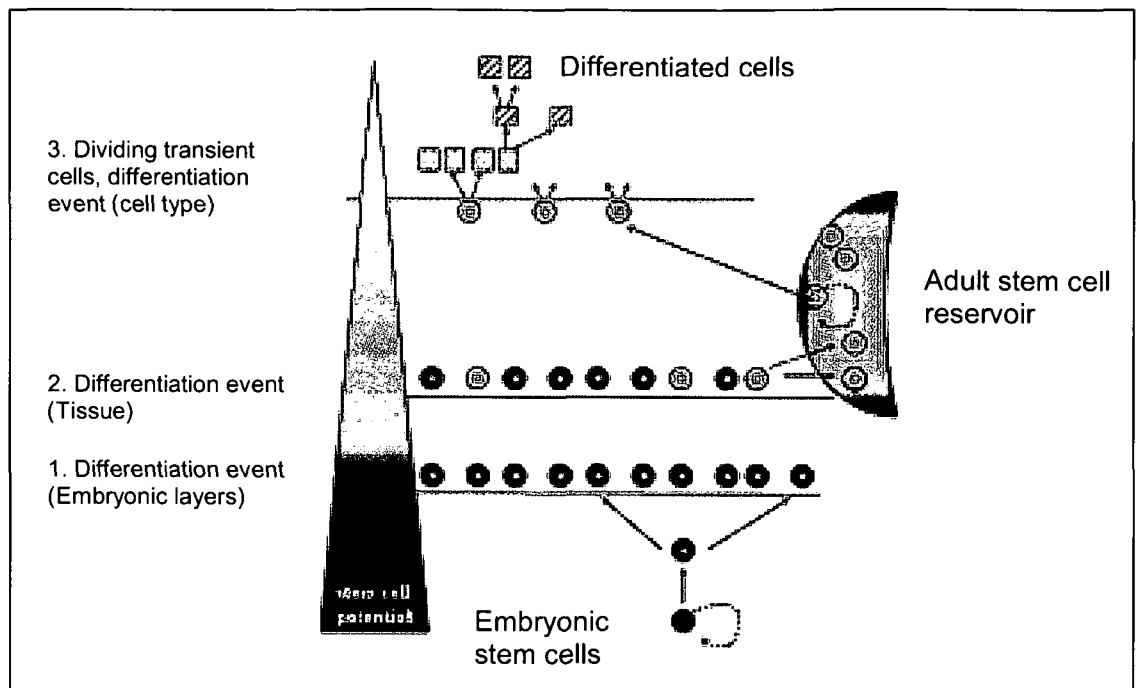


*Fig 1.1 Schematic illustrating the origins and differentiation states of mesenchymal stem cells in vivo. [33]*

From the perspective of development and evolution, the destiny of any complex, multicellular organism is to pass on its genes, ideally intact to subsequent generations. This process is orchestrated by the appropriate exploitation of somatic cells by their precursor germ cells [148]. The germ line is a vector for the genome from one generation to the next and is the only cell lineage that retains its true, complete developmental totipotency: The capacity to form any cell in an organism. In this context, it can be realised that all somatic cells are descendants from the germ line and facilitate germ cells in their role of gene multiplication [151].

The earliest of all cells, the zygote derives directly from the fusion of two compatible germ cells (female oocyte and male sperm) as the most

primitive totipotent stem cell, having the capability to form both embryonic and extraembryonal tissues (placenta). In the zygote, haploid DNA derived from an oocyte is combined with haploid DNA from sperm. Thus, the zygote could be envisioned as a mother cell to both the germ and somatic lineages which ultimately will give rise to (A) more differentiated cells from the germ line and (B) other somatic lineages that will provide the soma (meso-, ecto-, and endoderm) of the terminal organism, which ensure transfer of DNA to the next generation [149-150].

Mesenchymal stem cells are no different from any other cell in an organism in that they derive from pluripotent embryonic stem cells in the early blastocyst (epiblast) after several precursor differentiation events during the course of development, tightly controlled by DNA methylation [147]. The first of these developmental steps is the formation of the cells of the three embryonic layers, the mesoderm, ectoderm and endoderm that further differentiate into tissues. Within each tissue, particularly those that undergo regular turnover of cells such as skin or intestinal epithelium, stem cell compartments are formed that are maintained in the adult organism. These will give rise to transient amplifying cells that undergo differentiation to give rise to the mature tissue and serve as a reservoir for tissue homeostasis and repair. At each developmental step, the differentiation potential of the stem cell is depleted. Recent experiments have demonstrated, however, that adult tissue stem cells, or even some undifferentiated cells, when exposed to a permissive or instructive environment, can reverse their phenotype to become cells with a less restricted differentiation potential (Fig. 1.1 [34]).

The origins and direction of mesenchymal stem cells to a particular niche in the adult organism is very vague. However one plausible hypothesis suggested for the rich harvest of adult pluripotent cells in the bone marrow can be hypothesised from the fact that bone marrow (BM), in addition to hematopoietic stem cells also contains a heterogeneous population of non-hematopoietic stem cells. It is therefore suggested that the presence of these various populations of stem cells in the marrow is a result of the



“developmental migration” of stem cells during ontogenesis and the presence of the permissive environment that attracts these cells to the BM tissue. Both hematopoietic and non-hematopoietic stem cells are actively chemoattracted by factors secreted by BM stroma cells and osteoblasts (e.g., stromal derived factor-1[SDF-1] and hepatocyte growth factor [HGF]) and colonize marrow by the end of the second and the beginning of the third trimester of gestation [144]. Accumulating evidence suggests that these non-hematopoietic stem cells residing in the bone marrow play some role in the homeostasis/turnover of peripheral tissues and when needed, are released/mobilized from the BM into the circulation during tissue injury and stress, thus facilitating the regeneration of damaged organs [145-146].

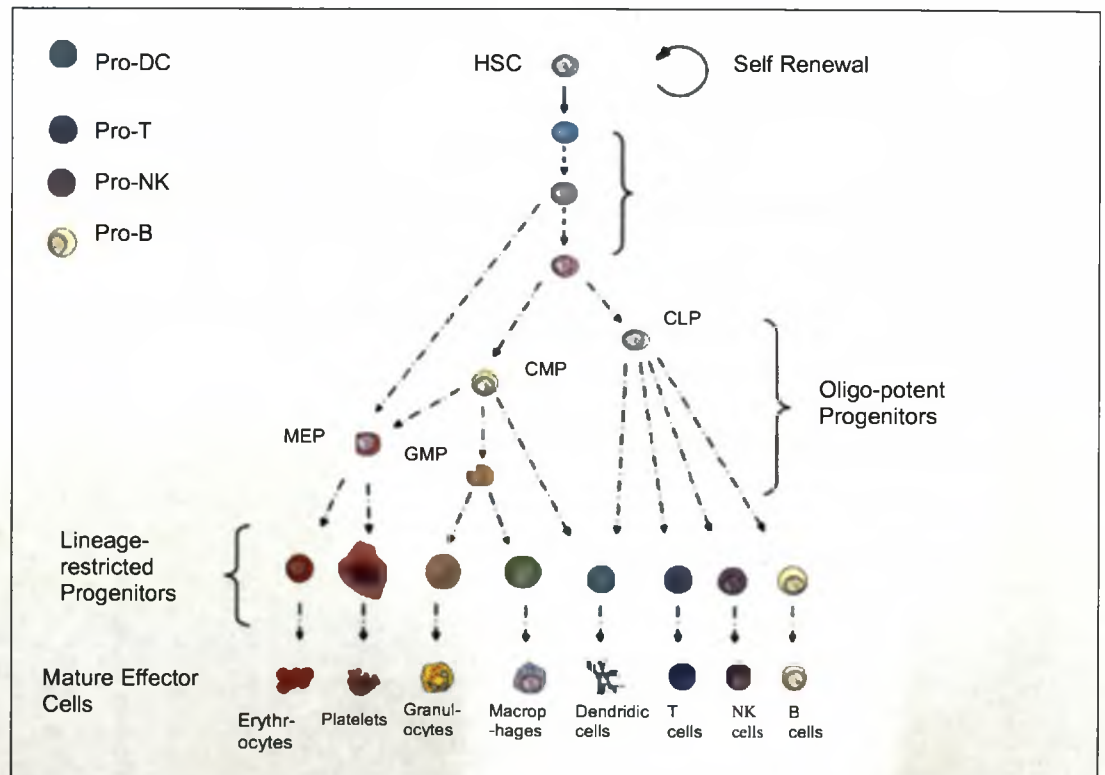


*Fig 1.2 Schematic illustrating the origins and differentiation states of Hematopoietic stem cells in vivo (Kamminga L.M. & De Haan G., 2006,[ 35])*

Hematopoietic stem cells are a further class of adult stem cell derived from bone marrow. Developmentally, the first potent adult-repopulating hematopoietic stem cells are generated from an embryonic stem cell precursor in the aorta within the region known as the AGM (aorta-gonad-

mesonephros). Hematopoietic stem cells are also found in the umbilical and vitelline arteries during ontogenesis. Later in embryogenesis, hematopoietic stem cells appear in the placental vasculature. All these tissues may *de novo* generate hematopoietic stem cells. The fetal liver is thought to become colonized by hematopoietic stem cells at a later point in fetal development and serve as a reservoir until the time of birth, when they migrate and colonize the bone marrow [156].

HSCs are responsible for differentiation into non-adherent cells such as erythrocytes and cells of the immune system [155]. Because mature blood cells are predominantly short lived, stem cells are required throughout life to replenish multilineage progenitors and the precursors committed to individual hematopoietic lineages. Hematopoietic stem cells reside as rare cells in the bone marrow in adult mammals and give rise to a number of less plastic multipotent progenitor cell types [152-153]. These pluripotent progenitor cells derive multipotent progenitors including the common lymphoid progenitor, which divide into mature B lymphocytes, T lymphocytes, and natural killer cells. The common myeloid progenitor gives rise to granulocyte-macrophage progenitors, which differentiate into monocytes/macrophages and granulocytes, and megakaryocyte/erythrocyte progenitors, which differentiate into megakaryocytes/platelets and erythrocytes. Both Common myeloid and common lymphoid progenitor cells have been proposed to give rise to dendritic cells *in vivo* (Fig.1.2 [35-38]). Critically, hematopoietic stem cells are defined operationally by their capacity to reconstitute the entire blood system. Importantly these cells can also undergo self renewal in addition to differentiation. Evidence is also available to suggest that in addition to their role in the repopulation of the hematopoietic system, hematopoietic stem cells may also play a role in differentiation into adherent cells such as fibroblasts (154, 157).

### 1.v Dental Pulp Derived Stem Cells

Stem cells derived from dental pulp are potentially superior to other types of adult stem cell as teeth are easy to access, either shed as part of development or extracted routinely throughout life, and the cells are located in both adult and deciduous teeth of even more importance is the ability to secure DPSCs at a young age and store it for the future usage. Potentially, a personalized stem cell can then be created from DPSCs without using procedures that may cause ethical concerns [158]. Stem cells derived from dental pulp share similar gene expression profiles and differentiation capability to that of more familiar bone marrow derived stem cells [159-160] and are derived from migrating neural crest cells during development, therefore considered an 'early' cell with an particularly uncommitted phenotype, as a result dental pulp is made of both ectodermic and mesenchymal components, containing neural crest cells that display plasticity and multipotent capability [161-162, 167]. It has been demonstrated that, like all adult stem cell compartments, dental pulp is heterogeneous, although interestingly despite the heterogeneity of the cell population, all of the cells within the pulp cavity share a common +Thy-1 (CD90) phenotype, a marker of undifferentiated stem cells, in addition to more heterogeneously expressed stem cell markers such as CD29, CD44, CD105, STRO-1 and stem cell factor (SCF) [164-165, 171]. *In vitro*, dental pulp-derived stem cells have shown extensive plastic potential, and using suitable stimuli and substrates have been differentiated into osteoblasts, to the point of bone chip formation, functional neurons, adipocytes, myocytes, and chondrocytes [163, 168, 170, 172]. From a tissue engineering perspective, these cells have demonstrated themselves as ideal candidates for implantation and subsequent host integration and differentiation with osteogenic, myogenic and adipogenic tissues demonstrated to form *in vivo* from dental pulp derived stem cells using immunosuppressed animal models implanted in conjunction with a suitable supportive matrix [166, 169].

1.vi Cell Culture – A Brief History

The maintenance of cells *ex vivo* began over a century ago in 1880 when English physiologist Sydney Ringer developed salt solutions containing the chlorides of sodium, potassium, calcium and magnesium suitable for maintaining the beating of an isolated animal heart outside of the body [46, 174-175]. In 1885 this research was furthered when Wilhelm Roux, a German anatomist and embryologist first cultivated cells derived from chick embryos in simple balanced salt solutions *in vitro* for periods of a few days [176]. Cell culture advanced rapidly and in 1898 the discovery was made that that skin fragments could be kept alive for extended periods of time and in some cases be re-transplanted back to the donor, arguably the dawn of tissue engineering.

Over the subsequent decades major leaps were made in the culture of cells by several individuals that are widely referred to today, including Alexis Carrel who in 1913 furthered Roux's work by demonstrating that cells can grow for long periods in culture provided they are fed regularly under aseptic conditions. Later in 1948 Earle and colleagues isolated single cells of the L cell line and showed that they had the capacity of form clones in tissue culture. Earle is considered by many to be one of the forefathers of cell culture with his salt solution 'Earles salts' forming the basis of many contemporary culture media. In 1955 Eagle published several papers which set about defining exact concentrations of nutrients including sugars, vitamins and amino acids necessary to sustain growth of mammalian cells in culture for extended periods of time. This work became a milestone in cell culture and for many, defined classical cell culture medium with many of his defined nutrient formula still existing in cell culture media today [47-49]. Up to this point cell growth in culture always required the presence in the medium of whole or dialysed serum, serum proteins or unknown factors dialysed into the media from serum. The first work in defining serum-free cell culture parameters was carried out by R.G. Ham in 1965, whose chemically defined medium, totally

devoid of serum derived adducts was demonstrated to be capable of sustaining the growth of mammalian cells through several passages [50].

#### 1.vii Adult Stem Cell Growth ex vivo

Adult stem cells are anchorage dependent cells and expand in adherent monolayer populations on tissue culture polystyrene, typically exhibiting fibroblastic morphologies [39]. Conversely, hematopoietic stem cells prefer to grow in suspension [61]. When grown in optimal conditions mesenchymal stem cells demonstrate a population doubling time of roughly 7 to 48 hours depending on optimization of culture parameters, harvesting procedures, source tissue, and the species from which they were collected. Their growth in culture does not diverge greatly away from classical cell culture protocols involving a mixture of serum, generally of fetal calf origin at concentrations of between 5%-20% and a bespoke culture media defined specifically for their expansion and phenotype maintenance *in vitro* [40-43]. Mesenchymal stem cell specific culture medium is now responsible for making large revenues for its producers with several multinational biotechnology companies including Cambrex®, Gibco® and Invitrogen® launching mesenchymal stem cell specific media over the last five years. Stem cell growth media is typically supplemented with basic fibroblast growth factor (bFGF / FGF2) as this protein has been shown to increase mesenchymal stem cell proliferation and play a role in the maintenance of an undifferentiated plastic stem cell phenotype and suppress differentiation *in vitro* [44-45].

#### 1.viii Serum Exploitation in Cell Culture – the Need for an Alternative

Although serum has proved to be an invaluable tool in the development of cell culture technologies, it has long been recognized (hence the work of Ham as early as 1965) that serum is far from adequate to facilitate the culture of cells intended to be moved from the laboratory to the clinic due

to the undefined, variable nature of the constituent components [178-181]. Serum is a fraction purified from blood. It is a mixture of proteins, carbohydrates, fats, cytokines and growth factors to name but a few components [182].

Its precise composition has a vast number of determinants and can vary dependent on season [191-192], point in photoperiod [192,196], species [183-184], donor gender [185-187, 189], age [191, 193], diet [188, 190-191] and time of collection. For example, an estrous female animal will have a different serum protein composition to a non estrous animal [194-195]. These are mere examples of factors determining the protein content and composition of a serum sample. Often serum batch tests analyzing a range of serum samples provided from the same company can yield vastly different results, not only on cell proliferation rate but more crucial, phenotype maintenance. Serum used in cell culture can be derived from a range of species including bovine [201], equine [199-200], porcine [197], canine [198] and human [202-203].

Typically the serum of choice in the laboratory is of fetal calf origin, which is extracted from pregnant cows at the point of slaughter. The role of fetal calf serum in cell culture is to provide the cells with all the necessary proteins that are required for maintenance and proliferation. The main economic advantage of fetal calf serum is its availability due to the abundance of cattle, particularly in countries with massive expanses of land devoted to cattle ranches such as Australia and several South American countries such as Argentina and Brazil. It has been estimated that around half a million litres of raw fetal calf serum is produced each year worldwide which equates to the harvesting of more than one million bovine fetuses annually [51]. However, in addition to the undefined nature of serum, there are many other disadvantages. Cells for implantation simply could not be grown in a solution containing adducts which are xenogeneic, due to the likelihood of histocompatibility issues resulting from the cells adapting to the bovine protein containing media. Serum, being an animal derived product may contain contamination of a

viral, prion or mycoplasmal nature. The cross contamination risks between flask and implant are too great to take into the operating theatre [204-206].

In addition to these factors, there will always be the obvious ethical issues surrounding the collection procedures from unborn calves which involves cardiac puncture of the unanaesthetised calf either *in situ* in the mother when the pregnancy is recognized prior to evisceration, or the mothers uterus containing the calf foetus being removed during the evisceration process. In both cases, the blood is vacuumed into a sterile collection bag, after which serum is isolated by refrigerated centrifugation. A bovine foetus of 3 months yields about 150 ml of raw serum, at 6 months 350 ml and at 9 months (near-term) 550 ml. The *in situ* method for collection is preferred due to a reduction in possible contamination of the collected serum as the calf never comes into contact with the outside environment. During these collection protocols it is still not clear whether the calf experiences pain. In the instance of bleeding after uterus evisceration, it is hypothesised that the resultant hypoxia of the calf incurred as a result of no longer having an umbilical connection to the mother will cause a loss of consciousness. However, when blood is extracted *in situ*, the calf is thought to be conscious throughout. [52, 207-208, 222].

#### 1.ix Alternatives to Serum

Since the work of Ham in 1965, serum alternatives have advanced significantly, with different grade serum replacement products available tailored to suit many complex cell culture scenarios. The various grades of serum free media and media replacements are summarized in table 1.

Abbreviation	Definition
Animal Derived Component Free (ADCF)	Product free of animal derived components
Chemically Defined (CD)	Chemically defined, no animal derived components, no unknown substances included
Complete Serum Free Medium (CSFM)	Serum free medium needing no further supplementation
Protein Free (PF)	Formulation lacking proteins, may include animal derived components
Serum Free (SF)	Product without serum (components)
Serum Free Medium (SFM)	Serum free product, may need supplementation
Serum Replacement (SR)	Serum replacement product of varying origin/composition

*Table.1. The various grades of serum free media/media supplements available commercially at time of writing*

All of these formulations can be broadly divided into two classes, chemically defined and protein free. Animal derived component free and chemically defined medium may still contain protein. The animal derived component free formulations may contain autologous animal proteins made recombinantly in bacteria, eukaryotic cells, or purified from whole serum itself [209-211, 213, 220]. Classically, three proteins are used in protein containing serum replacements at various concentrations, these are; insulin [212, 214, 216-217, 154], transferrin [212, 215-217, 228] and serum albumin [218-220]. In serum substitutes, these may be purified from bovine blood or organs (pancreas in the case of insulin), however as mentioned previously, in an animal component free media supplement these will be synthesized recombinantly and subsequently purified [53]. These defined media formulations are extensively exploited, and can be optimized to maintain proliferation rates higher than their serum containing counterparts [54-57, 221]. Recombinant proteins come at a price however; extensive purification and characterization are required before the bacterial derived proteins can enter mammalian cell culture systems. Bacteria may not fold a given protein in the same way as a



mammalian cell thus resulting in decreased affinity for the mammalian receptor [223-225]. In addition to this, bacterial production of protein for cell culture adds another possible route of infection which removal of calf serum sought to eliminate. This brings the necessity for development of protein free chemically defined media. This may involve the addition of extra essential ions such as selenium, molybdenum, and nickel to replace those found in serum [226-228]. Protein by can be replaced by chemical counterparts such as aurintricarboxylic acid, tropolone and pyridoxal isonicotinoyl hydrazone (Figs 1.3-1.5) a group of synthetic iron chelating molecules which can potentially alleviate the need for Transferrin as an iron delivery system in certain cell culture applications. [58, 229-230].

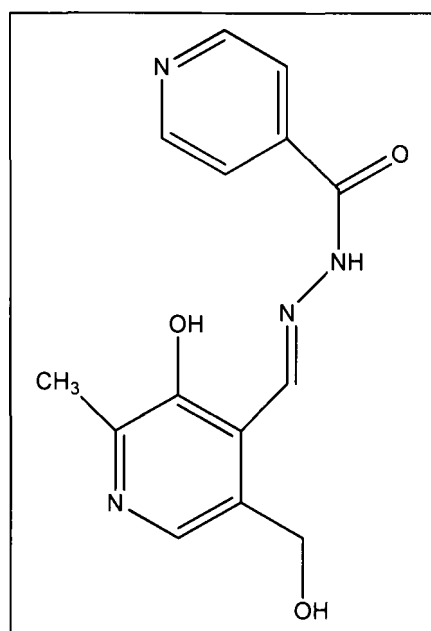


Fig.1.3. The molecular structure of the synthetic iron carrier pyridoxal isonicotinoyl hydrazone

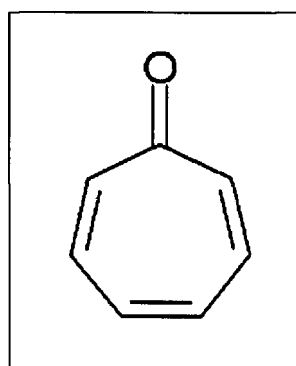


Fig.1.4. The molecular structure of the synthetic iron carrier Tropolone

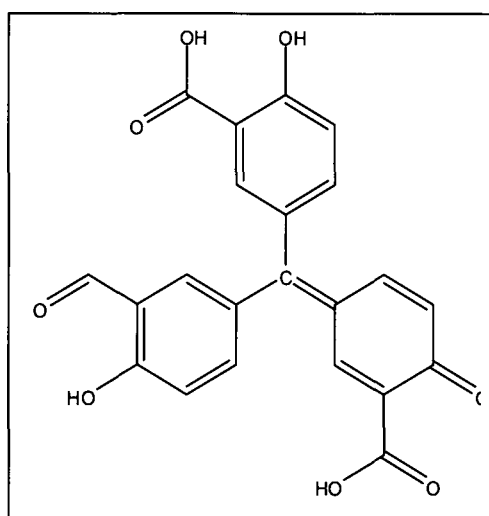


Fig.1.5. The molecular structure of the synthetic iron carrier Aurintricarboxylic acid

These iron chelating molecules have the difficult task of equilibrating the ferric and ferrous iron in tissue culture scenarios, a fine balance between necessity and toxicity. Ferric iron is the stable oxidative state of iron in aerobic conditions, and the normal oxidative state utilised by mammalian cells for its role in oxygen provision, electron transport and cofactorial catalysis.

In a solution at physiologic pH, ferric iron that is not bound by a chelator (ferritin *in vivo*) or carrier (transferrin *in vivo*), will form ferric hydroxide complexes that are virtually insoluble, rendering it useless. *In vitro*, ferric iron can be reduced to ferrous iron by reducing agents in the medium, namely ascorbate in routine use culture media. Both the loss of ferric iron due to precipitation and its reduction to ferrous iron are undesirable events in the extracellular milieu. Iron in the ferrous oxidative state that is free to participate in Fenton chemistry is a major source of oxidative stress in media. This involves the ferrous iron-catalyzed conversion of hydrogen peroxide into a hydroxide ion and a hydroxyl free radical with the concurrent oxidation of ferrous iron to ferric iron. This reaction is profoundly important in cell culture, because when it occurs, it creates the most damaging agent found in the cell culture system: the hydroxyl free radical. This radical will react with virtually any molecule in the medium or cell. It is so reactive that it typically reacts very close to its site of formation. A major action of hydroxyl free radicals in cell culture involves the initiation of lipid and DNA peroxidation.

Pluronic 68 a non-ionic surfactant which has a role similar to that of albumin in culture: protecting cells from shear forces induced during maintenance, can be used to replace this protein in cell culture. However, it has been shown to be internalized into cells and only eliminated from certain cell types. One phenotype demonstrated to accumulate Pluronic 68 is human chondrocytes, questioning the suitability of this molecule for certain tissue engineering applications [231].

Additionally, an excess of ionic zinc can alleviate the requirement for insulin in cell culture, a further reduction in the protein component of culture media for certain cell culture applications [232-233]. Several other cellular molecules can be replaced by chemical substitutes such as  $\beta$ -mercaptoethanol, which present an -SH group and therefore act as a reducing agent, breaking down several toxic intracellular metabolites, replacing the need for glutathione, which is usually purified from serum [59, 234-235]. A second molecule capable of protecting cells from oxidative stress is ethanolamine which additionally can form part of the building blocks for phospholipids, precursors for numerous enzymes and cofactors [236-237]. Defined glycerides such as lipoic, oleic, linoleic and palmitic acids can replace the undefined fatty acids component of sera when necessary. In the case of cholesterol-dependant cell culture, several commercial synthetic cholesterol substitutes are available such as Synthecol<sup>TM</sup> from Sigma-Aldrich® [60]. All of these factors combined leave the chemist with a diverse palette from which to draw components for designing and optimising bespoke cell culture media.

### 1.x Stem Cell Differentiation in Vitro

Stem cell differentiation *ex vivo* is classically carried out by altering the cocktail of exogenous factors in the media in which they are cultured. Modulating the composition of the growth medium has been extensively characterized to influence the lineage determination of the stem cell, during differentiation culture. The phenotype of the stem cells is subjected to a range of analysis to observe the presence of molecules or structures associated with the defined lineage which the differentiation culture is designed to promote, characterizing the differentiation state of the cell. A simple example is that of cardiomyogenic differentiation of mesenchymal stem cells, which occurs after 12 days when the dimethylating agent 5-azacitidine is used exogenously in the conventional cell culture medium (Iscoves modified Dubeccos media, IMDM), characterised by the morphological presence of myotube structures and beating cells.

Additionally, the presence of the cardiomyocyte specific genes: ANP, BNP, GATA4, and Nkx2.5/Csx were characterised throughout the differentiated cardiomyocyte cell population. It is also worthy of note that in this particular study only 30% of the total mesenchymal stem cell population were found to differentiate into cardiomyocytes. This is suggestive of the heterogeneity of mesenchymal stem cell subsets, often harboring sub-populations of cells more predisposed to a particular differentiation event. This particular study also highlights another critical feature in the characterisation of differentiated cells: the observance of markers associated with functionality, particularly when considering a regenerative outcome for the cultured cells. It is difficult to base an assumption that the cells will behave as those of the same phenotype do natively when implanted as part of a tissue engineering therapy purely on the basis of morphology and protein expression of phenotype associated markers. For this reason it is important to analyse proteins or genes intimately associated with *in vivo* function of the cell. This particular group were able to observe adrenergic and muscarinic receptors in their differentiated populations of cardiomyocyte cells, proteins which play crucial roles in mediating heart rate, conduction velocity, contractility, and cardiac hypertrophy natively [69, 238-240].

The exploitation of single exogenous molecules as in the example of cardiomyocyte differentiation leads to an extremely simple differentiation medium; however, more often, media formulations for the directed differentiation of adult stem cells are considerably more complex. The combination of biotin, pantothenate, insulin, dexamethasone and 1-methyl-3-isobutylxanthine induces cells along an adipogenic lineage [241, 243]. Often the combinations of these molecules are applied with no regard for the function of the individual component. Recently, it has been demonstrated that in an adipogenic media, 1-methyl-3-isobutylxanthine (IBMX), a phosphodiesterase inhibitor, is the crucial mediator of this differentiation cocktail, mediating expression of the early adipocyte transcription factor KLF4, in time periods as short as 30 minutes post induction [240]. This perhaps provides a more sensible explanation for its

role over earlier hypotheses which suggested that its capacity to initiate differentiation down an adipocyte lineage was due to an inhibition of the expression of tumor necrosis factor (TNF), an event not directly linked with an adipocytes [242]. Adipocyte functionality is characterized by the morphological observation of lipid encapsulation within the cytoplasm of the cells. Additionally, the functional protein leptin can be identified; a critical molecule responsible for mediating the signaling role of adipocytes in dietary regulation *in vivo*.

The augmentation of basal cell culture media with  $\beta$ -glycerophosphate, ascorbate-2-phosphate, and dexamethasone is regarded as the gold standard for the initiation of osteogenic differentiation and maintenance of osteogenic phenotype [70]. In a manner similar to that of adipogenic differentiation mentioned previously, this media is often used with no regard for the roles of the particular exogenous components.

Dexamethasone, a glucocorticoid, is hypothesized to hold the critical role in maintenance of osteogenic progression. It may heighten the activation and differentiation of osteoblastic cells through an interaction with the early response gene cFos. Change in expression of cFos mRNA has been observed in cultures of osteoblasts containing dexamethasone. Interaction between glucocorticoid receptor and cFos mRNA has been demonstrated. cFos, is expressed as unspliced and spliced mRNAs. Treatment of osteoblastic cells with dexamethasone resulted in elevated levels of the spliced form of cFos mRNA: promoters of many developmentally regulated genes, including osteocalcin, a marker of osteoblast differentiation, contain AP-1 sites that bind cFos/Jun dimers. [245, 248]. Furthermore, it has been observed that cells transfected to hyper-express the osteogenic transcription factor osterix, do not undergo functional osteogenesis in the absence of dexamethasone [246]. Additional studies have demonstrated a role for dexamethasone in both early and late osteogenesis, acting at multiple points during differentiation to control the progression from pre-osteoblast to terminal osteoblastic phenotypes [247]. The terminal, functional differentiation of an osteoblast is characterised by the presence of a calcified extracellular matrix, typically using traditional

histology by Von Kossa staining. Furthermore, proteins associated with matrix mineralisation such as osteocalcin and osteonectin can be observed.

$\beta$ -glycerophosphate alone has been demonstrated to initiate chondrogenic differentiation [71], however most protocols for chondrogenic differentiation also incorporate the growth factor TGF- $\beta$ 1 into the medium to fully stimulate chondrogenesis [250]. Members of the transforming growth factor family have been shown to play a major role in bone and cartilage development. Recent studies have demonstrated that TGF- $\beta$ , BPM-2 and growth differentiation factor 5 (GDF-5) rapidly induce type II collagen gene expression, suggesting a critical role of the TGF- $\beta$  superfamily in chondrocyte specific gene expression [249]. Although TGF- $\beta$  superfamily molecules exert their intracellular signalling roles through the Smad pathway, it has been hypothesised that additional pathways are involved in chondrogenesis (Fig.1.6.).

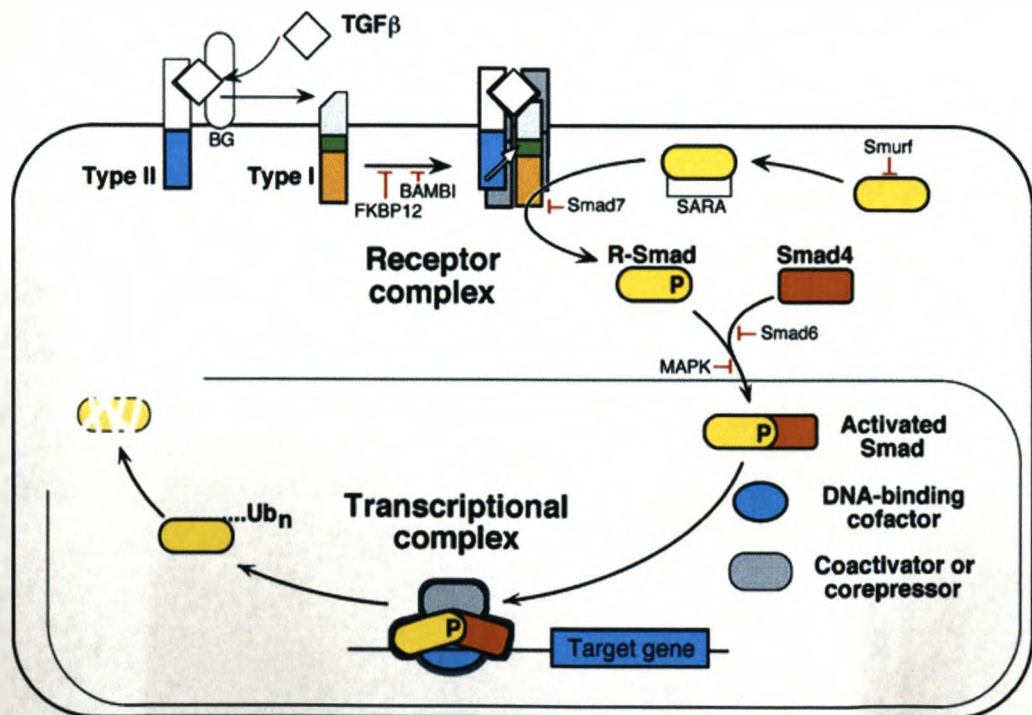


Fig.1.6. The role of TGF- $\beta$  in the Smad signalling cascade (Massagué J. & Wotton D, 2000, [264])

Extracellular signal related kinase 1/2 (ERK1/2) and c-Jun N terminal kinase (JNK) have been reported to be activated by TGF- $\beta$  signalling in certain chondrogenic cell lines [251]. More recent studies using knockout models have also demonstrated a role for ERK1/2 in chondrogenesis, demonstrating its necessity for type II collagen synthesis [252]. One particular review indeed suggested a role of Smad signalling in the up scaling of type I collagen synthesis [253], a phenomenon which occurs inversely during chondrogenesis, therefore further suggesting that although Smad is the classical intracellular signalling pathway induced by the TGF- $\beta$  superfamily, further crosstalk between pathways, most likely ERK1/2 mediated signalling occurs intracellularly to induce terminal chondrogenesis. In addition to exogenous factors, chondrogenesis permits demonstration of a differentiation event in which the three dimensional environment around the cells can potentially have large implications upon their phenotype. Many groups undertake chondrogenic differentiation using pellet culture conditions. This technique relies on spinning the cells to a pellet aggregate and maintaining them in this manner throughout culture. During culture the 'core' of the pellet becomes hypoxic, mimicking the native cartilage niche in which these cells reside *in vivo*, therefore facilitating differentiation or maintenance of a chondrogenic phenotype. This technique still requires the addition of exogenous TGF- $\beta$  superfamily molecules, however many groups report a higher yield of chondrocytes after differentiation using this culture strategy. Additionally, hydrogel systems have been exploited to mimic the three dimensional matrix in which these cells reside *in vivo* [254-256]. It has been noted too that during chondrogenic culture cells derived from the bone marrow often show a predisposition to an ossification, possibly an artefact of the proximity to bone and potential predisposition towards an osteoblastic cell *in vivo*. Chondrocyte functionality can be assayed by observation of the presence of extracellular matrix glycosaminoglycans. These large branching carbohydrate structures associate with large numbers of water molecules thus allowing the chondrocytes to 'lubricate' the joint which their cartilage tissue lines *in vivo*. However, difficulties arise during chondrogenic differentiation studies, terminating the differentiation at a



the point of an articular chondrocyte phenotype before the cells begin to resemble more closely a hypertrophic or osteochondral chondrocyte cell, characterised by the expression of hypertrophic collagen, collagen type X, in addition to proteins associated with extracellular matrix calcification such as osteocalcin. It is interesting to note therefore, that RUNX2, the osteogenic master gene, a transcription factor responsible for initiating osteogenesis is a DNA binding cofactor capable of binding a Smad complex generated by TGF- $\beta$  superfamily initiated signalling, natively by one of the bone morphogenic proteins (BMP) members of the family.

Neural differentiation of mesenchymal stem cells is possibly one of the most targeted differentiation events from the point of view of direction towards a particular cell signalling event. Focus in neural differentiation lies in subjecting the cells to exogenous conditions which will elevate the concentration of intracellular cAMP, which has been demonstrated to be crucial in the differentiation from a stem to a neural cell phenotype. The cAMP pathway, via the cAMP-dependent protein kinase A (PKA), activates the transcription factor CREB (cAMP response element-binding protein) by phosphorylation. It has been demonstrated that CREB is capable of dephosphorylating and subsequently activating the proneural homeodomain transcription factor Phox2a which is a key regulator in the differentiation of neural cells generating noradrenergic neurons of the both the central and peripheral nervous systems [257-258] The cAMP pathway is detailed in Fig.1.7 shown innervated by its native ligand, Wnt

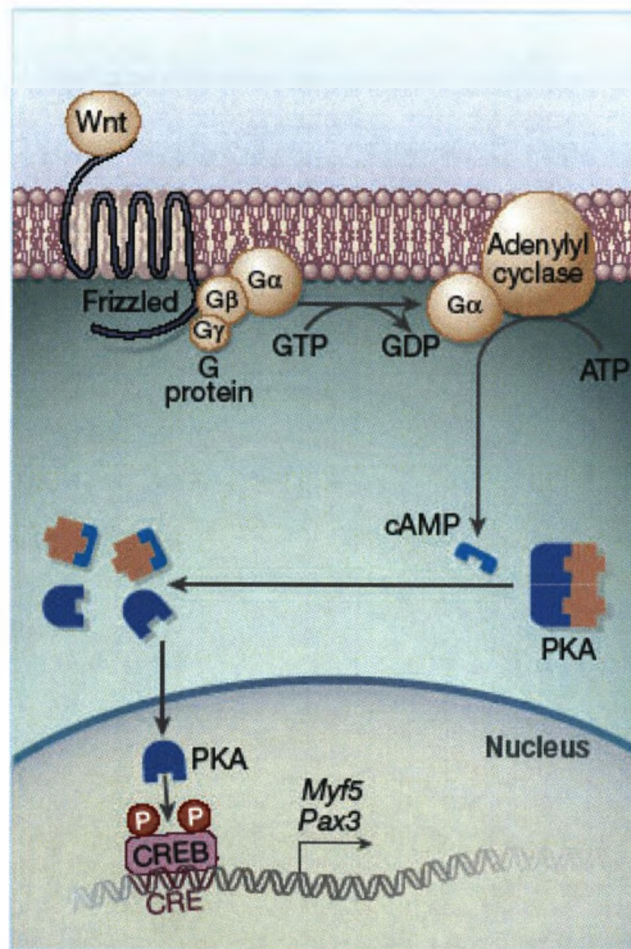


*Fig. 1.7. Wnt signalling mediated via cAMP (Pourquié O., 2005 [265])*

Therefore, efforts have focussed on subjection of stem cells to molecules which have the potential to increase intracellular concentrations of cAMP. Studies have successfully achieved neural differentiation of adult stem cells exploiting this technique using the membrane permeable cAMP analogue; dibutyryl cAMP to elevate intracellular cAMP. The influence of such a molecule can be heightened when used in conjunction with a non-specific phosphodiesterase inhibitor such as IBMX. This is merely one example. Forskolin is another molecule commonly exploited for its function in increasing intracellular cAMP concentrations in conjunction with the alkaloid K252a, a synthetic non-specific phosphodiesterase inhibitor [74, 259]. Numerous groups are also focussing on the differentiation of stem cells into a neural cell phenotype using retinoic acid

as a stimulus. Retinoic acid can play a role in an extensive number of intracellular processes. It interacts with retinoic acid and retinoid X receptors in the cell nucleus and can control apoptosis, cell cycle regulation and differentiation, including modulation of the tumour suppressor p53. Although these roles are diverse and critical in cellular fate, the mechanism by which they are coordinated is largely unknown. In neurogenesis it has been identified that the two isoforms of the retinoic acid receptor can dimerise which results in the transcription of several early neural lineage commitment genes such as *mash-1*, *ngn-1*, *prox-1*, and *neuro-D*, however the precise mechanisms of this transcription are undefined [260-262]. Characterisation of functional neurogenesis can be carried out by observation of molecules which permit neural cells to fulfil their role *in vivo* such as the neurotransmitter molecules noradrenalin, 5-hydroxytryptamine dopamine, and by electrophysiological assays to elucidate the potential of the neurons to electrically excite [263].

Differentiation of mesenchymal stem cells towards a hepatic fate is heavily dependent on one of a number of growth factors and cytokines, which have been shown to include hepatocyte growth factor (HGF), epidermal growth factor (EGF), transforming growth factor- $\beta$  (TGF- $\beta$ ), acidic FGF/FGF1, insulin and insulin-like growth factor (IGF). Additionally, an extensive group of non-proteinaceous chemical compounds have been demonstrated to promote hepatic differentiation and/or phenotype maintenance *in vitro* and include dexamethasone, retinoic acid, sodium butyrate, nicotinamide, norepinephrine, and dimethylsulfoxide [266]. Furthermore hepatic differentiation allows demonstration of a further event which favours a suitable three dimensional matrix over monolayer culture. It has been demonstrated that extensive cell-cell contact between hepatocytes grown in aggregates promotes the formation of gap junctions, tight junctions, and bile canaliculi that are important for stabilizing the hepatocyte phenotype, therefore suggesting the requirement for three dimensional culture matrices for the differentiation and lineage commitment to a hepatocyte phenotype [267-268]. As a result of this 3D spheroidal cultures have proven ideal culture systems for the

differentiation of mesenchymal stem cells along a hepatic lineage, although this did not alleviate the requirement for exogenous growth factors [269]. It has been demonstrated that umbilical cord derived stem cells cultured in a monolayer under hepatic conditions did not express markers associated with terminal hepatogenesis although they did express early hepatic markers and morphologically took on a hepatocyte appearance, initially suggesting that a monolayer culture is not satisfactory to complete hepatic differentiation of adult stem cells [270]. However, a similar study in which adipose derived mesenchymal stem cells were subjected to monolayer culture under hepatic conditions resulted in the differentiation into mature, functional hepatocyte cells, suggesting that a monolayer culture system is capable of stimulating hepatogenesis, however umbilical cord stem cells may be an unsuitable candidate for hepatic tissue engineering [271].

# DERIVATION OF DEFINED MEDIA FOR THE PHENOTYPE MAINTENANCE AND DIRECTED DIFFERENTIATION OF PRIMARY HUMAN PLURIPOTENT CELLS

## Chapter 2. Materials & Methods

### 2.i Immunohistochemistry

Staining was carried out *in situ* whilst the TCP cover slip was still in place in the well plate in which the cells were cultured. Samples were washed with PBS at room temperature for 5 minutes, followed by fixation using a solution of ddH<sub>2</sub>O containing formaldehyde and sucrose (Sigma-Aldrich, UK) at a concentration of 4% and 2% respectively (v/v) for 15 minutes at 37°C.

Post fixation, a further wash with PBS for 5 minutes at room temperature was carried out prior to permeabilisation using a solution of PBS containing the surfactant, Triton-X100 (Sigma-Aldrich, UK), at a concentration of 0.005% (v/v). After a further 5 minute wash at room temperature to remove residual Triton-X100, 50µL of a primary antibody (table.2.1.) was added to the samples, diluted to the working concentrations shown in table 2.1 using PBS containing bovine serum albumin (BSA) (Sigma-Aldrich, UK) at a concentration of 1% (v/v). Samples were incubated with primary antibody solutions for 1 hour at 37°C.

After incubation with primary antibody, samples were washed 3 times, for 5 minutes, at room temperature using PBS, again containing Triton-X100 at a concentration of 0.005% (v/v) to ensure that cells were still adequately permeable to permit entry of a secondary antibody. After re-permeabilisation, samples received 50µL of a relevant fluorochrome conjugated secondary antibody diluted to the working concentration illustrated in table 2.2 using PBS containing BSA to a concentration of 1%

(v/v) in an identical manner to primary antibody dilutions (table.2.1.). Samples were incubated with secondary antibodies for 1 hour at 37°C. After this time had elapsed samples were subjected to treatment with 50µL of Phalloidin, a phalloxin isolated from the death cap fungi (*Amanita phalloides*) that has the property of binding and stabilizing F-Actin filaments. This molecule was conjugated to the fluorochrome; 2',7'-difluorofluorescein (Oregon Green), (Ex 496nm, Em 524nm) (Invitrogen, Molecular Probes, UK) permitting visualisation of F-Actin filaments. The working dilution of Phalloidin was 1:100. Finally, samples were washed using PBS for 5 minutes at room temperature and further counterstained with vector shield fluorescence mounting media containing one of two DNA collating dyes; 4',6-diamidino-2-phenylindole (DAPI) (Vector Laboratories, UK) , (abs 358nm, em 461nm) or the monomeric cyaninie, TO-PRO-3 (abs 642nm, em 661nm) (Invitrogen, Molecular Probes, UK). These molecules were utilized interchangeably as a nuclear stain, the preference dependant on the laser system used to ultimately analyze the samples (UV or He-Ne Respectively). DAPI was utilized at the working concentration at which it was provided and TO-PRO-3 was diluted 1000 fold using vector shield (Vector Laboratories, UK). Immediately after nuclear staining, samples were mounted and observed using laser scanning confocal microscopy.

For particular applications the Phalloidin step of the protocol was replaced with a second primary antibody to create a 'dual stain'. In the case of these samples after removal of the initial secondary antibody a blocking step was carried out using 3 drops of horse serum in PBS for 15 minutes at 4°C, after which the protocol commenced again from the post fixation step with the F-actin counter staining removed. Nuclear staining proceeded as standard.

Controls to assess the extent of non-specific binding and hence fluorescence of secondary antibodies were carried out by replacing primary antibodies with PBS. Furthermore isotype controls were performed in which non-specific immunoglobins of the identical isotype

and speciation of the target antibody were used to replace the primary antibody used in immunohistochemical investigations in order to assess the levels of background non-specific staining caused by the target primary antibody at binding sites not specific to the desired target antigen.

Antigen	Speciation	Reactivity	Conjugate	Supplier	Dilution
IgG	Chicken	Rabbit	Alexa Fluor 488	Invitrogen, UK	1/100
IgG	Chicken	Rabbit	Alexa Fluor 594	Invitrogen, UK	1/100
IgG	Chicken	Mouse	Alexa Fluor 488	Invitrogen, UK	1/100
IgG	Donkey	Sheep	Alexa Fluor 594	Invitrogen, UK	1/100
IgG	Goat	Rabbit	Alexa Fluor 568	Invitrogen, UK	1/100
IgG	Goat	Mouse	Alexa Fluor 488	Invitrogen, UK	1/100
IgG	Goat	Rabbit	Texas Red	Invitrogen, UK	1/1000
IgG	Goat	Mouse	Rhodamine	ICN Biochemicals, Germany	1/500
IgG	Rabbit	Goat	Alexa Fluor 594	Invitrogen, UK	1/100

Table.2.2. Secondary antibodies used throughout immunohistochemical investigations

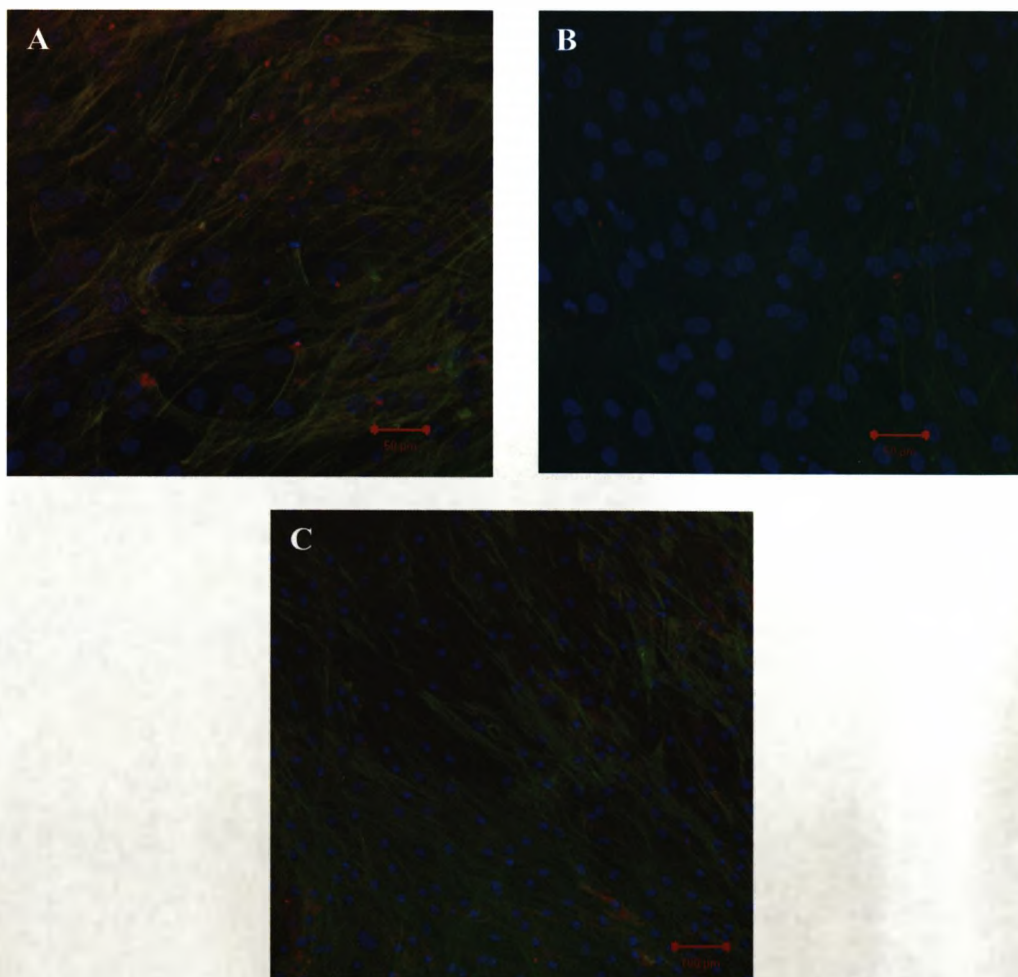


Fig.2.1. Isotype controls carried out in the obtaining of A; Fig. 2.32A, B; Fig. 3.24 and C; 3.25. Non-specific IgG interaction, F-actin & Nuclei



Antigen	Speciation	Reactivity	Clonality	Supplier	Dilution
Oct-4	Mouse	Human	Monoclonal	abcam, UK	1/100
5B5/D7-Fib	Mouse	Human	Monoclonal	abcam, UK	1/100
Adiponectin	Rat	Human	Monoclonal	R&D Sysytems, UK	1/100
Aggrecan	Mouse	Human	Monoclonal	Serotec, UK	1/100
$\alpha$ -feto-protein	Mouse	Human	Monoclonal	abcam, UK	1/100
$\beta$ -III-Tubulin	Rabbit	Human	Polyclonal	abcam, UK	1/100
CBFA1/RUNX2	Mouse	Human	Monoclonal	abcam, UK	1/100
CD205	Mouse	Human	Monoclonal	abcam, UK	1/100
CD25	Goat	Human	Monoclonal	R&D Sysytems, UK	1/100
CD3	Goat	Human	Polyclonal	abcam, UK	1/100
CD31	Rabbit	Human	Polyclonal	Serotec, UK	1/100
CD5	Mouse	Human	Monoclonal	abcam, UK	1/100
CD68	Mouse	Human	Monoclonal	abcam, UK	1/100
CHOP	Mouse	Human	Monoclonal	abcam, UK	1/100
CNTF	Mouse	Human	Monoclonal	R&D Sysytems, UK	1/100
Collagen I	Mouse	Human	Monoclonal	abcam, UK	1/100
Collagen II	Rat	Mouse	Monoclonal	Serotec, UK	1/200
Cripto1	Rat	Mouse	Monoclonal	Serotec, UK	1/100
Cytokerain-18	Rat	Mouse	Monoclonal	Serotec, UK	1/200
GAD153/CHOP	Rat	Mouse	Monoclonal	Serotec, UK	1/100
GFAP	Rat	Mouse	Monoclonal	Serotec, UK	1/200
Leptin	Human	Mouse	Monoclonal	Serotec, UK	1/100
Macrophage	Mouse	Human	Monoclonal	Alexis Biochemicals, USA	1/100
MBP	Rabbit	Human	Polyclonal	abcam, UK	1/100
MHCII	Rabbit	Human	Polyclonal	abcam, UK	1/100
Nestin	Mouse	Human	Monoclonal	abcam, UK	1/100
Neurofilament	Rabbit	Human	Polyclonal	abcam, UK	1/100
NGF	Mouse	Human	Monoclonal	abcam, UK	1/100
Nucleostemin	Mouse	Human	Monoclonal	R&D Sysytems, UK	1/100
Neutrophil	Mouse	Human	Monoclonal	abcam, UK	1/100
Osteocalcin	Mouse	Human	Monoclonal	R&D Sysytems, UK	1/100
P75-NGFR	Mouse	Human	Monoclonal	Sigma-Aldrich, UK	1/100
PPAR- $\gamma$	Mouse	Human	Monoclonal	abcam, UK	1/100
REST	Rabbit	Human	Monoclonal	Millipore, UK	1/100
S100	Mouse	Human	Monoclonal	abcam, UK	1/100
Serum Albumin	Rabbit	Human	Polyclonal	abcam, UK	1/100
SOX2	Sheep	Human	Polyclonal	abcam, UK	1/100
STRO-1	Mouse	Human	Monoclonal	abcam, UK	1/100
Substance P	Mouse	Human	Monoclonal	abcam, UK	1/100
TBR2	Mouse	Human	Monoclonal	Sigma-Aldrich, UK	1/1000
TRA-1-81	Mouse	Human	Monoclonal	Serotec, UK	1/100
VE-Cadherin	Mouse	Human	Monoclonal	Serotec, UK	1/100

Table.2.1. Primary antibodies used throughout immunohistochemical investigations



## 2.ii Fluorescence in situ hybridisation

Prior to hybridisation the following solutions were prepared. 20x sodium chloride, sodium citrate (20x SSC) using 87.6g NaCl (Sigma-Aldrich, UK) and 44.1g  $\text{NaH}_2(\text{C}_3\text{H}_5\text{O}(\text{COO})_3)$  (Sigma-Aldrich, UK) dissolved in 500ml ddH<sub>2</sub>O and pH adjusted to 7.4 using 10N HCl (Sigma-Aldrich, UK). This solution was then diluted 10 fold to make a working concentration of 2x SSC with the remainder stored at 4°C.

A denaturation solution was prepared using 70% HCONH<sub>2</sub> (v/v) (Sigma-Aldrich, UK) diluted using 2xSSC. Finally a working solution of porcine pepsin (Sigma-Aldrich) was prepared initially by production of a 1% solution of pepsin (w/v) in ddH<sub>2</sub>O, followed by subsequent dilution of 500 $\mu$ L of this stock with 49.5ml of 10mM HCl to produce a working concentration of the enzyme.

3-aminopropyl triethoxysilane (APTES) (Sigma-Aldrich, UK) coated slides were produced by immersing glass slides in a solution of acetone containing APTES at a concentration of 2% (v/v) for 5 minutes. Slides were then removed and placed in 100% acetone for a further 5 minutes followed by two 5 minute washes in ddH<sub>2</sub>O. Slides were then left to dry at 37°C overnight. Experimental samples were generated by the production of 6 $\mu$ m thick sections from frozen tissue explants using an OTF cryostat (Hacker-Bright, UK) and applied to APTES-coated slides followed by fixation for 15 minutes in ice cold 100% acetone (VMR, UK). Samples were then dehydrated in 100% ethanol for 5 minutes and dried at room temperature for 1 hour. Samples were then incubated in the working solution of pepsin for 5 minutes at room temperature followed by 2 washes using 2x SSC and a further wash using ddH<sub>2</sub>O. Samples were then re-dehydrated using a gradient of ethanol (VWR, UK); 70%, 90% and 100% (v/v) for two minutes in each, and dried at room temperature for 1 hour.

'Ready to use' cytochrome-3 labelled chromosome probes for human Y chromosome and chromosome 1 (Cambio, UK) were warmed to 37°C and

briefly centrifuged. Probes were denatured for 10 minutes at 65°C and held at 37°C for 1 hour.

Samples were incubated for 1 hour at 65°C after which were treated with denaturation solution, also pre-warmed to 65°C, for 2 minutes. Samples were then quenched in ice cold 70% (v/v) ethanol, followed by a further ethanol gradient dehydration and subsequent drying as performed above. After this point hybridisation was carried out by the application of 15µL of labelled probe to each sample. Samples were covered with a glass cover slip; air bubbles expelled using a pencil, and the union between the edge of the cover slip and the slide below sealed using superglue. Samples were then placed in an airtight, humidified chamber and incubated over night at 37°C in total darkness, after which point detection was carried out using laser scanning confocal microscopy.

### 2.iii RNA Isolation

Prior to the commencement of RNA isolation the following solutions were prepared. 10µL of 1M β-HOCH<sub>2</sub>CH<sub>2</sub>SH (Sigma-Aldrich, UK) was added to 1mL of buffer RLT. Additionally 44mL of 100% ethanol was added to 6mL of buffer RPE.

Samples were allowed to remain in tissue culture wells and subjected to three 5 minute washes using PBS at room temperature, after which 350µL of buffer RLT was added to each well and incubated for 5 minutes, also at room temperature. The subsequent cell lysate was removed and transferred to a QIAshredder column and spun at  $1.3 \times 10^4$  rpm for 2 minutes. Liquid that had been eluted from the column was diluted using 250µL 100% ethanol and added to an RNeasy mini column and spun at  $1.3 \times 10^4$  rpm for 15 seconds. 500µL of buffer RW1 was then added to the column and incubated for 5 minutes at room temperature, followed by a further  $1.3 \times 10^4$  rpm centrifugation step for 15 seconds. Proceeding this, 500µL of buffer RPE was added to the column followed by a 15 second spin at

1.3x10<sup>4</sup> rpm. Finally a further 500µL of buffer RPE was added to the column followed by 2 minutes of centrifugation at 1.3x10<sup>4</sup> rpm. To elute the RNA, the column was inserted into a clean, RNase-free eppendorf tube, 30µL of RNase free ddH<sub>2</sub>O was added, incubated at room temperature for 10 minutes, and spun for 1 minute at 1.3x10<sup>4</sup> rpm. Samples were then frozen at -80°C. Unless otherwise stated, all reagents were purchased from Qiagen, UK.

#### 2.iv DNA Isolation from Crude Tissue

Tissue sections of approximately 5mm<sup>3</sup> were isolated from whole tissue explants and macerated using surgical scissors. The following solutions were then produced: DNA buffer, containing 20mL 1M Tris pH 8.0 (Sigma-Aldrich, UK), 20mL 0.5M ethylenediaminetetraacetic acid (EDTA) (Invitrogen, UK) and 100mL ddH<sub>2</sub>O. Proteinase K solution containing 100mg of proteinase K (600 mU/ml) (Qiagen, UK) in 10mL of DNA buffer.

Macerated tissue was centrifuged at 1.5x10<sup>3</sup> rpm for 2 minutes at 4°C, the supernatant removed and the remaining pellet washed twice using DNA buffer and recovered by 2 minutes of centrifugation at 5x10<sup>3</sup> rpm. Post-washing, to the pellet was added 100µL Proteinase K and 240µL 10% (v/v) Sodium-dodecyl sulphate (Sigma-Aldrich, UK) was added to the pellet followed by overnight incubation at 45°C. After incubation, 2.4mL of 1M phenol (Sigma-Aldrich, UK) was added which was then agitated by hand for 10 minutes and spun at 3.0x10<sup>3</sup> rpm for 5 minutes at 10°C. The resulting supernatant was removed to a fresh tube to which was added a further 2.1mL 1M phenol and 1.2mL chloroform/isoamyl alcohol (24:1) (Sigma-Aldrich, UK). This solution was further agitated by hand for 10 minutes and spun at 3.0x10<sup>3</sup> rpm for 5 minutes at 10°C.

The resulting supernatant was removed to a fresh tube to which was added 25µL 3M sodium acetate (pH5.2) and 5mL 100% ethanol. In this solution,

the DNA precipitated after gentle shaking by hand. DNA could be carefully removed using a molecular biology grade 100 $\mu$ L pipette and transferred to a clean eppendorf where it was dissolved, facilitated by rolling in 1mL of ddH<sub>2</sub>O overnight at 4°C. The resultant DNA was stored at 4°C.

### 2.v Reverse Transcription / cDNA Generation

Prior to commencement of reverse transcription, the following stock solutions were created. Stock 1: 1 $\mu$ l 50 $\mu$ M Oligo(dT)<sub>20</sub>, 1 $\mu$ l 10mM dNTP cocktail, 9 $\mu$ L RNase free ddH<sub>2</sub>O. Stock 2: 4 $\mu$ L 5x first-strand buffers, 1 $\mu$ L 0.1M DTT, 1 $\mu$ L RNaseOUT recombinant RNase inhibitor (40 U/ $\mu$ L) and 1 $\mu$ L Superscript III RT (200 U/ $\mu$ L). The above stock solutions were suitable quantities for the reverse transcription of one sample (2 $\mu$ L) of RNA generated from the previously stated RNA isolation protocol (15-200  $\mu$ g/mL total RNA) and were scaled up accordingly for larger volumes of sample.

2 $\mu$ L of RNA solution was added to stock 1 and the resulting solution was denatured at 65°C for 5 minutes followed immediately by a 1 minute chill at -20°C. Stock 2 was then added, the resulting solution heated for 40 minutes at 50°C, immediately followed by a further 15 minutes heating at 70°C. The resulting cDNA solution was stored at 4°C. All reagents were purchased from Invitrogen, UK.

### 2.vi Real-Time Polymerase Chain Reaction (qRT-PCR)

qRT-PCR reactions were assembled containing 2 $\mu$ L cDNA previously diluted 100 fold using molecular biology grade ddH<sub>2</sub>O (Invitrogen, UK), 0.5 $\mu$ L of sense primer (100 $\mu$ M), 0.5 $\mu$ L antisense primer (100 $\mu$ M) (Sigma-Aldrich, UK), 7.5 $\mu$ L Sybr green single tube real time PCR master mix (Bio-Rad, UK) and 4.5 $\mu$ L molecular biology grade ddH<sub>2</sub>O. The stated

volumes quoted are per sample and were scaled up accordingly with stock solutions containing, primers, master mix and ddH<sub>2</sub>O made when required. All Primers (table 2.3.) were designed in house with the exception of Topoisomerase-3 (TOP-3) which was purchased pre-designed from Primer Design Ltd, UK.

Reactions were carried out in clean RNase free 96 well plates (Bio-Rad, UK) in a total reaction volume of 15 $\mu$ L. The cDNA was added to each well first, followed by 13 $\mu$ L of PCR reagent stock. All steps were carried out using filtered RNase free pipette tips (Scientific Laboratory Supplies, UK). Controls devoid of template cDNA were included in all plates by replacement of template cDNA with molecular biology grade ddH<sub>2</sub>O as to identify potential contaminant DNA than may have been introduced into the reaction components.

PCR reactions were performed using a Bio-Rad i-cycler machine and the standard i-cycler operating platform (Bio-Rad, UK) as follows. Plates were initially denatured for 3 minutes at 95°C. Immediately proceeding this were 40 cycles of amplification consisting of 95°C for 30 seconds followed directly by 30 seconds of the pre-calculated optimum annealing temperature ( $T_{a_{opt}}$ ) for the specific primer employed in the reaction, illustrated in table 2.3.  $C_t$  values were calculated when the increase in fluorescence generated as a result of the Sybr green molecule binding double stranded DNA during amplification entered its exponential phase (Ex 497nm, Em 520nm when bound to dsDNA).

After completion of amplification, melt curve analysis of the product was performed. Plates were subjected to an increase in temperature at an increment of 1°C per second commencing at 55°C and terminating at 95°C. This process quantifies the decrease in fluorescence as a result of the dsDNA becoming denatured, the two strands dissociating and thus the sybr green emission decreasing. As the 'melting' temperature of dsDNA varies as a result of its base composition this method was an ideal indicator of the identity of the amplification products when compared against the melting

temperature of a confirmed target product for a particular primer (Fig.2.2).  
When required, amplification products were stored at 4°C.

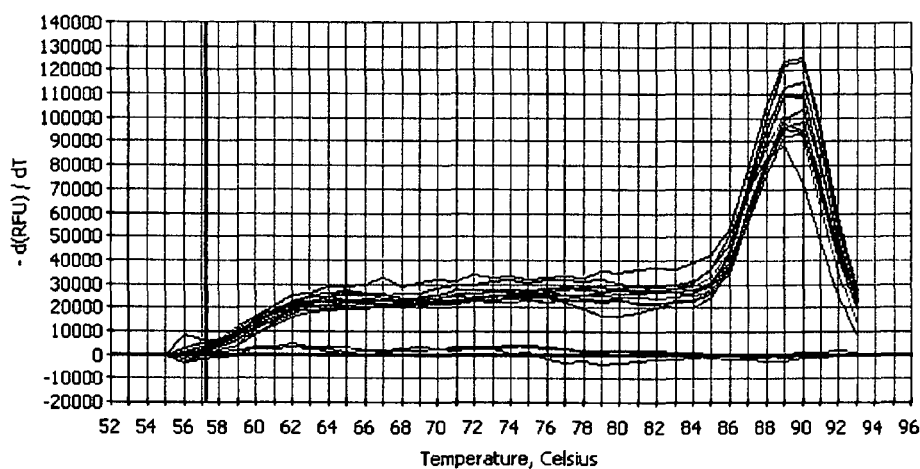


*Fig.2.2. Melt curve analysis of  $\beta$ -actin primer pair amplicon. Flat lines represent no cDNA template controls*

Fold differences in gene expression were calculated based threshold cycle values ( $C_t$ ). Mean  $C_t$  values from differentiation media were subtracted from mean  $C_t$ 's for a defined reference gene ( $\beta$ -actin) from the same cDNA sample for each time point investigated (Step 1.). Additionally the same calculation was performed on an identical cell type cultured under basal parameters (Step 2.). The difference in  $C_t$  induced by differentiation media could then be calculated by a simple subtraction (Step 3.) which then provided a value for input into a standard equation for equating  $C_t$  values to fold changes in gene expression ( $2^{-\Delta C_t}$ ) (Step 4.). This process is detailed progressively below.

Step 1:

$$C_t \text{ of gene of interest}_{\text{differentiation media}} - C_t \text{ reference gene}_{\text{differentiation media}}$$

Step 2:

$$C_t \text{ of gene of interest}_{\text{basal media}} - C_t \text{ reference gene}_{\text{basal media}}$$

Step 3: Step 1 – Step 2

Step 4:  $2^{-\text{Step}}$

Target Gene	Acession Number	Sense (5'-3')	Antisense (3'-5')	Ta opt (°C)
$\beta$ -Actin	NM001101	GGACCTGACTGACTACCTC	GCCATCTCTTGCTCGAAG	53.9
Collagen II	NM001844	GAGCAGCAAGAGCAAGGAGAAG	TGGACAGCAGGCGTAGGAAG	54.3
Sox9	X65665	CTACTCCACCTTCACCTAC	TGTGTAGACGGGTTGTTC	52.6
Osteopontin	NM000582	GCGAGGCGTTGAATGGTG	CTTGTGGCTGTGGGTTTC	53.9
Osterix	AF477981	CCACAACTCTCATCTCAG	GGACAGCAGGAAATAAGC	54.1
Osteonectin	BC008011	GCTGGATGATGAGAACAACAC	AAGAAGTGGCAGGAAGAG	53.4
CBFA1/RUNX2	AH005498	GGCAGTTCCCAAGCATTTC	GCAGGTAGGTGTGGTGTG	54.5
Aggrecan	BC036445	GTCTACCTCTACCCTAACC	TCTTGCTCTGATGGATGG	56.3
Collagen I	NM000088	GCCACTCCAGGTCCTCAG	CCACAGCACCAGCAACAC	54.5
Chondroadherin	AF371328	TTATCTACTTGTACCTGTCC	AAGATGAAGAGGTTGACC	54.9
$\beta$ -3-Tubulin	BC003021	AGGTGCGTGAGGAGTATC	GAAGCAGATGTCGTAGAGC	56.9
Adiponectin	EU420013	ATATGAAGGATGTGAAGGTC	CAGCATAGAGTCCATTACG	54.1
Alkaline Phosphatase	X55958	GGCATCCCAGTACCAGTTG	CCAAGAAAGCAGGAAAGTCAG	55.3
Neurofilament	NM006158	CTTCCAGAAGCCAAGACTCCAG	GAAGCAGATGTCGTAGAGC	55.0
Nestin	NM006617	GGAAAGTCAAAGGAATCTG	CTTCTCCACCGTATCTTC	53.7
Nerve Growth Factor	BC032517	GCAGACCCGCAACATCACTG	ATCTCCAACCCAACACACTGACA	61.0
PPAR- $\gamma$	NM005037	GACCACTCCCCTCCTTTG	GTGAATGGAATGTCTTCGTAATG	50.7
REST	BC017822	GCATCACATCAGTGTTACAG	CAGCGGTCACAGCGAATG	54.5
D7-Fib	AX772981	AGGAACAGAGCACAGGCCTTAGTG	AAGACCCCTCCCAGATAGATGG	55.0
Substance P	NM013996	TTCTTGTCTCCACTCAGC	GAATCAGCATCCCCTTTG	54.2
Fibronectin	U42594	TCATCCGTGGTTGTATCAG	GTCTCAGTCTTGTTCTCC	54.2
Fibrillin-1	AB177803	AGGCTGTGTAGATGAGAATGAATG	GGCACTCGTCCTGGTTGG	56.5
Elastin	AH007100	GAGTTGGTGCTGGTGTTTC	AGGTGCTGAGAGGAGGAG	56.2
Laminin	Z15008	ACTATTGCCTCATATTGCCTCTG	CCAACACTGCTCACTTCTTCC	52.9
$\alpha$ -SMA	AL157394	TCCACCTTCCAGCAGATG	CCACAGGACATTCACAGTTG	53.6
Smoothelin B	Y13492	GAGTCCATGACCGATGTG	TCTCTTGAGCCACTGTTG	55.9
GAPDH	NM002046	GAAGGTGAAGGTCGGAGT	CATGGTGAATCATGTTGGAA	53.5
Topoisomerase-III	D87012	NA	NA	60.0

Table.2.3. Parameters of primers used throughout PCR studies

### 2.vi Oil Red O Staining Protocol for Visualisation of Lipid Droplets

0.5% (w/v) Oil Red O solution was generated by dissolving 0.5g Oil Red O (Sigma-Aldrich, UK) in 100% CH<sub>3</sub>CHOHCH<sub>2</sub>OH (Sigma-Aldrich, UK) at 95°C, taking care not to allow the solution to reach 100°C. After the Oil Red O had dissolved, the resultant solution was filtered through coarse filter paper (Whatman, UK) overnight then stored at room temperature. Samples were air dried for 30 minutes and fixed using ddH<sub>2</sub>O containing formaldehyde and sucrose at a concentration of 4% and 2% respectively (v/v) for 15 minutes at 37°C followed by a 5 minute wash at room temperature using PBS. Samples were then placed in 100% CH<sub>3</sub>CHOHCH<sub>2</sub>OH for 5 minutes at room temperature. Staining then followed. The samples were submersed in 0.5% (w/v) Oil Red O solution for 8 minutes at 60°C and subsequently rinsed in 100% CH<sub>3</sub>CHOHCH<sub>2</sub>OH for 5 minutes at room temperature, followed by a 5 minute wash in ddH<sub>2</sub>O. Samples were counter stained using Gill's haematoxylin (Sigma-Aldrich, UK) for 30 seconds and 'blued' under running ddH<sub>2</sub>O for 3 minutes. Samples were then washed twice for 5 minutes using ddH<sub>2</sub>O and observed using transmitted light microscopy. Using this method, lipid droplets encapsulated within cells took on red staining.

### 2.vii Alcian Blue Staining Protocol for Visualisation of Glycosaminoglycans

Prior to staining the following solutions were prepared: 3% acetic acid solution (v/v) (Sigma-Aldrich, UK), 1% alcian blue solution (w/v) by dissolving 1g of alcian blue 8GX (Sigma-Aldrich, UK) in 3% acetic acid), and nuclear fast red solution synthesised by taking 100µg nuclear fast red (Sigma-Aldrich, UK) dissolving in ddH<sub>2</sub>O containing 5% Al<sub>2</sub>(SO<sub>4</sub>)<sub>3</sub> (w/v) (Sigma-Aldrich, UK) and to this was added 1-3g of thymol (Sigma-Aldrich, UK). Samples were fixed using ddH<sub>2</sub>O containing formaldehyde and sucrose at a concentration of 4% and 2% respectively (v/v) for 15 minutes at 37°C followed by a 5 minute wash at room temperature using



PBS. After fixation was complete, samples were placed in 3% acetic acid solution for 3 minutes. Immediately after this samples were placed in 1% alcian blue solution for 30 minutes followed by 2 minutes of continuous washing under running ddH<sub>2</sub>O. Samples were then counter-stained using the nuclear fast red solution for 5 minutes and rinsed using running ddH<sub>2</sub>O. Finally samples were dehydrated through gradients of ethanol; 70%, 90% and 100% (v/v) for two minutes in each, cleared using xylene (VWR, UK) and observed using transmitted light microscopy. All steps post fixation were carried out at room temperature. Using this method cells which contained surface glycosaminoglycans were stained turquoise blue.

#### 2.viii Von Kossa Staining Protocol for Visualisation of Calcification

Samples were fixed using ddH<sub>2</sub>O containing formaldehyde and sucrose at a concentration of 4% and 2% respectively (v/v) for 15 minutes at 37°C followed by a 5 minute wash at room temperature using PBS and 3 changes of ddH<sub>2</sub>O lasting 5 minutes each. After washing had been completed, samples were submersed a solution of 1% AgNO<sub>3</sub> (w/v) (Sigma-Aldrich, UK) made using ddH<sub>2</sub>O and placed under UV excitation for 1 hour. Once this time had elapsed, samples were subjected to three further changes of ddH<sub>2</sub>O each lasting 5 minutes followed by counter staining using Harris haematoxylin (Sigma-Aldrich, UK) for 5 minutes. 'Blueing' of the haematoxylin was carried out by placing the samples under running ddH<sub>2</sub>O for 5 minutes. Finally, samples were differentiated using ethanol containing 1% 1M HCl (v/v) for 10 seconds, washed using 3 changes of ddH<sub>2</sub>O and observed using transmitted light microscopy. All steps post fixation were carried out at room temperature. Using this method, calcified extracellular matrix appeared navy blue/black.

### 2.ix Methylene Blue Staining for Observation of Cell Morphology

Samples were fixed using ddH<sub>2</sub>O containing formaldehyde and sucrose at a concentration of 4% and 2% respectively (v/v) for 15 minutes at 37°C followed by a 5 minute wash at room temperature using PBS. After washing samples were subjected to staining using 0.04% (v/v) diluted using ddH<sub>2</sub>O from a 1.4% (w/v) stock dissolved in 95% ethanol (Sigma-Aldrich). Samples were incubated with the stain for 3 minutes at 37°C then washed for 5 minutes using PBS followed by a further 5 minute wash using ddH<sub>2</sub>O before being observed using transmitted light microscopy.

### 2.x Cell Culture

Cells were maintained on conventional plasma-treated tissue culture polystyrene (TCP) unless stated otherwise (Scientific Laboratory Supplies, UK). Prior to passage, cell culture media was removed from the tissue culture vessel and resultant adherent cells washed with PBS for 5 minutes to remove residual serum proteins which might have inhibited trypsinisation. After washing was completed, PBS was replaced by a solution of 5g porcine trypsin, 2g EDTA in 100mL of 0.9% sodium chloride (Sigma-Aldrich, UK) diluted to a working concentration of 10% (v/v) using PBS. Trypsinisation was performed at 37°C for between 5-10 minutes until approximately 75% of cells became detached from the substrate, observed by transmitted light microscopy. Cell/trypsin suspension was then diluted in an equal volume of appropriate basal cell culture media, pre-warmed to 37°C, containing 5% fetal calf serum (v/v) (Lonza, UK) 10,000 U/ml penicillin and 10 mg/ml streptomycin in 0.9% sodium chloride UK) to inhibit the trypsinisation reaction and thus prevent protease-induced cell damage during subsequent steps. Diluted trypsin/cell suspension was then spun at  $1.5 \times 10^3$  rpm for 5 minutes at 4°C to retrieve the cells, and the resultant cell pellet resuspended in an appropriate volume of suitable basal cell culture media. This solution was then distributed

throughout the desired number of tissue culture vessels and diluted further in a defined volume of cell culture media to permit long term culture.

Culture media was refreshed every 4<sup>th</sup> day by aspiration of spent media followed by replacement using fresh cell culture media, pre-warmed to 37°C. This process was repeated until cells became a confluent monolayer, at which point passaging was repeated. All cells were reseeded at 1/3 of the confluent cell density and incubated at 37°C, in a humidified atmosphere, containing 5%CO<sub>2</sub>.

#### 2.xi Protein Extraction

Media was aspirated and samples washed three 3 times for 5 minutes at room temperature to remove residual serum protein. After the final wash, PBS was replaced by a suitable volume of 1% (w/v) sodium-dodecyl sulphate dissolved in ddH<sub>2</sub>O and incubated at room temperature for 5 minutes. Resultant lysate was collected and transferred to an eppendorf tube and further denatured for 5 minutes at 95°C. Samples could be stored at -20°C until required. All plastics used (pipettes and eppendorf tubes) were protein free and purchased from Scientific Laboratory Supplies, UK.

#### 2.xii Enzyme-Linked Immunosorbent Assay (ELISA) – Human Serum Albumin

Prior to commencement of the assay the following solutions were prepared. Coating buffer: 0.05M sodium bicarbonate, pH 9.6. Wash solution: 50mM Tris, 0.14M NaCl, 0.05% Tween 20, pH 8.0. Blocking solution: 50mM Tris, 0.14M NaCl, 1% BSA, pH8.0. Sample diluent: 50mM Tris, 0.14M NaCl, 1% BSA, 0.05% Tween 20, pH8.0. All solutions were prepared using ddH<sub>2</sub>O were appropriate.

The required numbers of wells of a clean, molecular biology grade 96 well plate were coated with a 100 $\mu$ L of a coating solution containing 10 $\mu$ g/mL goat anti human albumin antibody diluted from 1mg/mL stock using the previously prepared coating buffer. Plates were incubated at room temperature for 1 hour after which the coating solution was aspirated and the plate was washed 3 times using 200 $\mu$ L of washing solution.

After washing, the antibody-coated substrata was blocked by the addition of 200 $\mu$ L of blocking solution to each well followed by 30 minutes of incubation at room temperature. Once this time had elapsed, the blocking solution was aspirated and the plate subjected to three further washes using washing solution.

To permit the generation of a calibration curve from which unknown sample serum albumin concentrations could be extrapolated, defined standard concentrations of human serum albumin were produced using human serum with a previously elucidated concentration of serum albumin. Human serum albumin was serially diluted with sample diluent such that the final concentrations of serum albumin used as standards were 1.0 $\times 10^4$ , 400, 200, 100, 50, 25, 12.5, 6.25, 3.12 and 1.6ng/mL.

Experimental samples, which consisted of cell lysates and media aspirates were then diluted also using sample diluent, based on predicted serum albumin concentrations, such that the sample concentrations would fall within the limitations of the calibration values (1:10). 100 $\mu$ L of samples and calibrators were added to the appropriate coated wells and incubated for 60 minutes at room temperature, after which, wells were aspirated and washed 5 times using 200 $\mu$ L of washing buffer. Controls included in the assay were samples which were replaced by an identical volume of ddH<sub>2</sub>O to identify non-specificity.

Horseshoe peroxidase conjugate was then diluted 1:7.5 $\times 10^4$  using sample diluent and 100 $\mu$ L applied to each well, followed by 60 minutes of incubation at room temperature, removed by aspiration, and 5 washes

using 200 $\mu$ L washing buffer. Enzyme substrate: 3, 3', 5, 5'-tetramethylbenzidine (TMB), was prepared immediately prior to use, by mixing equal volumes of the two provided substrate reagents. 100 $\mu$ L of substrate was added to each well after washing was completed and incubated at room temperature for 30 minutes. After this final incubation was complete the reaction was terminated using 100 $\mu$ L of 2M H<sub>2</sub>SO<sub>4</sub>, and the plate read immediately at 450nm using a  $\mu$ Quant microwell plate reader in conjunction with the operating platform KC Junior (BIO-TEK Instruments, USA). All reagents unless stated otherwise were purchased from Bethyl Laboratories. Inc, USA.

To calculate final concentrations of target protein in experimental samples the equation was generated to represent the curvature of the calibration curve:

$y = 0.3279\ln(x) + 0.0602$  and transposed such that x becomes the subject;  $x = e^{[(y-0.0602)/0.039]}$  where y is the absorbance and x is the target protein concentration. The absorbance for unknown samples was then used to calculate the concentration of human serum albumin therein.

#### 2.xiii Enzyme-Linked Immunosorbent Assay (ELISA) – Human Transferrin

Prior to commencement of the assay the following solutions were prepared. Standards were prepared by serial dilution using mix diluent of a 1mg/mL standard solution of human apo-transferrin such that final concentrations for generation of the standard curve were 750, 375, 118, 59, 29, 15, 7.5, 3.8, 1.9, 1.0, 0.5 and 0.25ng/mL. Experimental samples which consisted of cell lysates and media aspirates were also diluted using mix diluent such that expected concentrations fell within the limitations of the calibration values (1:10). 50 $\mu$ L of standards and samples were loaded to appropriate wells of a 96 well plate, pre-coated with polyclonal goat anti human apo-transferrin antibody and incubated at room temperature for 2 hours. Controls were included in which samples were replaced by an identical volume of ddH<sub>2</sub>O to identify non-specificity.

After this incubation had elapsed samples were aspirated from the plate which was then washed 5 times using 200 $\mu$ L of wash buffer. After the final wash was removed, wells were subjected to a second incubation at room temperature lasting 1 hour with 50 $\mu$ L of an 80X solution of a biotinylated polyclonal goat anti human transferrin antibody, diluted a working concentration using mix diluent. Once this incubation was complete, antibody was aspirated from the wells and the plate was washed 5 times using 200 $\mu$ L of wash buffer. Samples were then subjected to 30 minutes of incubation at room temperature with 50 $\mu$ L of a 100X streptavidin-peroxidase conjugate diluted to a working concentration using mix diluent, after which, the conjugate was aspirated and samples washed a further 5 times using 200 $\mu$ L of wash buffer. Finally, 50 $\mu$ L of 3, 3', 5, 5'-tetramethylbenzidine was added to the wells at the working concentration provided and incubated for 10 minutes at room temperature. The reactions were then terminated using 0.5M HCl. Immediately after termination, the plates were read at 450nm using a  $\mu$ Quant microwell plate reader in conjunction with the operating platform KC Junior (BIO-TEK Instruments, USA). All reagents unless stated otherwise were purchased from ASSAYPRO, USA.

To calculate final concentrations of target protein in experimental samples the equation was generated to represent the curvature of the calibration curve:

$y = 0.1521\ln(x) + 0.0716$  and transposed such that x becomes the subject;  
 $x = e^{[(y-0.0716)/0.1521]}$  where y is the absorbance and x is the target protein concentration. The absorbance for unknown samples was then used to calculate the resultant concentration of human apo-transferrin.

#### 2.xiv Alamar Blue Assay

Media was aspirated from cells seeded in a 24 well tissue culture plate (Scientific Laboratory Supplier, UK). Cells were then washed with PBS

three times for 5 minutes at room temperature. Once washing was completed cells were subjected to staining with 200 $\mu$ L of a 10% (v/v) dilution of alamar blue (AbD Serotec, UK) made using ddH<sub>2</sub>O. Samples were incubated for 90 minutes at 37°C, in a humidified atmosphere containing 5% CO<sub>2</sub>. After incubation had been completed the resultant solution was transferred to a black 96 well plate and read using an FL<sub>x</sub>800 microplate fluorescence reader in conjunction with the KC Junior operating platform (BIO-TEK Instruments, USA). This technique relies on the molecule: resazurin, a nontoxic, non-fluorescent, cell permeable redox indicator dye, which is continually converted to bright red-fluorescent resorufin via the reduction reactions of viable, metabolically active cells (Fig.2.3.). As a result of this, the absorbance maxima of the molecule shifts from 530nm to 590nm and can be quantified using appropriate colourimetric techniques.

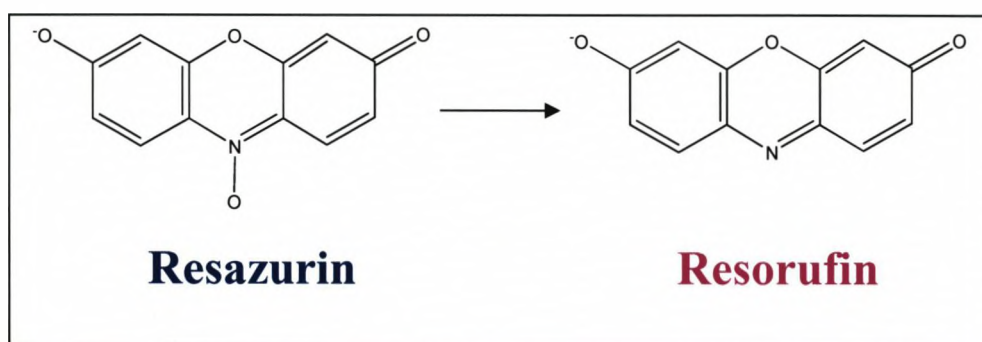


*Fig.2.3. Molecular schematic of the reduction of Resazurin to Resorufin which occurs in metabolically active cells*

### 2.xv Flow-Cytometry

Prior to analysis adherent cells were washed using PBS for 5 minutes at room temperature. After washing was completed PBS was replaced by a solution of 5g porcine trypsin, 2g EDTA in 100mL of 0.9% sodium chloride (Sigma-Aldrich, UK) diluted to a working concentration of 10% (v/v) using PBS. Trypsinisation occurred at 37°C for between 5-10 minutes until approximately 75% of total cells became detached from the substrate, observed by transmitted light microscopy. Cell/trypsin

suspension was then diluted in an equal volume of appropriate basal cell culture media, pre-warmed to 37°C, containing 5% Fetal calf serum (v/v) (Lonza, UK) and 1% (v/v) 10,000 U/ml penicillin and 10mg/ml streptomycin in 0.9% sodium chloride (Sigma-Aldrich, UK) to inhibit the trypsinisation reaction and thus prevent protease induced cell damage during subsequent steps. Diluted trypsin/cell suspension was then spun at  $1.5 \times 10^3$  rpm for 5 minutes at 4°C to retrieve the cells, and the resultant cell pellet resuspended in an appropriate volume of PBS and aliquotted into suitable clean, flow-cytometry tubes (ELKAY, UK) such that the total number of cells per tube was between  $5.0 \times 10^4$  and  $6.0 \times 10^4$  in a total volume of 10µL of PBS. To each tube was then added 2µL of a defined fluorochrome conjugated antibody (table 2.5.) resulting in a final concentration of approximately 1.0µg IgG per  $1.0 \times 10^6$  cells. Samples were then incubated at 4°C for 15 minutes. After incubation 190µL of sheath fluid (BD-Biosciences, UK) was added to each tube before analysis using a FACSort flow cytometer (BD-Biosciences, UK).

Non specific fluorescence was compensated for by incorporating conjugated isotype controls. Antibodies with a defined antigenicity were replaced at the same concentration with a non-specific IgG of an identical isotype (table.2.4.), speciation and conjugation to the specific antibody. This permitted the quantification of fluorescence as a result of binding of the IgG to cells, without target to a particular antigen. The isotype fluorescence peak was then subtracted from the specific antigen peak to elucidate the true fluorescence resulting from positive staining, illustrated in Fig.2.4.

Fig.2.5. Illustrates a number of MSC antigens used throughout flow cytometric analysis of mesenchymal stem cell phenotype detailing overlays of isotype controls.



Isotype	Speciation	Reactivity	Clonality	Conjugate	Supplier
IgM	Mouse	Human	Monoclonal	PE	Santa Cruz Biotechnology, USA
IgG1	Goat	Human	Monoclonal	FITC	Serotec, UK
IgG2a	Rat	Human	Monoclonal	FITC	Serotec, UK
IgG2a	Mouse	Human	Monoclonal	FITC	Serotec, UK
IgG1	Mouse	Human	Monoclonal	FITC	Serotec, UK
IgG1	Mouse	Human	Monoclonal	PE-Cy5	BD Biosciences, UK
IgG1	Mouse	Human	Monoclonal	PE	BD Biosciences, UK
IgG2b	Mouse	Human	Monoclonal	FITC	Serotec, UK
IgG2b	Mouse	Human	Monoclonal	PE	BD Biosciences, UK

Table.2.4. Isotype control antibodies used throughout flow-cytometry investigations

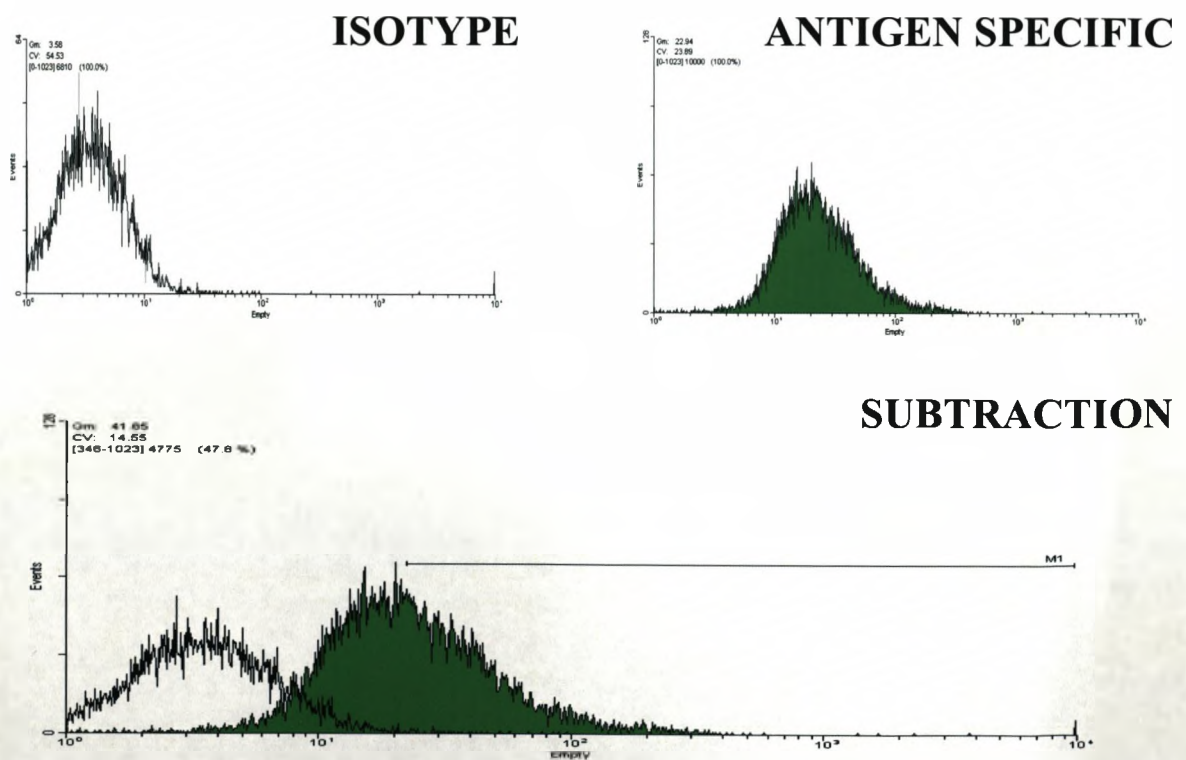


Fig.2.4. Flow-Cytograms illustrating the reference to non-specific IgG-Cell interactions when generating data

Antigen	Speciation	Reactivity	Clonality	Conjugate	Isotype	Supplier
CD9	Mouse	Human	Monoclonal	<b>FITC</b>	IgG2b	Serotec, UK
CD19	Mouse	Human	Monoclonal	<b>Per-CP</b>	IgG1	BD Biosciences, UK
CD29	Mouse	Human	Monoclonal	<b>PE-Cy5</b>	IgG1	BD Biosciences, UK
CD30: FITC	Mouse	Human	Monoclonal	<b>FITC</b>	IgG2a	Serotec, UK
CD31	Mouse	Human	Monoclonal	<b>PE</b>	IgG1	BD Biosciences, UK
CD34	Mouse	Human	Monoclonal	<b>FITC</b>	IgG1	BD Biosciences, UK
CD34 Class II	Mouse	Human	Monoclonal	<b>FITC</b>	IgG1	Serotec, UK
CD34 Class III	Mouse	Human	Monoclonal	<b>FITC</b>	IgG2a	Serotec, UK
CD44	Mouse	Human	Monoclonal	<b>PE</b>	IgG2b	BD Biosciences, UK
CD45	Mouse	Human	Monoclonal	<b>FITC</b>	IgG1	BD Biosciences, UK
CD50: FITC	Mouse	Human	Monoclonal	<b>FITC</b>	IgG1	Serotec, UK
CD51/CD61	Mouse	Human	Monoclonal	<b>FITC</b>	IgG1	BD Biosciences, UK
CD56	Mouse	Human	Monoclonal	<b>FITC</b>	IgG2a	Serotec, UK
CD62E	Mouse	Human	Monoclonal	<b>FITC</b>	IgG2a	Serotec, UK
CD64	Mouse	Human	Monoclonal	<b>FITC</b>	IgG1	BD Biosciences, UK
CD73	Mouse	Human	Monoclonal	<b>PE</b>	IgG1	BD Biosciences, UK
CD90	Mouse	Human	Monoclonal	<b>FITC</b>	IgG1	Serotec, UK
CD106	Mouse	Human	Monoclonal	<b>PE</b>	IgG1	BD Biosciences, UK
CD105	Mouse	Human	Monoclonal	<b>FITC</b>	IgG1	Serotec, UK
CD117	Mouse	Human	Monoclonal	<b>PE</b>	IgG1	BD Biosciences, UK
CD133	Mouse	Human	Monoclonal	<b>PE</b>	IgG1	Miltenyi Biotec
CD146	Mouse	Human	Monoclonal	<b>FITC</b>	IgG1	Serotec, UK
CD166	Mouse	Human	Monoclonal	<b>PE</b>	IgG1	BD Biosciences, UK
CD271 (NGFR)	Mouse	Human	Monoclonal	<b>PE</b>	IgG1	BD Biosciences, UK
HLA-B27	Mouse	Human	Monoclonal	<b>FITC</b>	IgG2a	Serotec, UK
HLA-DR	Rat	Human	Monoclonal	<b>FITC</b>	IgG2a	Serotec, UK
STRO-1	Mouse	Human	Monoclonal	<b>PE</b>	IgM	Santa Cruz Biotechnology, USA
VWF	Sheep	Human	Polyclonal	<b>FITC</b>	IgG1	Serotec, UK
$\alpha$ -SMA	Mouse	Human	Monoclonal	<b>FITC</b>	IgG2a	Sigma-Aldrich, UK

Table.2.5. Antibodies used throughout flow-cytometric investigations



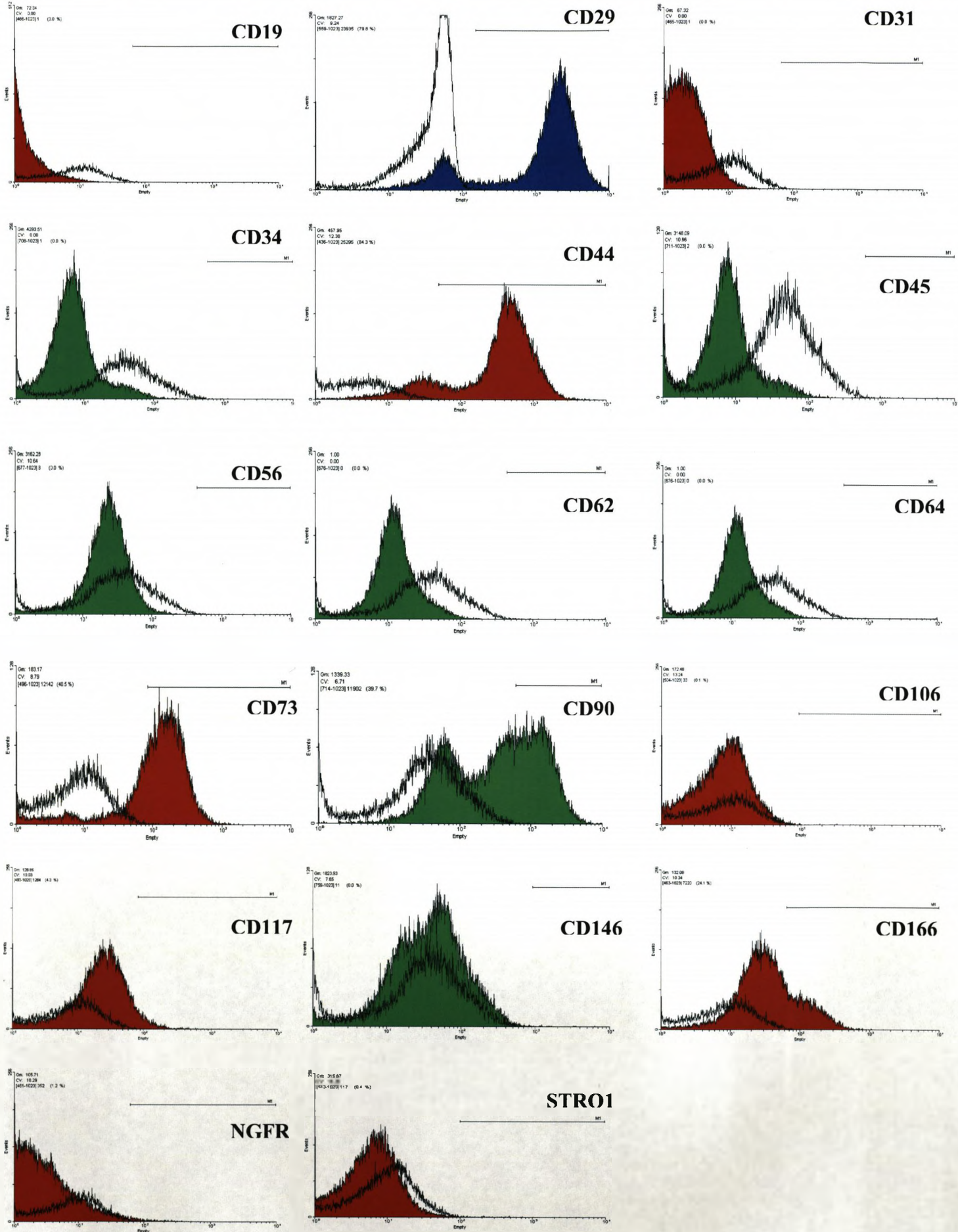


Fig.2.5. Antigens used throughout flow cytometric analysis of MSC phenotype showing isotype overlay (Shown MSC passage 2, serum free parameters)

### 2.xvi Plasma Isolation

20mL of peripheral blood was isolated by vein puncture from experimental groups containing at least 6 healthy donors of both genders, decanted into sterile plastic, and immediately prevented from coagulating using 10% (v/v) 10mM sodium citrate (Sigma-Aldrich,UK). This inhibited clotting by chellation of  $Ca^{2+}$ , an ion critical for progression of the blood coagulation cascade. The conversion of prothrombin (factor II) to thrombin (factor I) is  $Ca^{2+}$  dependant, and is rate limiting in blood clotting because thrombin cleaves fibrinogen to form fibrin, the scaffold material in a blood clot. Citrated blood samples were sealed and allowed to remain at room temperature for a period of 2 hours before being incubated overnight at 4°C to allow blood cells and blood plasma to form 2 distinct fractions. Following this incubation, samples were centrifuged at 500 rpm for 10 minutes and the resultant supernatant collected, and blood cell containing pellet discarded. Supernatants were then subjected to further centrifugation for at 500 rpm for 10 minutes to ensure maximal extraction of any residual blood cells. The resultant citrated, platelet poor plasma was pooled then either used immediately or frozen at -20°C until required.

### 2. xvii In Vitro Hydrogel Synthesis

Citrated, platelet poor, blood plasma was defrosted and pre-warmed to 37°C. Simultaneously, culture media base was prepared and pre-warmed to 37°C; Dubecco's modified Eagles media (DMEM), 4,500mgL<sup>-1</sup>, + L-glutamine, + phenol red (Gibco, UK) was combined with 1% (v/v) 10,000 U/ml penicillin and 10mg/ml streptomycin in 0.9% sodium chloride (Sigma-Aldrich, UK). DMEM was used as a basal medium for the routine culture and maintenance of human cells using the hydrogel system. The base culture media could potentially be modulated to become any  $Ca^{2+}$  containing culture media and was modified for particular usage in cell specific applications such as the differentiation of mesenchymal stem cells,

which may require defined differentiation, with increased exogenous stimulation media in place of conventional DMEM.

Following suitable media selection, the blood plasma fraction was added to the basal media at a concentration of 10% (v/v) in a suitable TCP vessel and returned to 37°C, in a humidified atmosphere, containing 5% CO<sub>2</sub>. After approximately 3-5 minutes of incubation, a stable hydrogel formed as a result of combination of the two solutions. Gels were generally cast 3mm in thickness.

The Ca<sup>2+</sup> laden culture media replaced the Ca<sup>2+</sup> which was removed from the blood coagulation cascade as a consequence of citration. Replacement of Ca<sup>2+</sup> resulted in the progression of thrombus formation, which, in conjunction with the liquid component of the media formed a nutrient rich hydrogel.

#### 2.xvii Cell Culture – Hydrogel Substrate

Prior to introduction to the hydrogel, cells were maintained on conventional plasma treated tissue culture polystyrene (TCP) unless stated otherwise (Scientific Laboratory Supplies, UK). Prior to passage, cell culture media was removed from the tissue culture vessel and resultant adherent cells washed with PBS for 5 minutes to remove residual serum proteins which may have compromised trypsinisation. After washing was completed PBS, was replaced by a solution of 5g porcine trypsin, 2g EDTA in 100mL of 0.9% sodium chloride (Sigma-Aldrich, UK) diluted to a working concentration of 10% (v/v) using PBS. Trypsinisation occurred at 37°C for between 5-10 minutes until approximately 75% of cells became detached from the substrate, observed by transmitted light microscopy. Cell/trypsin suspension was then diluted in an equal volume of appropriate basal cell culture media, pre-warmed to 37°C, containing 5% fetal calf serum (v/v) (Lonza, UK) and 1% (v/v) 10,000 U/ml

penicillin and 10 mg/ml streptomycin in 0.9% sodium chloride (Sigma-Aldrich, UK) to inhibit the trypsinisation reaction and thus prevent protease induced cell damage during subsequent steps. Diluted trypsin/cell suspension was then spun at  $1.5 \times 10^3$  rpm for 5 minutes at 4°C to retrieve the cells, and the resultant cell pellet resuspended in an appropriate volume of suitable basal cell culture media.

Cells were introduced to the hydrogel substrate in one of three ways: surface seeded, embedded or seeded beneath the gel. When seeding onto the surface of the gel, gels were cast as described. Cells were then introduced on to the gel surface by means of resuspension in a suitable volume of culture media as to achieve the desired seeding density, loaded gently onto the surface of the gel, and distributed across the surface by slight rocking of the vessel before being allowed to adhere and proliferate.

To embed cells in the gel, they were resuspended in the 37°C basal media/citrated platelet poor plasma solution before being introduced to a suitable vessel, and thus becoming entrapped in the hydrogel during gelation. Finally, cells seeded under the gel were introduced to tissue culture plastic in suitable media containing 5% fetal calf serum (v/v) (Lonza, UK) and 1% (v/v) 10,000 U/ml penicillin and 10mg/mL streptomycin in 0.9% sodium chloride after retrieval from centrifugation, allowed to adhere for a period of 4-5 hours at 37°C in a humidified atmosphere of 5% CO<sub>2</sub>. Media was then aspirated and replaced by basal media/citrated platelet poor plasma solution which then set, sandwiching the cells below the hydrogel. The culture media on cells seeded on top of the hydrogel was routinely refreshed every 4<sup>th</sup> day by aspiration of spent media followed by replacement with a suitable volume of fresh culture media. Cells could be removed from the hydrogel by the complete destruction of the gel matrix using a standard solution of 5g porcine trypsin, 2g EDTA in 100mL of 0.9% sodium chloride (Sigma-Aldrich, UK) diluted to a working concentration of 10% (v/v) using PBS. Gels were incubated at 37°C in a humidified atmosphere of 5% CO<sub>2</sub> for 30 minutes, after which the gel was destroyed and cells could be harvested.

The cell/liquid gel volume was doubled using a suitable cell culture media, pre-warmed to 37°C, containing 5% Fetal calf serum (v/v) (Lonza, UK) and 1% (v/v) 10,000 U/ml penicillin and 10 mg/ml streptomycin in 0.9% sodium chloride (Sigma-Aldrich, UK) to terminate the trypsinisation. Cells were then collected by means of centrifugation at  $1.5 \times 10^3$  rpm for 5 minutes at 4°C before undergoing reseeding onto a suitable substrate or further analysis.

### 2.xviii Cell Tracking Dyes

Prior to introduction to the hydrogel, cells were maintained on conventional plasma treated tissue culture polystyrene (TCP) unless stated otherwise (Scientific Laboratory Supplies, UK). Prior to passage, cell culture media was removed from the tissue culture vessel and resultant adherent cells washed with PBS for 5 minutes to remove residual serum proteins which may have compromised trypsinisation. After washing was completed PBS was replaced by a solution of 5g porcine trypsin, 2g EDTA in 100mL of 0.9% sodium chloride (Sigma-Aldrich, UK) diluted to a working concentration of 10% (v/v) using PBS. Trypsinisation occurred at 37°C for between 5-10 minutes until approximately 75% of cells had become detached from the substrate, observed by transmitted light microscopy. Cell/trypsin suspension was then diluted in an equal volume of appropriate basal cell culture media, pre-warmed to 37°C, containing 5% Fetal calf serum (v/v) (Lonza, UK) and 1% (v/v) 10,000 U/ml penicillin and 10 mg/ml streptomycin in 0.9% sodium chloride (Sigma-Aldrich, UK) to inhibit the trypsinisation reaction and thus prevent protease induced cell damage during subsequent steps.

Diluted trypsin/cell suspension was then spun at  $1.5 \times 10^3$  rpm for 5 minutes at 4°C to retrieve the cells, and the resultant cell pellet resuspended in an appropriate volume of DMEM, 4,500mg/L, + L-glutamine, + phenol red (Gibco, Uk) in the absence of serum, at a density of  $1.0 \times 10^6$  cells/mL. 5µl of DiD (Ex 644nm, Em 665nm), DiL (Ex 549nm, Em 565nm) or DiO (Ex

484nm, Em 501nm) cell tracking dye (Invitrogen, UK) were added per mL of cell laden media and mixed by gentle vortexing. These dyes were used interchangeably using an identical protocol with preference being made depending on the laser system available to observe the subsequent specimens. Cells were incubated at 37°C in a humidified atmosphere containing 5% CO<sub>2</sub> for 15 minutes followed by retrieval using 5 minutes of 1.5x10<sup>3</sup>rpm centrifugation at 4°C. After centrifugation, media was aspirated and the remaining pellet washed by resuspension in 5mL of PBS prewarmed to 37°C for 5 minutes. Cells were then collected after 5 minutes of centrifugation at 1.5x10<sup>3</sup>rpm at 4°C and subsequently introduced into culture or subjected to appropriate analysis.

#### 2.xix In vivo cell growth and defect site delivery model

Six week old, immuno deficient CH1 nude mice received four implants as injections, 2 into the subcutaneous (SC) tissue above each shoulder and either 2 subcutaneous injections above each hip joint or 2 intramuscular injections (IM) into the quadriceps femoris muscle. The site of implantation (IM or SC) was determined by the phenotype of the implanted cells, and the gender of the experimental animals determined by the nature of subsequent planned analyses. Two primary human cell types were employed in animal validations: Human dermal fibroblasts were chosen as the model for soft tissue generation and were delivered solely to SC sites. Human osteoblasts which were exploited as a model for ectopic bone tissue formation due to their ability to drive osteogenesis in clinical applications, and additionally determined the validity of data published previously suggesting the requirement for a solid scaffold for the synthesis of ectopic bone *in vivo*, were delivered to both SC and IM sites.

Implantation was carried out using defined cell numbers between 1.0x10<sup>5</sup> and 2.0x10<sup>6</sup> taken from passage 6. Each animal received a defined number of primary cells in a total injection volume of 300µl.



Citrated platelet poor plasma (v/v) and cell-loaded DMEM, 4,500mg/L, + L-glutamine, + phenol red (Gibco, Uk) in the absence of serum were pre-warmed and combined at 10% plasma:media (v/v), immediately prior to implantation then injected into the animals in one of the candidate implantation sites per animal. Animals were sacrificed at 4, 6, 8 and 10 weeks post implantation using asphyxiation with CO<sub>2</sub>, and ectopic tissue excised for analysis to determine tissue formation and host integration. To achieve gelation *in vivo*, implantation was performed using a three way stopcock tap system (Smiths Medical, UK). Cells and media were contained in one syringe with blood plasma in another (Fig.2.6). Both solutions were prewarmed to 37°C. The two solutions were then transfused into one syringe by means of the three way tap to allow mixing and, following a further turn of the tap, injected through a 21 gauge needle into the desired implantation site. All *in vivo* experimental procedures were conducted in accordance with the U.K. Home Office regulations under licence and were approved by Research Ethics Committee.

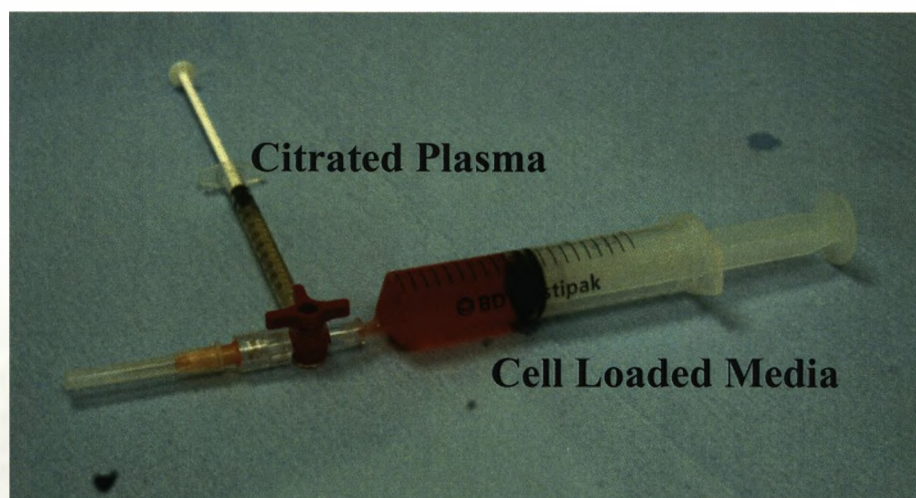


*Fig.2.6. Illustration of the implantation system employed for the delivery of cell loaded hydrogel to a desired in-vivo site*

### 2.xx Cryo-Scanning Electron Microscopy (CryoSEM)

CryoSEM presents a valuable technique for the visualisation of materials that have a high water content whose structure might be altered or destroyed by dehydration and cross linking. Fresh tissue samples were

washed using PBS then immediately snap frozen in liquid nitrogen. The frozen samples were then transferred under vacuum to a Gatan Alto 2500 preparation chamber (Gatan Inc. USA) and warmed to  $-95^{\circ}\text{C}$  for 15 minutes to allow the vitreous ice layer to sublime. Once the water was removed from the surface of the sample it was fractured under vacuum using a scalpel blade to reveal internal structures and subsequently sputter coated with gold to create a conductive pathway across the surface of the sample. The sample was then transferred under vacuum to the cold stage of the scanning electron microscope, where it was observed at 3kV using a working distance of 8mm.

#### 2.xxi Histopathology and Antigen Preservation

To retain tissue antigenicity whilst providing excellent tissue morphology, samples were placed directly into periodate-lysine-paraformaldehyde fixative post explantation, which was prepared as follows. Initially a 0.2M lysine-HCl solution was prepared by dissolving 10.96g of Lysine-HCl (Sigma-Aldrich, UK) in 300mL of ddH<sub>2</sub>O. Secondly a 0.1M solution of Na<sub>2</sub>HPO<sub>4</sub> was prepared by dissolving 1.42g of Na<sub>2</sub>HPO<sub>4</sub> (Sigma-Aldrich, UK) in 100mL of ddH<sub>2</sub>O, 60mL of which was then added to 300mL of Lysine-HCl to result in a solution with a pH of 7.4. Next, a 0.1M phosphate buffer was prepared by dissolving 0.476g NaH<sub>2</sub>PO<sub>4</sub> (Sigma-Aldrich, UK) and 2.24g Na<sub>2</sub>HPO<sub>4</sub> in 400mL ddH<sub>2</sub>O. 240mL of this phosphate buffer was added to the Lysine-HCl/Na<sub>2</sub>HPO<sub>4</sub> solution resulting in a 0.1M concentration of Lysine-HCl. A solution of 2% (w/v) paraformaldehyde (Sigma-Aldrich, UK) was then prepared by dissolving 2g of paraformaldehyde in 100mL of ddH<sub>2</sub>O with gentle heating.

Immediately prior to use, 300mL of the phosphate buffered lysine-HCl solution was combined with 100mL of 2% (w/v) paraformaldehyde and to this was added 0.855g of sodium periodate (Sigma-Aldrich, UK) resulting

in a concentration of 0.1M. The fixative was then chilled to 4°C prior to use. Samples were placed under periodate-lysine-paraformaldehyde fixation on a roller for 24hrs at 4°C. Fixative was aspirated from samples and replaced with cold washing solution, which consisted of the previously described 0.1M phosphate buffer modified to contain 7% sucrose (Sigma-Aldrich, UK) and 40mM NH<sub>4</sub>Cl (Sigma-Aldrich, UK) Samples were gently rolled at 4°C for 24 hours. After this time had elapsed cold washing solution was aspirated and replaced by ice-cold acetone to remove phosphate crystals and dehydrate the specimens, for 24 hours at 4°C, whilst being rolled.

Once samples were suitably dehydrated they were immersed in 100% glycol methacrylate (GMA) (TAAB, UK) for 24 hours at 4°C, after which, samples were then moved to ice cold Technovit infiltration solution (TAAB, UK) for a further 24 hours at 4°C. Specimens were then cast in place in an appropriately sized mould, orientated carefully for optimum cutting (TAAB, UK) and submersed in Technovit embedding solution (TAAB, UK). The pre-resin surface was covered with mineral oil (Sigma-Aldrich, UK) to prevent oxidation and evaporation, sealed with aluminium foil and placed at -55°C to infiltrate for 4 days. After this time had passed, the incubation temperature was then increased to -20°C for 2 days to facilitate polymerisation of the resin.

After successful setting followed by subsequent removal from the moulds, tissue blocks were sectioned (6µm thick sections) using a polycut microtome (Reichert-Jung, USA) and placed onto microscope slides coated with 3-aminopropyl triethoxysilane (APTES) (Sigma-Aldrich, UK) by immersion in a solution of acetone containing APTES at a concentration of 2% (v/v) for 5 minutes. Slides were then removed and placed in 100% acetone for a further 5 minutes followed by two 5 minute washes in ddH<sub>2</sub>O. Slides were then left to dry at 37°C overnight.

### 2.xxii Immunohistochemistry – Resin Embedded Samples

Masked epitopes of 6 $\mu$ m resin embedded sections were exposed by digestion with 0.1% trypsin type III (Sigma-Aldrich, UK) in 0.1% (w/v) CaCl<sub>2</sub> (Sigma-Aldrich, UK), pH 7.8 produced using ddH<sub>2</sub>O, for 15 minutes at 37°C followed by a 5 minute wash at room temperature using PBS. Non-specific binding was then blocked using horse serum (Sigma-Aldrich, UK) suitably diluted by mixing 3 drops of serum in 10mL of PBS. Samples were blocked for 30 minutes at 37°C, under normal atmospheric conditions.

Primary antibodies were diluted to working concentrations (table.2.1.) using a 1% (w/v) solution of BSA (Sigma-Aldrich) dissolved in PBS. After receiving antibodies, samples were incubated for 24 hours at 4°C. Samples were then washed using PBS for 5 minutes at room temperature prior to incubation with secondary antibodies, followed by a 5 minute wash in PBS. Secondary antibodies were diluted using to working concentrations (table.2.2.) using PBS and after application to the samples incubation lasted 60 minutes at 37°C under normal atmospheric conditions. Slides were then washed in PBS for 5 minutes at room temperature and exposed to mouse ABC/AP tertiary antibody kit, following the manufacturers instructions (Vector laboratories, UK) for 30 minutes at room temperature, directly proceeded by a further wash in PBS. Slides were then incubated at room temperature for 20 minutes with alkaline phosphatase kit (Vector laboratories, UK) in 0.1M Tris-HCl (Sigma-Aldrich, UK) pH 8.2, followed by two final 5 minute washing steps in PBS and ddH<sub>2</sub>O. Tissue histopathology was performed on the stained samples using a combination of microscopical techniques: laser scanning confocal; fluorescent and visible light microscopy.

### 2.xxiii Haematoxylin and Eosin Staining for Observation of Tissue Structures

Samples were hydrated using ddH<sub>2</sub>O before being submersed in Harris' haematoxylin (Sigma-Aldrich) for 5 minutes at room temperature. Stained samples were then 'blued' under running ddH<sub>2</sub>O for 3 minutes before differentiation using ethanol containing 1% 1M HCl (v/v) for 10 seconds. Samples were then washed under running ddH<sub>2</sub>O before being subjected to 3 minutes of staining at room temperature with 1% eosin (Sigma-Aldrich, UK) prepared using ddH<sub>2</sub>O. Finally samples were dehydrated using gradient of ethanol; 70%, 90% and 100% (v/v) for two minutes in each, cleared using xylene (VWR, UK) and observed using transmitted light microscopy. Staining in this manner permitted visualisation of differing tissular structures in varying shades of red/pink.

### 2.xxiv Primer Design

RT-PCR primers were designed in house using the Beacon Designer V.7.21 platform (Premierbiosoft International, USA) using the following methodologies. Initially a gene of interest for a particular application was selected and the coding strand cDNA sequence (CDS) identified using the bioinformatics database maintained by the National Centre for Biotechnology Information (NCBI) (<http://www.ncbi.nlm.nih.gov/>). For purposes of explanation the design of a primer for the commonly used marker of chondrogenesis, aggrecan will be explained. Searching the 'protein' database with the search string of aggrecan, *homo sapiens*, provides the amino acid sequence for the peptide and additionally the coding strand CDS for that particular peptide assembly in FASTA format (Fig.2.7.). The database also provides an accession number, a unique identifier of this gene transferable across genomic disciplines (BC036445).

```

atgaccactt tactctgggt tttcgtgact ctgagggtca tcaactgcagc tgtcactgta
gaaacttcag accatgacaa ctcgctgagt gtcagcatcc cccaaccgtc cccgctgagg
gtcctcctgg ggacctccct caccatcccc tgctatttca tcgaccccat gcaccctgtg
accaccgccc cttctaccgc cccactggcc ccaagaatca agtggagccg tgtgtccaag
gagaaggagg tagtgctgct ggtggccact gaagggcgcg tgcgggtcaa cagtgcctat
caggacaagg tctcactgcc caactaccog gccatcccca gtgacgccac cttggaagtc
cagagcctgc gctccaatga ctctggggtc taccgctgcg aggtgatgca tggcatcgag
gacagcgagg ccaccctgga agtcgtgggt aaaggcatcg tgttccatta cagagccatc
tctacacgct acaccctcga ctttgacagg ggcagcggg cctgcctgca gaacagtgcc
atcattgcca cgcctgagca gctgcaggcc gcctacgaag acggcttcca ccagtgtgac
gccggtggtc tggtgacca gactgtcaga taccocatcc acactccccg ggaaggctgc
tatggagaca aggatgagtt tcttgggtgt aggacgtatg gcatccgaga caccaacgag
acctatgatg tgtactgctt cgccgaggag atggagggtg aggtctttta tgcaacatct
ccagagaagt tcaccttcca ggaagcagcc aatgagtgcc ggcggctggg tgcccggctg
gccaccacgg gccagctcta cctggcctgg caggctggca tggacatgtg cagcgcgggc
tggctggccg accgcagcgt gcgctacccc atctccaagg cccggcccaa ctgcgggtggc
aacctcctgg cgtgaggac cgtctacgtg catgccaacc agacgggcta ccccgacccc
tcatcccgtc acgacgccat ctgctacaca ggtgaagact ttgtggacat cccagaaaac
ttctttggag tggggggtga ggaggacatc accgtccaga cagtgcctg gcctgacatg
gagctgccac tgctcgaaa catcaactgag ggtgaagccc gaggcagcgt gatccttacc
gtaaagccca tcttcgaggt ctccccagt cccctggaac ccgaggagcc cttcacgttt
gcccctgaaa taggggccac tgcttctgct gagggtgaga atgagactgg agaggccacc
aggccctggg gctttcccac acctggcctg ggccctgcca cggcattcac cagtgaggac
ctcgtcgtgc aggtgaccgc tgtccctggg cagccgcatt tgccaggggg ggtcgtcttc
cactaccgcc cgggaccac ccgctactcg ctgacctttg aggaggcaca gcaggcctgc
ctgcgcacgg gggcggcatc tgctcgcgcg gaggcagctcc aggcgccta cgaagcaggc
tatgagcagt gtgacgcgg ctggtcggg gaccagaccg tcagataccc cattgtgagc
ccccggaccc catgcgtggg tgacaaggac agcagcccag ggtcaggac ctatggcgtg
cgccatcaa cagagacctc cgatgtctac tgctttgtag acagacttga gggggagggtg
ttcttcgcca cacgccttga gcagttcacc ttccaggaag cactggagtt ctgtgaatct
cacaatgcca cgtggccac cacgggccag ctctacgcgc cctggagccg cggcctggac
aagtgctatg ccggctggct ggccgacggc agcctcgcct accccatcgt caccccaagg
cctgcctgcg gtggggacaa gccaggcgtg agaacggtct acctctaccc taaccagacg
ggcctcccag accactgtc ccggaccat gccttctgct tccagggtat gcagcctcac
ttcggctcca acagcccctt ttgtctggag aggaccccac tgggttcacc ggatcctgcc
accaccagt atcccatcca tcagagcaag aaaatgtcag tcctctggg gcagagccag
ctctga

```

Fig.2.7. Full coding sequence of the human Aggrecan transcript provided by the National Centre for Biotechnology Information (<http://www.ncbi.nlm.nih.gov/entrez/viewer.fcgi?val=22209082&from=346&to=2511&view=gbwithparts>)

After identification of a suitable target CDS, this data was imputed into the Beacon Designer platform with suitable primer search criteria to identify primers optimal for Sybr green based RT-PCR; an optimal annealing temperature ( $T_a$ ) of  $55^{\circ}\text{C} \pm 5^{\circ}\text{C}$ , a primer length of between 18 and 24 nucleotides and an optimal amplicon length of between 75 and 200 base pairs. The program then searches the CDS and identifies a suitable candidate area of the CDS for optimal amplification, identified in red in

Fig.2.8. Potential amplicons were then analysed using the DNA folding platform 'European mfold'

(<http://frontend.bioinfo.rpi.edu/applications/mfold/cgi-bin/dna-form1.cgi>) in order to identify problematic hairpins or other DNA tertiary structures which could hinder primer annealing at the temperature defined by the primer design platform ( $56.3^{\circ}\text{C}$ ).

After successful identification of suitable unobstructed binding sequences for the primers at the annealing temperature specified, primers were then synthesised at a production scale of 25nM. All primers were purchased from Invitrogen, UK.



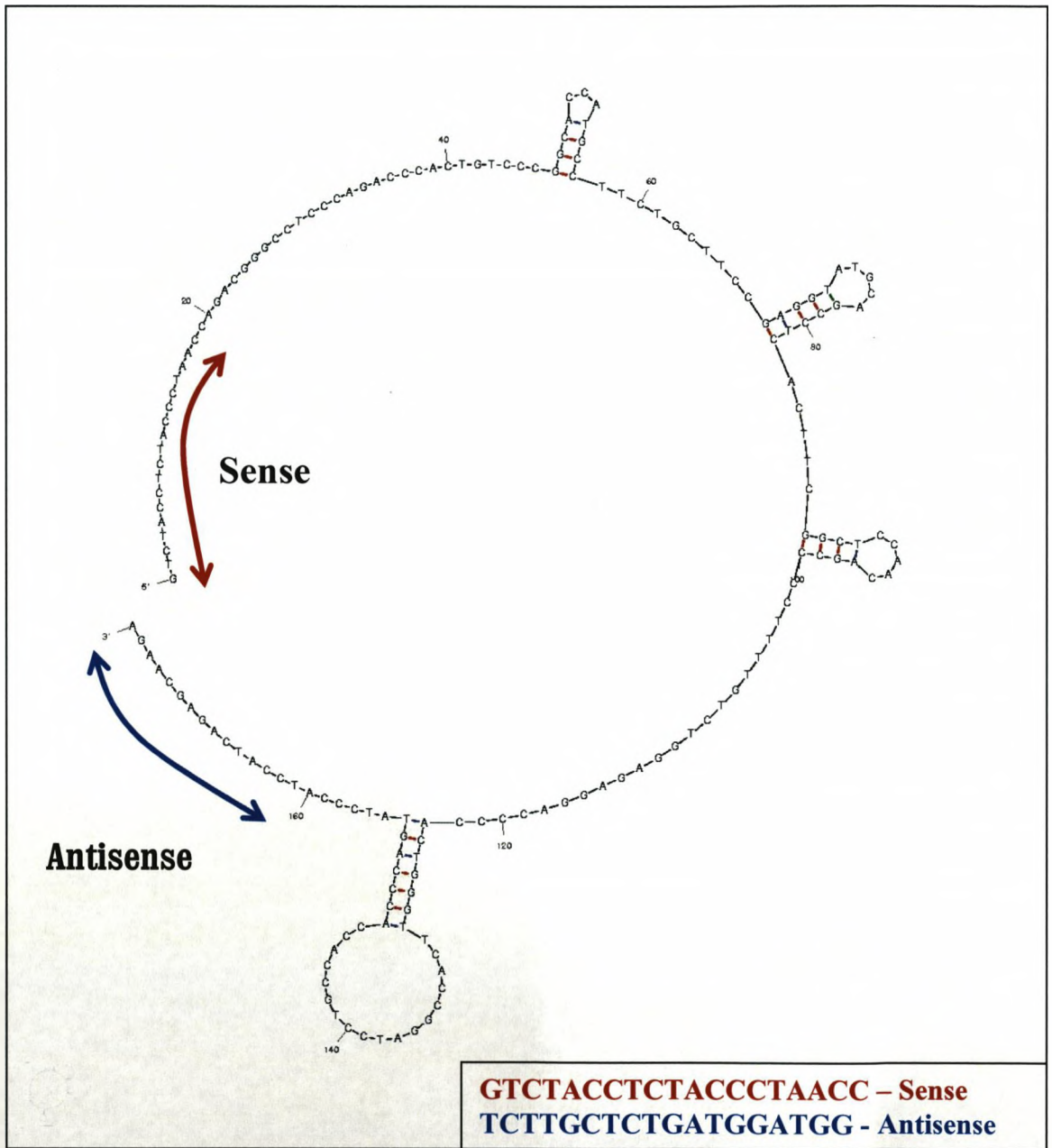


Fig.2.8. Predicted tertiary structure for a target amplicon within the Aggrecan CDS, generated using European mfold (<http://frontend.bioinfo.rpi.edu/applications/mfold/cgi-bin/dna-form1.cgi>) illustrating primer binding domains.



### 2.x xv Statistics

Statistical analyses were carried out using independent sample T-tests and one way ANOVA statistical tests using the software package SPSS ver.15. Unless stated otherwise confidence intervals were set such that \*P<0.05, \*\*P<0.01, \*\*\*P<0.001

### 2.x xvi Dynamic Contact Angle

Clean filter paper 'dog bone' carriers for the platelet poor plasma derived hydrogel were cut using an appropriately sized stamp from larger disks such that the final dimensions were as stated in Fig.2.9.

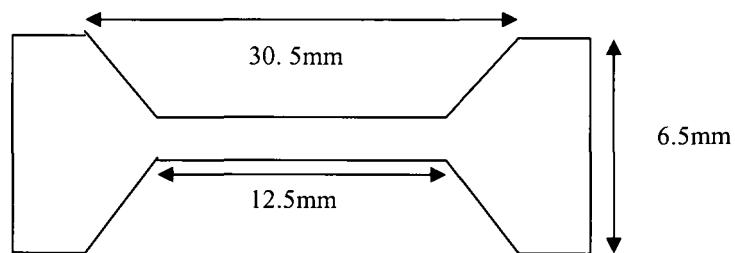


*Fig.2.9. Schematic illustrating the dimensions of the filter paper carrier of the platelet poor plasma derived hydrogel during dynamic contact angle studies*

Platelet poor plasma hydrogel was synthesised in the manner detailed in section 2.xvii. and immediately after additions of plasma (10%, v/v) and media components (DMEM + 4500mg/L glucose, Gibco, UK) 500 $\mu$ L of the solution was applied gently to each dog bone and allowed to completely gellate for 30 minutes at 37°C, suspended vertically. Hydrogel-laden dog bones were then subjected to dynamic contact angle analysis using a CDCA 100F tensiometer (Camtel Ltd, UK) in conjunction with the standard software platform supplied by the manufacturer. Solvents used were prepared from fetal calf serum (Cambrex, UK) and cell culture media (DMEM + 4500mg/L glucose; Gibco, UK) by means of simple combinations in a non sterile atmosphere. Samples were immersed in the

solution to a depth of 10mm before being retracted and the advancing and receding contact angles calculated dynamically using the Wilhelmy plate method throughout. A final contact angle was defined for each set of conditions by taking a mean advancing contact angle from the entire length of the immersion. Receding contact angles were not measurable due to the sample being totally wetted during derivation of an advancing contact angle. Samples were subjected to analysis in triplicate.

# DERIVATION OF DEFINED MEDIA FOR THE PHENOTYPE MAINTENANCE AND DIRECTED DIFFERENTIATION OF PRIMARY HUMAN PLURIPOTENT CELLS

## Chapter 3. Media Definition

### 3.i Introduction

The field of regenerative medicine focuses on the utilisation of biocompatible and/or bioactive materials in conjunction with a cellular component; either autologous or allogeneic, to augment or restore function to damaged tissues or organs. This strategy, fundamentally, has the ability to change the way that a vast plethora of medical conditions are treated essentially using the patients own intrinsic physiology to 'incubate' a replacement tissue *in situ* by facilitating proliferation of the cells delivered to the repair site, with complementary synergistic cues from the biomaterial mediating additional factors such as cellular adhesion, selection and differentiation.

Lineage committed cells have a defined functionality to enable them to fulfil their role within a specific *in vivo* niche. For example, osteoblasts produce calcified extra-cellular matrix which gives bone its mechanical strength whilst chondrocyte cells produce large amounts of hydrophilic branching glycosaminoglycans in their extra cellular matrix which enables the matrix to retain large amounts of water thus maintaining joints in a lubricated state. As a lineage committed cell ages this functionality is lost. During extended culture chondrocytes take on a fibroblastic phenotype losing the particular matrix components that confer their function. Similarly, osteoblasts do not retain the capacity to reliably calcify matrix thus bone generated from aged osteoblasts would be mechanically unsuitable for tissue augmentation. Often, large numbers of cells are required for cell based regenerative therapies ( $1.0 \times 10^7$ - $1.0 \times 10^8$  cells per implant, dependent on application), which can be generated in two ways; either by large initial biopsies to harvest extensive numbers of cells

therefore minimising the extent of *ex vivo* expansion required.

Alternatively, extended culture passages thus generating large yields of cells from smaller masses of initial tissue.

Neither of these strategies is ideal; large enough biopsies of a particular tissue to yield appropriate cell numbers for neotissue synthesis are rarely possible particularly after a tissue has already undergone trauma.

Additionally, culture of primary cells through extended passages ages the cells to the extent that functionality is questionable, therefore reducing their appeal for exploitation in biomedicine.

Therefore an alternative is needed. Whilst lineage committed cells provide the reassurance of being derived from a particular tissue with identical properties to the tissue destined for repair, lineage uncommitted cells have considerably more variable outcome in their terminal tissue destiny but provide more flexibility when considered for a regenerative therapy.

Lineage uncommitted stem cells can be obtained from a range of adult tissues which would generally not be critically damaged as a result of injury and therefore their potential harvest compromised, such as bone marrow, dental pulp and adipose. The number of tissues into which these cells can be differentiated is questionable. When first isolated, the hypothesis was suggested that a stem cell obtained from adult tissue only possessed the capacity to become a cell involved in forming tissues derived from the mesodermal embryonic germ layer, however this is now known not to be the case.

Potentially, a pluripotent cell can differentiate into one type of cell from an ever increasing set of different cell types from all three germ layers; these are capable of being used in a range of tissue repair strategies. *In vitro* differentiation into the previous mesodermal examples of osteoblast and chondrocytes are now common place and termed, along with adipose; 'tri-lineage differentiation confirmation', proof of a cell whose lineage is undefined. Stem cells are advantageous over those of a defined phenotype due to their plasticity, the ability to take a cell from a layer of abundant

and often surplus, subcutaneous adipose and generate cells forming tissues as diverse as neural and cardiac is just one potential example of the obvious benefits of these cells over their lineage committed counterparts.

In order to manipulate these cells to their maximum potential, the differentiation state of the phenotype of plastic cells needs to be controlled. Crude differentiation strategies can result in little more than a population of heterogeneous cells in various states of lineage commitment and phenotype, which could potentially be unsuccessful when used in conjunction with a regenerative medical repair strategy. Therefore, it is necessary to define parameters for maintaining adult stem cells in an undifferentiated plastic state in addition to concluding conditions which will control and influence their lineage commitment into a pre-defined terminal phenotype.

Current manipulation strategies when working with primary cells, including those of a pluripotent phenotype, relies on the use of suitable culture parameters in which the cells are maintained. Typically this is made of a basal component containing salts to maintain the osmolarity and pH of the media, sugars to provide an energy source for the cells contained within, amino acids for use in protein synthesis and selected vitamins necessary for facilitating defined critical intracellular roles. This mixture, despite its complexity is still unable to maintain extended cellular expansion and maintenance due to the fact that there are undefined soluble factors missing from the growth milieu, a proteinaceous component which facilitates cellular adhesion, and expansion. In contemporary cell culture strategies, this element is provided by the augmentation of the basal cell culture media with serum, typically fetal calf in origin.

Whilst providing a simple, accessible source of protein, cytokines, growth factors and other soluble exogenous regulatory molecules required by the primary cells *ex vivo*, serum is far from an ideal. From the perspective of cells destined solely for experimental *in vitro* manipulation, the lack of definition and consistency of the composition of serum introduced as

cumulation of factors from the donor including: diet, lineage, age and gender, induces variations in the cellular responses during culture in sera obtained from different donors. This may include rates of proliferation and metabolic activity, apoptosis and crucially from the point of view of pluripotent cells, phenotype modification.

From a tissue engineering standpoint, for the derivation of cells of a clinical grade, serum is a completely unsuitable component of the cell maintenance matrix. One obstacle of serum based cell culture systems in conjunction with regenerative medicine is the possibility of the introduction of zoonotic pathogens to a patient which could be transferred when the cells are delivered. Additionally, the undefined nature of the protein and growth factor component renders it difficult to stringently control the phenotype of stem cells grown in media containing serum. Furthermore, it is possible for autologous cells to adapt immunogenically to culture under non-host serum, further complicating the lengthy immunosuppression as a result of implantation.

Therefore, it was necessary to refine growth parameters for the maintenance of a range of candidate cells for exploitation in bioengineering strategies under conditions completely chemically defined, most importantly, devoid of serum. This strategy would further need to be modulated with defined exogenous components to control and coordinate the differentiation of pluripotent primary human cells into one of a range of clinically relevant cell types. Successful optimisation of such conditions would provide a means of overcoming a vital milestone in tissue engineering, deriving clinically applicable conditions for the manipulation of cells directly acceptable to regenerative medical applications, thereby providing a means of progressing tissue engineered strategies from the laboratory to the operating theatre.

### 3.ii Definition of basal media – Lineage committed cells

Initially it was important to develop a defined basal media which, with the addition to fetal calf serum would support the expansion of human cells. The ultimate goal of the study was to define media formulations which were devoid of animal sera, although for optimisation of basal media formulations it was required to reduce the amount of variable factors influencing cellular fate. Taking into account the proven capacity of serum to provide an adequate source of components to support cellular expansion that are absent in basal media formulations, development of defined basal parameters focussed on deriving a minimal mixture of salts, amino acids, sugars and other components that performed in a comparable manner to commercially available basal counter parts with additions of sera at identical concentrations.

An optimal basal media formulation was concluded on the basis of the ability of the media to maintain the cellular expansion and morphology of terminally differentiated primary human dermal fibroblasts. These cells were chosen on the basis of their robustness to maintain their fibroblastic phenotype. It was necessary to define optimal basal parameters initially using lineage committed cells due to the likelihood of introducing further variables in terms of lineage fate if using a plastic cell type for these early studies.

Media were synthesized *de novo* from raw components outside of a laminar flow area using ddH<sub>2</sub>O generated using reverse osmosis when necessary. Salt powders were blended dry, devoid of calcium containing salts. Mass salt mix and calcium containing salts were dissolved separately, then combined with minimal kinesis, addition of calcium in powder form with the total salt fraction resulted in precipitation and subsequent loss of necessary elements from the total media. Compounds insoluble in water were dissolved at stock concentrations in 70% ethanol when required such that the ultimate volume of ethanol in culture media

was kept to a minimum (<0.1%). After complete synthesis, the pH of the media was checked and adjusted to 7.4 from the approximate general pH of 6.8 of freshly mixed constituents using a minimum volume of 10N NaOH. After correct pH was achieved antibiotics were administered to the media at a standard concentration of 1% (v/v) 10,000 U/ml penicillin and 10 mg/ml streptomycin in 0.9% sodium chloride. Subsequently, media was filter-sterilized manually using 0.2 $\mu$ m syringe filter disks under minimal pressure applied by hand. It was not possible to autoclave this media due to precipitation occurring during the autoclave process. Media was pre-warmed to 37°C prior to use.

The optimum concentration of media constituents found to maintain the expansion of primary human dermal fibroblasts is detailed in table.3.1. in combination with fetal calf serum at a concentration of 5% (v/v). In conjunction with an initial standard seeding density of 5.0x10<sup>4</sup> cells/cm<sup>2</sup> dermal fibroblasts reached confluence in culture periods of 7 days with refreshment of media occurring at day 5. Repeated division of the cells into two equal densities of 5.0x10<sup>4</sup> cells/cm<sup>2</sup> when confluent resulted in demonstration of the defined basal media in addition to fetal calf serum to support dermal fibroblasts through 50 culture passages. Cells maintained their fibroblastic morphology throughout, as illustrated in Fig.3.1. taken from passage 10.



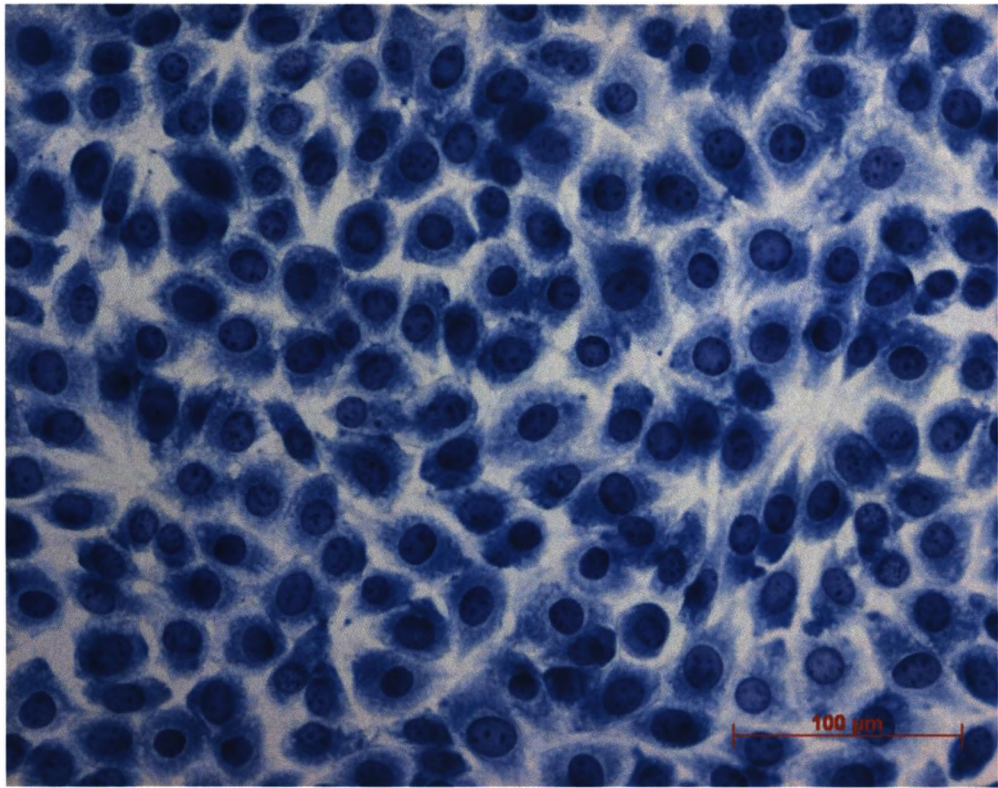


*Fig.3.1. Light microscopic observation of methylene blue stained dermal fibroblast cells demonstrating associated fibroblastic morphology in defined basal media with additions of fetal calf serum of 5%*

Salts	Conc (g/L)	Vitamins	Conc (mg/L)	Amino Acids	Conc (mg/L)	Other components	Conc
CaCl <sub>2</sub> ·2H <sub>2</sub> O	0.26	Choline Chloride	1	Glycine	7.5	Glucose	1.0 g/L
MgSO <sub>4</sub>	0.1	Calcium Pantothenate	1	Alanine	8.9	pyruvate	60 mg/L
KCl	0.4	Folic Acid	1	Asparagine	13.2	L-Analyl-L-Glutamine	2mM
NaHCO <sub>3</sub>	2.2	Inositol	2	Aspartic acid	13.3		
NaCl	6.8	Nicotinamide	1	Glutamic Acid	14.7		
NaH <sub>2</sub> PO <sub>4</sub>	0.12	Pyridoxal Hydrochloride	1	Proline	11.5		
		Riboflavin	0.1	Serine	10.5		
		Thiamine Hydrochloride	1	Argenine	126.4		
		Ascorbalte-2-phosphate	60	Cysteine	24		
				L-Histine-Hydrochloride	42		
				Isoleucine	54.2		
				Leucine	54.2		
				Lysine	72.5		
				Methionine	15.1		
				Phenylalanine	33		
				Threonine	47.6		
				Thyptophan	10.2		
				Tyrosine	36		
				Valine	48.6		

Table.3.1. Composition of defined basal media.

In order to define a suitable combination of factors to replace serum to act in conjunction with this basal media, dermal fibroblasts were again chosen as the candidate cell type due to their reported lack of susceptibility to phenotypic transformation.

<b>Serum replacement compounds</b>	<b>Conc<sup>n</sup></b>
Bovine serum albumin	2.8mg/ml
Insulin	10 $\mu$ g/ml
Apo Transferrin	10 $\mu$ g/ml
SeO <sub>2</sub>	5ng/ml
Ethanolamine	2 $\mu$ g/ml
Hydrocortisone	25 $\mu$ M
Fe <sub>2</sub> NO <sub>3</sub>	0.1mg/L

*Table.3.2. Components of serum replacement*

The optimal combination and concentrations of serum replacement compounds is illustrated in table.3.2. Bovine serum albumin was added directly to the basal media and allowed to dissolve passively. Insulin, apo-transferrin, sodium selenite and ethanolamine were made in ROH<sub>2</sub>O as a 100x stock, then added to the media after complete dissolution of bovine serum albumin. Hydrocortisone was dissolved as a powder in 70% ethanol as a 1000x stock then added to the media followed by Fe<sub>2</sub>NO<sub>3</sub> which was added finally from a 1000x stock made in ROH<sub>2</sub>O. When synthesising serum free media, pH was adjusted after the addition of all serum replacement compounds followed by antibiotic addition, filter sterilization and pre-warming. Both holo- and apo-transferrins were trialled with no observable difference in cellular maintenance between the two. Unused proteinaceous stocks were frozen at -20°C until required.

Degradation and the resultant decreases in efficacy of proteinaceous components in serum free media formulations is considered to be a factor influencing their ability to sustain cellular development for extended periods. In whole sera, the concentration of total protein is considerably higher than in serum free media, therefore sterically stabilising individual

protein components. This stabilising factor is not present in serum free media due to the minimal concentrations of individual proteins. Therefore it was necessary to deduce the rate at which protein, particularly apo-transferrin due to its crucial role in iron delivery to cells, degraded under normal incubation conditions.

Fresh serum free media was synthesised and incubated at 37°C, in a humidified atmosphere of 5% CO<sub>2</sub>, contained in a standard tissue culture vessel. Media aspirates were removed at defined time points between days 1 and 21 (a typical cell culture time scale) and the concentration of apo-transferrin quantified using the ELISA method detailed in section 2.xiii. This data demonstrated that the 21 day incubation period resulted in no significant decrease in the concentration of apo-transferrin, thus proving its stability in this optimal serum free media (Fig.3.2.).

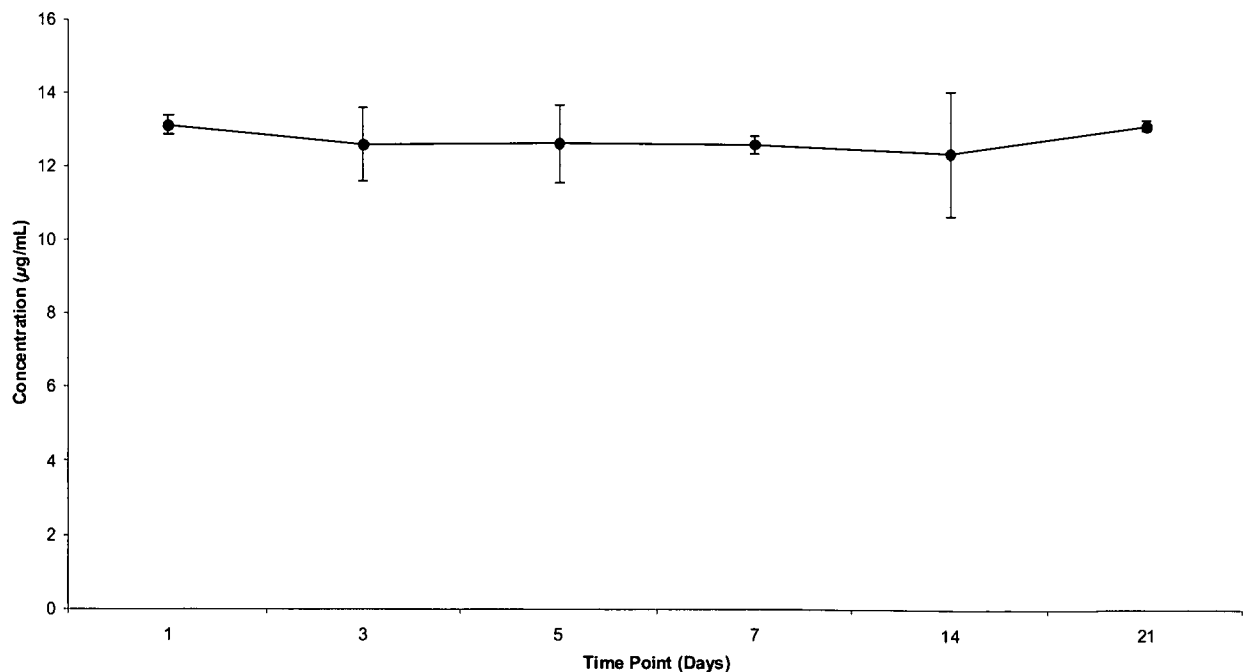


*Fig. 3.2. Stability of human Apo-transferrin in serum free cell culture media quantified using the ELISA method. Error bars represent 1 standard deviation from the mean, n=3*

### 3.iii Expansion of Primary Human Cells in Conjunction with Defined Serum Free Parameters – Dermal Fibroblast Cells

Cells were subjected to maintenance under conditions devoid of serum, using the serum free media in a manner identical to when cells were routinely cultured using proprietary serum containing formulations detailed in section 2.x. Human dermal fibroblasts were removed at passage 4 and seeded at a density of  $5.0 \times 10^4$  cells/cm<sup>2</sup>. Cells were cultured for 14 days with media refreshment occurring at day 7. The metabolic activity of these cells cultured under serum free and serum containing conditions was compared using the Alamar blue method outlined in section 2.xiv.

Data from this is shown in Fig.3.3. DMEM containing serum at 10% (v/v) is the proprietary media recommended for the growth of these cells. Defined basal media is the basal media derived *de novo* summarised in table 3.1 with 5% (v/v) fetal calf serum additions. During optimisation of serum free media formulations the effects of the presence of iron (0.1mg/L, as shown in table 3.2) on metabolic activity of primary cells was observed due to the contrasting literature contradicting the requirement of this iron in routine cell culture media formulations.

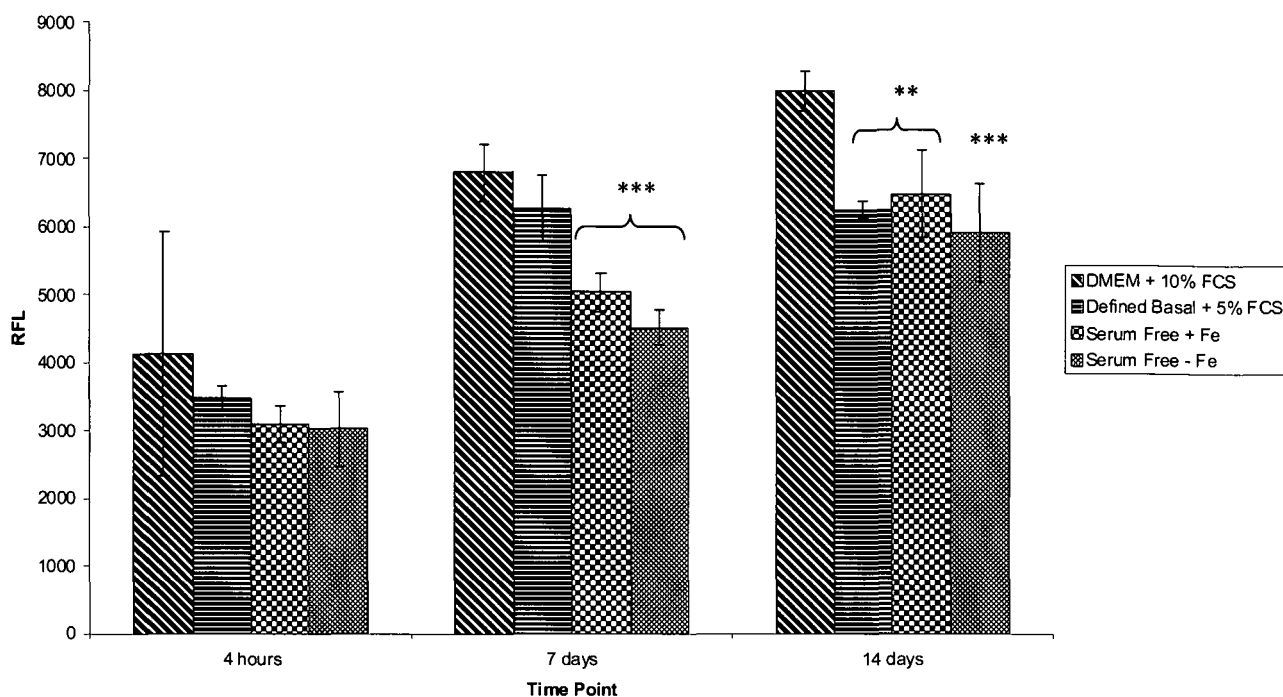


*Fig.3.3. Comparison of the metabolic activities of human dermal fibroblast cells in a range of serum free and serum containing media formulations using the Alamar blue method. Error bars represent 1 standard deviation from the mean, n=3, \*P<0.05, \*\*P<0.01, \*\*\*P<0.001 compared to serum containing basal DMEM No correction for change in cell number was made*

This data illustrates significant differences between media containing serum at 5% to either of the media formulations devoid of serum in their capacity to support cellular metabolism during this 14 day culture period. After 7 days of culture, cells in the serum containing formulations were significantly more metabolically active than in the conditions devoid of serum. However, by 14 days there was no significant difference between the formulation containing 5% FCS and the iron containing serum free formulation, although these are both reduced significantly when compared to the 10% containing formulation. The cells reached confluence and it was possible to demonstrate that the iron containing-free media allowed the cells to act metabolically in a statistically similar manner to the 5% serum containing formulation

Additionally, it was also critical to observe that the fibroblasts had not undergone any phenotypic transformations, which was confirmed using

immunohistochemical staining to assess the presence of the D7-Fib antigen, a protein specific to the cytoplasm of fibroblasts. Cells were stained after 21 days of culture in conjunction with serum-free media containing iron, illustrated in Fig.3.4. Positive red staining for the fibroblast specific marker was observed throughout the entire population, further confirmed by the presence of a typical fibroblastic morphology demonstrated by the cytoskeletal F-actin staining shown in green. This data therefore provided strong evidence that the serum-free formulation maintained the phenotype and morphology of human dermal fibroblasts after *in vitro* culture.

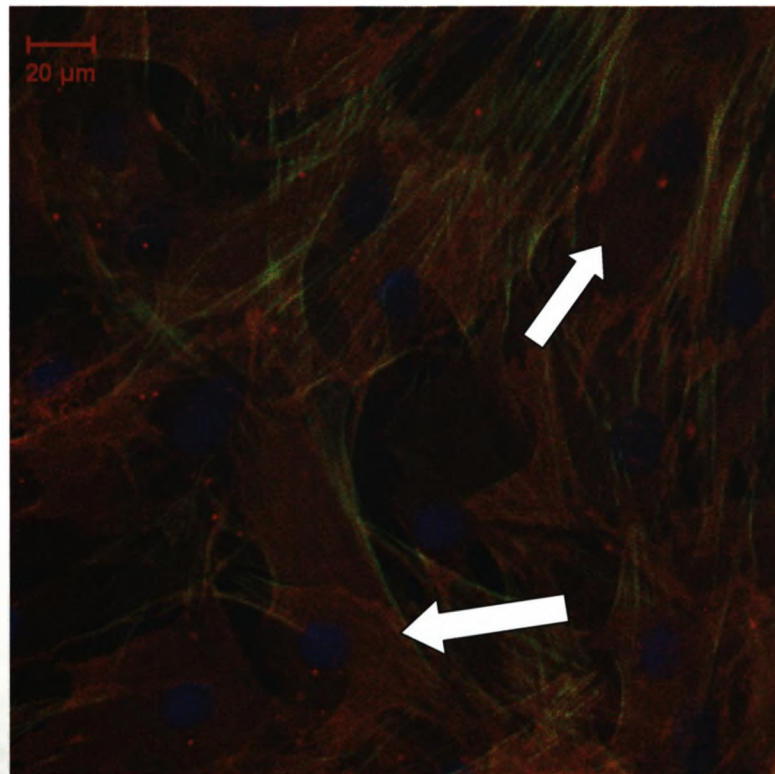


*Fig.3.4. Fluorescent microscopic observation of the immunohistochemical staining for the Fibroblast specific D7-Fib antigen and additionally; F-actin and Nucleii after 21 days of serum free culture (positive staining illustrated by arrows)*

3.iv Expansion of Primary Human Cells in Conjunction with Defined Serum Free Parameters – Osteoblasts

As a further primary human cell type, human osteoblasts were chosen as a candidate after consideration of their contrasting *in vivo* niche to dermal fibroblasts in addition to their relevance in a multitude of regenerative medical therapies. Passage 4 osteoblasts were subjected to expansion in the identical serum free media to which dermal fibroblasts were maintained. Control media was changed to proprietary osteogenic media made from 1.0g/L glucose DMEM containing of 50 $\mu$ M ascorbate, 100nM dexamethasone, 10mM  $\beta$ -glycerophosphate and 10% fetal calf serum. Serum-free osteogenic parameters were created using the above modifications to defined basal media, replacing the 10% serum component with the constituents from table 3.2. Osteoblast cells were cultured under these conditions for 14 days after an initial seeding of 5.0x10<sup>4</sup> cells/cm<sup>2</sup>, metabolic-activity was compared throughout culture using the Alamar blue method and media refreshed at day 7.

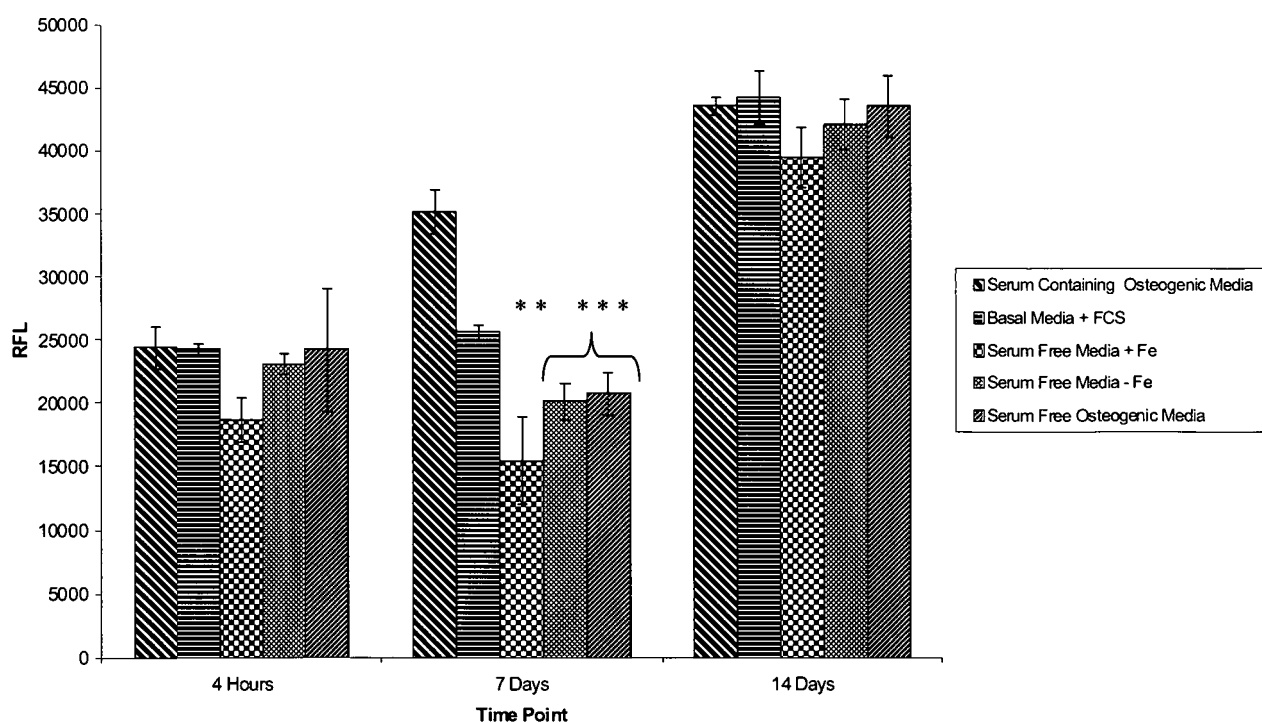


*Fig.3.5. Comparison of the metabolic activities of human osteoblast cells in a range of serum free and serum containing media formulations using the Alamar blue method. Error bars represent 1 standard deviation from the mean, n=3, \*P<0.05, \*\*P<0.01, \*\*\*P<0.001 compared to serum containing Osteogenic medium. No correction for change in cell number was made*



Although a significant decrease in metabolic activity was observed throughout all *de novo* derived media formulations at day 7, overall, by termination of culture at day 14 there were no significant differences in the metabolic activity of the osteoblasts when cultured in serum-containing and defined serum free-media formulations in the presence or absence of iron. There was also no significant difference between media with proprietary osteogenic modifications and basal media without these additions both containing serum. These data suggested that the derived serum free media was capable of maintaining cellular metabolism of primary human osteoblasts in a manner comparable to serum containing osteogenic modified proprietary counterparts.

### 3.v Expansion of Primary Human Cells in Conjunction with Defined Serum Free Parameters – Arterial Smooth Muscle Cells

Arterial smooth muscle cells, used at passage 4, were subjected to expansion in defined serum free media as a final candidate cell lineage-committed cell due to their clinical relevance in tissue engineering strategies for the repair of cardiovascular defects and also, from an experimental point of view, their ability to modulate their phenotype between contractile and synthetic states.

In this instance, the basal media chosen was Media 231 (Invitrogen, UK) due to its popularity in *ex vivo* smooth muscle cell culture applications. Defined basal and serum free media formulations were modified to contain 4.5g/L glucose due to the widely publicised higher glucose requirement of smooth muscle cells during *in vitro* culture. Cells were seeded at  $5.0 \times 10^4$  cells/cm<sup>2</sup> and cultured for 14 days with media refreshment occurring at day 7. Metabolic activity was observed throughout culture using the alamar blue method previously stated (Fig.3.6.).

This data illustrates that the overall trend in metabolic activity of smooth muscle cells during culture was increased up to day 7 and decreased by

day 14. It was hypothesised that this phenomenon could be as a result of contact inhibition and subsequent quiescence of these cells once confluence is reached. In a similar manner to the two previous primary human cell types, no significant difference in metabolic activity was observed between serum-free and serum-containing formulations by termination of culture, however a small significant difference was observed at day 7 between the serum free and serum containing formulations. No significant differences were recorded between formulations with iron present or absent.

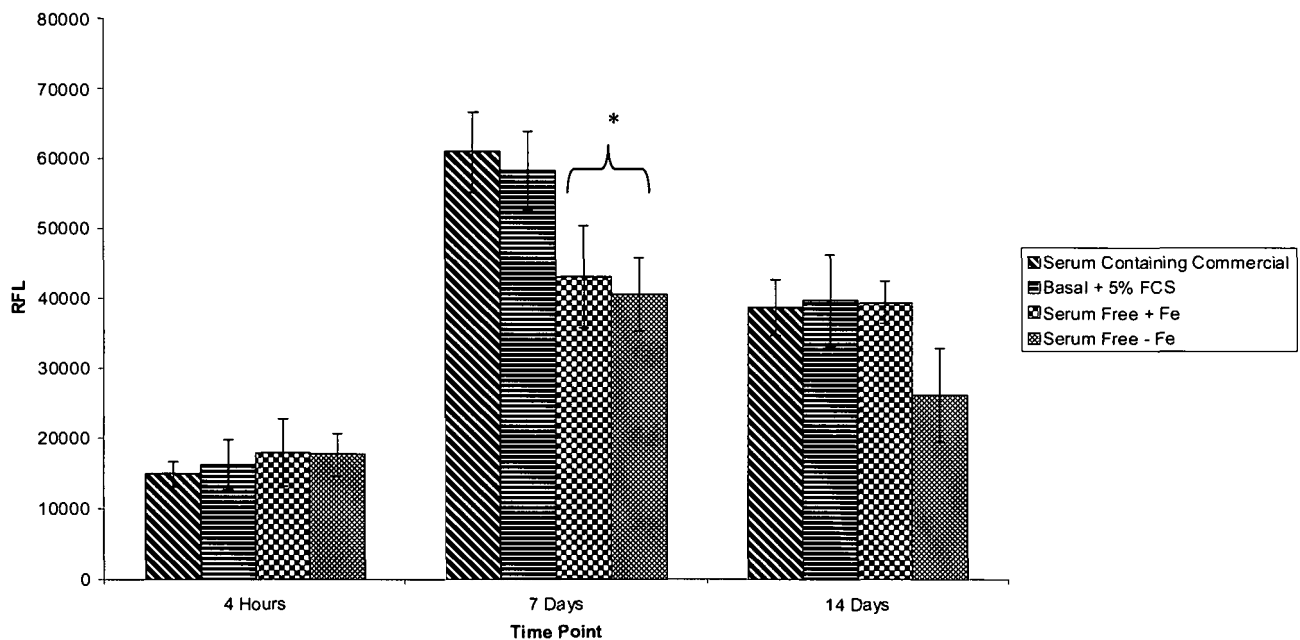


*Fig.3.6. Comparison of the metabolic activities of human arterial smooth muscle cells in a range of serum free and serum containing media formulations using the Alamar blue method. Error bars represent 1 standard deviation from the mean, n=3, \*P<0.05, \*\*P<0.01, \*\*\*P<0.001 compared to serum containing commercial medium. No correction for change in cell number was made.*

Characterisation of crude smooth muscle phenotype was carried out using immunohistochemical observation, as outlined in section 2.i, of smooth muscle actin at day 14. Fig.3.7. illustrates this data demonstrating the presence of this smooth muscle cell-specific protein throughout the cell population, confirming the maintenance of phenotype.

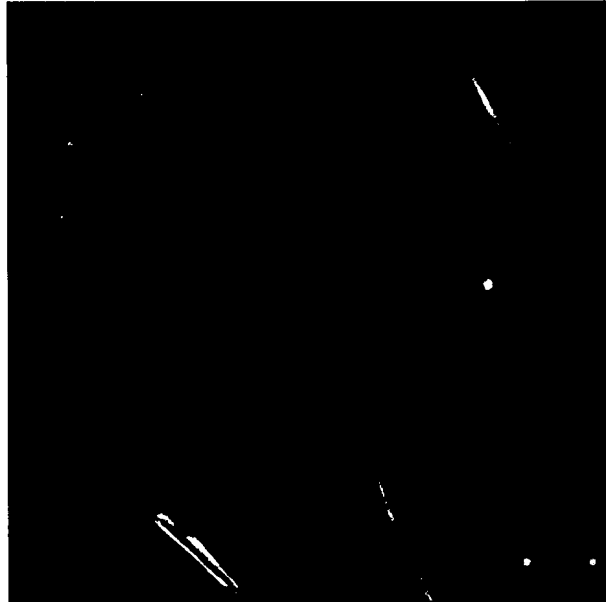


*Fig.3.7. Fluorescent microscopic observation of immunohistochemical staining of arterial smooth muscle cells for the smooth muscle specific  $\alpha$ -smooth muscle actin after 14 days of serum free culture*

Smooth muscle actin was further characterised using flow cytometry as outlined in section 2.xv. Serum free media in the presence and absence of iron and defined basal media containing 5% FCS were compared in their ability to promote smooth muscle actin expression after 14 days of culture (Fig.3.8.).

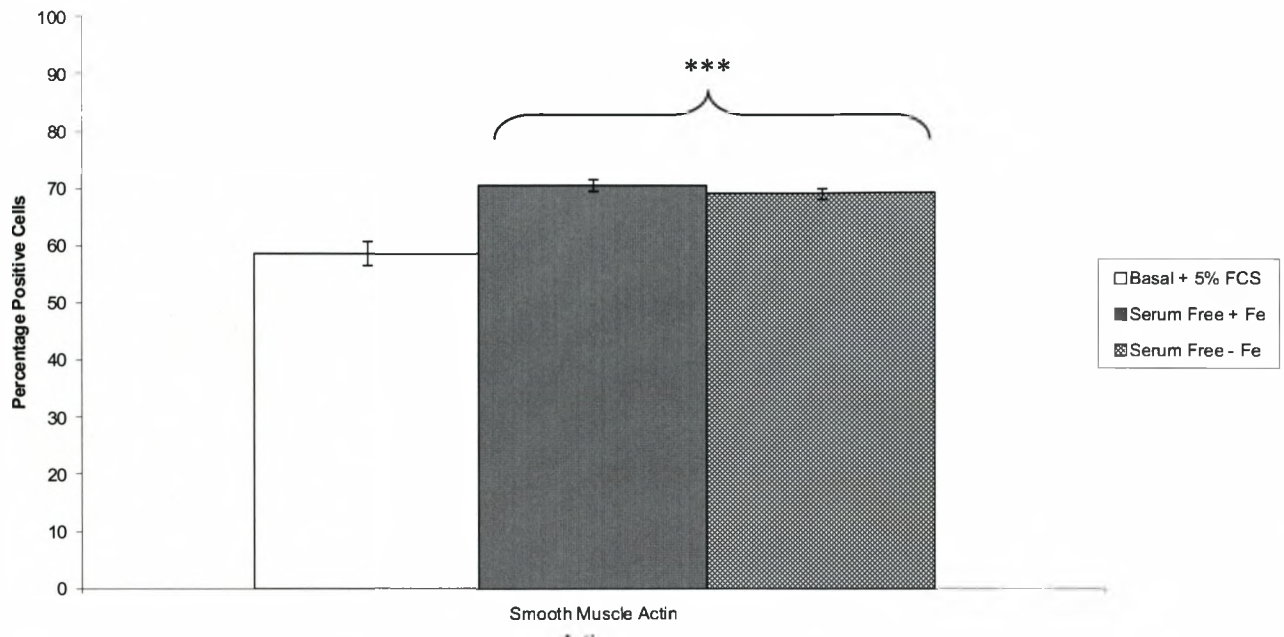


Fig.3.8. Flow cytometric analysis of the presence of  $\alpha$ - smooth muscle actin in populations of arterial smooth muscle cells cultured in serum free and serum containing media formulations. Error bars represent 1 standard deviation from the mean,  $n=3$ ,  $*P<0.05$ ,  $**P<0.01$ ,  $***P<0.001$  compared to serum containing basal medium

Flow cytometric analysis illustrated, quantifiably, a strongly significant increase in the capacity of defined serum free over serum containing basal media formulations to support the expression of smooth muscle actin, a conclusive indicator of smooth muscle cell phenotype.

Further analysis was carried to confirm the phenotype of the arterial smooth muscle cells using real time-PCR. cDNA libraries were generated from RNA obtained from cell lysates of arterial smooth muscle cells cultured under defined serum free conditions in the presence and absence of iron, in the manner explained in section 2.vi. This intricate molecular analysis was conducted in order to determine, in greater detail the effect of serum free growth on the phenotype of this potentially phenotypically plastic cell. All primers and appropriate annealing temperatures are shown in table 2.3. Target genes were normalised to the level of expression of the house keeping gene  $\beta$ -actin based on  $C_t$  values. These values were then

further normalised to their level of expression in Media 231 to provide a value corresponding to a change in expression caused as a result of subjection to the experimental serum free parameters.

In an identical manner to previous trials involving smooth muscle cells, cells were seeded at an initial density of  $5.0 \times 10^4$  cells/cm<sup>2</sup> and cultured for 14 days under defined serum free conditions prior to lysis. Fig.3.9. further illustrates the presence of smooth muscle actin, showing small decreases in transcription when cultured under both serum free parameters. However, this decrease was smaller in serum free media which did not contain iron.

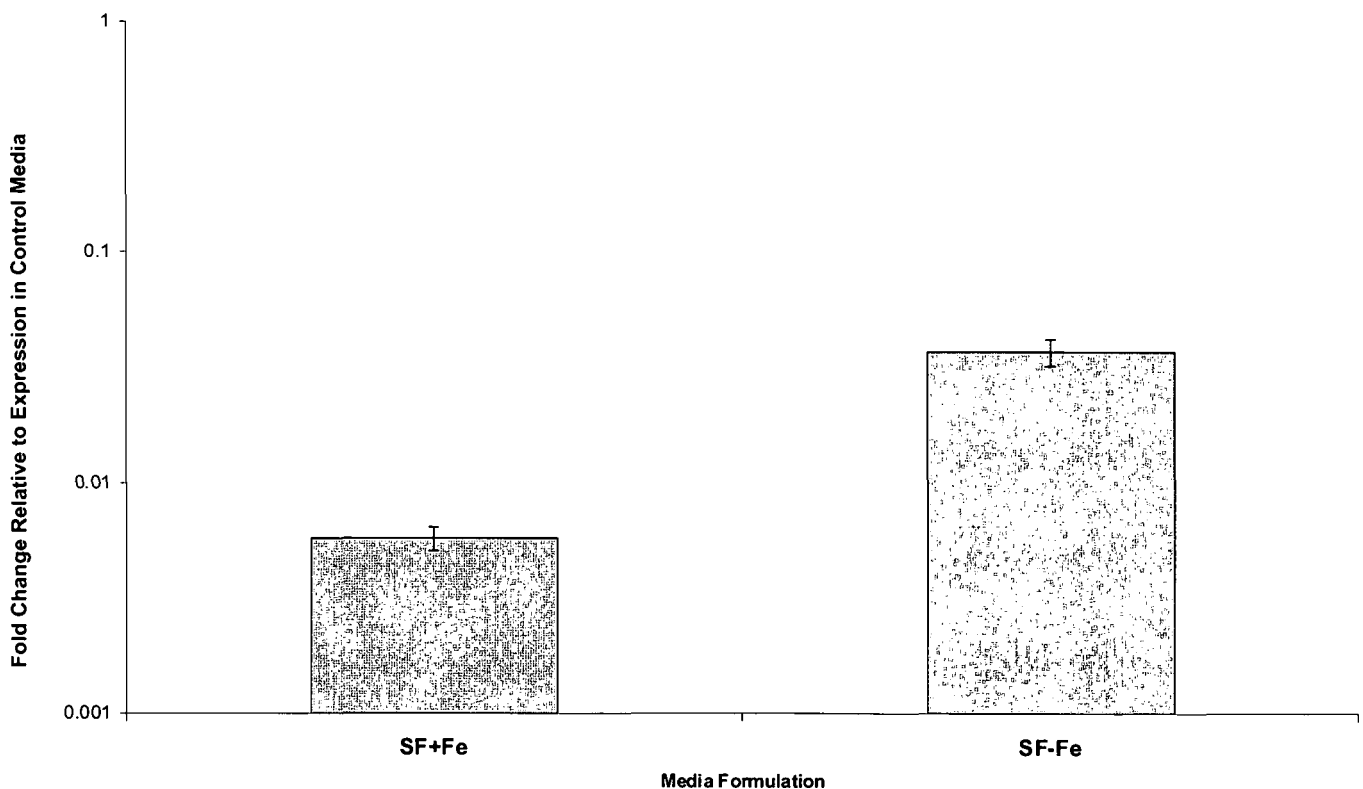


*Fig.3.9. Real time-PCR comparison of the expression of  $\alpha$ -smooth muscle actin in arterial smooth muscle cells cultured in conjunction with serum free media formulations in the presence (SF+Fe) and absence (SF-Fe) of iron after 14 days. Error bars represent 1 standard deviation from the mean, n=6*

Elastin is a protein expressed extensively in connective tissue, particularly smooth muscle cells. It is an elastic molecule in the tissues of mammals and used in places where mechanical energy is required to be dispersed. This protein demonstrated a similar expression profile to smooth muscle

actin, expressed to a lesser extent than basal in both serum containing media formulations, with the smallest decrease in transcription occurring in media devoid of iron (Fig.3.10.).

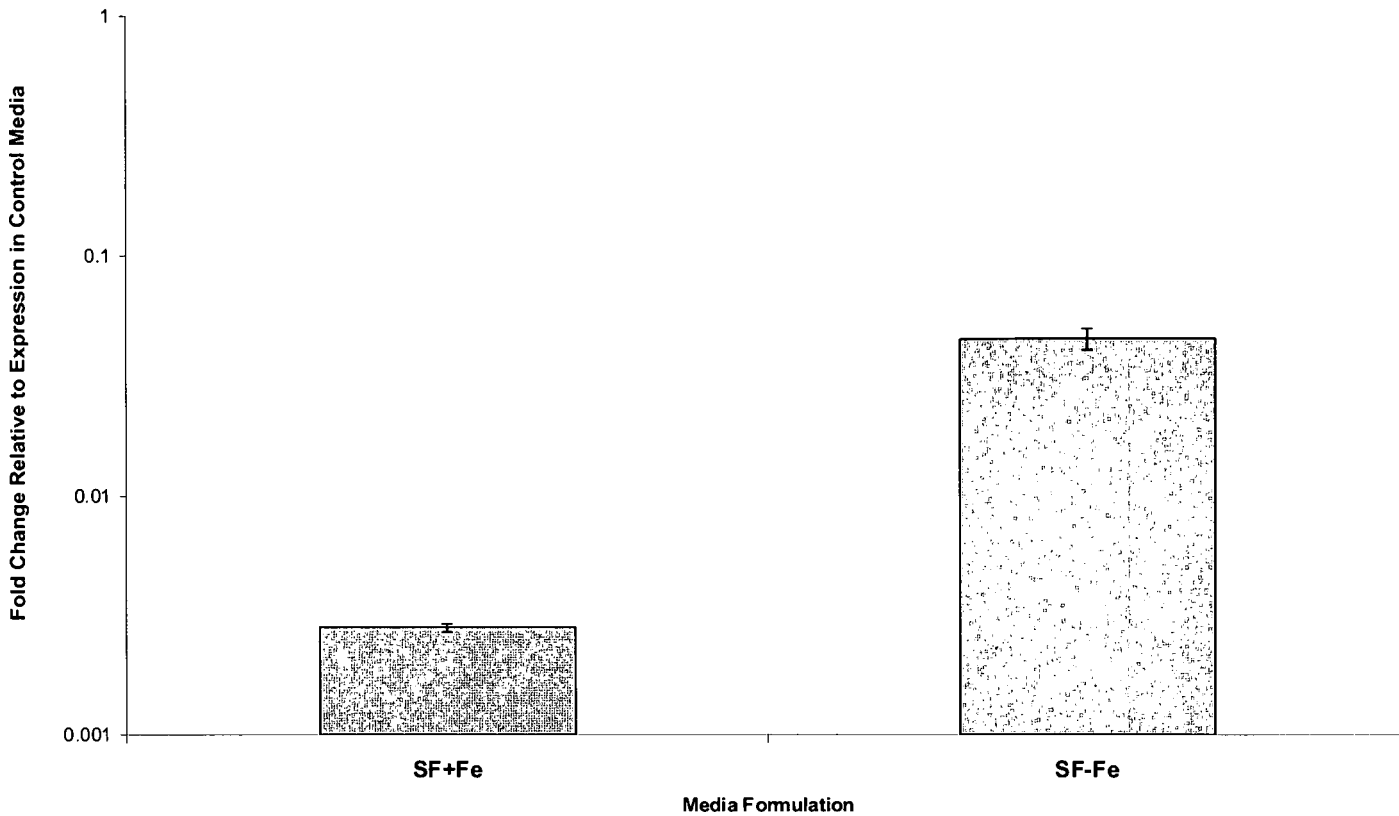
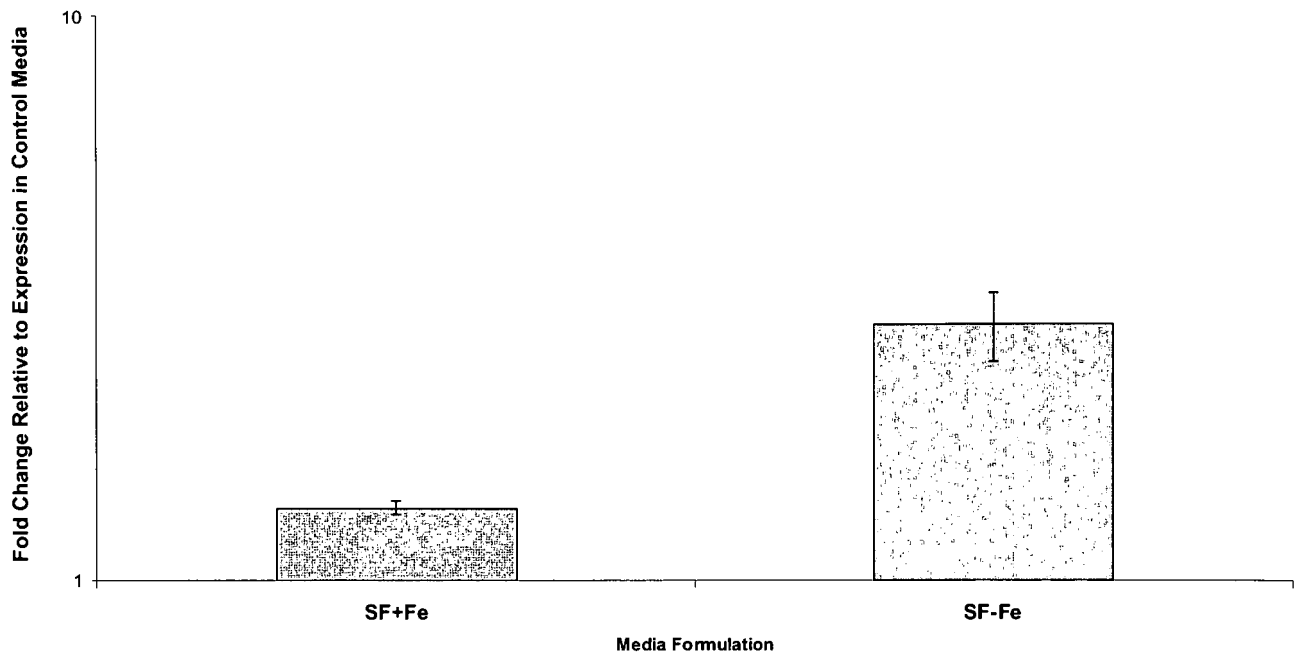


Fig.3.10. Real time-PCR comparison of the expression of Elastin in arterial smooth muscle cells cultured in conjunction with serum free media formulations in the presence (SF+Fe) and absence (SF-Fe) of iron after 14 days. Error bars represent 1 standard deviation from the mean, n=6

As a further indicator of smooth muscle cell phenotype, the expression of fibrillin-1, an extracellular matrix glycoprotein was measured. This protein is a component of microfibril quaternary structure, which forms part of the cytoskeletal elastic fibres. Elastic fibres are essential for the function of flexible structures such as the vasculature, throughout the *in vivo* niche from which these arterial smooth muscle cells were derived. Fig.3.11. demonstrates the changes observed in the expression of this peptide as a result of culture under serum-free conditions. As with previous target genes, both formulations stimulated small decreases in transcription, the smallest decrease in serum-free media devoid of iron.



*Fig.3.11. Real time-PCR comparison of the expression of fibrillin-1 in arterial smooth muscle cells cultured in conjunction with serum free media formulations in the presence (SF+Fe) and absence (SF-Fe) of iron after 14 days. Error bars represent 1 standard deviation from the mean, n=6*

Fig.3.12. shows the modulation in expression of fibronectin. Fibronectin is an extracellular glycoprotein associated with mediation of cellular adhesion, growth, migration and differentiation through its role as a ligand for a number of integrin receptors. Fibronectin also interacts directly with components of the extracellular matrix such as collagen and fibrin to form a structural component in this intercellular scaffold. Although this protein is not exclusively a marker of a smooth muscle cell phenotype, extensive down regulation would be indicative of a smooth muscle cell population in a state of decline as a result of an unsuitable environment. Fig.3.12. clearly demonstrates no significant difference in the expression of fibronectin when cultured in either serum-free media formulation over serum-containing basal media.

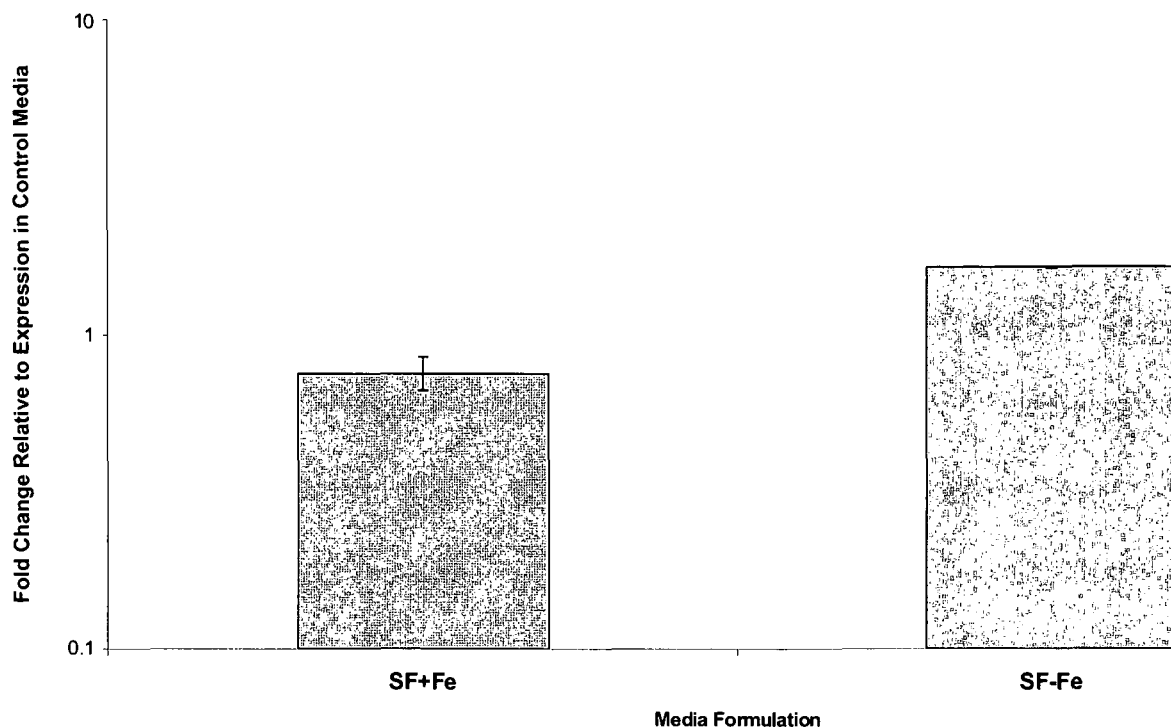
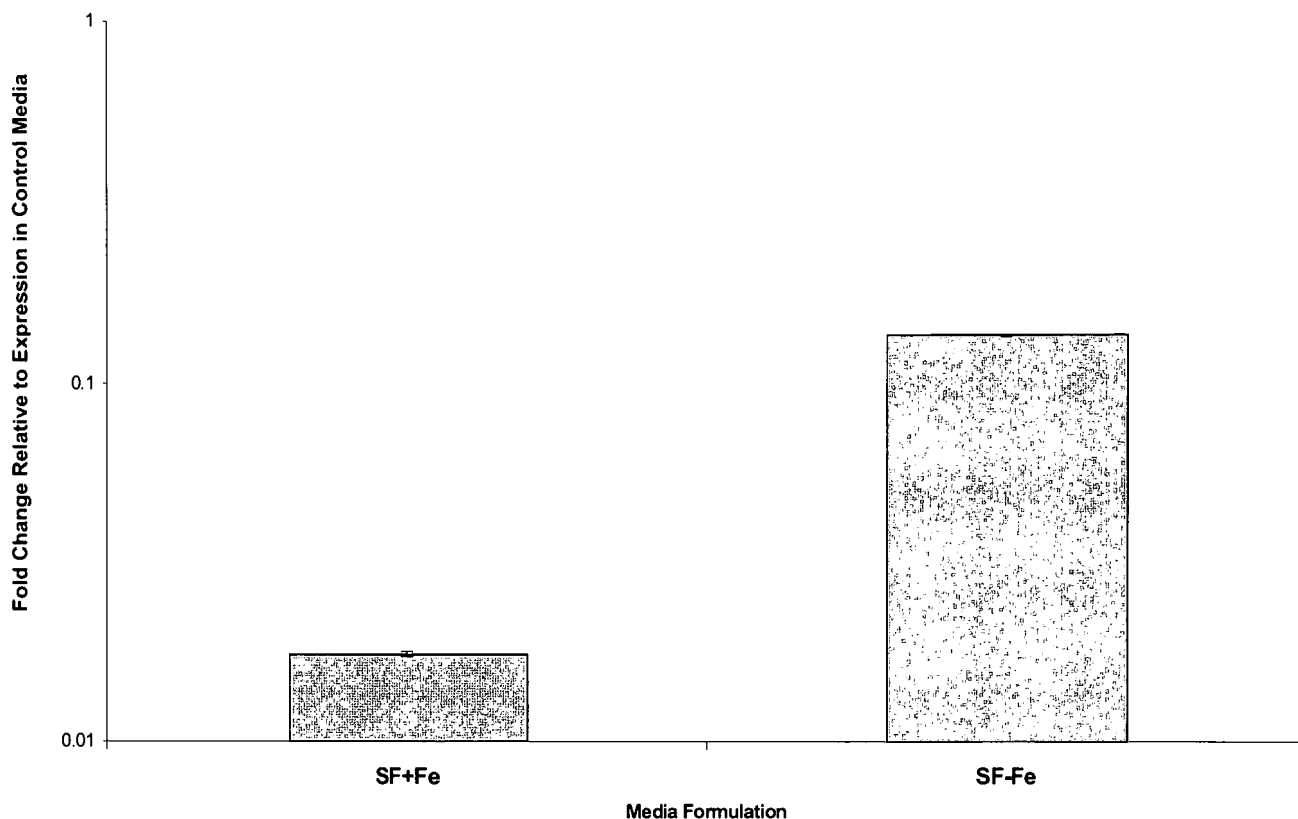


Fig.3.12. Real time-PCR comparison of the expression of fibronectin in arterial smooth muscle cells cultured in conjunction with serum free media formulations in the presence (SF+Fe) and absence (SF-Fe) of iron after 14 days. Error bars represent 1 standard deviation from the mean.  $n=6$

Laminin is a further component of the extracellular matrix, with a particular role in formation of basal lamina. Increase in the expression of this protein would suggest that the smooth muscle cells are attempting to form basal lamina, the surface on which they reside *in vivo*. Laminin also contains the tri-peptide RGD sequence, the specific three amino acid motif documented extensively for its adhesive role in cellular control. Fig.3.13. demonstrates the modulations of expression of laminin in the smooth muscle cells cultured under serum-free conditions. Similarly to other proteins, both defined serum-free media formulations stimulated an decrease in the expression of this molecule, with the smallest decrease observed in the media devoid of iron, further emphasising its suitability for the expansion of primary smooth muscle cells.





*Fig.3.13. Real time-PCR comparison of the expression of Laminin in arterial smooth muscle cells cultured in conjunction with serum free media formulations in the presence (SF+Fe) and absence (SF-Fe) of iron after 14 days. Error bars represent 1 standard deviation from the mean, n=6*

Smoothelin is a critical molecule in the characterisation of smooth muscle cell phenotype. This protein is a component of the smooth muscle cell cytoskeleton and is regarded as a marker of smooth muscle cell differentiation, being exclusively expressed on fully differentiated smooth muscle cells; those with a contractile phenotype. Fig.3.14. illustrates the modulation of expression of smoothelin after 14 days of culture. Under serum-free conditions, it is apparent that iron has the potential to act as a switch between a contractile and synthetic phenotype. Under serum free conditions in the presence of iron no expression of smoothelin was observed, however in the absence of iron a significant increase was apparent from that recorded under basal parameters. These data suggests a possible inhibitory effect of iron on the transformation of smooth muscle cells into a functional phenotype, or considerably more interesting, a de-differentiation from a contractile into a synthetic phenotype.

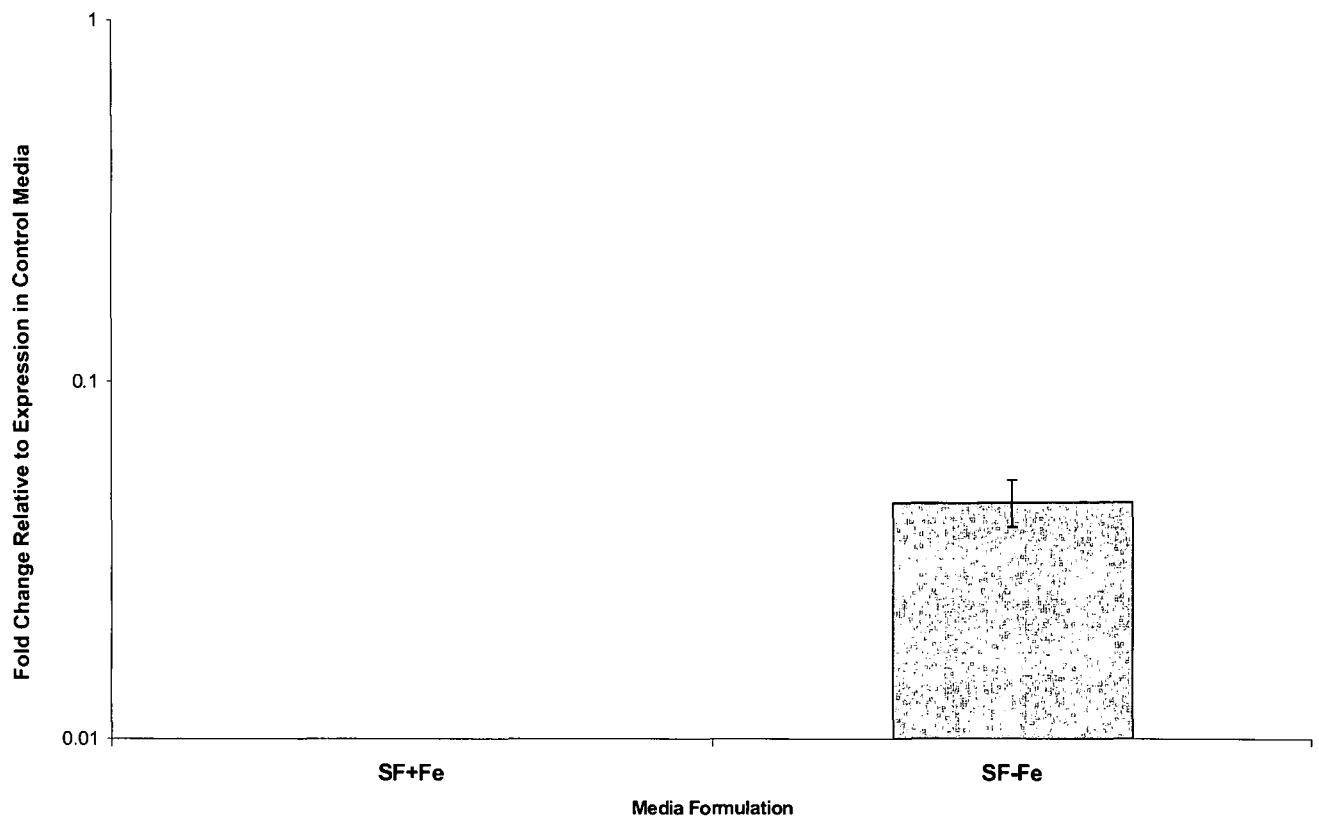


*Fig.3.14. Real time-PCR comparison of the expression of smoothelin in arterial smooth muscle cells cultured in conjunction with serum free media formulations in the presence (SF+Fe) and absence (SF-Fe) of iron after 14 days. Error bars represent 1 standard deviation from the mean, n=6*

From this data, it was possible to conclude that defined serum-free media formulations were developed and validated against human dermal fibroblasts, human osteoblasts and finally human arterial smooth muscle cells. In all cells there was very little significant difference between proprietary brands of media containing fetal calf serum, defined basal media containing 5% fetal calf serum and two serum free media formulations with iron both present and absent. Generally, metabolic activity increased throughout a 14 day culture period unless halted by contact inhibition as in the case of smooth muscle cells.

Defined serum-free basal media demonstrated the capacity to maintain the phenotype of both dermal fibroblast and smooth muscle cells. Extensive analysis of smooth muscle cell phenotype demonstrated the preference of these cells for media devoid of iron to the extent that a possible role of iron as a mediator of smooth muscle cell phenotype functionality could be

suggested, characterised by the absence of smoothelin in the iron containing media formulation. This highlights a major benefit of utilising intricately defined media formulations for cell culture applications, in enabling discrimination of the precise molecule responsible for mediating a particular cellular response.

### 3.vi Expansion of Primary Pluripotent Human Cells in Conjunction with Defined Serum Free Parameters – Bone Marrow Derived Mesenchymal Stem Cells

As a result of successful validation of the defined serum-free media formulation for the expansion and phenotypic maintenance of lineage committed human cells, validation of the media was required using primary human stem cells and subsequently, further defined modifications carried out on the media formulation to permit modulation of the stem cell phenotype.

Two factors would need to be addressed. Initially the media would need to be characterised for its capacity to maintain mesenchymal stem cells in an undifferentiated plastic state and secondly, it would need to be possible to use exogenous factors in the media, whilst maintaining the definition of the media, to guide a multipotent stem cell to a predetermined terminally differentiated cell fate.

Combinatorially, a defined, clinically acceptable formulation in addition to autologous or allogeneic stem cells would overcome several milestones in the progression of tissue engineering strategies from the laboratory to the clinic. The media component provides a pharmacopeia grade parameter for the culture and delivery of the cells whilst the stem cells themselves in conjunction with a mechanically suitable biomaterial provide a means of repopulating a vast array of damaged tissues, limited only by the degree of plasticity exhibited by a particular cell source.

Bone marrow-derived mesenchymal stem cells (Cambrex, UK) were cultured to passage 4 and subjected to 14 days of culture under defined serum free conditions in the presence and absence of iron. The media chosen as the control medium was Cambrex mesenchymal stem cell basal media (MSCBM) which contains fetal calf serum at a concentration undisclosed by the manufacturer. During this culture period the metabolic activity of the stem cells was characterised using the almar blue method

(Fig.3.15.). Throughout this culture period, there was a notably significant difference between the effects of serum containing and serum free media formulations on the metabolic activity of the cells. The overall trend was an increase in metabolism up to day 7, followed by a decrease at day 14 across all media, in a similar manner to smooth muscle cells. This was hypothesised to be a result of confluence mediating contact inhibition of growth and the resultant quiescence leading to a decrease in metabolic activity. Although a statistically significant decrease in metabolic activity was characterised at day 7, the culture cumulated in a strongly significant increase in metabolic activity in mesenchymal stem cells cultured in both iron containing and iron free parameters devoid of serum, the most significant increase relative to commercial media occurring in the iron containing formulation ( $P < 0.001$ ).

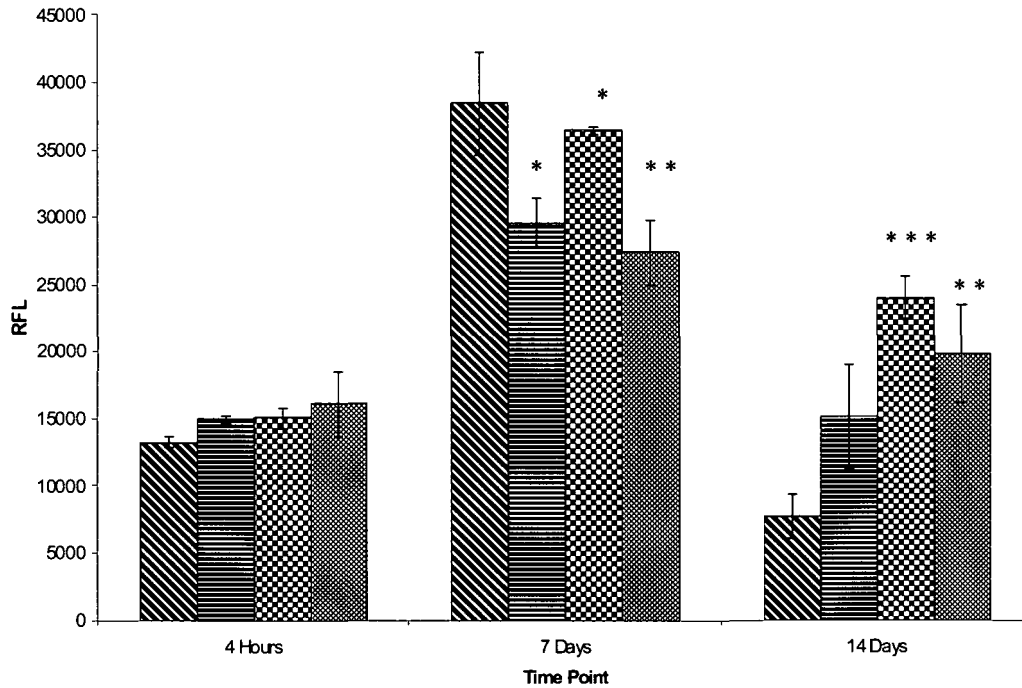


*Fig.3.15. Comparison of the metabolic activities of human bone marrow derived mesenchymal stem cells in a range of serum free and serum containing media formulations using the Alamar blue method. Error bars represent 1 standard deviation from the mean, n=3, \*P<0.05, \*\*P<0.01, \*\*\*P<0.001 compared to Cambrex MSCBM. No correction for change in cell number was made*

Bone marrow derived mesenchymal stem cells maintained their fibroblastic morphology throughout this culture period in serum free media (Fig.3.16.), with observation of confluence confirming contact inhibition (and resultant contact mediated quiescence) as a potential for the drop in metabolism observed at day 14 using the alamar blue method, to be a result of contact inhibition.

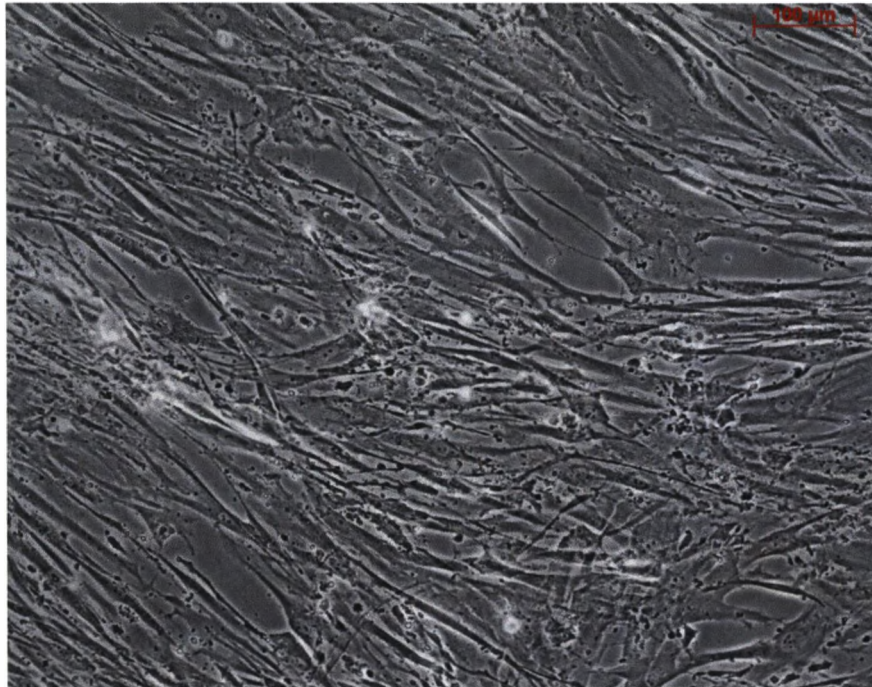


*Fig.3.16. Light microscopic observation of confluent bone marrow derived mesenchymal stem cells in serum free media containing iron after 14 days of culture*

Further analysis was carried out to confirm the phenotypic state of these cells using flow cytometry as outlined in section 2.xv, in conjunction with a subset of target proteins chosen to assess stem cell plasticity in addition to early lineage commitment. Mesenchymal stem cells are widely reputed to reduce in plasticity as they age in culture. To account for this factor, mesenchymal stem cells were compared from a progression of early through to late passages (passage 2 to passage 7) and cultured in Cambrex MSCBM and serum free media until confluent, then analysed (figs 3.17-3.22). The iron containing serum-free formulation was chosen, given the earlier demonstration of a significant preference of the cells for this formulation during the determination of metabolic activity.

Markers chosen to represent a mesenchymal stem cell phenotype were CD29, CD44, CD73, CD90, CD117, CD166, NGFR (CD271) and STRO-1. CD34 was included as a hematopoietic stem cell marker in addition to CD45, a marker of hematopoietic lineage progression. CD56 (neural cell adhesion molecule; NCAM) is expressed on the surface of neural and glial

cells in addition to skeletal muscle and would indicate spontaneous transformation to a neural lineage. CD31 (platelet endothelial cell adhesion molecule; PECAM), CD62 and CD106 (vascular cell adhesion molecule; VCAM) are both cell adhesion molecules expressed exclusively on endothelium and thus would indicate endothelial cell lineage commitment, additionally CD146 (melanoma cell adhesion molecule; MCAM), is a marker of endothelial progenitor cells also expressed on terminally differentiated endothelium. CD64, a marker of monocyte and macrophage cells and CD19, a marker of dendritic cells, encompasses a group of proteins describing terminal myeloid and lymphoid differentiation [250, 313, 319-321].

Overall, throughout the investigation, markers associated with a stem cell phenotype were observed that under serum free conditions stem cells maintained at statistically significantly increased levels to when maintained in serum containing media. This data suggests that the undefined nature of the cytokine and growth factor component of serum may be influencing the lineage commitment of the stem cells during culture. Removal of this exogenous variability using media devoid of serum enabled the cells to maintain their plasticity for extended periods of time. Additionally, to support this data, as the cell passage number increased, cells began to express markers associated with differentiation much more heterogeneously, further supporting their transgression away from a stem cell phenotype. However, lineage commitment markers were generally reduced in serum-free over serum-containing media, particularly in the final passage of cells analysed, passage 7. These data demonstrated the suitability of the defined serum free media formulation for the culture of bone marrow derived mesenchymal stem cells whilst also demonstrating its advantage over serum-containing counterparts by demonstration of the exogenous nature of the proteinaceous component of serum stimulating spontaneous, non-defined heterogeneous differentiation of the stem cell population, summarised in table 3.3. Furthermore table 3.4 illustrates a direct quantitative statistical comparison between the potential



to maintain stem phenotype of both serum containing and serum free media formulations. This is based on a subtraction of lineage commitment markers from markers of a stem cell phenotype based on the number of degrees of statistical significance in the case of each media ( $*P < 0.05$ ,  $**P < 0.01$ ,  $***P < 0.001$ ), demonstrating the superiority of serum free over serum containing media at maintaining stem phenotype in 4 of the 6 passages characterised [250, 313, 319-321].

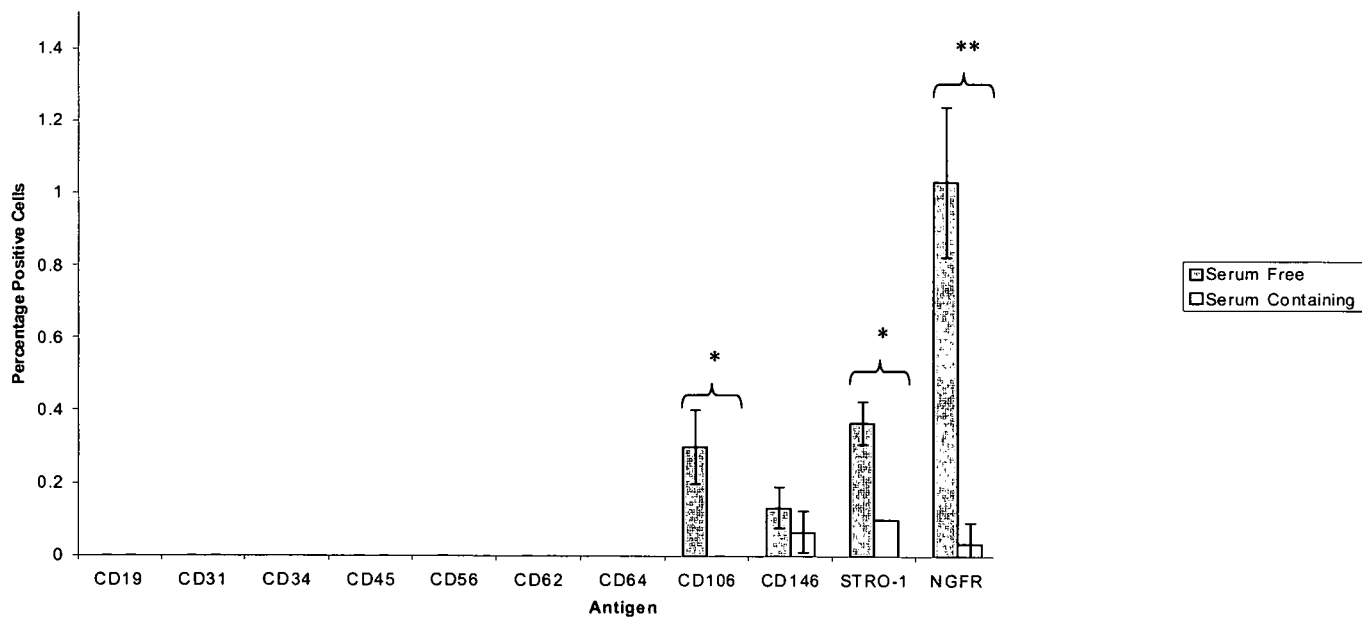
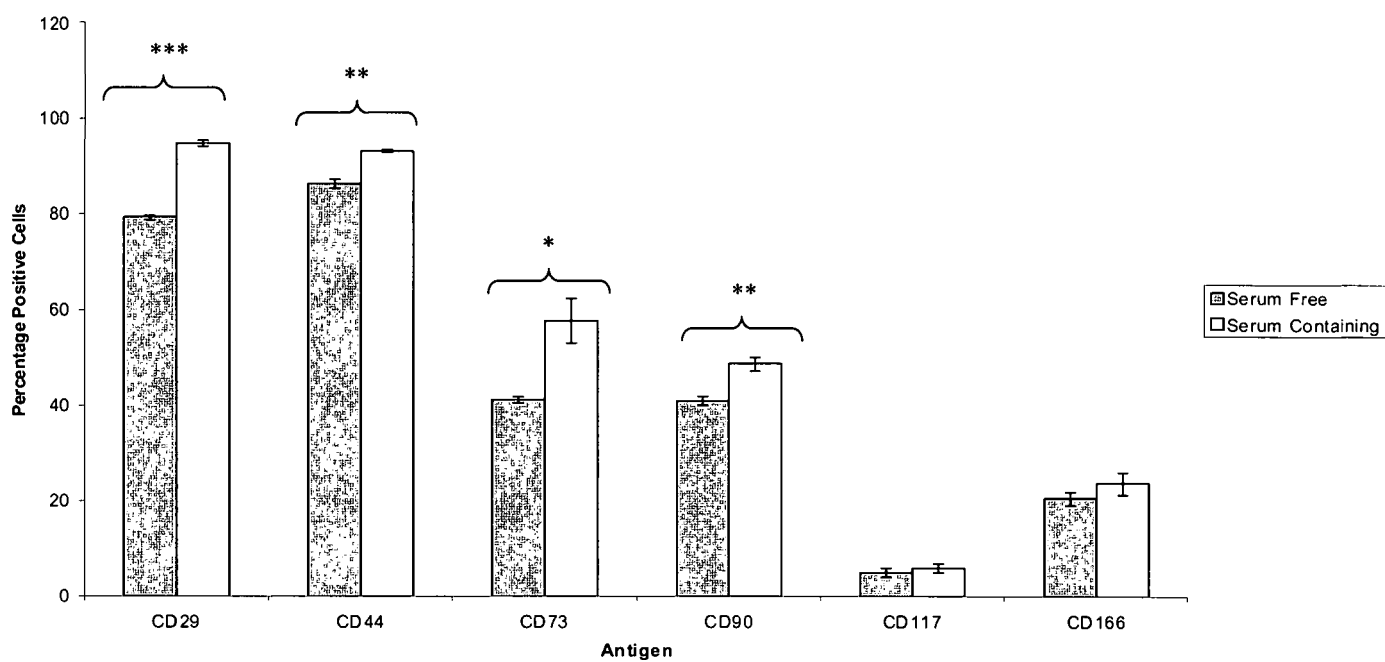


Fig.3.17. Comparison of a subset of cellular antigens of bone marrow derived mesenchymal stem cells cultured in serum free and serum containing (Cambrex MSCBM) media formulations at confluence, at passage 2, observed using flow cytometry. Error bars represent 1 standard deviation from the mean, n=3, \*P<0.05, \*\*P<0.01, \*\*\*P<0.001

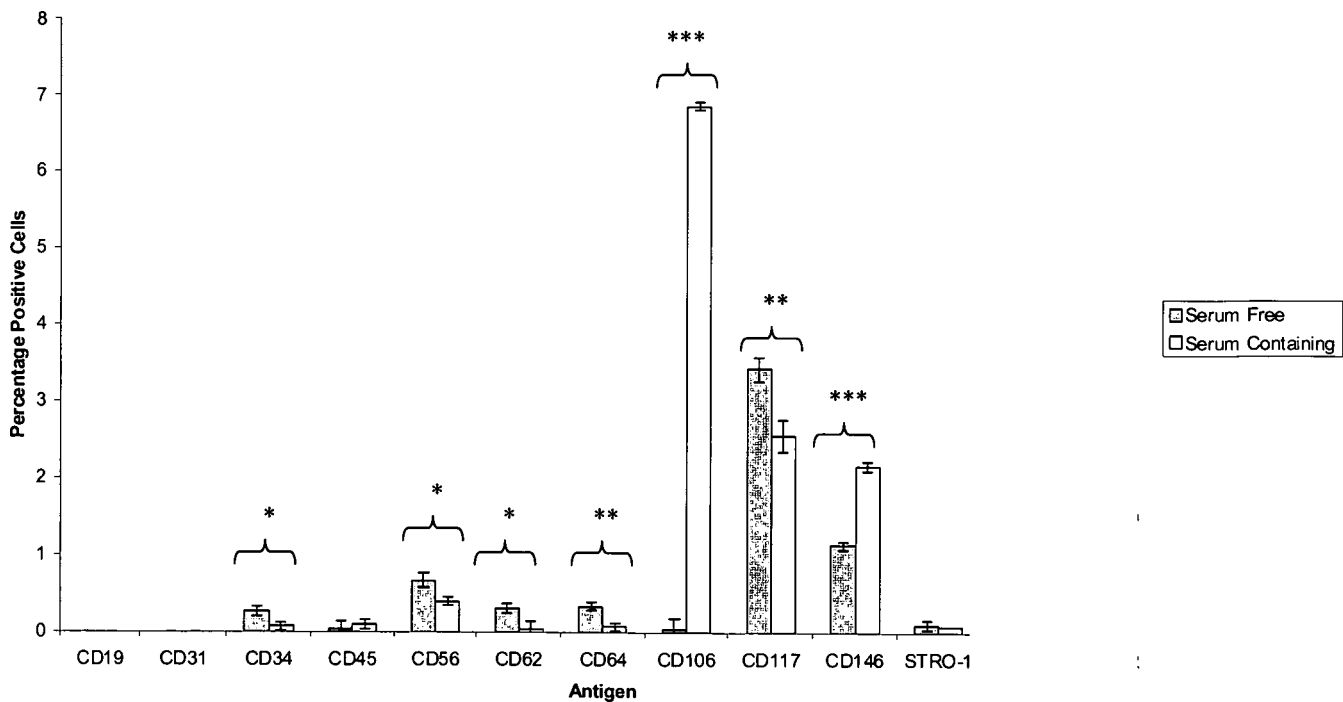
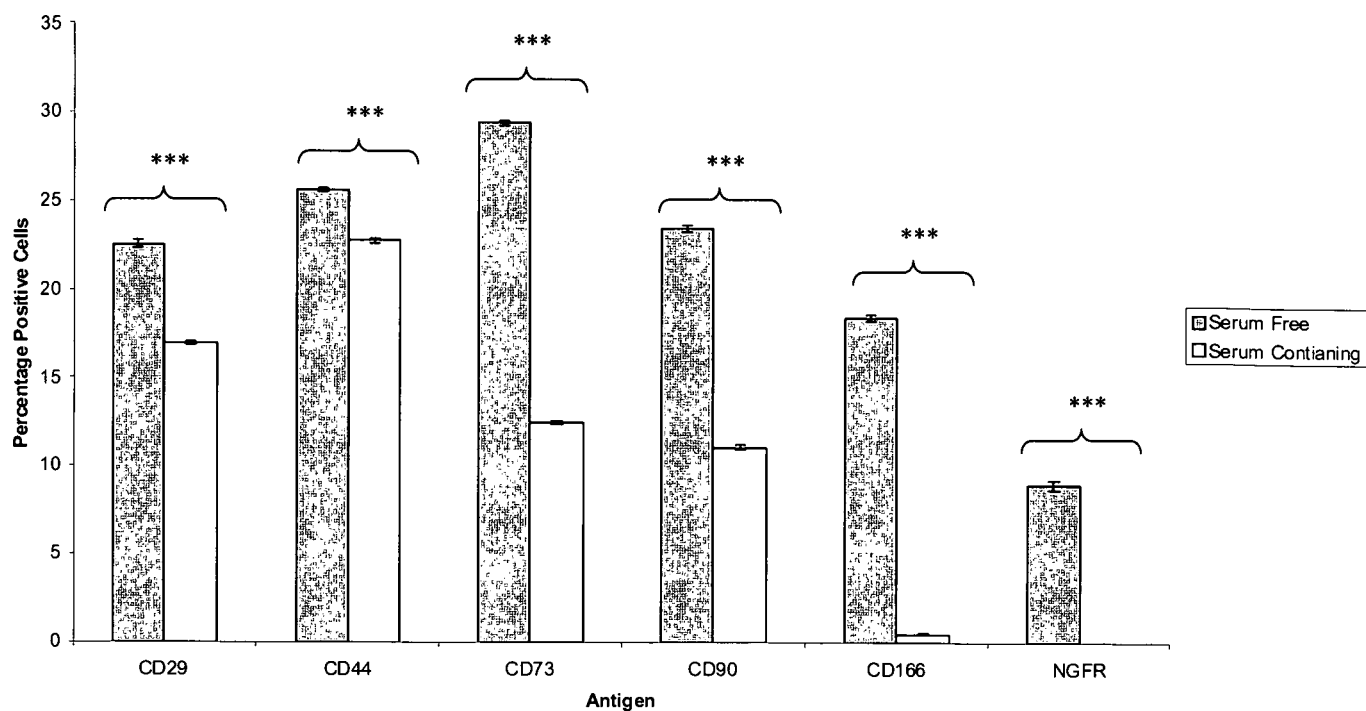


Fig.3.18. Comparison of a subset of cellular antigens of bone marrow derived mesenchymal stem cells cultured in serum free and serum containing (Cambrex MSCBM) media formulations at confluence, at passage 3, observed using flow cytometry. Error bars represent 1 standard deviation from the mean, n=3, \*P<0.05, \*\*P<0.01, \*\*\*P<0.001

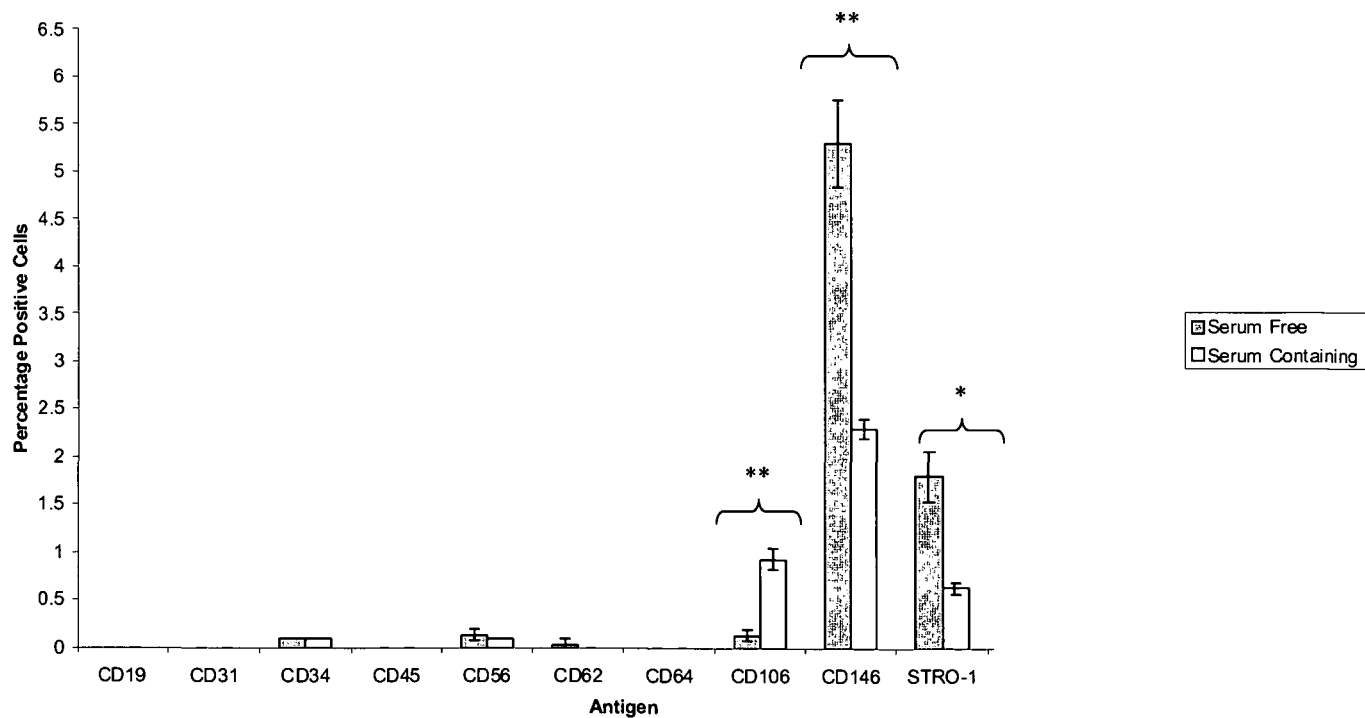
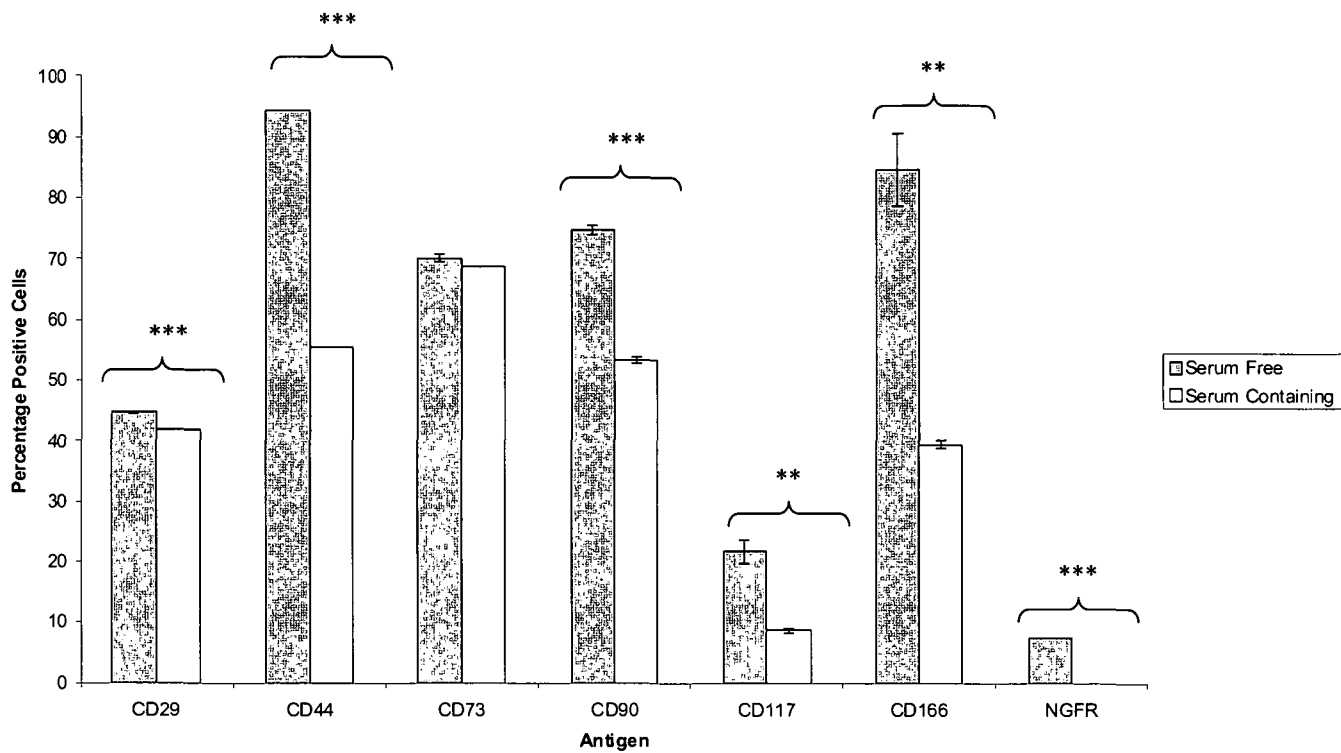


Fig.3.19. Comparison of a subset of cellular antigens of bone marrow derived mesenchymal stem cells cultured in serum free and serum containing (Cambrex MSCBM) media formulations at confluence, at passage 4, observed using flow cytometry. Error bars represent 1 standard deviation from the mean,  $n=3$ , \* $P<0.05$ , \*\* $P<0.01$ , \*\*\* $P<0.001$

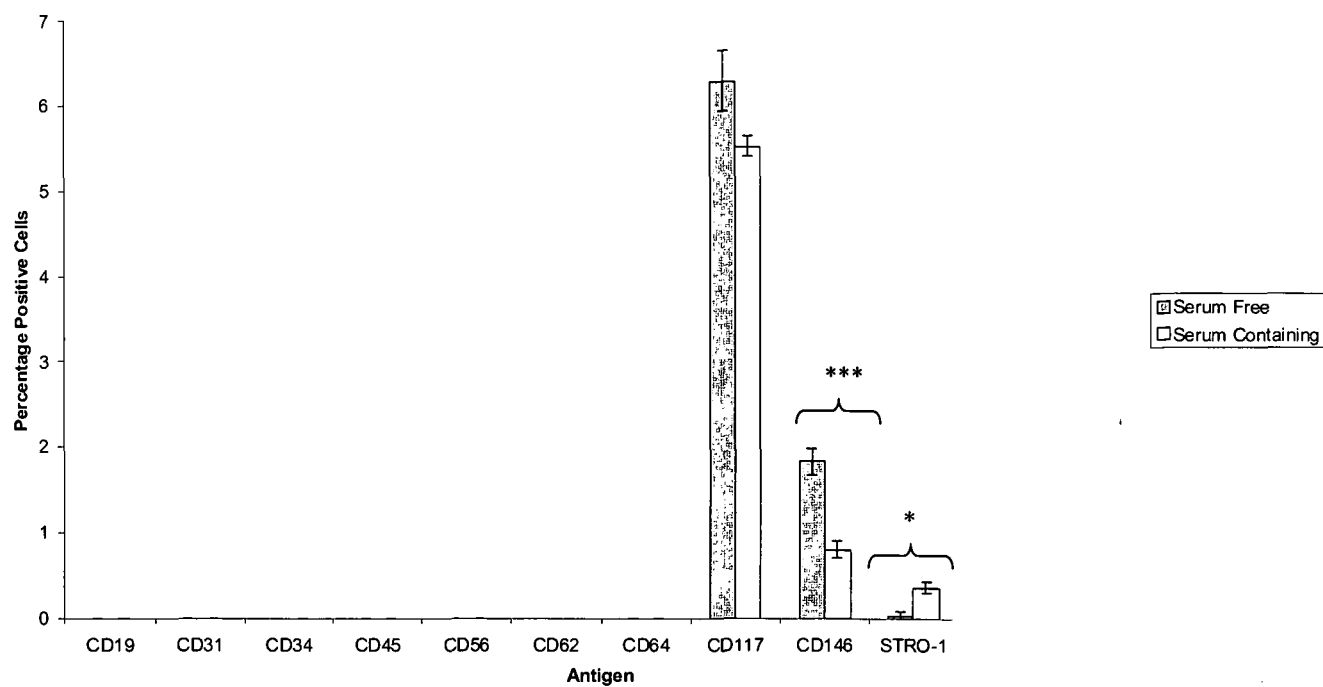
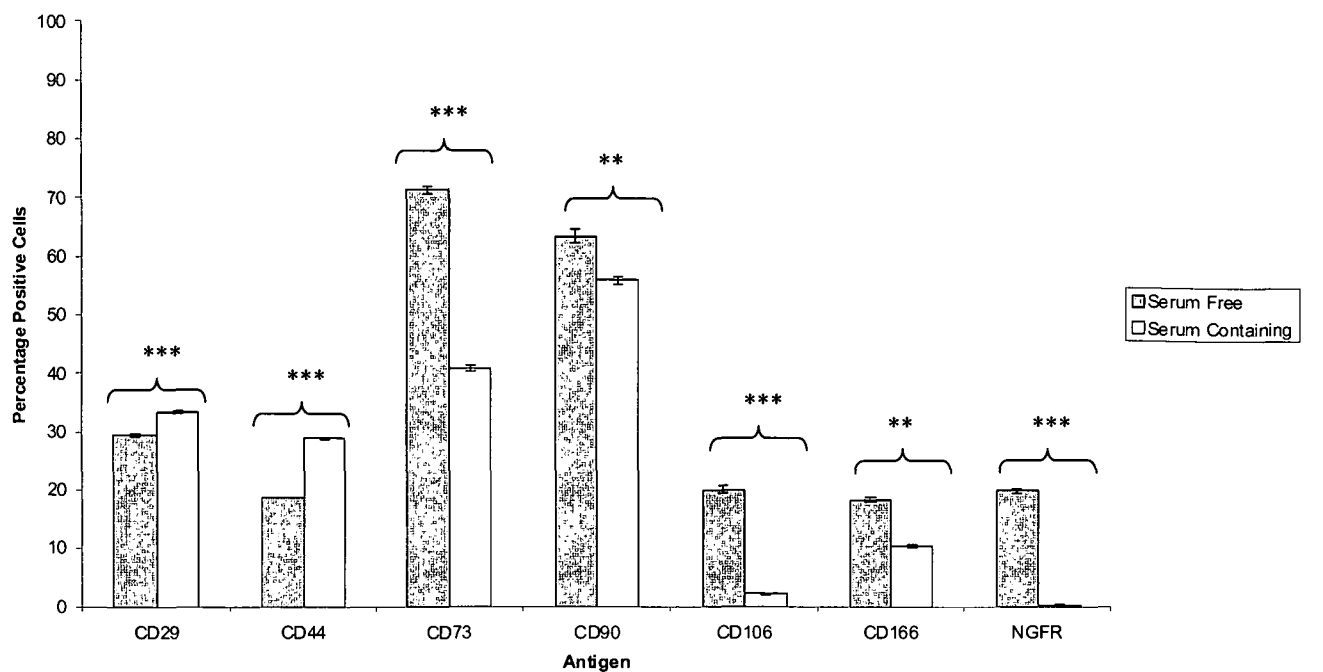
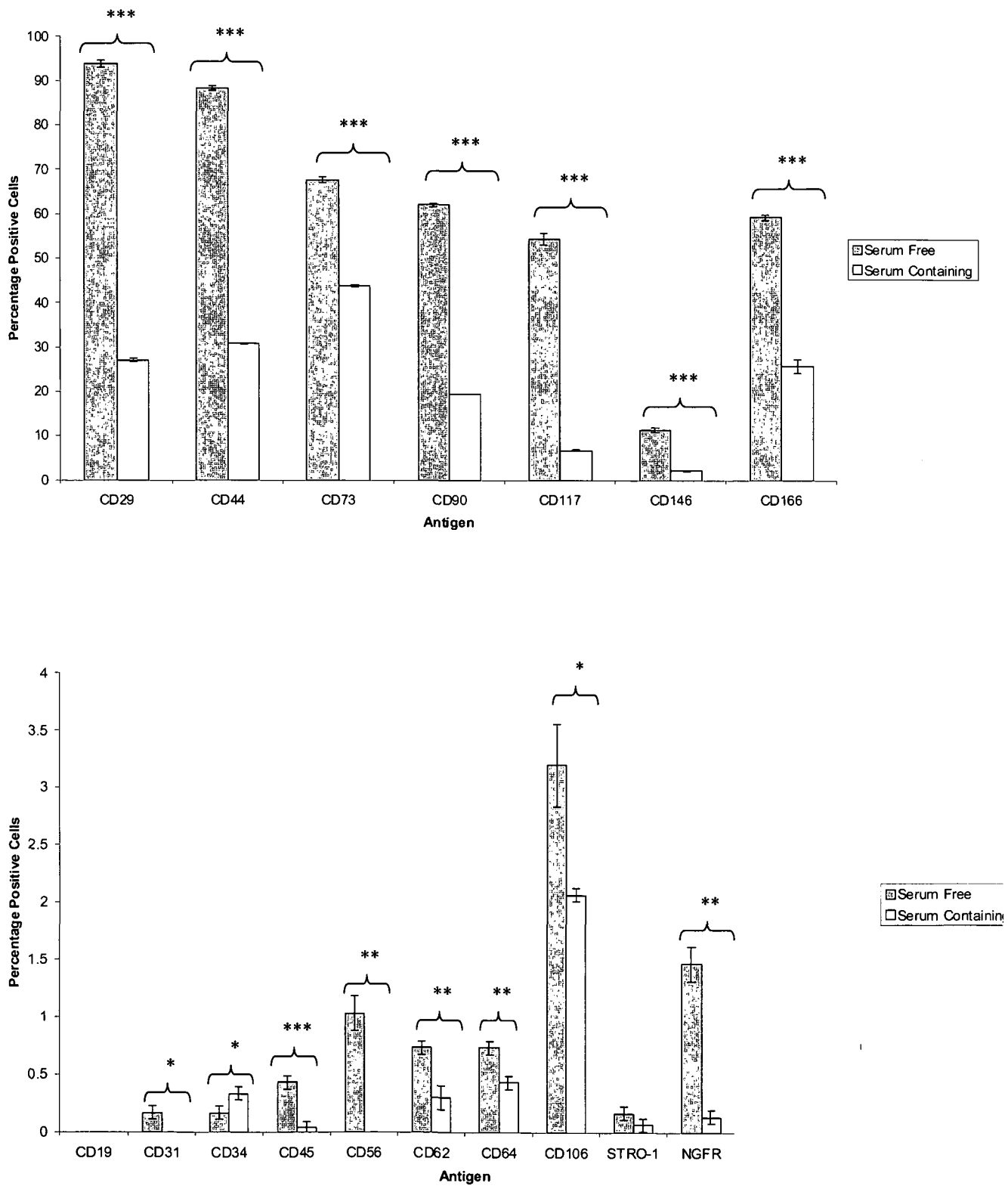


Fig.3.20. Comparison of a subset of cellular antigens of bone marrow derived mesenchymal stem cells cultured in serum free and serum containing (Cambrex MSCBM) media formulations at confluence, at passage 5, observed using flow cytometry. Error bars represent 1 standard deviation from the mean,  $n=3$ , \* $P<0.05$ , \*\* $P<0.01$ , \*\*\* $P<0.001$



*Fig.3.21. Comparison of a subset of cellular antigens of bone marrow derived mesenchymal stem cells cultured in serum free and serum containing (Cambrex MSCBM) media formulations at confluence, at passage 6, observed using flow cytometry. Error bars represent 1 standard deviation from the mean, n=3, \*P<0.05, \*\*P<0.01, \*\*\*P<0.001*

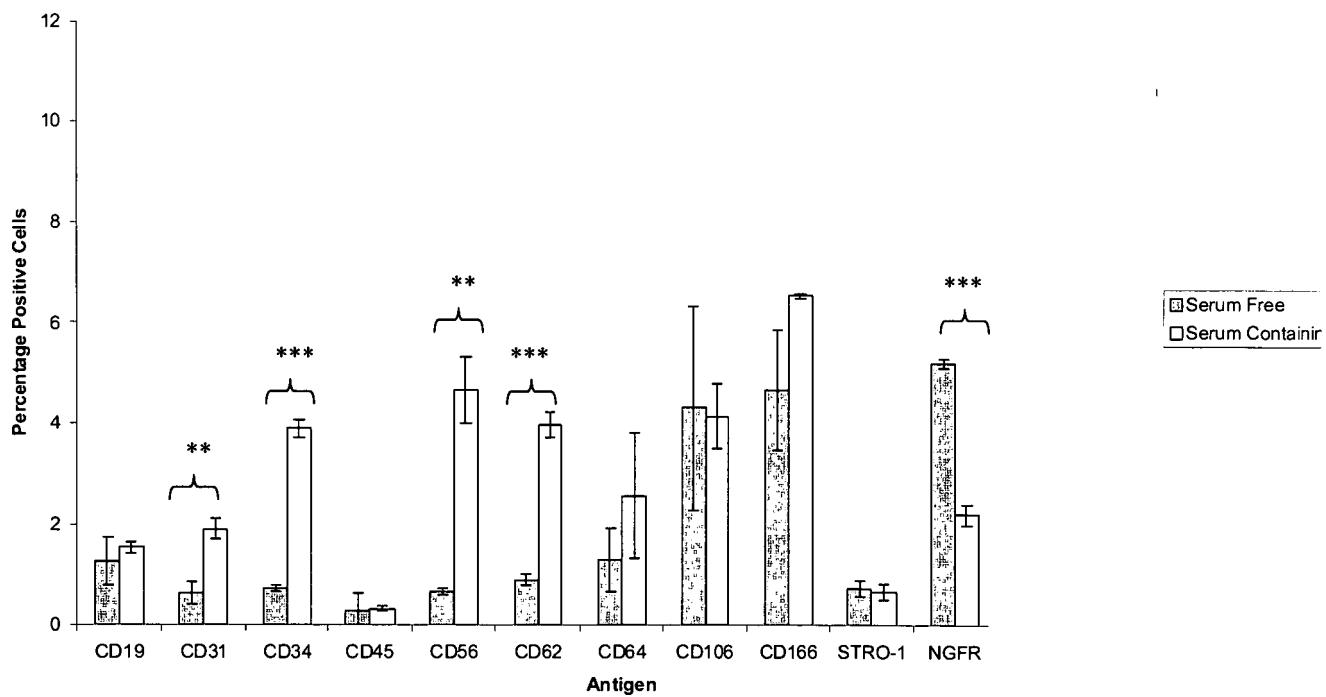
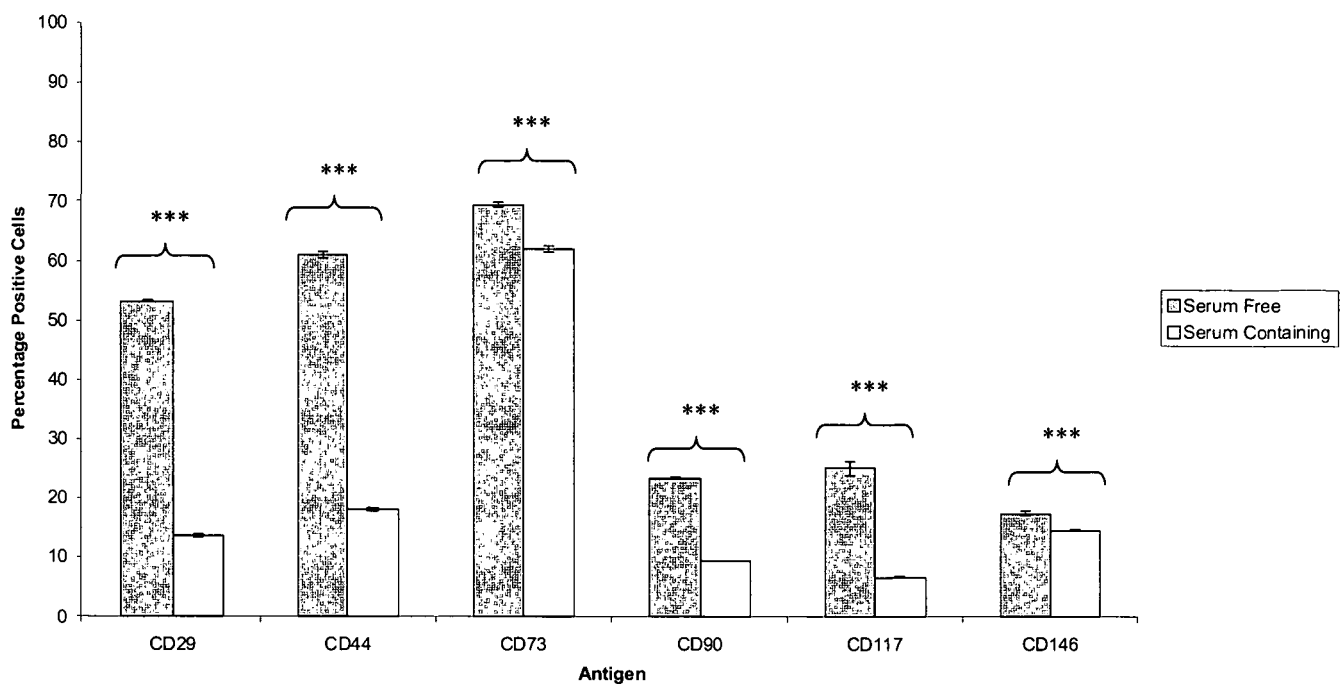


Fig.3.22. Comparison of a subset of cellular antigens of bone marrow derived mesenchymal stem cells cultured in serum free and serum containing (Cambrex MSCBM) media formulations at confluence, at passage 7, observed using flow cytometry. Error bars represent 1 standard deviation from the mean, n=3, \*P<0.05, \*\*P<0.01, \*\*\*P<0.001

	Passage 2		Passage 3		Passage 4		Passage 5		Passage 6		Passage 7	
	SC	SF	SC	SF	SC	SF	SC	SF	SC	SF	SC	SF
CD19	0.00	0.00	0.00	0.00	0.00	0.00	0.00	0.00	0.00	0.00	1.53	1.27
CD29	33.2***	29.30	17.00	22.6***	42.00	44.7***	33.3***	29.30	27.10	93.9***	13.80	53.2***
CD31	0.00	0.00	0.00	0.00	0.00	0.00	0.00	0.00	0.00	0.17*	1.9**	0.63
CD34	0.00	0.00	0.07	0.27*	0.10	0.10	0.00	0.00	0.33	0.17*	3.9***	0.73
CD44	93.3**	86.40	22.70	25.6***	55.50	94.4***	27.8***	18.70	30.90	88.4***	18.10	60.9***
CD45	0.00	0.00	0.10	0.03	0.00	0.00	0.00	0.00	0.03	0.43***	0.30	0.30
CD56	0.00	0.00	0.40	0.67*	0.10	0.13	0.00	0.00	0.00	1.03**	4.7**	0.67
CD62	0.00	0.00	0.03	0.3*	0.00	0.03	0.00	0.00	0.30	0.73**	4***	0.90
CD64	0.00	0.00	0.07	0.3**	0.00	0.00	0.00	0.00	0.43	0.73**	2.60	1.30
CD73	57.8*	41.20	12.50	29.4***	68.80	70.20	41.20	71.3***	43.90	67.9***	61.90	69.4***
CD90	48.6**	41.00	11.10	23.4***	53.40	74.9***	56.00	63.4**	19.40	62.1***	9.60	23.5***
CD106	0.00	0.3*	6.9***	0.03	0.93**	0.13	2.10	20.1***	2.07	3.2*	4.13	4.30
CD117	5.70	5.00	2.60	3.4**	8.70	21.7**	5.30	6.30	6.80	54.4***	6.80	25.2***
CD146	0.07	0.13	2.20	1.1**	2.30	5.3**	0.80	1.8***	2.10	11.3***	14.60	17.5***
CD166	23.50	20.40	0.47	18.4***	39.40	84.7**	10.30	18.2**	25.80	59.3***	6.53	4.67
STRO-1	0.10	0.36*	0.07	0.10	0.63	1.8*	0.36*	0.03	0.07	0.17	0.67	0.73
NGFR	0.03	1.03**	0.00	8.90	0.00	7.5***	0.23	19.6***	0.13	1.47**	2.20	5.2***

Table.3.3. Comparison summary of the mean antigenicity of bone marrow derived mesenchymal stem cells in serum free and serum containing media (Cambrex MSCBM) over a number of passages, demonstrated using flow cytometry, \*P<0.05, \*\*P<0.01, \*\*\*P<0.001

Colour	Antigen Subset	Passage 2		Passage 3		Passage 4		Passage 5		Passage 6		Passage 7	
		SC	SF	SC	SF	SC	SF	SC	SF	SC	SF	SC	SF
	Mesenchymal Stem	8	3	0	17	0	17	7	10	0	20	0	18
	Hematopoietic	0	0	0	1	0	0	0	0	0	4	3	0
	Myeloid/Lymphoid	0	0	0	2	0	0	0	0	0	2	0	0
	Lineage Commitment	0	0	3	4	2	2	0	6	0	9	7	3
	Ambiguous	0	0	0	3	0	0	0	0	0	2	0	0
	<b>(Stem) - (Lineage Commitment)</b>	<b>8</b>	<b>3</b>	<b>-3</b>	<b>9</b>	<b>-2</b>	<b>15</b>	<b>7</b>	<b>4</b>	<b>0</b>	<b>3</b>	<b>-10</b>	<b>15</b>

Table.3.4. Comparison of serum containing and serum free media formulations on their capacity to maintain mesenchymal stem cell phenotype by normalisation based on number of statistical significances, \*P<0.05, \*\*P<0.01, \*\*\*P<0.001



Further characterisation of the mesenchymal stem cell phenotype was carried out using immunohistochemical observation of 3 markers indicative of a plastic cell phenotype. After 21 days of culture under defined serum free parameters passage 4 stem cells were demonstrated to express STRO-1, nucleostemin and CD105, three markers of multipotency, further demonstrating the suitability of this media formulation in facilitating the maintenance of the undifferentiated phenotype of bone marrow derived mesenchymal stem cells (Fig.3.23.).

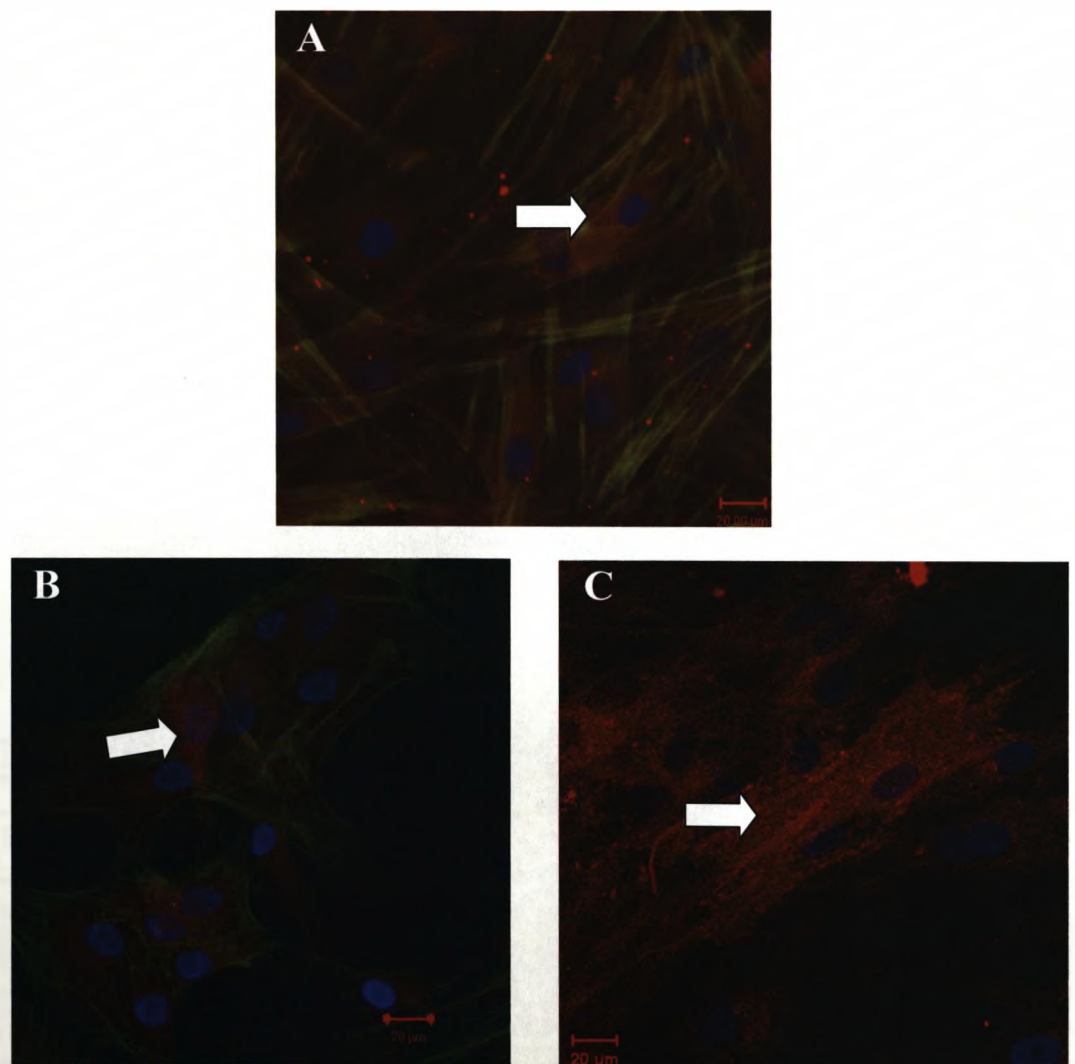


*Fig.3.23. Fluorescent microscopic observation of immunohistochemical staining for: A; Nucleostemin, F-Actin, Nuclei. B; STRO-1, F-Actin, Nuclei and C; CD105, Nuclei after 21 days of defined serum free culture (positive staining illustrated by arrows)*

After successful demonstration that basal defined serum free media maintained the undifferentiated phenotype of primary human bone marrow mesenchymal stem cells, it was necessary to define and subject the cells to controlled differentiation parameters in order to confirm their capacity to lineage commit in the absence of serum. Bone marrow derived stem cells were selected from passage 4 and seeded at a standard density for differentiation of  $5.0 \times 10^4$  cells/cm<sup>2</sup>. The mesenchymal stem cells were subjected to tri lineage differentiation using the defined serum free formulations for osteogenic, chondrogenic and adipogenic differentiation media given in table 3.5. In these cases, the additions quoted in the table were added to complete iron containing serum free media, the pH of the media was adjusted to 7.4 followed by filter sterilization. Cells were seeded under basal conditions for 24 hours after which basal media was aspirated and replaced with differentiation media. Stem cells were cultured under differentiation conditions for 21 days with media refreshment occurring every 7<sup>th</sup> day, a standard culture period for differentiation assays and analysed throughout.

<b>Osetogenic</b> Ascorbate Dexamethasone $\beta$ -Glycerophosphate	<b>Conc</b> 50 $\mu$ m 100nm 10mM	<b>Chondrogenic</b> Pyruvate Ascorbate Dexamethasone TGF $\beta$ 1 Glucose	<b>Conc</b> 1mM 50 $\mu$ m 100 $\mu$ m 10ng/ml 3.5g/L
<b>Adipogenic</b> Dexamethasone Hydrocortisone	<b>Conc</b> 1 $\mu$ m 50 $\mu$ m	<b>Hepatic</b> HGF bFGF aFGF	<b>Conc</b> 20ng/ml 20ng/ml 10ng/ml
<b>Neural</b> Retinoic Acid	<b>Conc</b> 300ng/ml		

*Table.3.5. Composition of defined serum free differentiation media used throughout differentiation assays*

Stem cells subjected to osteogenic differentiation criteria expressed the osteogenic master gene core binding factor- $\alpha$ -1 (CBFA1/RUNX2) [404]; observed using immunohistochemistry, after a culture period of 5 days,

indicating the commencement of osteogenic induction as a result of stimulation using defined serum free osteogenic media (Fig.3.24.).

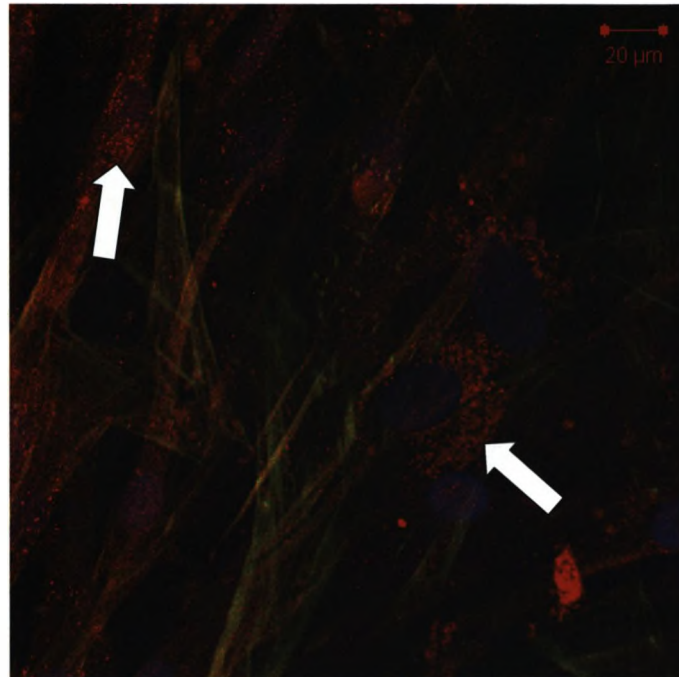


*Fig.3.24. fluorescent microscopic observation of immunohistochemical staining of bone marrow derived mesenchymal stem cells for **CBFA1/RUNX2**, F-Actin and Nuclei after 5 days of defined serum free osteogenic culture (positive staining illustrated by arrows)*

After completion of the 21 day culture period under defined osteogenic stimuli, cells were observed immunohistochemically to express osteocalcin, a marker indicative of terminal, functional osteogenesis (Fig.3.25.) [405]. Osteocalcin, a transcription factor, was evident in both nuclear and cytoplasmic locations after osteogenic differentiation culture.

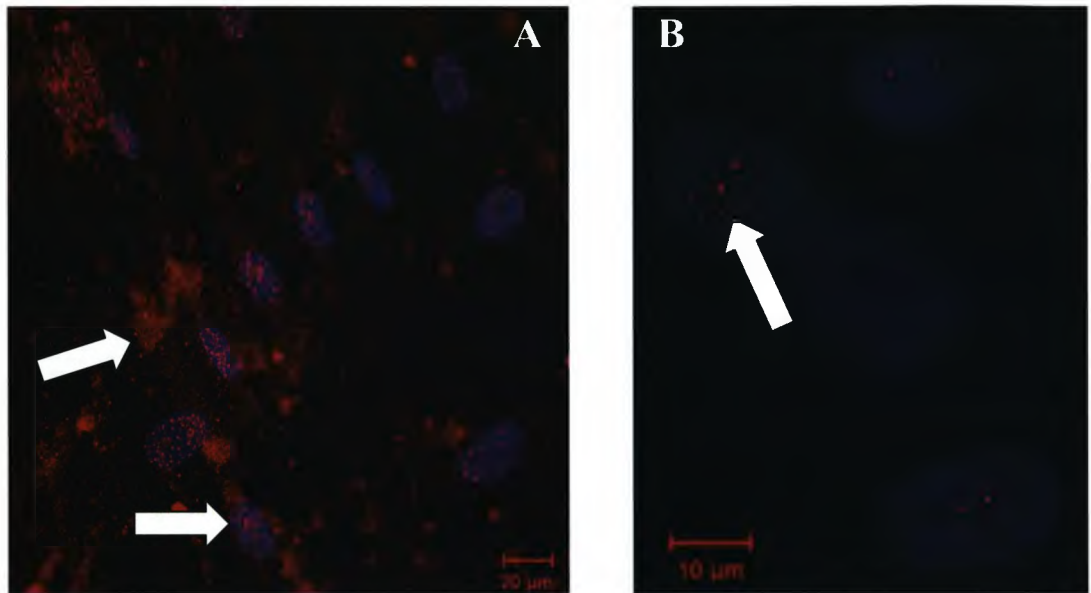


*Fig.3.25. Fluorescent microscopic observation of immunohistochemical staining of bone marrow derived mesenchymal stem cells for **Osteocalcin**, **F-Actin** and **Nuclei** after 21 days of osteogenic culture (positive staining indicated by arrows)*

Further analysis using real time-PCR in conjunction with cDNA samples generated from stem cells after 21 days of osteogenic differentiation culture as detailed in section 2.v, confirmed the expression of a subset of osteogenic genes after 21 days of culture under defined osteogenic parameters (all primers and corresponding annealing temperatures are given in table.2.3). Gene expression levels were compared based on  $C_t$  values for differentiation marker genes normalised to the house keeping gene:  $\beta$ -actin under differentiation parameters then this value further subtracted from the level of the target marker present in basal parameters to elucidate a true representation to compare modulations in gene expression when applied to the  $2^{-\Delta Ct}$  calculation, an equation used to represent the exponential nature of DNA amplification during a real time-PCR reaction (Fig.3.26.).



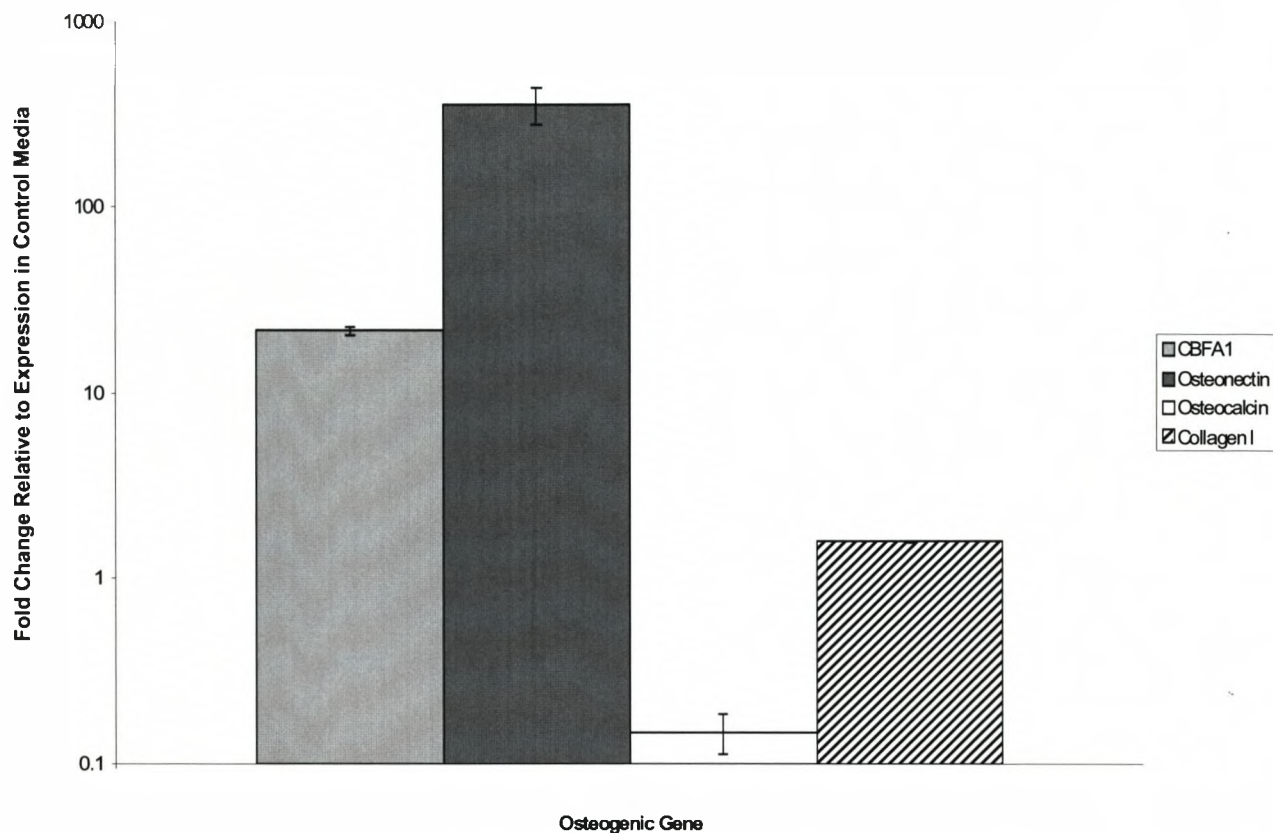


*Fig.3.26. Real time-PCR characterisation of a subset of osteogenic genes after 21 days of osteogenic culture of bone marrow derived mesenchymal stem cells. Error bars represent 1 standard deviation from the mean, n=6*

These data demonstrated increases in expression of CBFA1/RUNX2, and osteonectin, two proteins associated intimately with osteogenesis, after 21 days under osteogenic culture conditions. A slight increase in collagen I was also observed during this study which, although interesting, is not directly related specifically to osteogenesis. Therefore using the real time-PCR analysis in conjunction with immunohistochemistry it was possible to conclude that bone marrow derived stem cells in conjunction with defined serum free osteogenic media underwent differentiation into lineage committed osteoblasts after 21 days of culture.

Using an identical seeding strategy to osteogenic differentiation parameters, bone marrow derived stem cells were additionally subjected to defined chondrogenic differentiation media using the formulation detailed

in table.3.5. Cells were again taken from passage 4, seeded under basal conditions for 24 hours at  $5.0 \times 10^4$  cells/cm<sup>2</sup> after which basal media was aspirated and replaced with defined, serum free chondrogenic differentiation media. Unlike many chondrogenic differentiation strategies, cells were not cultured using pellet style culture systems, with a monolayer being preferred due to ease of analysis. After 21 days of culture cells were analysed for the presence of type II collagen, a fibre forming collagen specific to chondrocyte cells which *in vivo*, allows cartilage to associate with proteoglycan as well as provide tensile strength to the tissue. Fig.3.27. illustrates the presence of type II collagen after the 21 day chondrogenic culture period using immunohistochemistry.

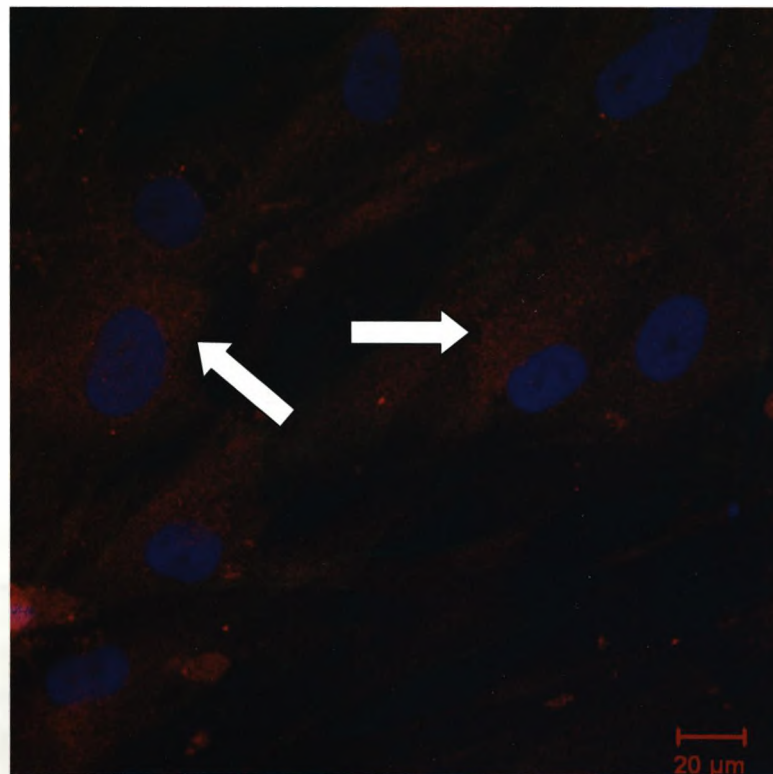


*Fig.3.27. Fluorescent microscopic observation of immunohistochemical staining of bone marrow derived stem cells after 21 days of chondrogenic culture for Collagen II, F-Actin and Nuclei (positive staining illustrated by arrows)*

Further confirmation of a chondrogenic phenotype was carried out using real time-PCR analysis, again characterizing the presence of the type II collagen using cDNA libraries generated from bone marrow derived stem cells, after 21 days of chondrogenic culture. Normalization was performed

as described previously and the appropriate primers and annealing temperatures detailed in table 2.3. Fig.3.28. demonstrates the findings from the real time analysis, also included for comparison is type I collagen.

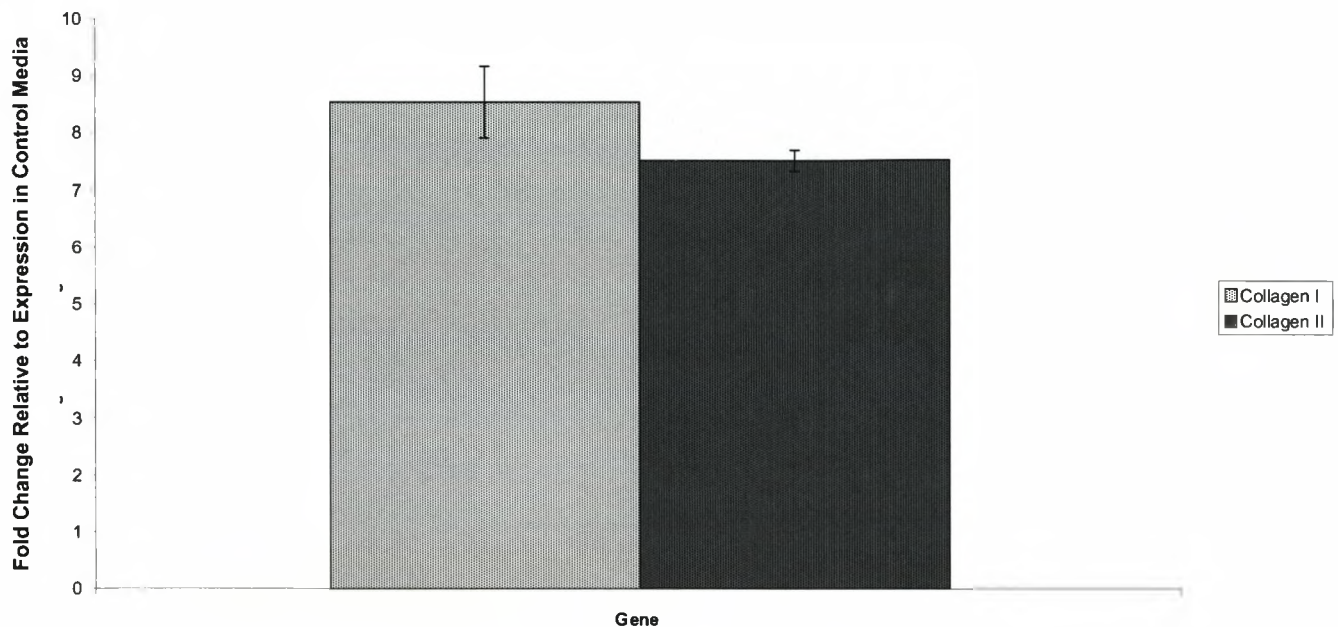


*Fig.3.28. Real time-PCR characterisation of type I and II collagen after 21 days of chondrogenic culture of bone marrow derived mesenchymal stem cells. Error bars represent 1 standard deviation from the mean, n=6*

Real time analysis demonstrated an increase in the expression of both collagen type I and II at similar fold levels. Ultimately, in a terminally differentiated articular chondrocyte collagen II occupies approximately 90% of total collagen. Therefore this data could suggest that more extended differentiation culture periods are required for terminal chondrogenesis under these conditions. However, given the specificity of type II collagen to chondrocytes, these data confirm that differentiation towards a terminal chondrogenic lineage is certainly facilitated under these defined serum-free chondrogenic parameters.

Defined serum-free adipogenic media was synthesized as per table 3.1/3.2 and bone marrow derived mesenchymal stem cells were subjected to



differentiation culture in an identical manner to the osteogenic and chondrogenic differentiation studies in which passage 4 cells were seeded in a monolayer of  $5.0 \times 10^4$  cells/cm<sup>2</sup>, adhesion permitted for 24 hours under basal parameters before cells were subjected to 21 days of differentiation culture. Throughout this culture period cells were subjected to conventional histological staining using the Oil Red O method detailed in section 2.vi to observe the presence of lipid vesicles within the cells therefore characterizing their differentiation into an adipogenic lineage. Lipid encapsulation in the cytoplasm of the cells was observed after time periods as rapid as 5 days post induction (Fig.3.29). After this time the cells still retained the fibroblastic morphology associated with bone marrow derived mesenchymal stem cells with the additional lipid vesicles associated with adipose cells.

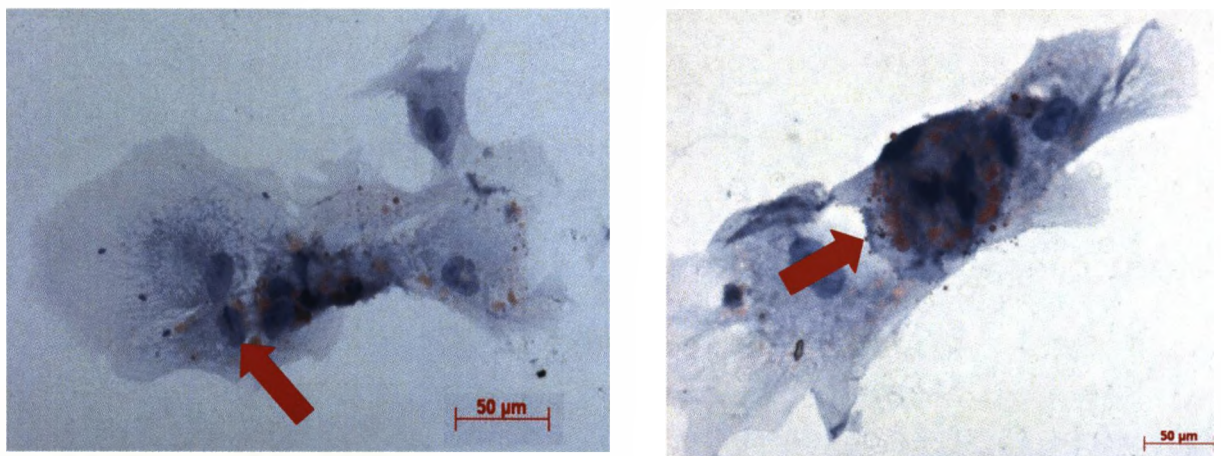


*Fig.3.29. Microscopic observation of Oil Red O and haematoxylin stained bone marrow derived mesenchymal stem cells after 5 days of adipogenic culture (positive staining illustrated by arrows)*

After 21 days of adipogenic culture the bone marrow derived stem cells no longer retained their fibroblastic morphology demonstrating a more rounded typical adipocyte like appearance. Additionally, further Oil Red O staining confirmed extensive lipid encapsulation throughout the entire cytoplasmic compartment of the cell (Fig.3.30.).



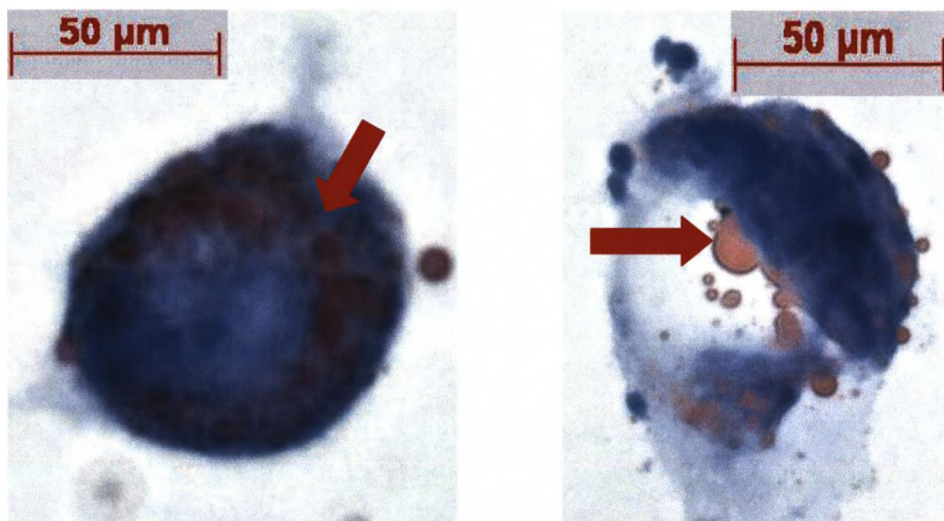


*Fig.3.30. Microscopic observation of Oil Red O and haematoxylin stained bone marrow derived mesenchymal stem cells after 21 days of adipogenic culture (positive staining illustrated by arrows)*

It was possible, therefore, to conclude that defined serum-free media was capable of maintaining the undifferentiated phenotype and plasticity of bone marrow derived mesenchymal stem cells. In the case of late passage stem cells, it was further possible to demonstrate that the serum free media formulation enhanced the expression of markers associated with an undifferentiated phenotype and inhibited the expression of certain antigens associated with lineage commitment.

Additionally, defined modifications of exogenous components to the basal media formulation was demonstrated capable of mediating 'tri-lineage' differentiation of bone marrow derived stem cells into osteoblast, chondrocyte and adipocyte cells in a culture period of 21 days.

3.vii Expansion of Primary Pluripotent Human Cells in Conjunction with Defined Serum Free Parameters – Dental Pulp Derived Mesenchymal Stem Cells

Additional studies into differentiation involved the exploitation of dental pulp derived stem cells. These cells have significant benefits for *ex-vivo* manipulation over bone marrow derived mesenchymal stem cells.

Developmentally, cells found within the dental pulp niche are derived from the embryonic neural crest. As a result of this it is hypothesized that these cells would yield an increased plasticity, being closer in the cellular lineage commitment hierarchy to embryonic stem cells than classical bone marrow derived mesenchymal stem cells. In culture these cells appear considerably more robust than most stem cell sources with more rapid population doubling times and a substantially higher longevity. From a practical point of view these cells are also easy to obtain, schemes are in place to coordinate banking of infant ‘milk’ teeth as a stem cell source for potential autologous tissue regeneration later in life, however, teeth derived from adult donors, removed as part of routine dental practice also yield plastic populations of cells.

In this study dental pulp stem cells were obtained from adult donors as a result of consented routine dental practice. Cells were maintained routinely, using the tissue culture protocol outlined in section 2.x. Under basal serum free conditions in the presence of iron dental pulp cells maintained cobblestone morphology, identical to serum containing media formulation, as illustrated in Fig.3.31. using methylene blue staining in conjunction with passage 6 dental pulps derived stem cells as outlined in section 2.ix.

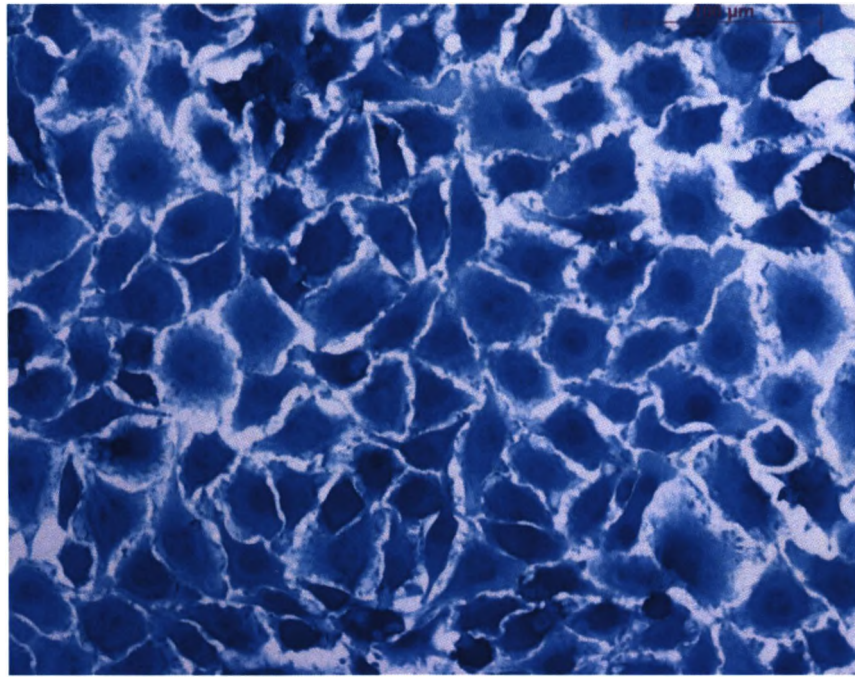


*Fig.3.31. Microscopic observation of methylene blue stained dental pulp derived stem cells cultured to confluence under serum free basal conditions*

Metabolic activity of dental pulp derived stem cells in conjunction with defined basal serum free media was quantified using the almar blue method (Fig.3.32.). These data demonstrated a trend similar to that observed with bone marrow-derived mesenchymal stem cells, an increase in metabolic activity up to confluence at day 7, after which contact inhibition resulted in a plateau (Fig.3.15).

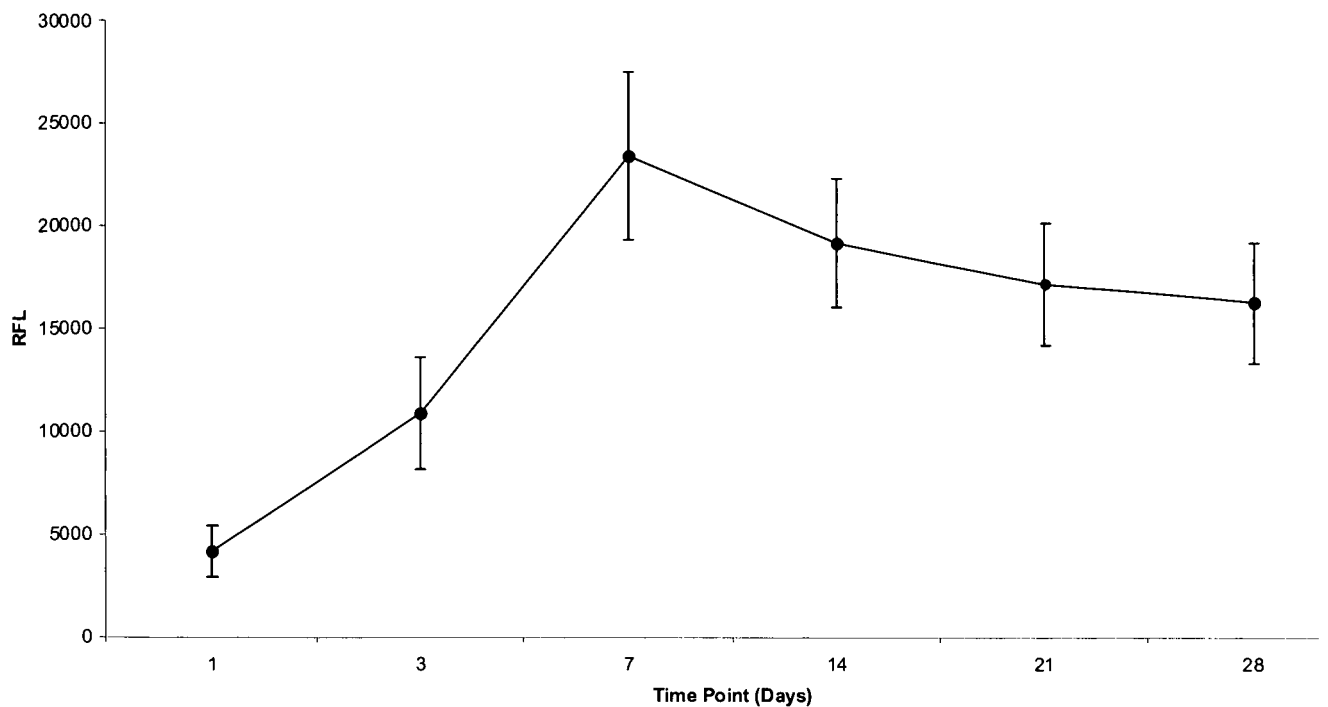


*Fig.3.32. Change in the metabolic activity of human dental pulp derived stem cells cultured in conjunction with basal serum free parameters using the Alamar blue method. Error bars represent 1 standard deviation from the mean, n=3. No correction for change in cell number was made*

In a similar manner to bone marrow derived mesenchymal stem cells it was concluded that dental pulp derived stem cells maintained their undifferentiated phenotype following observation of the stem cell markers STRO-1 and nucleostemin by immunohistochemistry (Fig.3.33A). Furthermore, in stem cells from this particular source it was also possible to observe proteins associated with an undifferentiated embryonic stem cell phenotype Oct-4, Sox2 and TRA-1-81 (Fig.3.33.). This therefore not only concludes the plasticity of the cells is maintained but also furthers the belief that these cells are considerably further removed from lineage commitment than their bone marrow derived counterparts.

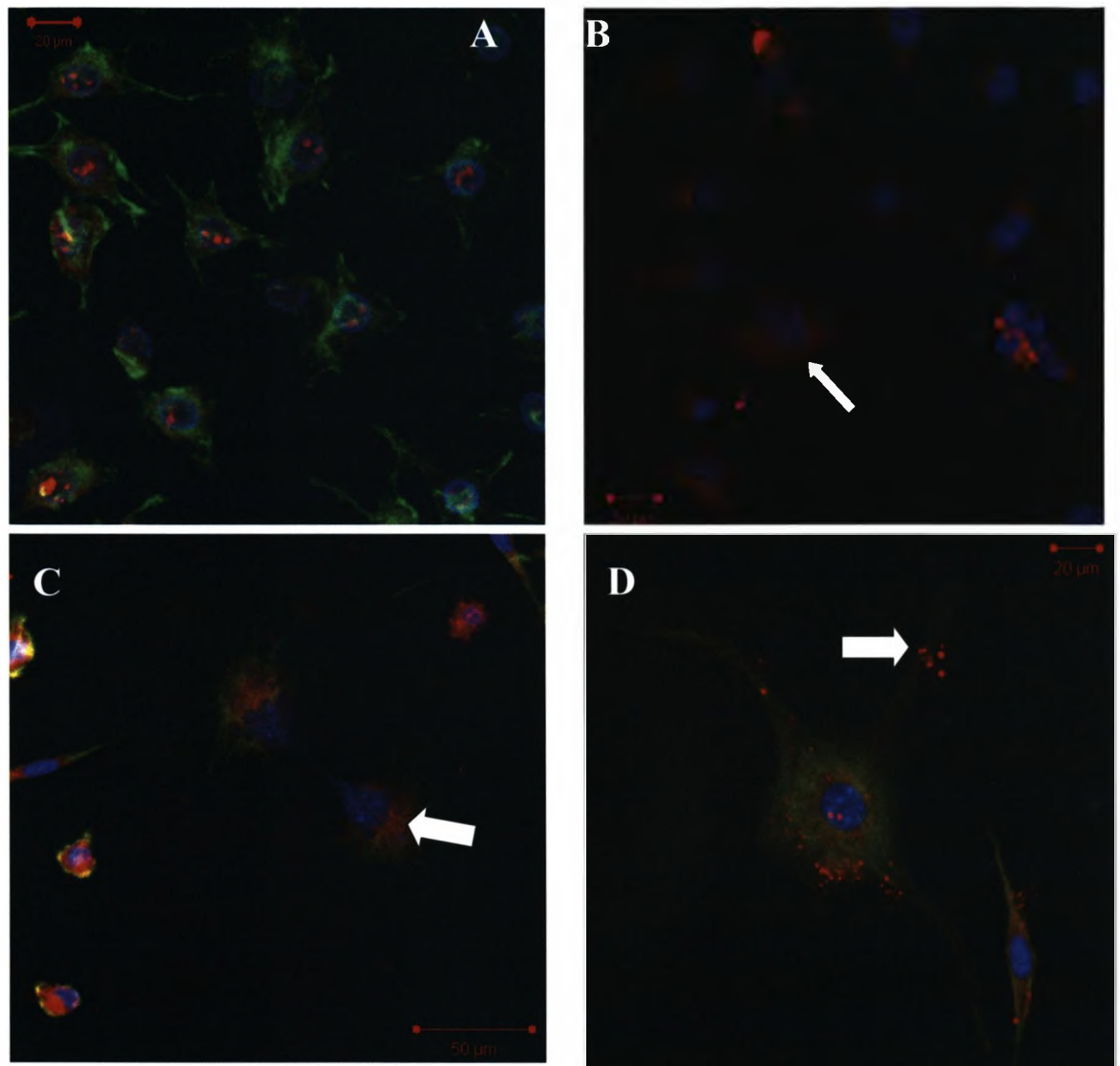


*Fig.3.33. Flourescent microscopic observation of immunohistochemical staining for A; Stro-1, Nucleostemin, Nuclei, B; TRA-1-81, F-Actin, C; Sox2, F-Actin, Nuclei and D; Oct-4, F-Actin, Nuclei after 21 days of defined serum free basal culture (positive staining illustrated by arrows)*

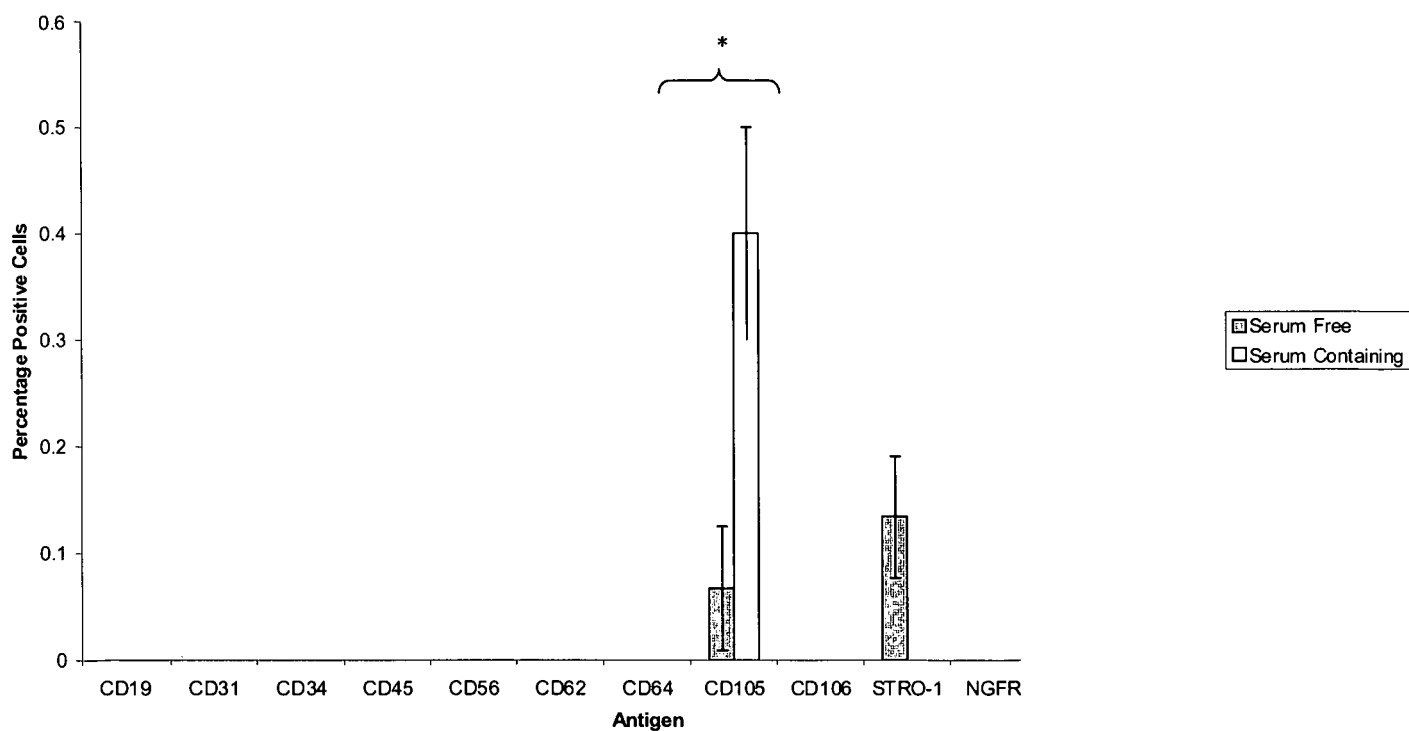
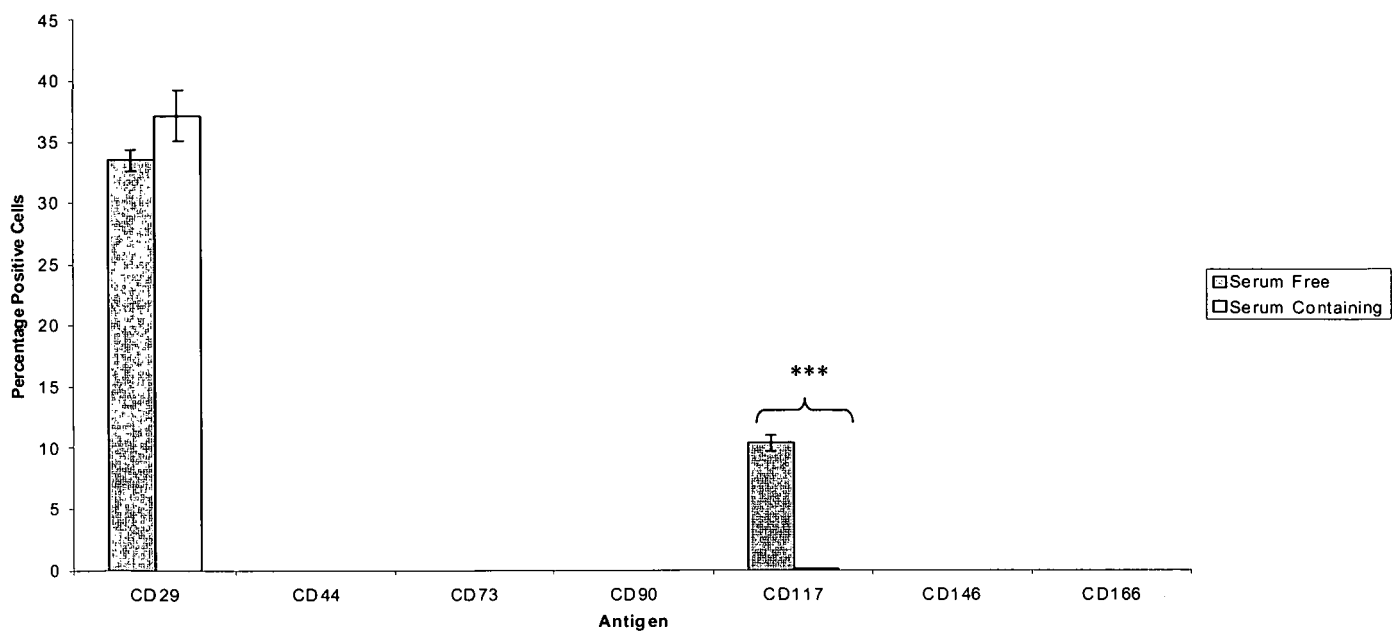


Fig.3.34. Comparison of a subset of cellular antigens of dental pulp derived stem cells cultured in serum free and serum containing (Cambrex MSCBM) media formulations at confluence, at passage 4, observed using flow cytometry. Error bars represent 1 standard deviation from the mean,  $n=3$ , \* $P<0.05$ , \*\* $P<0.01$ , \*\*\* $P<0.001$

Fig.3.34. demonstrates flow cytometric observations of an identical subset of cellular antigens to those used to characterise bone marrow derived mesenchymal stem cells to a minimum positive level of 0.1% (Figs.3.17.-3.22.). It is clear that dental pulp derived stem cells do not express many of the proteins commonly associated with 'stemness' such as CD90, CD44, CD90 and CD166 although expression of the stem cell associated CD29 is retained. STRO1 was also solely observed in these cells in conjunction with defined serum free media, expression of the mesenchymal stem cell antigen CD117 was found to be strongly significantly increased in serum free media. Additionally, given the limited amount of expression witnessed using the identical antigens used to characterise bone marrow derived mesenchymal stem cells, an additional adult stem cell marker was included, CD105, which demonstrated small amounts of expression which were found to be significant in serum containing media. Considering this data, it was not possible to conclude a superiority of either media at maintaining a stem phenotype due to the lack of expression of a subset of mesenchymal stem markers.



### 3.viii Defined Chondrogenic Differentiation of Dental Pulp Derived Stem Cells

Chondrogenic differentiation of dental pulp derived stem cells was carried out using an identical strategy to that used to differentiate bone marrow derived mesenchymal stem cells. Cells were seeded in a monolayer at a defined density of  $5.0 \times 10^4$  cells/cm<sup>2</sup>, in conjunction with the defined chondrogenic media formulation detailed in table 3.5. Cells were allowed to adhere under defined basal conditions for 24 hours before media was replaced with serum free differentiation media. Cells were cultured for 21 days with media refreshment occurring at day 7.

At defined time points throughout this culture period cells were lysed and the resulting RNA collected and reverse transcribed as described in section 2.vi. This provided a representation of the real time modulation of expression of a subset of chondrogenic associated genes by dental pulp derived stem cells throughout differentiation culture.

SOX9 is a transcription factor with a high mobility group (HMB) DNA binding domain and has a well documented early role in the initiation and control of chondrogenesis. SOX9 null knockout stem cells lack the capacity to differentiate along a chondrogenic lineage and additionally SOX9 binding has been demonstrated to activate chondrocyte specific enhancer elements involved in the transcription of the crucial chondrocyte protein, type II collagen [401,402].

Fig.3.35. illustrates the modulation of expression of SOX9 in dental pulp derived stem cells throughout chondrogenic culture normalised to the amount of the gene observed under basal culture. SOX9 is clearly observable throughout chondrogenic culture after day 3. The greatest increase of approximately  $1.0 \times 10^4$  fold occurred after 14 days. The presence of SOX9 confirmed populations of cells undergoing early stage chondrogenic differentiation at all time periods throughout chondrogenic culture.



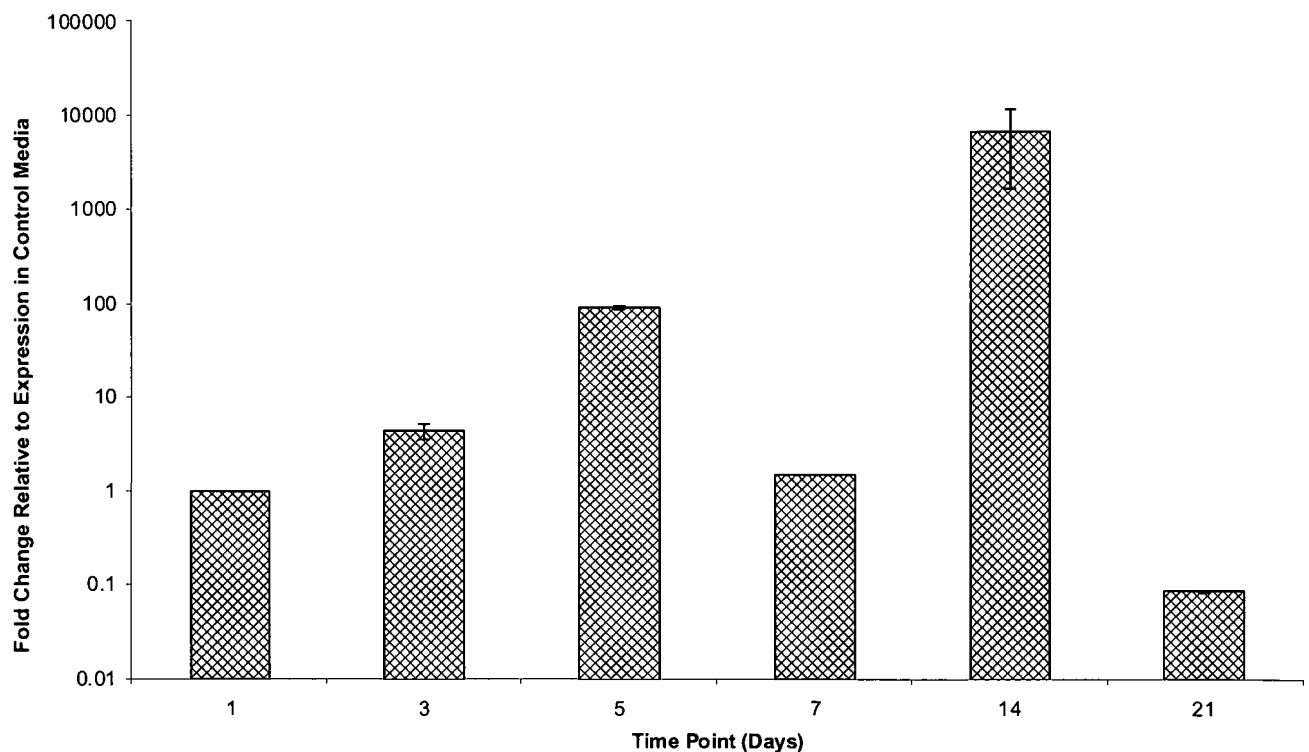
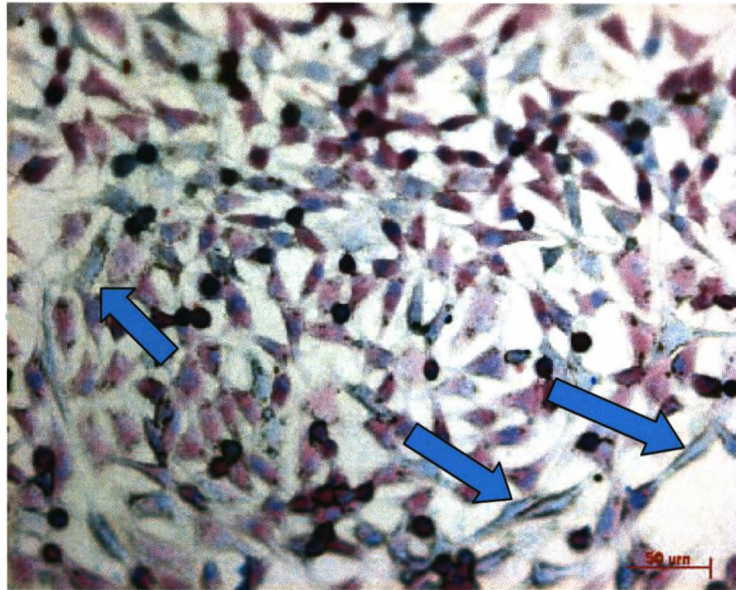


Fig.3.35. Real time-PCR observation of the change in expression of SOX9 relative to basal conditions at any specified time point as a result of chondrogenic stimuli. Error bars represent 1 standard deviation from the mean, n=6

One of the critical properties of a chondrocyte, which permits them to fulfill their role *in vivo*, is the elevated concentrations of glycosylated proteins on the cell surface. These proteoglycans are hydrophilic and as a result cause the attraction of large quantities of water molecules to the surface of the cell which makes them ideal for the lubrication of joints in their anatomical niche, cartilage [406].

Fig.3.36. Illustrates the presence of proteoglycans using the alcian blue method described in section 2.vii in dental pulp stem cells after 21 days of chondrogenic culture. Positive staining is clearly observed in the form of turquoise/blue cells, however it can be noted from this figure that not all cells within the population demonstrate positive staining, an indication of the heterogeneity of the original population of primary cells.



*Fig.3.36. Microscopic observation of Alcian blue stained dental pulp derived stem cells after 21 days of defined chondrogenic culture (positive blue staining indicated by arrows)*

One protein which forms a major constituent of the proteoglycan component of the chondrocyte extracellular matrix is aggrecan. Fig.3.37. shows real-time PCR analysis of aggrecan expression in dental pulp derived stem cells during defined chondrogenic culture. This data demonstrated a small increase in expression relative to basal after as little as 3 days of defined chondrogenic culture. However, 21 days of culture under chondrogenic stimuli results in almost 100 fold increase in the expression of this chondrocyte associated protein by dental pulp derived stem cells.

Fig.3.38. further confirms the presence of the aggrecan protein after 21 days of defined chondrogenic culture using immunohistochemistry. Images show aggrecan at days 3, 5 and 21. This confirms the presence of this protein throughout defined chondrogenic culture after the initial presence of RNA at day 3.

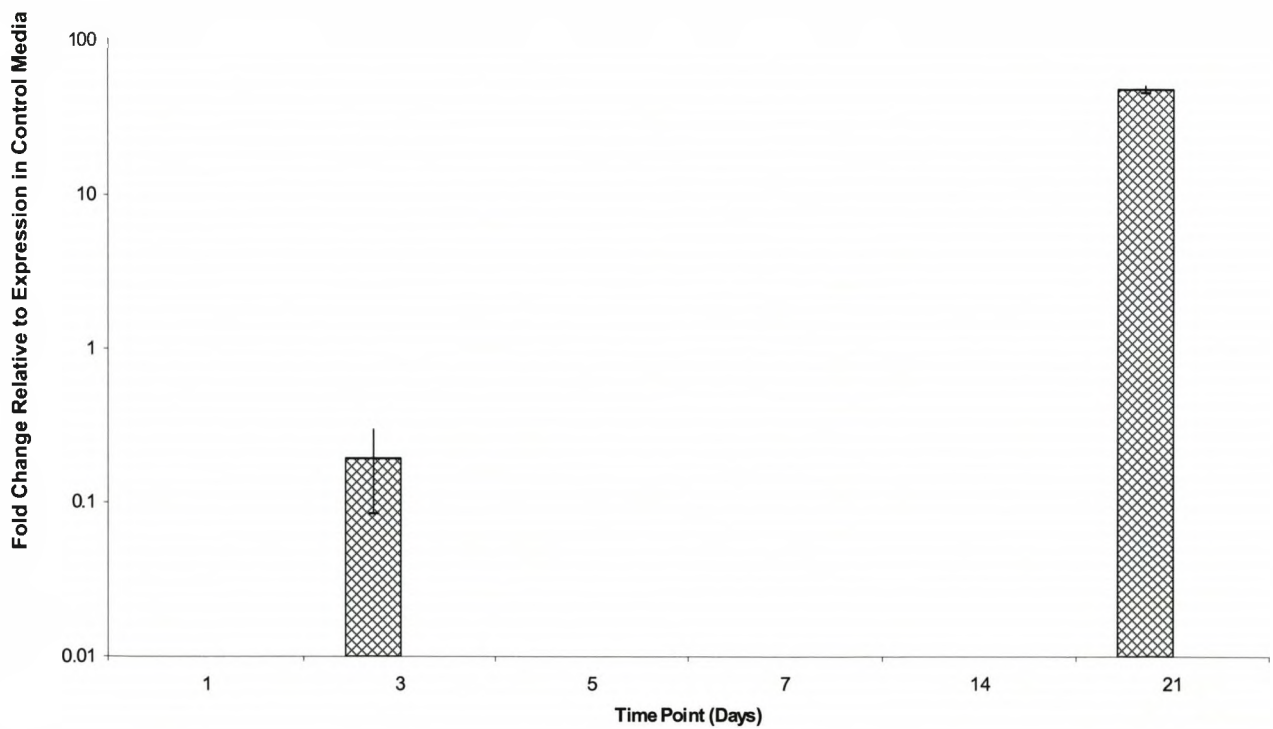


*Fig.3.37. Real time-PCR observation of the change in expression of Aggrecan relative to basal conditions at any specified time point as a result of subjection to chondrogenic stimuli. Error bars represent 1 standard deviation from the mean, n=6*

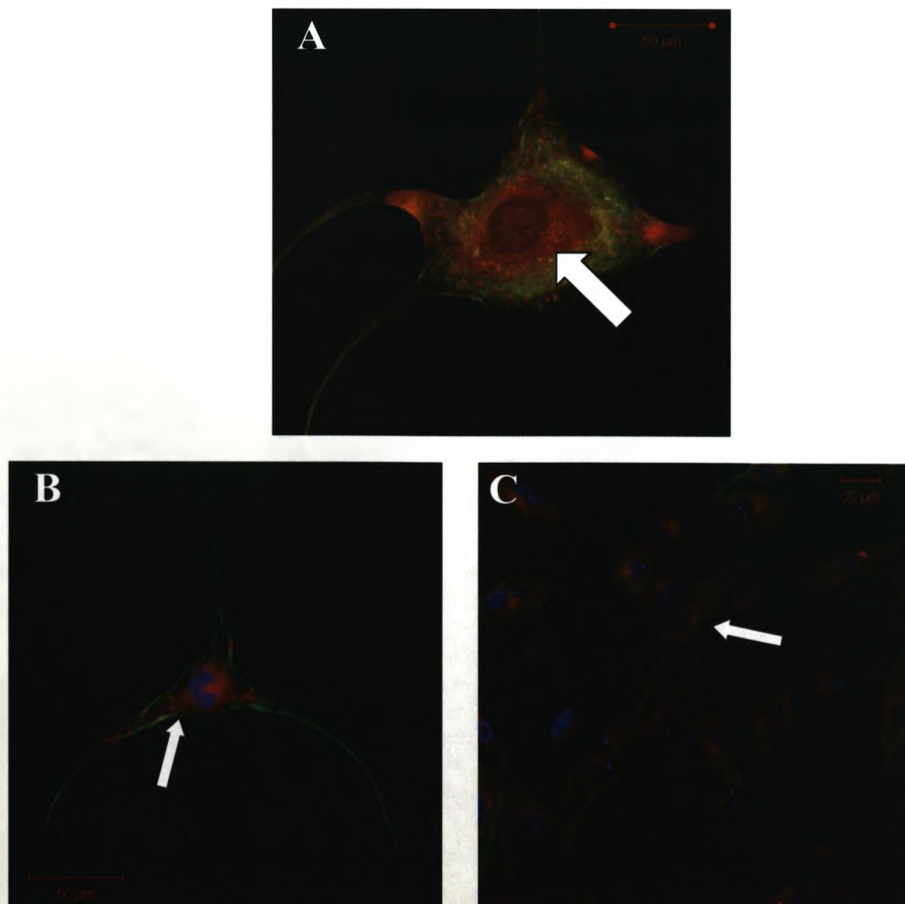


*Fig.3.38. Fluorescent microscopic observation of immunohistochemical staining for Aggrecan in dental pulp derived stem cells during chondrogenic culture after A; 21 days, B; 3 days and C; 5 days (Aggrecan, F-Actin, Nuclei)*

Terminal articular chondrogenesis was characterised by observation of type II collagen, which in a terminally differentiated chondrocyte forms 50% of total extracellular matrix protein, and 70-80% of total collagen [407]. Fig.3.39. shows real time-PCR analysis of collagen II expression showing increases in expression above basal level at day 5. Furthermore, immunohistochemical observation demonstrated the presence of collagen II and the absence of collagen I after 21 days of defined chondrogenic culture (Fig.3.40.).

Further conformation of the transformation of the dental pulp derived stem cells into a chondrogenic phenotype was identification of the presence of chondroadherin (3.41.). This protein associates with collagen II in the chondrocyte extracellular matrix at defined loci of the collagen II molecule. It is hypothesised that this association has a role in matrix stabilisation but also in chondrocyte growth and proliferation. Large scale increases in expression of this protein relative to basal were observed at days 5, 7 and 14 with expression still evident although reduced at day 21.

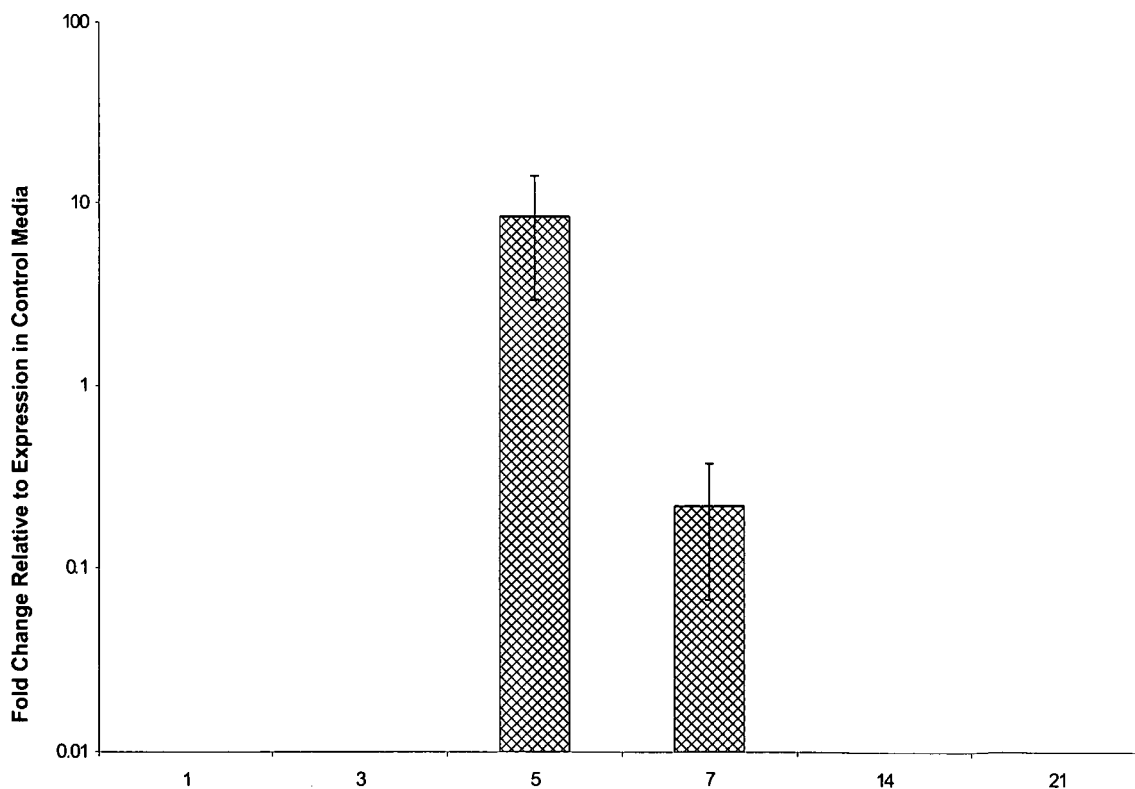


*Fig.3.39. Real time-PCR observation of the change in expression of Collagen II relative to basal conditions at any specified time point as a result of subsection to chondrogenic stimuli. Error bars represent 1 standard deviation from the mean, n=6*



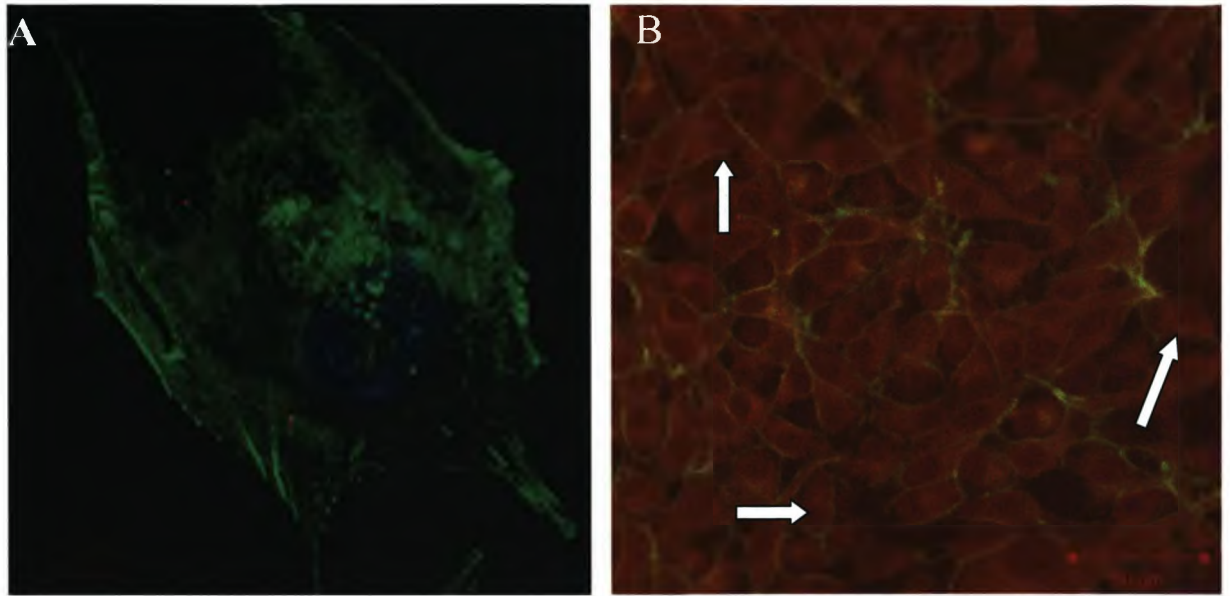


Fig.3.40. Fluorescent microscopic observation of immunohistochemical staining for **A**; Collagen I, F-Actin, Nuclei and **B**; Collagen II, F-Actin, Nuclei after 21 days of chondrogenic

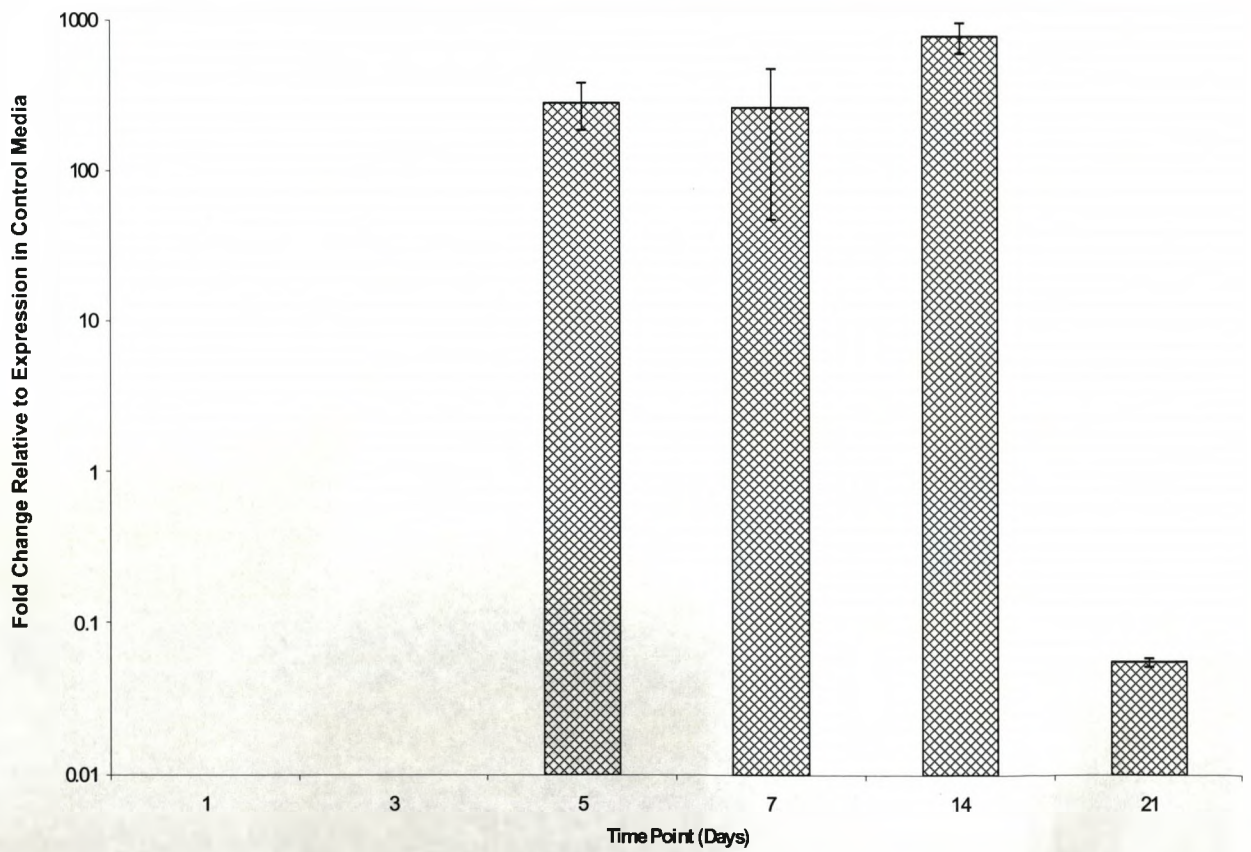


Fig.3.41. Real time-PCR observation of the change in expression of Chondroadherin relative to basal conditions at any specified time point as a result of subjection to chondrogenic stimuli. Error bars represent 1 standard deviation from the mean, n=6

Chondrogenic differentiation was further confirmed by scanning electron microscopic analysis of a rounded, ball like morphology in these cells, a morphology associated with functional articular chondrocytes, illustrated after 21 days, in Fig.3.42.

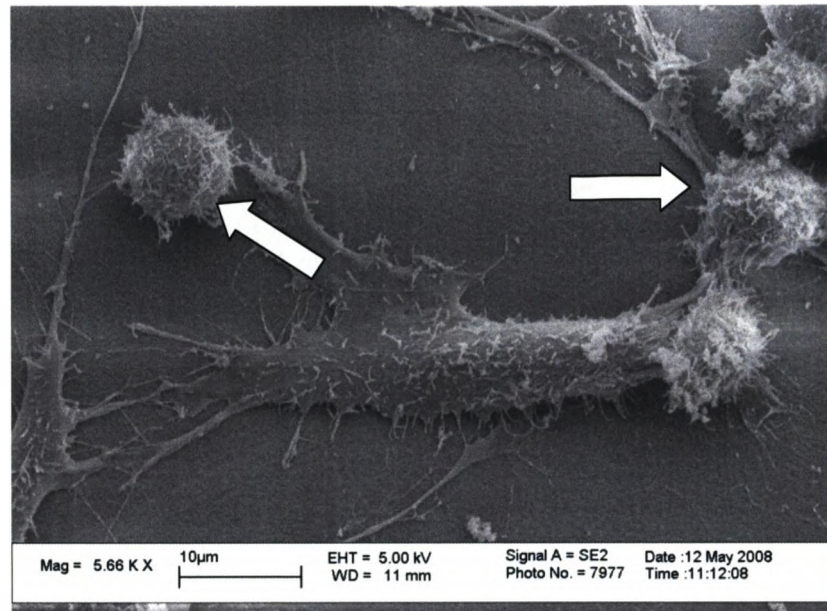


Fig.3.42. Scanning electron microscopic analysis of dental pulp derived stem cells after 21 days of defined chondrogenic culture (indicated by arrows)

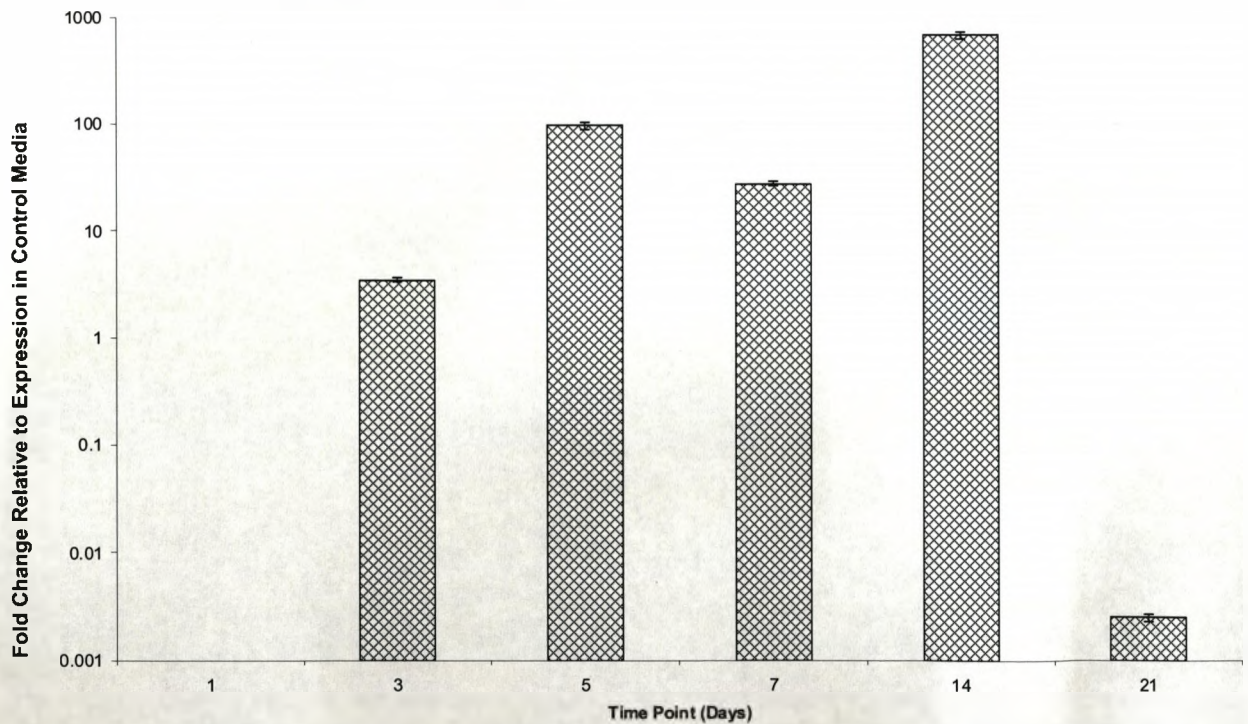
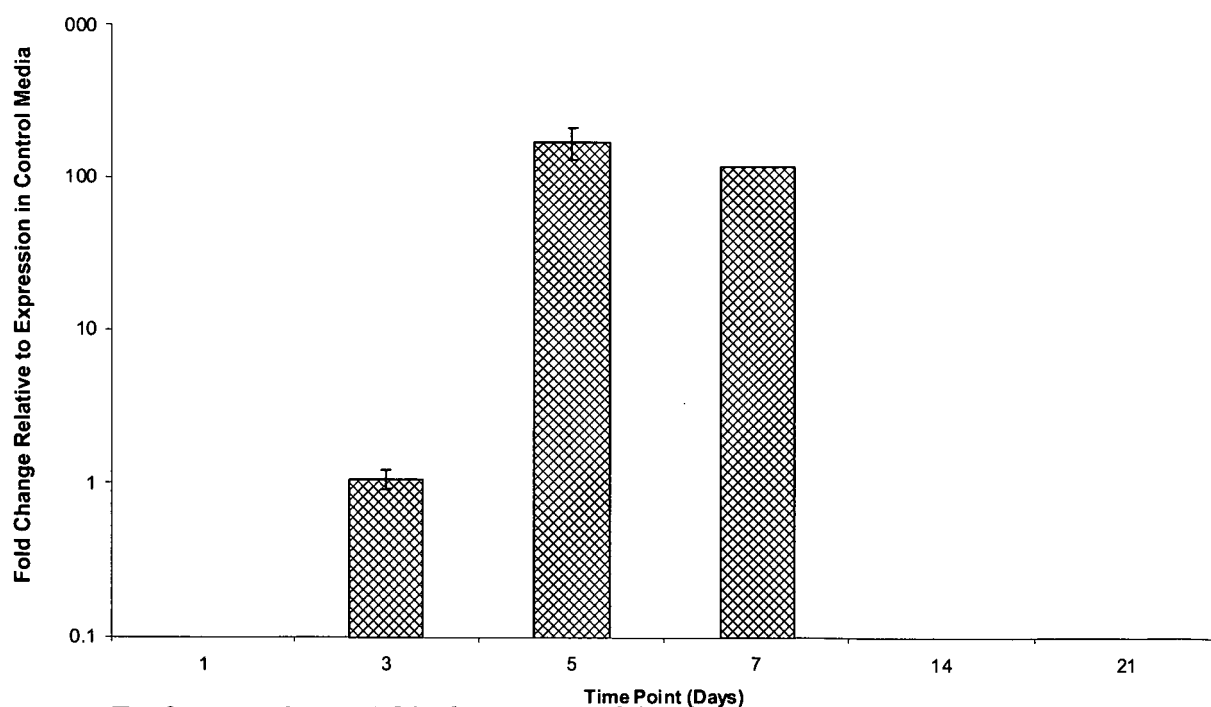


Fig.3.43. Real time-PCR observation of the change in expression of CBFA1/RUNX2 relative to basal conditions at any specified time point as a result of subjecting to chondrogenic stimuli. Error bars represent 1 standard deviation from the mean, n=6

Real time-PCR characterisation of cells under chondrogenic stimulation also demonstrated modulation in the expression of CBFA1/RUNX2 (Fig.3.43.). Although this gene is commonly regarded as a marker of osteogenesis it has been observed in cells of a chondrogenic lineage with a tendency to terminate in hypertrophic rather than articular cartilage, therefore mimicking the total cartilage niche in which, as hypoxia decreases as the cells encroach towards bone, the properties of the cells change in order to compensate for the differing mechanical and physical strains [404].

An increase in the bone-associated gene osteopontin was also observed during chondrogenic culture (Fig.3.44.). In a similar manner to CBFA1/RUNX2 this gene is also associated with hypertrophic cartilage and additionally preosteoblast cells, further suggesting a heterogenic differentiation into both articular and hypertrophic chondrocytes or possibly the progression of the chondrocytes through a series of osteochondral intermediate phenotypes into osteoblasts [408].



*Fig.3.44. Real time-PCR observation of the change in expression of Osteopontin relative to basal conditions at any specified time point as a result of subjection to chondrogenic stimuli. Error bars represent 1 standard deviation from the mean, n=6*



Further confirmation of a progression to an osteoblastic phenotype was concluded by observation of a large increase in expression of osteonectin after 14 days of chondrogenic culture (Fig.3.45.). This protein is an extracellular matrix component with an affinity for calcium which as a result plays a role in calcification and bone mineralization [409]. This, therefore concludes the presence of a functional osteogenic population of dental pulp stem cells derived under defined chondrogenic culture conditions.

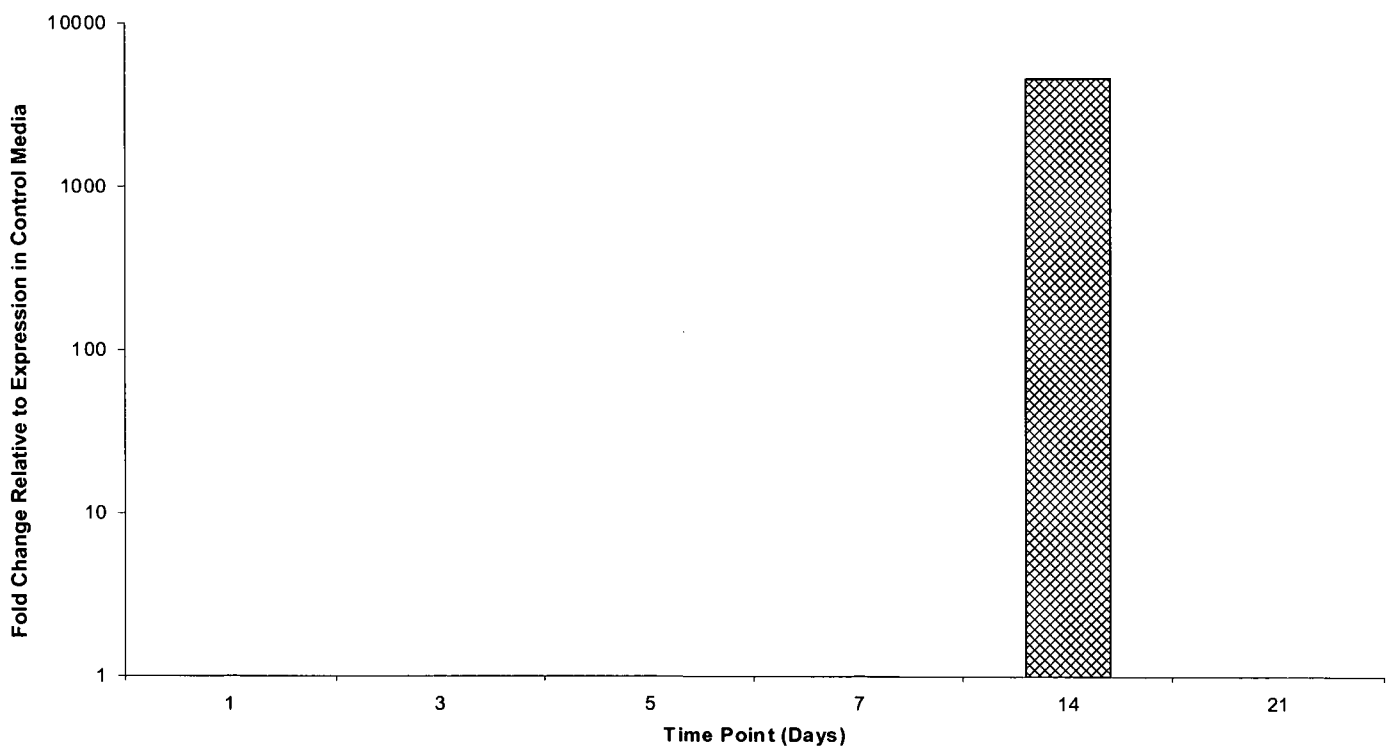


*Fig.3.45. Real time-PCR observation of the change in expression of Osteonectin relative to basal conditions at any specified time point as a result of subjection to chondrogenic stimuli. Error bars represent 1 standard deviation from the mean, n=6*

It was possible to conclude that defined serum-free chondrogenic culture conditions permitted the differentiation of dental pulp derived stem cells down a terminal chondrogenic lineage. Additionally, it was also possible to prove the presence of an ossifying population of cells formed during chondrogenic culture. This could have been a representation of the heterogeneity of the original primary population of cells, thus demonstrating a subset more predisposed to osteogenesis rather than



chondrogenesis. However, these finding could also represent the non-termination of chondrogenesis at the point of articular chondrocyte derivation, forming ossifying cells through an osteochondral hypertrophic intermediate.

### 3.ix Defined Osteogenic Differentiation of Dental Pulp Derived Stem Cells

Osteogenic differentiation of dental pulp derived stem cells was carried out using an identical strategy to that used to stimulate chondrogenic differentiation in conjunction with the defined osteogenic parameters detailed in table.3.5. Cells were seeded in a monolayer at a defined density of  $5.0 \times 10^4$  cells/cm<sup>2</sup>, allowed to adhere under defined basal conditions for 24 hours before media was replaced with defined serum free differentiation media. Cells were cultured for 21 days with media changes refreshment occurring at day 7.

Initiation of osteogenesis by means of the transcription factor CBFA1/RUNX2, widely accepted as the osteogenic master gene was observed in dental pulp derived stem cells under defined osteogenic culture parameters at day 5 using real time-PCR analysis [404]. This gene was then found to be present at levels higher than those observed in basal media for a further 11 days of culture (Fig.3.46.).

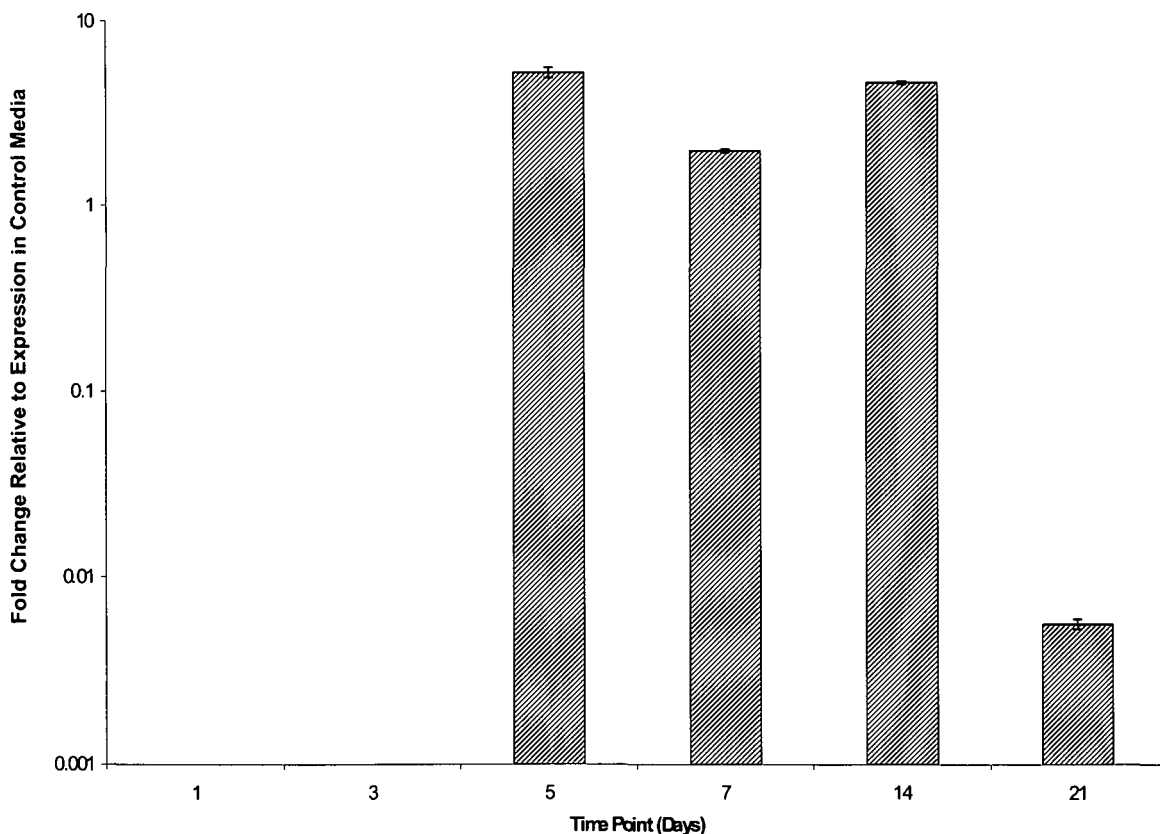


*Fig.3.46. Real time-PCR observation of the change in expression of CBFA1/RUNX2 relative to basal conditions at any specified time point as a result of subjection to osteogenic stimuli. Error bars represent 1 standard deviation from the mean, n=6*

Further characterisation of the presence of CBFA1/RUNX2 induced in these cells using defined osteogenic culture conditions was performed using immunohistochemistry, shown in Fig.3.47, day 21 post induction.

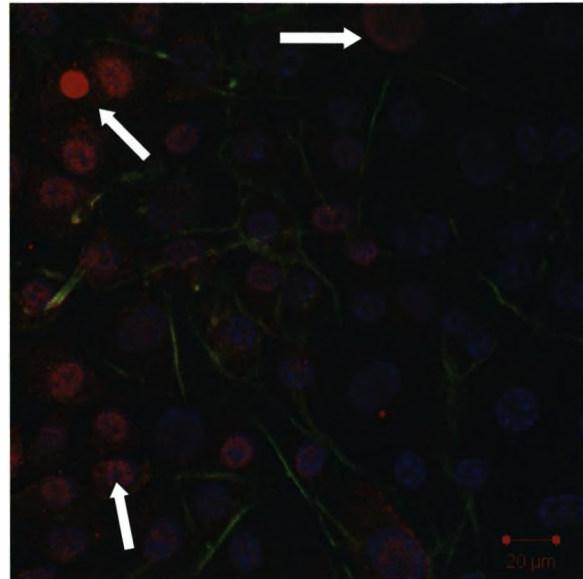


*Fig.3.47. Fluorescent microscopic observation of immunohistochemical staining for **CBFA1/RUNX2**, **F-Actin** and **Nuclei** after 21 days of osteogenic culture (positive staining indicated by arrows)*

A further critical transcription factor which acts downstream of CBFA1/RUNX2 is osterix, a zinc finger containing transcription factor, with a rate limiting role in bone formation and skeletogenesis [330, 404]. Fig.3.48. demonstrates that a slight increase in the expression of osterix was observed as rapidly as 24 hours post induction. However a large increase in the expression of this molecule is detectable at day 14, in excess of  $1.0 \times 10^4$  fold over basal levels as a result of defined osteogenic induction parameters. Further to earlier data suggesting the ossification of dental pulp derived stem cells as a result of chondrogenic stimuli, it was noted that osterix was undetectable throughout the chondrogenic culture period [403]. Further to these data, osteopontin, a mid marker of osteogenesis was observed throughout osteogenic culture until day 7, with the greatest increase in expression of almost 1000 fold occurring after 24 hours (Fig.3.49.) [408].

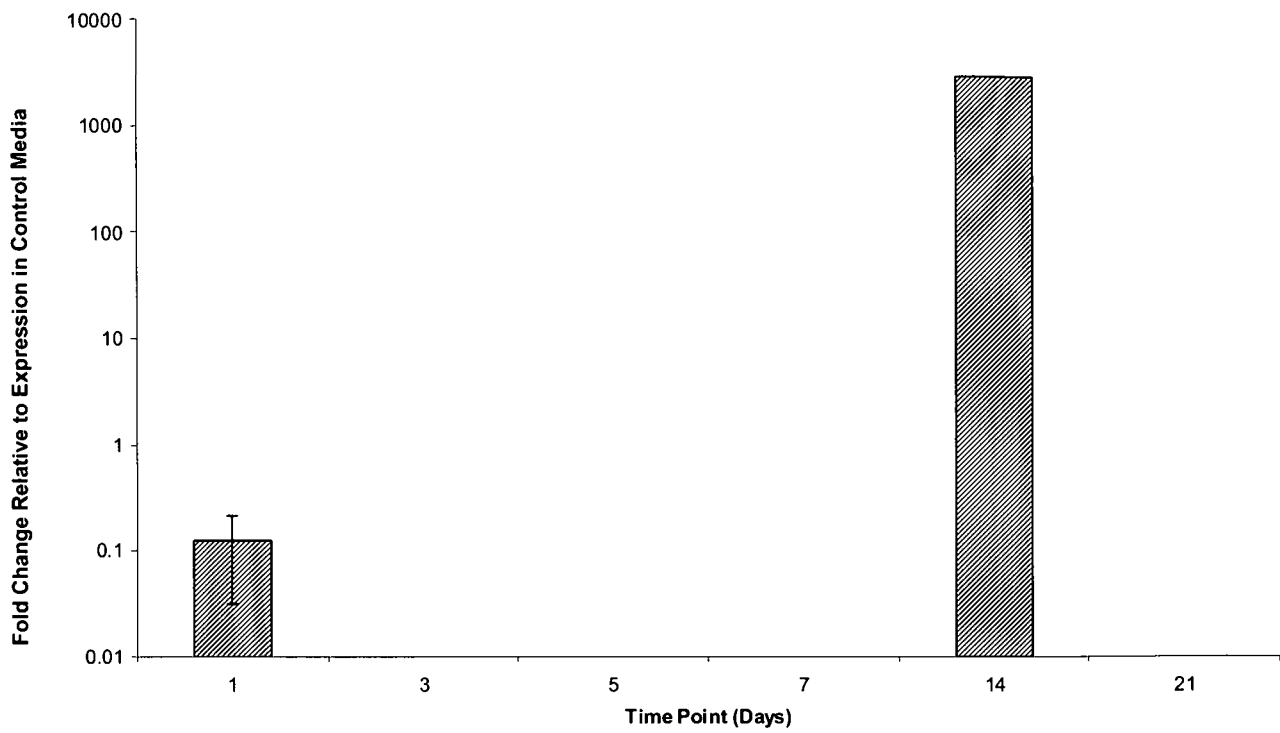


Fig.3.48. Real time-PCR observation of the change in expression of osterix relative to basal conditions at any specified time point as a result of subjection to osteogenic stimuli. Error bars represent 1 standard deviation from the mean, n=6

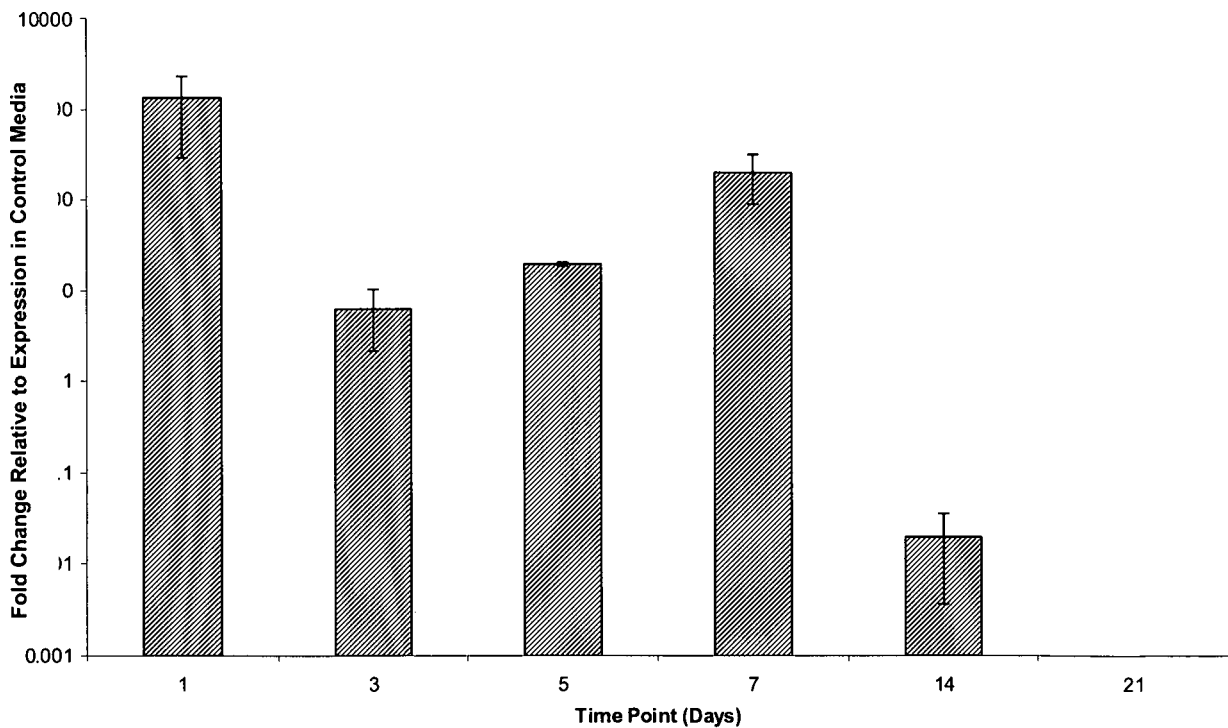
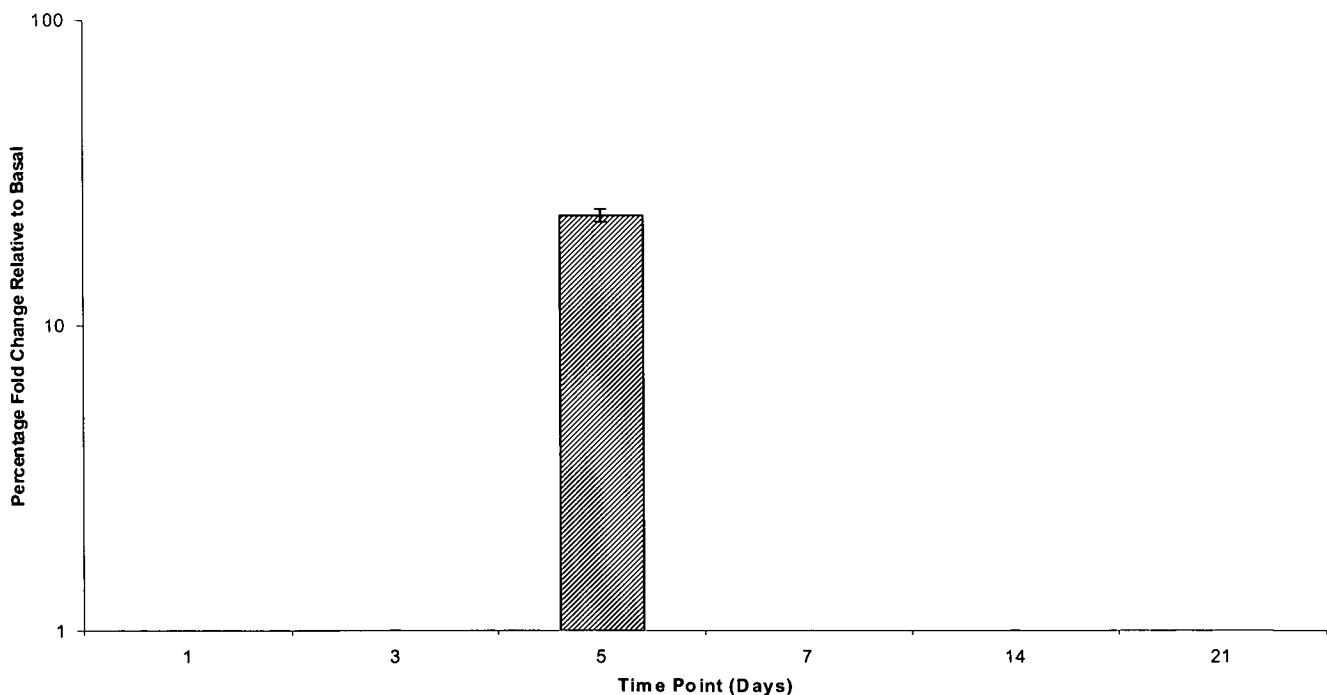


Fig.3.49. Real time-PCR observation of the change in expression of Osteopontin relative to basal conditions at any specified time point as a result of subjection to osteogenic stimuli. Error bars represent 1 standard deviation from the mean, n=6

An increase in osteonectin expression was observed at day 5 post induction (Fig.3.50.), demonstrating the cumulation of the dental pulp derived stem cells to terminal functional osteogenesis given the critical role of this protein in matrix mineralization [409]. This was further confirmed by the observation of osteocalcin, a second extracellular matrix protein with functions involving calcium ion binding and subsequent matrix mineralisation using immunohistochemistry [405]. Fig.3.51. illustrates the presence of osteocalcin in dental pulp derived stem cells after 21 days of defined osteogenic culture.



*Fig.3.50. Real time-PCR observation of the change in expression of Osteonectin relative to basal conditions as a result of subjection to osteogenic stimuli. Error bars represent 1 standard deviation from the mean, n=6*

Conventional histology using Von Kossa staining as detailed in section 2.viii further confirmed the presence of calcification of these cells, shown in Fig.3.52, after 21 days. Positive staining is indicated by brown nodules throughout the monolayer of cells.

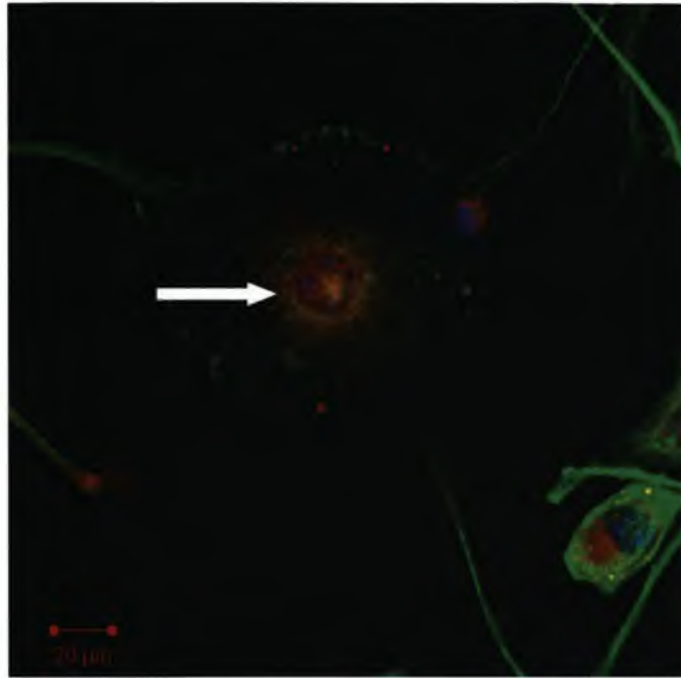


*Fig.3.51. Fluorescent microscopic observation of immunohistochemical staining for **Osteocalcin**, **F-Actin** and **Nuclei** after 21 days of osteogenic culture (positive staining illustrated by arrow)*

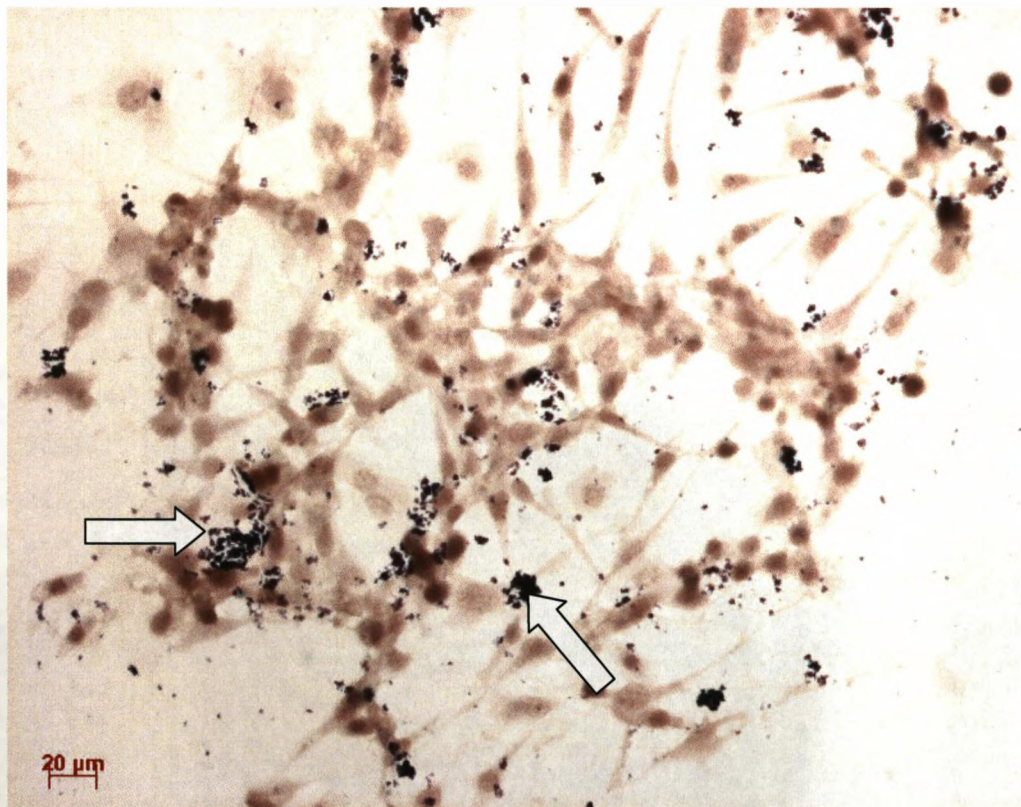


*Fig.3.52. Microscopic observation of Von Kossa stained dental pulp derived stem cells after 21 days of defined osteogenic culture (positive staining illustrated by arrows)*

In a similar manner to chondrogenic differentiation stimulation, there was evidence to suggest hypertrophy was occurring during osteogenic culture. Small increases in SOX9, the transcription factor involved in chondrocyte differentiation, were observed between days 3 and 14 of osteogenic differentiation culture (Fig.3.53) [401, 402].

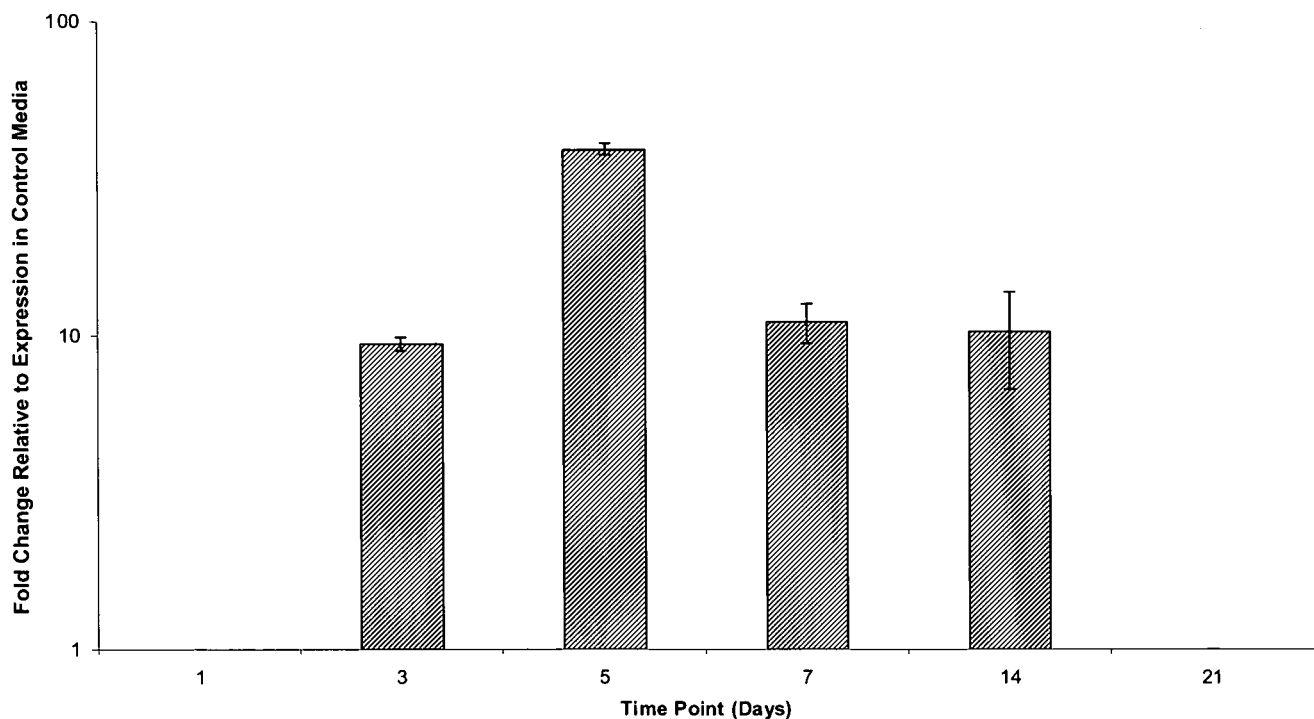


*Fig.3.53. Real time-PCR observation of the change in expression of SOX9 relative to basal conditions at any specified time point as a result of subjection to osteogenic stimuli. Error bars represent 1 standard deviation from the mean, n=6*

Furthermore, type X collagen was observed immunohistochemically in dental pulp derived stem cells after 21 days of osteogenic culture (Fig.3.55.). This extracellular matrix component is specific to hypertrophic cartilage further confirming the presence of a small subset of chondrocyte forming cells under these stimuli from the heterogenic population of dental pulp derived stem cells [410].



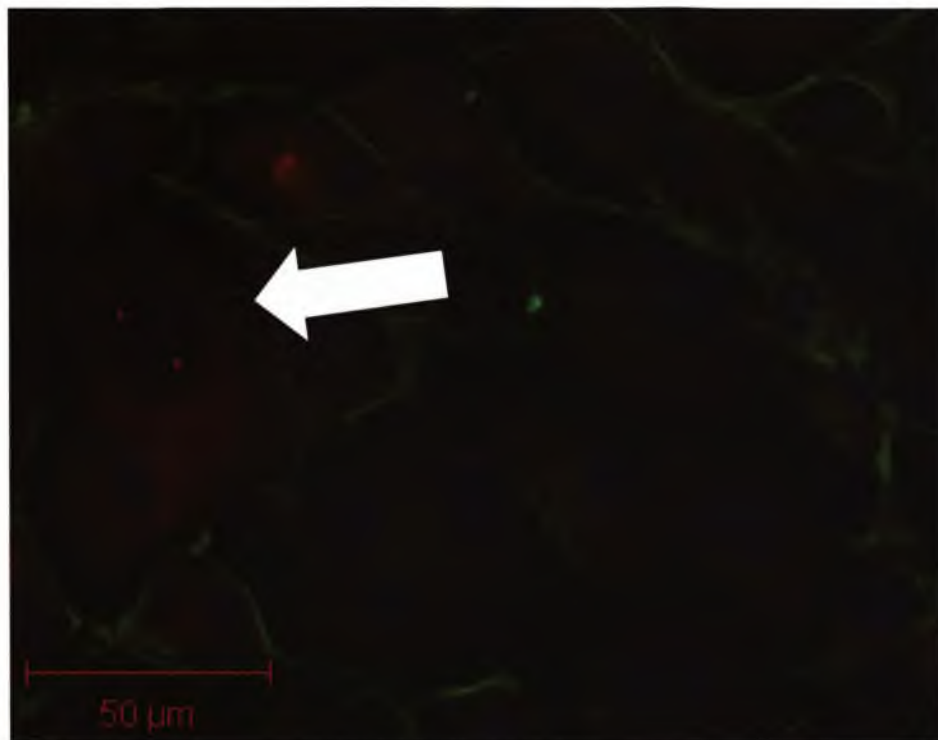


*Fig.3.55. Fluorescent microscopic observation of immunohistochemical staining for **Collagen X**, **F-Actin** and **Nuclei** after 21 days of osteogenic culture (positive staining indicated by arrow)*

Using defined serum free osteogenic media it was possible to differentiate primary dental pulp derived stem cells into osteoblasts during a differentiation culture period of 21 days.

Osteogenesis occurred rapidly with an increase in expression of osteogenic transcription factors detectable as early as 24 hours post induction. Terminal osteogenesis and subsequent osteoblast function was characterised by the presence of osteonectin, an osteoblast extracellular matrix protein responsible for matrix mineralisation and subsequent resulting ossification. Furthermore physical calcification was characterised histologically, 21 days post induction.

In a similar manner to chondrogenic stimulation, it was evident that osteogenic differentiation was not homogeneous with the presence of several proteins which would suggest an osteochondral overlap of cellular fate preference of the dental pulp derived stem cells during differentiation under these conditions. Although increase in expression of SOX9 and



Aggrecan were observed, at no point during osteogenic culture were chondroadherin or type II collagen found to be present. Increases in chondrogenic markers under osteogenic conditions were considerably smaller than those in osteogenic associated proteins under chondrogenic stimulation, therefore suggesting a more homogeneous differentiation of these cells was possible under osteogenic stimuli, possibly suggesting a predisposition of stem cells from this source towards an osteoblastic lineage.

### 3.x Defined Adipogenic Differentiation of Dental Pulp Derived Stem Cells

To complete the demonstration that defined serum-free media could stimulate trilineage differentiation of primary human dental pulp derived stem cells, adipogenic differentiation was carried out using the serum free defined adipogenic media formulation stated in table 3.5. Cells were seeded in a monolayer at a defined density of  $5.0 \times 10^4$  cells/cm<sup>2</sup>, allowed to adhere under defined basal conditions for 24 hours before media was replaced with defined serum free differentiation media. Cells were cultured for 21 days with media refreshment occurring at day 7.

Initiation of adipogenesis was characterised by observation of a slight increase in the expression of the receptor complex PPAR $\gamma$ 2. PPAR $\gamma$ 2 forms a part of the peroxisome proliferator activated receptor family, which upon activation by its ligand (a prostaglandin), homodimerises with the retinoid X receptor (RXR) to form a transcription factor complex capable of binding DNA and promoting transcription of defined genes involved in the regulation of adipocyte development [411]. Confirmation of PPAR $\gamma$ 2 presence was confirmed using immunohistochemistry on dental pulp derived stem cells taken from day 21 post adipogenic initiation (Fig.3.56.).

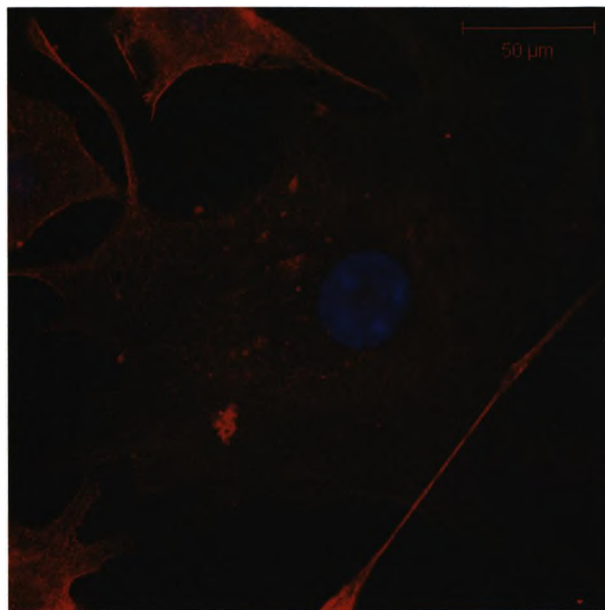


Fig.3.56. Fluorescent microscopic observation of immunohistochemical staining for *PPAR-Gamma*, and Nuclei after 21 days of adipogenic culture

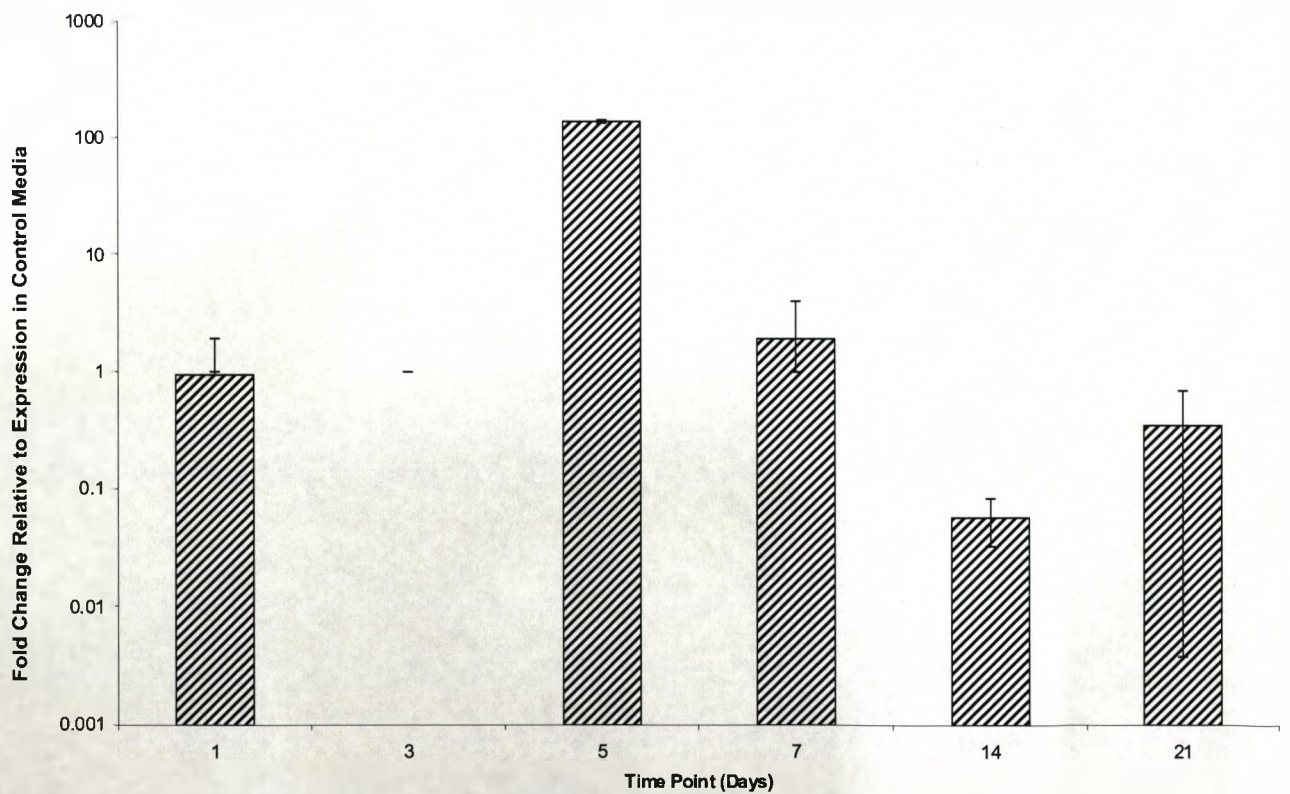
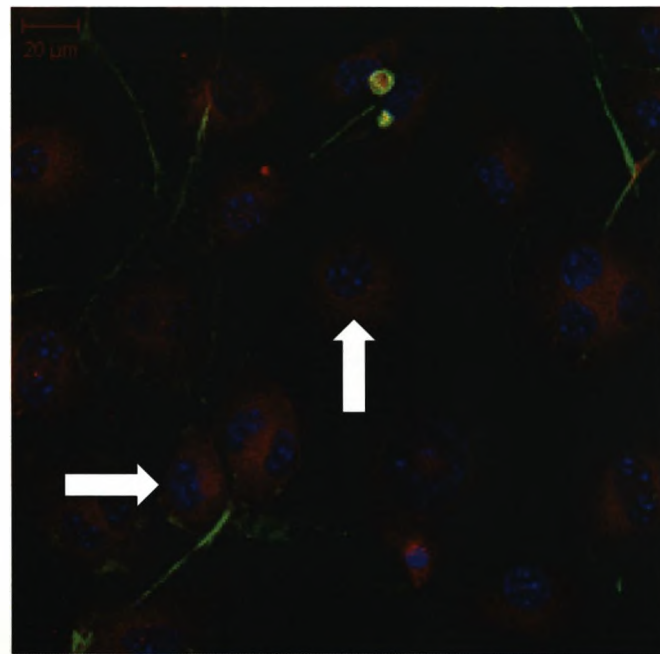


Fig.3.57. Real time-PCR observation of the change in expression of *Adiponectin* relative to basal condition at any specified time point as a result of subjection to adipogenic stimuli. Error bars represent 1 standard deviation from the mean,  $n=6$

Adiponectin is commonly associated with preadipose however, despite its expression in these cells it is an abundant transcript in terminal adipose tissue. Adiponectin was identified at an increase relative to basal levels of in excess of 100 fold 5 days post adipogenic initiation (Fig.3.57). *In vivo* this hormone is secreted by adipose tissues and has regulatory roles in glucose and lipid metabolism, its presence demonstrating the functionality of the differentiating cells [412]. The presence of this molecule was further demonstrated using immunohistochemistry, illustrated in Fig.3.58, at 7 days post induction.



*Fig.3.58. Fluorescent microscopic observation of immunohistochemical staining for Adiponectin, F-Actin and Nuclei after 7 days of adipogenic culture (positive staining illustrated by arrows)*

A further significant bioactive secreted product of adipocyte cells is leptin. Leptin is a crucial hormone *in vivo* which is involved in dietary modulation through appetite regulation. Leptin works through interaction with leptin receptors located in the hypothalamus of the brain. Its binding stimulates inhibition of the activity of neurons which contain the neurotransmitter; neuropeptide Y, a key element in the regulation of appetite [413]. Mutations to the leptin gene are commonly associated with

obesity through lack of efficacy of the molecule at its receptor and subsequent dietary deregulation [413]. Leptin was observed immunohistochemically in dental pulp derived stem cells subjected to defined adipogenic culture conditions at 21 days post induction, shown in Fig.3.59.

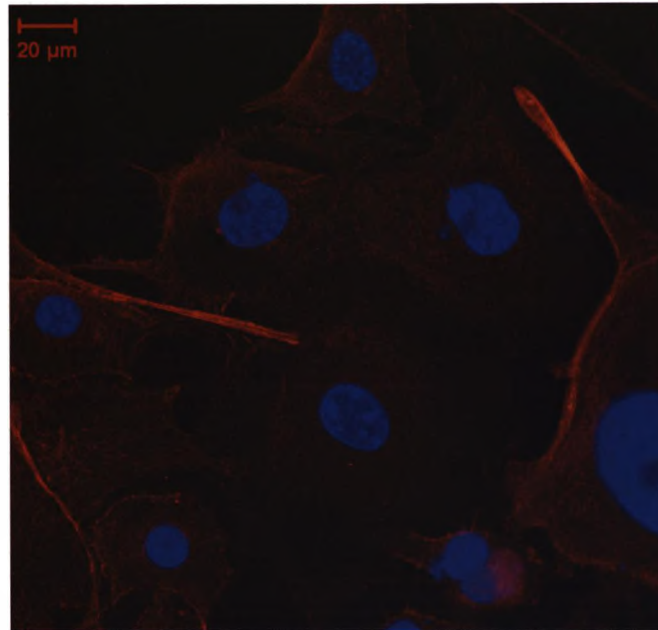


*Fig.3.59. Fluorescent microscopic observation of immunohistochemical staining for **Leptin** and **Nuclei** after 21 days of adipogenic culture*

Perilipin was also observed immunohistochemically in dental pulp derived stem cells under adipogenic stimuli after 21 days of culture (Fig.3.60.). This protein appeared diffuse throughout the cytoplasm of the cells under adipogenic stimuli. Perilipin is exclusively expressed in adipocyte cells and has the function of encapsulating lipid vesicles within the cell body thus preventing their digestion by lipase enzymes present natively in the cytoplasm [414].

Further confirmation of adipose vesicle incorporation in the cytoplasm of the cells was acknowledged using conventional Oil Red O staining as outlined in section 2.vi. Fig.3.61. illustrates the initial presence of lipid



capsules after 7 days of culture and additionally the extensive lipid vacuole present throughout the population of cells by 14 days post initiation [415].

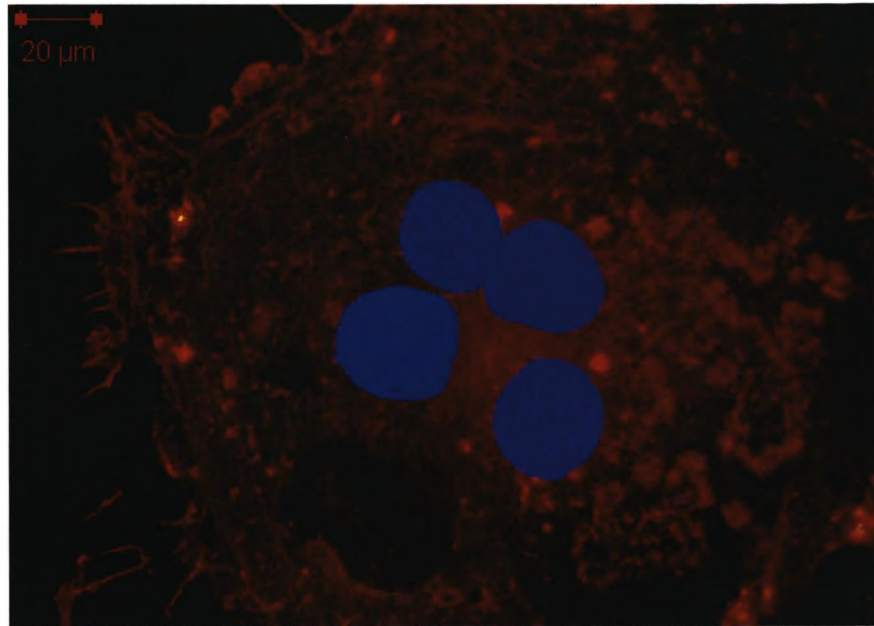


*Fig.3.60. Fluorescent microscopic observation of immunohistochemical staining for **Perilipin** and Nuclei after 21 days of adipogenic culture*

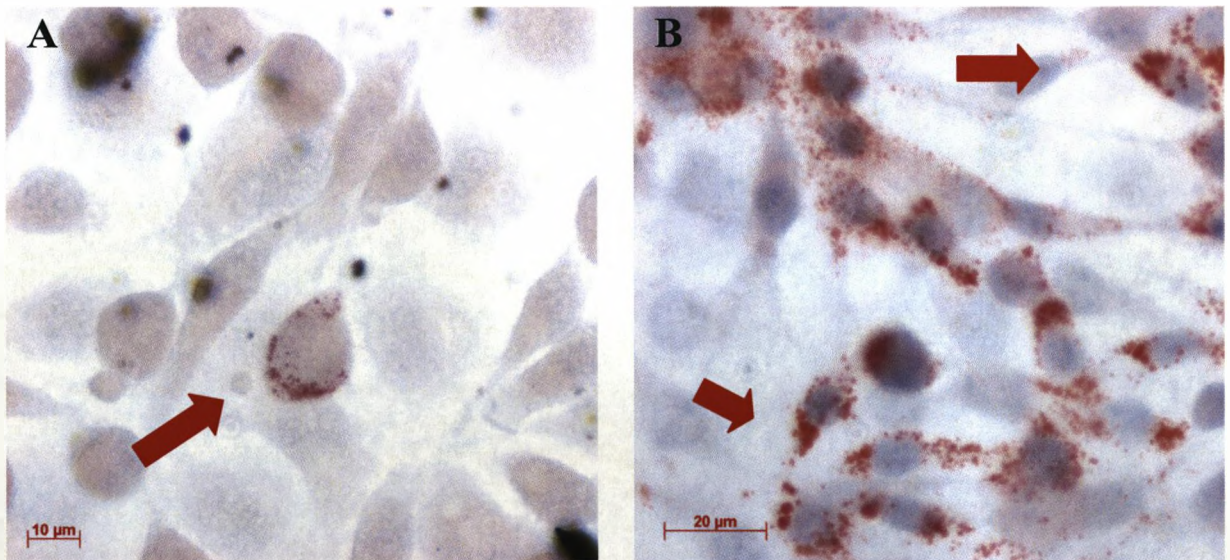


*Fig.3.61. Microscopic observation of dental pulp derived stem cells under defined adipogenic stimuli subjected to Oil Red O and haematoxylin staining after **A**; 7 days and **B**; 14 days (positive staining illustrated by arrows)*

After 14 days of adipogenic culture lipid vesicles were observable using light microscopy without the aid of additional histological staining, illustrated in Fig.3.62.

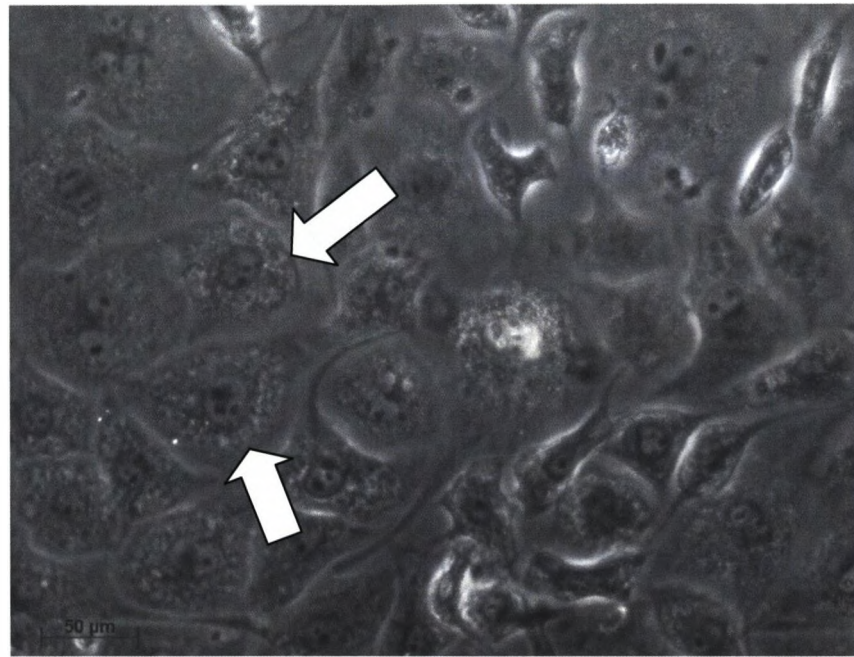


*Fig.3.62. Light microscopic observation of the granularity of dental pulp derived stem cells after 14 days of adipogenic culture due to lipid droplet encapsulation (examples given using arrows)*

It was possible to conclude that defined serum free adipogenic differentiation parameters were capable of differentiating dental pulp derived stem cells into lineage committed adipocytes after a culture period of 14 days.

These cells expressed several proteins associated with an adipogenic phenotype including a subset intimately associated with the regulatory and homeostatic role of adipose tissue *in vivo*, confirming the functionality of these *in vitro* derived adipose cells.

The final confirmation of adipogenic phenotype was the presence of lipid vacuoles within the cell body, a morphological feature exclusive to adipocytes, additionally confirmed by the presence of perilipin, a protein

associated with the formation and maintenance of these cytoplasmic structures.

### 3.xi Defined Neural Differentiation of Dental Pulp Derived Stem Cells

Transgermal differentiation was demonstrated using the defined serum free neural media shown in table 3.5 Dental pulp derived stem cells were an excellent candidate for this given the proximity of these cells to the neural crest during embryogenesis. It was sensible to hypothesise that dental pulp derived stem cells would be more likely to undergo neurogenesis than stem cells derived from bone marrow or another mesenchymal adult source.

As with previously discussed differentiation studies, cells were seeded in a monolayer at a defined density of  $5.0 \times 10^4$  cells/cm<sup>2</sup>, allowed to adhere under defined basal conditions for 24 hours before media was replaced with defined serum free differentiation media. Cells were cultured for 21 days with media refreshment occurring at day 7

As a marker of early neurogenesis, nestin was considered to be an appropriate candidate. Nestin expression is usually transient and does not continue into lineage committed cells, as a result of this it is not easy to detect due to rapid switching and termination of translation, resulting in an overall small copy number. However, nestin is still widely regarded as an optimal candidate marker for neuronal precursor cells. Nestin is an intermediate filament protein expressed in dividing cells during the early stages of development in both the central and peripheral nervous systems [416]. Upon differentiation, nestin becomes down regulated and is replaced by tissue-specific intermediate filament proteins such as neurofilament and  $\beta$ -III-tubulin.

Shown in Fig.3.63. is staining for nestin in dental pulp derived stem cells under neural differentiation parameters 5 days post induction.



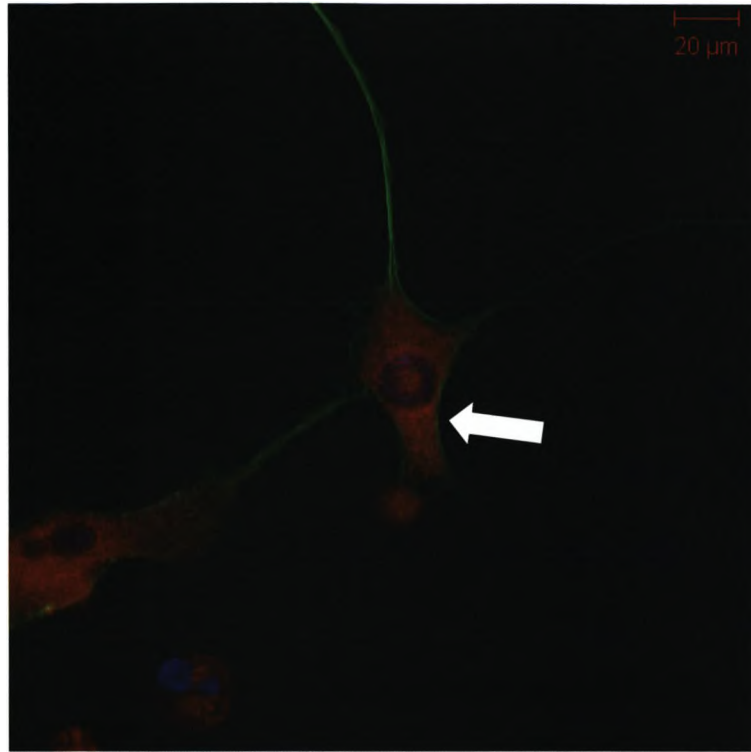


*Fig.3.63. Fluorescent microscopic observation of immunohistochemical staining for **Nestin**, **F-Actin** and **Nuclei** after 5 days of neural culture (positive staining illustrated by arrow)*

Neural growth factor (NGF) is a neurotrophin associated with neural growth and differentiation. On binding, its receptor on the surface of neural cells it is internalised and can play a role in the intracellular initiation of one of a number of signalling cascades terminating in gene transcription. NGF responses can include Egr and CREB mediated signalling. The Egr family of transcription factors and the Mek/Erk pathway contribute to NGF-induced neurite formation. Furthermore, the CREB family of transcription factors are involved in NGF-induced survival of sympathetic neurons [417] It was possible to observe an increase in the expression of NGF throughout the neural culture period up to 14 days post stimulation (Fig.3.64), confirming the attempt of these dental pulp derived stem cells to become neurite cells when considering the role of NGF in the mediation of overall neurite integrity. Furthermore, it was also possible to demonstrate the presence of NGF using immunohistochemistry shown after 21 days of neural culture, in Fig.3.65.

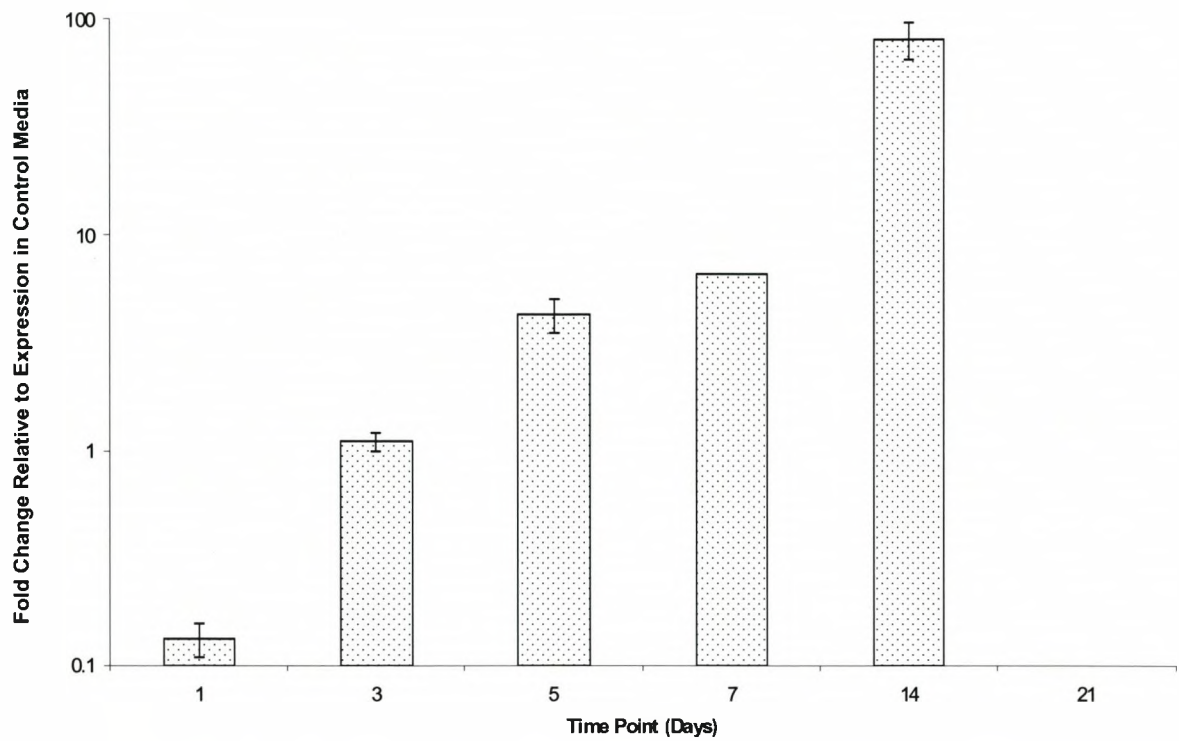


*Fig.3.64. Real time-PCR observation of the change in expression of Neural Growth Factor relative to basal conditions at any specified time point as a result of subjection to neural stimuli. Error bars represent 1 standard deviation from the mean, n=6*

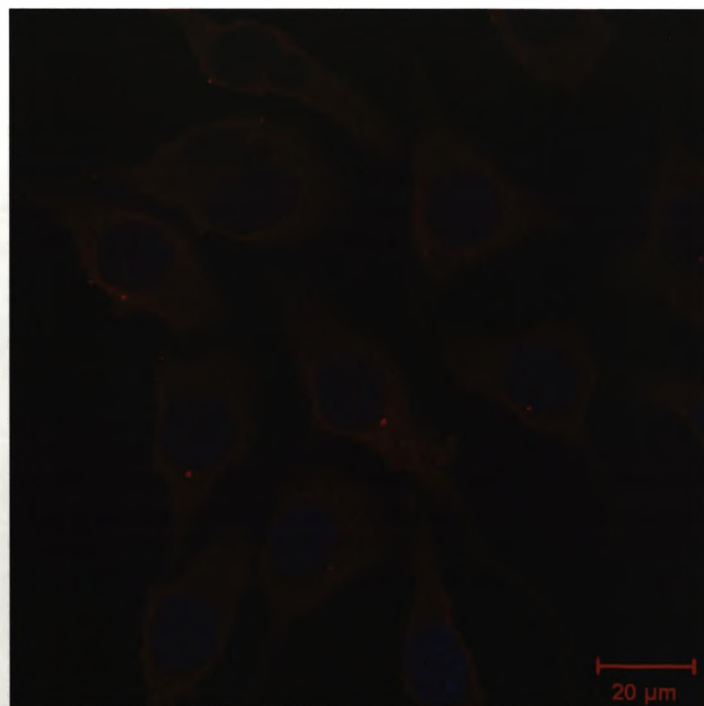


*Fig.3.65. Fluorescent microscopic observation of immunohistochemical staining for NGF and Nuclei after 14 days of neural culture*

During neurogenesis, nestin becomes replaced by terminal neuron associated intermediate filament proteins, the most common of which is neurofilament. This protein has a role in neurite development by mediating axonal growth. Neurofilament has a polymeric structure made of several differing subunits. During axonal elongation, subunits are deposited at either end of an ever lengthening neurofilament molecule in a dynamic process. The polarity of neurofilaments makes them repulsive, so this protein can control the diameter of an axon by repulsion, therefore causing the axon to expand [418].

Neurofilament could be observed immunohistochemically, in the cell nucleus at day 7 and diffusely throughout the cytoplasm of the cells by day 14 which also demonstrates cell hypertrophy as a neurite morphology is established (Fig.3.66.)

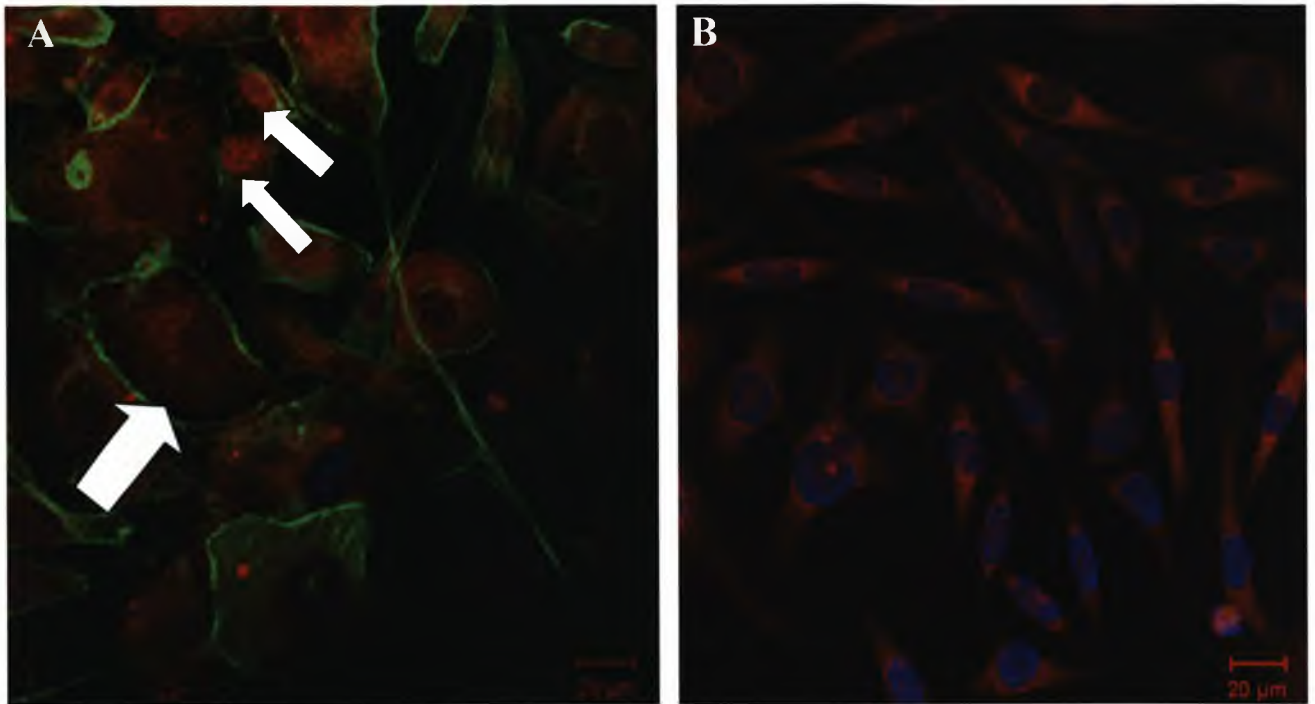


Fig.3.66. Fluorescent microscopic observation of immunohistochemical staining for *Neurofilament*, *F-Actin* and *Nuclei* after *A*; 7 days (located both nuclear and cytoplasmic, indicated by arrows), and *B*; 14 days of neural culture

$\beta$ -III-tubulin is a structural component of the neuronal cytoskeleton. Tubulins are a class of proteins which form microtubules through dimerisation of  $\alpha$  and  $\beta$  tubulin subunits. Although tubulins are present in most tissues, the  $\beta$ -III isoform is specific to nervous tissue and therefore a suitable candidate marker for neuronal differentiation and lineage commitment [419].

Fig.3.67. illustrates real time-PCR analysis of the changes in expression of this neuronal specific cytoskeletal element during neural culture of dental pulp derived stem cells. From this it can be concluded that an increase in expression is evident as early as 24 hours post induction, demonstrating a population of neural cells undergoing an increase in cytoskeletal arrangement and stabilisation. Most significant is the increase in expression of in excess of  $1.0 \times 10^4$  fold, 14 days post induction.

Further demonstration of  $\beta$ -III-tubulin expression was observed using immunohistochemistry after 21 days of culture, shown in Fig.3.68.



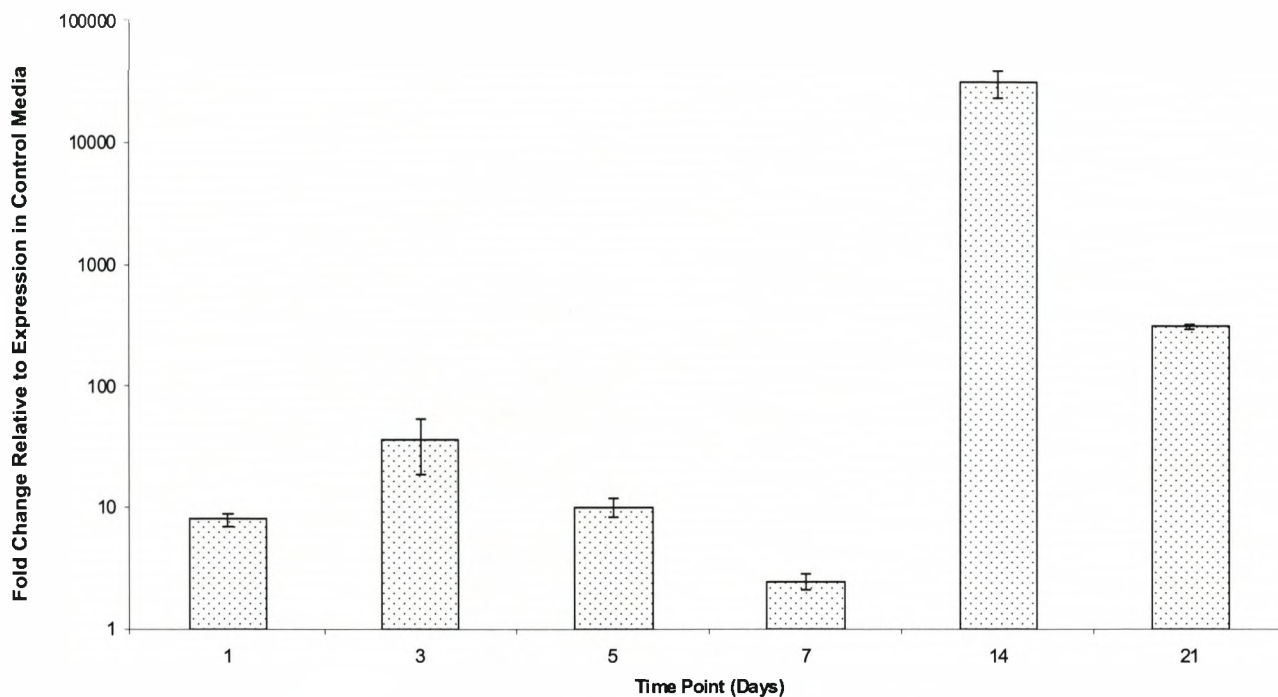


*Fig.3.67. Real time-PCR observation of the change in expression of  $\beta$ -III-Tubulin relative to basal conditions at any time point specified as a result of subjection to neural stimuli. Error bars represent 1 standard deviation from the mean, n=6*

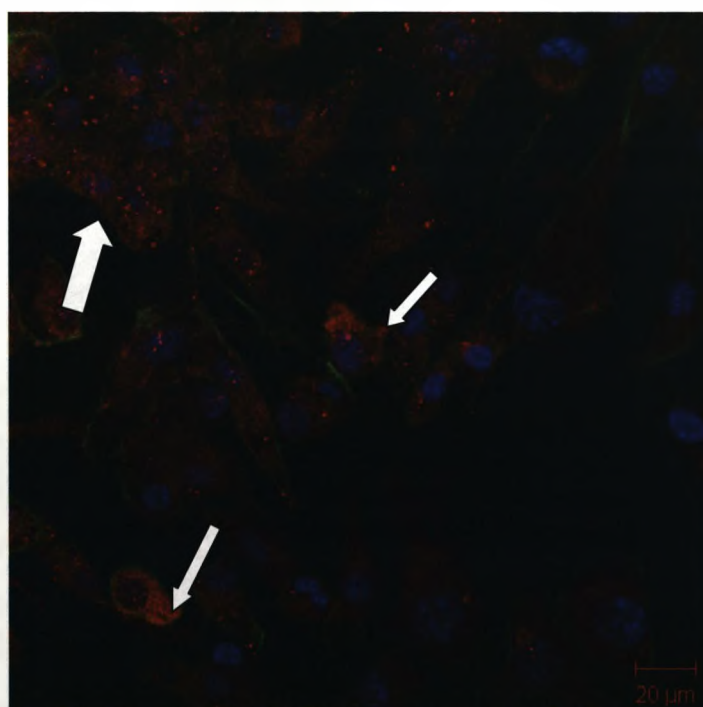


*Fig.3.68. Fluorescent microscopic observation of immunohistochemical staining for  $\beta$ -III-Tubulin, F-Actin and Nuclei after 21 days of neural culture (positive staining illustrated by arrows)*

Immunohistochemistry after 21 days of neural culture also allowed demonstration of the neuron specific vesicle glycoprotein synaptophysin and additionally synaptic vesicle protein, both molecules associated with structural construction of the mechanics for synapse formation therefore providing evidence to confirm the functionality of the neural cells (Fig.3.69.) [420].

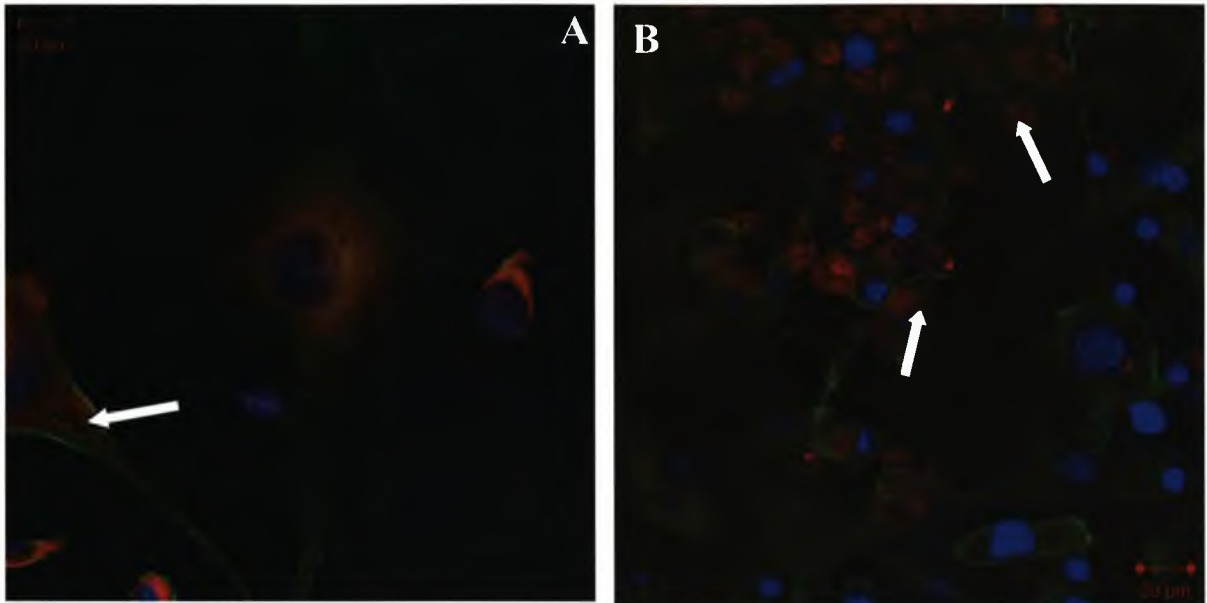


*Fig.3.69. Fluorescent microscopic observation of immunohistochemical staining for **A**; Synaptophysin, F-Actin, Nuclei and **B**; Synaptic vesicle protein, F-Actin, Nuclei after 21 days of neural culture (positive staining illustrated by arrows)*

REST is a crucial protein involved in coordination of central nervous system development. REST regulates the transitions from pluripotent to neural stem/progenitor cell and from progenitor to mature neuron, through its function as a gene silencing transcription factor at a critical DNA element involved in mediation of neuronal development, the RE1 site. In the transition to progenitor cell, REST is degraded to levels just sufficient to maintain neuronal gene chromatin in an inactive state that is nonetheless poised for expression. As progenitors differentiate into neurons, REST and its corepressors dissociate from the RE1 site, triggering activation of neuronal genes. In some genes, the level of expression is adjusted further in neurons by CoREST/MeCP2 repressor complexes. Therefore REST

defines a gene set subject to plasticity in mature neurons, whilst also potentially permitting fine tuning in response to specific stimuli [421].

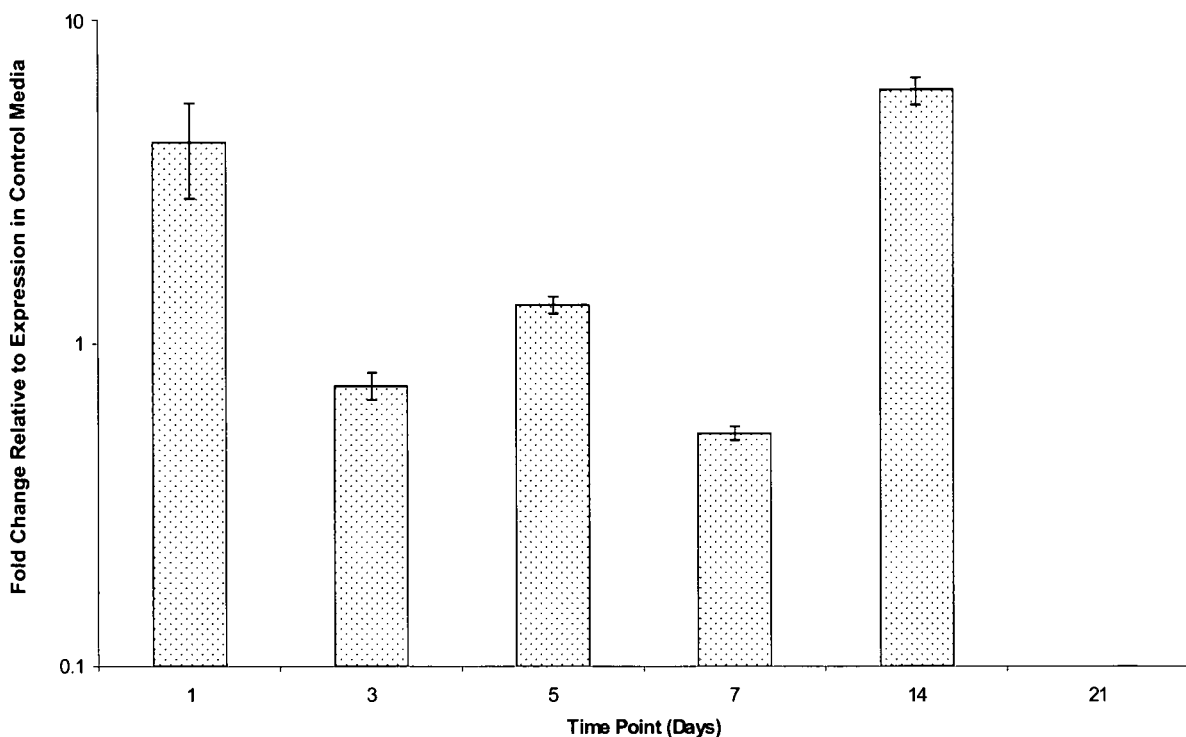


*Fig.3.70. Real time-PCR observation of the change in expression of REST relative to basal conditions at any specified time point as a result of subjection to neural stimuli. Error bars represent 1 standard deviation from the mean, n=6*

Fig.3.70. illustrates real time-PCR characterisation of REST throughout culture under defined serum free neural conditions. It is possible to observe the hypothesised decrease in REST expression from day 1 – 7. An increase in expression is apparent at day 14, possibly reflective of CoREST/MeCP2 fine tuning of the fate of the neural cells developed under this stimulus. However the clear reduction in rest levels during the first week of neural culture is indicative of the transition from a stem cell to a neural progenitor phenotype.

To confirm the functionality of the neural cells, it was decided to use the neurotransmitter substance P as a candidate molecule to elucidate the formation of a functional neuron capable of neurotransmitter mediated signalling. Substance P is a tachykinin neuropeptide which is released from the terminals of specific sensory neurons. The main endogenous role

of substance P *in vivo* is in pain perception and it is released from peripheral terminals of sensory neurons in various areas of the body as a result to pain stimuli. It has receptors (neurokinin 1, NK1-receptor) widely distributed throughout the brain [422].

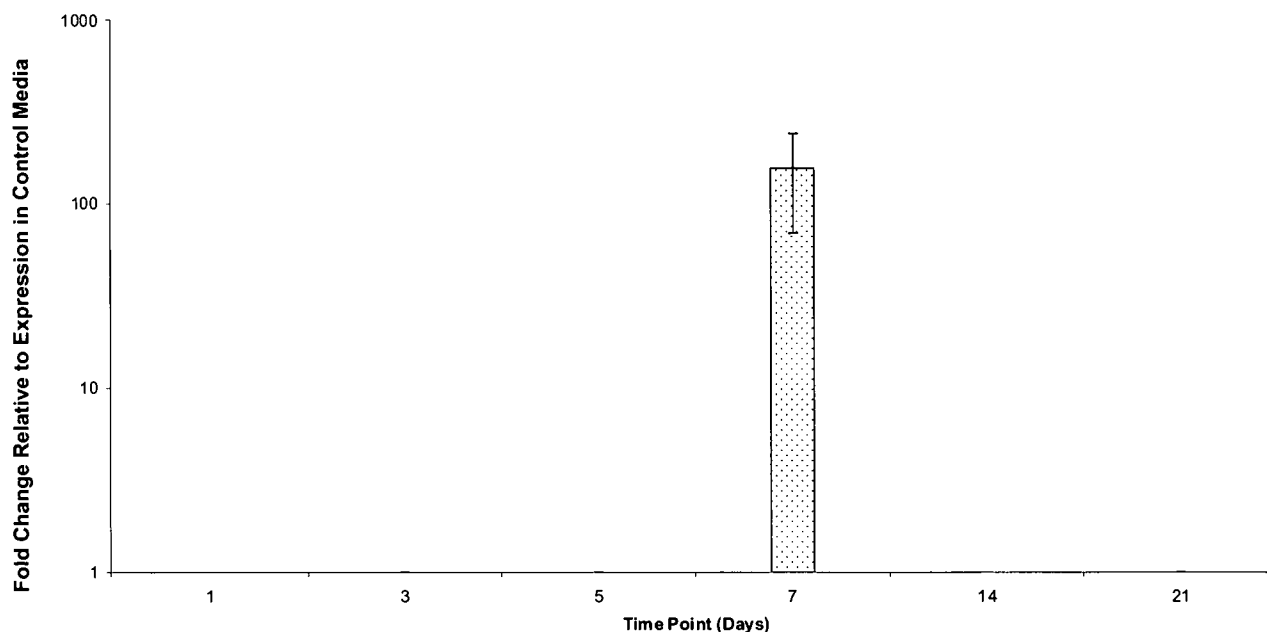


*Fig.3.71. Real time-PCR observation of the change in expression of Substance P relative to basal conditions at any specified time point as a result of subjection to neural stimuli. Error bars represent 1 standard deviation from the mean, n=6*

Fig.3.71. illustrates real time-PCR analysis of the presence of substance P in defined neural dental pulp stem cell cultures. It is clear to observe a significant increase in the expression of this functional neuropeptide at day 7. This was further validated using immunohistochemistry, shown in fig.3.72. The presence of substance P presence observed in dental pulp derived stem cells after 21 days of defined neural culture.

In addition to the confirmed presence of synaptophysin and synaptic vesicle protein this data confirmed the presence of potentially functional synapse formation by these neo-neuronal cells derived under serum free defined neural parameters. Fig.3.72. also demonstrates the neurite-like



morphology of the cells after neural culture. The familiar cobblestone, endothelial-like morphology is lost in favour of a considerably more dendritic spindle shaped structure, further illustrated in Fig.3.73. after 14 days after neuronal initiation.

Furthermore it was also possible to subject umbilical cord derived stem cells to defined neural stimuli and initiate differentiation into a neuronal phenotype, shown as an immunohistochemical overview after 21 days, using passage 4 primary derived umbilical cord stem cells used at passage 4 (Fig.3.74).

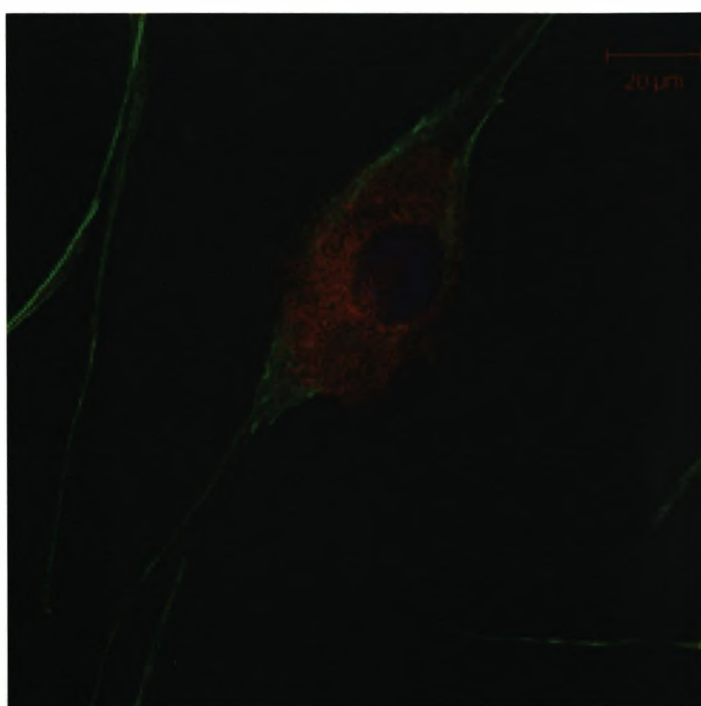


*Fig.3.72. Fluorescent microscopic observation of immunohistochemical staining for Substance P, F-Actin and Nuclei after 21 days of neural culture*

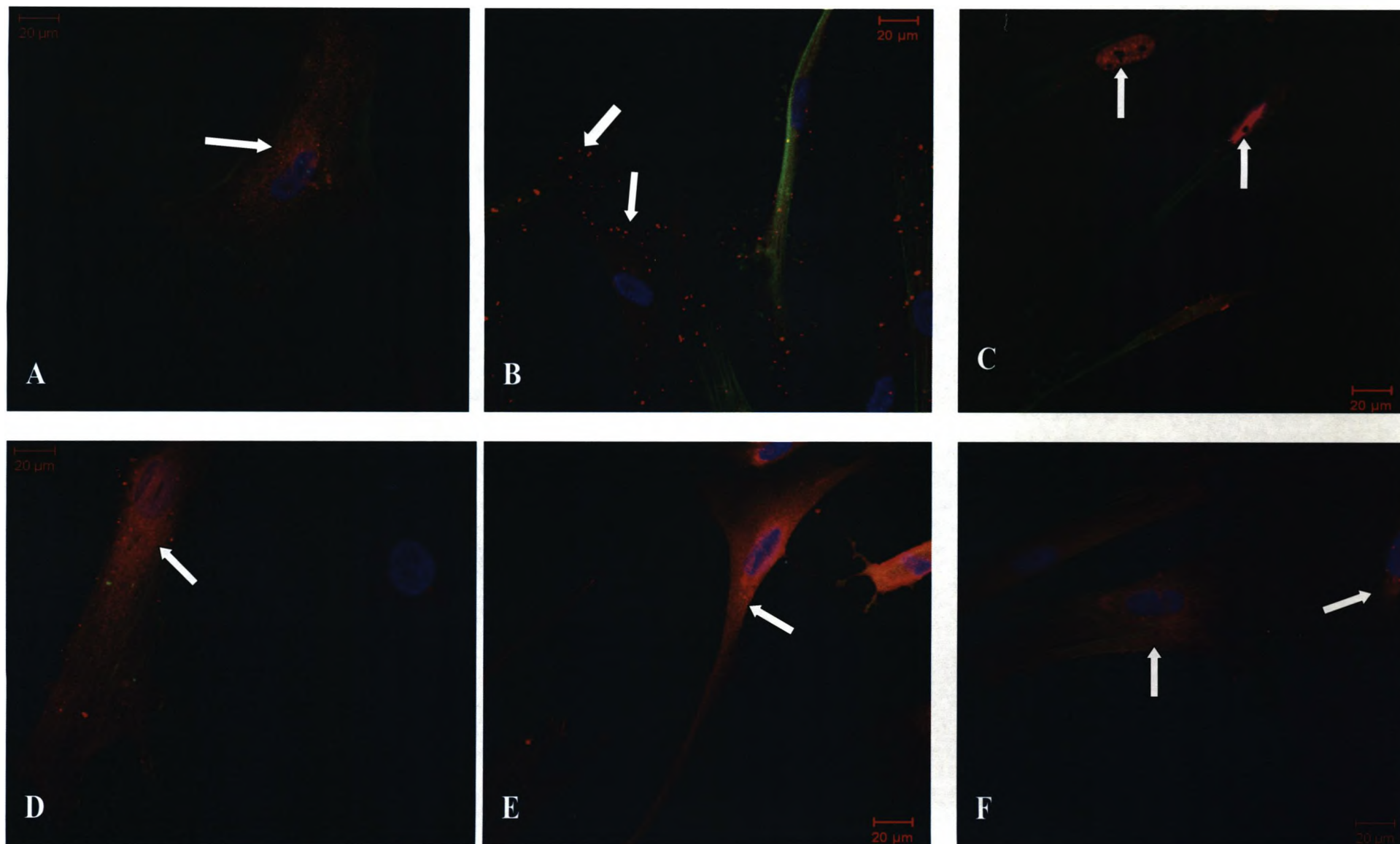
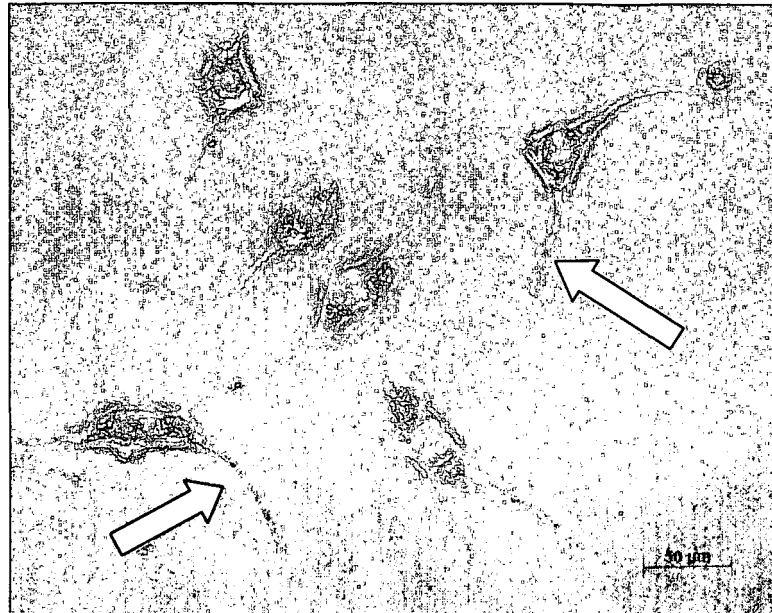


Fig.3.74. Fluorescent microscopic visualisation of immunohistochemical staining of umbilical cord derived stem cells after 21 days of neural culture for **A**; *GFAP*, *F-Actin*, *Nuclei*, **B**; *Synaptophysin*, *F-Actin*, *Nuclei*, **C**; *Neurofilament*, *F-Actin*, *Nuclei*, **D**; *Beta-III-Tubulin*, *F-Actin*, *Nuclei*, **E**; *NGF*, *F-Actin*, *Nuclei* and **F**; *Nestin*, *F-Actin*, *Nuclei* (positive staining illustrated by arrows)



*Fig.3.73. Light Microscopic observation of neurite morphology of dental pulp derived stem cells after 14 days of culture under defined neural conditions, illustrating neurite processes (arrow)*

From these data, therefore, it was possible to conclude that defined serum free neural differentiation media was capable of differentiating dental pulp-derived stem cells into a neuronal lineage in a culture period of 14 days. These neo-neuronal cells demonstrated an extensive number of proteins associated with specific neuronal progenitor and lineage commitment, in addition to molecules associated with *in vivo* functionality and synaptic transmission. The cells also modulated their morphology into a typical neuronal dendritic structure.

Furthermore, it was also possible to differentiate umbilical cord derived stem cells into a neuronal phenotype using an identical media formulation. Interestingly these cells expressed glial fibrillary acidic protein (GFAP), a peptide expressed in glial cells but not terminal neurones, suggesting a more heterogeneous differentiation into a population of both glial and neuronal cells. Dental pulp derived stem cells did not express GFAP at any point throughout their culture, neither did they express S100, a second marker associated with glial cells confirming a homogeneous preference of neuronal over glial phenotypes by dental pulp-derived stem cells under these serum free neural stimuli.

### 3.xii Defined Hepatic Differentiation of Dental Pulp Derived Stem Cells

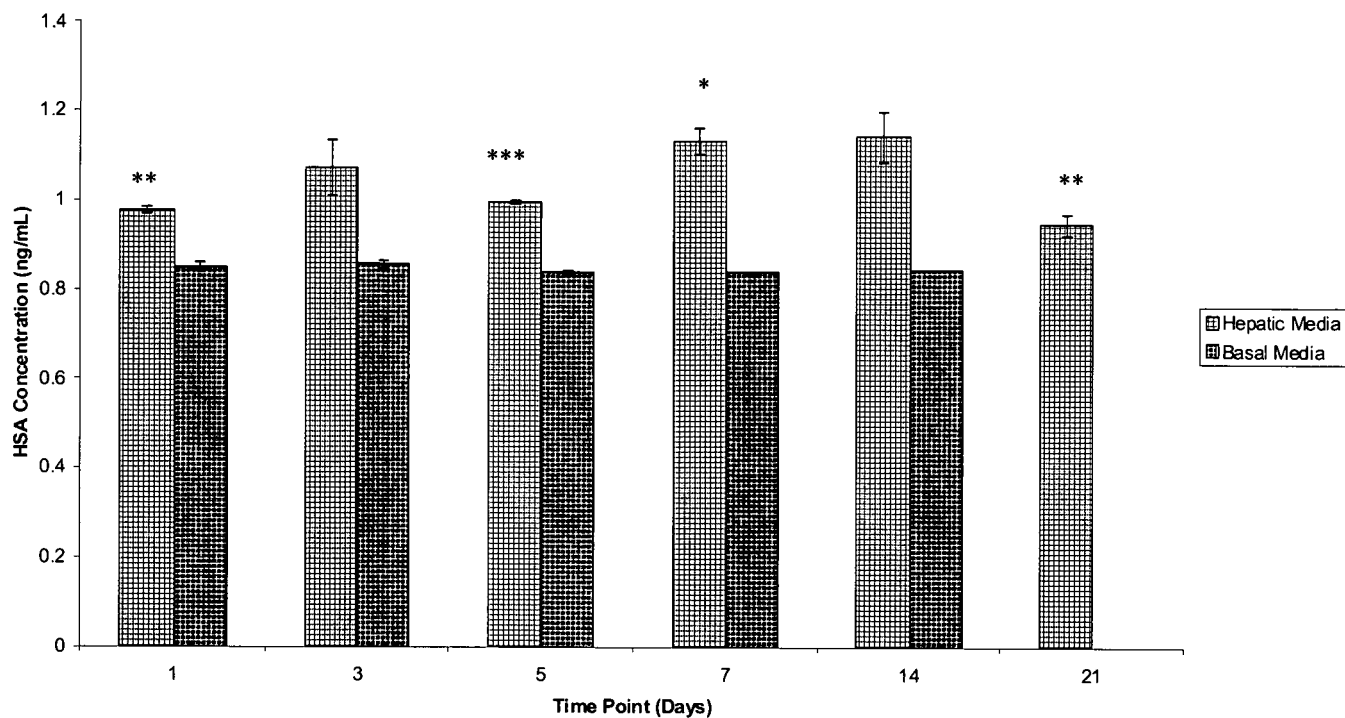
A second transgermal differentiation event was characterised using the defined serum free hepatic media shown in table 3.5. After extensive demonstration that the stem cells derived from dental pulp possessed the capacity to differentiate into neural cells, hepatocytes were chosen as a target phenotype in order to demonstrate if the cells were indeed considerably more plastic than bone marrow derived stem cells or was the ease of neural differentiation an artefact of the proximity of these cells to the neural crest during development, predisposing them to a neural phenotype in conjunction with suitable stimulation.

As with previously discussed differentiation studies, cells were seeded in a monolayer at a defined density of  $5.0 \times 10^4$  cells/cm<sup>2</sup>, and allowed to adhere under defined basal conditions for 24 hours before media was replaced with defined serum free differentiation media. Cells were cultured for 21 days with media refreshment occurring at day 7.

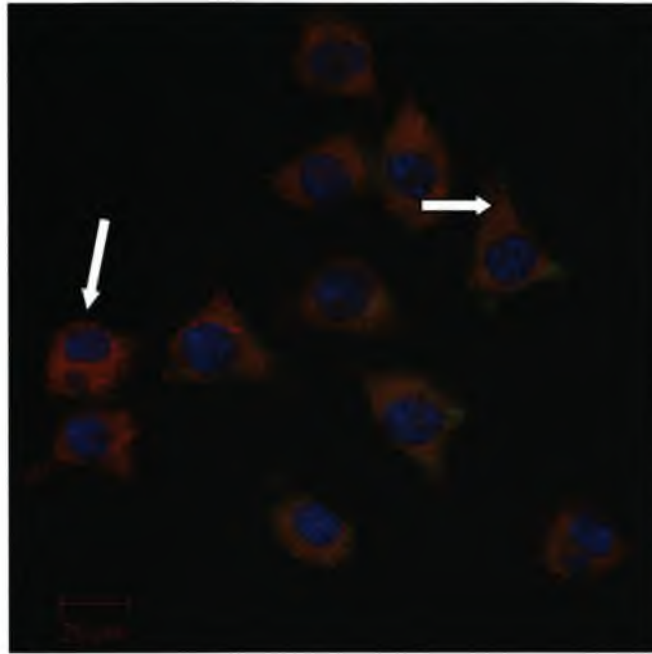
One of the major secretory products of hepatocyte cells *in vivo* is serum albumin. This is the most abundant protein in blood plasma, comprising approximately 50% of total serum protein. The major function of this protein is its role in maintenance of the osmotic balance of blood, additionally though it also has functions in hormone binding and transport, fatty acid movement around the body and also a role in maintenance of the pH buffering system in blood plasma [432,424].

Fig.3.75. demonstrates quantification of human serum albumin in cell culture media aspirates taken from dental pulp cells cultured under basal and hepatic conditions calculated using the ELISA method stated in section 2.xii. The data demonstrates significant increases in secreted albumin from cells under hepatic stimuli over those in basal culture throughout culture period until after 21 days post stimulation. Basal cells no longer produced any detectable albumin, whilst cells under hepatic stimulation remained secreting this vital plasma protein. It was also

confirmed prior to data analysis that no cross reaction occurred with bovine serum albumin present in the media, using this method.



*Fig.3.75. Quantification of the concentration of human serum albumin in culture media aspirates taken from dental pulp derived stem cells under basal and hepatic culture conditions confirmed using the ELISA method. Error bars represent 1 standard deviation from the mean, n=3, \*P<0.05, \*\*P<0.01, \*\*\*P<0.001 relative to basal media*



*Fig.3.76. Fluorescent microscopic observation of immunohistochemical staining for **Serum Albumin**, **F-Actin** and **Nuclei** after 21 days of hepatic culture (positive staining illustrated by arrows)*

The presence of serum albumin was further confirmed using immunohistochemistry after 21 days of hepatic culture and illustrated in Fig.3.76 [423, 424].

Interestingly  $\alpha$ -fetoprotein was also detected in dental pulp derived stem cells under hepatic stimuli. This is an early protein, expressed by the liver during fetal development hypothesized to play a series of comparable roles to serum albumin in the developing infant. *In vivo* levels of  $\alpha$ -fetoprotein decrease gradually during the first year of life, and although present in very low amounts in adults it does not have any known role [425].

Fig.3.77. illustrates  $\alpha$ -fetoprotein immunohistochemically which further supports the hypothesis of the origins of these cells in early development, forming extensively a protein which would not typically be transcribed in any great amount in a terminal adult cell, shown here after 21 days of hepatic culture.



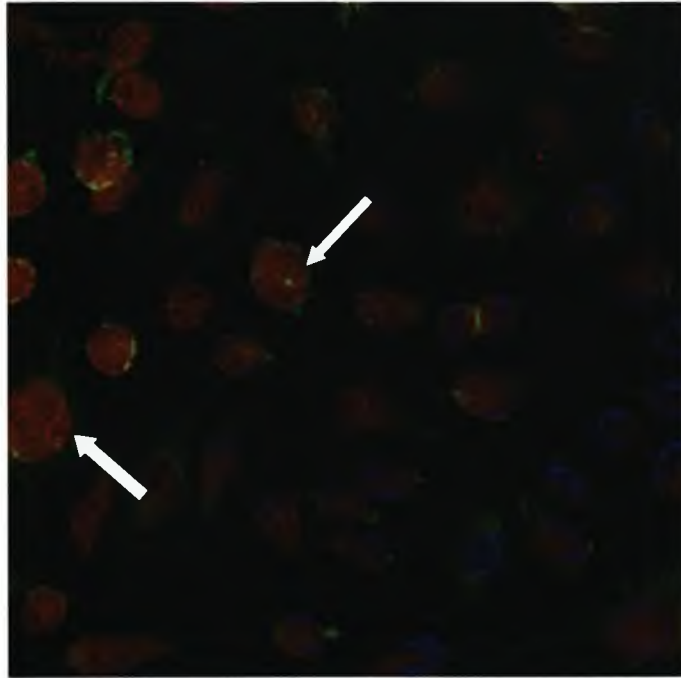


*Fig.3.77. Fluorescent microscopic observation of immunohistochemical staining for  $\alpha$ -fetoprotein, F-Actin and Nuclei after 21 days of hepatic culture (positive staining illustrated by arrows)*

Additionally, cytokeratin18 was observed immunohistochemically in the dental pulp derived hepatocyte cells after 21 days of culture (Fig.3.78.). This molecule is one of a large family of tissue specific intermediate filament keratins involved in cytoskeletal formation. The 18 isoform, a high molecular weight acidic cytokeratin is a hepatocyte specific element, further confirming the lineage commitment of the dental pulp derived stem cells under hepatic stimuli [426].

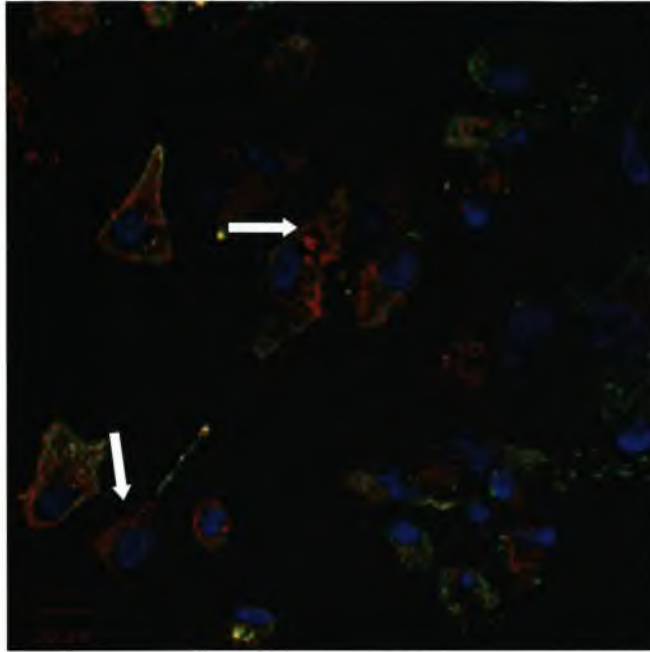


*Fig.3.78. Fluorescent microscopic observation of immunohistochemical staining for Cytokeratin 18, F-Actin and Nuclei after 21 days of hepatic culture (positive staining illustrated by arrows)*

Therefore, it was possible to conclude that under defined serum free hepatic stimuli dental pulp cells could be differentiated into hepatocyte cells characterised by the presence of cytokeratin18, a hepatocyte specific cytokeratin and additionally serum albumin, confirming part of their *in vivo* functionality [426].



3.xiii Metabolic Activity of Dental Pulp Derived Stem Cells in Conjunction with Serum Free Differentiation Media Formulations

The metabolic activities of dental pulp derived stem cells under serum free basal and differentiation media formulations were compared using the Alamar blue method (Fig.3.79 & Fig.3.32.).

Consistent with previous studies, using these cells in conjunction with the defined media formulations, cells were seeded in a monolayer at a defined density of  $5.0 \times 10^4$  cells/cm<sup>2</sup>, allowed to adhere under defined basal conditions for 24 hours before media was replaced with defined serum free differentiation media. Cells were cultured for 21 days with media refreshment occurring at day 7.

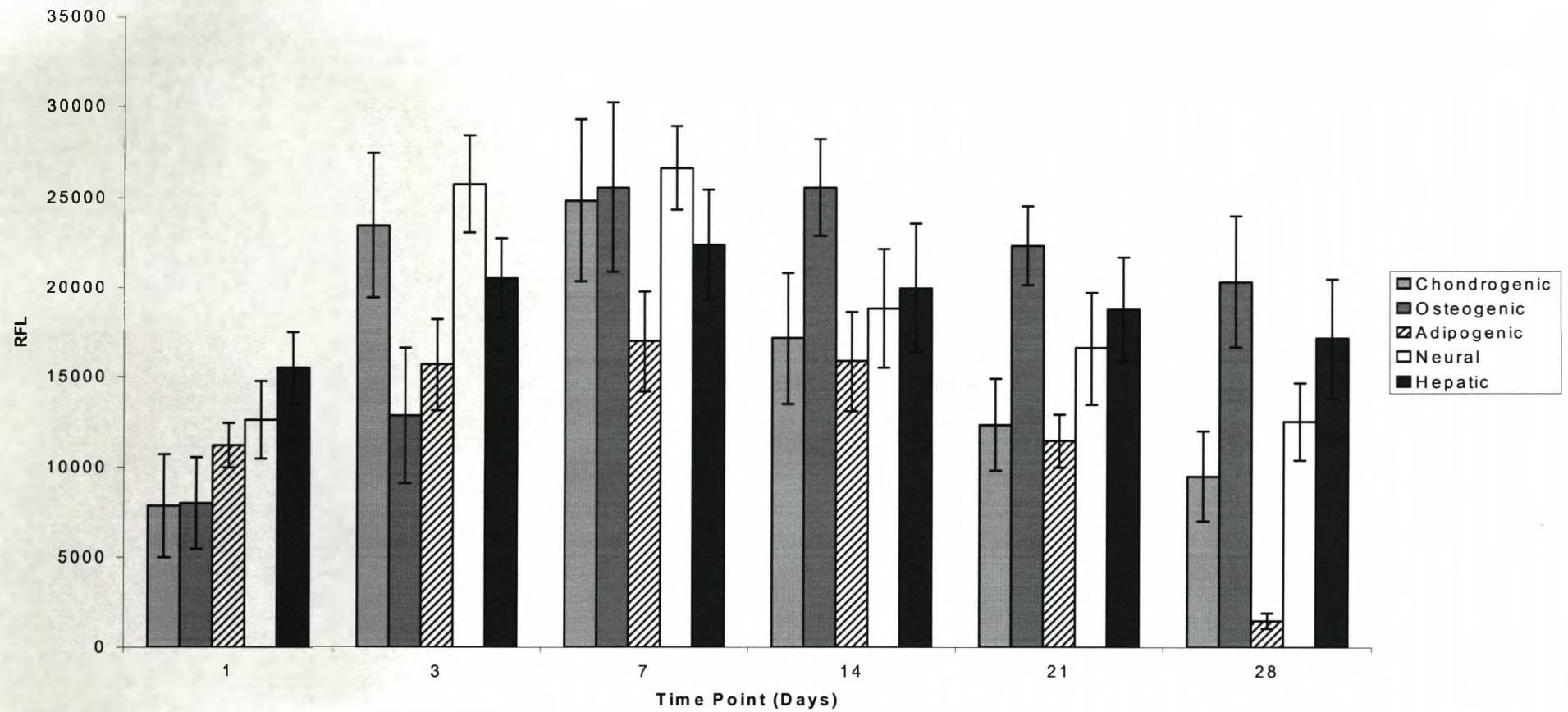


Fig.3.79. Metabolic activity of human dental pulp derived stem cells under defined serum free differentiation conditions using the Alamar blue method. Error bars represent 1 standard deviation from the mean, n=3. No correction for change in cell number was conducted

These data demonstrated that the general trend in metabolic activity was a familiar one, an increase in metabolic activity during the first week of culture, followed by a plateau in the case of basal culture and a decrease in the case of the differentiation culture. The phenomenon of a decrease in proliferation during differentiation is a common occurrence; this is a result of a cell becoming non-proliferative due to its status in mid-lineage commitment

In a similar manner to bone marrow-derived stem cells, the metabolic activity plateau observed under basal conditions can be confirmed microscopically to be a result of contact inhibition.

### 3.xiv Summary

Serum free defined basal cell culture media was designed and synthesised *de novo* from individual components incorporating salts, vitamins, amino acids and energy sources. Initially, the media formulation was trialled using primary human dermal fibroblast cells which was demonstrated to maintain morphology, metabolic activity at similar rates to serum containing media formulations. Crucially, phenotype was confirmed by identification of the fibroblast specific D7-Fib antigen after extended culture in conjunction with the serum free basal media formulation. The media also proved itself as a suitable candidate for the expansion of primary human osteoblasts.

An increase in the concentration of glucose in the defined serum free media identified it as a suitable candidate media for the expansion of primary human arterial smooth muscle cells, with metabolic activity again almost identical to serum containing media formulations. Overall smooth muscle phenotype maintenance was confirmed by the presence of smooth muscle actin using various methods. Interestingly, the serum free basal formulation identified iron as a potential candidate moiety responsible for the switch between a synthetic and contractile phenotype, hypothesised on the basis of the cells lack of expression of smoothelin in the media formulation devoid of iron.

Bone marrow derived mesenchymal stem cells were introduced into the media and furthermore showed metabolic activities comparable to serum containing media formulations. Under defined serum free basal conditions, it was demonstrated extensively that these cells maintained their fibroblastic morphology and also their undifferentiated phenotype. In a subset of specific examples it was also demonstrated that the serum free basal media halted the spontaneous differentiation of bone marrow derived stem cells during basal culture by the observation of increases over serum containing media of markers associated with plasticity as the cells were aged in culture.

Defined serum free basal media could be modified to contain controlled exogenous factors which were demonstrated capable of inducing tri-lineage differentiation of bone marrow-derived mesenchymal stem cells. Cells were differentiated into osteoblast, chondrocyte and adipocyte cells in culture periods of 21 days in conjunction with defined serum free media formulations.

Defined serum free media was used in conjunction with a considerably more obtainable source of stem cells: those derived from dental pulp. As with bone marrow-derived stem cells, these cells were to maintain a plastic phenotype under basal serum free conditions characterised by the presence of several markers of pluripotency including proteins associated with an embryonic stem cell phenotype such as TRA-1-81 and Oct4 [427, 428].

In conjunction with defined serum free differentiation parameters these cells were capable of carrying out tri-lineage differentiation, which was characterised extensively throughout a 21 day differentiation culture period. Furthermore it was also confirmed that dental pulp-derived stem cells were capable of trans-germal differentiation (differentiation into a lineage of a germ layer different to the developmental origin of the stem cell), made possible by the use of defined neural and hepatic differentiation media formulations. Additionally, the serum free defined neural media was also demonstrated capable of differentiating stem cells derived from an umbilical cord source into a terminal trans-germal neural lineage.

**DEVELOPMENT AND VALIDATION OF A DEFINED STRATEGY  
FOR THE SITE DIRECTED DELIVERY OF CLINICAL GRADE  
PRIMARY HUMAN CELLS**

4.i. Introduction

Treatment of conditions that compromise homeostasis and normal physiological function often requires tissue implantation or transplantation. The ideal paradigm is to introduce cells or tissues that are normally native to the damaged organ. Early indications are that treatment in this way using cell therapy or tissue engineering is feasible only when the correct environmental conditions are determined and well defined. To take this regenerative approach to the clinical end point, the development of injectable scaffolds for the minimally invasive delivery of appropriate cells to a defect site is highly desirable. Potentially, a single versatile material would provide a biotherapeutic approach to the regeneration of general and focal defects of a multitude of hard and soft tissues *in situ* with minimal surgical intervention. In order to achieve this, a suitable candidate material should be biodegradable, histocompatible and have mechanical properties closely resembling living tissue, providing a transient dynamic matrix for the delivery of pluripotent or lineage-committed cells. The scaffold material should interact with the host to achieve a fully integrated autogenous tissue, free of any foreign body [429-431].

A large variety of materials, both organic and inorganic are already being exploited for biomedical devices, and are being investigated further as interactive open porous scaffolds. Generally, these are designed to be application-specific for a tissue defect or disorder but do not anticipate the host's innate and specific defence mechanisms. These can be predicted and should be utilised in the functional delivery of the treatment regime. Therapies

for bone regeneration are predominantly based on injectable osteogenic tri-calcium phosphate cements [274]. These form micro-porous structures and are favoured for bone repair because they are more efficiently absorbed than hydroxyapatite and are more similar to host bone in their mechanical properties [275]. Several other materials have been used for scaffold fabrication including poly-L-lactic acid (PLLA) for injectable soft tissue augmentation [276]. As nanofibre structures, these mimic the extra cellular matrix (ECM), providing a familiar fibrous meshwork in which cells can attach and proliferate [277]. The fibres can then be 'decorated' through progressive synthetic chemistry to include functional groups that may direct the host response or increase clinical suitability through modulation of the polymer's physicochemical properties [278-280].

Polymers provide the possibility of designing matrices with high water content approaching that of natural tissues. Hydrogels are a class of covalently-linked polymers that exhibit excellent potential as candidate media for cellular delivery due to their hydrophilicity, high water content and compliant physical properties [281]. A further property of hydrogels that make them exciting candidates for implantation is their isotropic swelling, meaning that their dry shape is maintained post water absorption. Hydrogels can be utilised to elute drugs or present cell-signalling molecules to influence the cells that they contain or the tissue into which they are delivered [282-283]. Polymer gels can be chemically modified to modulate cell phenotype and proliferative status [284].

The aim of this research was to investigate a unique approach to producing hydrogels for use in cell therapies and tissue engineering processes, to drive specific tissue formation via autologous mechanisms. Gels were derived from autologous host plasma, thus providing a totally natural material for cell expansion and implantation, overcoming potential complex histocompatibility issues associated with organic implantable biomaterials.

ECM hydrogels have been utilised as vectors for cellular delivery in tissue regeneration for several years. These materials may consist of a mixture of purified undefined ECM components or defined, well characterised molecules associated with cell adhesion and recognition such as collagen, keratin, elastin and fibrin which have been used for tissue engineering applications such as nerve conduits [285-287]. These components provide an ideal substrate for cellular delivery and *in vivo* culture. The hydrogel developed in this study exploits this practice in conjunction with the well defined coagulation cascade mediated via molecules present in host plasma to generate a mechanically stable, self forming hydrogel matrix composed of fibrin. Citration of blood immediately following exsanguination prevents immediate clotting and preserves the components of the clotting cascade in place. Injecting culture media containing a high concentration of free calcium concurrently with the host plasma and cells during implantation results in clot formation and therefore *in situ* delivery of a cell-loaded protein scaffold at the defect site. Hydrogels formed in this way are superior to conventional hydrogels due to the lack of a significant foreign body response and the absence of factors which could be antigenic. In addition, specifically chosen variations in culture media composition can be exploited during hydrogel formation to influence cell lineage, particularly when used in conjunction with stem cells or uncommitted progenitor cells. This system therefore would be directly translatable to a range of clinical therapies due to the pharmacopeia grade standards in which the media component can be synthesised in combination with the autologous nature of the plasma and cellular elements.



#### 4.ii. Dynamic Contact Angle

Surface energy can be defined as the disruption of intermolecular bonds that occurs as the result of a surface being created; the excess energy at the surface of the material in comparison to the bulk. Fundamentally, the surface has to be intrinsically less energetically favourable than the bulk of the material, otherwise there would be a driving force for surfaces to be created, resulting in a material with no bulk, solely surface [432].

In biomaterial surface characterisation this is quantified by exploitation of the relationship that the force balance between a liquid-vapour surface tension ( $\gamma_{lv}$ ) and the interfacial tension between a material and the liquid ( $\gamma_{sl}$ ) is manifested through the contact angle ( $\cos\theta$ ) of the material with the liquid (Fig.4.1). This relationship can be used to characterise the surface energy ( $\gamma_{sv}$ ) of a material using a modified version of Young's equation:

$$\gamma_{sv} = \gamma_{sl} + \gamma_{lv} \cos\theta$$

The surface energy, and therefore contact angle has a strong correlation with biological interaction. The amount of free energy at a surface can greatly alter the way a cell adheres and possibly differentiates so for this reason it was critical to calculate contact angles associated with the platelet poor plasma derived hydrogel surface.

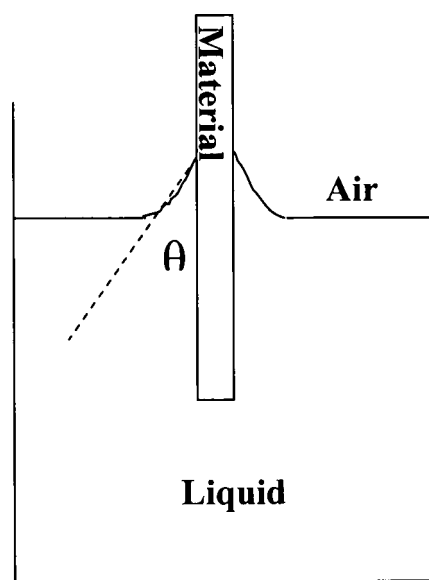


*Fig.4.1. Demonstration of role of the necessary components of the dynamic contact angle method for quantification of surface energy*

The solvent chosen to form the basis of the analysis was serum, in various incremental concentrations, as this was more biologically relevant than other liquids commonly used for dynamic contact angle investigations such as water, ethanol or chloroform. When dealing with the hydrogel as either *in vitro* or *in vivo* cell culture systems, it will be in contact with serum in various concentrations, thus this method would allow measurement of a contact angle directly applicable to the surface as it appears functionally in these applications. One particular variable of note using serum as a solvent concerned the equilibrium of total protein; the protein in solution and the protein adsorbed to the various components of the direct contact angle system, particularly the glass vessel in which it was held. The time taken to reach this equilibrium was examined by calculating the contact angle clean glass coverslips in serum which had remained *in situ* in the DCA system for 1-10 minutes at 1 minute intervals. No difference in contact angle was observed

during this time, allowing the assumption to be made that the equilibrium of protein in the solution had been reached after the initial minute.

In its liquid phase, the hydrogel was adsorbed onto clean filter paper and allowed to gellate at 37°C. After which it was subjected to submersion in a defined concentration of fetal calf serum in cell culture media and the contact angle between the gel and the liquid surface measured throughout the advancement of the material into the solution.

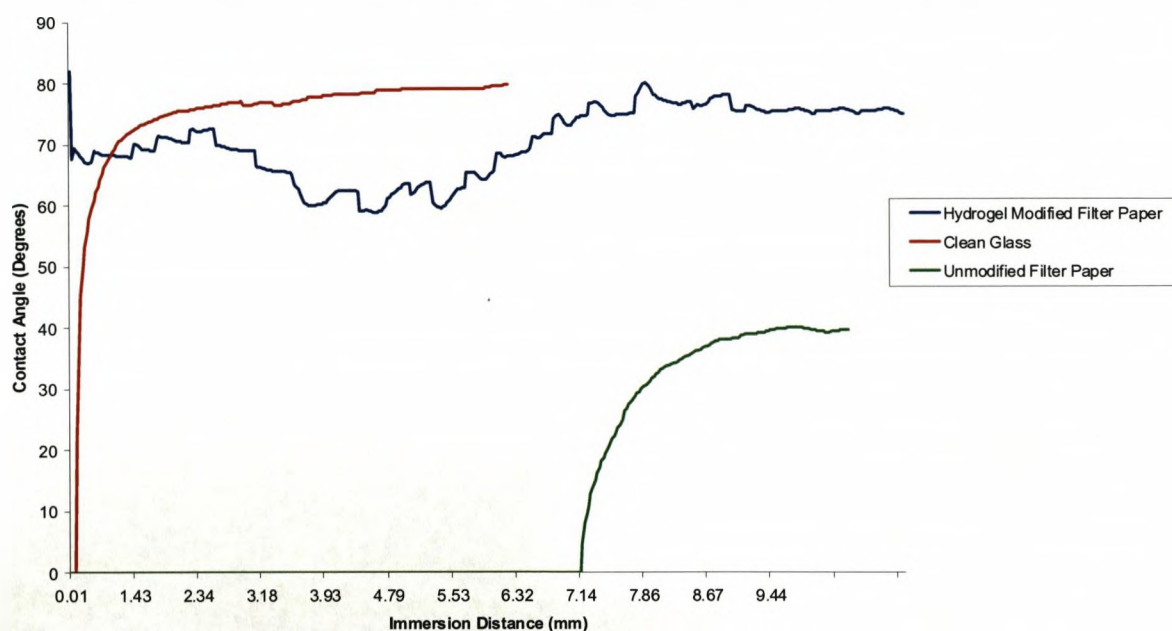


Fig.4.2. Advancing contact angles of three test surfaces during immersion into 5% fetal calf serum (v/v) measured using the dynamic contact angle method,  $n=3$

Fig.4.2 illustrates the contact angle profiles of the hydrogel modified filter paper and unmodified filter paper in comparison to clean tissue culture glass coverslips throughout submersion in a fetal calf serum concentration of 5% (v/v), a concentration widely used across *in vitro* tissue culture applications.

Across the range of fetal calf serum concentrations used, the contact angle of the hydrogel with the liquid interface remained almost unchanged. The angle was only slightly less than glass (although statistically this was regarded as being highly statistically significant), widely regarded as being an ideal material to facilitate the adhesion and proliferation of primary human cells, when subjected to an identical set of conditions (Fig.4.3). This data illustrates the similarity of the hydrogel surface to glass in this crucial first stage parameter for cell acceptance and compliance with a surface, contact angle.

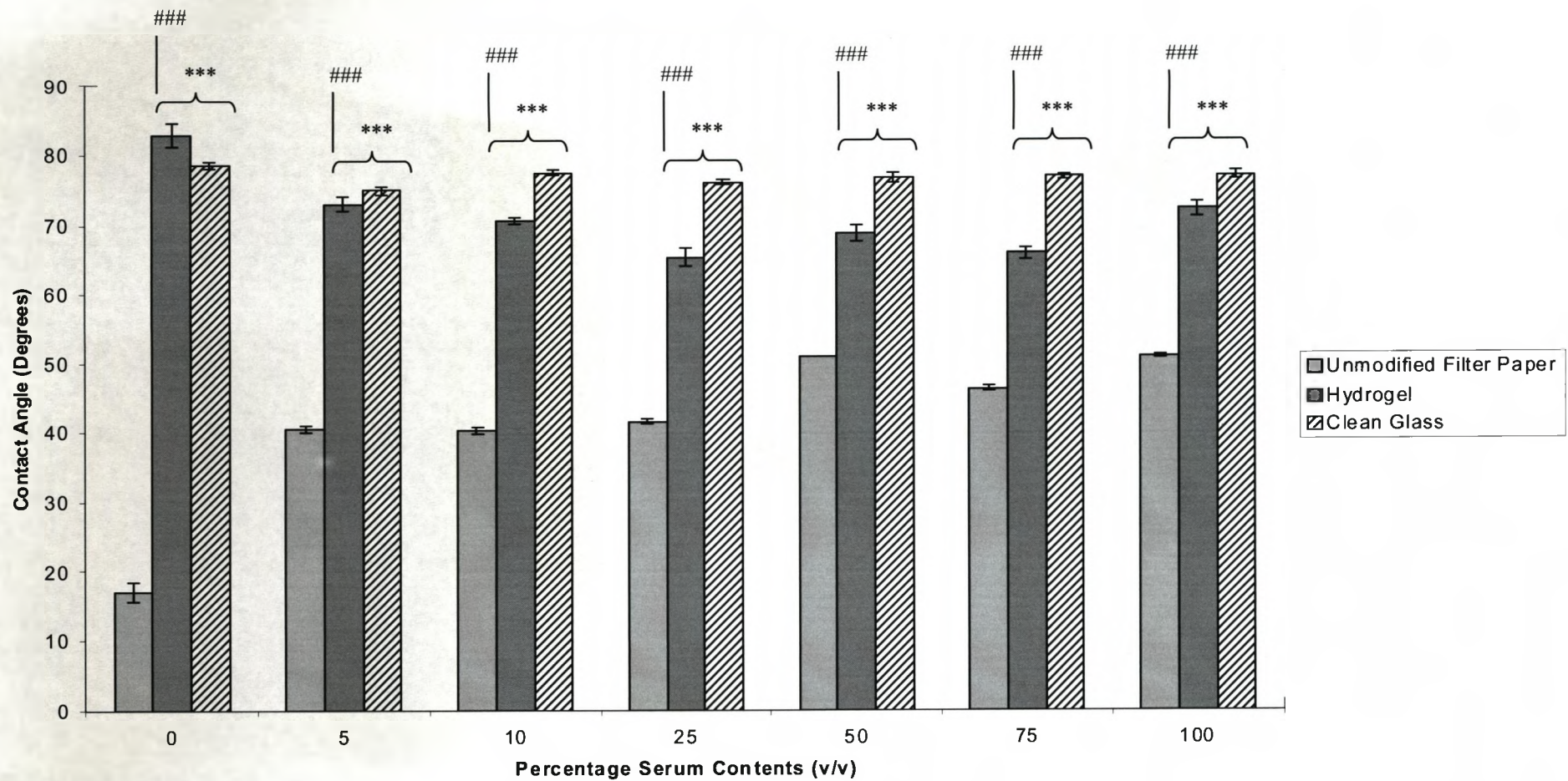


Fig.4.3. Comparison of the dynamic contact angle of blood plasma derived hydrogel and plain glass tissue culture substrate across a range of concentrations of fetal calf serum. Error bars represent 1 standard deviation from the mean,  $n=3$ , \* $P<0.05$ , \*\* $P<0.01$ , \*\*\* $P<0.001$  relative to unmodified filter paper; # $P<0.05$ , ## $P<0.01$ , ### $P<0.001$  hydrogel relative to clean glass

#### 4.iii Hypoxic Cell Maintenance Model

Human articular chondrocytes were chosen as an ideal candidate cell for validation of the platelet poor plasma derived hydrogel system as a supportive medium for the growth of primary cells contained within a specific niche *in vivo*, a niche deep within poorly vascular tissue which reflects the cells adaptation to an anoxic environment. The expansion and, crucially, phenotypic maintenance of chondrocytes *ex vivo* relies on a controlled hypoxic environment in which they can be cultured. The phenotype of a chondrocyte is dynamic, with rapid differentiation into more fibroblastic or osteochondral cells in the absence of suitable environmental stimuli. The chondrocyte is a cell type that with optimised conditions for its maintenance has vast potential for exploitation in regenerative therapies due to the plethora of potential cartilage defect-related diseases that could be treated using autologous or allogeneic chondrocyte constructs after *ex vivo* expansion. Current strategies rely on the expansion of these cells in pellet culture. The cells are spun down to a tight pellet and the hypoxic environment in the centre of the pellet which occurs as a result of the compaction of the outer cells causes the chondrocytes to maintain their phenotype. It was hypothesised that the platelet poor plasma derived hydrogel would provide an ideal medium for the expansion of chondrocytes given the controlled hypoxia conferred upon the cells by a hydrogel block above. Additionally, the high water content of the hydrogel would permit efflux of waste compounds from the monolayer of cells in culture below [433-435].

Human articular chondrocytes were taken from passage 6 and introduced to the hydrogel system in the manner stated previously in section 2.xvii for culture of cells below the gel. Cells were seeded at a density of  $5.0 \times 10^3$  cells/cm<sup>2</sup> and cultured under 10mm thick gels for a period of 21 days after which time the gel was aspirated from the monolayer of cells adhered to the tissue culture plastic below and were stained using the Alcian blue method stated in section 2.vii. Alcian blue is a cationic copper containing phthalocyanine dye which stains

mucopolysaccharides and glycosaminoglycans blue or turquoise green. These molecules are expressed extensively on the surface of chondrocyte cells, and are used not only as a marker of maintenance of cell phenotype but also as an indicator of chondrocyte functionality. Mucopolysaccharides and glycosaminoglycans, long, unbranched polysaccharides permit the role of chondrocytes in the lubrication of joints by attracting water to the cell surface due to the anionic nature of these molecules.

Fig.4.5. Demonstrates human articular chondrocyte cells stained after 21 days of culture under hydrogel culture clearly illustrating the blue staining associated with lineage committed chondrocytes using the Alcian blue method. This confirms the hydrogel system as a suitable candidate for the *ex vivo* maintenance and expansion of these clinically relevant primary cells.



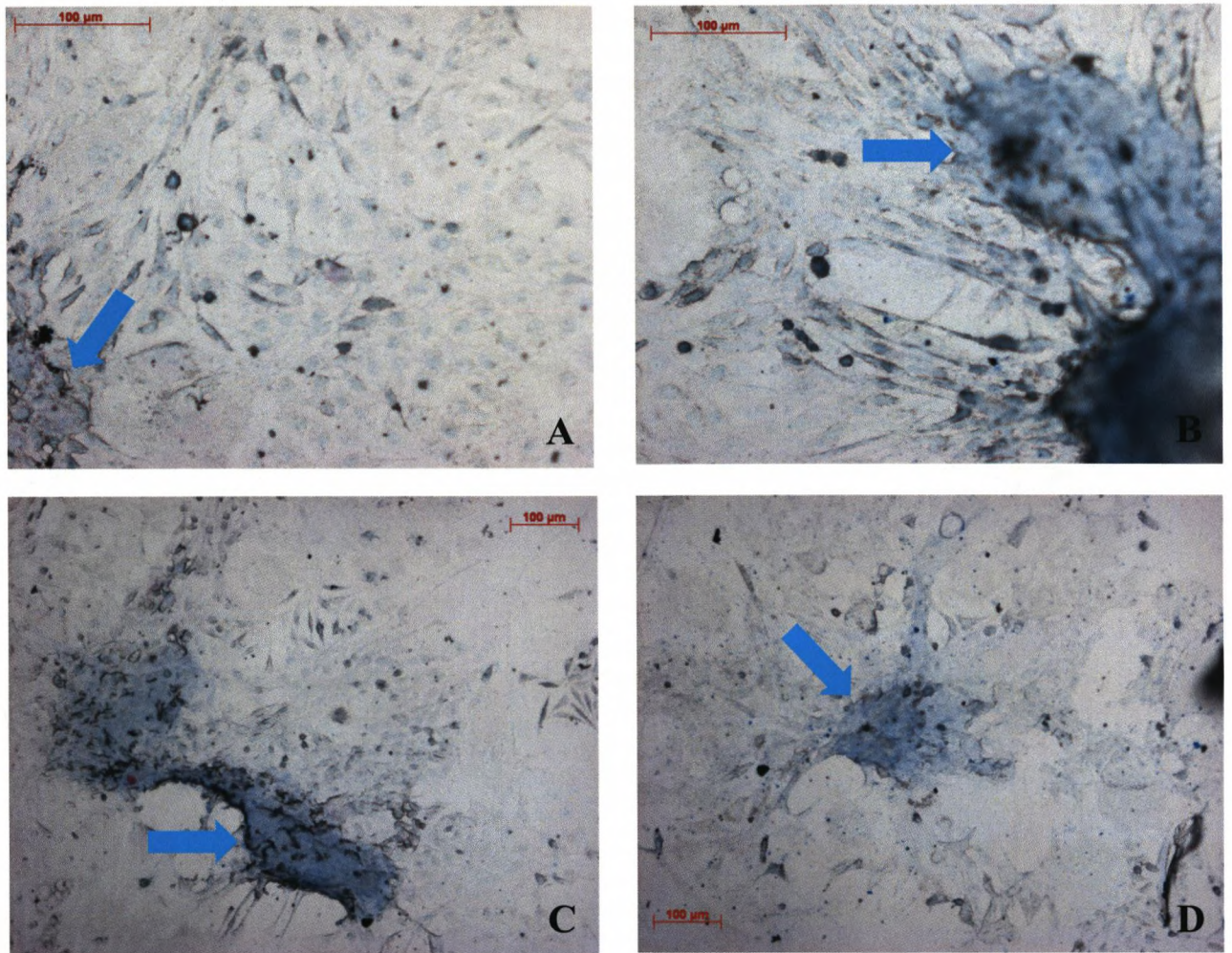


*Fig.4.5. Light microscopic observation of human articular chondrocytes cultured under platelet poor plasma derived hydrogel for 21 days stained using the Alcian blue method (Positive staining illustrated using arrows)*

#### 4.iv Gel Surface Validation

Human dental pulp derived stem cells were chosen as a candidate for the validation of the surface of the platelet poor plasma-derived hydrogel as a suitable medium for the expansion of primary human cells. The hypothesis was founded on the basis that the scaffold component of the gel is ultimately fibrin



combined with extra cellular matrix. This environment will provide a much more realistic substitute to the cells native niche than uncoated TCP, thus permitting the expansion and maintenance of the native phenotype of the cells to be considerably more facilitated than when grown on plastic. When seeded on TCP, dental pulp derived stem cells proliferate uncharacteristically rapidly when compared to adult stem cells from other sources such as adipose and bone marrow. On TCP, the cells exhibited a cobblestone, endothelial cell like morphology *in vitro*, without contact inhibition.

Interestingly, dental pulp derived stem cells, unlike bone marrow or umbilical cord stem cells do not possess the ability to undergo expansion on a commercially available Matrigel surface, an undefined extracellular tumour mass deived matrix hydrogel commonly used for the selection of haematopoietic subsets from a crude stem cell population based on their ability to divide on this particular substrate (Figs. 4.6 & 4.7).

Hetrogeneous populations of dental pulp cells were taken from passage 7 and introduced to the surface of 3mm thick gels in the manner previously illustrated in section 2.xvii. Cells were seeded at  $5.0 \times 10^3$  cells/cm<sup>2</sup> and maintained under Medium 199 containing 5% fetal calf serum and 1% penicillin/streptomycin until confluent. At the same time, dental pulp-derived stem cells were introduced onto Matrigel at an identical seeding density and the subsequent adhesion and proliferation observed microscopically.

Fig.4.6. Illustrates the heterogeneous population of dental pulp derived stem cells seeded onto both platelet poor plasma derived hydrogel and Matrigel substrates at periods of 3, 5 and 7 days post introduction. The cells on the Matrigel surface, as predicted, failed to proliferate. In contrast, the cells introduced into the blood plasma-derived hydrogel proliferated until confluent after 7 days. This therefore highlights the potential of the gel as a means of supporting the culture of this highly proliferative cell type *ex vivo*. However,

this data could also hypothetically highlight the lack of a hematopoietic population within the crude population of dental pulp stem cells, considering the absence of proliferative cells on the Matrigel, and also demonstrating the non-cell-specific nature of the blood plasma derived hydrogel in its capacity to support *in vitro* proliferation.

Metabolic activity of dental pulp derived stem cells was quantified using the almar blue method discussed in section 2.xiv. Cells were seeded at  $5.0 \times 10^3$  cells/cm<sup>2</sup> and cultured for 1, 7 and 14 days on a 3mm thick hydrogel surface under medium 199 containing 5% fetal calf serum and 1% penicillin/streptomycin (Fig.4.6.). This data further illustrates the potential of the gel as a tissue culture substrate, the dental pulp derived stem cells increasing in metabolic activity throughout the 14 day experimental culture timescale.

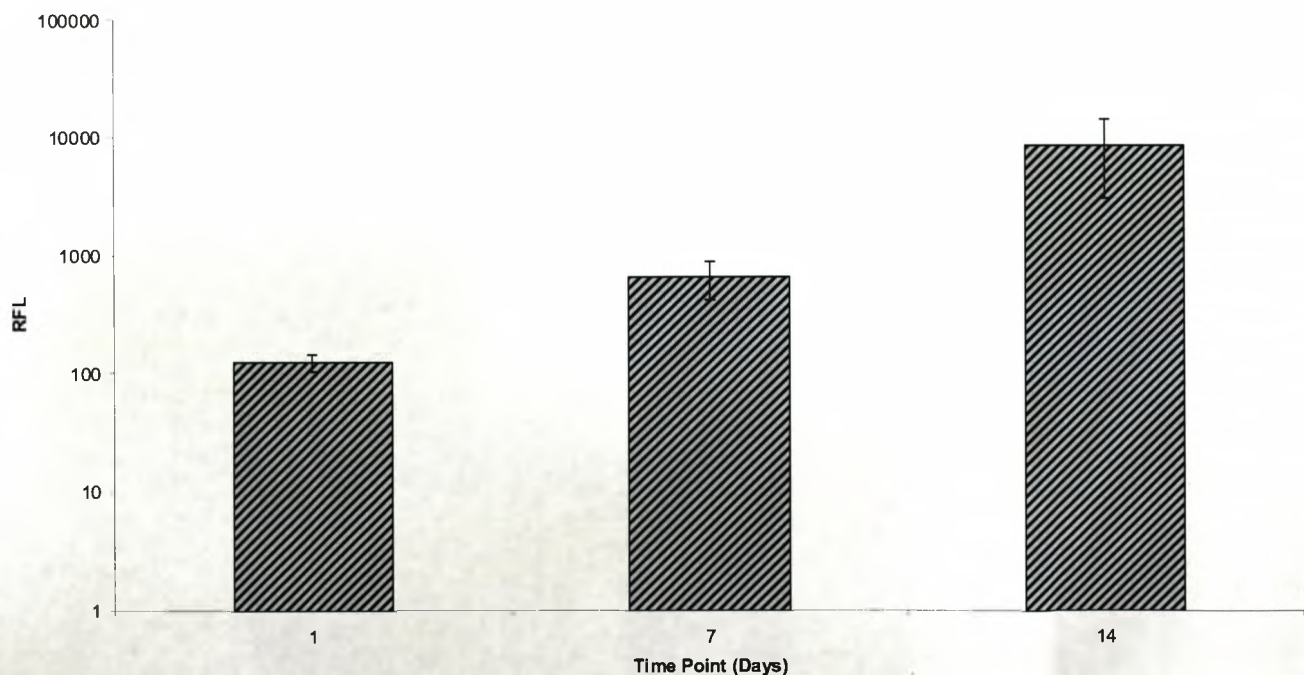
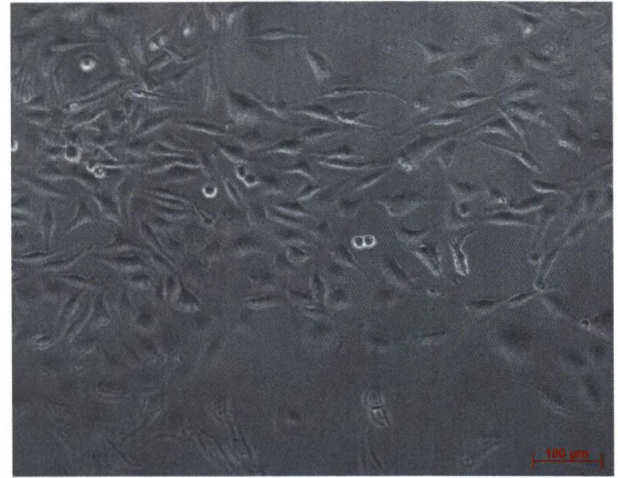
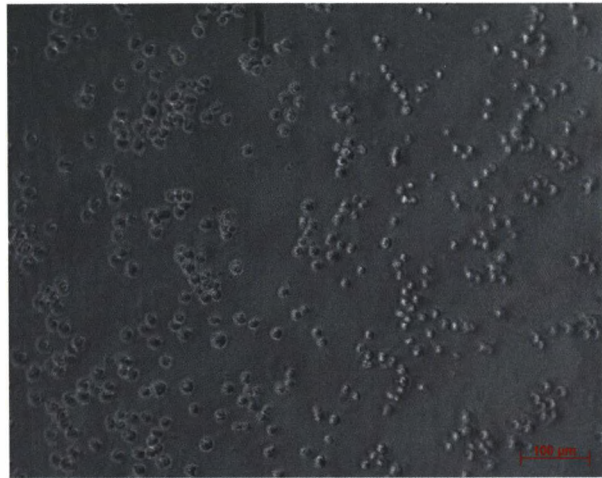


*Fig.4.6. Metabolic activity of dental pulp derived stem cells cultured on platelet poor plasma derived hydrogel surface, using the Almar blue method. Error bars represent 1 standard deviation from the mean, n=3. No correction for change in cell number was made*

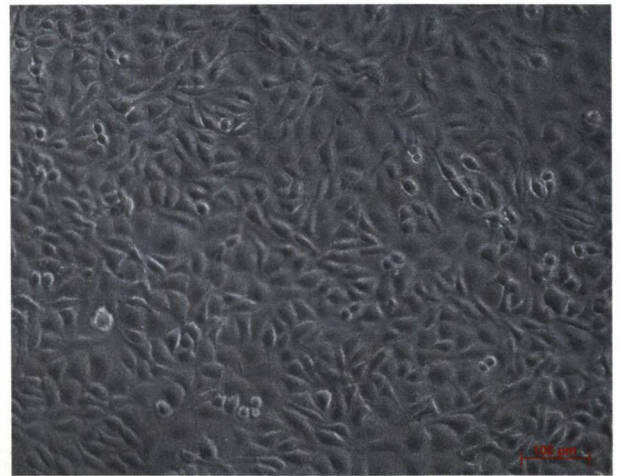


### Matrigel

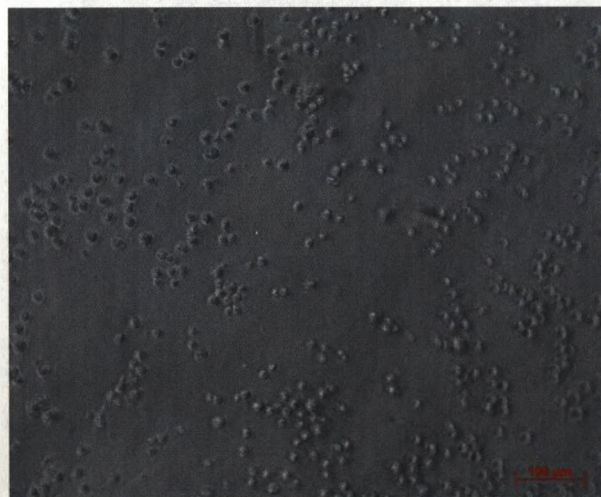
### Blood Plasma Derived Hydrogel



3 Days



5 Days



7 Days

*Fig.4.7. Light Microscopic comparison of the expansion of dental pulp derived stem cells on Matrigel and platelet poor plasma derived hydrogel*

The inability of dental pulp-derived stem cells to undergo expansion on Matrigel highlighted a possible lack of hematopoietic potential of this cell source. Given the similar scaffold properties of Matrigel and platelet poor plasma derived hydrogel it was difficult to hypothesise an explanation for the proliferation observed on one media over the other. In order to identify the potential of platelet poor derived hydrogel as a suitable medium for the expansion of hematopoietic cells, a homogeneous population of dental pulp derived stem cells was isolated from the crude cell population based on hematopoietic characteristics.

Cells were isolated from the primary population based on their ability to efflux Hoechst 33342 dye, a DNA binding molecule which in the presence of DNA fluoresces at 420-505nm. Hematopoietic cells possess a pump system which transects the cell membrane called the ABCG2 pump. This system confers upon the cells the ability to remove the dye from their cytosol prior to DNA binding. Therefore, a population of cells which contains a hematopoietic sub-population can have that population homogeneously isolated using flow-cytometric methods based on a negative fluorescence in the blue area of the spectrum. Cells discriminated for in this manner are referred to as the Hoechst<sup>dull</sup> fraction [436, 437].

These cells were cultured as detailed in section 2.x, by seeding on normal TCP, with Medium 199 containing 5% fetal calf serum and 1% penicillin/streptomycin. Hoechst<sup>dull</sup> cells form discrete colony forming units, a feature characteristic of hematopoietic stem cells, shown both micro- and macroscopically in Fig.4.8. The yield of Hoechst<sup>dull</sup> cells from a population of crude primary dental pulp derived stem cells was approximately 0.1%.



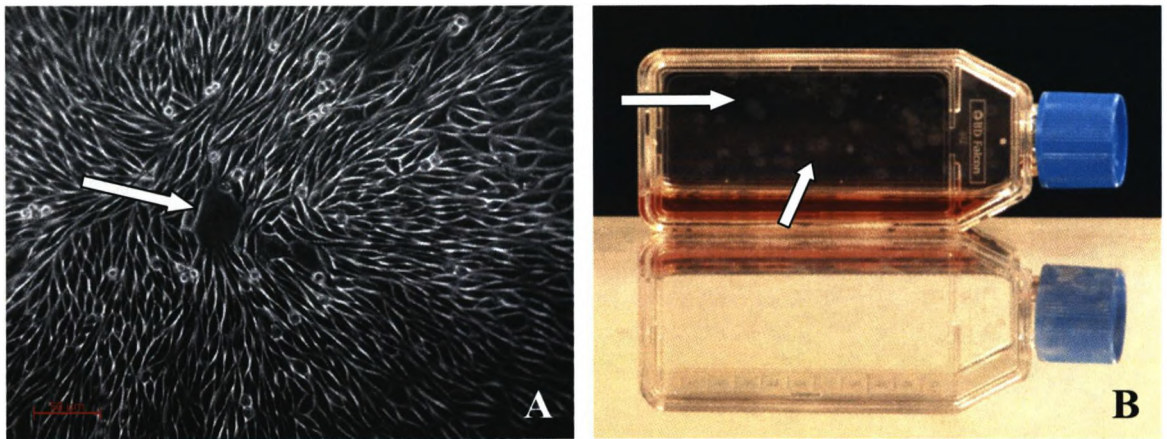


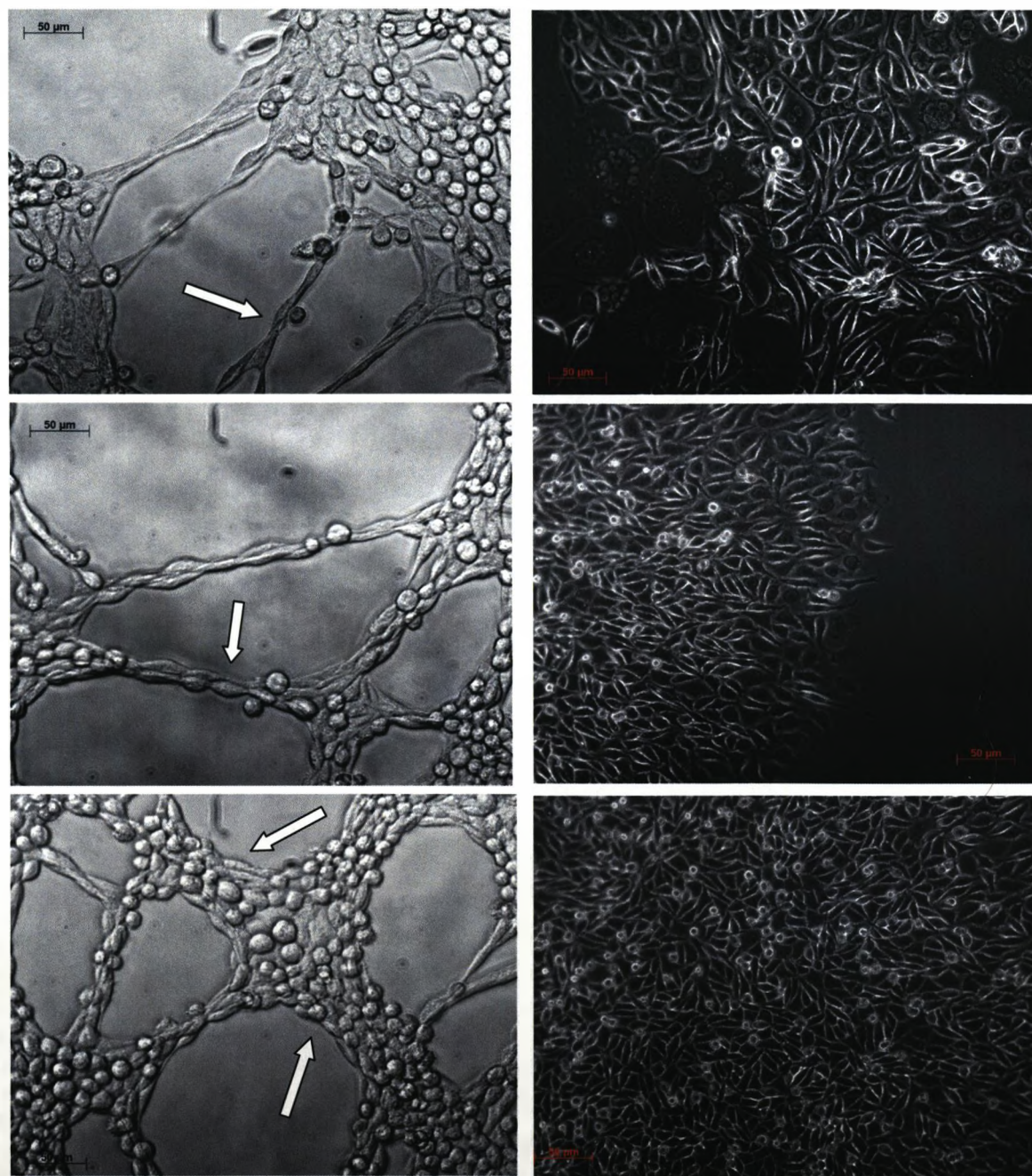
*Fig.4.8. A. Phase contrast microscopic and B. Macroscopic visualisation of colony forming units formed from Hoechst<sup>dull</sup> isolated dental pulp derived stem cells (colony forming units indicated by arrows)*

A further characteristic of haematopoietic/endothelial precursor stem cells is their capacity to form microvascular assemblies in conjunction with a hydrogel substrate [438, 439]. Cells were introduced into the 3mm thick gel surface at a density of  $5.0 \times 10^3$  cells/cm<sup>2</sup> under medium 199 containing 5% fetal calf serum and 1% penicillin/streptomycin and the subsequent morphological changes observed microscopically. Cells organised into microtube-like structures after culture periods of 5 days and proceeded to form densely organised microtube structures throughout the 14 day culture period. This phenomenon was substrate-dependant and did not occur on TCP, with the cells reverting to their more regular cobblestone-like morphology on this less biologically comparable substrate (Fig.4.9). Fig.4.10. illustrates the intimacy of the association and organisation of the Hoechst<sup>dull</sup> cells in these microtubular structures observed using light microscopy while Fig.4.11, further demonstrates the nature of the microtubular assembly using the cytoplasmic cell tracking dye DiO in conjunction with fluorescent microscopy, as detailed in section 2.xviii.



## Blood Plasma Derived Hydrogel

## TCP



5 days

10 days

14 Days

*Fig.4.9. Phase contrast microscopic observation of morphological changes of Hoechst<sup>dull</sup> subset of dental pulp derived stem cells cultured on TCP and platelet poor plasma derived hydrogel (example microvascular like assemblies indicated using arrows)*



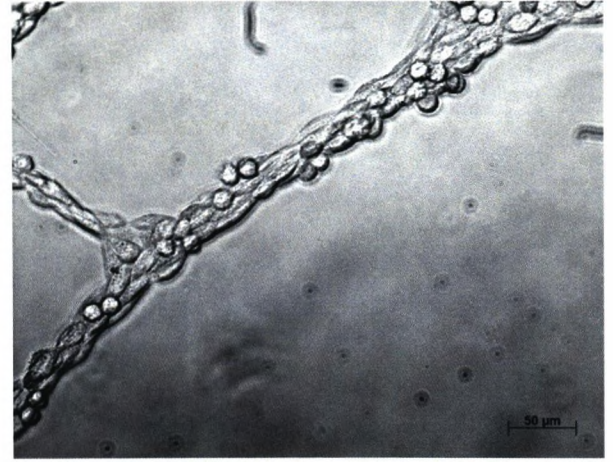
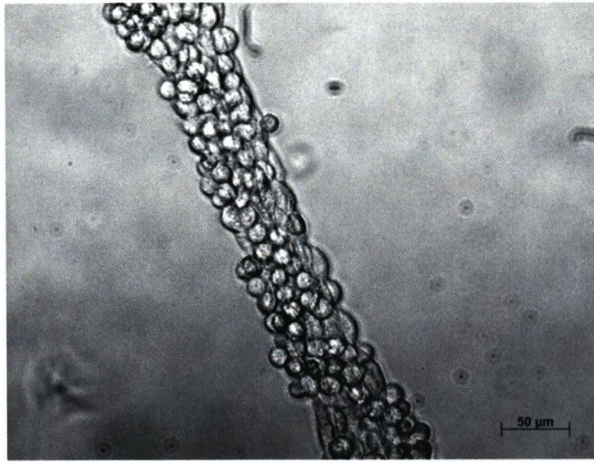


*Fig.4.10. Phase contrast microscopic observation of the intimacy of organisation between Hoechst<sup>stull</sup> sorted dental pulp stem cells cultured on platelet poor plasma derived hydrogel after 14*

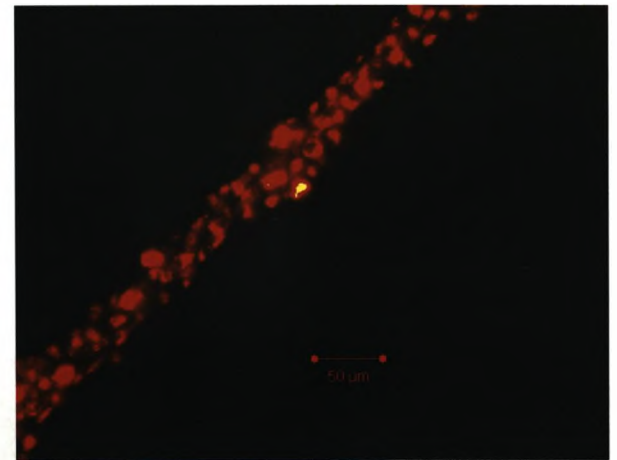
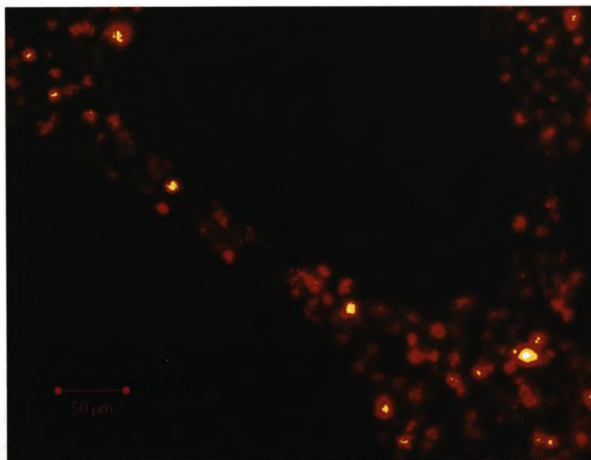


*Fig.4.11. Fluorescent microscopic observation of the cellular intimacy during microvascular assembly using fluorescent cytoplasmic cell tracking*

Cells were subjected to analysis to elucidate their phenotype after formation of microtubular structures to assess if these *Hoechst<sup>dull</sup>* cells had undergone differentiation to form the tubular arrangement or, if this is phenomenon a characteristic of these cells in their native state when cultured in conjunction with this substrate. Typically, formation of microtubular structures in culture is a phenomenon associated with microvascular endothelial cells, the primary cell responsible for forming the inner lining of microvasculature *in vivo*, which, in combination with a suitable three dimensional substrate, forms tubular structures resembling their vascular *in vivo* niche, *ex vivo* [440, 441].

*Hoechst<sup>dull</sup>* cells were analysed immunohistochemically using the protocol outlined in section 2.i to confirm the presence of a subset of cellular antigens associated with a terminal, functional endothelial cell lineage after 14 days of culture on platelet poor plasma derived hydrogel matrix after microscopic observation of microtube formation. Antigens selected were as follows; Von Willebrand Factor, a large glycoprotein involved in haemostasis which is produced in an exclusive subset of cells including endothelium [443]. CD31 (platelet endothelial cell adhesion molecule, PE-CAM) a protein expressed on endothelial cells in addition to selected myeloid cells and is associated with platelet recognition by expressing cells [442]. Finally, VE-Cadherin (CD144), a molecule associated with functionality of endothelial cells by mediating cohesion and organization of the intercellular junctions [444].

Fig.4.12. illustrates fluorescent micrographs obtained from the immunohistochemical staining. *Hoechst<sup>dull</sup>* cells post culture on the platelet poor plasma derived hydrogel demonstrated expression of Von Willebrand factor and CD31 in the cytoplasm of the cells in addition to VE-Cadherin located around the cell periphery. F-actin staining also allowed demonstration of the correct cobblestone morphology associated with endothelial cells *in vitro*, which, although also a feature of primary dental pulp cells is conserved through



Hoechst sorting and the subsequent transition to functional endothelial lineage commitment.

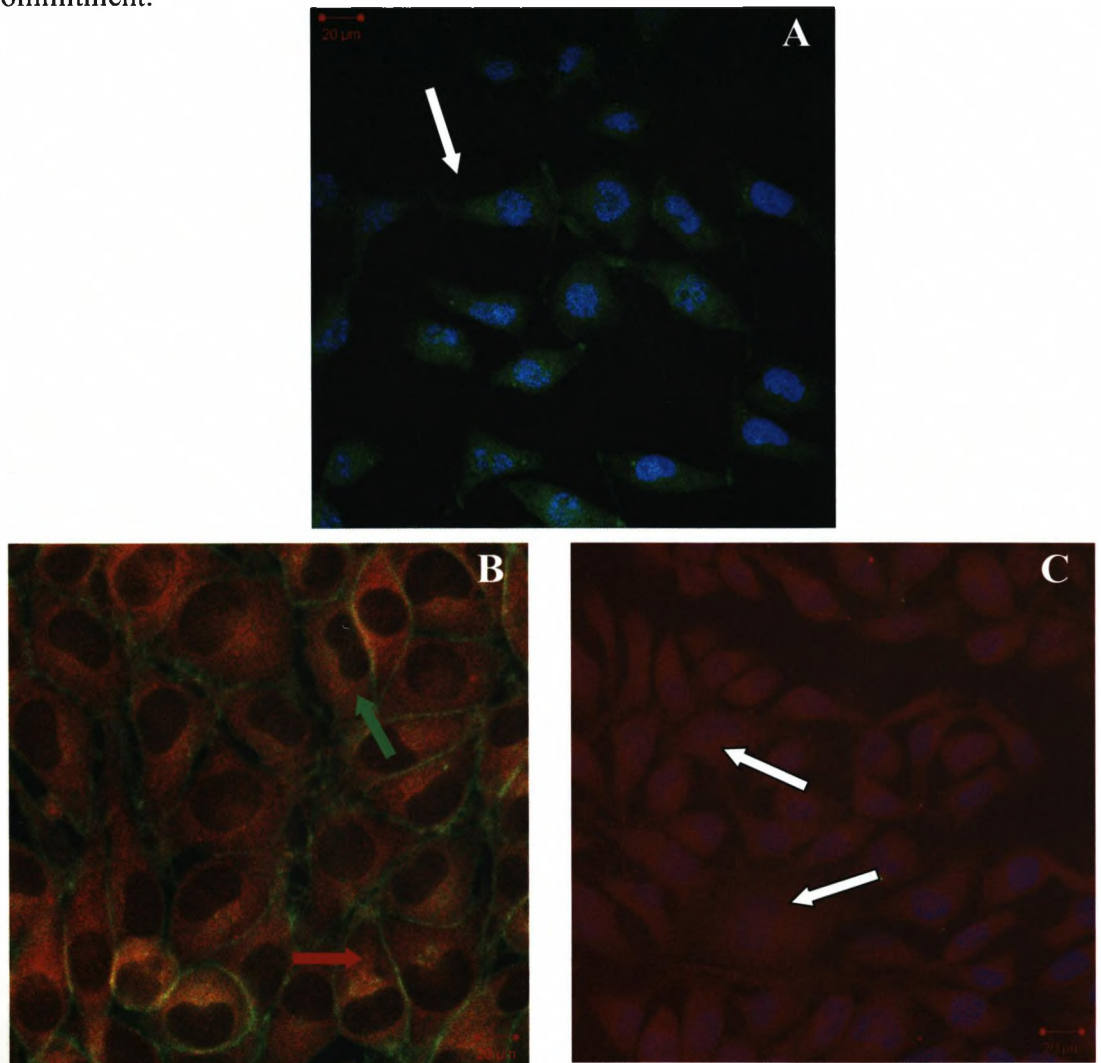


*Fig.4.12. Fluorescent microscopic observation of immunohistochemical staining of dental pulp stem cell derived endothelial cells for **A**; Von Willebrand Factor, Nuclei, **B**; VE-Cadherin, CD31 and **C**; CD31 and nuclei after 14 days culture in conjunction with platelet poor plasma derived hydrogel (positive staining illustrated by arrows)*

In addition to immunohistochemistry, Hoechst<sup>dull</sup> cells cultured on platelet poor plasma derived hydrogel surface were subjected to quantitative antigenic analysis by means of flow cytometry after 14 days of culture and subsequent microtube formation, using the method outlined in section 2.xv (Figs 4.13. & 4.14.). Antigens were chosen as candidate molecules for flow-cytometric

analysis based on their presence on endothelial cells and to determine conversion onto other cellular phenotypes.

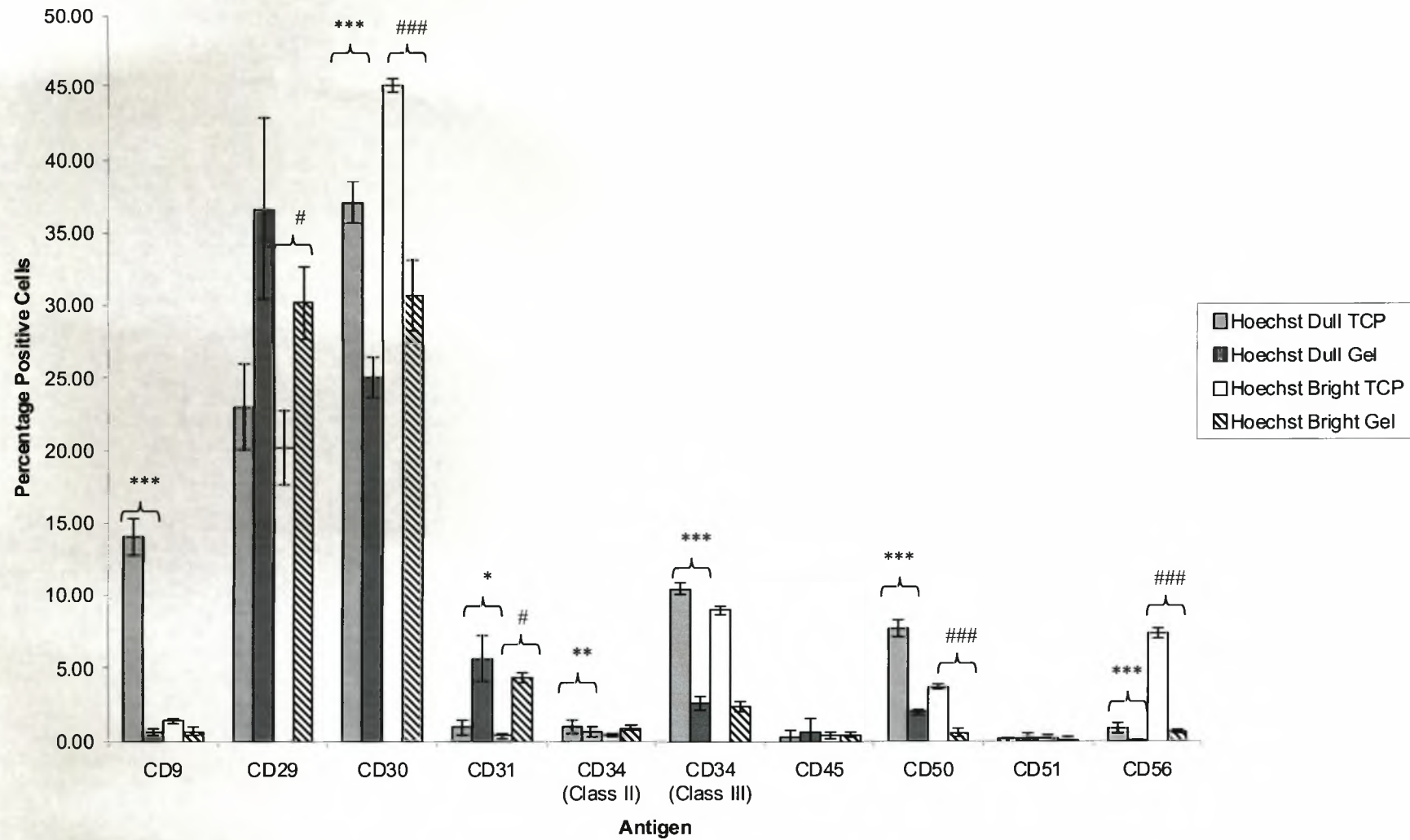


Fig.4.13. Flow-cytometric comparison of the antigenicity of sorted and unsorted dental pulp derived stem cells post differentiation culture in conjunction with platelet poor plasma and tissue culture plastic substrate. Error bars represent 1 standard deviation from the mean, n=3, \*P<0.05, \*\*P<0.01, \*\*\*P<0.001 Hoechst dull TCP relative to gel; #P<0.05, ##P<0.01, ###P<0.001 Hoechst bright TCP relative to gel

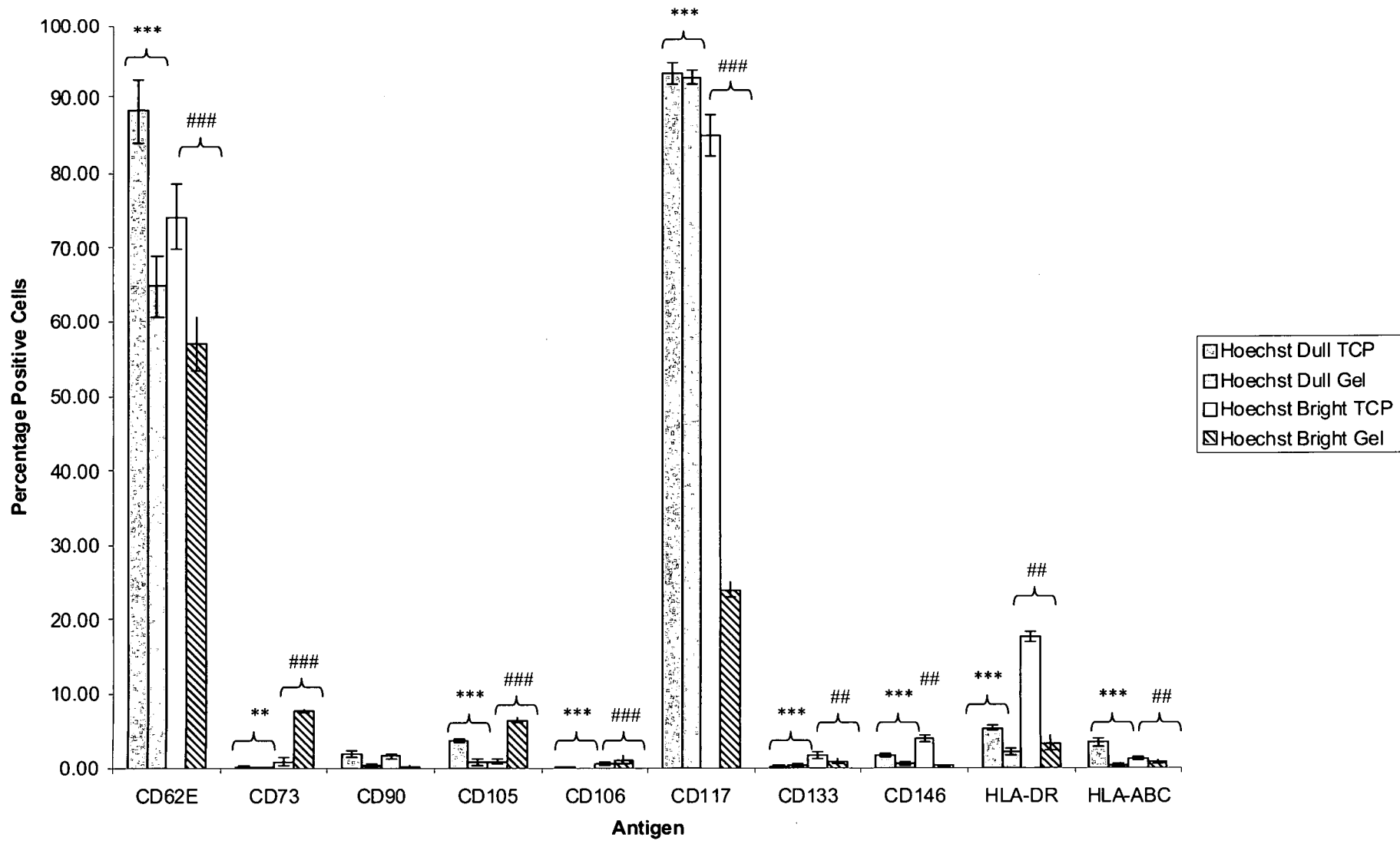


Fig.4.14. Flow-cytometric comparison of the antigenicity of sorted and unsorted dental pulp derived stem cells post differentiation culture in conjunction with platelet poor plasma and tissue culture plastic substrate. Error bars represent 1 standard deviation from the mean, n=3, \*P<0.05, \*\*P<0.01, \*\*\*P<0.001 Hoechst dull TCP relative to gel; #P<0.05, ##P<0.01, ###P<0.001 Hoechst bright TCP relative to gel

Flow cytometry further supported immunohistochemical data by demonstration that Hoechst<sup>dull</sup> cells express markers associated with endothelial cell phenotype cultured on both TCP and platelet poor plasma-derived hydrogel, CD62E (E-Selectin), a cell adhesion molecule expressed exclusively on endothelial cells which is completely absent in heterogeneous dental pulp derived stem cells cultured on TCP [445]. This marker is expressed to a greater extent in cells cultured on TCP which suggests that endothelial cells exist in both populations of cells however the hydrogel substrate is required to facilitate their subsequent formation to microvascular structures. In contrast CD31, a second marker of endothelial cell phenotype, was increased in both populations in contact with the hydrogel substrate suggesting this protein to be a more representative marker of endothelial functionality [442]. Interestingly, expression of CD117, a receptor tyrosine kinase, the cell recognition molecule for stem cell factor, which was thought to be expressed on the surface of haematopoietic stem cells, is maintained pre and post sort suggesting a lack exclusivity of this marker to multipotent cells associated solely with haematopoiesis [446]. In contrast to this, haematopoietic antigens associated with adult stem cells of a mesenchymal lineage decrease as cells take on an endothelial phenotype. CD29, an integrin receptor subunit, which although associated with late integrins is widely regarded as a marker of plasticity, and greatly reduced during culture on hydrogel substrate [447]. Additionally CD90 (Thy-1), a heavily glycosylated surface protein, considered to be a marker of a stem cell phenotype, also decreased during differentiation culture on the hydrogel but not plastic substrates in both cell populations [448]. Although Hoechst<sup>dull</sup> cells maintained on both TCP and hydrogel substrates both exhibited antigens indicative of differentiation to an endothelial lineage, microvascular endothelial tubular superstructure is only apparent when cultured with a suitable three dimensional matrix, in this instance platelet poor plasma derived hydrogel.

The metabolic activities of heterogeneous dental pulp stem cells and Hoechst<sup>dull</sup> selected dental pulp cells cultured on platelet poor plasma derived hydrogel were compared. Cells were seeded at identical densities of  $5.0 \times 10^3$  cells/cm<sup>2</sup>, under medium 199 containing 5% fetal calf serum and 1% penicillin/streptomycin was compared at days 1, 7 and 14 using the almar blue method detailed in section 2.xiv, illustrated in Fig.4.15. During the 14 day time course, a general trend in both populations of dental pulp derived stem cells of a progressive increase in metabolic activity throughout the culture period was concluded, although overall the metabolic activity of the Hoechst<sup>dull</sup> population appeared reduced in comparison to the heterogeneous dental pulp derived stem cells, although this was only found to be statistically

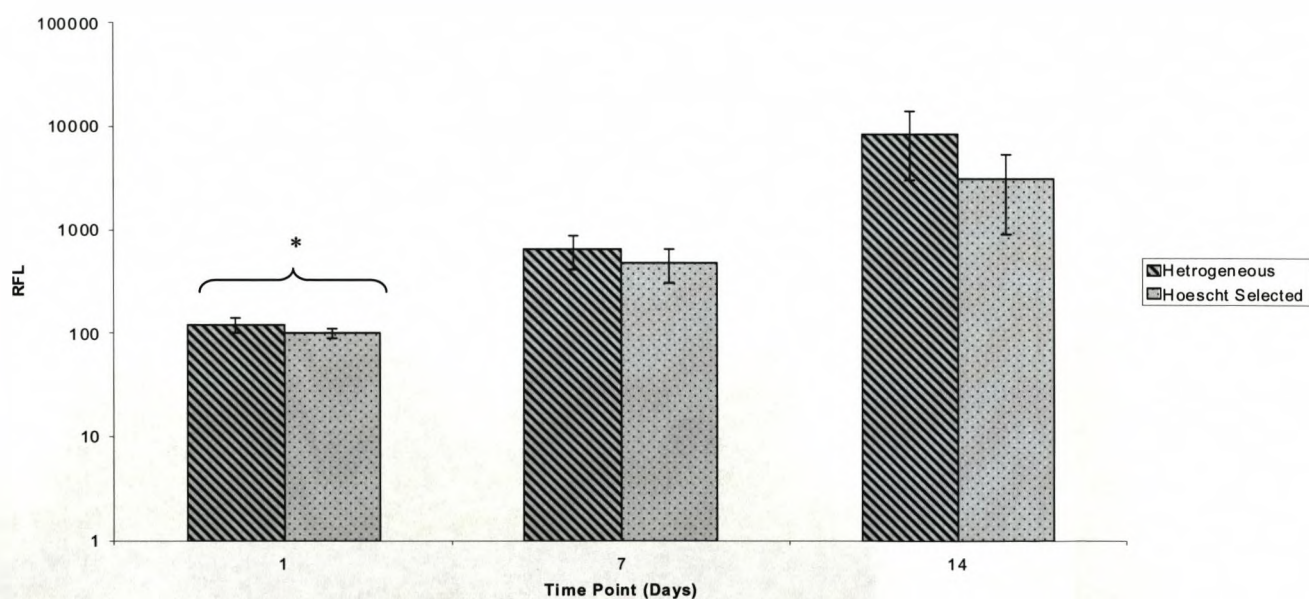


Fig.4.15. Comparison of the metabolic activity of Hoechst<sup>dull</sup> selected and heterogeneous populations of dental pulp derived stem cells cultured on blood plasma derived hydrogel matrix using the Almar blue method. Error bars represent 1 standard deviation from the mean, n=3, \*P<0.05, \*\*P<0.01, \*\*\*P<0.001 No correction for change in cell number was made



#### 4.v Cell growth and migration in vitro, embedded within gel

Human articular chondrocytes were again selected as a candidate cell for assessment of the degree of cellular migration through the hydrogel matrix. As a potential biomaterial, the hydrogel not only needed to sustain adequate cellular expansion as a two dimensional substrata for primary human cells but equally as critical, had to demonstrate the capacity to facilitate free cell movement through the material, as it is this property which permits integration with host tissues when implanted *in vivo*. Chondrocytes were an ideal cell to demonstrate migration due to their proven preference of a hypoxic environment, allowing the hypothesis to be made that their preferred areas would occur towards the base of the gel block [449]. Articular chondrocytes were harvested at passage 6 and embedded in the gel, as discussed in section 2.xvii, in two layers each 20mm in thickness. A cell laden gel was cast, allowed to set thus trapping the cells inside and immediately after setting, a second gel was cast directly onto of the first, in an identical manner. Each block contained  $2.5 \times 10^5$  cells and the cells contained within each layer were identifiable using fluorescent microscopy in conjunction with contrasting cytoplasmic cell tracking dyes.

Fig.4.16. illustrates the data obtained using this method after 5 days of culture. Viewing the figure from left to right progressively down the figure, demonstrates a series of images taken from the z plane (viewing from the surface to the base) of the overall gel block, in proximity to the interface between the two gel layers. It is clear that the chondrocytes have migrated freely through the gel blocks resulting in an even dispersion of cells and no aggregation. The interface between the two layers is also evident and interestingly, sections are present which contain both of the two differently stained cell populations demonstrating the high mobility between the interfaces separating the two independent gel masses. Furthermore, as



hypothesised, the deepest sections taken from the gel contain the greatest number of cells, demonstrating that as the gel becomes thicker, the lower regions become more hypoxic and thus favoured for expansion of primary chondrocytes.

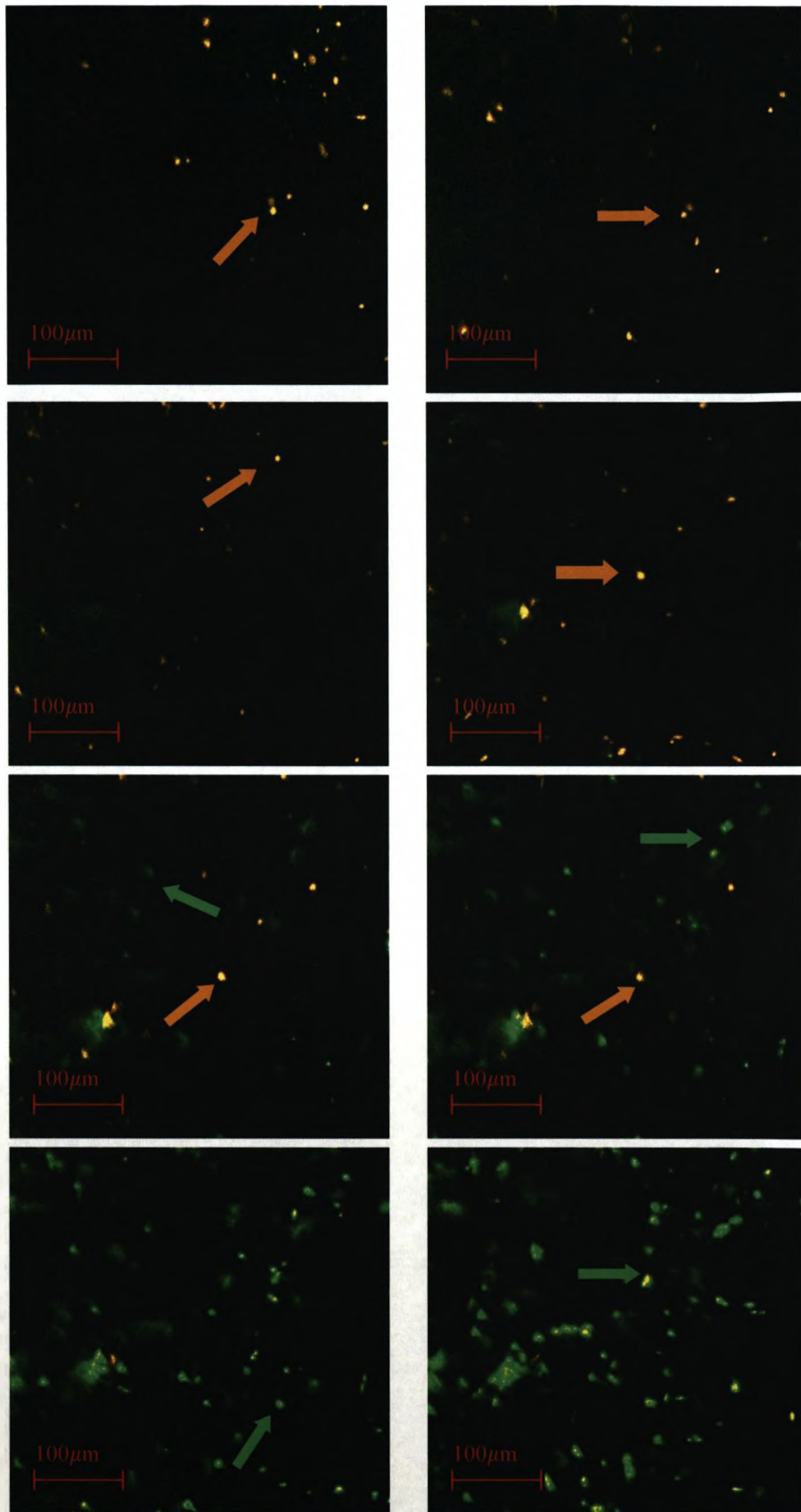


*Fig.4.16. Fluorescent micrographs showing sections taken through the z plane of human articular chondrocyte cells cultured embedded in a platelet poor plasma derived hydrogel block*

#### 4.vi Optimisation of suitable cell phenotype for ectopic soft tissue formation model

*In vitro*, the platelet poor plasma derived hydrogel demonstrated a versatile capacity for the maintenance of primary human cells, using a variety of different methods (Sections: 4.iii-4.v). Ultimately, further exploitation of this system would rely on the gel not only being a suitable media for the facilitation of cell growth *ex vivo*, but also demonstration of its suitability for cell delivery as a component of a tissue augmentation or repair strategy suitable for use in regenerative medical therapies.

Potentially, the platelet poor plasma derived hydrogel was an ideal candidate for the site-directed localisation of primary cells in biomedical technologies. The fluidic nature of the two components of the gellation system meant that this scaffold could be implanted as a liquid by injection, forming a gel matrix under physiological conditions *in situ* in the host. Therefore no incision is required to deliver the material; the entire cell loaded gel construct can be deployed using solely local puncturation.

The system chosen to test the feasibility of the hydrogel as a candidate scaffold for cell delivery *in vivo* employed two syringes connected via means of a 3 way stopcock tap system as outlined in section 2.xix. Media loaded with cells of a defined phenotype were maintained in one syringe, the other contained platelet poor plasma at such volumes that plasma would be at a concentration of 10% (v/v) when combined, an identical method as used to construct the gel *in vitro*. Immediately prior to implantation, the two solutions were infused into one syringe using the tap, then with a further rotation of the tap were directed to the needle and thus injected into the subject.

Initially, this was tested using three cell types, in order to decide an optimum phenotype for progression to further studies to assess the potential of the gel to form tissue *in vivo*. In this model primary human dermal fibroblasts taken from passage 10 human articular chondrocytes at passage 6 and human bone marrow derived mesenchymal stem cells at passage 4 were implanted subcutaneously into 6 week old male NOD/SCID mice using the delivery strategy discussed in section 2.xix at a density of  $5.0 \times 10^5$  cells in a  $300 \mu\text{L}$  total injection volume. Additionally, acellular gel was also implanted in an identical manner using media with no cellular component, to investigate the possible synergistic roles of combined cell and hydrogel elements in the generation of neotissue.

Animals were sacrificed at three weeks post implantation and subsequent ectopic tissue formation observed macroscopically (n=4). Prior to dissection, subcutaneous lumps with no evidence of surrounding inflammation were observed at the sites of hydrogel delivery (Fig.4.17). Dissection revealed that dermal fibroblasts and articular chondrocytes both formed clearly visible neotissues in conjunction with the platelet poor plasma derived hydrogel scaffold (Fig.4.18). This tissue attached to the underlying subcutaneous tissue of the host and was clearly observed to be vascular with noticeable supply from the peripheral circulation of the animal. Mesenchymal stem cells did not form any retrievable tissue. Additionally, the site which had received the acellular hydrogel was also completely devoid of tissue suggesting that the formation of tissue in this manner involves combined roles of both cells and hydrogel matrix.



*Fig.4.17. Macroscopic observation of subject post sacrifice indicating visible subcutaneous tissue formation prior to dissection (1:3)*

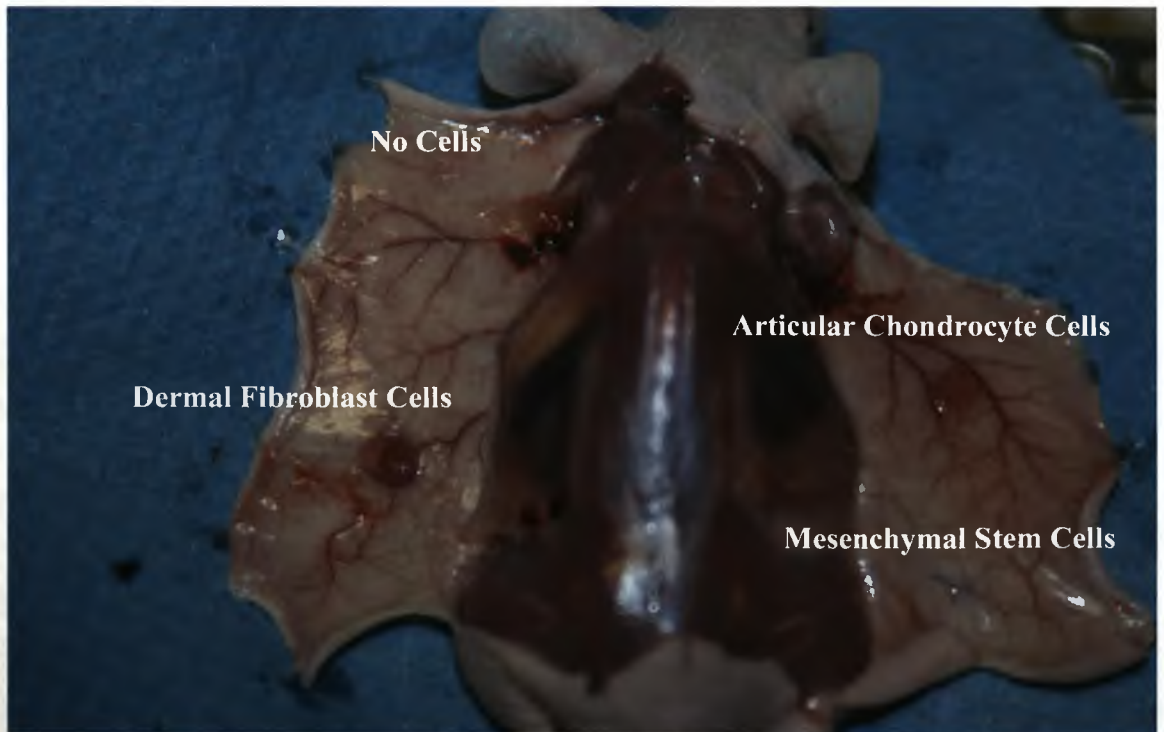


*Fig.4.18. Macroscopic visualisation of neotissue formation after 3 weeks as a result of implantation of primary human cells in conjunction with platelet poor plasma derived hydrogel (1:3)*



Explanted tissues were prepared as outlined in section 2.xxi and subjected initially to tinctural staining using haematoxylin and eosin as described in section 2.xxiii. This allowed demonstration of the densely cellular nature of the neo-tissue with extensive matrix production around the cells. The tissue formed a discrete mass confined within the gel construct at the site of implantation, with no observable bidirectional migration of cells from the surrounding tissue or subsequent infiltration into the surrounding host tissue. The tissue interfaced with the host by means of a ribbon of connective tissue between itself and the underlying host subcutaneum (Fig.4.19).

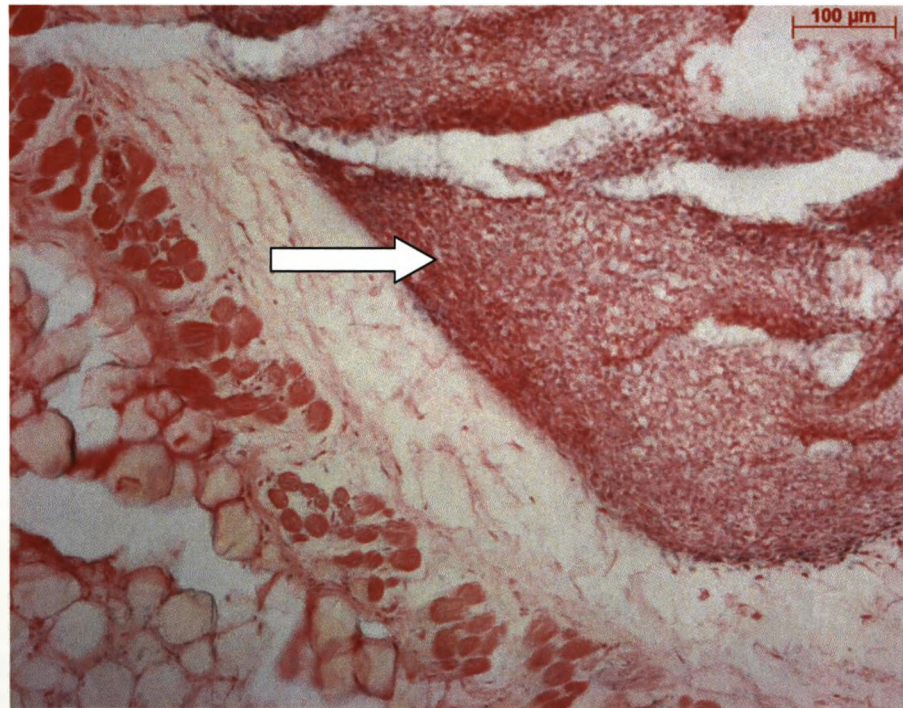


*Fig.4.19. Light microscopic analysis of Haematoxylin and Eosin staining of explanted human dermal fibroblast neo tissue after 3 weeks of in-vivo culture (ectopic gel mass indicated by arrow)*

As a result of this data, dermal fibroblasts were chosen as the candidate cell for further *in vivo* studies using this system after demonstrating the most rapid and reproducible tissue formation in this initial set of animal models.

#### 4.vii Tissue Formation Model

After initial data demonstrated the capability of human dermal fibroblasts in conjunction with blood plasma derived hydrogel scaffold to reliably produce cellular, ectopic tissue in animal models, an additional series of experiments was designed to further validate the hydrogel system as a tool for site-directed cellular delivery. Importantly, it was necessary to elucidate if hydrogel derived tissue would increase in bulk further if incubated *in vivo* for periods longer than was permitted for the initial group of experimental animals (3 weeks), or alternatively, would the tissue eventually become immunogenic or necrotic and ultimately disappear possibly resulting in the premature death of the animal? Furthermore, after demonstrating that acellular gels did not form tissue, it was required to discover the threshold number of cells that was required to facilitate the synergy of neo-tissue formation in conjunction with the hydrogel matrix. In conjunction, it would also be possible to elucidate if the initial cell number at the point of implant was ultimately reflected in the mass of the tissue at the point of explantation. Further characterisation of the tissue would also be required using techniques to determine the contribution of various cell types in forming the bulk of the tissue. Crucially, did the human dermal fibroblasts implanted in the initial injection fraction remain in the tissue throughout *in vivo* culture? Finally, characterisation of the matrix within the tissue would be required to qualify its biodegradability during *in vivo* cell culture.

Animals received defined numbers of dermal fibroblasts, taken from passage 6 of between the upper and lower limits of  $1.0 \times 10^5$  and  $2.0 \times 10^6$  cells in an injection volume of  $300 \mu\text{L}$  using the previously validated model of 4 subcutaneous implantation sites per male 6 week old, NOD/SCID mouse.

In order to identify the ability of the platelet poor plasma derived scaffold system to maintain the integrity of the ectopic tissues, experimental animals



were maintained post implantation for periods as long as 10 weeks. Fig.4.20 shows one of these subjects and the respective cell number per injection site. This clearly illustrates the presence of tissue after this extended time period demonstrating the capacity of the hydrogel to maintain a stable environment for the cells contained within to proliferate for the desired time course necessary for the augmentation of a particular tissue defect. The neotissue develops its own vasculature from the host peripheral circulation, further emphasising this observation from earlier implants. Therefore, necrosis of even large tissue masses is prevented by rapid angiogenesis, ensuring an adequate supply of nutrients and oxygen in addition to removal of waste compounds into the host circulation. Furthermore, the hypothesised immunocompatibility of the implant with the host reduces macrophage mediated degradation allowing the tissue to expand unhindered.

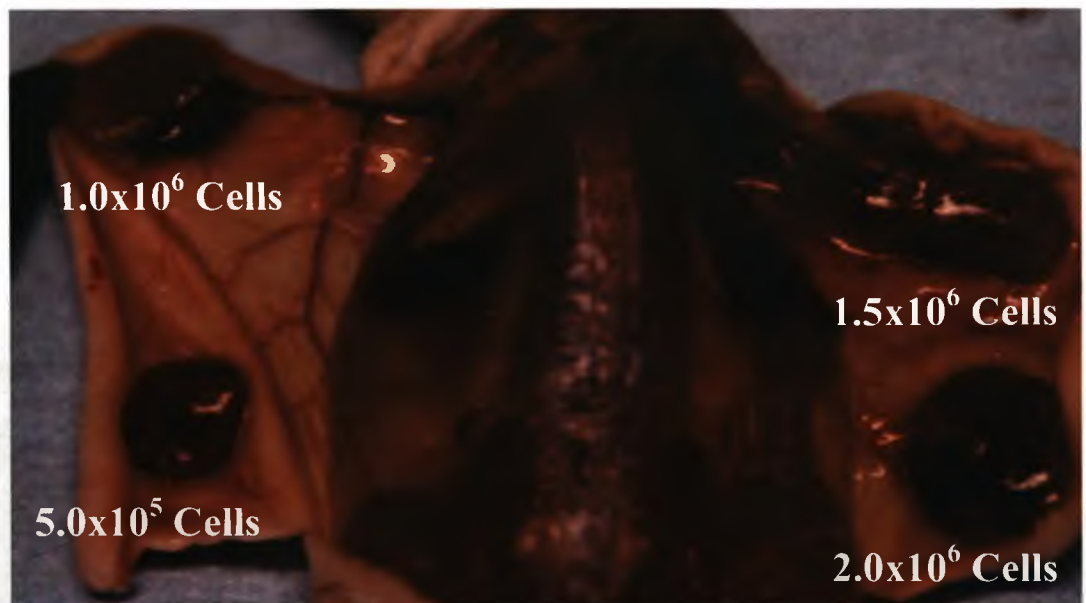


*Fig.4.20. Macroscopic observation of human dermal fibroblast cells after 10 weeks of in-vivo incubation in conjunction with platelet poor plasma derived hydrogel matrix*

Implanting smaller numbers of cells than previously demonstrated ectopic tissue formation and allowed for the calculation of a threshold number of cells

per scaffold that was capable of forming neo-tissue within the platelet poor plasma derived hydrogel. It was elucidated that  $2.0 \times 10^5$  human dermal fibroblasts per injection was the threshold number capable of forming ectopic tissue using this model. Any cell number lower than this did not result in tissue formation even with *in vivo* implantation periods of up to 10 weeks. As previously hypothesised, the formation of neo-tissue from cells implanted in conjunction with the hydrogel matrix is synergistic, the fibrin scaffold within the hydrogel providing a suitable three dimensional meshwork in which the cells can attach and proliferate. Additionally, however the extra cellular matrix laid down by the cells contained within provides stability and further cross linking to enhance the longevity of the scaffold *in vivo*.

Evidence was also required to determine the extent to which the initial number of cells in the implant contributed to the ultimate bulk of the neo-tissue. In regenerative applications, having control such that a defect of a defined size could be implanted with a number of cells pre-calculated to generate a suitable quantity of tissue to precisely fill a defect would be invaluable. The first stage of evaluating this potential however, is deciding the magnitude of the role that the cells delivered to the scaffold play in influencing the terminal size of the subsequent tissue. Fig 4.21 illustrates incremental defined numbers of human dermal fibroblast cells in an animal sacrificed after 6 weeks of *in vivo* culture, externally visible lumps pre-dissection clearly demonstrated the increase in subcutaneous tissue size resulting from higher numbers of initial cells.

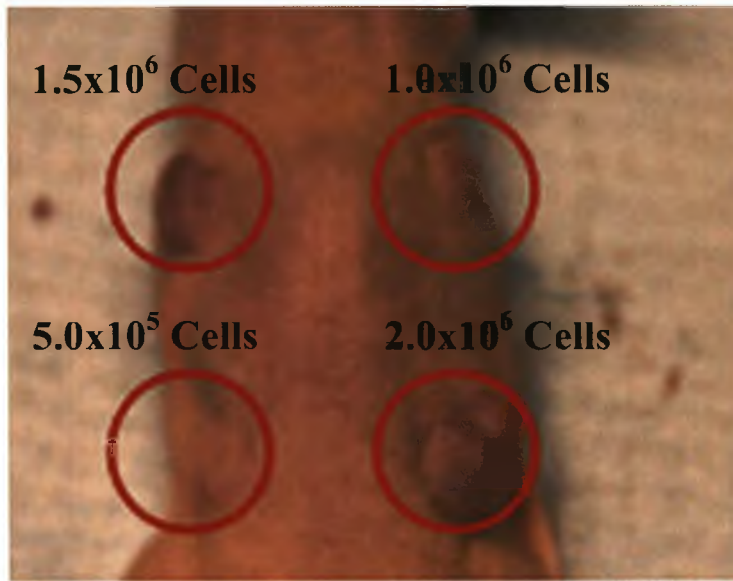


*Fig.4.21. Macroscopic demonstration of the influence of initial cell number on terminal tissue bulk (1:3)*

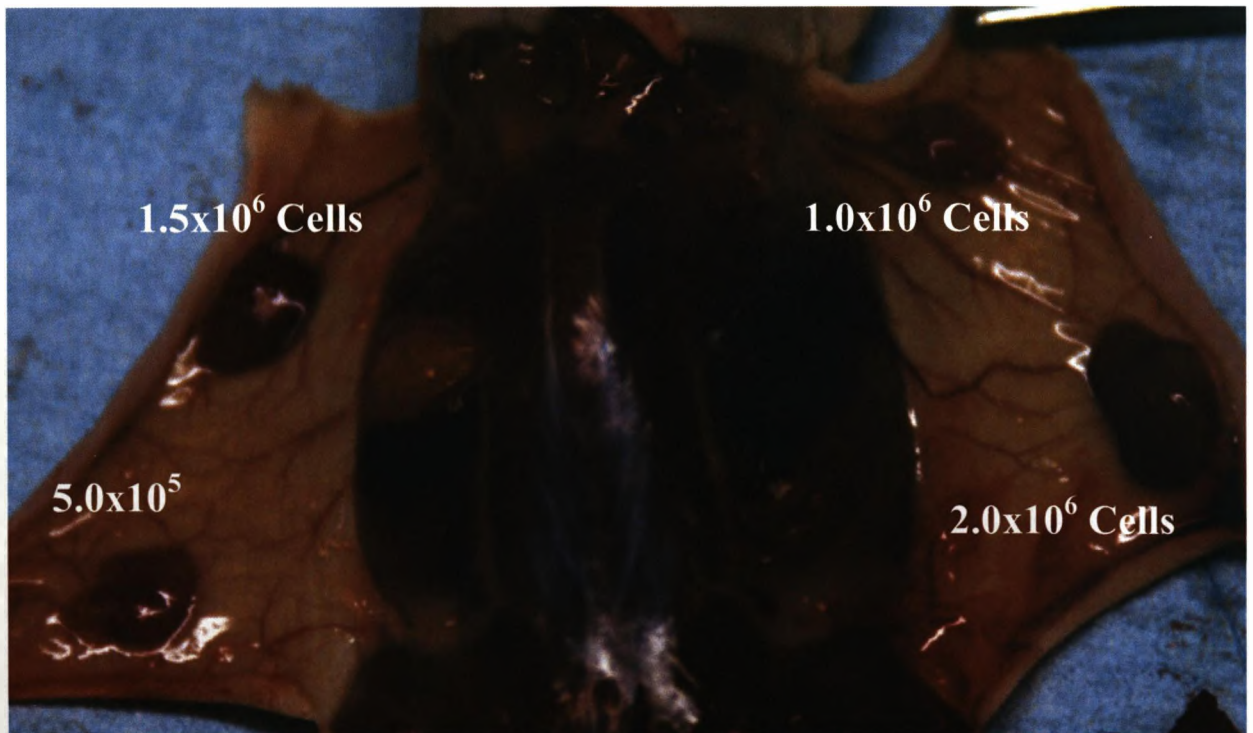
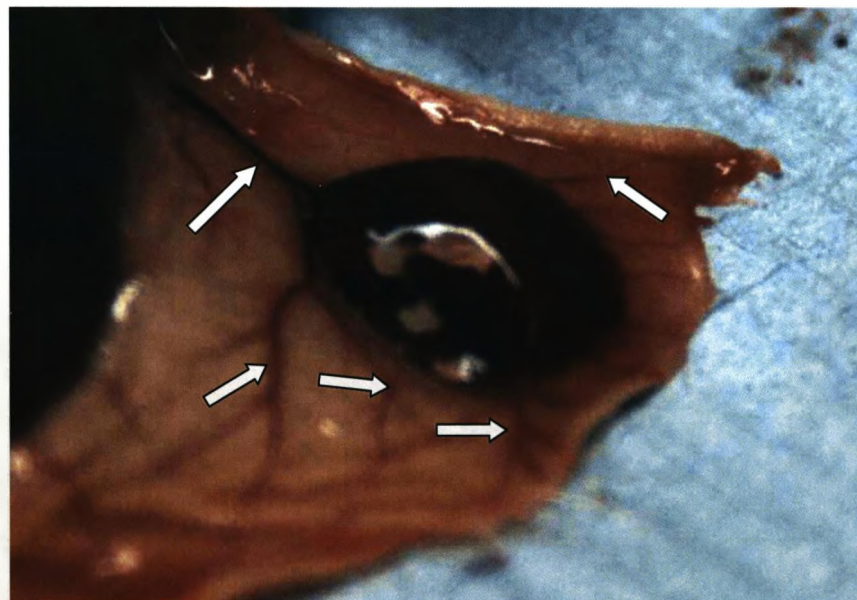


*Fig.4.22. Macroscopic comparison of cell seeding number and neotissue bulk at after 6 weeks of in-vivo culture (1:4)*



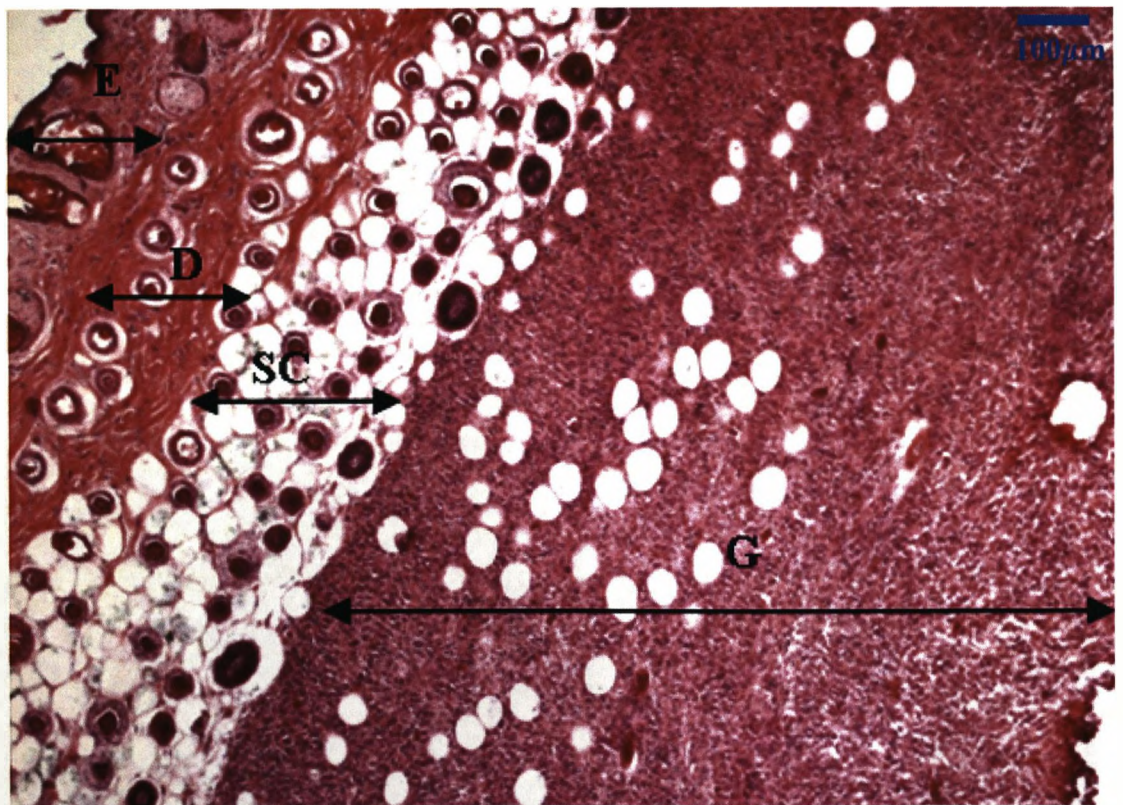
At the point of explantation, Fig.4.22 illustrates the same specimen as Fig.4.21. Immediately the differences in the size of the neo-tissues are clear and furthermore become incrementally larger as the number of human dermal fibroblast cells in the implant was increased. Therefore, the cell number introduced in the implanted hydrogel was proportional to the bulk of the tissue that formed ectopically as a result of the cellularisation of the scaffold.

Fig.4.23, taken from an implant containing  $2.0 \times 10^6$  dermal fibroblast cells after 6 weeks of *in vivo* culture demonstrates prior to histopathology, the extent of the vascularisation of the ectopic tissue. From this figure the neo-vascular network can be observed converging into the gel from the periphery of the host, then subsequently radiating from the ectopic tissue into the host sub-dermis, further demonstrating the degree of the host infiltration.



*Fig.4.23. Macroscopic observation of the vascularisation of a neo-tissue after 6 weeks of in-vivo culture (vasculature indicated using arrows) (1:4)*

Processing of explanted neotissue as detailed in section 2,xxii, followed by subsequent histological examination further demonstrated the consistency in the structure of the ectopic mass. The cellularised mass formed below the subcutaneous layer at the site of injection in all implantation sites, with no adhesion to the underlying musculature of the host animal. Fig.4.24 illustrates the cellularised gel mass stained using haematoxylin and eosin to observe the position of the gel in reference to anatomical structures associated with the native tissue of the host. The ectopic tissue formed exclusively below the dermal layers, with no observable penetration of the gel mass through the subcutaneous layer of host tissue.



*Fig.4.24. Light microscopic observation of Haematoxylin and Eosin stained explanted tissue, demonstrating proximity to host tissue. (E; Epidermis, D; Dermis, SC; Subcutaneous layer and G; Gel mass)*



As hypothesised, the cell loaded hydrogel formed extensively cellular tissues with substantial deposition of extracellular matrix from the cells contained within the implant; this is demonstrated using haematoxylin and eosin staining in Fig.4.25. The extent of matrix deposition combined with the apparent non-myeloid morphology of the cells observed using these histological techniques suggested they were not cells associated with the murine immune system which may have been the case, essentially forming a large immunogenic mass as a result of host immunostimulation. Immune cell recruitment may possibly have occurred as a result of an endogenous component of the gelation system; the platelet poor plasma or a component of the culture media or the cell component; the human dermal fibroblasts contained within the implant. However, this data; showing fibroblastic like morphologies as well as the rapid proliferation and colonisation of the three dimensional environment which would be expected from dermal fibroblasts when considering their rapid population doubling time *in vitro* was suggestive that the cells responsible for the generation of these tissues were the human dermal fibroblast cells which were directed to the site in the initial implant.

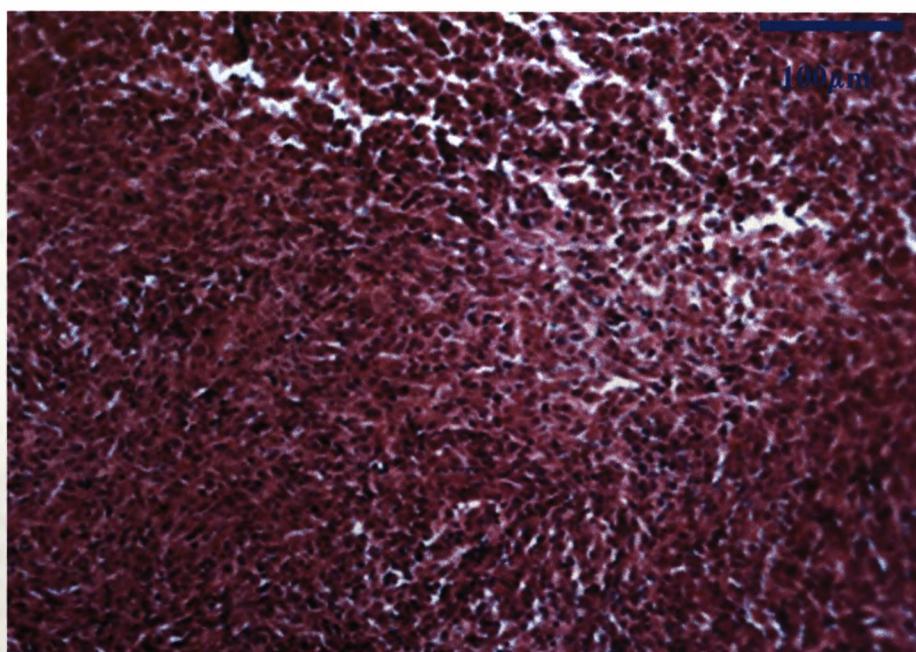


*Fig.4.25. Light microscopic characterisation of haematoxylin and eosin stained ectopic tissue showing the densely cellular nature of the hydrogel derived tissue mass*

The ability of the platelet poor plasma hydrogel to deliver cells delivery was further confirmed by the observation of infiltration of of host structures into the neo-tissue mass. Fig.4.26 illustrates the beginnings of the migration of adipose cells from the subcutaneous tissue of the host into the ectopic tissue mass.

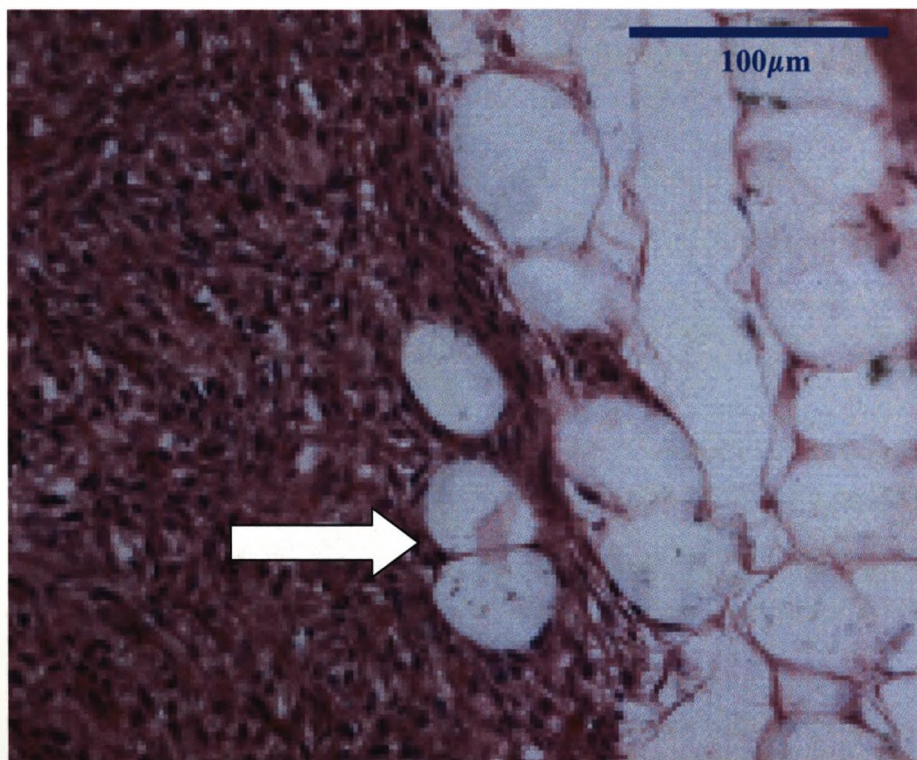


*Fig.4.26. Light microscopic observation of haematoxylin and eosin stained explanted tissue demonstrating the progression of adipose infiltration into the hydrogel derived tissue mass (adipose cells indicated by arrow)*

During extended periods of *in vivo* culture of the hydrogel derived tissue, adipocyte infiltration became more extensive, characterised by adipocytes



observable throughout the entire mass of the neo-tissue, illustrated in Fig.4.27. Throughout all explanted tissues there was no observation of fibrous capsule formation further emphasising the immunocompatibility of the foreign tissue derived using this system.

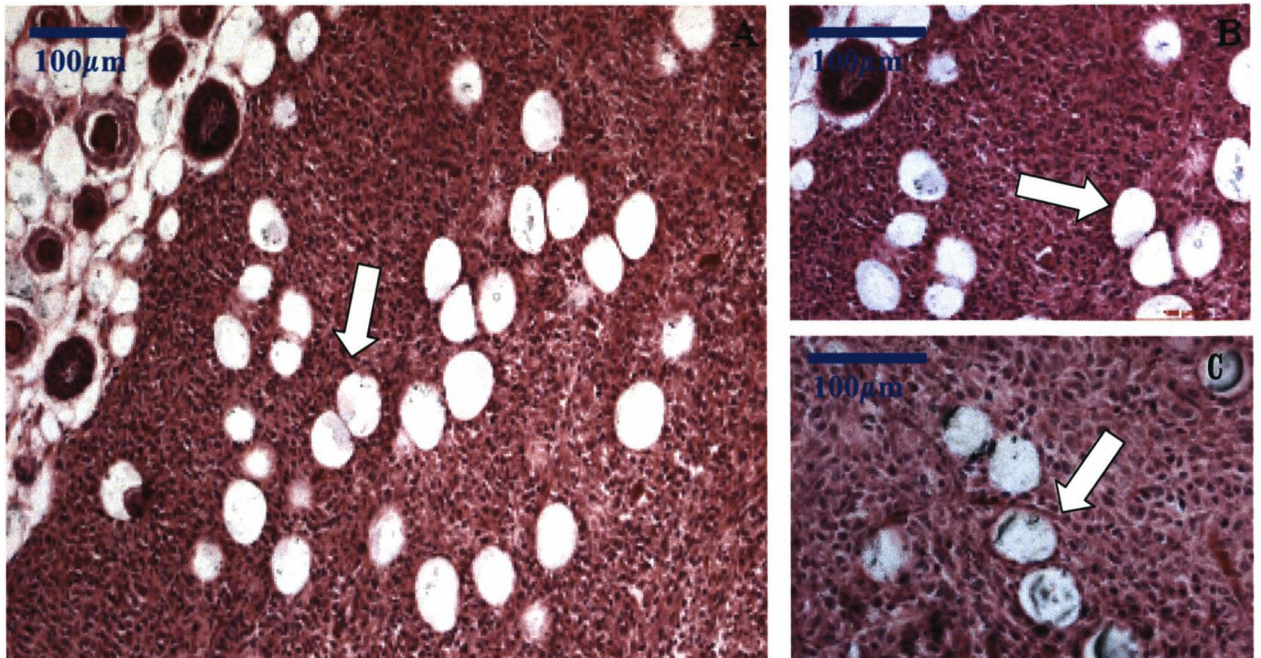
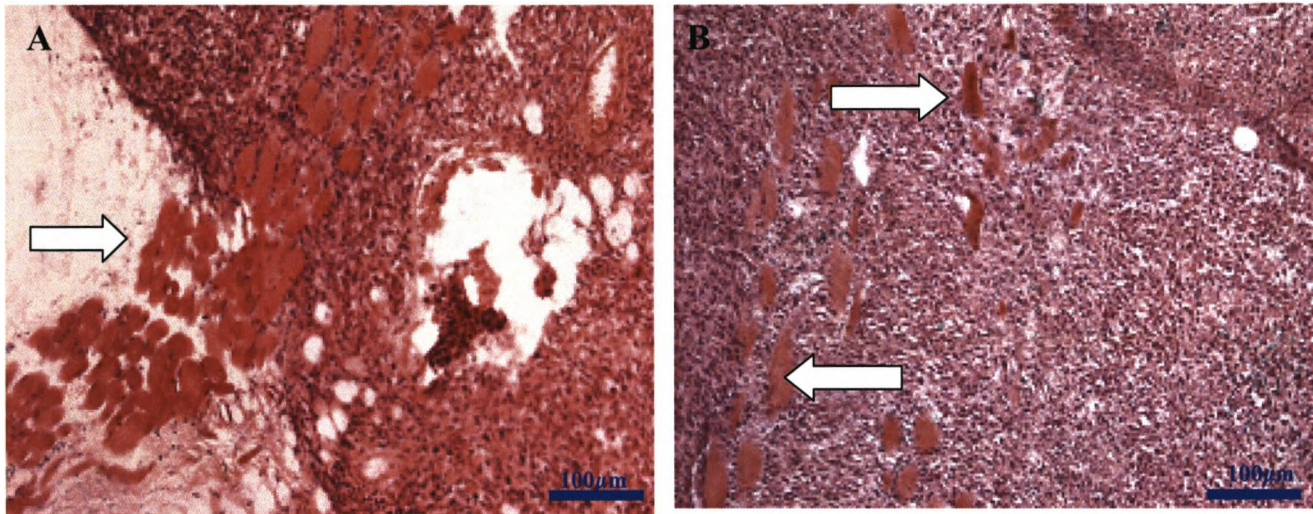


Fig.4.27. Microscopic observation of haematoxylin and eosin stained explanted tissue illustrating extensive infiltration of host adipose into the hydrogel derived tissue mass (adipose cells indicated using arrows)

Ectopic tissues further demonstrated excellent integration with the host tissue by the infiltration of host musculature of the tissue mass. In tissues explanted after the shortest time of *in vivo* incubation (4 weeks) this phenomenon was observed by the presence of small aggregates of host muscle fibres entering the tissue from the host sub-dermis. However, as periods of *in vivo* incubation became more prolonged (6-10 weeks) this early muscle penetration progressed into the development of a completely neo-muscle block, infiltrating the tissue on the sub-dermal face and exiting the tissue on the opposite side, forming a continuous ribbon of host musculature through the



foreign tissue. Both early stage infiltration, in addition to full muscle block formation and infiltration are characterised in Fig.4.28.



*Fig.4.28. Microscopic observation of haematoxylin and eosin stained ectopic tissue demonstrating A. complete continuation of a neo-muscle block through the hydrogel derived tissue and B. early infiltration of muscle fibres into the cellular gel mass (muscle fibres indicated by arrows)*

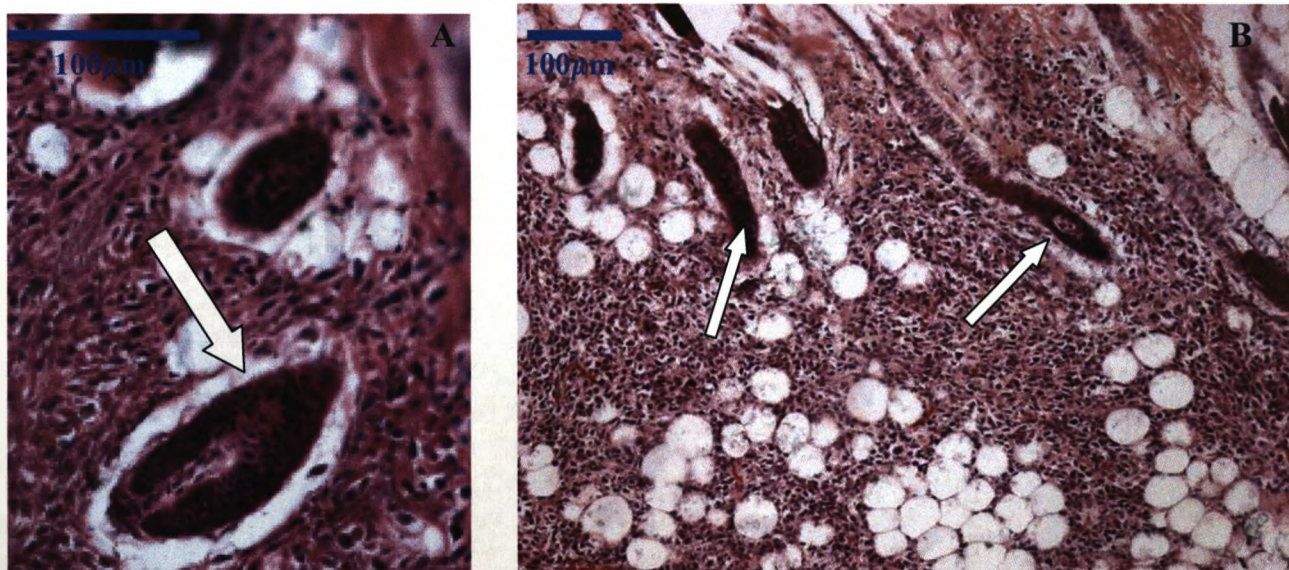


*Fig.4.29. Microscopic observation of haematoxylin and eosin stained ectopic tissues illustrating infiltration of host hair follicles into the hydrogel derived tissue mass. (Hair follicles indicated using arrows)*



Acceptance of the implanted cellular scaffold with the host tissues was further characterised by consistent observation of the appearance of host hair follicles infiltrating the tissue from the sub-dermal layer of tissue, illustrated in Fig.4.29.

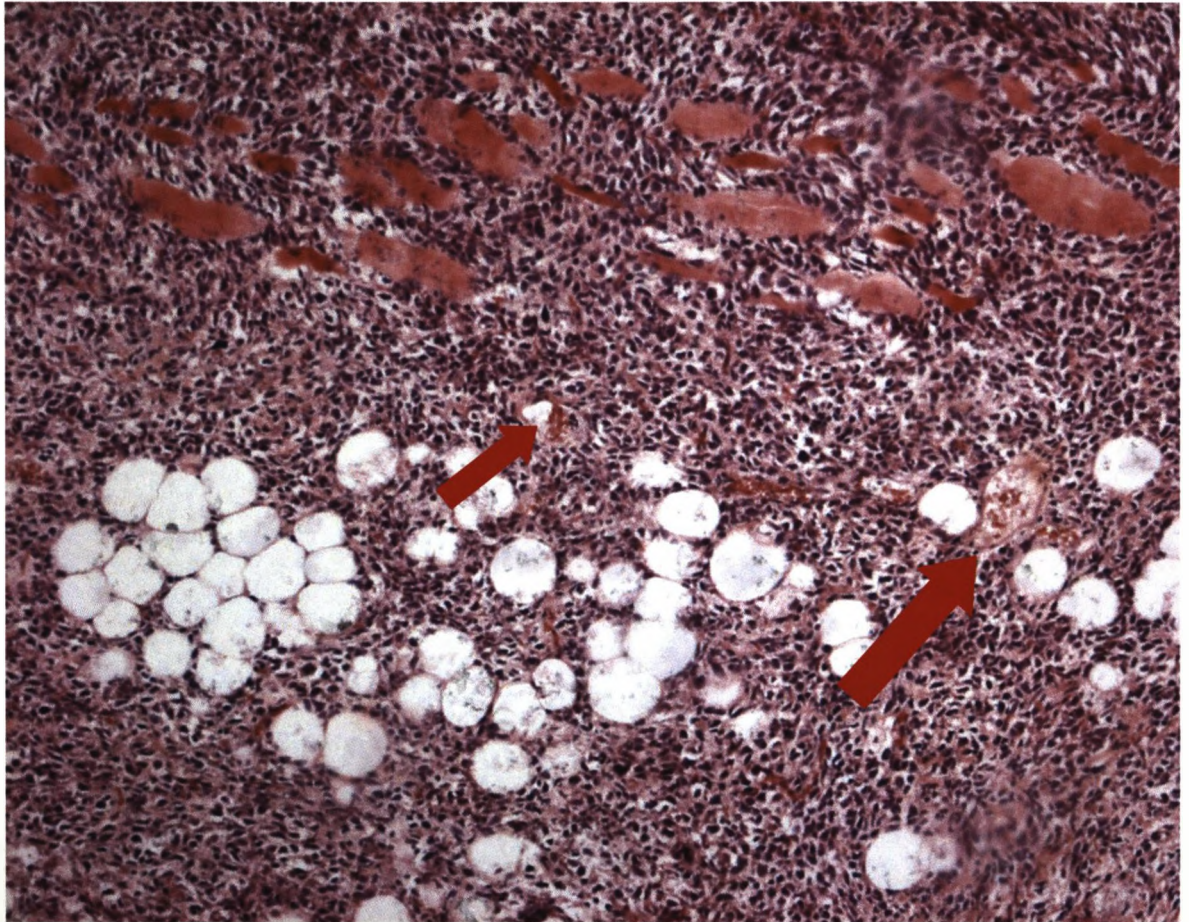


*Fig4.30. Microscopic analysis of hematoxylin and eosin stained ectopic tissue indicating the areas of apparent host microvasculature(microvasculature indicated using arrows)*

Macroscopic observation of host vasculature infiltration was further confirmed by the regular observation, microscopically, of host microvasculature throughout the explanted hydrogel derived tissues. The functionality of the vasculature was additionally confirmed by the presence of

erythrocytes in the transverse sections through the neo-vascular network penetrating the ectopic tissue (Fig.4.30).

If platelet poor plasma derived hydrogel was to be confirmed as a mechanism for delivery of cells in regenerative medical therapies the scaffold would not only have to possess the ability to facilitate cellularisation of the area into which it was delivered, the process would need to be defined. Cells implanted as part of a directed tissue engineering strategy in conjunction with this hydrogel system would need to be of a suitable phenotype to augment the repair of a particular damaged tissue. Therefore the hydrogel would have to be capable of maintaining the location and also the original phenotype of the implanted cells through suitable *in vivo* culture periods which would facilitate tissue repair in a true regenerative medical application.

Crucially, it was necessary, therefore, to confirm hypotheses suggested on the basis of conventional histology (Fig.4.24) that the cells responsible for the cellularisation and resulting expansion of the implanted hydrogel derived tissue were indeed the cells that were introduced with the scaffold material at the point of implantation. Secondly, characterisation of the cells within the tissue was also required to elucidate if not only were the cells within the tissue the original cells that were delivered in the implant, but also to assess to what extent did the three dimensional hydrogel matrix permitted the cells to maintain their fibroblastic phenotype *in vivo*.

Female NOD/SCID mice were implanted with platelet poor plasma derived hydrogel containing  $1.0 \times 10^6$  human dermal fibroblast cells derived from a male donor, in an identical manner to that previously described. Carrying out the implantation using a defined, controlled gender of both cells and animals in this manner would permit the observation of human Y chromosomes in frozen slices of explanted tissue using fluorescence *in situ* hybridisation as explained in section 2.ii. Given that this chromosome would not be present in

the female murine cells native to the host, this method would provide a definitive method of discriminating between native and implanted cells.

Fig.4.30. Illustrates the data obtained from the fluorescence *in situ* hybridisation studies clearly allowing observation of aggregates of cells containing Y chromosomes, an impossible structure for host cells to contain, thus proving both the origin and the speciation of the cells contained within the neotissue.

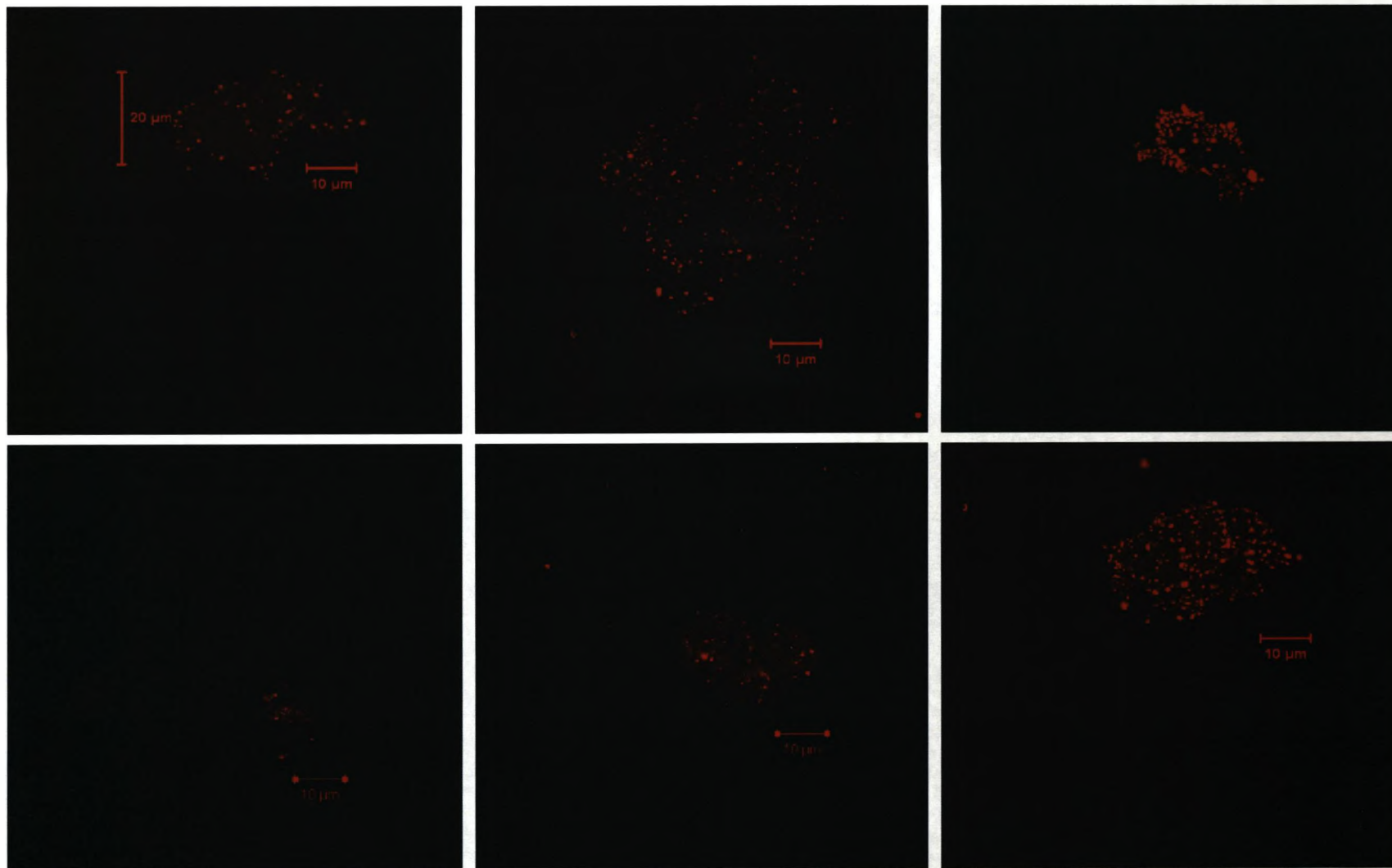


*Fig.4.30. Fluorescent microscopic observation of fluorescent in-situ hybridisation of explanted tissue with probes targeted against the human Y chromosome*



Confirmation of the maintenance of the original phenotype of the cells contained within the implant was demonstrated using immunohistochemistry targeted against the fibroblast specific D7-Fib antigen, illustrated in Fig.4.31. This data shows the typical position of the hydrogel derived tissue mass, made familiar from the conventional histological staining with immunohistochemical analysis performed *in situ*. It is clear from observation of abundant red positive staining that cells expressing D7-Fib are present in the tissue. This data combined with the observation of cells with fibroblastic morphologies using haematoxylin and eosin staining and the presence of human Y chromosomes using fluorescence *in situ* hybridisation is conclusive proof that the cells responsible for the formation and expansion of the ectopic tissue are the human dermal fibroblast cells which were delivered in conjunction with the hydrogel scaffold.

Further evidence of the origin of the cells in the neo-tissue was provided by observing selected implants in which the cells had been incorporated with a fluorescent cell tracking dye as previously detailed in the *in vitro* investigations. Shown in Fig.4.32 are the results of this data taken from mice implanted with human dermal fibroblasts after 6 weeks of culture. The composite image proves the origin of the cells in the gel is indeed the implanted human dermal fibroblasts by means of preservation of fluorescence.



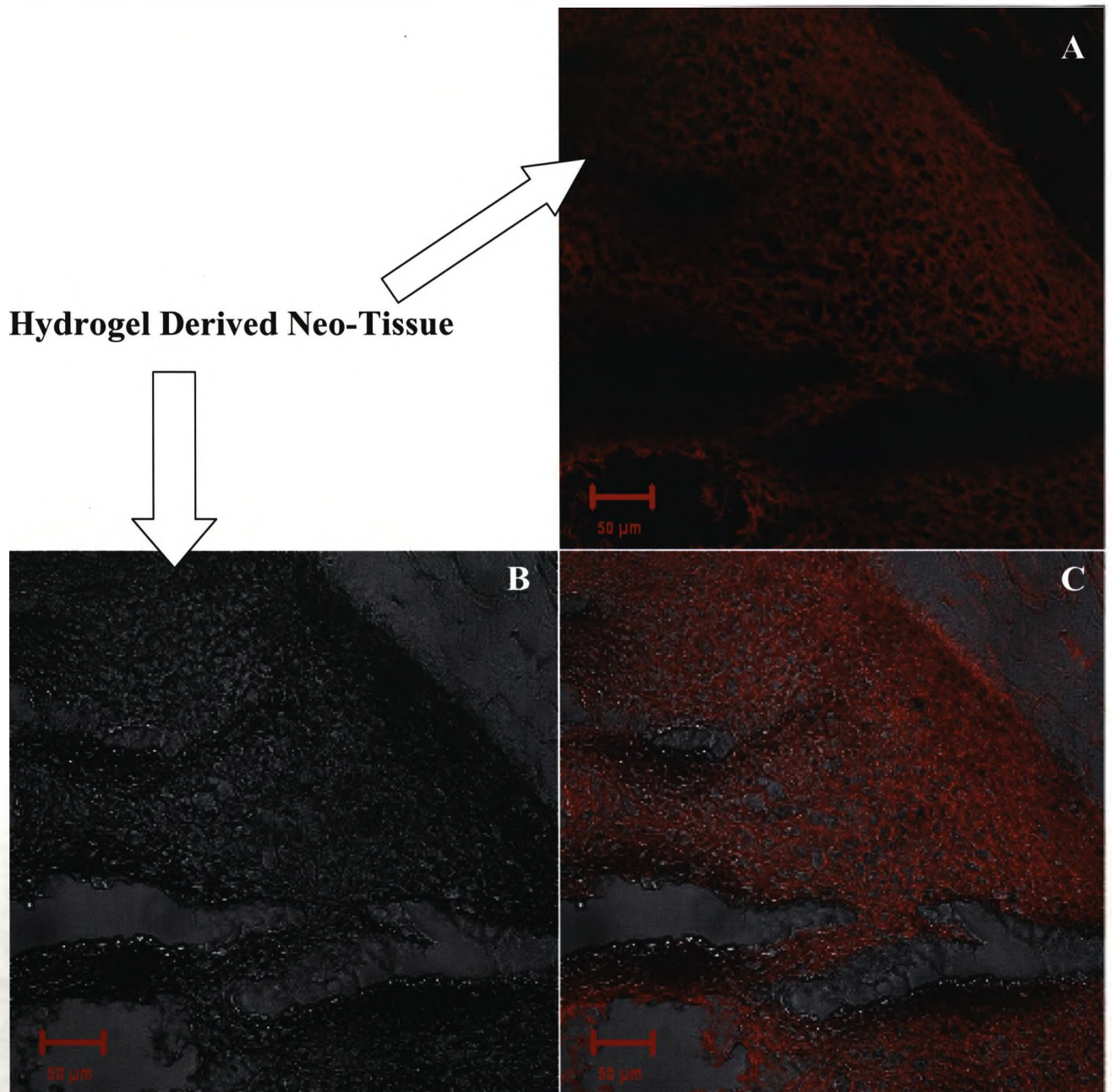


*Fig.4.32. Confirmation of the human dermal fibroblast origin of the cells in the platelet poor plasma derived neo-tissue. A; immunoflourescent cell tracking dye alone, B; transmitted light alone and C; composite of both immunoflourescent cell tracking and transmitted light images*



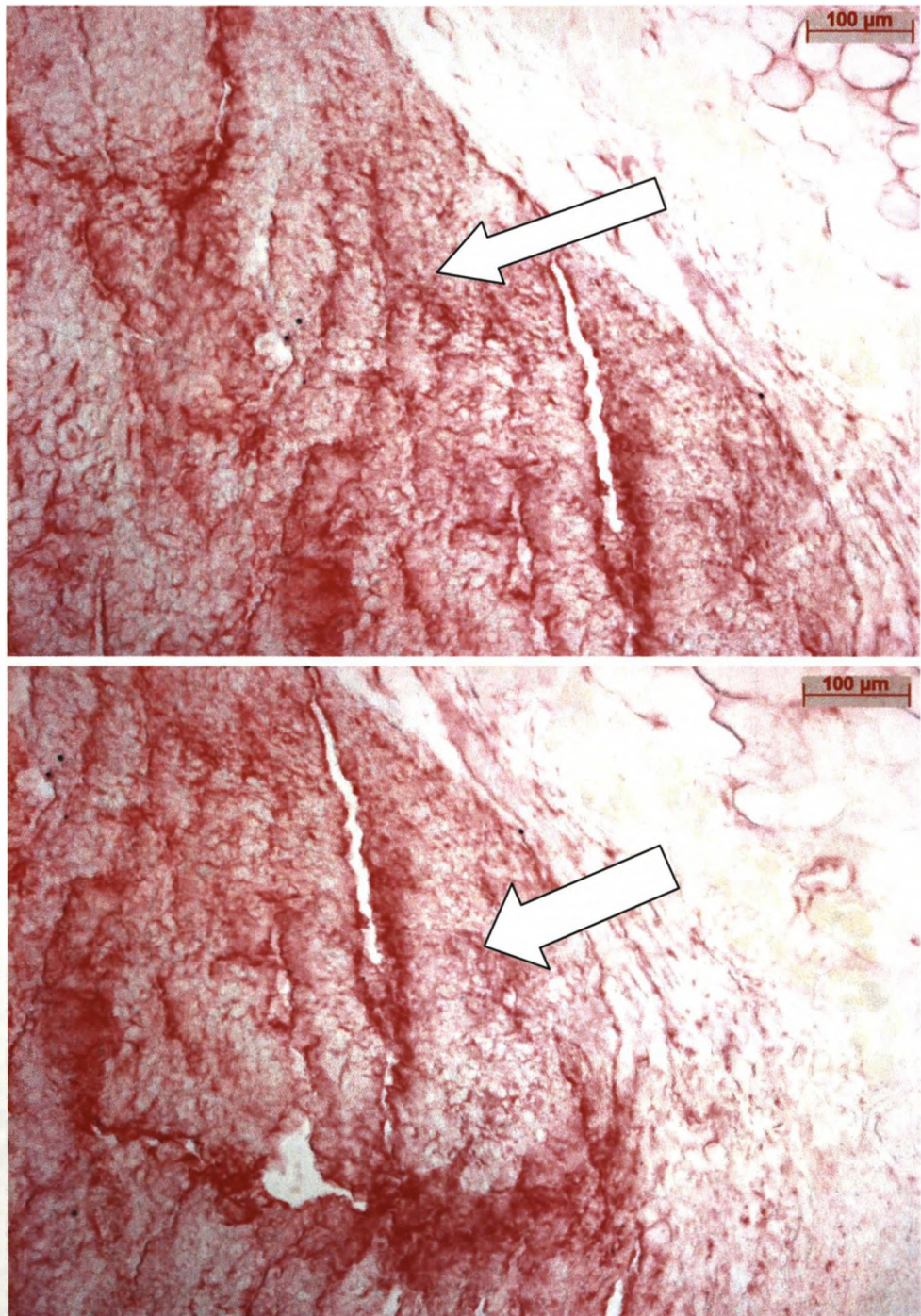


*Fig.4.31. Light microscopic visualisation of explanted tissue immunohistochemically stained for the presence of the D7-Fib antigen (positive staining indicated using arrows)*

In order to further determine the origin of the cells within ectopic tissues, real time PCR analysis was carried out on both ectopic and native tissues.

Hydrogel derived tissues were isolated and dissected into three regions, G1, G2 and G3. G1 was taken from the centre of the tissue, G3 was taken from the periphery, and G2 was taken from the region in between. Additionally, tissue was also removed from the liver of the animal and also the dermis surrounding the implanted hydrogel. RNA was isolated at the point of explantation and reverse transcribed as described in section 2.iv. Tissue was then subjected to real time PCR analysis, using the method described in section 2.iv, to confirm the presence of human D7-Fib; fibroblast specific protein, to further confirm the presence of human fibroblasts. Additionally, tissues were also probed for the presence of 2 human house keeping genes, glutaraldehyde phosphate dehydrogenase (GAPDH) and DNA topoisomerase-3. Samples were compared by means of normalisation of threshold cycle values ( $C_t$ ) to  $C_t$  values achieved using a non-species specific  $\beta$ -actin primer, under identical reaction conditions.

Fig.4.33 illustrates D7-Fib expression across the samples, demonstrating a progressive decrease in detection from the centre to the periphery of the tissue, with small amounts of this cell specific gene observed in the liver of the host, suggesting a possible mobilisation of the human fibroblasts in the circulation. Additionally, even smaller amounts were detected in the dermis surrounding the implant, suggesting that, although no infiltration of cells into the host surrounding tissue is observed histologically, molecular analysis does suggest cross-over of cells from the hydrogel to the host. This trend was conserved when considering the house keeping genes (Figs 4.34 and 4.35) with the highest detection of the gene in samples taken from the core of the construct with progressively less apparent towards the periphery. Both genes were present in the liver of the animal, supporting further, the mobility of the human cells by means of the circulation developed throughout the ectopic tissue, and although GAPDH was not detectable in the skin, DNA

Topoisomerase-3 was present, further suggesting possible crossover of cells from the gel mass to the surrounding tissues. Presence of human genes in the surrounding dermis could be explained by becoming deposited there as an artefact of the initial implantation. Furthermore, the presence of human RNA in the liver could be representative of a small population of human cells which have been phagocytised by host macrophage cells as a result of either apoptosis of immuno-stimulation. The resulting human cellular debris, including genomic and transcriptomic material is processed in the liver after secretion from the macrophage, permitting its detection using this technique.

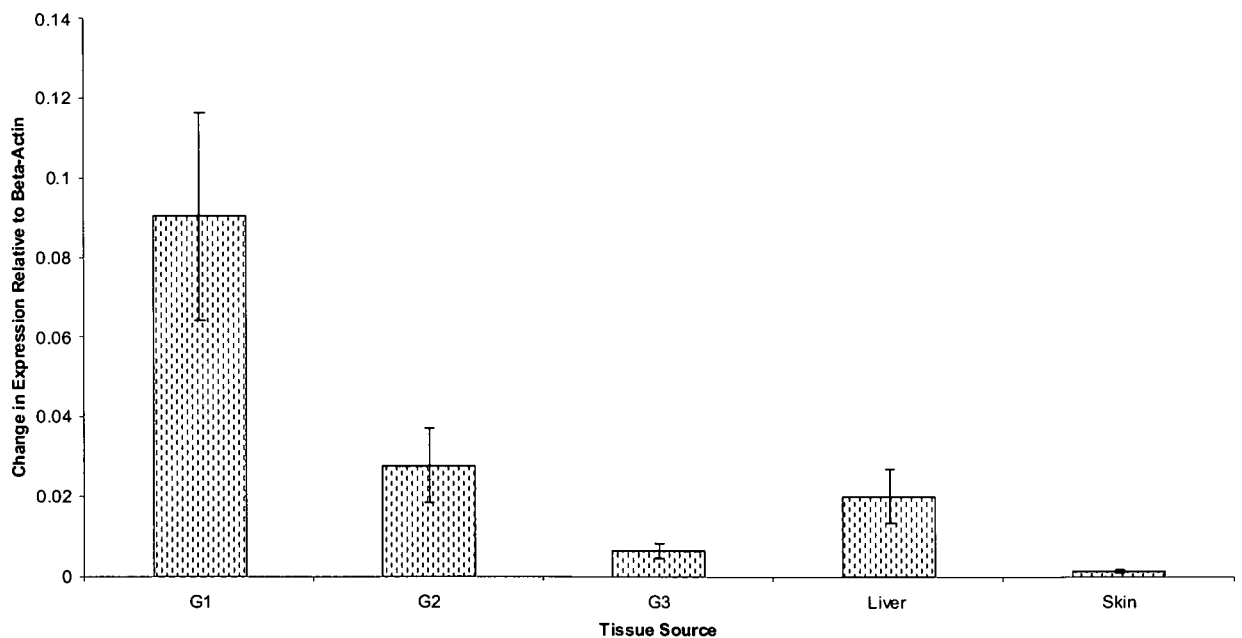


*Fig.3.33. Real time PCR observation of the human D7-Fib gene in tissues explanted from experimental subjects after 6 weeks of in-vivo culture. Error bars represent 1 standard deviation from the mean, n=6*

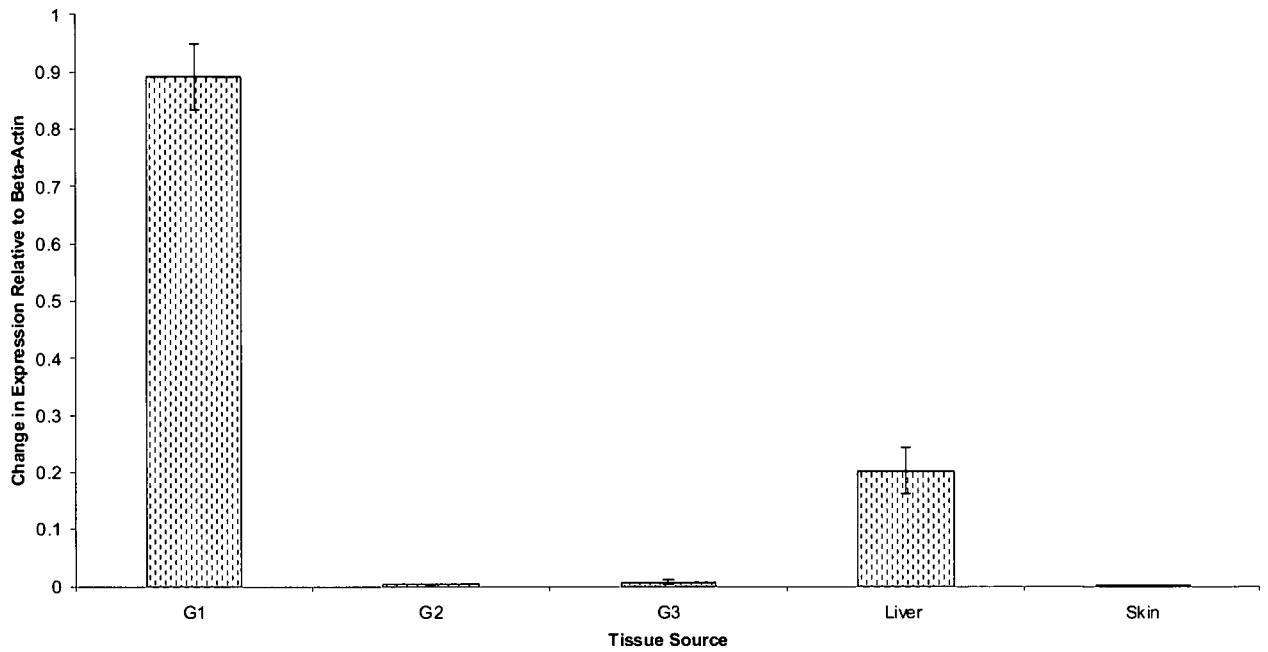


Fig.4.34 Real time PCR observation of the human GAPDH gene in tissues explanted from experimental subjects after 6 weeks of in-vivo culture. Error bars represent 1 standard deviation from the mean, n=6

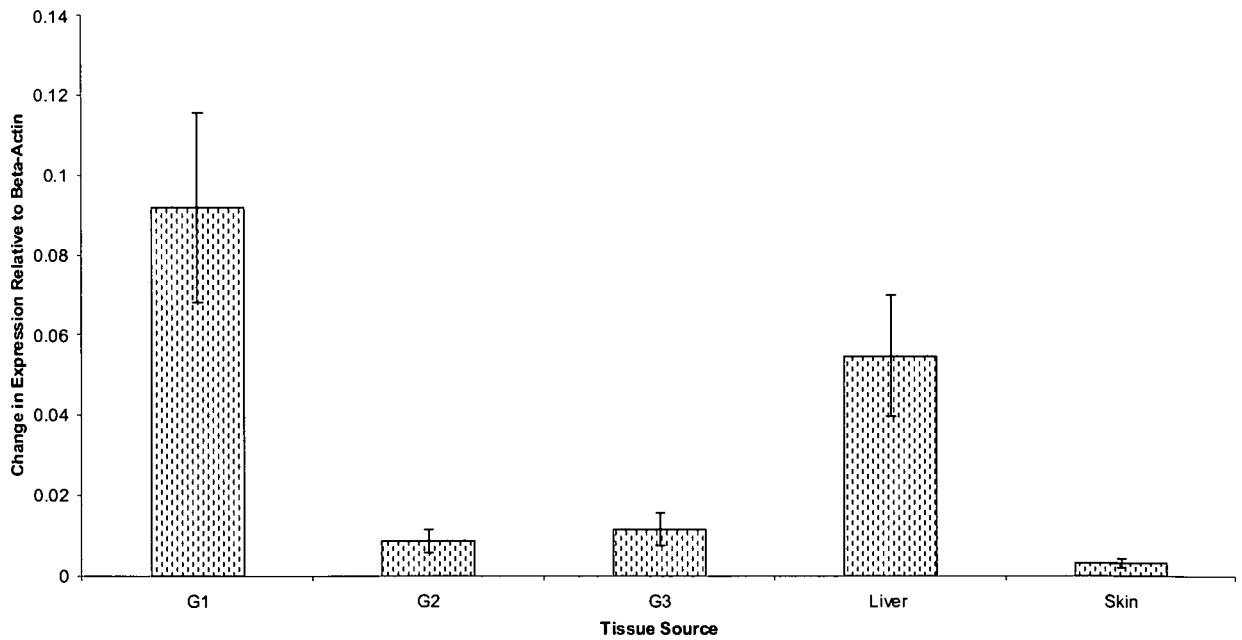
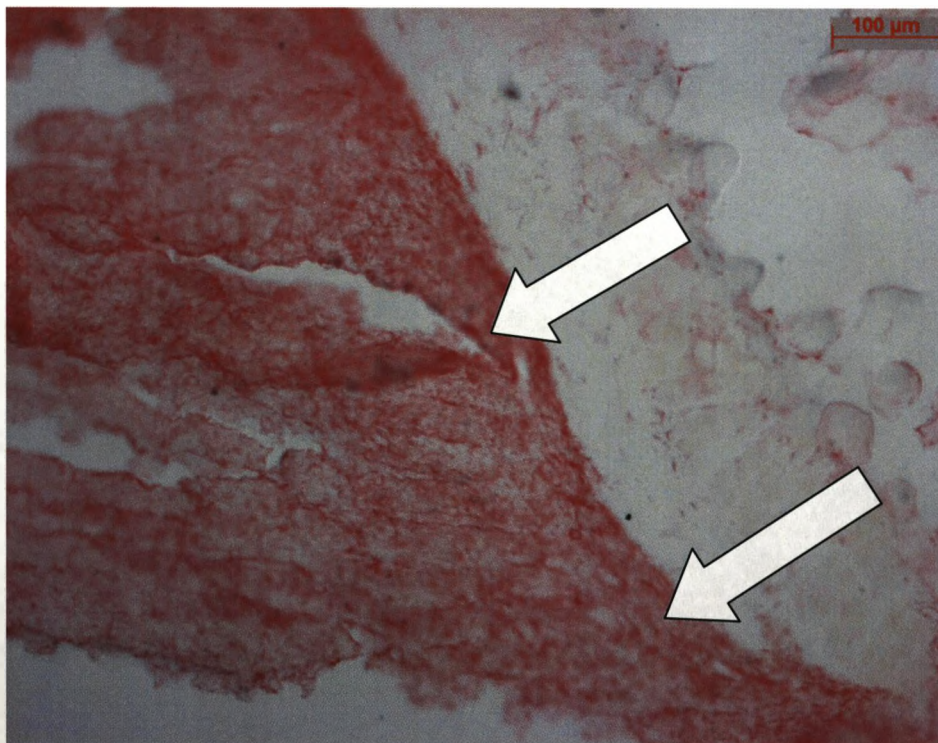


Fig.4.35. Real time PCR observation of the human DNA Topoisomerase-3 gene in tissues explanted from experimental subjects after 6 weeks of in-vivo culture. Error bars represent 1 standard deviation from the mean, n=6



Immunohistochemistry was used to characterise the immune response raised by the host in response to implantation of the hydrogel. Initially, neotissue was subjected to staining using an antibody raised against murine macrophages which demonstrated extensive macrophage infiltration into the non-host tissue (Fig.4.36). This was expected when considering the multitude of potential immuno-stimulatory factors which, as previously stated, were part of the gellation system, in the form of the human platelet poor plasma or a culture media component. Alternatively it may be due too the human dermal fibroblasts or an exogenous factor such as a cytokine or growth factor secreted during their expansion.

Despite the presence of macrophages in the ectopic tissues, there was little evidence to support their activation, and subsequent destruction of the tissue. CD68, a surface protein expressed by activated macrophage cells was not present in any of the cases where macrophages were observed to have infiltrated the hydrogel-derived tissues (Fig.4.37).



*Fig.4.36. Light microscopic observation of immunohistochemical identification of the presence of host macrophage cells in explanted neotissue (positive staining illustrated by arrows)*



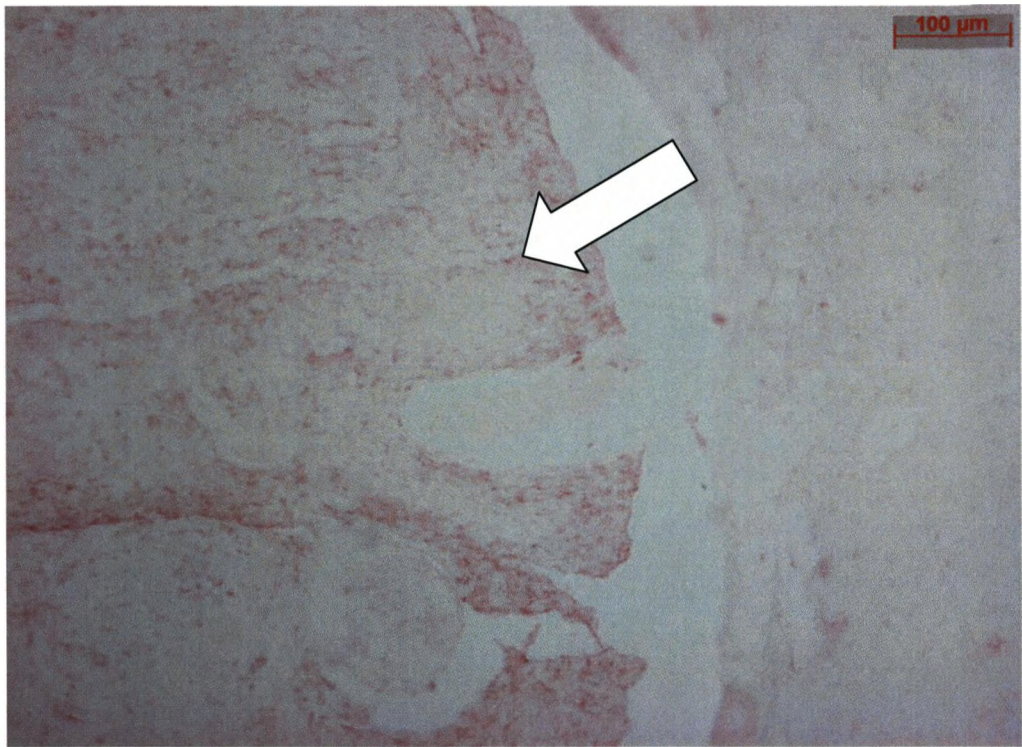


*Fig.4.37. Light microscopic observation of immunohistochemical identification of the presence of host CD68 positive cells in explanted neotissue (positive staining illustrated using arrows)*

Neutrophils were also observed immunohistochemically (Serotec, MCA771G antibody, an IgG capable of binding a 40kDa antigen expressed on neutrophil but not macrophage cells), but in lower concentrations than macrophages. These phagocytotic cells possess a characteristic polymorphonuclear morphology, making them obvious during histological analysis. However, although conventional histological analyses did not support the presence of these cells, immunohistochemistry did suggest their presence in limited amounts, as illustrated in Fig.4.38.

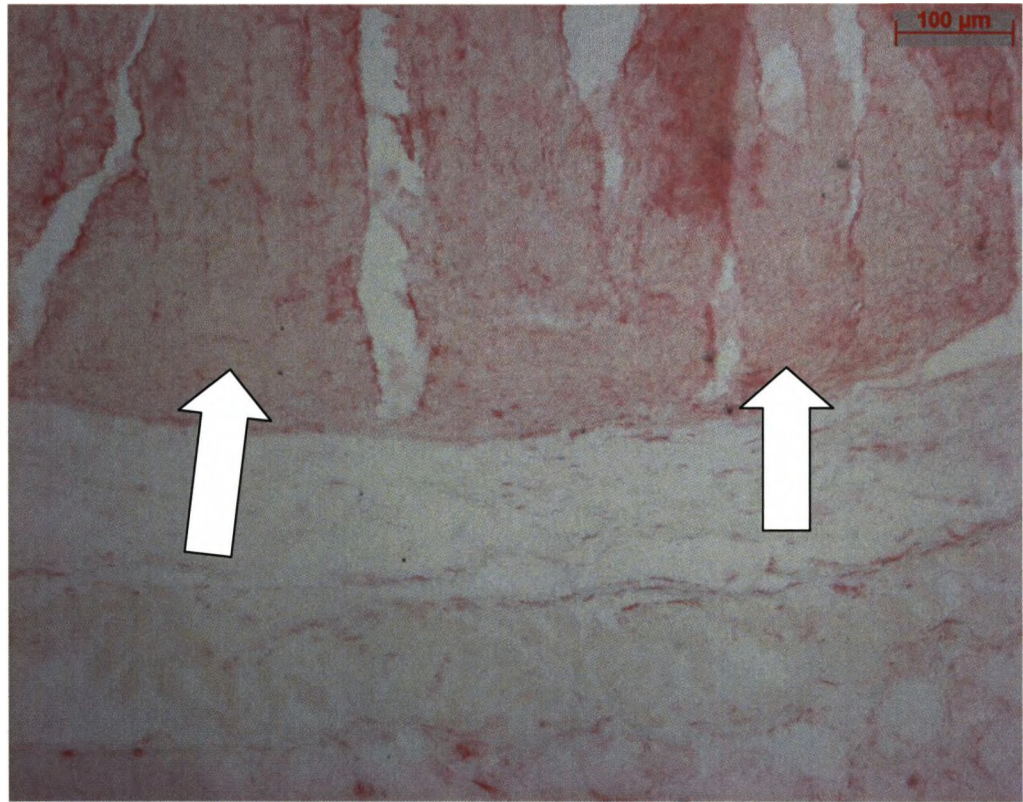


*Fig.4.38. Light microscopic observation of immunohistochemical identification of the presence of host neutrophil cells in explanted neotissue (positive staining illustrated using arrows)*

The lack of antigenicity of the hydrogel system was further characterised by the absence of antigen presenting dendritic cells, confirmed by the absence of the dendritic cell protein CD205 (Fig.4.39) [452]. Further absence of antigen presentation was characterised by immunohistochemical targeting for major histocompatibility class II (MHCII) molecule, the tether molecule, responsible for correct presentation of antigens on the surface of lymphoid cells (Fig.4.40) [453].



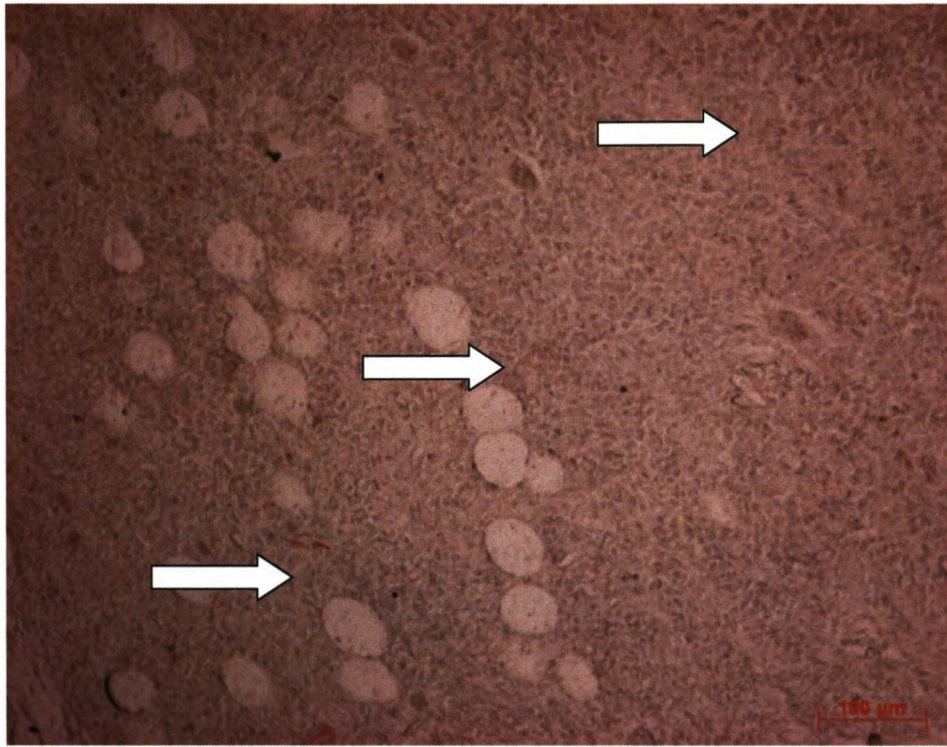


*Fig.4.39. Light microscopic observation of immunohistochemical confirmation of the absence of host CD205 positive cells in explanted neotissue (neo-tissue area subjected to staining indicated using arrows)*

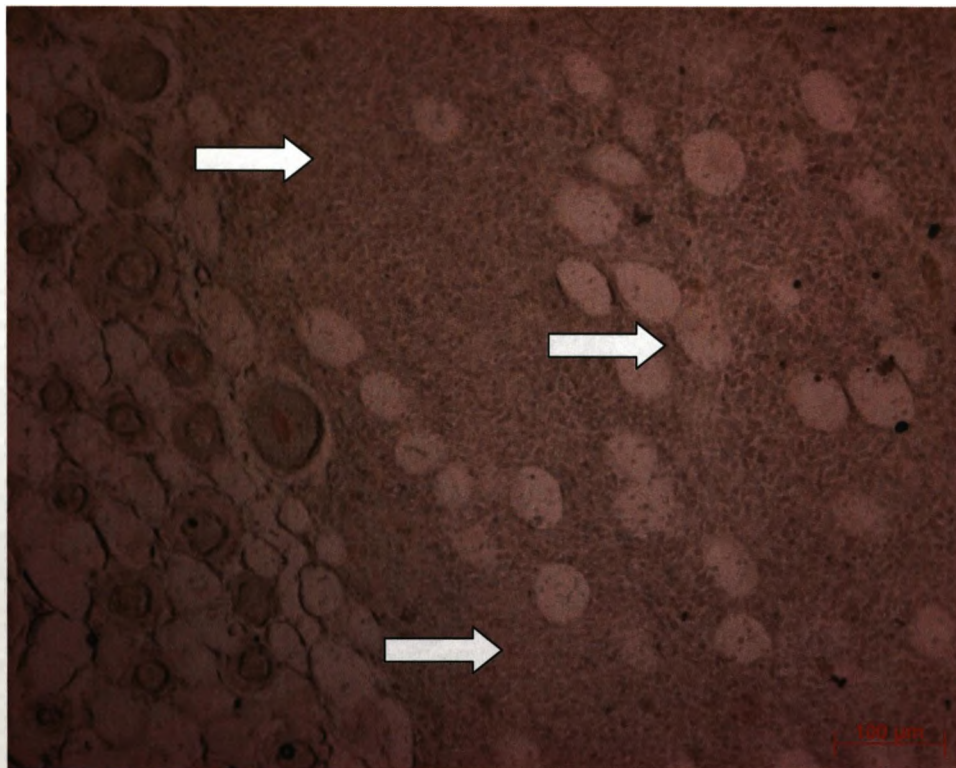


*Fig.4.40. Light microscopic observation of immunohistochemical confirmation of the absence of host MHCII positive cells in explanted neotissue (neo-tissue area subjected to staining indicated using arrows)*

In order to assess the biodegradation of the fibrin meshwork responsible for formation of the scaffold that permits tissue formation, ectopic tissues were analysed using cryogenic scanning electron microscopy using the protocol outlined in section 2.xx, to observe fibrin fibres still present in the tissues after successful colonisation of human dermal fibroblasts and therefore extended periods of *in vivo* incubation. Analysis in this manner would also permit visualisation of the nature of the association of cells with the hydrogel itself.

Tissues explanted after 6 weeks of *in vivo* incubation were immediately frozen in liquid nitrogen at the point of explantation before being chipped using a scalpel to reveal internal cellular structures. Fig.4.42. illustrates the appearance of the surface of the tissue. The extensive cobblestone morphology demonstrates the density of the cellular colonisation of the hydrogel-derived scaffold. Fig.4.41. illustrates the surface of the tissue using an increased magnification with the presence of the fibrin fibre scaffold clearly visible.

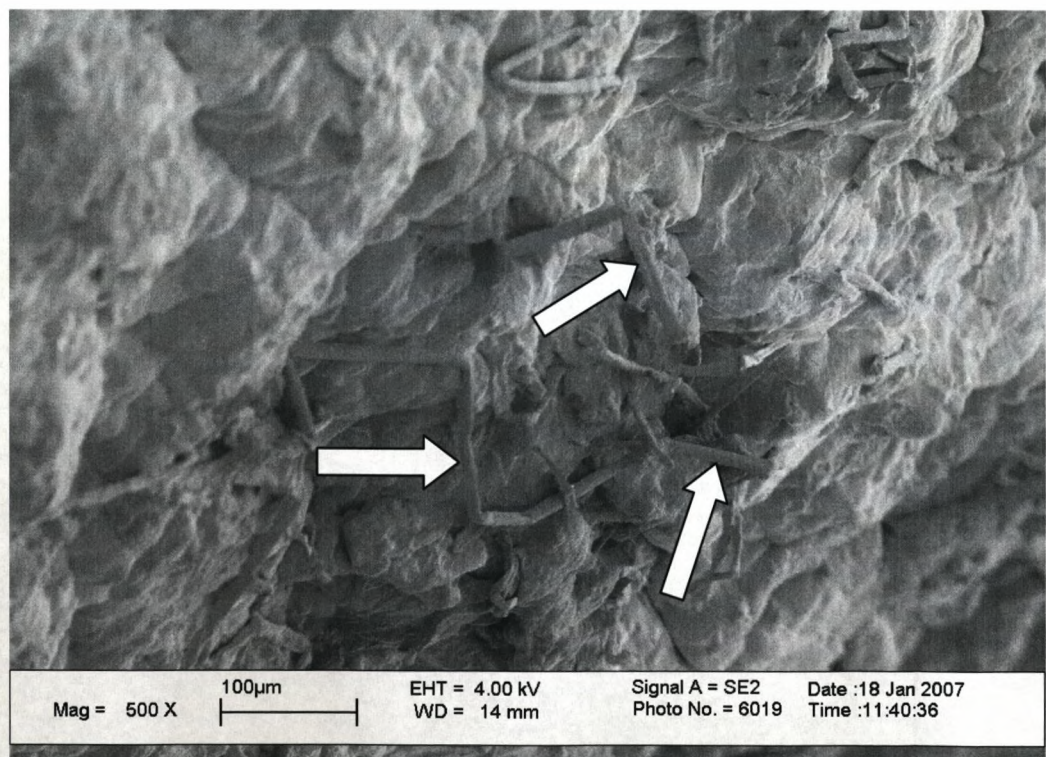


*Fig.4.41. Electron micrograph of the surface of the ectopic tissue demonstrating the interaction between cells and fibrin meshwork (fibrin scaffold indicated using arrows).*



Post chipping of the frozen tissue the fibrin meshwork was clearly observable after 6 weeks of *in vivo* culture as demonstrated in Fig.4.42. Furthermore, it was possible to observe intimately, the association between scaffold and cells, shown in Fig.4.43.

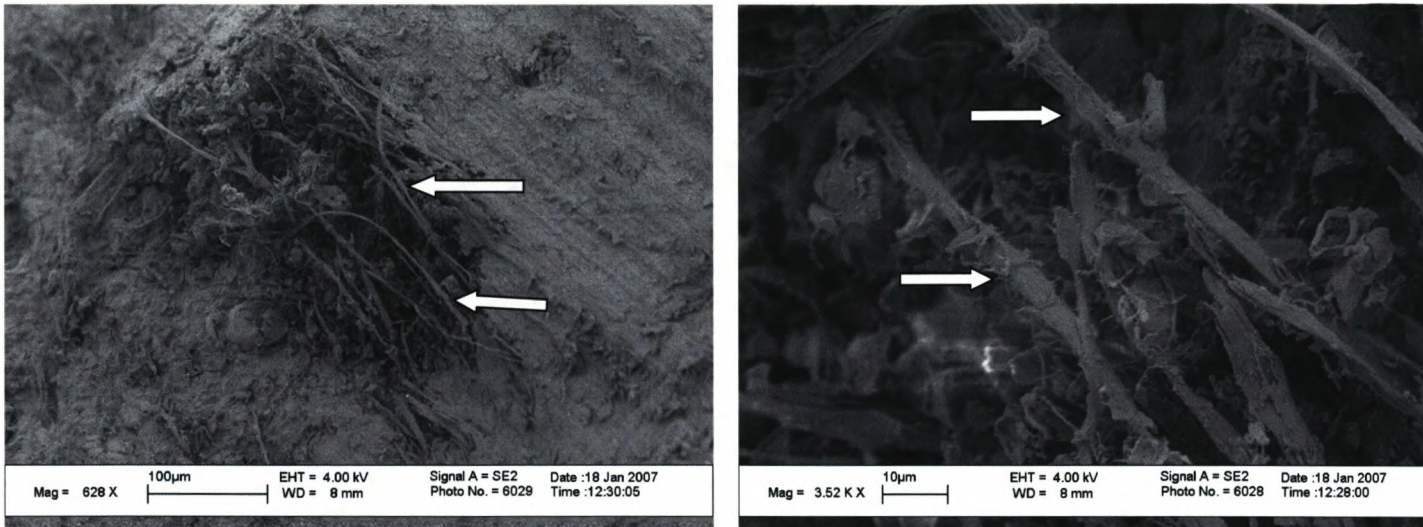


Fig.4.42. Electron micrograph confirming the presence of a fibrin meshwork in the neo-tissue after *in-vivo* culture (fibrin fibres indicated using arrows).

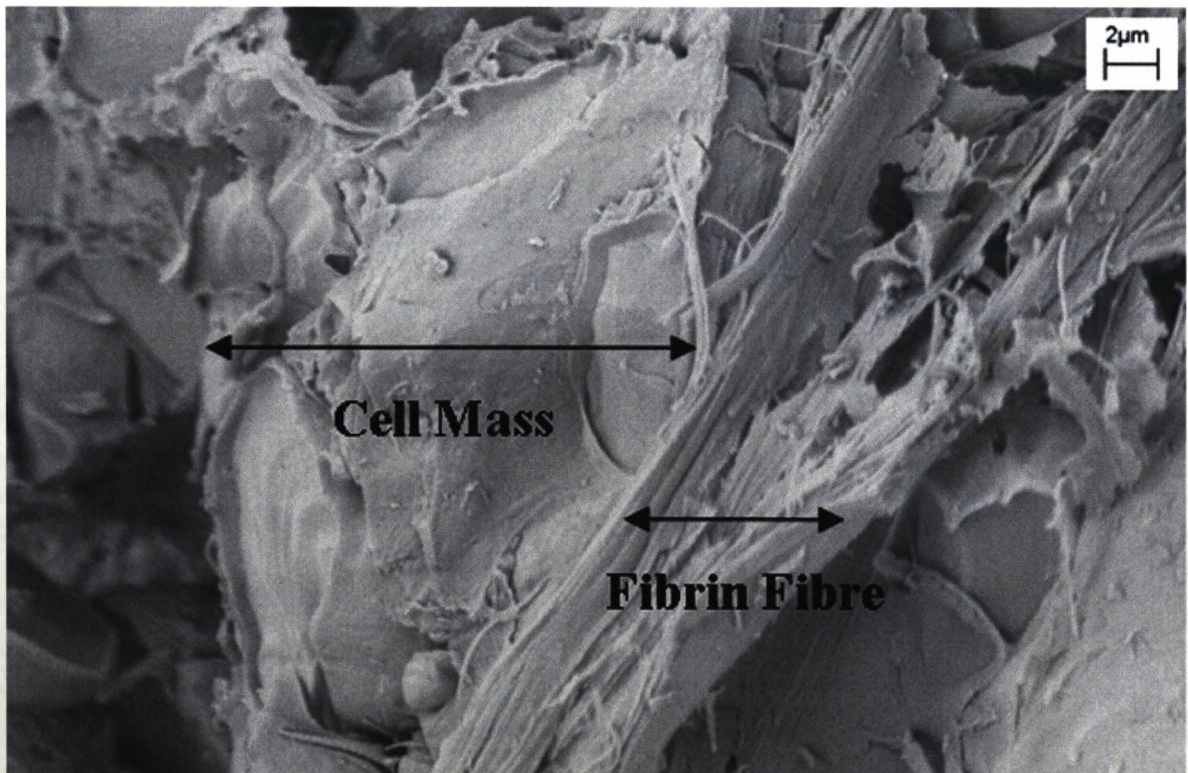


Fig.4.43. Electron micrograph demonstrating the interaction between scaffold fibres and cells in the ectopic tissue

In addition to validation of the capacity of the platelet poor plasma derived hydrogel to maintain the expansion of human dermal fibroblasts and subsequent successful formation of soft tissue, it was also decided that it was necessary to validate the system for its capacity to form ectopic hard tissue. In proving this the potential scope of tissue engineering applications in which the hydrogel could be exploited becomes greatly enlarged incorporating a wide range of possible bone related debilitating diseases in addition to other biomedical morbidities where neo-bone is required to be generated such as injury or cosmetic surgery.

Since the target tissue in regenerative therapies of hard tissue is bone, the implanted cell chosen for this application was primary human osteoblasts, taken from passage 6. These cells were delivered using an identical injection based implantation strategy to intramuscular sites in the quadriceps femoris muscle in the hind legs of the subjects. Intramuscular sites were chosen based on previous evidence that formation of calcified bone using a subcutaneous hydrogel as scaffold material was not possible; however studies have been successful in forming ectopic bone using intramuscular delivery of primary osteoblasts in conjunction with more complex, polymer hydrogel.

6 week old, male, NOD/SCID mice were implanted with  $1.0 \times 10^6$  primary human hip osteoblasts (Promocell, UK) and sacrificed 6 weeks post implantation. Ectopic tissue was clearly visible at the point of sacrifice, having formed within a capsule inside the muscle block of the host quadriceps femoris. Tissue was white in appearance, resembling bone; however texture was malleable suggesting an absence of calcification.

Histological analysis after excision of the neo-tissue demonstrated the magnitude of cellularisation of the hydrogel scaffold with a dense colonisation of cells producing extensive matrix, in a manner similar to the dermal fibroblast containing subcutaneous implants (Fig.4.44)



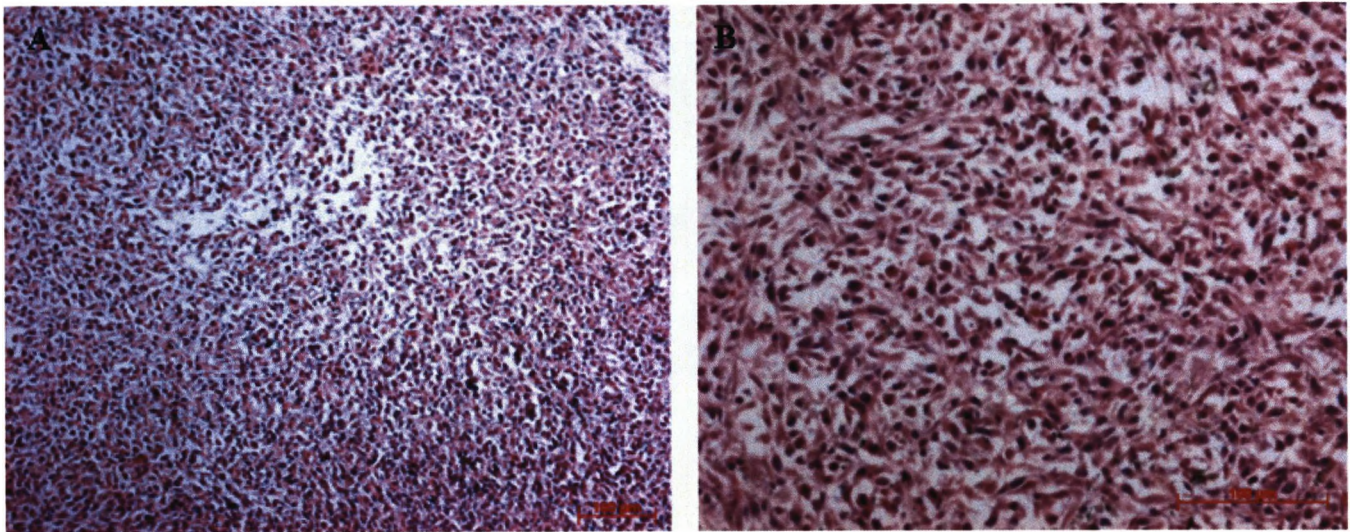


*Fig.4.44. Light microscopic observation of haematoxylin and eosin stained ectopic tissue derived from platelet poor plasma hydrogel in conjunction with human osteoblast cells showing the degree of cellularisation*

In order to confirm the phenotype of the cells in the ectopic tissue, sections were subjected to immunohistochemical staining to observe the presence of human core binding factor- $\alpha$  (CBFA1/RUNX2), a transcription factor involved in osteogenesis, widely regarded as the osteogenic master gene [404]. Presence of this protein was observed throughout the tissue, confirming the maintenance of osteogenic phenotype of the cells contained within, demonstrated in Fig.4.45, which also illustrates the vascularisation of the neo-tissue by the presence of a large erythrocyte cell laden vessel at the bottom left of the figure.

Ectopic tissue was subjected to histological analysis using Von Kossa staining described in section 2.viii to detect calcification and therefore assess the functionality of the osteoblast cells (Fig.4.46). Calcification (brown/grey staining) was observed sporadically throughout tissue confirming, in conjunction with the presence of CBFA1/RUNX2, that the process of

ossification was occurring although further *in vivo* incubation was necessary to facilitate generation of tissue mechanically resembling bone.

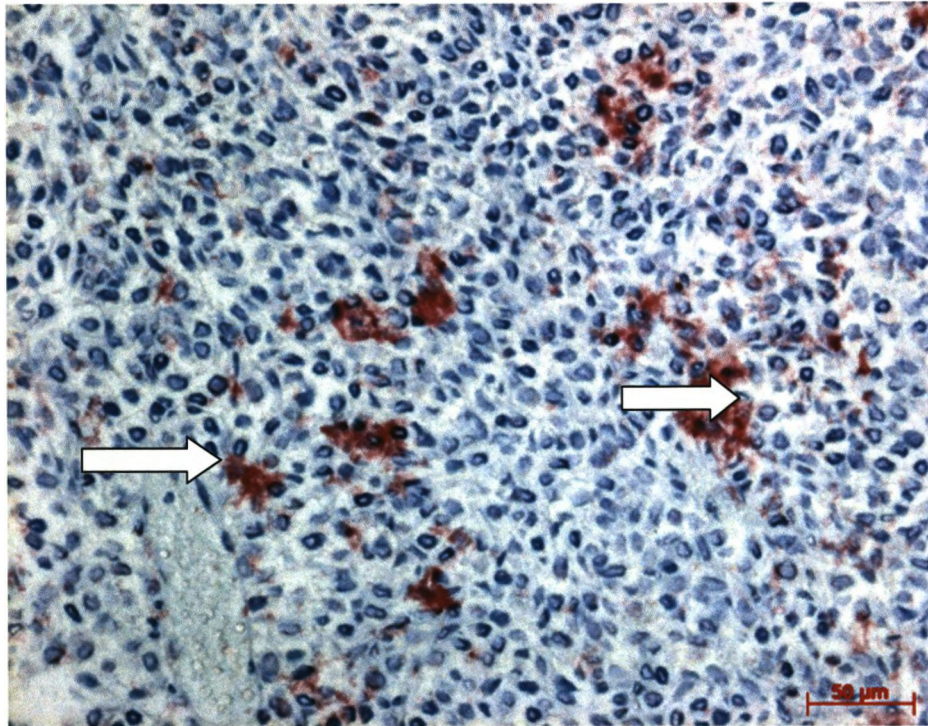


*Fig.4.45. Microscopic observation of immunohistochemical recognition of human Cbfa1/Runx2 (positive staining illustrated using arrows)*



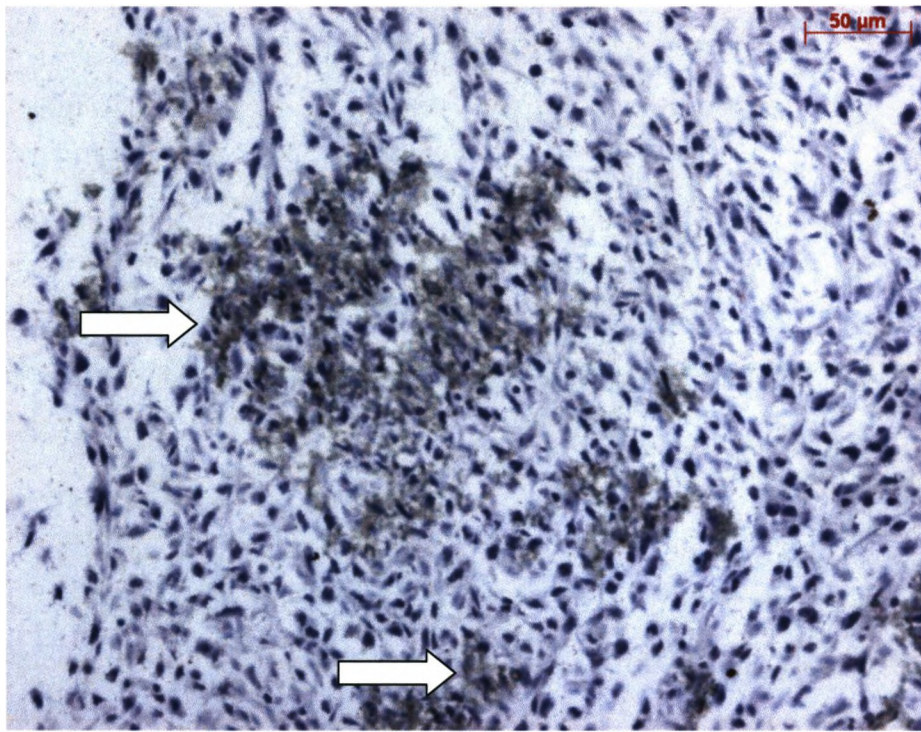


*Fig.4.46. Light microscopic observation of Von-Kossa stained ectopic tissue (positive staining illustrated using arrows)*

Human osteoblast-derived tissues had an identical immune cell recruitment profile to the dermal fibroblast derived tissues. Macrophage and neutrophil cells were observed although, seemingly inactive, characterised by no observable expression of CD68. Additionally there was no antigen presenting cells detectable in the explanted neo-tissues.

#### 4.viii Summary

The combination of citrated platelet poor plasma derived from mixed gender healthy donors possessed intrinsically the capacity to form a hydrogel when combined with cell culture media containing calcium. The scaffold of the hydrogel was composed of fibrin, with gelation occurring as a result of replacement of calcium ions, which had been removed from the plasma as a result of citration, using the culture media to initiate fibrinogenesis, exploiting the innate clotting machinery present in the plasma.

Characterisation of the gel using the dynamic contact angle method demonstrated a consistent contact angle when subjected to immersion in a range of concentrations of sera relevant to both *in vivo* and *in vitro* cell culture applications. The contact angle throughout was similar to clean glass, regarded widely as the gold standard comparison for tissue culture substrates.

*In vitro* cell studies demonstrated the hydrogel substrate to be an ideal candidate media for the maintenance of human articular chondrocytes, using a block of hydrogel cast on top of a cell monolayer, the gel created the controlled hypoxic environment in which chondrocyte cells thrive, whilst still permitting the influx of nutrients and efflux of cellular waste products. The chondrocytes maintained their phenotype, demonstrated by the presence of glycosaminoglycans using the alcian blue method.

The surface of the hydrogel proved to be a suitable substrate for the growth and differentiation of primary plastic human cells. Human dental pulp-derived stem cells proliferated on the gel surface followed by differentiation into microvascular endothelial cells after pre-selection using Hoechst staining, demonstrated by observation of endothelial cell specific proteins using immunohistochemistry and flow cytometry. The platelet poor plasma derived hydrogel demonstrated superiority over commercially available Matrigel for

maintaining these cells *in vitro*, with introduction to a Matrigel surface resulting in the death of dental pulp derived stem cells.

Cells exhibited excellent motility through the hydrogel blocks, demonstrated by cell tracking in conjunction with human articular chondrocytes. Motility of the cells was followed using cell tracking, illustrating the migration of the chondrocytes to the increasingly hypoxic lower regions of the hydrogel blocks.

The hydrogel system proved itself an ideal candidate for minimally invasive introduction of cells to a defect site for exploitation in bioengineering applications. The platelet poor plasma derived hydrogel could be delivered in a liquid phase, with the two components (platelet poor plasma and cell loaded culture media) combined at the point of implantation, with gellation occurring *in situ* in the host.

The hydrogel scaffold demonstrated the capacity to maintain the phenotype and expansion of primary human dermal fibroblast cells delivered subcutaneously to immunosuppressed animals. Furthermore, the scaffold also permitted the formation of a completely novel tissue at the site of implantation. The tissue formation was a synergistic combination of the fibrin scaffold of the hydrogel maintained in structure by the extra cellular matrix of the cells contained within. Acellular gels and cells contained solely in media did not form tissue when implanted.

Tissues formed below the subcutaneous layer of skin, with minimal adhesion to the underlying host connective tissues. Ectopic tissues were vascular, with clearly observable neovasculature diversions from the peripheral circulation of the host animal, visible both macro and microscopically. Furthermore, histological analysis demonstrated the degree of infiltration of host tissues into

the neo-tissue with adipose, musculature and hair follicles all present in the hydrogel derived tissue mass.

Primary human dermal fibroblasts were characterised in the explanted tissues by the presence of D7-Fib antigen observed by immunohistochemistry, a fibroblast specific protein, further qualified by the presence of human genes in the tissues using real time-PCR. This data confirmed the presence of the fibroblasts throughout the tissue mass, certifying their responsibility for neo-tissue formation. Furthermore, the presence of human Y chromosomes in ectopic tissues in female animals illustrated the speciation of the cells responsible for formation of the ectopic tissue.

The hydrogel also demonstrated its potential as a media to support the formation of hard tissues using primary human osteoblasts implanted into intramuscular sites. Tissue formed inside capsules within muscle blocks of the host, with very limited adhesion to the surrounding muscle. These tissues were also vascularised and the phenotype of the cells was confirmed by the immunohistochemical observation of the osteogenic master gene CBFA1/RUNX2. Initiation of calcification was confirmed by observation of the presence of positive staining using the Von Kossa method.



## DERIVATION OF DEFINED MEDIA FOR THE PHENOTYPE MAINTENANCE AND DIRECTED DIFFERENTIATION OF PRIMARY HUMAN PURIPOTENT CELLS

### Chapter 5. Discussion

#### 5.i Transferrin Degradation Studies

Chemically defined media, completely devoid of whole serum could be synthesised completely *de novo* from individual basic components, containing three exogenous proteins: Insulin, transferrin and serum albumin. ELISA-based techniques demonstrated no significant degradation in transferrin; a critical protein present in the media formulation, during a 21 day acellular incubation under standard tissue culture conditions (Fig.3.2). This is contrary to previous studies which have demonstrated the susceptibility of transferrin to degradation into smaller peptide fragments particularly in the presence of ascorbate (vitamin C) which incidentally is also present in the defined media formulation [288]. The previous study [288] did not discuss the nature of the transferrin used with respect to its iron saturation and binding (apo-transferrin; unbound to iron, holo-transferrin; iron bound) and used a system devoid of iron which, when considering the intimacy of this protein with iron under physiological conditions is not an ideal model for the assessment of degradation under tissue culture or physiological conditions. It should also be stated that the ELISA method chosen to measure the concentrations of transferrin in conjunction with the defined serum free media formulation studies was specific to both apo- and holo-transferrin. Although previous studies used holo-transferrin in cell culture systems [290-291], defined media for this study utilised apo-. It was hypothesised that when considering the binding affinity of transferrin for iron (present in the culture media) allowing the transferrin to saturate with iron passively, the inclusion of apo-transferrin (non-iron bound) would provide a more appropriate iron bound/iron unbound equilibrium to that present physiologically in the native

environment of primary cells. Transferrin binds iron avidly, with a dissociation constant of approximately  $10^{22} \text{ M}^{-1}$  in the presence of an anion which is typically carbonate; an abundant media component [289]. The previous study [288] found that the degradation of transferrin was facilitated by ascorbate but also did not consider the synergistic effects of other proteins in proximity to transferrin. In the chemically defined media it is possible that the other two proteins present, particularly albumin could have a steric protective role in the maintenance of transferrin structure.

### 5.ii Lineage committed cells – Dermal Fibroblasts

The *de novo* synthesised chemically defined serum free media demonstrated the capacity to support the metabolic activity of primary human dermal fibroblasts at rates statistically similar to media containing serum at a concentration of 5% (Fig.3.3). In contrast, Previously published data concluded serum free media was not capable of maintaining the viability of dermal fibroblast cells at a level similar to that which could be obtained in serum containing media formulations, using the proprietary serum free formulation; ultraCULTURE, of which the composition is undisclosed [292]. In contrast, a second previously published study using ultraCULTURE in combination with fibroblasts did report an increase in cell number during a 96 hour culture period, by means of simple cell counting, which equated to approximately 1 population doubling during this culture period. This investigation did not compare this increase in cell number to serum containing media formulations [294]. Therefore, presenting two conflicting reports on the viability of dermal fibroblasts in conjunction with an identical serum containing formulation highlighting the ambiguities which arise when using sera replacements, typically as a result of an increased/decreased serum preference of a particular population of cells.

From a tissue engineering perspective several groups are working on optimising conditions for the maintenance of fibroblast cells due to the necessity of these cells as feeder cells for the expansion of keratinocytes

for organotypic culture of skin. One study in particular although, again, using viability as opposed to metabolic activity demonstrated that the decrease in viability observed using serum free culture strategies for this cell type was dependent on the anatomical origin of the particular cells; with fetal lung fibroblasts showing the smallest decrease in viability as a result of 5 days of culture in the absence of serum, similarly to the previously mentioned study, no serum free media formulations were disclosed [293], further emphasising the point made previously regarding the variable preference of serum dependency of an individual cell population. A further investigation into the relationship between keratinocytes and fibroblast cells using serum free media formulations detailed that no proliferation of fibroblasts was observed in serum free media, however the same serum free media which was pre-conditioned using keratinocytes triggered the dermal fibroblasts to proliferate. It was hypothesised that the presence of a unknown keratinocyte secreted factor was necessary in addition to the serum free media to permit fibroblast expansion. The serum free media used in this fibroblast/keratinocyte case was undisclosed [296]. A study into the role of various wound fluid-derived exogenous components on fibroblast cell viability disclosed a serum free media formulation containing holo-transferrin, sodium selenite, linoleic acid, bovine serum albumin, epidermal growth factor and insulin and reported that fibroblast cells did not proliferate under these conditions after replacement from serum containing conditions; naming these cells 'non-replicating but reactive fibroblasts', the cells maintained a fibroblastic morphology but did not increase in number [295].

Therefore, it was possible to conclude from the data presented in this thesis that the chemically defined serum free media synthesised *de novo* was potentially superior to those available commercially or previously described in conjunction with dermal fibroblasts. The metabolic activity of fibroblasts increased progressively during the 21 day experimental time course which was longer than any of the time scales observed in the previously published work dealing with fibroblasts and serum free media formulations. Only one of these aforementioned studies reported an

increase in cell number, with the general observation being a loss or no significant change in viability during culture under serum free parameters. Additionally, none of the previous studies using fibroblasts in conjunction with defined serum free conditions characterised the phenotype of the cells after culture. Using the chemically defined serum free media formulation presented herein, the phenotype of the cells was characterised by immunohistochemical detection of the fibroblast specific D7-Fib antigen which was found to be present after 21 days of defined serum free culture (Fig.3.4).

### 5.iii Lineage committed cells – Osteoblasts

Using defined osteogenic modifications to the serum free basal media it was possible to conclude that a serum free osteogenic formulation was capable of maintaining the metabolic activity of primary human osteoblasts during a 21 day culture time scale, because after 14 days of culture there were no significant differences in the metabolic activity of osteoblasts maintained in osteogenic modified media with or without serum at concentrations as high as 10% (Fig.3.5). Previously published data demonstrated that under serum free conditions, proliferation of primary non-immortalised osteoblasts cells was massively reduced when compared to identical formulations but containing serum. However, coating of the tissue culture surface with vitronectin could restore cellular proliferation to levels comparable to serum containing formulations in conjunction with serum free media, although vitronectin added as an exogenous component of the media formulation (not as a substrate coating) showed little effect on proliferative status [297]. Similarly, another study into the effect of substrate interactions in overcoming the dependence on serum of osteoblasts in culture reported no increase in cell number when osteoblasts were cultured in serum free media (alpha-MEM). However, when cells were cultured on fetuin-coated surfaces, cell number increased, and furthermore, coating a hydroxyapatite surface with this protein increased cell number more than fetuin-coated tissue culture plastic

alone [298]. This further illustrates a previous understanding of the dependency on a suitable substrate matrix to permit proliferation of osteoblasts in the absence of serum, which was not deemed necessary using the *de novo* derived serum free media presented in this research.

It has been possible to hypothesise that this substrate dependency is a result of integrin-mediated stimulation or proliferation: One particular group demonstrating the superior capacity of fibronectin, an RGD sequence containing peptide, as a coating for facilitation of osteoblast proliferation in the absence of serum. This particular study reported similar data to the previously stated works [297-298] in that no increase beyond the initial cell seeding number was observed in primary human osteoblasts cultured under serum free conditions on unmodified tissue culture plastic. This previous study into the role of RGD peptides in serum free osteoblast proliferation supplemented serum free media with bovine serum albumin alone as a protein source [299].

Therefore it could be concluded from previously reported data that in general, no increase in overall osteoblastic cell number could be achieved in conjunction with serum free media using unmodified tissue culture plastic as a substrate. Chemically defined serum free media synthesized *de novo* supported osteoblast metabolic activity at levels comparable to that observed when cells were cultured in serum containing media formulations. Additionally, it was also possible to observe an increase in metabolic activity of these cells during a 14 day culture time scale, a considerably longer time course than was used in any of the previously mentioned publications (6 days being the longest of the previously published data sets), without the need for exogenous protein coating.

#### 5.iv Lineage committed cells – Arterial Smooth Muscle Cells

Arterial smooth muscle cells in conjunction with smooth muscle cell modified chemically defined media (increase to 4.5g/L glucose)

demonstrated a differing trend in metabolic activity to the two previously discussed primary cells (dermal fibroblasts and osteoblasts). The smooth muscle cells increased their metabolism for the first week of culture, after which metabolism decreased to a level which was still higher than the initial time point. This trend was observed in serum containing media, not solely serum free and, similarly to the previous cell types, there were no significant differences between metabolic activity in serum free and serum containing media formulations after 14 days of culture (Fig.3.6). A decrease in metabolic activity during smooth muscle cell culture is supported by previously published data which demonstrated that proliferation in populations of smooth muscle cells decreases as cell density becomes increased; therefore it is suggested that this phenomenon was responsible for the decrease in metabolic activity which occurred as cells became confluent [300].

Previously published work reported that there were no proliferating cells present in populations of smooth muscle cells cultured under serum free conditions, with cell numbers gradually reducing over the first three days of culture. Furthermore, populations of these cells cultured under serum free conditions possessed high percentages of necrotic cells when compared to serum containing media formulations. The particular serum free media used to make these claims was unclear from the literature [301, 302]. A further observation of the effect of the chemically defined serum free media reported in this thesis on primary smooth muscle cells was the ability of the medium to induce the change from a synthetic to contractile phenotype, characterised by the presence of the smoothelin, a marker of contractile smooth muscle cells (Fig.3.14). This data supports previous studies and one in particular which used transferrin, insulin and selenium as a serum substitute and also observes an identical phenotype modification of smooth muscle cells characterised by the presence of smoothelin. From the limited details of the media formulation in this publication, it was not possible to support the claim derived from the medium in this thesis of a role of exogenous iron in facilitating the switch between synthetic and contractile phenotype. Interestingly however, in



contrast to the data presented in this thesis, this same publication suggests a role for serum in the up regulation of the matrix protein laminin. However, data presented in this research (Fig. 3.13) contradicts this, showing small decreases in laminin expression when normalised to serum containing media formulations [303].

A second previous study which confirmed the presence of smoothelin as a result of culture under serum free conditions also confirmed (as was concluded from this research also) the presence of  $\alpha$ -smooth muscle actin throughout culture in both contractile and synthetic phenotypes [304]. The presence of  $\alpha$ -smooth muscle actin throughout smooth muscle cell differentiation was also elucidated in [305]. Previous work has also demonstrated this increase in contractile phenotype as a result of serum deprivation, additionally demonstrating a possible role for insulin (a component of the defined media derived in this thesis) in hyper-stimulation of contractile phenotype beyond that which was recorded when cells were cultured purely in the absence of serum [302]. Furthermore, an insulin mimetic molecule has been demonstrated to interact with vascular smooth muscle cells, although phenotype was not characterised. The cells exhibited a significant decrease in proliferation suggestive of a contractile over a synthetic phenotype induced by bio-mimetic stimulation of an insulin mediated pathway [303]. Decreases fibronectin expression (Fig.3.13) observed in this thesis were in agreement to previously obtained data which had demonstrated an increase in fibronectin synthesis as a function of increased serum concentration [308].

Therefore it was possible to conclude that smooth muscle cells behaved in a similar manner under the chemically defined serum free conditions derived herein, to data previously published using similar experimental conditions. Cells demonstrated density dependent decreases in metabolic activity and expressed  $\alpha$ -smooth muscle actin throughout culture (Figs 3.7-3.9). Additionally, the smooth muscle cells expressed smoothelin, a marker indicative of a contractile smooth muscle cell phenotype, which was supported by a multitude of previous data which elucidates a role for

serum deprivation in the modulation of functional smooth muscle cell phenotype. Furthermore, during this study it was possible to demonstrate that the phenotypic switch in these cells was dependent on the absence of iron, as defined serum free culture media in which iron was present did not demonstrate the facilitation of the formation of a contractile phenotype. In support to one previous study, smooth muscle cells under defined serum free conditions decreased the expression of fibronectin, and additionally laminin, elastin and fibrillin-1, 3 molecules associated with smooth muscle cell integrity in which no previous data had been published contrasting the expression of these molecules in serum free and serum containing media formulations. Although it is widely regarded that populations of contractile smooth muscle cells are 100% positive for expression of laminin and fibronectin (Figs 3.9-3.14), explaining the observation of increases in the expression of these genes as a population switches phenotype [309].

#### 5.v Lineage uncommitted cells – Adult Tissue Derived Mesenchymal Stem Cells

When used in conjunction with bone marrow derived stem cells, the chemically defined serum free media demonstrated its capability of maintaining the metabolic activity of these cells in a similar manner to a widely used bespoke commercially available serum containing counterpart (Cambrex MSCBM). Ultimately, the cells increased in metabolic activity for the initial week of culture before decreasing by day 14. This was an identical trend to that observed with the serum containing media formulation with the resultant drop in metabolism hypothesised to be a result of contact mediated quiescence in a manner similar to that of smooth muscle cells. Interestingly, the metabolic activity of these cells at 14 days, although decreased from day 7 was significantly higher in serum free over serum containing media formulations (Fig.3.14). This observation is contrary to published data which suggests that bone marrow derived mesenchymal stem cells decrease in cell number when cultured under serum free media and also do not progress from G0/G1 phase of the cell

cycle suggesting cell dormancy. The serum free media formulation used in this particular study was not disclosed [310]. However, the data reported in [310] is similar to that obtained in research using rat bone marrow derived mesenchymal stem cells which showed that under serum free conditions containing similar constituents to those deemed optimal in this thesis (insulin, serum albumin and transferrin), mesenchymal stem cell number did not increase overall during an expansion period of 10 days. However, additions of two further exogenous components, basic fibroblast growth factor and platelet derived growth factor restored proliferation to a comparable rate to serum. Both of these components were found to be unnecessary in the data presented in this thesis. This study [240] was also able to elegantly demonstrate the role of insulin in mediating the proliferation of mesenchymal stem cells, due to its role as a mitogen and its involvement in glycogen synthesis. The publication hypothesises that insulin is required in hyper-physiological concentrations due to insulin like growth factor receptors having a high affinity for insulin like growth factors and a low affinity for insulin, therefore permitting insulin like growth factor mediated signalling when used in idiosyncratically high concentrations in comparison to an *in vivo* cellular environment [316]. This is supported by previous data obtained using the serum substitute B27 (Gibco, UK) and basic fibroblast growth factor which demonstrated a 5 fold increase in mesenchymal stem cell number during a culture period of 21 days in the absence of serum [317]. A study using bone marrow derived mesenchymal stem cells in conjunction with ultraCULTURE serum substitute, of which the formulation is undisclosed, described contradicting reports. The data from this study [317] suggests higher cell numbers are obtained in conjunction with the serum substitute when compared to media containing 15% fetal calf serum. This data shows considerably more rapid proliferation is obtained when using ultraCULTURE supplemented medium over a fetal calf serum containing alpha-MEM. They report that primary bone marrow derived mesenchymal stem cells expanded approximately 19-fold in 18 days whereas the same number of cells cultured in conjunction with ultraCULTURE supplemented media expanded 38-fold during an in the time period. This data suggests a

superiority for a serum free formulation in supporting the expansion of mesenchymal stem cells at a considerably higher level than the serum free media formulation developed in this thesis, which demonstrated the ability to support expansion at a rate comparable to serum containing formulations rather than surpassing them. Given the undisclosed nature of the ultraCULTURE components it is difficult to elucidate a reason for why this is the case.

More comparable with the data obtained using chemically defined serum free media presented in this thesis was the antigenic profile of the cells derived using ultraCULTURE. These cells demonstrated positivity for CD29, CD44, CD166 and CD73 in addition to negativity for CD34 and CD45, an almost identical antigenic profile to mesenchymal stem cells cultured using the serum free media presented in this research (Figs 3.17-3.22), although the exact values for the extent of positivity of these antigens were not published in the ultraCULTURE study. Additionally with the addition of exogenous factors (osteogenic: dexamethasone, ascorbate and  $\beta$ -glycerophosphate; adipogenic: indomethacin, dexamethasone and insulin; chondrogenic: FCS, insulin, ascorbate and TGF- $\beta$ ) ultraCULTURE demonstrated the capacity to support trilineage differentiation of the cells in a similar time frame to that was used for the data obtained using the *de novo* derived chemically defined media presented herein (2-3 weeks). One contrasting media component between the ultraCULTURE study and this research was the addition of serum in the ultraCULTURE chondrogenic differentiation matrix, which was not found to be necessary using the serum free media defined herein (Table 3.5). Whether a completely serum free chondrogenic differentiation strategy was attempted in the ultraCULTURE study was not stated in the publication (serum has in fact been demonstrated to inhibit chondrogenesis [318]). The adipogenic differentiation media using ultraCULTURE contained completely different components than was deemed necessary in the adipogenic defined serum free media formulation derived in this research (dexamethasone and hydrocortisone) (Table 3.5), whilst the osteogenic additions were identical [311]. A further study which reported

the antigenicity of bone marrow derived mesenchymal stem cells cultured under defined conditions also reported an antigenic profile of CD90, CD73, CD44 positive and CD34 and CD45 negative similar to this research (Figs 3.17-3.22). However, although the 'defined' media used in this particular publication contained insulin, transferrin and serum albumin, components which it shares with the media derived herein, it also contains 2% serum, rendering the claim to its defined nature made within the publication invalid [313]. Multiple reports using serum as a component of the cell culture matrix confirm that the antigenic profile analysis during serum free culture reported in this thesis are that which would be associated with a 'model' mesenchymal stem cell *in vitro*; including [319] CD29, CD44, CD90, CD105 positive, CD34 and HLA-DR negative. Interestingly, this publication discussed the negativity of CD146 in mesenchymal stem cells which was observed to increase in both serum free and serum containing cultures as cells increased in passage in the data presented in this research (Figs.3.17-3.22). Unfortunately, cell aging was not a factor that was considered in that previous publication [319]. Similarly [319] HLA-DR was significantly increased in both serum free and serum containing cultures by passage 7, although the increase in serum free media was not found to be significant in this thesis. Similar research states CD105, CD29, CD44 positive and CD34, CD45 negative [250]; CD90, CD105 and STRO-1 positive and CD31 negative (interestingly this report suggests CD146 to be positive and stably so throughout culture passages, contrary to the previous publication) [321] and CD105 positive [322].

A previously published study using umbilical cord derived mesenchymal stem cells demonstrated similar data to that obtained in this thesis using bone marrow derived mesenchymal stem cells when using a serum substitute containing comparable proteins (insulin, transferrin and serum albumin). During a 5 day expansion culture it was noted that although growth profiles were not identical, ultimately numbers of umbilical cord derived mesenchymal stem cells in the serum free and serum containing media formulations terminated at almost identical amounts. Interestingly,

this publication suggests a necessity for basic fibroblast growth factors as media components for optimal expansion, and is not alone in this suggestion. In conjunction with the media formulation presented in this thesis, basic fibroblast growth factor showed no effect on increasing the extent of proliferation under serum free conditions. The same publication also demonstrates the potential of serum free derived stem cells to undertake trilineage differentiation, however it does employ an osteogenic differentiation media containing 20% fetal calf serum, a component which was not deemed necessary in this research. It was not stated whether serum free osteogenic differentiation strategies were trialled. Additionally, the adipogenic medium derived was considerably more complex (dexamethasone, insulin, IBMX and indomethacin) than what was deemed minimal in this study (Table 3.5) [312].

A previous study has been conducted into the effect of serum deprivation on mesenchymal stem cell selection and it has been shown that stem cell populations selected on the basis of their ability to survive serum deprivation have long telomeres, and enhanced expression of genes which occur primarily in early progenitor cells. At the same time, the serum deprived cells retained most of the characteristics of mesenchymal stem cells in that they generated single cell-derived colonies and they differentiated into osteoblasts, chondrocytes, and adipocytes. This study used solely alpha-MEM as a maintenance media, therefore completely devoid of protein. Whether these findings are therefore relevant to those reported herein is difficult to conclude, however the observation of retention of stem cell associated characteristics and trilineage differentiation potential is consistent with findings reported in this research (Section 3.vi.) [314].

A further previous publication reported similar findings using bone marrow derived stem cells. This study used Knockout serum replacement which is produced commercially and as a result the formulation is undisclosed but does contain protein. Additionally, the media was supplemented with basic fibroblast growth factor and cells were cultured



on a matrix of gelatin rather than tissue culture plastic. This study examined proliferation and noted that a 4-5 fold increase occurred in the serum free over serum containing media formulation when cultured on a gelatin substrate. On tissue culture plastic, proliferation levels were massively reduced in serum free over serum containing medium. Additionally, however, it was reported that cells expressed nanog, Oct-4, nestin and frizzled-9, all proteins associated with early stem cell phenotype when cultured under serum free conditions. This, although similar to findings reported in [314] demonstrated that less severe serum deprivation was possible for inducing a more plastic phenotype in adult stem cells [315].

Gene expression data presented in this thesis in conjunction with bone marrow derived mesenchymal stem cells subjected to stimulation with defined serum free osteogenic differentiation media was remarkably similar to that obtained by a similar previous study (Fig.3.26). It was shown that after 18 days of culture of mesenchymal stem cells under osteogenic conditions, an increase in expression of approximately 10 fold was observed for CBFA1 and 1 fold was observed for type I collagen, data almost identical to that presented here, however, in contrast this previous data reported expression of osteocalcin was approximately 10 fold higher than that presented in this thesis. This previous study utilized a significantly more complex media formulation which, although devoid of serum (containing an insulin, transferrin and selenium based serum substitute) also contained basic fibroblast growth factor, fibroblast growth factor-8, fibroblast growth factor-10, insulin like growth factor, vascular endothelial growth factor, stem cell factor, transforming growth factor-beta, sonic hedgehog homologue, parathyroid hormone and bone morphogenic protein-6; therefore achieving similar data using a considerably more complex, costly and less defined media formulation [323]. A previous report demonstrated a relationship between dexamethasone and CBFA1, illustrating that CBFA1 gene expression decreases as the concentration of dexamethasone increases. This publication reported that at 100nM (the concentration of dexamethasone

used in the defined osteogenic media derived herein) there was an increase of approximately 55 fold relative to basal in CBFA1 gene expression after 48 hours of culture. When considering the early role of this gene in osteogenesis it is sensible to hypothesise that after 21 days of culture (the time scale used in this thesis) a decline in expression to the 10 fold reported both in this research (Figs.3.24 & 3.26) and in the previous publication [323] would be expected [324].

Another study into gene expression profiles of bone marrow derived stem cells during osteogenesis also reported an increase in the expression of osteonectin and no observable increase in the expression of osteocalcin (although exact levels are not stated) after 28 days of culture using a commercially available undefined osteogenic induction media [325]. This is similar to data presented herein (Figs 3.25 & 3.26), although a small increase in osteocalcin expression was observed after 21 days of culture under serum free defined osteogenic conditions. An elegant study examining a range of osteogenic associated proteins during osteogenic differentiation of bone marrow derived stem cells which also examined osteonectin and osteocalcin expression demonstrated contrasting data to that presented in this thesis, showing after 20 days in serum and FGF-2 containing osteogenic induction media, cells demonstrated expression of osteonectin roughly 100 fold lower, and osteocalcin 100 fold higher than that observed using chemically defined osteogenic induction media reported in this thesis. This publication also demonstrated the large extent of donor variability on gene expression of osteogenic markers during osteo-induction, therefore providing a possible explanation for the variation observed between these findings and the findings reported herein. Interestingly, the mean change in expression of CBFA1 reported in this study is approximately 10 fold after 20 days, consistent with previously discussed publications and data reported here [326].

A report using an almost identical serum free chondrogenic differentiation strategy based around TGF- $\beta$ 1 and an insulin, transferrin and selenium based serum substitute detailed an increase in type II collagen of

approximately 10 fold less than was reported in this thesis after an identical culture period of 21 days (Figs 3.27 & 3.28). This study highlighted a difference in chondrogenic gene expression levels as a factor of original isolation protocol, a possible explanation for the differences observed between this published data and data in this thesis [327]. In contrast, a further publication suggests increases of type II collagen expression during chondrogenic differentiation of approximately double those presented in this thesis were obtained using an identical chondrogenic differentiation strategy as was stated in [327] with the substitution of TGF- $\beta$ 1 for TGF- $\beta$ 3, suggesting a possible role of the TGF- $\beta$  isoform in the introduction of variability into the chondrogenic differentiation process [328].

Therefore it was possible to identify that the data previously published regarding the capacity of serum free media formulations to support bone marrow derived stem cell expansion *in vitro* is ambiguous. The consequences of introduction of bone marrow derived stem cells to serum free condition have been reported to be as diverse as apoptosis and cell cycle arrest versus multiple population doublings comparable and even surpassing that achieved using serum, making comparisons with existing data difficult. The serum replacements ultraCULTURE and B27 were reported to show numerous population doublings, however, their undisclosed formulation make deductions as to why this may be the case impossible. The disclosed serum free formulations without additions of exogenous growth factors generally resulted in no increases in cell number, or alternatively apoptosis: Basic fibroblast growth factor and platelet derived growth factor were identified as candidate molecules for maintaining mesenchymal stem cell proliferation at rates comparable to serum. As previously stated, a direct comparison with these data and the data presented in this thesis is difficult, however it can still be clearly concluded that the chemically defined serum free media derived presented herein demonstrated the capacity to maintain the metabolic activity of bone marrow derived stem cells at a rate directly comparable, and ultimately surpassing, that which was observed in serum containing media

formulations, leading cells to confluence and subsequent contact inhibition.

It was also possible to demonstrate from previous literature that serum starvation/deprivation resulted in selection of developmentally 'earlier' subpopulations of adult stem cells, a phenomenon which was also observed in media containing a protein component, allowing a possible hypothesis to be drawn that this could be occurring in the serum free defined media presented herein. Interestingly, the ambiguities which arise in the interpretation of data from serum free and serum containing media trials in conjunction with stem cells is reviewed concisely here [329]. Data presented in this thesis regarding maintenance of stem cell phenotype (Figs 3.17-3.23) were supported by extensive previous data into the surface antigenicity of bone marrow derived mesenchymal stem cells, allowing demonstration that the media supports the undifferentiated phenotype of these cells, in an almost identical manner to serum containing media counterparts. Additionally, in the case of certain subsets of antigens promoted an increase in expression of markers of plasticity over serum containing formulations (supporting the hypothesis that a serum free media could be selecting more plastic cells). Furthermore, the data also permitted demonstration of a decrease in markers of plasticity and a subsequent increase in markers associated with lineage commitment, as the cells increased in culture passage (Figs 3.17-3.22). Defined differentiation parameters enabled trilineage differentiation under conditions completely devoid of serum. Adipogenic differentiation was completed in media considerably less complex than any previous studies had reported (Table 3.5 & Figs 3.29-3.30). Additionally, chondrogenic and osteogenic differentiation was able to be carried out in a manner devoid of serum and characterised by cell type specific gene expression profiles in conjunction with immunohistochemistry similar to several previous studies in the differentiation of mesenchymal stem cells down these two lineages; often containing serum.

The chemically defined serum free medium displayed excellent potential when used in conjunction with the readily obtainable, ethically acceptable source of early pluripotent cells; dental pulp derived stem cells (Section 3.vii). The metabolic profile of the dental pulp derived cells under defined serum free conditions was similar to that observed using stem cells derived from bone marrow: an increase up until the 7<sup>th</sup> day of culture after which a plateau was observed. Cells at this point were confirmed by light microscopy to be confluent, therefore allowing the interpretation to be made that the drop in plateau in metabolic activity was a result of contact mediated inhibition of growth (Fig.3.32). These data are similar to that obtained previously using dental pulp derived stem cells in conjunction with the previously mentioned B27 serum supplement for which the formulation is undisclosed, but includes basic fibroblast growth factor and epidermal growth factor. These data only reported cell expansion under these conditions for the first 96 hours of culture, however the increase in cell number reported during this time corresponds to the increase in metabolic activity observed in the data presented herein (dental pulp cells were observed to have an increased metabolic activity to bone marrow derived stem cells under serum free conditions; confirmed by previously published data using a serum containing formulation [312]). Additionally these data also characterise the dental pulp stem cells used throughout the publication and states they are Sox2 positive, CD34, CD45, CD90 negative, a phenotype confirmed in this research (Figs 3.33 & 3.34), in conjunction with defined serum free medium. Interestingly, this report highlights dental pulp derived stem cells as CD117 and Oct4 negative; however it was possible to observe small amounts of CD117 positive and extensive amounts of Oct4 positive dental pulp derived stem cells in conjunction with the serum free medium defined herein (Figs 3.33 & 3.34). The maintenance of Oct4 is of particular note, being a transcription factor arguably associated with early plasticity [330]. The expression of Oct4 has been further confirmed in undifferentiated dental pulp derived stem cells, along with the presence of nestin, possibly suggesting a predisposition to a neuronal phenotype. Nestin was only evident in cells under defined neuronal stimuli in the data presented herein, and was not

present in undifferentiated dental pulp derived stem cells [336]. A further embryonic stem cell marker Tra-1-81 was observed in dental pulp cells cultured under defined serum free basal conditions (Fig.3.33). This was confirmed by previous studies that also observed this molecule when dental pulp derived stem cells were grown in media containing 20% serum. Interestingly this study reported that Oct4 expression ceased when cells were cultured under Knockout serum replacement (Invitrogen) for which the formulation is undisclosed. This was not found to be the case using the serum free media formulation derived in this research (Fig.3.33) [337].

Studies in which dental pulp derived stem cells are cultured under serum free parameters are scarce, seemingly having not gained significant commercial interest to warrant the development of clinically acceptable conditions to allow exploitation in tissue engineering. Further to previously discussed data, an additional study which characterized the plasticity of cells isolated from a range of oral tissues, confirmed, in consistency with data presented here (Fig 3.34), the presence of CD29 in stem cells derived from dental pulp. This study employed classical alpha-MEM medium containing 10% fetal calf serum and obtained similar expression data to that obtained here in using the defined serum free media formulation. In addition, this publication also confirmed the differentiation of dental pulp derived stem cells down an osteogenic lineage by the presence of CBFA1 and calcification after 21 days of culture under serum containing osteogenic medium. Again, this is similar to data obtained in this research using chemically defined media (Figs 3.46-3.47 & 3.52), with the presence of CBFA1 observed from day 5 then throughout the remainder of culture, and identically, calcified nodules were observed 21 days post induction under serum free osteogenic conditions. This study also detailed the differentiation of dental pulp derived stem cells down an adipogenic lineage after 21 days of culture although this used a protein (LPL; lipoprotein lipase) which was not used as part of the characterization in this thesis [331]. In conjunction with alpha-MEM media and 20% fetal calf serum a further study demonstrated the



expression of the marker of undifferentiated stem cells, STRO-1, in dental pulp derived stem cell populations. This was achieved in this research using the chemically defined media devoid of serum (Fig.3.33). This study carried on to differentiate the dental pulp derived stem cells and was able to demonstrate that the cells could differentiate into chondrocytes confirmed by the presence of type II collagen and sulphated glycosaminoclycans (alcian blue) after 3 weeks of culture in a chondrogenic media which consisted solely of alpha-MEM, 20% fetal calf serum basal media supplemented with 5% horse serum. This is consistent with data presented here, which detailed the presence of glycosaminoglycans and type II collagen (at the protein level) after 21 days of culture (Figs 3.36 & 3.40). The presence of type II collagen transcripts was observed initially 5 days post induction under chemically defined chondrogenic parameters (Fig 3.39). Furthermore this publication detailed adipogenic differentiation of dental pulp derived stem cells in a complex media (alpha-MEM, IBMX, dexamethasone, insulin, indomethacin) which contained 10% fetal calf serum. Interestingly, this was shown not to result in 'terminal' adipogenesis. Although the adipogenic gene, PPAR- $\gamma$  was detected after 21 days, no lipid vesicle formation was observed by Oil red O. In conjunction with the serum free adipogenic media derived here in PPAR- $\gamma$  was observed after 5 days of culture, and furthermore, complete adipogenesis was characterised by the presence of lipid droplets both using light microscopy and tinctural staining (Figs 3.56-3.57 & 3.61-3.62). Similarly to previously discussed data, this publication also detailed osteogenic differentiation of dental pulp derived stem cells by the presence of calcified nodules after 21 days of osteogenic culture (containing serum) consistent with the data presented in this research, in the absence of serum (Fig.3.52) [332].

Further previous accounts of chondrogenic differentiation of dental pulp derived stem cells are scarce. One study used porcine and canine dental pulp derived stem cells in a particularly complex medium containing 10% fetal calf serum, an insulin, transferrin, selenium based serum substitute, bovine serum albumin, dexamethasone, ascorbate and TGF- $\beta$ 3, which

furthermore then required the cells to be maintained in pellet culture, concluded that the dental pulp derived stem cells had become chondrogenic by the observation of aggrecan and type II collagen after 21 days of culture. This was similar to data presented here in using a media devoid of serum and monolayer culture. Both of these proteins were observed after 21 days of culture, and associated increases in gene expression for the precursor transcripts observed during the culture period (Figs 3.37-3.40) [250, 352].

The confirmation of adipogenesis presented herein is more consistent with data published by Gronthos *et al* which confirmed that the adipogenic potential of dental pulp derived stem cells by the presence of PPAR- $\gamma$  and additionally lipid vesicle encapsulation after 5 weeks of culture under adipogenic conditions. This publication also further confirmed CD29 as an integral marker of pluripotent dental pulp derived stem cells. Adipogenesis was confirmed in the data presented as part of this research after a shorter time course than that previously published and additionally, the Gronthos differentiation study employed 10% fetal calf serum in the media (Figs 3.56-3.63) [338-339]. The presence of CD29 and STRO-1 (the presence of STRO-1 as an indicator of dental pulp derived stem cells was also stated in the following [239-241, 245]) in dental pulp derived stem cells has been further confirmed although this particular study detailed higher levels of expression than that observed from the data presented herein (99% to approximately 30%). This study also observed the stem cell marker CD90 in dental pulp derived stem cells, which was not found to be present here (Fig 3.34). This publication detailed the osteogenic induction of dental pulp derived stem cells using osteo-induction media containing 10% serum and after 14 days obtained a comparable set of gene expression data to that presented in this research (Figs 3.46-3.51). The serum containing osteogenic media demonstrated an approximately 2 fold increase in CBFA1 after 14 days of culture, in conjunction with the defined serum free media derived here in an increase of approximately 7 fold was observed after an identical time scale (Fig 3.46). Osteopontin expression

increased a mean of 20 fold and a maximum of 100 fold in the serum containing osteogenic media formulation after 14 days of culture. In conjunction with serum free osteogenic medium increases in osetopontin was observed earlier; between day 5 and 7 post osteo-induction (Fig 3.49). Also reported is an increase in osteocalcin after 14 days using serum containing osteogenic media in conjunction with dental pulp derived stem cells which was reported in this research at the protein level using defined osteogenic media (Fig 3.51). This publication also elegantly stated 'Findings point towards DPSCs having higher internal heterogeneity possibly due to subpopulations of varying degrees of commitment or origin. The dental pulp also contains neuronal and vascular cells'. This may provide an explanation for the discrepancies observed between serum free over the published serum containing media formulation.

Quite possibly the cells used for the study detailed in this thesis may contain a subpopulation pre-destined to osteogenesis, hence earlier osteogenic gene detection and increased levels of expression under the serum free osteogenic parameters [323]. The presence of subpopulations of cells with discrete gene expression profiles was concluded in a second similar study by observing the response of cells isolated on the basis of their clonality to sets of arbitrary PCR primers [344]. Furthermore, similarly to bone marrow derived mesenchymal stem cells, variability in characterization of dental pulp derived stem cells has been shown to be influenced by the method of collection [264]. A further study into the osteogenic potential of dental pulp derived stem cells using direct stimulation with BMP-4 under serum containing conditions reported up regulations in CBFA1 and osterix after 24 hours of culture. This data is similar to that presented here in: In conjunction with defined osteogenic parameters osterix was observed 14 days post stimulation, however CBFA1 was not determined to be present until day 5 post induction (Figs 3.46 & 3.48). However, when considering the role of CBFA1 in early osteogenic induction, the presence of osterix (a precursor molecule to CBFA1 in osteogenesis) is suggestive that CBFA1 had been previously transcribed at this time although the mRNA was not remaining in tact in

the cell at the time lysates were taken [239]. A further study which differentiated dental pulp derived stem cells down an osteogenic lineage in osteo-inductive media containing 20% fetal calf serum confirmed the presence of osteonectin post induction, although the exact time frame at which the molecule became apparent was unpublished. Osteonectin was observed in defined serum free osteogenic medium after 5 days of culture (Fig 3.50). Furthermore, this publication confirmed the presence of CBFA1 and osteocalcin in osteogenic differentiated dental pulp derived stem cells [340]. A second study incorporating 20% fetal calf serum as part of the osteo-induction strategy also confirmed the presence of CBFA1, osteonectin and osteocalcin, similarly to the data presented in this research obtained without the use of serum (Figs 3.46-3.47 & 3.50, 3.51) [341].

It has been suggested that dental pulp derived cells secrete neurotrophic factors when residing in their niche *in vivo*. A characterising factor of dental pulp that was differentiated down a neuronal lineage was the expression of NGF. A previous study suggested that this molecule, along with GDNF and BDNF are expressed by dental pulp cells natively, however this was not found to be the case in the data presented herein, this molecule (NGF) only being expressed after neural induction under defined serum free neural stimulation (Figs 3.64-3.65). Consistent with the data reported in this thesis however, the same publication details the expression of  $\beta$ -III-tubulin under neural conditions containing 10% fetal calf serum (direct stimulation using exogenous dopamine). Although the precise time points at which this molecule became apparent are unreported, it is consistent with data reported herein, with increases in expression in excess of 10,000 fold over basal evident after 14 days of defined serum free neuronal culture (Figs 3.67-3.68) [235]. The presence of  $\beta$ -III-tubulin was also defined after neural induction [237]. This publication used a similar differentiation strategy to that presented here, using Knockout serum replacement (Invitrogen) in conjunction with retinoic acid. Although these cells were demonstrated to express  $\beta$ -III-tubulin, a marker of neural lineage commitment, they were also shown to express GFAP,

suggestive of a sub population more predisposed to a glial rather than neuronal fate, the precise time scale at which these molecules were recognisable after initial induction was not published. The presence of GFAP was not observed during the serum free neuronal culture of dental pulp derived stem cells detailed in this research. However, it was present in umbilical cord derived stem cells under the same stimuli along with a similar subset of neuronal lineage markers to dental pulp derived cells, suggestive of a more homogeneous neuronal differentiation of dental pulp over umbilical cord derived stem cells (Fig 3.74). This publication reported that the sites of neuronal differentiation were spheroid bodies within the population of cells. These structures were not recognisable in the cultures performed in this project. A similar study, which utilised a second commercially available serum replacement; B27 (Gibco) as part of the neural differentiation media in addition to basic fibroblast growth factor and epidermal growth factor reports similar findings. Cells were demonstrated to express  $\beta$ -III-tubulin, nestin, and neurofilament after neural induction, although the time scale after which these molecules were apparent was not published. All of these markers of neurogenesis were evident in dental pulp derived stem cells under the serum free neural parameters defined in this research (Figs 3.63, 3.66 & 3.67-3.68). In a similar manner to the previously discussed work, this publication records the presence of GFAP under neural stimulation, a phenomenon which as mentioned previously was not observed in dental pulp derived stem cells under defined neural differentiation parameters [239]. A second publication which used identical stimulation [239] detailed the presence of the nestin and  $\beta$ -III-tubulin proteins, although detailed that at the RNA level these genes were down regulated relative to basal conditions after 3 weeks of culture. This data is contrary to that presented in this study which details a large increase in expression of  $\beta$ -III-tubulin after 3 weeks of culture although similarly nestin was not found to be present at this time point (Figs 3.67-3.68 & 3.63) [243].

Differentiation of dental pulp derived stem cells towards a hepatic lineage had not previously been reported. However, comparisons can be made

with previous data obtained using adult stem cells from alternative tissues. One previous study which used umbilical cord blood derived stem cells characterised hepatic differentiation using a considerably more complex induction strategy than was described in this thesis (Table 3.5). Cells were initially subjected to differentiation media containing Hepatocyte growth factor, dexamethasone and an insulin, transferrin & selenium based serum substitute for 14 days, after which this media was removed and replaced by a maturation medium containing the same serum substitute in addition to oncostatin M and dexamethasone for a further 14 days. After the 28<sup>th</sup> day, the cells expressed serum albumin, cytokeratin 18 and alpha-fetoprotein, the same subset of markers which was confirmed present in dental pulp derived stem cells after 21 days of culture under the considerably more straightforward defined serum free hepatic differentiation protocol detailed in this study (Figs 3.75-3.78) [346]. An similar technique using umbilical cord blood derived stem cells under identical stimuli to that stated in [346] with the modification that the induction media contained 10% fetal calf serum reported identical data: presence of serum albumin, cytokeratin 18 and alpha-fetoprotein after 28 days of culture [348]. An equally as complex 2 step protocol was demonstrated to differentiate bone marrow derived stem cells down a hepatocyte lineage. This involved a 10 day induction in media containing hepatocyte growth factor, FGF-4, nicotinamide and an insulin, transferrin, selenium based serum substitute followed by a 20 day maturation period in media containing the same serum substitute, oncostatin M and dexamethasone. In a manner similar to that in [346] after differentiation these cells possessed serum albumin, cytokeratin 18 and alpha-fetoprotein, the same subset of proteins used to define dental pulp derived stem cell differentiation using the considerably less complex approach reported in this study (Figs 3.75-3.78). This previous data [346] was also able to demonstrate the preservation of mesodermal proteins such as vimentin and fibronectin in hepatocyte cells derived from mesenchymal stem cells. A further study using an identical differentiation protocol as was detailed in [347] demonstrated the necessity of bone marrow derived stem cells to be maintained in pellet culture to initiate hepatocyte differentiation. This was



not found to be the case using defined serum free medium in conjunction with dental pulp derived stem cells, nor was it this culture strategy was deemed necessary for the hepatic differentiation of bone marrow derived stem cells in the publication using an identical media formulation [348]. Adipose derived stem cells have also demonstrated hepatic potential, illustrated using a comparatively simple media formulation; dimethyl sulfoxide, hepatocyte growth factor and oncostatin M in the absence of serum or serum substitute compounds. In a similar manner to the previous studies, these cells possessed serum albumin and cytokeratin 18 proteins after 28 days of culture, further confirming these proteins as suitable indicators of terminal hepatogenesis [349].

The metabolic profile of dental pulp derived stem cells was similar to that of bone marrow derived stem cells cultured under chemically defined serum free parameters. Cells increased in metabolic activity until confluence after which contact mediated inhibition resulted in a decrease in metabolism. There have been very few previous studies examining the proliferative capacity of dental pulp derived stem cells under serum free conditions. One which was available detailed an increase in cell proliferation during the initial 96 hours of culture, which was consistent with the increase in metabolism observed during this time under the chemically defined conditions detailed herein. The dental pulp derived stem cells maintained their associated undifferentiated phenotype under serum free conditions in a manner comparable to that which has previously been reported in serum containing media formulations. This included a subset of markers associated with early plasticity: Oct4, Tra-1-81 and Sox2 in addition to the markers of an undifferentiated adult stem cell phenotype: STRO-1 and nucleostemin (the presence of nucleostemin had not previously been reported in dental pulp derived stem cell populations). Discrepancies did occur when contrasting phenotype characterization data with that previously obtained. However, the well documented donor variability in antigenic profiles of dental pulp derived stem cells and the existence of discrete sub-populations which can be selected under certain stimuli may account for this. The dental pulp derived stem cells were

differentiated down an osteogenic lineage which has not previously been reported under defined serum free parameters. As a result of subjection to these conditions the cells expressed a familiar subset of osteogenic genes in addition to histological confirmation of calcification which was consistent with several previous studies using these cells in conjunction with serum containing osteogenic media formulations. Previous data into chondrogenic differentiation of dental pulp derived stem cells was limited. However, the cells expressed aggrecan and type II collagen as a result of serum free chondrogenic stimuli which was consistent with the small number of previous attempts at this component of tri-lineage differentiation, and did not require three dimensional culture. Furthermore, the cells were shown to express Sox9 and chondroadherin, under defined chondrogenic stimuli, two chondrogenic transcription factors which had previously not been targeted in characterisation of chondrogenic differentiation of dental pulp derived stem cells (Figs 3.35 & 3.41), in addition to the typical rounded morphology of functional chondrocytes concluded using scanning electron microscopy (Fig 3.42). Interestingly, the cross over between osteogenic genes under chondrogenic stimuli and chondrogenic genes under osteogenic stimuli was observed, suggesting a progression in both cases to a hypertrophic cartilage intermediate, concluded particularly by the presence of type X collagen in the cells under defined osteogenic stimuli (Fig 3.55). This phenomenon had not previously been characterised using dental pulp derived stem cells although is often concluded using stem cells from more conventional adult tissues [351]. Previous data detailed the onset of adipogenesis in dental pulp derived stem cells through the observation of PPAR- $\gamma$  and lipid vesicle formation within the cell cytoplasm. This was consistent with the data presented herein, which also used other adipocyte associated proteins: perilipin, adiponectin and leptin to characterise the transdifferentiation of dental pulp cells into adipocytes under defined serum free adipogenic conditions, three proteins never previously reported as part of this characterisation (Figs 3.58-3.61). Neural differentiation had previously been achieved under serum free parameters using the serum substitute B27 and data presented herein was consistent and considerably more extensive

than that previously published. Previous studies had characterized neural differentiation on the basis of small subsets of neural proteins with the presence of  $\beta$ -III-tubulin often reported as adequate confirmation of neural differentiation. Under stimulation with a particularly simple defined serum free neural differentiation media it was reported in this data that the dental pulp derived stem cells differentiated down a neural lineage and expressed  $\beta$ -III-tubulin, nestin, NGF and neurofilament (consistent with previous reports) in addition to Synaptophysin, synaptic vesicle protein, and substance P, three molecules associated with neural functionality which had not previously been reported in characterization of neural differentiation of dental pulp derived stem cells (Figs 3.69 & 3.71). Additionally under defined serum free conditions the dental pulp derived stem cells exhibited a neural morphology and an overall decrease in the repressor of neural differentiation REST was observed at the RNA level (Fig 3.70). Hepatic differentiation of dental pulp derived stem cells had not previously been documented. Herein a defined serum free strategy was reported which was considerably less complex than previous data obtained using adult stem cells from alternative sources and resulted in similar protein expression, the presence of serum albumin, cytokeratin 18 and alpha-fetoprotein. Furthermore the metabolic activity during various differentiation stimuli had not previously been documented however the overall trend presented here; an increase in metabolic activity initially followed by either a plateau or a decline is consistent with the arrest of cellular proliferation and overall reduction in cell number as a plastic cell is induced to lineage commitment (Fig 3.79).

### 5.vi Hydrogel Characterisation

The platelet poor plasma derived hydrogel was characterised using dynamic contact angle. The contact angles which were recorded were similar to that of unmodified, clean glass. Glass is regarded as one of the optimal substrates for facilitating cellular adhesion and proliferation. A critical milestone in the early compatibility of primary cells with a substrate is the surface energy of the substrate (directly related to contact angle by;  $\gamma_{sv} = \gamma_{sl} + \gamma_{lv} \cos\theta$ ) therefore the demonstration that the contact angles of the platelet poor plasma derived hydrogel were similar to that of glass was indicative of a compliant surface energy for facilitation of cellular adhesion. Varying concentrations of sera were used as a solvent in dynamic contact angle experiments to give a more realistic representation of the surface characteristics of the hydrogel when used in both *in vitro* and *in vivo* tissue culture scenarios. There was no significant variation in the contact angle of the hydrogel throughout 0-100% serum, likewise no variation in the contact angle of glass with an identical set of solvents was recorded either (Fig.4.3). Previous studies have also identified the potential of hydrogels as suitable candidate materials for tissue engineering, particularly in cartilage repair. One publication stated: 'Hydrogels, cross linked hydrophilic polymers, have many advantages that make them prime candidates for cartilage tissue engineering applications: relative biocompatibility, tissue-like water contents and tissue-like elasticity, which can encapsulate cells when they crosslink. In addition, hydrogels, three-dimensional networks of hydrophilic polymers that are able to swell, retaining large amounts of water, can be made to resemble the physical characteristics of soft tissue' [353]. Previously characterised in a similar manner was a considerably more complex hydrogel for the purpose of cell culture, a photo-crosslinkable poly (ethylene glycol) diacrylate based hydrogel. The contact angles reported for this hydrogel are considerably less than were elucidated for the platelet poor plasma derived hydrogel. Additionally [353] reported how the contact angles vary, with the introduction of 2-hydroxymethacrylate into the polymer matrix to increase cross linking (100% PEDGA/0% HEMA = 52° – 60% PEDGA/40%

HEMA = 33°). Although these differences were significant when compared the hydrogel presented herein and the suitability of the PEDGA based hydrogel in cartilage tissue engineering was suggested, no cellular compatibility investigations were reported, this study also used water as its solvent [353]. In contrast, an equally chemically complex hydrogel designed for cell culture purposes reported a considerably higher contact angle than that presented in [353]. Similarly, this study also used 2-hydroxymethacrylate combined in this instance with poly(dimethylsiloxane). Here again it was noted that the contact angle decreased with the addition of HEMA, however overall the contact angle measurements were more comparable to that of the platelet poor plasma derived hydrogel (80%PDMS/20%HEMA = 97.1°, 60%PDMS/40%HEMA = 88.3° and 40%PDMS/60%HEMA = 61.5°). Similarly again to [353], it is hypothesised that this hydrogel would be cellularly compatible, however, no data is presented to support this. Furthermore, the publication stated how only rarely cell based data is presented to support compatibility claims based on characterisation measurements [354]. A study which compared the effect of contact angle on a plastic substrate (polypropylene) demonstrated data contrary to [353] and [354], suggesting that HEMA was responsible for increasing contact angles versus their base polymer; diethylene glycol methacrylate. This particular study published data that suggested very little difference in contact angle between the plastic substrate and a completely HEMA hydrogel. Diethylene glycol methacrylate additions, however decreased the contact angle (untreated polypropylene = 95°, HEMA hydrogel coated polypropylene = 91° and DEGMA hydrogel coated polypropylene = 69°). These contact angles are also in the range of the platelet poor plasma derived hydrogel (maximum approx. 82° in PBS) therefore demonstrating similar characteristics with significantly simpler chemistry. Furthermore, this study also quotes no cell data but does suggest suitability in biomaterial applications [355]. Similarly, high contact angles were observed in hydrogels generated using poly(ethylene oxide) and poly(tetramethylene oxide) (89.7°-109° dependent on ratios of the two components) [358]. A major use of hydrogels in current clinical

biomaterials is intraocular lenses. These lenses need to be biocompatible, as associated publication [356] states 'Contact angle readings in particular assess surface hydrophilicity, which can be used as a reliable parameter for predicting uveal and capsular biocompatibility'. This publication used contact angle as an indicator characteristic extrapolatable to biocompatibility and assessed a number of currently commercially produced intra ocular lenses and discovered a maximum contact angle of  $199^\circ$  (Silens 6/Bausch & Lomb; PDMS) and a minimum of  $56.5^\circ$  (CeeOn 811C/Pharmacia HSM; PMMA). This publication further presented no cell data to suggest these materials were biocompatible however this is implied by their current presence on the market. The range of contact angles is explained by the need for materials of differing mechanical properties to fulfil the same role in different patients, for example, certain ocular complications may require lenses to be more flexible to fit into a particular space or more hydrophilic in the case of a patient with chronic uveitis. This suggests a range of contact angles are capable of being biocompatible, with variations in contact angle being more to tailor a material to a particular function rather than to make it more cellular compatible [356]. A semi-organic hydrogel made from a poly(N-isopropylacrylamide)-g-methylcellulose copolymer was reported to have similar contact angles to the completely organic platelet poor plasma derived hydrogel ( $80.8^\circ$ - $88.1^\circ$ ; dependent on methylcellulose concentration) although similarly to the previous publications, a biocompatibility was suggested but not supported with any cell-based data [357]. Furthermore, a completely organic homogeneous collagen gel was demonstrated to have an almost identical contact angle of  $82^\circ$ . This gel also demonstrated cellular compatibility demonstrating excellent adhesion of tendon derived primary human fibroblasts [359]. Therefore, it was possible to conclude that the hydrogel derived from blood plasma had a similar contact angle to several previously described polymers. Generally, the previously synthesised polymers were chemically considerably more complex and had only been hypothesised to be biocompatible. Furthermore, the two polymers previously studied with an organic component showed remarkably similar contact angles to that stated for the



platelet poor plasma-derived hydrogel. In the case of the collagen gel, this material has been documented extensively to support cellular adhesion and expansion, having a contact angle almost identical to that of the platelet poor plasma-derived hydrogel.

#### 5.vii In-Vitro Cell Culture in Conjunction with Platelet Poor Plasma Derived Hydrogel

The platelet poor plasma derived hydrogel demonstrated the capacity to maintain the phenotype of primary articular chondrocytes. Cells seeded under the gel were demonstrated to maintain their phenotype after a culture period of 21 days, confirmed by the presence of sulphated extracellular matrix glycosaminoglycans (Fig 4.5). Articular chondrocytes have a tendency to change phenotype into a more fibroblast resembling cell in the absence of a suitable culture matrix. In particular, these cells favour culture under controlled hypoxia as this is mimetic of their *in vivo* niche inside articular cartilage. Several previous studies have confirmed this data using alternative hydrogel systems. These include one particular study which compared an organic hydrogel made from agarose with an inorganic polymer hydrogel made from a copolymer of poly(N-isopropylacrylamide) and acrylic acid (PNiPAAmco-Aac) which both demonstrated identical data to that obtained with the platelet poor plasma derived hydrogel: maintenance of chondrogenic phenotype confirmed by the presence of glycosaminoglycans after 21 days of culture inside blocks of the hydrogels [360]. A further synthetic polymer hydrogel, poly(ethylene glycol) dimethacrylate (PEGDM), reported identical data: presence of glycosaminoglycans after culture inside the hydrogel confirming the maintenance of a chondrogenic phenotype [367]. Alginate, a naturally occurring polymer has also been used to demonstrate similar data, cells cultured inside the gel maintained matrix glycosaminoglycans after 42 days of culture. Interestingly, this gel system did contain an additional exogenous factor, TFG- $\beta$  which was deemed unnecessary in the platelet poor plasma derived hydrogel [361]. Additionally, the presence of

glycosaminoglycans has been demonstrated in collagen gels after defined culture periods. These systems often rely on non-host serum as a component of the culture medium surrounding the cell laden hydrogels [362-363, 366]. Furthermore, gels synthesised from fibrin, have demonstrated an identical capacity to maintain chondrogenic phenotype after extended culture, demonstrated by the presence of several chondrogenic genes (type II collagen, aggrecan and versican) post hydrogel culture [364]. The use and success of fibrin-based gels as a material for the expansion and phenotype maintenance of chondrocytes is reviewed here [365]. Therefore it could be concluded that the platelet poor plasma derived hydrogel demonstrated the same biological properties as a vast multitude of predecessor hydrogels, the capacity to support chondrogenic phenotype. In general, previously published gels required either complex chemistry or the addition of exogenous serum or more defined factors (TGF- $\beta$ , PDGF) to achieve this, which were not deemed necessary components of the culture media when using the platelet poor plasma derived hydrogel.

The surface of the platelet poor plasma derived hydrogel was demonstrated to be an ideal substrate for the growth of primary human cells. The gel surface was used in conjunction with a sub-population of dental pulp derived pre-endothelial stem cells, discriminated from the main population on the basis of the presence of an ABCG2 membrane pump and subsequent efflux of Hoechst dye, to support the differentiation into microvascular endothelial cells and resultant formation of three dimensional microtube/microcapillary structures (Figs 4.9-4.11). Interestingly, these structures did not form on a Matrigel surface, an undefined extracellular matrix hydrogel (Fig 4.6). The endothelial cells expressed CD31, Von Willebrand factor and VE-cadherin (cadherin 5) (Fig 4.12), three molecules associated with functional vessel endothelium. Similar data has been presented previously using type I collagen gels. In this particular study, terminally differentiated endothelial cells harvested from a range of tissues (human umbilical vein endothelial cells, adult and neonatal human dermal microvascular endothelial cells and human blood

outgrowth endothelial cells) were seeded onto type I collagen gels additionally containing exogenous basic fibroblast growth factor, vascular endothelial growth factor and phorbol myristate. In this instance, the publication reports that microtubular organisation was apparent after 48 hours of culture. However, from the data presented, this formation does not appear as extensive and organised as that achieved with platelet poor plasma and Hoechst<sup>dull</sup> dental pulp derived stem cells. The endothelial phenotype of these cells was not characterised after culture in conjunction with the hydrogel, however, it was detailed that prior to seeding they were CD31, Von Willebrand factor and VE-cadherin positive, demonstrating that the phenomenon was this not differentiation but the provision of a suitable matrix for the cells to adopt a native organisation. The platelet poor plasma gel demonstrated the generation of considerably more extensive microvascular network formation from a cell source which was not previously endothelial although selected on a marker which was suggestive of its predisposition to become a cell of this phenotype. Additionally, no further exogenous additions were required to facilitate this, with the constituents of the human plasma being sufficient to support endothelialisation of the gel surface [368]. One early study using a fibrin-based gel as a supporting matrix for microvascular formation demonstrated that the embedding of large portions of bovine pulmonary artery containing endothelium and luminal layers resulted in microvascular migration into the surrounding hydrogel to an extent which resembled that which was observed using Hoechst<sup>dull</sup> dental pulp derived stem cells in conjunction with the platelet poor plasma derived hydrogel. The study reported that when isolated homogeneous endothelial cells were seeded onto the gel surface, the cells formed a monolayer. Additions of basic fibroblast growth factor and vascular endothelial growth factor caused the cells to elongate and begin to organise into a microvascular like arrangement. As stated previously, these exogenous additions were not deemed necessary using platelet poor plasma derived hydrogel. The publication also elucidated a role of supportive cells in the generation of ectopic microvasculature. In this case vascular smooth muscle cells and pericytes were used, however, again this was not deemed necessary using

the platelet poor plasma derived matrix [369]. The suggestion of a cell supportive role being necessary for the complete facilitation of microtubule formation was also hypothesised previously using fibroblasts in conjunction with fibrin gels [372]. The necessity for basic fibroblast growth factor and vascular endothelial growth factor was further elucidated using primary derived microvascular endothelial cells in conjunction with a type I collagen gel. This particular study clearly demonstrated a synergy between the two growth factors in the support of these two angiogenic molecules in microvascular arrangement and suggested that this proposed mechanism could play a role in vascular direction *in vivo*. In this study, the extent of arrangement resembled that which was observed using the platelet poor plasma derived hydrogel, again stimulated without the need for additional exogenous additions [370, 373]. A further study again obtained, an almost identical extent of vascular outgrowth to that observed using the platelet poor plasma derived hydrogel, across a type I collagen gel using primary endothelial cells. However, in this investigation platelet derived growth factor was identified as a necessary exogenous addition to support microvascular organisation [371].

Therefore it was possible to elucidate that the platelet poor plasma derived hydrogel was capable of providing a suitable surface matrix in which dental pulp derived stem cells, selected on their predisposition to an endothelial phenotype could form microtubular structures in an identical manner to several previously published works using fibrin and collagen gels. Typically, previous data suggested the necessity for additions of defined exogenous factors to stimulate *in vitro* angiogenesis, however, using the platelet poor plasma derived hydrogel matrix this was not deemed necessary. However, that was not to say that factors such as basic fibroblast growth factor and vascular endothelial growth factor were not present natively in the plasma used to construct the gel. Their molecular roles in neo-vascularisation may be correct, however no further supplementation outside of the platelet poor plasma was necessary. After differentiation and subsequent microtubule arrangement the Hoechst<sup>dull</sup> -

selected dental pulp derived stem cells expressed CD31, Von Willebrand factor and VE-cadherin, three molecules associated with functional endothelial cells. Hematopoietic stem cells have been reported to contain a subpopulation of endothelial progenitor cells, one previous publication states 'circulating CD34+ cells expressing VEGFR-2 and AC133 constitute a phenotypically and functionally distinct population of circulating endothelial cells that may play a role in neo-angiogenesis [374]. It is this population that was selected for using Hoechst based cell sorting exploiting Hoechst efflux from hematopoietic cells based on their possession of a specific membrane pump, the ABCG2 pump, which elutes the dye, then combined with a suitable growth substrate in the form of the platelet poor plasma derived hydrogel. These cells did not form microtubes when cultured on conventional tissue culture plastic, reiterating the suitability of the hydrogel substrate for this application and additionally did not successfully form microtubes in conjunction with the undefined extracellular matrix hydrogel Matrigel for reasons which were not possible to elucidate. During the period of hydrogel culture the dental pulp derived stem cells also decreased their expression of stem cell markers such as CD29, CD73, CD90, CD105 and CD106 confirming their progression towards a particular fate. The Hoechst<sup>dull</sup> cells cultured in conjunction with platelet poor plasma derived hydrogel also expressed the endothelial specific molecule CD62E, however, this molecule was also expressed by the Hoechst<sup>bright</sup> population of cells in a substrate independent manner in both cases. Interestingly, this molecule was expressed in only a very small percentage of the dental pulp derived stem cells when present in a heterogeneous population and while the sort stimulated expression of this marker equally in all populations is an interesting artefact of this study it highlights the lack of suitability of CD62E as an exclusive marker of endothelial cell phenotype. In a similar manner the expression of the stem cell marker CD117 was conserved post sort at similar amounts independent of substrate suggesting its lack of suitability as a marker of undifferentiated pluripotent cells (Figs 4.13-4.14). Furthermore the surface of the platelet poor plasma derived hydrogel facilitated an overall increase in the metabolic activity of the both populations of pulp derived

cells throughout culture in conjunction with the hydrogel substrate further emphasizing its suitability as a tissue culture substrate (Fig 4.15).

The platelet poor plasma derived hydrogel demonstrated the capacity to support the migration of primary cells throughout the gel. This was demonstrated using human articular chondrocytes seeded in two layers and their dispersion throughout the gel block 'tracked' using cytoplasmic cell tracking dyes (Fig 4.16). Similar data has been presented using alternative hydrogel polymers and cell types. Previous data has shown the capacity of polyethylene glycol and type I collagen hydrogels to support the migration of primary human fibroblast, bone marrow derived stem and cardiomyocyte cells. These data did not demonstrate this as clearly as those herein. The presence of cells was only noted in one section and additionally the gels cast were significantly smaller, only 1  $\mu$ L in volume [375]. A further study using an artificial polymer hydrogel of poly(N-isopropylacrylamide-co-acrylic acid) demonstrated its supportive properties for osteoblast migration demonstrated by placement of a pellet of osteoblasts inside a block of gel and monitoring the outgrowth from the pellet using phase contrast microscopy, thus demonstrating the capacity of the hydrogel to facilitate migration and cell outgrowth without elucidating the extent of migration in three dimensions [306]. A second study using osteoblasts reported their capacity to migrate through a poly(propylene fumarate-co-ethylene glycol)-based hydrogel only when the gel was cross linked with an RGD sequence containing peptide. Again, the cell migration through the hydrogel was only qualified by observation of cell outgrowth from an initial population in two dimensions [377]. Another similar study which populated poly(ethylene glycol) hydrogels with various RGD containing peptide motifs claimed the gel supported migration of dermal fibroblast and arterial smooth muscle cells although again, only demonstrated this as a two dimensional outgrowth from a pellet [378]. One study of note did demonstrate three dimensional migrations of cells through an agarose gel again populated with RGD containing peptides. However, in this instance channels were generated in



the gel to guide dorsal root ganglia cells from the surface into the bulk of the gel, and no data was presented to suggest whether this would have occurred without the guidance channels [379]. Three dimensional migration was again noted in a study which used smooth muscle cells in conjunction with a hybrid gel of poly(ethylene glycol) and fibrinogen. This publication presents images similar to those presented herein, of fluorescent cells embedded within the hydrogel. However no complete Z section is presented and the image is taken shortly after gel casting so ultimately cell migration in three dimensions is not elucidated when all that is presented is an initial seeding of a cell block. Alternatively the typical cell outgrowth from a pellet of cells is shown, again only detailing two dimensional outgrowth rather than infiltration through the hydrogel [380]. Therefore it was possible to conclude that the data presented here in detailing the migration of articular chondrocytes through the platelet poor plasma derived hydrogel was comparable or superior to previously published studies. In general, previous data only detailed the infiltration of cells in two dimensions through the various hydrogels. Additionally, several studies employed protein modifications to their hydrogels to stimulate migration. In the case of the platelet poor plasma derived hydrogel three dimensional migration was clearly observed and additionally, no further exogenous modifications to the gel were necessary to facilitate this.

#### 5.viii In Vivo Cell Culture in Conjunction With Platelet Poor Plasma Derived Hydrogel

The platelet poor plasma derived hydrogel extensively demonstrated its potential as an *in vivo* candidate biomaterial for cell delivery and provision of a degradable stable environment for cellular expansion by injection through a study in which primary human dermal fibroblasts were implanted in conjunction with the hydrogel subcutaneously into immunosuppressed mice. The gel could be delivered by means of two syringes, one containing cell loaded media and the other containing platelet poor

plasma. The two solutions could be combined by means of a stopcock tap system immediately prior to implantation allowing gellation to occur *in situ*, entrapping the primary cells within the hydrogel matrix. The cells proliferated within the gel causing the reliable ectopic formation of subcutaneous neotissue composed of human dermal fibroblasts (Fig 4.24). These tissues were well vascularised (Fig 4.23) and showed limited adhesion to the underlying host connective tissue (Fig 4.22). The origin of the cells at the point of explantation was confirmed as human by a combination of immunohistochemistry, real time-PCR, fluorescent cell tracking and fluorescent *in situ* hybridisation observation of human Y chromosomes in the delivered human male cells in female host animals (Figs 4.30-4.35). The tissues showed several features which emphasise their compatibility with the host tissue including infiltration of several host structures into the hydrogel derived neo-tissue such as adipose (Figs 4.26-4.27), hair follicles (Fig 4.29) and muscle blocks (Fig 4.28). The cell loaded hydrogel raised a minimal immune response in the host animal. Although macrophages and neutrophils were observed (Figs 4.36 & 4.38), immunohistochemistry suggested only limited activation (Fig 4.37). In addition antigen presenting cells were also only rarely present further confirming the immuno-compatibility of the neotissue (Figs 4.40). A previous study attempted to elucidate the molecule responsible for angiogenesis in a hydrogel. This comparable hydrogel system could provide an explanation for the extent of vascularisation which was observed throughout the dermal fibroblast neo-tissues. This particular study implanted gels derived from heparin (6-O-desulfated heparin) which eluted FGF2. It was observed that this molecule stimulated a degree of vascularisation in these gels that was comparable to that observed in the platelet poor derived hydrogel derived tissues in similar sized gels when implanted subcutaneously. Vascularisation was not observed in gels without FGF2 (nor was it observed in platelet poor plasma gel without fibroblasts) which suggests that it may have been this molecule, secreted by fibroblasts, which was responsible for guiding angiogenesis towards the fibroblast laden tissue. Furthermore, in the osteogenic hydrogel-derived tissues, only very limited vascularisation was observed both macro and

microscopically when compared to the extensively vascularised fibroblastic tissues. Therefore, based on this and previous data it was hypothesised that FGF2 was responsible for the degree of angiogenic response witnessed in platelet poor plasma/human dermal fibroblast derived tissues (Figs 4.23 & 4.30). Similar data regarding the angiogenic effect of FGF2 has also been demonstrated using gels derived from chitosan [381-383, 388]. Previously, similar studies had been carried out using oligo(poly(ethylene glycol) fumarate) hydrogels in conjunction with primary human fibroblasts. In this experiment, the animal model was identical to that used to validate the platelet poor plasma derived hydrogel. Although the cell number used is not clear, each animal (NOD/SCID mice) received a 300 $\mu$ L subcutaneous implantation by injection which allowed gellation and subsequent cell entrapment to occur *in situ*. Additionally, the gels were populated with various RGD containing peptide modifications which demonstrated variation in the rates of cellular expansion on the gel *in vitro*. This study reported data resembling that which was observed using the platelet poor plasma derived hydrogel as a means of fibroblastic tissue generation. The publication reported that using the oligo(poly(ethylene glycol) fumarate) hydrogels there were no signs of biological incompatibility, for example necrosis or damage to the surrounding tissues, which was also the case using the hydrogel system presented herein. Furthermore, this study reported that the cell free hydrogels gellated *in situ*, however, did not form tissues and were degraded after 4 weeks of implantation. This data is similar to that of the platelet poor plasma derived hydrogel, with respect that acellular gels did not form tissue, however the degradation time was considerably shorter than 4 weeks (24hrs). The publication reports that the fibroblasts within the oligo(poly(ethylene glycol) hydrogels proliferated and were analysed by the presence of pro-collagen positive staining and after 8 weeks of *in vivo* culture, uniform fibrous tissue had formed in the gels. The gel modifications with various peptides did not show any influence on improving the capacity of the gels to form tissue. Similarly the platelet poor plasma derived hydrogel formed uniform fibroblastic tissue in time periods of 4 weeks, less than the 8 weeks that was reported to be required

in the oligo(poly(ethylene glycol) hydrogel study using the same cell type [384, 389]. An experiment by the same group as the previous two publications carried out a similar set of experiments using fibroblasts in conjunction with a hyaluronan hydrogel and reported identical data, no damage or necrosis in the tissues surrounding the subcutaneous implant and the cells proliferated and maintained their phenotype by immunohistochemical confirmation of the presence of human fibronectin in the neo-tissues [390]. Several studies have presented data which illustrates the effect of culturing mesenchymal stem cells in hydrogel systems *in vivo* which report contrary data to that which was obtained using the platelet poor derived plasma hydrogel in conjunction with the same pluripotent cells. One study in particular demonstrated the formation of adipose tissue in a hydrogel composed of PEGDA using subcutaneously implanted bone marrow derived mesenchymal stem cells which had been pre-cultured in adipogenic media. The publication reported that tissues formed which were PPAR- $\gamma$ /Oil-red-O positive with fibrous encapsulation of the tissue and no subsequent invasion of the host cells. Several components of this data are contrary to that from the platelet poor plasma derived hydrogel study. The gels which were implanted containing mesenchymal stem cells did not form ectopic tissue, however in the study presented here, no previous induction culture had been undertaken to direct the cells to a particular terminal lineage. Furthermore, the tissues which formed as a result of the successful cell types did not demonstrate fibrous encapsulation and reliably permitted the migration of host cells/structures into the neo-tissue. When considering the similar physical properties of adipose to hydrogels in general, adipose is quite possibly a tissue in which mesenchymal stem cells require only limited induction to differentiate towards when the physical and mechanical components of the scaffold so much resemble the native environment of the cells [385].

Articular chondrocytes were demonstrated to form tissue in conjunction with the platelet poor plasma derived hydrogel although the degree of tissue formation was not as extensive as that which was observed in implants containing dermal fibroblasts (Fig 4.18). Previous studies have

achieved comparable data using hydrogel systems. One particular study of note was performed using porcine articular chondrocytes in hydrogels composed of fibrin derived from fibrinogen, a similar gellation mechanism to that which was ultimately involved in forming the platelet poor plasma derived hydrogel. Interestingly however, this publication reports that after 4 population doublings which equated to one passage *in vitro*, the chondrocytes were no longer capable of forming matrix *in vivo*. This was not demonstrated to be the case in conjunction with hydrogel derived from platelet poor plasma with the chondrocytes used at passage 6. Of the fibrinogen derived hydrogel this publication reports 'It is immunologically inactive, not hostile to cells, adequately rigid for shape-specific tissue production, easily attainable from an autologous source, injectable, and its final strength and rate of polymerization can be controlled' elegantly summing up its findings and detailing a list of similarities between the hydrogel composed of pure fibrin and the hydrogel composed of crude platelet poor plasma detailed herein [386]. A second study which implanted chondrocytes subcutaneously into NOD/SCID mice used an agarose/chitosan hydrogel. The histology of tissues derived in this manner were contrary to the previously discussed chondrocyte/hydrogel derived tissues and much more resembled those which were reported in conjunction with the platelet poor plasma derived hydrogel. In this study each animal received  $2.0 \times 10^6$  cells per implant, in a  $400 \mu\text{L}$  gel volume both a larger cell number and injection fraction than was used in conjunction with articular chondrocytes and platelet poor plasma derived hydrogel. In this publication the histological data reports infiltration of host cells and vascularisation in the chondrocyte derived neo-tissues after 7-9 weeks of *in vivo* culture. Furthermore, it was also demonstrated that this gel was still present, and in fact had formed tissue containing host cells after this time when implanted without cells. Therefore, although the host response was similar to the platelet poor plasma derived hydrogel in this instance, the capacity of acellular gels to form tissues was not [387]. Studies have been carried out using similar gel systems exploiting components of blood to form structurally stable hydrogels. Typically in these systems wound healing and cell migration responses are contributed

to factors secreted by platelets. However, in the case of the platelet poor plasma derived hydrogel, the plasma preparation should ensure no residual platelets remain in the hydrogel matrix. One such study in which an equine cutaneous defect model was used, a platelet rich plasma derived hydrogel delivered to a topical cutaneous wound accelerated epithelial differentiation and collagen alignment in the host tissues surrounding the wound to form a cover of autologous tissue of similar mechanical properties to the surrounding tissues. The publication attributed this to a combination of a number of the secretory products from platelets including TGF- $\beta$ 1, thrombin, epidermal growth factor, fibroblast growth factor, platelet derived growth factor, thrombospondin and fibronectin. However in the case of the platelet poor plasma derived hydrogel, it is unlikely that the level of integration and cell proliferation in the gel was facilitated by any factor derived from platelets, therefore relying on secreted molecules from the human cells within the gel, residual molecules present in the gel obtained from platelets or signalling molecules diffusing into the gel from the surrounding host tissue [391]. Platelet rich plasma derived gels have also been demonstrated to be suitable candidate materials in the healing of critical sized corneal defects in rabbit models. The platelet rich plasma gel was applied to the defect and as a result the animal re-grew tissue of identical morphology and mechanical strength to the surrounding native tissue, a component of which relied on the activation and differentiation of endothelial cells, contributing to one or several of the secreted molecules of platelets present in the plasma used to form the gel [392].

Therefore, in summary, previous studies in which primary cells have been delivered to a subcutaneous or pre-defined wound site by means of injection and encapsulation in a hydrogel matrix are plentiful. However, no previous data has documented the fate and efficiency of the cells and delivery strategy with the completeness of the study presented here in. It was possible to culture dermal fibroblasts *in vivo* to the point of ectopic tissue formation in conjunction with the platelet poor plasma derived hydrogel. Previous studies have also demonstrated this using either organic or inorganic but not autologous polymer gels. In these studies, the limited



post explant analysis demonstrated that the fibroblast cells had maintained their phenotype by the presence of pro-collagen and fibronectin and that there was little immuno-activation by means of a lack of microscopic observation of necrosis in the tissues surrounding the hydrogel derived neo-tissues. The study presented here essentially achieved similar data using a considerably more elegant approach to the analysis of explanted tissues. Fibroblasts were tracked through the tissue using cell tracking dyes proving their origin. Disputes arise however regarding *in vivo* cell tracking dye studies that fluorescence can arise as a result of host macrophages phagocytising orphan fluorochrome or fluorescent cells in their entirety. This factor was eliminated by observance of human Y chromosomes in female animals in the neo-tissues, further confirming the presence of human cells. This however was still not adequate to confirm the phenotype of the cells, merely their origin. Therefore immunohistochemical observation of the D7-Fib antigen, a molecule expressed exclusively on human fibroblasts was carried out to that no phenotypic transformations had taken place. This was superior to the similar previous study due to the fact that both pro-collagen and in particular fibronectin are expressed on a multitude of cell types other than fibroblasts. Furthermore, the presence of a group of human mRNAs including the D7-Fib transcript was confirmed in the neo-tissues by real time PCR analysis. Immuno-compliance of the neo-tissues was confirmed histologically in the same manner which had previously demonstrated contradicting data regarding infiltration of host cells and structures into hydrogel derived tissues. In the platelet poor plasma derived hydrogel it was possible to observe host adipose, musculature, vasculature and hair follicles in the neo-tissue, with no evidence of fibrous encapsulation. None of the reported previous studies had documented the influence of host cells on the composition of the neo-tissue in this manner, merely stating the presence of host cells without elucidating their phenotype. Furthermore, it was possible to elucidate the extent of the immunogenicity of the cell loaded hydrogel by means of a series of immunohistochemical observations. Macrophages and neutrophils were confirmed to be present in limited numbers, although CD68, a marker of activated macrophages was only rarely observed. These

factors coupled with the lack of fibrous capsule formation demonstrate the degree of immuno-acceptance. Absence of MHC class II molecules illustrated a lack of antigen presentation. The immunogenicity of a hydrogel derived tissue had not previously been characterised to the extent presented herein. Furthermore, previous studies had attributed the success of plasma derived hydrogels in tissue augmentation to various platelet-derived factors, which was not the case here given the degree of platelet depletion which had occurred prior to utilisation in the hydrogel system (the ambiguities and mixed host responses which occur as a result of variability in platelet releasates are reviewed here 393,394). Contrary to previous data involving hydrogels and mesenchymal stem cells, the platelet poor plasma derived hydrogel did not form tissue when implanted with mesenchymal stem cells. Previous studies involving mesenchymal stem cells and hydrogels *in vivo* often focused on the direction of mesenchymal stem cells to an adipogenic lineage with pre-induction in adipogenic media facilitated by the mechanical similarity of hydrogel to adipose tissue. No pre-induction was undertaken during the platelet poor plasma derived hydrogel study using mesenchymal stem cells, which could possibly provide an explanation for the lack of neo-tissue formation. The platelet poor plasma derived hydrogel also formed tissue in conjunction with primary chondrocytes, which was superior to one previous report which suggested that chondrocyte cells could only form a stable matrix *in vivo* prior to undertaking 4 population doublings (1 passage). This was not demonstrated to be the case in conjunction with the platelet poor plasma derived hydrogel which facilitated tissue formation of articular chondrocytes after 6 passages.

The platelet poor plasma derived hydrogel demonstrated the potential to facilitate the formation of tissue when implanted intramuscularly in conjunction with primary human osteoblasts. This tissue formed after an *in vivo* incubation period of 6 weeks. The tissue was densely cellular (Fig 4.44) and the cells within maintained their osteoblastic phenotype as characterised by the presence of the osteogenic master transcription factor CBFA1/RUNX2 by immunohistochemistry (Fig 4.45). The cells also

demonstrated calcification by the presence of positive von Kossa staining although this was sporadic and not present throughout the entire tissue (Fig 4.46). Immunologically, the tissues resembled the tissues derived with human dermal fibroblasts, with very little immunoreactivity. Macrophage and neutrophils were present although CD68 was predominantly absent suggesting a lack of activation and molecules associated with antigen presentation such as MHCII were also lacking. Tissues were vascular, although not to an extent as great as the dermal fibroblast cell derived neo-tissues. Previous studies in the area of hydrogel derived bone tissues generally employ a combination of pluripotent cells such as bone marrow derived mesenchymal stem cells and bone morphogenic factors such as BMPs to derive osteogenic tissues. Furthermore, previous studies generally utilise critical sized osteogenic defects rather than attempting to generate bone ectopically. One such previous study [395] demonstrated the importance of synergy between the cell, growth factor and scaffold component of the neo-tissue forming matrix. In this study a hydrogel composed of a hyaluronic acid polymer was used in conjunction with BMP-2 and bone marrow-derived mesenchymal stem cells implanted into a rat cavial defect of a critical size. This study demonstrated that the hydrogel alone was not capable of reforming tissue. However, additions of BMP-2 or mesenchymal stem cells demonstrated an increase in calcified tissue where the hydrogel was implanted by either recruitment of host osteoblasts into the gel or differentiation of implanted mesenchymal stem cells. To complete the study, stem cells were implanted into the gel in combination with BMP-2. This group demonstrated complete healing of the critical sized defect with bone that was difficult to discern from host bone tissue. The tissue was organised, calcified and contained extensive hematopoietic stromal areas with an abundance of cells after 4 weeks of *in vivo* culture, thus concluding that under suitable stimuli and cells, a hydrogel is capable of forming neo-bone tissue. The bone formed in this publication was also vascular to a similar extent as the bone formed in conjunction with osteoblasts and the platelet poor plasma derived hydrogel [395]. A study in which ectopic bone was generated employed a hydrogel composed of hydroxypropylmethylcellulose in which were incorporated

particles of hydroxyapatite to provide a familiar osteogenic scaffold for the cells to adhere within the confines of an injectable hydrogel. This study demonstrated that this hydrogel system could form bone ectopically, implanted subcutaneously in conjunction with bone marrow derived mesenchymal stem cells. This system formed osteogenic tissues after 4 weeks of *in vivo* culture with complete woven bone visible 8 weeks post implantation. Histologically, these explanted tissues resembled the tissues derived using the platelet poor plasma derived hydrogel with dense cellularisation and sporadic calcified extracellular matrix staining. Furthermore, this study also described a lack of fibrous encapsulation and inflammation at the site of delivery, two further features in common with the osteoblastic tissue derived from platelet poor plasma derived hydrogel [396, 399]. A second study which involved the use of osteogenic scaffolds embedded in hydrogel reported similar data. In this study, solid tricalcium phosphate lattices were seeded with mesenchymal stem cells then coated with a hydrogel of fibrin, alginate or collagen. Bone formed after 8 weeks in all gels and was validated by staining for extracellular matrix calcification, suggesting that in both of these subcutaneous implantation studies the calcified inorganic matrix may have played a part in the generation of bone rather than the hydrogel [400]. A similar study to that presented herein, implanted various hydrogel polymer scaffolds intramuscularly and rather than incorporating growth factors into the hydrogel matrix, engineered bone marrow derived mesenchymal stem cells to hyper-express BMP-2. In this instance, all of the hydrogels used formed osteogenic tissues (collagen, alginate, hyaluronic acid, agarose and fibrin). Interestingly the fibrin gel, the scaffold most closely resembling the platelet poor plasma derived hydrogel, formed the smallest amount of bone tissue. The extent of bone formation varied dependent on the composition of the hydrogel. However, tissues formed in this study were considerably more heterogeneous than that which formed in conjunction with the platelet poor plasma derived hydrogel. This publication reported the presence of cartilage in all but the fibrin derived hydrogel, in some instances at similar densities to the neo-bone tissue which was generated. Additionally in this publication the presence of bone was identified solely

by microscopy in conjunction with tinctural staining (haematoxylin and eosin) and no experimental qualification of calcification was reported [397]. A second study which involved an intramuscular implantation technique employed an acellular alginate hydrogel into which was incorporated a short recombinant peptide sequence mimicking the functional site of BMP-2. This study reported similar results to [397] without the use of cells. A heterogeneous tissue containing bone and cartilage was formed within the muscle quadriceps muscle block of the host. This is contrary to [397] which reported no tissue formation at an intramuscular site from a number of hydrogels including alginate in the absence of cells, which was also the case using acellular platelet poor plasma derived hydrogels. The publication hypothesises that the presence of osteogenic tissue is a result of the migration of host mesenchymal stem and osteoblast cells to the implantation site as a result of chemotaxis induced by the recombinant peptide [398]. Therefore it was possible to conclude that the platelet poor plasma derived hydrogel demonstrated equal or increased performance of previously published predecessor hydrogels in the generation of ectopic bone. Previous studies in which ectopic bone had been generated in combination with a hydrogel relied on the exploitation of a solid substrate previously proven to stimulate osteogenesis embedded within the hydrogel. These hybrid materials form bone; however the role or necessity for the hydrogel is questionable when the system becomes so reliant on a solid component to the gel that is no longer injectable. Furthermore, previous systems employed BMP-2 for the stimulation of bone formation either by incorporation into the hydrogel or transduction into the cells. Addition of any exogenous factor removes the autologous nature from implantation strategy and furthermore transduced cells are not currently accepted for clinical applications. The platelet poor plasma derived hydrogel also demonstrated the formation of an osteogenic tissue outside of a critical sized defect. In the instance of such a defect the cells within the scaffold are stimulated by the native cells of an identical phenotype within the surrounding bone, enhancing the potential of the cells within the gel to remain osteogenic. This was not deemed necessary

in the formation of bone using the platelet poor plasma derived hydrogel system.



# DERIVATION OF DEFINED MEDIA FOR THE PHENOTYPE MAINTENANCE AND DIRECTED DIFFERENTIATION OF PRIMARY HUMAN PURIPOTENT CELLS

## Chapter 6. Conclusions

### 6.i. Derivation of Defined Media

A basal media formulation was generated from component salts, amino acids, vitamins and energy sources which demonstrated the capacity to support the expansion of primary human cells in conjunction with additions of fetal calf serum at a concentration of 5% (v/v), a concentration identical to that used in combination with commercially available basal media formulations. This was demonstrated initially using primary human dermal fibroblasts. Furthermore, it was possible to use this basal media formulation in conjunction with a serum substitute derived *de novo* to generate a culture media formulation, completely defined chemically, and entirely devoid of whole serum.

This serum free media formulation demonstrated its suitability as a routine cell culture media by maintenance of a range of primary human cells both morphologically and phenotypically including human osteoblasts, extensively characterised smooth muscle cells and dermal fibroblasts. In all cases the serum free media formulation resulted in a metabolic activity profile similar to that obtained using the commercially available culture media for the particular cell type in conjunction with undefined fetal calf serum. The extent of the definition of the culture media also permitted demonstration of a possible role of iron in the modulation of smooth muscle cells between a synthetic and functional phenotype demonstrated by real time-PCR observation of smoothelin, a marker of contractile smooth muscle cells solely in the serum free media formulation devoid of iron.

The defined serum free basal media formulation was also demonstrated as a suitable candidate media for the maintenance of a plastic cell type of particular interest for tissue engineering and regenerative medical exploitation, the mesenchymal stem cell. Primary human mesenchymal stem cells derived from bone marrow were subjected to multiple passages in the defined serum free media which was demonstrated to maintain the plasticity of the cells during this extended culture period. This was qualified by the observation of several proteins associated with pluripotency including STRO-1, nucleostemin and CD105. Furthermore, using flow cytometric analysis it was possible to demonstrate that throughout serum free culture markers of undifferentiated mesenchymal stem cells were often expressed at increased levels and markers of differentiation were decreased when compared to identical cells cultured in serum containing commercial media.

Controlled, defined exogenous modifications to the media formulation resulted in tri-lineage differentiation of bone marrow derived mesenchymal stem cells along osteogenic, chondrogenic and adipogenic lineage fates in culture periods similar or identical to those which had previously been reported often in conjunction with serum.

The media formulation also demonstrated its potential for culture of a potentially invaluable source of adult stem cells, which were obtained from dental pulp. Dental pulp derived stem cells have a substantial capacity to overcome bone marrow derived stem cells as a candidate plastic cell for tissue engineering. These possibly autologous cells are simple to obtain from either routine dental practice or milk tooth banking of deciduous teeth. Additionally, arguably these stem cells have a higher plastic potential over those obtained from bone marrow given their origin in the neural crest, an embryonic region of highly differentiating cells, during embryogenesis. The defined serum free media formulation exhibited the potential to maintain the expansion of these cells in an identical manner to media formulations containing serum. Similarly to previously stated primary human cells, the dental pulp derived stem cells

maintained a metabolic profile comparable with serum containing media formulations. The cells also retained their plasticity when cultured using the defined serum free basal media formulation characterised by the presence of typical mesenchymal stem cell markers such as STRO-1 and nucleostemin and additionally molecules more intimately associated with an embryonic stem cell origin such as Sox2, Oct-4 and Tra-1-81, further emphasising the hyper-plasticity of these cells over bone marrow derived stem cells whilst illustrating the capability of the defined serum free basal media to maintain an undifferentiated stem cell phenotype.

Defined additional exogenous factors facilitated the differentiation of dental pulp derived stem cells into chondrocytes, a differentiation event not previously extensively documented in conjunction with dental pulp derived stem cells. Cells were characterised on the basis of several molecules associated with a functional chondrogenic phenotype including type II collagen and glycosaminoglycans and furthermore demonstrated rounded typical chondrogenic morphology by scanning electron microscopy. The cells under chondrogenic stimulation also demonstrated a differentiation into an osteochondral or hypertrophic chondrocyte intermediate characterised by the presence of several markers of an osteogenic lineage.

Dental pulp derived stem cells were differentiated into an osteogenic lineage using defined serum free osteogenic differentiation media characterised by the presence of several osteogenic proteins including the osteogenic master gene, the transcription factor CBFA1/RUNX2 and additional molecules associated with functional osteogenesis such as osteocalcin. Tinctural staining illustrated the presence of calcified extracellular matrix after culture under defined osteogenic conditions confirming completion of osteogenic differentiation. Interestingly, increases in chondrogenic markers under osteogenic conditions were considerably smaller than the increases in osteogenic associated proteins under chondrogenic stimuli, therefore suggesting a more homogeneous differentiation of these cells was possible under osteogenic stimuli,

emphasising a predisposition of stem cells from this source towards an osteoblastic lineage. This is consistent with data previously published which illustrates the ease at which these cells reliably form osteoblastic cells, possibly due to the proximity of the cells to dentin and the similarity of this substance to bone.

Chemically defined adipogenic differentiation media demonstrated its capacity to differentiate dental pulp derived stem cells down an adipogenic lineage. This was characterised using tinctural staining to observe the presence of lipid vesicles within the cells, a morphological property exclusive to adipocytes and further confirmed by the presence of several molecules associated with functional adipocytes including leptin, a protein critical to the role of adipocytes *in vivo* in the regulation of food intake. This differentiation event occurred considerably more rapidly than had previously been described using much more complex adipogenic differentiation strategies which often involved serum. This was also the case with bone marrow derived mesenchymal stem cells.

The simple addition of retinoic acid to the chemically defined media allowed the generation of a defined neural differentiation media. It was hypothesised that given the proximity of these cells to the neural crest during development, differentiation into a neuronal lineage would be possible, which was proven to be the case using this media formulation. Cells formed neurite like morphologies rapidly and expressed several markers associated with functional neurogenesis including neurofilament, synaptophysin and substance P. Interestingly, the dental pulp cells did not express proteins associated with a glial phenotype highlighting a homogeneous differentiation to a neuronal phenotype which was not the case with adult stem cells from alternative sources which formed a heterogeneous culture of neural and glial cells. The defined neural differentiation media was also demonstrated capable of differentiating primary umbilical cord derived stem cells down a neuronal lineage.

Defined hepatic differentiation media was synthesised and proven again using dental pulp derived stem cells which formed hepatocytes after 21 days of serum free hepatic culture. This particular differentiation event had not been reported previously with stem cells from a dental pulp source. Post differentiation the cells expressed a subset of proteins associated with hepatocyte cells including albumin, a critical component of the hepatocyte secretome and the most abundant serum protein *in vivo*.

## DEVELOPMENT AND VALIDATION OF A DEFINED STRATEGY FOR THE SITE DIRECTED DELIVERY OF CLINICAL GRADE PRIMARY HUMAN CELLS

### 6.ii Synthesis of Autologous Hydrogel

The addition of citrated platelet poor plasma to one of a palette of calcium containing basal cell culture media resulted in a stable potentially autologous hydrogel at 37°C. This gel was demonstrated to have a contact angle similar to glass. The proximity of this critical first parameter in the compatibility of cells with a surface to an extensively pre-validated substrate highlighted its potential as a tissue culture substrate. The hydrogel was used as a matrix for the culture of human articular chondrocytes. The management of these cells *ex vivo* relies on the use of a controlled hypoxic environment to mimic their *in vivo* niche and therefore prevent phenotypic modifications. Primary human articular chondrocyte cells were cultured under blocks of platelet poor plasma derived hydrogel with the additions of no additional exogenous factors. After 21 days of culture beneath the hydrogel, the chondrocytes demonstrated their phenotype had been maintained by observation of the presence of glycosaminoglycans using tinctural staining. This method was considerably less complex than previously published hydrogel/chondrocyte culture strategies which involve chemically more complex hydrogels or additional exogenous factors to maintain the chondrocyte phenotype including transforming growth factors, furthermore previous studies lack the possibility to generate an autologous system that the platelet poor plasma derived hydrogel delivers.

The surface of the hydrogel was also characterised as a culture substrate using dental pulp derived stem cells sorted on the basis of their capacity to efflux a Hoechst dye. In conjunction with the platelet poor plasma derived hydrogel surface these cells demonstrated their potential to differentiate down an endothelial lineage and further form morphologically correct microvascular endothelial structures. These cells were characterised post



differentiation and were shown to express a subset of markers associated with endothelial cell phenotype including markers of functionality such as Von Willebrand factor and VE-cadherin. Interestingly, Hoechst negative selected dental pulp derived stem cells did not maintain this characteristic to differentiate towards a vascular endothelial lineage in conjunction with a Matrigel surface, a commercially available extracellular matrix hydrogel. The hydrogel demonstrated its potential to support cellular migration through gel blocks using primary articular chondrocyte cells in conjunction with cell tracking dyes.

The gel was characterised as a candidate material for the formation of soft tissue *in vivo* using primarily human dermal fibroblasts but also to a lesser extent articular chondrocytes which both formed ectopic neo-tissues when implanted subcutaneously into an immunosuppressed animal model. Tissues formed reliably after culture periods as short as 3 weeks with characteristic morphology observed throughout all neo-tissues. The hydrogel-derived tissue formed a densely cellular mass with extensive matrix deposition beneath the host subcutaneous layer. The tissues were well vascularised with minimal adhesion to the underlying host subcutaneous tissues. The size of the explanted tissue was found to be proportional to the number of cells delivered with the hydrogel at the point of implantation and gels which were delivered devoid of cells did not form retrievable tissues. Cells were well integrated with the host tissues and neo-tissues held several structures to support this including host adipose, hair follicles and musculature. The origin of the cells within the implants was proven to be human by means of cell tracking, fluorescent *in situ* hybridisation and furthermore the phenotype was confirmed to remain fibroblastic by means of observation of the D7-Fib antigen, a protein found exclusively in fibroblasts. Interestingly, the presence of human cells was recorded by real time-PCR in the surrounding dermis and the liver suggesting either migration of the human cells by means of simple passage through the gel block into the surrounding tissues or by means of the circulation. However, these results could also be explained by the presence of orphan human DNA within these host tissues due to cellular apoptosis or

macrophage mediated cell destruction. Macrophage cells were observed in the neo-tissues in addition to neutrophil cells however no markers were observed to suggest their activation.

The hydrogel also demonstrated its potential as a bone forming matrix. Human osteoblasts were delivered into intramuscular sites of immunosuppressed animals and tissues formed after a period of 6 weeks. These neo-tissues were considerably more homogeneous than those which were generated using human fibroblasts with no observation of host structures within other than host vasculature. The degree of immun acceptance was similar to that of the subcutaneous fibroblast derived tissues. The human osteoblasts maintained their phenotype, confirmed by observation of the osteogenic master gene CBFA1/RUNX2 and produced limited calcified extracellular matrix confirmed by tinctural staining. This suggested that, although the cells maintained their osteogenic lineage, a more extended *in vivo* incubation time was required for the generation of fully functional bone tissue.

**DERIVATION OF DEFINED MEDIA FOR THE PHENOTYPE  
MAINTENANCE AND DIRECTED DIFFERENTIATION OF  
PRIMARY HUMAN PURIPOTENT CELLS**

Chapter 7. References

1. Langer. R. & Vacanti. J.P. (1993) Tissue Engineering. Science. 260. 920-926
2. El-Amin. F.S., *et al.* (2005) Human osteoblast cells: isolation, characterisation, and growth on polymers for musculoskeletal tissue engineering. Journal of Biomedical Materials Research. 76A. 439-449
3. Nakase. Y. *et al.* (2006) Tissue engineering of small intestinal tissue using collagen sponge scaffolds seeded with smooth muscle cells. Tissue Engineering. 12. 403-412
4. Guan. Y. *et al.* (2006) Tissue engineering of urethra using human vascular endothelial growth factor gene-modified bladder urothelial cells. Artificial Organs. 32. 91-99
5. Tuan. S.R., *et al.* (2002) Adult mesenchymal stem cells and cell-based tissue engineering. Arthritis Research and Therapy. 5. 32-45
6. Zhdanov. P.V., *et al.* (2003) Simulation of morphogenesis: From a pluripotent stem cell to an ensemble of differentiated cells. Physical Chemistry Chemical Physics. 5. 1433-1439
7. De went. G., & Mummery. C. (2003) Human embryonic stem cells: research, ethics and policy. Human Reproduction. 18. 627-628
8. Henon. P.R. (2003) Human embryonic or adult stem cells: An overview on ethics and perspectives for tissue engineering. Tissue Engineering. 534. 27-45
9. Lim. J.Y., *et al.* (2006) Multiple stem cell traits of expanded rat bone marrow stromal cells. Experimental Neurology. 199. 416-426
10. Oesdayrajsingh-Varma. M.J., *et al.* (2006) Adipose tissue derived mesenchymal stem cell yield & growth characteristics are affected by the tissue-harvesting procedure. Cytotherapy. 8. 166-177
11. Zvalifler. N.J., *et al.* (2000) Mesenchymal precursor cells in the blood of normal individuals. Arthritis Research. 2. 477-488

12. Te-Chao. F., *et al.*. (2004) Adult stem cell plasticity: will engineered tissues be rejected. *International Journal of Experimental Pathology*. 85. 115-124
13. Raff. M. (2003) Adult stem cell plasticity: Fact of artifact. *Annual Review of Cell Developmental Biology*. 19. 1-22
14. Pittenger. M.F., *et al.*. (1999) Multilineage potential of adult human mesenchymal stem cells. *Science*. 184. 143-147
15. Johnstone. B., *et al.*. (1998) In vitro chondrogenesis of bone marrow-derived mesenchymal progenitor cells. *Experimental Cell Research*. 238. 265-272
16. Haynesworth. S.E., *et al.*. (1992) Characterisation of cells with osteogenic potential from human marrow. *Bone*. 12. 81-88
17. Kopen. G.C., *et al.*. (1999) Marrow stromal cells migrate throughout forebrain and cerebellum, and they differentiate into astrocytes after injection into neonatal mouse brains. *Proceedings of the National Academy of Science USA*. 95. 3908-3913
18. Fukuda. K. (2001) Development of regenerative cardiomyocytes from mesenchymal stem cells for cardiovascular tissue engineering. *Artificial Organs*. 25. 187-193
19. Bosnakovski. D., *et al.*. (2006) Gene expression profile of bovine marrow mesenchymal stem cell during spontaneous chondrogenic differentiation in pellet culture system. *Japanese Journal of Veterinary Research*. 53. 127-139
20. Mareschi. K., *et al.*. (2006) Expansion of mesenchymal stem cells isolated from paediatric and adult donor bone marrow. *Journal of Cellular Biochemistry*. 97. 744-754
21. Lu. F.Z., *et al.*. (2005) Characterization & gene transfer in mesenchymal stem cells derived from human umbilical-chord blood. *Journal of Laboratory & Clinical Medicine*. 146. 271-278
22. Romanov. Y.A., *et al.*. (2005) Mesenchymal stem cells from human bone marrow and adipose tissue: Isolation, characterization, and differentiation potentialities. *Bulletin of Experimental Biology and Medicine*. 140. 138-143
23. Covas. D.T., *et al.*. (2003) Isolation and culture of umbilical vein mesenchymal stem cells. *Brazilian Journal of Medical and Biological Research*. 36. 1179-1183
24. Gronthos. S., *et al.*. (2001) Surface protein characterisation of human adipose

- tissue-derived stromal cells. *Journal of Cellular Physiology*. 189. 54-63
25. Tondreau T., *et al.* (2005) Mesenchymal stem cells derived from CD133-positive cells in mobilized peripheral blood and cord blood: proliferation, Oct4 expression, and plasticity. *Stem Cells*. 23. 1105-1112
26. Huttmann. A., *et al.* (2006) Gene expression profiles in murine haematopoietic stem cells revisited: Analysis of cDNA libraries reveals high levels of translational and metabolic activities. *Stem Cells*. 24. 1719-1727
33. [www.etsr.org/bulletin12\\_1/section20.php](http://www.etsr.org/bulletin12_1/section20.php)
34. Lebrer M.S., *et al.* (1998). Strategies of epithelial repair: modulation of stem cell and transit amplifying cell proliferation. *Journal of Cellular Science*. 3. 2867-75
35. Kamminga. L.M. & De Haan. G. (2006) Cellular memory and, haematopoietic stem cell aging. *Stem Cells*. 24. 1143-1149
36. Forsberg E.C., *et al.* (2006). New evidence supporting megakaryocyte-erythrocyte potential of F1K2/F1t3(+) multipotent haematopoietic progenitors. *Cell*. 126. 415-426
37. Bhattacharya D, *et al.* (2000). Rapid lymphocyte reconstitution of unconditional immunodeficient mice with non-self-renewing multipotent haematopoietic progenitor. *Cell Cycle*. 5. 1135-1139
38. Akoshi K, *et al.* (2000). A clonogenic common myeloid progenitor that gives rise to all myeloid lineages. *Nature*. 404. 193-197
39. Li C. D., *et al.* (2005). Mesenchymal stem cells derived from human placenta suppress allogenic umbilical chord blood lymphocyte proliferation. *Cell Research*. 15. 539-547
40. Lee C. C. I, *et al.* (2006). Comparison of growth and differentiation of total and adult rhesus monkey mesenchymal stem cells. *Stem Cells and Development*. 15. 204-220
41. Campagnoli. C., *et al.* (2001) Identification of mesenchymal stem/progenitor cells in human first-trimester fetal blood, liver, and bone marrow. *Blood*. 15. 2396-2402
42. Oedayraj Singh-Varma M. J, *et al.* (2006). Adipose-tissue derived mesenchymal stem cell yield and growth characteristics are affected by the tissue harvesting procedure. *Cytotherapy*. 8. 166-177
43. Hoogdijn M. S, *et al.* (2006). Comparative characterization of hair follicle dermal stem cells and bone marrow mesenchymal stem cells. *Stem Cells and Development*. 15. 49-60

44. Benavente C. A, *et al.*. (2003). Subcellular distribution and mitogenic effect of bFGF in mesenchymal uncommitted stem cells. *Growth Factors*. 21. 87-94
45. Kalajzic. I., *et al.*. (2003) Stage specific inhibition of osteoblast lineage differentiation by FGF2 and noggin. *Journal of Cellular Biochemistry*. 88. 1168-1176
46. Ringer S. (1882). Concerning the influence exerted by each of the constituents of the blood on contraction of the ventricle. *Journal of Physiology*. 3. 380-393
47. Eagle H. (1955) The growth requirements of two mammalian cell lines in tissue culture. *Transactions of the Association of American Physicians*. 68. 78-81
48. Eagle H. (1955) Specific amino acid requirements of a mouse fibroblast and a human carcinoma cell in tissue culture. *Anatomical Record*. 121. 470
49. Eagle H. (1955) Nutrition needs of mammalian cells in tissue culture. *Science*. 122. 501-504
50. Ham R. (1965) Clonal growth of mammalian cells in a chemically defined, synthetic medium. *Proceedings of the National Academy of Sciences in the United States of America*. 53. 208-293
51. Carlo E. A, *et al.*. (2002) The use of fetal bovine serum: ethical or scientific problem? *Alternatives to Laboratory Animals*. 30. 219-227
52. Falkner E, *et al.*. (2004) Serum free cell culture media updated product guide. Centre for Alternative and Complimentary Methods to Animal Testing, Australia.
53. Zhany J & Robinson D. (2005) Development of animal free, protein free and chemically defined media for NSO cell culture. *Cytotechnology*. 48. 59-74
54. Wiles .V.M., & Johansson. M.B. (1999) Embryonic stem cell development in a chemically defined medium. *Experimental Cell Research*. 247. 241-248
55. Lennon. P.D., *et al.*. (1995) A chemically defined medium supports *in vitro* proliferation and maintains the osteochondral potential of rat marrow-derived mesenchymal stem cells. *Experimental cell research*. 219. 211-222

56. Meuleman N, *et al.* (2006). Human marrow mesenchymal stem cell culture: serum free medium allows better expansion than classical  $\alpha$ -MEM medium. *European Journal of Haematology*. 76. 309-316
57. Lu. J., *et al.* (2006) Defined culture conditions of human embryonic stem cells. *Proceedings of the National Academy of Sciences*. 103. 5688-5693
58. Bertheussen. K. (1993) Growth of cells in a new defined protein-free medium. *Cytotechnology*. 11. 219-231
59. Kim Y. D. (2005). Effects of supplementation of various medium components on Chinese hamster ovary cell culture producing recombinant antibody. *Cytotechnology*. 47. 34-49
60. Talley. D., *et al.* Synthecol<sup>TM</sup> synthetic cholesterol for cholesterol dependent cell culture-development of non-animal derived chemically defined NSO medium. Sigma-Aldrich corporation, PO Box 14508, Saint Louis, MO 63178 USA.
61. Ulloa-Montoya. F., *et al.* (2005) Culture systems for pluripotent stem cells. *Journal of Biological Sciences and Bioengineering*. 100. 12-27
68. Bancel S and Hu W. S. (1996). Confocal laser scanning microscopy examination of cell distribution in macroporous microcarriers. *Biotechnology Progress*. 12. 398-402
69. Gorenstaeva S. N. (2006). Myogenesis in haematopoietic tissue mesenchymal stem cell culture. *Cell Technologies in Biology and Medicine*. 2. 493-500
70. Gronthos S. (2001). Surface protein characterization of human adipose tissue derived stromal cells. *Journal of Cellular Physiology*. 189. 54-63
71. Zhang. Z.J., *et al.* (2006) Reorganisation of actin filaments enhances chondrogenic differentiation of cells derived from murine embryonic stem cells. *Biochemical and Biophysical Research Communications*. 348. 421-427
72. Mehlhorn. A.T., *et al.* (2006) Mesenchymal stem cells maintain TGF-beta-mediated chondrogenic phenotype in alginate bead culture. *Tissue Engineering*. 12. 1393-1403
73. Deng. W., *et al.* (2006) In vitro differentiation of human marrow stromal cells into early progenitors of neural cells by conditions that increase intracellular cyclic AMP. *Biochemical & Biophysical Research Communications*. 282. 148-152



74. Woodbury, D., *et al.*. (2000) Adult rat human bone marrow stromal cells differentiate into neurons. *Journal of Neuroscience Research*. 61. 364-370
75. Chen, Y., *et al.*. (2006) Coaxing bone marrow stromal mesenchymal stem cells towards neuronal differentiation: progress and uncertainties. *Cellular and Molecular Life Sciences*. 63. 1649-1657
75. Lin, Z., *et al.*. (2006) The chondrocyte: biology and clinical applications. *Tissue Engineering*. 12. 1971-1984
76. Ratajczak, M.Z., *et al.*. (2008) Hunt for pluripotent stem cell-Regenerative medicine search for almighty cell. *Journal of Autoimmunity*. 30. 151-162
77. Williams D.F. (2006) To reengineer is to create: the link between engineering and regeneration. *Trends in Biotechnology*. 24. 4-8
78. Korbling, M., *et al.*. (2003) Adult Stem Cells for Tissue Repair - A New Therapeutic Concept? *New England Journal of Medicine*. 349. 570-82
79. Simon, A; Frisen, J (2007) From stem cells to progenitors and back again. *Cell*. 128. 825-826
80. Flores, I., *et al.*. (2008) The longest telomeres – a general signature of adult stem cell compartments. *Genes and Development*. 22. 654-667
81. Cohen, S., *et al.*. (2006) Tissue engineering using human embryonic stem cells. *Stem Cells Tools and Other Experimental Protocols*. 420. 303-315
82. Conley, B.J., *et al.*. (2004) Derivation, propagation and differentiation of human embryonic stem cells. *International Journal of Biochemistry and Cell Biology*. 36. 555-567
83. Johnson, M.H. (2008) Human ES cells and a blastocyst from one embryo: Exciting science but conflicting ethics. *Cell Stem Cell*. 2. 103-104
84. Mauney, J.R. (2005) Role of adult mesenchymal stem cells in bone tissue-engineering applications: Current status and future prospects. *Tissue Engineering*. 11. 787-802
85. Bird, T.G., *et al.*. (2008) Activation of stem cells in hepatic diseases. *Cell and Tissue Research*. 331. 283-300
86. Martinez-Monedero, R., *et al.*. (2007) The potential role of endogenous stem cells in regeneration of the inner ear. *Hearing research*. 227. 45-52.

87. Bieibly R., *et al.* (2007) The role of mesenchymal stem cells in maintenance and repair of bone. *Injury*. 38. 26-32
88. Orlic D., *et al.* (2001) Bone marrow cells regenerate infarcted myocardium. *Nature*. 410. 701-705
89. Brazeton T.R., *et al.* (2000) From marrow to brain: Expression of neuronal phenotypes in adult mice. *Science*. 290. 1775-1779
90. Weibo Zhang, X., *et al.* (2006) Multilineage Differentiation Potential of Stem Cells Derived from Human Dental Pulp after Cryopreservation. *Tissue Engineering*. 13. 2813-2823
91. Chen Y., *et al.* (2007) In vitro differentiation of mouse bone marrow stromal cells into hepatocytes induced by conditioned culture media of hepatocytes. *Journal of Cellular Biochemistry*. 102. 52-63
92. Lock L.T., *et al.* (2007) Stem/progenitor sources of insulin-producing cells for the treatment of diabetes. *Tissue Engineering*. 13. 1399-1412
93. Nadri S., *et al.* (2008) Multipotent mesenchymal stem cells from adult human eye conjunctiva stromal cells. *Differentiation*. 76. 223-231
94. Sethe S., *et al.* (2006) Aging of mesenchymal stem cells. *Aging Research Reviews*. 5. 91-116.
95. Fukuchi Y., *et al.* (2004) Human placenta-derived cells have mesenchymal stem/progenitor cell potential. *Stem Cells*. 22. 649-658.
96. Secco M., *et al.* (2008) Multipotent stem cells from umbilical cord: cord is richer than blood. *Stem cells*. 26. 146-150.
97. Siegel N., *et al.* (2008) Stem Cells in Amniotic Fluid as New Tools to Study Human Genetic Diseases. *Stem cell reviews*. 3. 256-264
98. Janjanin S., *et al.* (2008) Human palatine tonsil: a new potential tissue source of multipotent mesenchymal progenitor cells. *Arthritis Research and Therapy*. 10. R83
99. Mancardi G. & Saccardi R. (2008) Autologous haematopoietic stem-cell transplantation in multiple sclerosis. *Lancet Neurology*. 7. 626-636
100. Devetten M. & Armitage J. (2007) Haematopoietic cell transplantation: progress and obstacles. *Annals of Oncology*. 18. 1450-1456
101. de Witte T., *et al.* (2007) Autologous and allogeneic stem cell transplantation for myelodysplastic syndrome. *Blood Reviews*. 21. 49-59

102. Riordan N.H., *et al.* (2007) Cord blood in regenerative medicine: do we need immune suppression? *Journal of Translational Medicine*. 5. Article Number: 8
103. de Buys P., *et al.* (2005) Hemopoietic stem cell transplantation in rheumatic diseases - an update. *Autoimmunity Reviews*. 4. 422-449
104. Le Blanc K. & Ringden O. (2005) Immunobiology of human mesenchymal stem cells and future use in haematopoietic stem cell transplantation. *Biology of Blood and Marrow Transplantation*. 11. 321-334
105. Banas A., *et al.* (2007) Stem cell plasticity: learning from hepatogenic differentiation strategies. *Developmental Dynamics*. 236. 3228- 3241
106. Heng B.C., *et al.* (2005) Factors influencing stem cell differentiation into the hepatic lineage *in vitro*. *Journal of Gastroenterology and Hepatology*. 20. 975-987
107. Ong S.Y., *et al.* (2006) Inducing hepatic differentiation of human mesenchymal stem cells in pellet culture. *Biomaterials*. 27. 4087-4097
108. Yang Q., *et al.* (2008) A simple and efficient method for deriving neurospheres from bone marrow stromal cells. *Biochemical and Biophysical Research Communications*. 372. 520-524
109. Barzilay R., *et al.* (2008) Induction of human mesenchymal stem cells into dopamine- producing cells with different differentiation protocols. *Stem Cells and Development*. 17. 547-554
110. Sheng H., *et al.* (2008) A critical role of IFN $\gamma$  in priming MSC-mediated suppression of T cell proliferation through up-regulation of B7-H1. *Cell Research*. 18. 846-857
111. Ren G., *et al.* (2007) Mesenchymal stem cell-mediated immunosuppression occurs via concerted action of chemokines and nitric oxide. *Cell Stem Cell*. 2. 141-150
112. Keating A. (2008) How Do Mesenchymal Stromal Cells Suppress T Cells? *Cell Stem Cell*. 2. 106-108
113. Gupta S. & Rosenberg E. (2008) Do stem cells exist in the adult kidney. *American Journal of Nephrology*. 28. 607-613
114. Anumanthan G., *et al.* (2008) Directed differentiation of bone marrow derived mesenchymal stem cells into bladder urothelium. *The Journal of Urology*. 180. 1778-1783

115. Greco S.J., *et al.* (2007) An interdisciplinary approach and characterization of neuronal cells transdifferentiated from human mesenchymal stem cells. *Stem Cells and Development*. 16. 811-826
116. Tseng P.Y., *et al.* (2007) Spontaneous differentiation of adult rat marrow stromal cells in a long term culture. *Journal of Veterinary Medical Science*. 69. 95-102
117. Kruse C., *et al.* (2006) Adult pancreatic stem/progenitor cells spontaneously differentiate in vitro into multiple cell lineages and form teratoma-like structures. *Annals of Anatomy*. 188. 503-517
118. Kruglyakov P.V., *et al.* (2006) In vitro and in vivo differentiation of mesenchymal stem cells in the cardiomyocyte direction. *Cell Technologies in Biology and Medicine*. 2. 503-506
119. Ishimura D., *et al.* (2008) Differentiation of adipose-derived stromal vascular fraction culture cells into chondrocytes using the method of cell sorting with a mesenchymal stem cell marker. *The Tohoku Journal of Experimental Medicine*. 216. 149-156
120. Weir C., *et al.* (2008) Mesenchymal stem cells: isolation, characterisation and *in vivo* fluorescent dye tracking. *Heart, Lung and Circulation*. 17. 395-403
121. Dvorakova J., *et al.* (2008) Isolation and characterization of mesenchymal stem cell population entrapped in bone marrow collection sets. *Cell Biology International*. 32. 1116-1125
122. Narita Y., *et al.* (2008) Effects of transforming growth factor-beta 1 and ascorbic acid on differentiation of human bone-marrow-derived mesenchymal stem cells into smooth muscle cell lineage. *Cell Tissue Research*. 333. 449-459
123. Kestendjieva S., *et al.* (2008) Characterization of mesenchymal stem cells isolated from the human umbilical cord. *Cell Biology International*. 32. 724-732
124. Romanov Y.A., *et al.* (2005) Mesenchymal Stem Cells from Human Bone Marrow and Adipose Tissue: Isolation, Characterization, and Differentiation Potentialities. *Bulletin of Experimental Biology and Medicine*. 140. 138-143
125. Mirmalek-Sani S.H., *et al.* (2006) Characterization and Multipotentiality of Human Fetal Femur-Derived Cells: Implications for Skeletal Tissue Regeneration. *Stem Cells*. 24. 1042-1053
126. Thomas R.J., *et al.* (2007) Manufacture of a human mesenchymal stem cell population using an automated cell culture platform. *Cytotechnology*. 5. 31-39

127. Zannettino A.C.W., *et al.* (2007) Human multipotential mesenchymal/stromal stem cells are derived from a discrete subpopulation of STRO-1(bright)/CD34(-)/CD45(-)/glycophorin-A-bone marrow cells. *Haematologica- the Haematology Journal*. 92. 1707-1708
128. Qiao C., *et al.* (2008) Human mesenchymal stem cells isolated from the umbilical cord. *Cell Biology International*. 32. 8-15
129. Satija M.K., *et al.* (2007) Mesenchymal stem cells: Molecular targets for tissue engineering. *Stem Cells and Development*. 16. 7-23
130. Yaghoobi M.M., *et al.* (2005) Nucleostemin, a coordinator of self-renewal, is expressed in rat marrow stromal cells and turns off after induction of neural differentiation. *Neuroscience Letters*. 390. 81-86
131. Tondreau T., *et al.* (2004) Isolation of BM mesenchymal stem cells by plastic adhesion or negative selection: phenotype, proliferation kinetics and differentiation potential. *Cytotherapy*. 6. 372-379
132. Nadri S., *et al.* (2007) Multipotent mesenchymal stem cells from adult human eye conjunctiva stromal cells. *Differentiation*. 76. 223-231
59. Lengner C.J., *et al.* (2008) The pluripotency regulator Oct4. *Cell Cycle*. 7. 725-728
133. Liedtke S., *et al.* (2008) Oct4 expression revisited: potential pitfalls for data misinterpretation in stem cell research. *Biological Chemistry*. 389. 845-850
134. Zhu Y., *et al.* (2008) Adipose-derived stem cell: a better stem cell than BMSC. *Cell Biochemistry and Function*. 26. 664-675
135. Battula V.L., *et al.* (2007) Prospective isolation and characterization of mesenchymal stem cells from human placenta using a frizzled-9-specific monoclonal antibody. *Differentiation*. 76. 326-336
136. Gonzalez R., *et al.* (2007) Pluripotent marker expression and differentiation of human second trimester Mesenchymal Stem Cells. *Biochemical and Biophysical Research Communications*. 362. 491-497
137. Battula V.L., *et al.* (2006) Human placenta and bone marrow derived MSC cultured in serum-free, b-FGF-containing medium express cell surface frizzled-9 and SSEA-4 and give rise to multilineage differentiation. *Differentiation*. 75. 279-291
138. Roche S., *et al.* (2007) Oct-4, Rex-1, and Gata-4 expression in human MSC increase the differentiation efficiency but not hTERT expression. *Journal of Cellular Biochemistry*. 101. 271-280

139. Lamoury F.M.J., *et al.* (2006) Undifferentiated mouse mesenchymal stem cells spontaneously express neural and stem cell markers Oct-4 and Rex-1. *Cytherapy*. 8. 228-242
140. Oldershaw R.A., *et al.* (2008) Notch signaling through jagged-1 is necessary to initiate chondrogenesis in human bone marrow stromal cells but must be switched off to complete chondrogenesis. *Stem Cells*. 26. 666-674
141. Patel S.A., *et al.* (2008) Immunological properties of mesenchymal stem cells and clinical implications. *Archivum Immunologiae et Therapiae Experimentalis*. 56. 1-8
142. Okitsu Y., *et al.* (2007) Regulation of adipocyte differentiation of bone marrow stromal cells by transcription factor GATA-2. *Biochemical and Biophysical Research Communications*. 364. 383-387
143. Trzaska K.A., *et al.* (2008) Loss of RE-1 silencing factor in mesenchymal stem cell-derived dopamine progenitors induces functional maturity. *Molecular and Cellular Neuroscience*. 39. 285-290
144. Kmiecik T.E., *et al.* (1992) Hepatocyte growth factor is a synergistic factor for the growth of haematopoietic progenitor cells. *Blood*. 80. 2454-2457
145. LaBarge M.A. & Blau H.M. (2002) Biological progression from adult bone marrow to mononucleate muscle stem cell to multinucleate muscle fiber in response to injury. *Cell*. 111. 589-601
146. Abbott J.D., *et al.* (2004) Stromal cell-derived factor-1 alpha plays a critical role in stem cell recruitment to the heart after myocardial infarction but is not sufficient to induce homing in the absence of injury. *Circulation*. 110. 3300-3305
147. Mann J.R. (2001) Imprinting in the germ line. *Stem Cells*. 19. 287-294
148. Kucia M., *et al.* (2006) The developmental deposition of epiblast/germ cell-line derived cells in various organs as a hypothetical explanation of stem cell plasticity? *Acta Neurobiology Experiments*. 66. 331-341.
149. Zwaka T.P. & Thomson J.A. (2005) A germ cell origin of embryonic stem cells? *Development*. 132. 227-233
150. Donovan P.J. (1998) The germ cell—the mother of all stem cells. *International Journal of Developmental Biology*. 42. 1043-1050.
151. Kucia M. (2007) Bone Marrow-Derived Very Small Embryonic-Like Stem Cells: Their Developmental Origin and Biological Significance. *Developmental Dynamics*. 236. 3309-3320

152. Orkin, S.H. (2000) Diversification of haematopoietic stem cells to specific lineages. *Nature Reviews Genetics*. 1. 57–64.
153. Orkin S.H. & Zon L.I. (2008) Hematopoiesis: an evolving paradigm for stem cell biology. *Cell*. 132. 631-644
154. Ebihara Y. *et al.* (2006) Haematopoietic origins of fibroblasts: II. *In vitro* studies of fibroblasts, CFU-F, and fibrocytes. *Experimental Hematology*. 34. 219-229
156. Jaffredo T., *et al.* (2005) From hemangioblast to haematopoietic stem cell: An endothelial connection? *Experimental Hematology*. 33. 1029-1040
157. Dzierzak E. (2005) The emergence of definitive haematopoietic stem cells in the mammal. *Current Opinion in Hematology*. 12. 197-202
158. Postlethwaite A.E., *et al.* (2004) Cellular origins of fibroblasts: possible implications for organ fibrosis in systemic sclerosis. *Current Opinion in Rheumatology*. 16. 733-738
159. Huang, A.H.C., *et al.* (2008) Isolation and characterization of dental pulp stem cells from a supernumerary tooth. *Journal of Oral Pathology and Medicine*. 37. 571-574
160. Gronthos S., *et al.* (2000) Postnatal human dental pulp stem cells (DPSCs) *in vitro* and *in vivo*. *Proceedings of the National Academy of Sciences*. 97. 13625–13630
161. Gronthos S., *et al.* (2002) Stem Cell Properties of Human Dental Pulp Stem Cells. *Journal of Dental Research*. 81. 531-535
162. Thesleff I. & Aberg T. (1999) Molecular regulation of tooth development. *Bone*. 25. 123–125
163. Peters H. & Balling R. (1999) Teeth. Where and how to make them. *Trends in Genetics*. 15. 59–65
164. Arthur A., *et al.* (2008) Adult Human Dental Pulp Stem Cells Differentiate Toward Functionally Active Neurons Under Appropriate Environmental Cues. *Stem Cells*. 26. 1787 – 1795
165. Suguro H., *et al.* (2008) Characterization of human dental pulp derived cell lines. *International Endodontic Journal*. 41. 609-616
166. Lindroos B., *et al.* (2008) Characterisation of human dental stem cells and buccal mucosa fibroblasts. *Biochemical and Biophysical Research Communications*. 368. 329-335



167. Zhang W., *et al.* (2008) *In vivo* evaluation of human dental pulp stem cells differentiated towards multiple lineages. *Journal of Tissue Engineering and Regenerative Medicine*. 2. 117-125
168. Kerkis, I., *et al.* (2006). Isolation and characterization of a population of immature dental pulp stem cells expressing OCT-4 and other embryonic stem cell markers. *Cells Tissues Organs*. 184. 105–116
169. d'Aquino R., *et al.* (2008) Dental Pulp Stem Cells: A Promising Tool for Bone Regeneration. *Stem Cell Reviews*. 4. 21-26
170. Otaki S., *et al.* (2007) Mesenchymal progenitor cells in adult human dental pulp and their ability to form bone when transplanted into immunocompromised mice. *Cell Biology International*. 31. 1191-1197
171. Yang X., *et al.* (2007) Multilineage potential of STRO-1<sup>+</sup> rat dental pulp cells *in vitro*. *Tissue Engineering and Regenerative Medicine*. 1. 128-135
173. Gagari E., *et al.* (2006) Expression of stem cell factor and its receptor, c-kit, in human oral mesenchymal cells. *European Journal of Oral Sciences*. 114. 409-415
174. Papaccio G., *et al.* (2006) Long-term cryopreservation of dental pulp stem cells (SBP-DPSCs) and their differentiated osteoblasts: A cell source for tissue repair. *Journal of Cellular Physiology*. 208. 319-325
175. Ringer S. (1883) A further contribution regarding the influence of different constituents of the blood on the contraction of the heart. *Journal of Physiology*. 4. 29-42
176. Nayler W.G. (1984) Sydney Ringer – Physician and Scientist. *Journal of Molecular and Cellular Cardiology*. 16. 113-116
177. Hamburger V. (1997) Wilhelm Roux: visionary with a blind spot. *Journal of the History of Biology*. 30. 229-238
178. Toffaletti J.G. & McDonnell E.H. (2008) Variation of serum creatine, cystatin C, and creatinine clearance tests in persons with normal renal function. *Clinica Chimica Acta*. 395. 115-119
178. Piccione G., *et al.* (2008) Daily rhythms of serum vitamin D-metabolites, calcium and phosphorus in horses. *Acta Veterinaria Brno*. 77. 151-157
179. Silvertri E., *et al.* (2008) Age-related changes in renal and hepatic cellular mechanisms associated with variations in rat serum thyroid hormone levels. *American Journal of Physiology-Endocrinology and Metabolism*. 294. 1160-1168

180. Greystoke A., *et al.* (2008) Optimisation of circulating biomarkers of cell death for routine clinical use. *Annals of Oncology*. 19. 990-995
181. Krebs H.A. (1950) Chemical composition of blood plasma and serum. *Annual Review of Biochemistry*. 19. 409-430
182. Matsuzawa T., *et al.* (1993) Clinical pathology reference ranges of laboratory animals. *Journal of Veterinary Medical Science*. 55. 351-362
183. Wilson A.C., *et al.* (1977) Biochemical Evolution. *Annual Review of Biochemistry*. 46. 573-639
184. Piccinni A., *et al.* (2008) Diurnal variation of plasma brain-derived neurotrophic factor (BDNF) in humans: An analysis of sex differences. *Chronobiology International*. 25. 819-826
185. Deepak K., *et al.* (2008) Gender variation in interleukin-13 production: A possible mechanism of differential *In vivo* growth of a T-cell lymphoma. *Scandinavian Journal of Immunology*. 67. 518-588
186. Banks R.E. (2000) Measurement of Cytokines in Clinical Samples Using Immunoassays: Problems and Pitfalls. *Critical Reviews in Clinical Laboratory Sciences*. 37. 131-182
187. das Dores C., *et al.* (2007) Relationship between diet and anticoagulant response to warfarin. *European Journal of Nutrition*. 46. 147-154
188. Cartmill J.A., *et al.* (2005) Leptin secretion in horses: Effects of dexamethasone, gender, and testosterone. *Domestic Animal Endocrinology*. 31. 197-210
189. Ma Y.S., *et al.* (2006) Association between dietary fibre and serum C-reactive protein. *American Journal of Clinical Nutrition*. 83. 760-766
190. Ma Y.S., *et al.* (2006) Association between fibre intake and serum lipids. *Journal of the American College of Nutrition*. 25. 155-163
191. Kratzsch J., *et al.* (2008) Reference intervals for TSH and thyroid hormones are mainly affected by age, body mass index and number of blood leucocytes, but hardly by gender and thyroid autoantibodies during the first decades of life. *Clinical Biochemistry*. 41. 1091-1098
192. Schlatt S., *et al.* (2008) Age-related changes in diurnal rhythms and levels of gonadotropins, testosterone, and inhibin B in male rhesus monkeys (*Macaca mulatta*). *Biology of Reproduction*. 79. 93-99
193. Stegner J.E., *et al.* (2004) Follicular dynamics and steroid profiles in cows during and after treatment with progestin-based protocols for synchronization of estrus. *Journal of Animal Science*. 82. 1022-1028

194. Alila-Johansson A., *et al.* (2003) Serum cortisol levels in goats exhibit seasonal but not daily rhythmicity. *Chronobiology International*. 20. 65-79
195. Garcia M.R., *et al.* (2002) Serum leptin and its adipose gene expression during pubertal development, the estrous cycle, and different seasons in cattle. *Journal of Animal Science*. 80. 2158-2167
196. Nagatani S., *et al.* (2000) Appearance of a Nocturnal Peak of Leptin Secretion in the Pubertal Rat. *Hormones and Behaviour*. 37. 345-352
197. Morigi M., *et al.* (1999) Xenogeneic Serum Promotes Leukocyte-Endothelium Interaction under Flow through Two Temporally Distinct Pathways. *Journal of the American Society of Nephrology*. 10. 2197-2207
198. Kharche S.D., *et al.* (2008) Effect of somatic cells co-culture on cleavage and development of in-vitro fertilized caprine embryos. *Indian Journal of Animal Sciences*. 78. 686-692
199. Woods T.L., *et al.* (1997) Conditions for the culture of bovine embryonic myogenic cells. *Tissue and Cell*. 29. 207-215
200. Liteplo R.G. & Jurewicz T.J. (1991) Serum has a differential effect on DNA replication in a human melanoma cell line cultured in methionine or 5'-deoxy-5'-methylthioadenosine. *Biochimica et Biophysica Acta*. 1088. 365-372
201. Perdikogianni, C., *et al.* (2008) Could cord blood be a source of mesenchymal stromal cells for clinical use? *Cytotherapy*. 10. 452-459
202. Hankey D.P., *et al.* (2001) Enhancement of human osteoblast proliferation and phenotypic expression when cultured in human serum. *Acta Orthopaedica Scandinavica*. 72. 395-403
203. Nimura A., *et al.* (2008) Increased proliferation of human synovial mesenchymal stem cells with autologous human serum. *Arthritis and Rheumatism*. 58. 501-510
204. Angulo, A.F., *et al.* (2000). *Acholeplasma vituli* sp. nov., from bovine serum and cell cultures. *International Journal of Systematic and Evolutionary Microbiology* 50. 1125-1131
205. Erickson G.A., *et al.* (1991) Viral contamination of fetal bovine serum used for tissue culture: risks and concerns. *Developments in Biological Standardization*. 75. 173-175

206. Kappeler A., *et al.* (1996) Detection of bovine polyomavirus contamination in fetal bovine sera and modified live viral vaccines using polymerase chain reaction. *Biologicals*. 131-135
207. Jochems C.E.A., *et al.* (2002) The use of fetal bovine serum: ethical or scientific problem? *Alternatives to Laboratory Animals*. 30. 219-227
208. Weihe, W.H. (1985) Use and misuse of an imprecise concept: alternative methods in animal experiments. *Laboratory Animals*. 19. 19-26.
209. Huang L.S., *et al.* (2005) Production of human serum albumin by sugar starvation induced promoter and rice cell culture. *Transgenic Research*. 14. 569-581
210. Keel B.A., *et al.* (1993) Purified human  $\alpha$ -fetoprotein inhibits follicle-stimulating hormone-stimulated estradiol production by porcine granulosa cells in culture. *Molecular and Cellular Endocrinology*. 94. 21-25
211. Hou L.T., *et al.* (2007) Modulation of osteogenic potential by recombinant human bone morphogenic protein-2 in human periodontal ligament cells: effect of serum, culture medium, and osteoinductive medium. *Journal of Periodontal Research*. 42. 244-252
212. Kanemura Y., *et al.* (2005) *In vitro* screening of exogenous factors for human neural stem/progenitor cell proliferation using measurement of total ATP content in viable cells. *Cell Transplantation*. 14. 673-682
213. Schmidt M., *et al.* (1999) Temperature-induced production of recombinant human insulin in high-cell density cultures of recombinant *Escherichia coli*. *Journal of Biotechnology*. 5. 71-83
214. Miyagawa S., *et al.* (2000) Insulin and insulin-like growth factor I support the proliferation of erythroid progenitor cells in bone marrow through the sharing of receptors. *British Journal of Haematology*. 109. 555-562
215. Keenan J., *et al.* (2006) Evaluation of recombinant human transferrin (DeltaFerrin<sup>TM</sup>) as an iron chelator in serum-free media for mammalian cell culture. *Cytotechnology*. 51. 29-37
216. Yeoman L.C., *et al.* (1996) Transferrin and insulin enhance human colon tumor cell growth by differentiation class specific mechanisms. *Oncology Research*. 8. 273-279
217. Karimullah A. Zirvi. (1991) Development of serum-free media for the growth of human gastrointestinal adenocarcinoma xenografts as primary

- tissue cultures. *Journal of Cancer Research and Clinical Oncology*. 117. 515-518
218. De Castro M., *et al.* (2006) Evaluation of human serum albumin as a substitute of foetal bovine serum for cell culture. *International Journal of Pharmaceutics*. 310. 8-14
219. Royer P.J., *et al.* (2006) Culture Medium and Protein Supplementation in the Generation and Maturation of Dendritic Cells. *Scandinavian Journal of Immunology*. 63. 401-409
220. Keenan J., *et al.* (1997) Recombinant human albumin in cell culture: evaluation of growth-promoting potential for NRK and SCC-9 cells in vitro. *Cytotechnology*. 24. 243-252
221. Tezel T.H. & Del Priore L.V. (1999) Serum-free Media for Culturing and Serial-Passaging of Adult Human Retinal Pigment Epithelium. *Experimental Eye Research*. 66. 807-815
222. van der Valk J., *et al.* (2004) The humane collection of fetal bovine serum and possibilities for serum-free cell and tissue culture. *Toxicology in Vitro*. 18. 1-12
223. Jenkins N., *et al.* (2008) Post-translational modifications of recombinant proteins: Significance for biopharmaceuticals. *Molecular Biotechnology*. 39. 113-118
224. Jenkins N. (2007) Modifications of therapeutic proteins: challenges and prospects. *Cytotechnology*. 53. 121-125
225. Georgiou G. & Segatori L. (2005) Preparative expression of secreted proteins in bacteria: status report and future prospects. *Current Opinion in Biotechnology*. 16. 538-545
226. Zhang J., *et al.* (2006) A novel function for selenium in biological system: Selenite as a highly effective iron carrier for Chinese hamster ovary cell growth and monoclonal antibody production. *Biotechnology and Bioengineering*. 95. 1188-1197
227. Zeng H. (2002) Selenite and selenomethionine promote HL-60 cell cycle progression. *Journal of Nutrition*. 132. 674-679
228. Kisiday K.D., *et al.* (2005) Evaluation of medium supplemented with insulin–transferrin–selenium for culture of primary bovine calf chondrocytes in three-dimensional hydrogel scaffolds. *Tissue Engineering*. 11. 141-151
229. Kaller H., *et al.* (2002) Evaluation of various serum and animal protein free media for the production of a veterinary rabies vaccine in BHK-21 cells. *Journal of Biotechnology*. 95. 195-204

230. Landschulz W., *et al.* (1984) A lipophilic iron chelator can replace transferrin as a stimulator of cell proliferation and differentiation. *The Journal of Cell Biology*. 98. 596-601
231. Gigout A., *et al.* (2008) The Fate of Pluronic F-68 in Chondrocytes and CHO Cells. *Biotechnology and Bioengineering*. 100. 975-987
232. Wong V.G., *et al.* (2004) Evaluation of insulin-mimetic trace metals as insulin replacements in mammalian cell cultures. *Cytotechnology*. 45. 107-115
233. Wong V.G., *et al.* (2005) Zinc as an insulin replacement in hybridoma cultures. *Biotechnology and Bioengineering*. 93. 552-563
234. Inomata M., *et al.* (1994) Culture of retinoblastoma cells from clinical specimens: growth-promoting effect of 2-Mercaptoethanol. *Journal of Cancer Research and Clinical Oncology*. 120. 149-155
235. Mobest D., *et al.* (1998) Serum-free ex vivo expansion of CD34<sup>+</sup> haematopoietic progenitor cells. *Biotechnology and Bioengineering*. 60. 341-347
236. Murakami H., *et al.* (1982) Growth of hybridoma cells in serum-free medium: ethanolamine is an essential component. *Proceedings of the National Academy of Sciences*. 79. 1158-1162
237. Spens E. & Haggstrom L. (2007) Defined protein and animal component-free NS0 fed-batch culture. *Biotechnology and Bioengineering*. 98. 1193-1194
238. Makino S., *et al.* (1999) Cardiomyocytes can be generated from marrow stromal cells in vitro. *The Journal of Clinical Investigation*. 103. 697-705
239. Hakuno D., *et al.* (2002) bone marrow-derived regenerated cardiomyocytes (CMG cells) express functional adrenergic and muscarinic receptors. *Circulation*. 105. 380-386
240. Tomita Y., *et al.* (2007) Application of mesenchymal stem cell-derived cardiomyocytes as bio-pacemakers: current status and problems to be solved. *Medical and Biological Engineering and Computing*. 45. 209-220
241. Birsoy K., *et al.* (2008) Transcriptional regulation of adipogenesis by KLF4. *Cell Metabolism*. 7. 339-347

242. Cousin W., *et al.* (2006) Inhibition of the anti-adipogenic Hedgehog signaling pathway by cyclopamine does not trigger adipocyte differentiation. *Biochemical and Biophysical Research Communications*. 349. 799-803
243. Hube F., *et al.* (1999) The phosphodiesterase inhibitor IBMX suppresses TNF-alpha expression in human adipocyte precursor cells: A possible explanation for its adipogenic effect. *Hormone and Metabolic Research*. 31. 359-362
244. Ding J., *et al.* (2003) Insulin-dependent adipogenesis in stromal ST2 cells derived from murine bone marrow. *Bioscience Biotechnology and Biochemistry*. 67. 314-321
245. Bielby R.C. *et al.* (2004). *In vitro* differentiation and *in vivo* mineralization of osteogenic cells derived from human embryonic stem cells. *Tissue Engineering*. 10.1518-1525
246. Fu H., *et al.* (2007) Osteoblast differentiation *in vitro* and *in vivo* promoted by Osterix. *Journal of Biomedical Materials Research Part A*. 83A. 770-778
247. Porter R.M., *et al.* (2003) Effect of dexamethasone withdrawal on osteoblastic differentiation of bone marrow stromal cells. *Journal of Cellular Biochemistry*. 90. 13-22
248. McCabe L.R., *et al.* (1996) Developmental expression and activities of specific Fos and Jun proteins are functionally related to osteoblast maturation: Role of Fra-2 and Jun D during differentiation. *Endocrinology*. 137. 4398- 4408
249. Fukumoto T., *et al.* (2003) Combined effects of insulin like growth factor-1 and transforming growth factor beta-1 on periosteal mesenchymal stem cells during chondrogenesis *in vitro*. *Osteoarthritis Cartilage*. 11.55-64
250. Han F., *et al.* (2005) Transforming Growth Factor-b1 (TGF-b1) Regulates ATDC5 Chondrogenic Differentiation and Fibronectin Isoform Expression. *Journal of Cellular Biochemistry*. 95. 750-762
251. Nakamura K., *et al.* (1999) p38 mitogen activated protein kinase functionally contributes to chondrogenesis induced by growth/differentiation factor-5 in ATDC5 cell. *Experimental Cell Research*. 250. 351-363
252. Lee J.W., *et al.* (2004) Chondrogenic differentiation of mesenchymal stem cells and its clinical applications. *Yonsei Medical Journal*. 45. 41-47
253. Miyazawa K., *et al.* (2002) Two major Smad pathways in TGF- b superfamily signalling. *Genes to Cells*. 7. 1191-1204



254. Shirasawa S., *et al.* (2006) In vitro chondrogenesis of human synovium-derived mesenchymal stem cells: optimal condition and comparison with bone marrow-derived cells. *Journal of Cellular Biochemistry.* 97. 84-97
255. Yang. I.H., *et al.* (2004) Comparison of phenotype characterisation between “alginate beads” and “pellet” culture systems as culture systems for chondrogenic differentiation models for human mesenchymal stem cells. *Yonsei Medical Journal.* 45. 891-900
256. Chang H.C., *et al.* (2008) Chondrogenesis from immortalized human mesenchymal stem cells: comparison between collagen gel and pellet culture methods. *Artificial Organs.* 32. 561-571
257. Chen S., *et al.* (2005) The cAMP pathway regulates both transcription and activity of the paired homeobox transcription factor Phox2a required for development of neural crest-derived and central nervous system-derived catecholaminergic neurons. *The Journal of Biological Chemistry.* 280. 41025-41036
258. Paris M., *et al.* (2006) Homeodomain transcription factor Phox2a, via cyclic AMP-mediated activation, induces p27Kip1 transcription, coordinating neural progenitor cell cycle exit and differentiation. *Molecular and Cellular Biology.* 26. 8826-8839
259. Jori J.P., *et al.* (2005) Molecular Pathways Involved in Neural In Vitro Differentiation of Marrow Stromal Stem Cells. *Journal of Cellular Biochemistry.* 94. 645-655
260. Sarkar S.A. & Sharma R.P. (2002) All-trans-retinoic acid-mediated modulation of p53 during neural differentiation in murine embryonic stem cells. *Cell Biology and Toxicology.* 18. 243-257
261. Farooqui A.A., *et al.* (2004) Retinoic acid-mediated phospholipase A<sub>2</sub> signalling in the nucleus. *Brain Research Reviews.* 45. 179-195
262. Zechel C. Requirement of retinoic acid receptor isotypes alpha, beta, and gamma during the initial steps of neural differentiation of PCC7 cells. *Molecular Endocrinology.* 19. 1629-1645
263. Xu R., *et al.* (2008) Functional Analysis of Neuron-like Cells Differentiated from Neural Stem Cells Derived from Bone Marrow Stroma Cells in vitro. *Cellular and Molecular Neurobiology.* 28. 545-558
264. J'Massagué J. & Wotton D. (2000) Transcriptional control by the TGF- $\beta$ /Smad signalling system. *The EMBO Journal.* 19. 1745-1754
265. Pourquié O. (2005) Signal transduction: A new canon. *Nature.* 433. 208-209

266. Banas A., *et al.* (2007) Stem cell plasticity: learning from hepatogenic differentiation strategies. *Developmental Dynamics*. 236. 3228-3241
267. Landry J., *et al.* (1985). Spheroidal aggregate culture of rat liver cells: histotypic reorganization, biomatrix deposition, and maintenance of functional activities. *Journal of Cellular Biology*. 101. 914-23
268. Abu-Absi S.F., *et al.* (2002) Structural polarity and functional bile canaliculi in rat hepatocyte spheroids. *Experimental Cell Research*. 274. 56-67.
269. Ong S.Y., *et al.* (2006) Inducing hepatic differentiation of human mesenchymal stem cells in pellet culture. *Biomaterials*. 27. 4087-4097
270. Campard D., *et al.* (2008) Native umbilical cord matrix stem cells express hepatic markers and differentiate into hepatocyte-like cells. *Gastroenterology*. 134. 833-848
271. Seo M.J., *et al.* (2005) Differentiation of human adipose stromal cells into hepatic lineage in vitro and in vivo. *Biochemical and Biophysical Research Communications*. 328. 258-264
272. Lysaght M.J. & Reyes J. (2001) The growth of tissue engineering. *Tissue Engineering*. 7. 485-493
273. Lavik E. & Langer R. (2004) Tissue engineering: current state and perspectives. *Applied Microbiology and Biotechnology*. 65. 1-8
274. Cazeau C. *et al.* (1999) Use of ceramics of calcium triphosphate in the repair of tibial plateau fractures: a series of 20 cases. *European Journal of Orthopaedic Surgery and Traumatology*. 9. 171-174
275. Bohner M. (2000) Calcium orthophosphates in medicine: from ceramics to calcium phosphate cements. *Injury*. 31. 37-47
276. Rotunda A. & Narins R. (2006) Poly-l-lactic acid: a new dimension in soft tissue augmentation. *Dermatologic Therapy*. 19. 151-158
277. Woo M.K., *et al.* (2007) Nano-fibrous scaffolding promotes osteoblast differentiation and biomineralization, *Biomaterials*. 28. 343-355
278. Ho M.H., *et al.* (2007) Efficient modification on PLLA by ozone treatment for biomedical applications. *Macromolecular Bioscience*. 7. 467-474
279. Porter K., *et al.* (2006) Regulation of osteoblast gene expression and phenotype by polylactide-fatty acid surfaces. *Molecular Biology Reports*. 33. 1-12

280. Jeon O., *et al.* (2007) Enhancement of ectopic bone formation by bone morphogenetic protein-2 released from a heparin-conjugated poly(l-lactic-co-glycolic acid) scaffold. *Biomaterials*. 28. 2763–2771
281. Zhu W. & Ding J. (2006) Synthesis and characterization of a redox injectable, biodegradable hydrogel. *Journal of Applied Polymer Science*. 99. 2375–2383
282. Xu X.D., *et al.* (2007) Fabrication and characterization of a novel composite PNIPAAm hydrogel for controlled drug release. *Journal of Biomedical Materials Research Part A*, 81A. 418–426
283. Ferreira L.S., *et al.* (2007) Bioactive hydrogel scaffolds for controllable vascular differentiation of human embryonic stem cells. *Biomaterials*. 28. 2706–2717
284. Hynd M.R., *et al.* (2007) Directed cell growth on protein-functionalized hydrogel surfaces. *Journal of Neuroscience Methods*. 162. 255–263
285. Wallace D.G. & Rosenblatt J. (2003) Collagen gel systems for sustained delivery and tissue engineering. *Advanced Drug Delivery Reviews*. 55. 1631–1649
286. Wang X.Y., *et al.* (2006) Fibrous proteins in tissue engineering. *Materials Today*. 9. 44–53
287. Nakayama K., *et al.* (2007) Enhancement of peripheral nerve regeneration using bioabsorbable polymer tubes packed with fibrin gel. *Artificial Organs*. 31. 500–508
288. Richheimer S.L. & Robinson A.B. (1977) Degradation of transferrin in the presence of ascorbic acid and oxygen. *Orthomolecular Psychiatry*. 6. 290–299
289. Aisen P. & Listowsky I. (1980) Iron transport and storage proteins. *Annual Review of Biochemistry*. 49. 357–393
290. Salis C., *et al.* (2002) HoloTransferrin but not ApoTransferrin prevents schwann cell de-differentiation in culture. *Developmental Neuroscience*. 24. 214–221
291. Chen Y.C., *et al.* (2008) NS21: Re-defined and modified supplement B27 for neuronal cultures. *Journal of Neuroscience Methods*. 171. 239–247
292. Lonergan D.M., *et al.* (2003) Growth factor profile of irradiated human dermal fibroblasts using a serum-free method. 111. 1960–1968

293. Bullock A.J., *et al.* (2006) Use of human fibroblasts in the development of a xenobiotic-free culture and delivery system for human keratinocytes. *Tissue Engineering*. 12. 245-255
294. Pollard J.D., *et al.* (2005) Effects of copper tripeptide on the growth and expression of growth factors by normal and irradiated fibroblasts. *Archives of Facial Plastic Surgery*. 7. 27-31
295. Chufa H.E., *et al.* (1999) Effects of chronic wound fluid on the bioactivity of platelet derived growth factor in serum-free medium and its direct effect on fibroblast growth. *Wound Repair and Regeneration*. 7. 97-105
296. Garner W.L. (1998) Epidermal regulation of Dermal Fibroblast Activity. *Plastic and Reconstructive Surgery*. 102. 135-139
297. Schleicher I. *et al.* (2005) Surface Modification by Complexes of Vitronectin and Growth Factors for Serum-Free Culture of Human Osteoblasts. *Tissue Engineering*. 11. 1688-1698
298. Xie J., *et al.* (2005) Adsorption of serum fetuin to hydroxylapatite does not contribute to osteoblast phenotype modifications. *Journal of Biomedical Materials Research Part A*. 73. 39-47
299. Cowles E.A., *et al.* (2000) Integrin-mediated signalling regulates AP-1 transcription factors and proliferation in osteoblasts. *Journal of Biomedical Materials Research*. 52. 725-737
300. Pelisek J., *et al.* (2001) Quiescence, cell viability, apoptosis and necrosis of smooth muscle cells using different growth inhibitors. *Cell Proliferation*. 34. 305-320
301. Markmann. A., *et al.* (2003) Expression of transcription factors and matrix genes in response to serum stimulus in vascular smooth muscle cells. *European Journal of Cell Biology*. 82. 119-129
302. Schaafsma D., *et al.* (2007) Insulin increases the expression of contractile phenotypic markers in airway smooth muscle. *American Journal of Physiology – Cell Physiology*. 293. C429- C439
303. Weber M.A., *et al.* (2000) A novel insulin mimetic without a proliferative effect on vascular smooth muscle cells. *Journal of Vascular Surgery*. 32. 1118-1126
304. Poliseño L., *et al.* (2006) Resting smooth muscle cells as a model for studying vascular cell activation. *Tissue and Cell*. 38. 111-120
305. Han M., *et al.* (2006) Serum deprivation results in redifferentiation of human umbilical vascular smooth muscle cells. *American Journal of Physiology –Cell Physiology*. 291. C50-C58.

306. Nelson C.M. & Chen C.S. (2002) Cell-cell signalling by direct contact increases cell proliferation via a PI3K-dependent signal. *FEBS Letters*. 514. 238-242
307. Mochizuki S., *et al.* (2002) Signalling pathways transduced through the elastin receptor facilitate proliferation of arterial smooth muscle cells. *Journal of Biological Chemistry*. 277. 44854-44863
308. Shiels I.A., *et al.* (1996) Homologous serum increases fibronectin expression and cell adhesion in airway smooth muscle cells. *Inflammation*. 20. 373-387
309. Baker S.C & Jennifer Southgate J. (2008) Towards control of smooth muscle cell differentiation in synthetic 3D scaffolds. *Biomaterials*. 29. 3357-3366
310. Akino K., *et al.* (2003) Bone morphogenetic protein-2 regulates proliferation of human mesenchymal stem cells. *Wound Repair and Regeneration*. 11. 354-360
311. Meuleman N., *et al.* (2006) Human marrow mesenchymal stem cell culture: serum-free medium allows better expansion than classical  $\alpha$ -MEM medium. *European Journal of Haematology*. 76. 309-316
312. Liu C.H., *et al.* (2007) Optimization of serum free medium for cord blood mesenchymal stem cells. *Biochemical Engineering Journal*. 33. 1-9
313. Roche S., *et al.* (2007) Oct-4, Rex-1, and Gata-4 expression in human MSC increase the differentiation efficiency but not hTERT expression. *Journal of Cellular Biochemistry*. 101. 271-280
314. Radhika R., *et al.* (2004) Serum deprivation of human marrow stromal cells (hMSCs) selects for a subpopulation of early progenitor cells with enhanced expression of OCT-4 and other embryonic genes. *Blood*. 103. 1647-1652
315. Battula V.L., *et al.* (2007) Human placenta and bone marrow derived MSC cultured in serum-free, b-FGF-containing medium express cell surface frizzled-9 and SSEA-4 and give rise to multilineage differentiation. *Differentiation*. 75. 279-291
316. Lennon D.P., *et al.* (1995) A chemically defined medium supports *in vitro* proliferation and maintains the osteochondral potential of rat marrow-derived mesenchymal stem cells. *Experimental Cell Research*. 219. 211-222

317. Magaki T., *et al.* (2005) Generation of bone marrow-derived neural cells in serum-free monolayer culture. *Neuroscience Letters*. 384. 282-287
318. Bilgen B., *et al.* (2007) FBS suppresses TGF- $\beta$ 1-induced chondrogenesis in synoviocyte pellet cultures while dexamethasone and dynamic stimuli are beneficial. *Journal of Tissue Engineering and Regenerative Medicine*. 1. 436-442
319. Lee R.H., *et al.* (2004) Characterization and expression analysis of mesenchymal stem cells from human bone marrow and adipose tissue. *Cellular Physiology and Biochemistry*. 14. 311-324
320. Shiota M., *et al.* (2007) Isolation and characterization of bone marrow-derived mesenchymal progenitor cells with myogenic and neuronal properties. *Experimental Cell Research*. 313. 1008-1023
321. Izadpanah R., *et al.* (2006) Biologic properties of mesenchymal stem cells derived from bone marrow and adipose tissue. *Journal of Cellular Biochemistry*. 99. 1285-1297
322. Barry F.P. & Murphy M.J. (2004) Mesenchymal stem cells: clinical applications and biological characterization. *The International Journal of Biochemistry & Cell Biology* 36. 568-584
323. Friedman M.S., *et al.* (2006) Osteogenic differentiation of human mesenchymal stem cells is regulated by bone morphogenetic protein-6. *Journal of Cellular Biochemistry*. 98. 538-554
324. Li X., *et al.* (2005) Steroid effects on osteogenesis through mesenchymal cell gene expression. *Osteoporosis International*. 16. 101-108
325. Egusa H., *et al.* (2007) Downregulation of extracellular matrix-related gene clusters during osteogenic differentiation of human bone marrow and adipose tissue-derived stromal cells. *Tissue Engineering*. 13. 2589-2600
326. Frank O., *et al.* (2002) Real-time quantitative RT-PCR analysis of human bone marrow stromal cells during osteogenic differentiation in vitro. *Journal of Cellular Biochemistry*. 85. 737-746
327. Mehlhorn A.T., *et al.* (2006) Differential expression pattern of extracellular matrix molecules during chondrogenesis of mesenchymal stem cells from bone marrow and adipose tissue. *Tissue Engineering*. 12. 2853-2862
328. Afizah H., *et al.* (2007) A comparison between the chondrogenic potential of human bone marrow stem cells (BMSCs) and adipose-derived stem cells (ADSCs) taken from the same donors. *Tissue Engineering*. 13. 659-666

329. Mannello F. & Tonti G.A. (2007) Concise review: No breakthroughs for human mesenchymal and embryonic stem cell culture: Conditioned medium, feeder layer, or feeder-free; Medium with fetal calf serum, human serum, or enriched plasma; Serum-free, serum replacement nonconditioned medium, or ad hoc formula? All that glitters is not gold! *Stem Cells*. 35. 1603-1609
330. Widera D., *et al.* (2007) Highly efficient neural differentiation of human somatic stem cells, isolated by minimally invasive periodontal surgery. *Stem Cells and Development*. 16. 447-460
331. Jo Y.Y., *et al.* (2007) Isolation and Characterization of Postnatal Stem Cells from Human Dental Tissues. *Tissue Engineering*. 13. 767-773
332. Zhang W., *et al.* (2006) Multilineage differentiation potential of stem cells derived from human dental pulp after cryopreservation. *Tissue Engineering*. 12. 2813-2823
333. Lindroos B., *et al.* (2008) Characterisation of human dental stem cells and buccal mucosa fibroblasts. *Biochemical and Biophysical Research Communications*. 386. 329-335
334. Huang G.T.J., *et al.* (2006) In vitro characterization of human dental pulp cells: various isolation methods and culturing environments. *Cell and Tissue Research*. 324. 225-236
335. Nosrat I.V., *et al.* (2004) Dental pulp cells provide neurotrophic support for dopaminergic neurons and differentiate into neurons in vitro; implications for tissue engineering and repair in the nervous system. *European Journal of Neuroscience*. 19. 2388-2398
336. Huang A.H.C., *et al.* (2008) Isolation and characterization of dental pulp stem cells from a supernumerary tooth. *Journal of Oral Pathology and Medicine*. 37. 571-574
337. Kerkis I., *et al.* (2006) Isolation and characterization of a population of immature dental pulp stem cells expressing OCT-4 and other embryonic stem cell markers. *Cells Tissues Organs*. 184. 105-116
338. Gronthos S., *et al.* (2002) Stem cell properties of human dental pulp stem cells. *Journal of Dental Research*. 81. 531-535
339. Miura M., *et al.* (2003) SHED: Stem cells from human exfoliated deciduous teeth. *Proceedings of the National Academy of Sciences of the United States of America*. 100. 5807-5812
340. Laino G., *et al.* (2006) An approachable human adult stem cell source for hard-tissue engineering. *Journal of Cellular Physiology*. 206. 693-701



341. Papaccio G., *et al.* (2006) Long-term cryopreservation of dental pulp stem cells (SBP-DPSCs) and their differentiated osteoblasts: A cell source for tissue repair. *Journal of cellular Physiology*. 208. 319-325
342. Gronthos S., *et al.* (2000) Postnatal human dental pulp stem cells (DPSCs) *in vitro* and *in vivo*. *Proceedings of the National Academy of Sciences of the United States of America*. 97. 13625-13630
343. Arthur A., *et al.* (2008) Adult human dental pulp stem cells differentiate toward functionally active neurons under appropriate environmental cues. *Stem Cells*. 26. 1787-1795
344. Suguro H., *et al.* (2008) Characterization of human dental pulp-derived cell lines. *International Endodontic Journal*. 41. 609-616
345. Liu H., *et al.* (2006) Dental pulp stem cells. *Methods in Enzymology*. 419. 99-113
346. Lee O.K., *et al.* (2004) Isolation of multipotent mesenchymal stem cells from umbilical cord blood. *Blood*. 103. 1669-1675
347. Lysy P.A., *et al.* (2008) Persistence of a chimerical phenotype after hepatocyte differentiation of human bone marrow mesenchymal stem cells. *Cell Proliferation*. 41. 36-58
348. Ong S.Y., *et al.* (2006) Inducing hepatic differentiation of human mesenchymal stem cells in pellet culture. *Biomaterials*. 27. 4087-4097
349. Hong S.H., *et al.* (2005) *In vitro* differentiation of human umbilical cord blood-derived mesenchymal stem cells' into hepatocyte-like cells. *Biochemical and Biophysical Research Communications*. 330. 1153-1161
350. Seo M.J., *et al.* (2005) Differentiation of human adipose stromal cells into hepatic lineage *in vitro* and *in vivo*. *Biochemical and Biophysical Research Communications*. 328. 258-264
351. Iohara K., *et al.* (2006) Side population cells isolated from porcine dental pulp tissue with self-renewal and multipotency for dentinogenesis, chondrogenesis, adipogenesis, and neurogenesis. *Stem Cells*. 24. 2493-2503
352. Ichinose S., *et al.* (2005) Detailed examination of cartilage formation and endochondral ossification using human mesenchymal stem cells. *Clinical and Experimental Pharmacology and Physiology*. 32. 561-570
353. Tan G., *et al.* (2008) Synthesis and characterization of injectable photocrosslinking poly (ethylene glycol) diacrylate based hydrogels. *Polymer Bulletin*. 61. 91-98

354. Abbasi F. & Mirzadeh H. (2003) Properties of poly(dimethylsiloxane)/hydrogel multicomponent systems. *Journal of Polymer Science: Part B: Polymer Physics*, 41, 2145–2156
355. Karlsson J.O. & Gatenholm P. (1996) Solid-supported wettable hydrogels prepared using ozone induced grafting. *Polymer*. 37. 4251-4256
356. Tehrani M., *et al.* (2004) Material properties of various intraocular lenses in an experimental study. *Ophthalmologica*. 218. 57–63
357. Liu W., *et al.* (2004) A rapid temperature-responsive sol–gel reversible poly(*N*-isopropylacrylamide)-*g*-methylcellulose copolymer hydrogel. *Biomaterials*. 25. 3005-3012
358. Park J.H. & Bae Y.H. (2002) Hydrogels based on poly(ethylene oxide) and poly(tetramethylene oxide) or poly(dimethyl siloxane): synthesis, characterization, in vitro protein adsorption and platelet adhesion. *Biomaterials*. 23. 1797-1808
359. Chen M.Y., *et al.* (2007) Substrate adhesion affects contraction and mechanical properties of fibroblast populated collagen lattices. *Journal of Biomedical Materials Research Part B – Applied Biomaterials*. 84B. 218-223
360. An Y.H., *et al.* (2001) Regaining chondrocyte phenotype in thermosensitive gel culture. *Anatomical Record*. 263. 336-341
361. Stevens M.M., *et al.* (2004) A rapid-curing alginate gel system: utility in periosteum-derived cartilage tissue engineering. *Biomaterials*. 25. 887-894
362. Galois L., *et al.* (2006) Bovine chondrocyte behaviour in three-dimensional type I collagen gel in terms of gel contraction, proliferation and gene expression. *Biomaterials*. 27. 79-90
363. Weiser L., *et al.* (1999) Effect of serum and platelet-derived growth factor on chondrocytes grown in collagen gels. *Tissue Engineering*. 5. 533-544
364. Malicev E., *et al.* (2007) Fibrin gel improved the spatial uniformity and phenotype of human chondrocytes seeded on collagen scaffolds. *Biotechnology and Bioengineering*. 96. 364-370
365. Peretti G.M., *et al.* (2006) Review of injectable cartilage engineering using fibrin gel in mice and swine models. *Tissue Engineering*. 12. 1151-1168
366. van Susante J.L.C., *et al.* (1995) Culture of chondrocytes in alginate and collagen carrier gels. 66. 549-556

367. Bryant S.J. & Anseth K.S. (2002) Hydrogel properties influence ECM production by chondrocytes photoencapsulated in poly(ethylene glycol) hydrogels. *Journal of Biomedical Materials Research*. 59. 63-72
368. Sieminski A.L., *et al.* (2005) Improved microvascular network *in vitro* by human blood outgrowth endothelial cells relative to vessel-derived endothelial cells. *Tissue Engineering*. 11. 1332-1345
369. Nehls V., *et al.* (1994) The effect of fibroblasts, vascular smooth muscle cells and pericytes on sprout formation of endothelial cells in a fibrin gel angiogenesis system. *Microvascular Research*. 48. 349-363
370. Pepper M.S. *et al.* (1998) Vascular endothelial growth factor (VEGF)-C synergizes with basic fibroblast growth factor and VEGF in the induction of angiogenesis *in vitro* and alters endothelial cell extracellular proteolytic activity. *Journal of Cellular Physiology*. 177. 439-352
371. Marx M., *et al.* (1994) Modulation of platelet-derived growth factor receptor expression in microvascular endothelial cells during *in vitro* angiogenesis. *Journal of Clinical Investigation*. 93. 131-139
372. Nehls V., *et al.* (1998) Contact-dependent inhibition of angiogenesis by cardiac fibroblasts in three-dimensional fibrin gels *in vitro*: implications for microvascular network remodelling and coronary collateral formation. *Cell and Tissue Research*. 293. 479-488
373. Mandriota S. & Pepper M.S. (1997) Vascular endothelial growth factor-induced *in vitro* angiogenesis and plasminogen activator expression are dependent on endogenous basic fibroblast growth factor. *Journal of Cell Science*. 110. 2293-2302
374. Toyoda T.K., *et al.* (2003) CD31 (PECAM-1)-bright cells derived from AC133-positive cells in human peripheral blood as endothelial-precursor cells. *Journal of Cellular Physiology*. 195. 119-129
375. Jongpaiboonkit L., *et al.* (2008) An adaptable hydrogel array format for 3-dimensional cell culture and analysis. *Biomaterials*. 29. 3346-3356
376. Kim Y., *et al.* (2005) Synthetic MMP-13 degradable ECMs based on poly(Nisopropylacrylamide- *co*-acrylic acid) semi-interpenetrating polymer networks. I. Degradation and cell migration. *Journal of Biomedical Materials Research Part A*. 75A. 73-88
377. Behraves E., *et al.* (2003) Adhesion and migration of marrow-derived osteoblasts on injectable *in situ* crosslinkable poly(propylene fumarate-*co*- ethylene glycol)-based hydrogels with a covalently linked RGDS peptide. *Journal of Biomedical Materials Research Part A*. 65A. 260-270

378. Man B.K., *et al.* (2001) Smooth muscle cell growth in photopolymerized hydrogels with cell adhesive and proteolytically degradable domains: synthetic ECM analogues for tissue engineering. *Biomaterials*. 22. 3045-3051
378. Luo Y., *et al.* (2004) A photolabile hydrogel for guided three dimensional cell growth and migration. *Nature Materials*. 3. 249-253
380. Dikovsky D., *et al.* (2006) The effect of structural alterations of PEG-fibrinogen hydrogel scaffolds on 3-D cellular morphology and cellular migration. *Biomaterials*. 27. 1496-1506
381. Nakamura S., *et al.* (2006) Controlled release of fibroblast growth factor-2 from an injectable 6-O-desulfated heparin hydrogel and subsequent effect on *in vivo* vascularisation. *Journal of Biomedical Materials Research Part A*. 78A. 364- 371
382. Nakamura S., *et al.* (2006) Effect of controlled release of fibroblast growth factor-2 from chitosan/fucoidan micro complex-hydrogel on *in vitro* and *in vivo* vascularisation. *Journal of Biomedical Materials Research Part A*. 85A. 619-627
383. Fujita M., *et al.* (2004) Vascularization *in vivo* caused by the controlled release of fibroblast growth factor-2 from an injectable chitosan/non anticoagulant heparin hydrogel. *Biomaterials*. 25. 699-706
384. Shu X.Z., *et al.* (2004) Attachment and spreading of fibroblasts on an RGD peptide-modified injectable hyaluronan hydrogel. *Journal of Biomedical Materials Research Part A*. 68A. 2. 365-375
385. Alhadlaq A., *et al.* (2005) Engineered adipose tissue from human mesenchymal stem cells maintains predefined shape and dimension: Implications in soft tissue augmentation and reconstruction. *Tissue Engineering*. 11. 556-566
386. Passaretti D., *et al.* (2001) Cultured chondrocytes produce injectable tissue-engineered cartilage in hydrogel polymer. *Tissue Engineering*. 7. 805-815
387. Hoemann C.D., *et al.* (2005) Tissue engineering of cartilage using an injectable and adhesive chitosan-based cell-delivery vehicle. *Journal of Biomaterials Science-Polymer Edition*. 18. 1181-1193
388. Cai S., *et al.* (2005) Injectable glycosaminoglycan hydrogels for controlled release of human basic fibroblast growth factor. *Biomaterials*. 26. 6054-6067
389. Shu X.Z., *et al.* (2006) Synthesis and evaluation of injectable, *in situ* crosslinkable synthetic extracellular matrices for tissue engineering. *Journal of Biomedical Materials Research Part A*. 79A. 902-912

390. Shu X.Z., *et al.* (2004) In situ crosslinkable hyaluronan hydrogels for tissue engineering. *Biomaterials*. 25. 1339-1348
391. Carter C.A., *et al.* (2003) Platelet-rich plasma gel promotes differentiation and regeneration during equine wound healing. *Experimental and Molecular Pathology*. 74. 244-255
392. Gimeno F.L., *et al.* (2006) Preparation of platelet-rich plasma as a tissue adhesive for experimental transplantation in rabbits. *Thrombosis Journal*. 4. 1-7
393. Borzini P. & Mazzucco L. (2005) Tissue regeneration in loco administration of platelet derivatives: clinical outcome, heterogeneous products, and heterogeneity of the effector molecules. *Transfusion*. 45, 1759-1767
394. Borzini P. & Mazzucco L. (2005) Platelet gels and releasates. *Current Opinions in Hematology*. 12. 473-479
395. Kim J., *et al.* (2007) Bone regeneration using hyaluronic acid-based hydrogel with bone morphogenic protein-2 and human mesenchymal stem cells. *Biomaterials*. 28. 1830-1837
396. Trojani C., *et al.* (2006) Ectopic bone formation using an injectable biphasic calcium phosphate/Si-HPMC hydrogel composite loaded with undifferentiated bone marrow stromal cells. *Biomaterials*. 27. 3256–3264
397. Xu X.L., *et al.* (2005) Evaluation of different scaffolds for BMP-2 genetic orthopaedic tissue engineering. *Journal of Biomedical Materials Research Part B – Applied Biomaterials*. 75B. 289-303
398. Suzuki Y., *et al.* (2000) Alginate hydrogel linked with synthetic oligopeptide derived from BMP-2 allows ectopic osteoinduction in vivo. *Journal of Biomedical Materials Research*. 50. 405-409
399. Trojani C., *et al.* (2005) Three-dimensional culture and differentiation of human osteogenic cells in an injectable hydroxypropylmethylcellulose hydrogel. *Biomaterials*. 26. 5509–5517
400. Weinand C., *et al.* (2007) Comparison of hydrogels in the in vivo formation of tissue-engineered bone using mesenchymal stem cells and Beta-Tricalcium Phosphate. *Tissue Engineering*. 13. 757-765
401. Kawakami Y., *et al.* (2005) Transcriptional coactivator PGC-1alpha regulates chondrogenesis via association with Sox9. *Proceedings of the National Academy of Sciences*. 102. 2414-2419

402. Furumatsu T., *et al.* (2005) Smad3 induces chondrogenesis through the activation of SOX9 via CREB-binding protein/p300 recruitment. *The Journal for Biological Chemistry*. 280. 8343-8349
403. Baek W.Y., *et al.* (2009) Positive Regulation of Adult Bone Formation by Osteoblast-Specific Transcription Factor Osterix. *Journal of Bone and Mineral Research*. 24. 1955-1065
404. Schroeder T.M., *et al.* (2005) Runx2: a master organizer of gene transcription in developing and maturing osteoblasts. *Birth Defects Research, Part C: Embryo Today: Reviews*. 75. 213-225
405. Nakamura A., *et al.* (2009) Osteocalcin Secretion as an Early Marker of In Vitro Osteogenic Differentiation of Rat Mesenchymal Stem Cells. *Tissue Engineering Part C – Methods*. 15. 169-180
406. Duer M.J., *et al.* (2009) The Mineral Phase of Calcified Cartilage: Its Molecular Structure and Interface with the Organic Matrix. *Biophysical Journal*. 96. 3372-378
407. Yingst S., *et al.* (2009) Characterization of collagenous matrix assembly in a chondrocyte model system. *Journal of Biomedical Materials Research Part A*. 90A. 247-255
408. Uenoyama M., *et al.* (2008) Osteopontin expression in normal and hypobaric hypoxia-exposed rats. *Acta Physiologica*. 193. 291-301
409. Yan Q. & Sage E.H. (1999) SPARC, a matricellular glycoprotein with important biological functions. *The Journal of Histochemistry and Cytochemistry*. 47. 1495-1506
410. Kuivaniemi. H. *et al.* (1997) Mutations in fibrillar collagens (types I, II, III, and XI), fibril-associated collagen (type IX), and network-forming collagen (type X) cause a spectrum of diseases of bone, cartilage, and blood vessels. *Human Mutation*. 9. 300-315
411. Greene M.E., *et al.* (1995) Isolation of the human peroxisome proliferator activated receptor gamma cDNA: expression in hematopoietic cells and chromosomal mapping. *Gene Expression*. 4. 281-299
412. Díez J.J. & Iglesias P. (2003). The role of the novel adipocyte-derived hormone adiponectin in human disease. *European Journal of Endocrinology*. 148. 293–300
413. Woods S.C. (2009) The control of food intake: behavioural versus molecular perspectives. *Cell Metabolism*. 9. 489-498
414. Tai E.S. & Ordovas J.M. (2007) The role of perilipin in human obesity and insulin resistance. *Current Opinions in Lipidology*. 18. 152-156

415. Beaudoin A. (2004) New technique for revealing latent fingerprints on wet, porous surfaces: Oil Red O. *Journal of Forensic Identification*. 54. 413-421
416. Michalczyk K. & Ziman M. (2005) Nestin structure and predicted function in cellular cytoskeletal organisation. *Histology and Histopathology*. 20. 665-671
417. Allen S.G. & Dawbarn D. (1979) Clinical relevance of the neurotrophins and their receptors. *Clinical Science*. 110. 175-191
418. Lalonde R. & Strazielle C. (2003) Neurobehavioral characteristics of mice with modified intermediate filament genes. *Reviews in the Neurosciences*. 14. 369-385
419. Singh R.P., et al. (2009) Retentive Multipotency of Adult Dorsal Root Ganglia Stem Cells. *Cell Transplantation*. 18. 55-68
420. Calhoun M.E., et al. (1996) Comparative evaluation of synaptophysin-based methods for quantification of synapses. *Journal of Neurocytology*. 25. 821-828
421. Ching G.Y. & Liem R.K.H. (2009) RE1 silencing transcription factor is involved in regulating neuron-specific expression of alpha-internexin and neurofilament genes. *Journal of Neurochemistry*. 109. 1610-1623
422. Datar P. et al. (2004) Substance P: structure, function, and therapeutics. *Current Topics in Medicinal Chemistry*. 4. 73-103
423. Shaklai N. et al. (1984) Nonenzymatic glycosylation of human serum albumin alters its conformation and function. *Journal of Biological Chemistry*. 259. 3812-3817
424. Mohamadi-Nejad A. et al. (2002). Thermodynamic analysis of human serum albumin interactions with glucose: insights into the diabetic range of glucose concentration. *International Journal of Biochemistry and Cell Biology*. 34. 1115-1124
425. Terentiev A.A. & Moldogazieva N.T. (2006) Structural and functional mapping of alpha-fetoprotein. *Biochemistry-Moscow*. 71. 120-132
426. Leifeild L., et al. (2009) Keratin 18 provides resistance to Fas-mediated liver failure in mice. *European Journal of Clinical Investigation*. 39. 481-488
427. Lamoury F. et al. (2006) Undifferentiated mouse mesenchymal stem cells spontaneously express neural and stem cell markers Oct-4 and Rex-1. *Cytherapy*. 8. 228-242



428. Inamdar M.S. et al (2009) Derivation and Characterization of Two Sibling Human Embryonic Stem Cell Lines from Discarded Grade III Embryos. *Stem Cells and Development*. 18. 423-433
429. Pal K., et al. (2009) Polymeric Hydrogels: Characterisation and Biomedical Applications. *Designed Monomers and Polymers*. 12. 197-220
430. Jia X.Q. & Kiick K.L. (2009) Hybrid Multicomponent Hydrogels in Tissue Engineering. *Macromolecular Bioscience*. 9. 140-156
431. Quaglia F. (2009) Bioinspired tissue engineering: The great promise of protein delivery technologies . *International Journal of Pharmaceutics*. 364. 381-297
432. Tadmor R. (2004) Line energy and the relation between advancing, receding and Young contact angles. *Langmuir*. 20. 7659-7664
433. Lin Z. et al. (2006) The chondrocyte: Biology and clinical application. *Tissue Engineering*. 12. 1971-1984
434. Heng B.C., et al. (2004) Directing stem cell differentiation into the chondrogenic lineage in vitro. *Stem Cells*. 22. 1152-1167
435. Wirth C. J. & Rudert M. (1996) Techniques of cartilage growth enhancement: A review of the literature. *Arthroscopy*. 12. 300-308
436. Mathew G., et al. (2009) ABCG2-mediated dyecycle violet efflux defined side population in benign and malignant prostate. *Cell Cycle*. 8. 1053-1061
437. Gradhand U. & Kim R.B. (2008) Pharmacogenomics of MRP transporters (ABCC1-5) and BCRP (ABCG2). *Drug Metabolism Reviews*. 40. 317-354
438. Rauch M.F., et al. (2009) Engineering angiogenesis following spinal cord injury: a coculture of neural progenitor and endothelial cells in a degradable polymer implant leads to an increase in vessel density and formation of the blood-spinal cord barrier. *European Journal of Neuroscience*. 29. 132-145
439. Rauch M.F., et al. (2008) Co-culture of primary neural progenitor and endothelial cells in a macroporous gel promotes stable vascular networks in vivo. *Journal of Biomaterials Science-Polymer Edition*. 19. 1469-1485
440. Nguyen V.A., et al. (2009) Endothelial cells from cord blood CD133(+)/CD34(+) progenitors share phenotypic, functional and gene expression profile similarities with lymphatics. *Journal of Cellular and Molecular Medicine*. 13. 522-534

441. Kassmeyer S., et al. (2009) New Insights in Vascular Development: Vasculogenesis and Endothelial Progenitor Cells. *Anatomia Histologica Embryologica*. 38. 1-11

442. Newman P.J. & Newman D.K. (2004) Signal transduction pathways mediated by PECAM-1: new roles for an old molecule in platelet and vascular cell biology. *Arteriosclerosis Thrombosis and Vascular Biology*. 23. 953-64

443. Sadler J.E. (1998) Biochemistry and genetics of von Willebrand factor. *Annual Review of Biochemistry*. 67. 395-424

444. Breviario F., et al. (1995) Functional properties of human vascular endothelial cadherin (7B4/cadherin-5), an endothelium-specific cadherin. *Arteriosclerosis Thrombosis and Vascular Biology*. 15. 1229-39

# APPENDIX 1

Nicholas Bryan, Nicholas P. Rhodes, John A. Hunt

Derivation and Performance of an Entirely Autologous Injectable Hydrogel  
Delivery System for Cell Based Therapies

Biomaterials. 30. 180-188



ELSEVIER

Contents lists available at ScienceDirect

## Biomaterials

journal homepage: [www.elsevier.com/locate/biomaterials](http://www.elsevier.com/locate/biomaterials)

## Derivation and performance of an entirely autologous injectable hydrogel delivery system for cell-based therapies

Nicholas Bryan, Nicholas P. Rhodes, John A. Hunt\*

Division of Clinical Engineering, UKCTE, School of Clinical Sciences, University of Liverpool, Duncan Building, Daulby Street, Liverpool L69 3GA, United Kingdom

## ARTICLE INFO

## Article history:

Received 22 July 2008

Accepted 3 September 2008

Available online 11 October 2008

## Keywords:

Stem cells

Injectable gel

Hydrogel

Fibrin

Animal model

## ABSTRACT

A host-derived hydrogel has been designed and validated as an entirely autologous, injectable delivery system for cells with potential for cell-based therapies and tissue engineering applications. Each individual has components in their blood from which can be formed a mechanically stable hydrogel having the capacity to maintain cellular phenotype and support cellular proliferation of multiple cell types through several culture passages *ex vivo*. The hydrogel can be triggered to gel at the time of implantation into the patient through an injection system that facilitates a liquid injection of components of the donor plasma and cells into the site of interest. This results in stable ectopic tissue formation at the site of implantation. Our studies have demonstrated excellent integration of the neotissue with host tissues with maintenance of the phenotype of implanted cells whilst observing minimal host innate immune cell recruitment. These findings could provide the fundamental basis for new hydrogel-based biomaterial therapies, overcoming the histocompatibility factors associated with implantable biomaterials whilst providing a stable three dimensional medium for cellular growth both *in vivo* and *ex vivo*.

© 2008 Elsevier Ltd. All rights reserved.

### 1. Introduction

Treatment of conditions that compromise homeostasis and normal physiological function often require tissue implantation or transplantation. The ideal paradigm is to introduce cells or tissues that are normally native to the damaged organ. Early indications are that treatment in this way using cell therapy or tissue engineering is feasible only when the correct environmental conditions are determined and well defined. To take this regenerative medicine approach to the clinical end point, the development of injectable scaffolds for the minimally invasive delivery of appropriate cells to a defect site is highly desirable. Potentially, a single versatile material could provide a biotherapeutic approach to the regeneration of general and focal defects of a multitude of hard and soft tissues *in situ* with minimal surgical intervention. In order to achieve this, a suitable candidate material should be biodegradable, histocompatible and have mechanical properties closely resembling living tissue, providing a transient dynamic matrix for the delivery of pluripotent or lineage-committed cells. The scaffold material should interact with the host to achieve a fully integrated autogenous tissue, free of any foreign body.

A large variety of materials, both organic and inorganic are already being exploited for biomedical devices, these are being

investigated further as interactive open porous scaffolds. Generally, these are designed to be application-specific for a tissue defect or disorder but do not anticipate the host's innate and specific defence mechanisms. These can be predicted and should be utilised in the functional delivery of the treatment regime. Therapies for bone regeneration are predominantly based on injectable osteogenic tricalcium phosphate cements [1]. These form micro-porous structures and are favoured for bone repair because they are more efficiently absorbed than hydroxyapatite and are more similar to host bone in their mechanical properties [2]. Several other materials have been used for scaffold fabrication including poly-L-lactic acid (PLLA) for injectable soft tissue augmentation [3]. As nanofibre structures, these mimic the extracellular matrix (ECM) providing a familiar fibrous meshwork in which cells can attach and proliferate [4]. The fibres can then be 'decorated' through progressive synthetic chemistry to include functional groups that may direct the host response or increase clinical suitability through modulation of the polymer's physicochemical properties [5–7].

Polymers provide the possibility of designing matrices with high water content approaching that of natural tissues. Hydrogels are a class of covalently linked polymers that exhibit excellent potential as candidate media for cellular delivery due to their hydrophilicity, high water content and compliant physical properties [8]. A further property of hydrogels that make them exciting candidates for implantation is their isotropic swelling, meaning that their dry shape is maintained post water absorption. Hydrogels can be utilised to elute drugs or present cell-signalling molecules to influence

\* Corresponding author. Tel.: +44 15 1706 5264; fax: +44 15 1706 4915.  
E-mail address: [huntja@liverpool.ac.uk](mailto:huntja@liverpool.ac.uk) (J.A. Hunt).

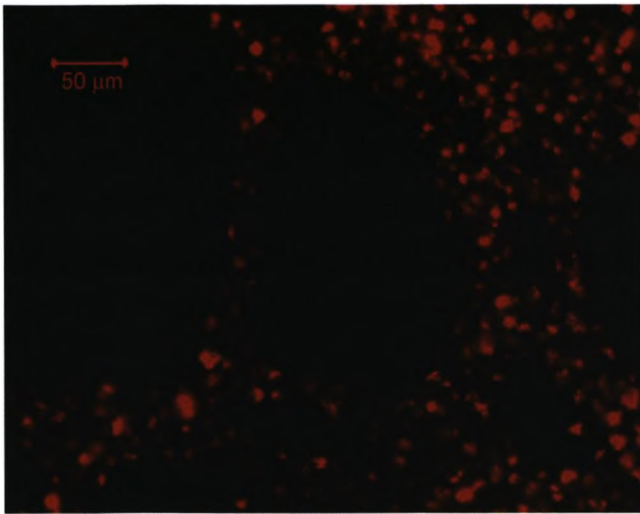


Fig. 1. Fluorescently-labelled human articular chondrocyte cells after 7 days of culture on extracellular matrix hydrogel substrate.

the cells that they contain or the tissue into which they are delivered [9,10]. Polymer gels can be chemically modified to modulate cell phenotype and proliferative status [11].

The aim of this research was to investigate a unique approach to produce hydrogels for use in cell therapies and tissue engineering processes, to drive specific tissue formation via autologous mechanisms. Gels were derived from autologous host plasma, thus providing a totally natural material for cell expansion and implantation, overcoming potential complex histocompatibility issues associated with organic implantable biomaterials.

ECM hydrogels have been utilised as vectors for cellular delivery in tissue regeneration for several years. These materials may consist of a mixture of purified undefined ECM components or defined, well characterised molecules associated with cell adhesion and recognition such as collagen, keratin, elastin and fibrin which have been used for tissue engineering applications such as nerve conduits [12–14]. These components provide an ideal substrate for cellular delivery and *in vivo* culture. Our hydrogel exploits this practice in conjunction with the well defined coagulation cascade mediated via molecules present in host plasma to generate a mechanically stable, self forming hydrogel matrix composed of fibrin. Citration of blood immediately following exsanguination reduces free calcium to less than  $10^{-6}$  M thus preventing immediate clotting and leaves the components of the coagulation cascade in

place. Injecting culture media containing a high concentration of free calcium concurrently with the host plasma and cells during implantation results in clot formation and therefore *in situ* delivery of a cell-loaded protein scaffold at the defect site. Hydrogels formed in this way are superior to their predecessors due to the lack of a significant foreign body response and the absence of factors which could be antigenic. In addition, specifically chosen variations in culture media composition can be exploited during hydrogel formation to influence cell lineage, particularly when used in conjunction with stem cells or uncommitted progenitor cells. This system therefore would be directly translatable to a range of clinical perspectives due to the pharmacopeia grade standards in which the media component can be synthesised in combination with the autologous nature of the plasma and cellular elements.

## 2. Methods

### 2.1. Material isolation

20 ml of peripheral blood was isolated by vein puncture from 6 healthy donors of both genders and immediately citrated with 10% (v/v) 10 mM sodium citrate (Sigma-Aldrich S1804, Poole, UK). Whole blood samples were sealed and left at room temperature for a period of 2 h and then placed overnight at 4 °C to allow blood cells and blood plasma to fractionate. Samples were then centrifuged at 1000 g for 10 min and the supernatant collected. Supernatants were then centrifuged for a second time at 1000 g for 10 min to remove any residual blood cells. At this point blood plasma was pooled and frozen at –20 °C.

### 2.2. In vitro hydrogel synthesis

Blood plasma was defrosted and pre-warmed to 37 °C. At the same time culture media base was prepared and pre-warmed to 37 °C; DMEM, 4500 mg L<sup>-1</sup>, +L-glutamine, +phenol red (Gibco 21063-029, Paisley, UK) was combined with penicillin/streptomycin solution (Sigma P4458, Poole, UK) to a concentration of 1%. The blood plasma fraction was then added to the basal media at a concentration of 10% (v/v) and returned to 37 °C, 5% CO<sub>2</sub>. After approximately 3–5 min a stable hydrogel was formed from the two solutions.

### 2.3. Cell selection

Primary human cells were used in all cases: human dermal fibroblasts (HDFs), human articular chondrocytes (HACs) and human osteoblasts (HOBs) were used at passages 10, 6 and 7, respectively. Human mesenchymal stem cells (MSCs) were obtained at passage 1 (Lonza, Slough, UK).

### 2.4. In vitro cell culture

Cells were introduced to the gel in one of three ways: surface seeded, embedded or seeded beneath the gel. Cells could be seeded onto the surface of the pre-formed gel using standard tissue culture protocols after removal from standard tissue culture polystyrene substrate (TCPS). Embedded seeding was carried out by adding cells to the gel formulation immediately after the addition of blood plasma and basal media thus trapping the cells in suspension during gelation. Seeding below the gel was carried out by applying the cells to standard TCPS in a minimal volume of media

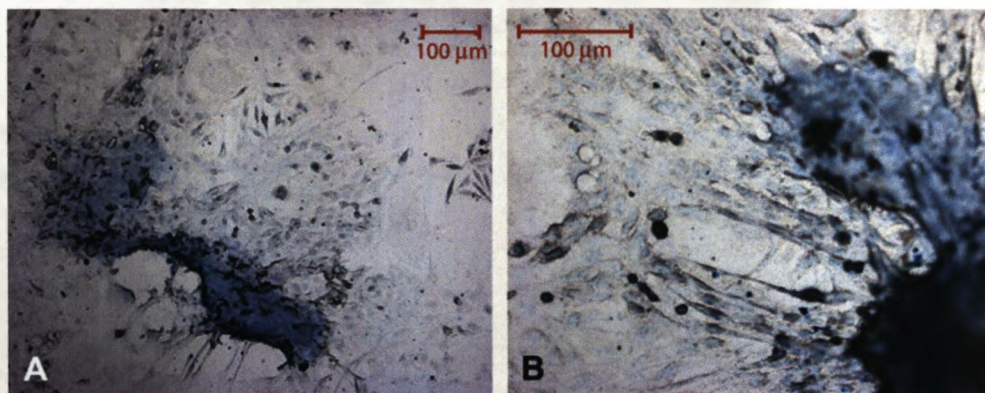


Fig. 2. HAC stained positive for the presence of glycosaminoglycans after 7 days under the plasma derived hydrogel matrix. (A. 20×, B. 40×).



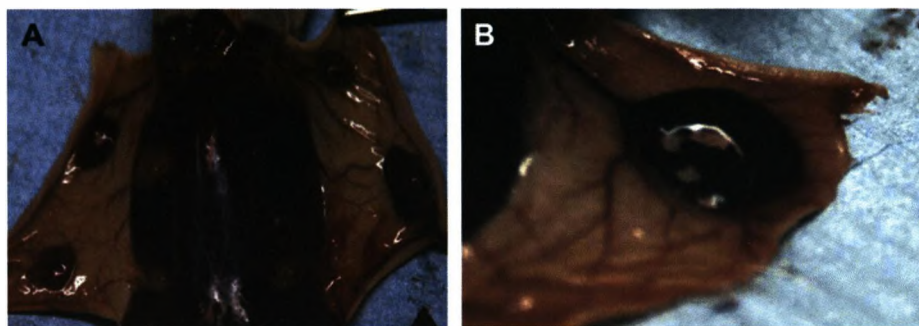


Fig. 3. A. Nude mouse at 4 weeks post implantation indicating ectopic tissue formation (scale 1.25 $\times$ ). B. Ectopic tissue demonstrating extensive vascularisation (scale 1.5 $\times$ ).

for 12 h, with the addition of foetal calf serum at 5% to allow adherence. Gel was cast on top of the pre-adhered cells after removal of the media.

#### 2.5. Cell tracking dyes

Cell tracking was used to differentiate implanted cells from host cells. Cells were suspended at a density of  $1.0 \times 10^6$  cells/mL<sup>-1</sup> in DMEM, 4500 mg L<sup>-1</sup>, +L-glutamine, +phenol red in the absence of serum. 5  $\mu$ l of DiD, DiL or DiO dye (Invitrogen V22889, Paisley, UK) were added per mL of cells and mixed by gentle vortexing. This suspension was then incubated at 37 °C for 15 min followed by a 5 min 1500 rpm (405 g) centrifugation. After centrifugation, the supernatant was removed and cells washed in pre-heated (37 °C) medium followed by a further 5 min 1500 rpm (405 g) centrifugation.

#### 2.6. In vivo cell growth and defect site delivery model

Six week old, male immuno deficient CH1 nude mice received four implants as injections, two into the subcutaneous (SC) tissue above each shoulder and two either subcutaneously above each hip joint or intramuscular (IM) into the quadriceps femoris muscle. The site of implantation (IM or SC) was determined by the cell type implanted. HDFs were delivered solely to SC sites whereas human osteoblasts (HOBs) were delivered to both IM and SC sites. Implantation was carried out using defined cell numbers between  $1.0 \times 10^5$  and  $2.0 \times 10^6$ . Each animal received a defined number of HDFs in a total injection volume of 300  $\mu$ l. 10% human plasma (v/v) and cell-loaded culture media were pre-warmed and combined immediately pre-implantation and injected into the animals in one of four SC implantation sites per animal, one above each shoulder and one above each hip. Animals were maintained for periods up to 10 weeks prior to sacrifice. Human osteoblasts (HOBs) were chosen as another tissue specific candidate for ectopic tissue formation due to their ability to drive osteogenesis in clinical applications, and additionally determined the validity of data published previously suggesting the requirement for a solid scaffold for the synthesis of ectopic bone *in vivo*. HOBs were delivered into IM sites. Animals were sacrificed at 4, 6, 8 and 10 weeks post implantation and ectopic tissue excised for analysis to determine tissue formation and host integration.

To achieve gelation *in vivo*, implantation was carried out using a three way stopcock tap system (Smiths Medical MX4341L, Watford, UK). Cells and media were contained in one syringe with blood plasma in another. Both solutions were pre-warmed to 37 °C. The two solutions were then transfused into one syringe by means

of the three way tap to allow mixing and, following a further turn of the tap injected through a 21 gauge needle into the desired implantation site. All *in vivo* experimental procedures were conducted in accordance with the U.K. Home Office regulations under licence and were approved by Research Ethics Committee.

#### 2.7. CryoSEM

CryoSEM presents a valuable technique for the visualisation of materials that have a high water content whose structure might be altered or destroyed by dehydration and cross linking. Samples were immediately washed in PBS and placed over liquid nitrogen prior to complete sublimation. They were freeze fractured to expose the interior structures then coated in platinum and moved directly onto the microscope cold stage where they were examined at 3 kV using a working distance of 8 mm.

#### 2.8. Histopathology and antigen preservation

To retain tissue antigenicity whilst providing excellent tissue morphology, samples were placed directly into periodate-lysine-paraformaldehyde fixative post explanation for 24 h at 4 °C then into cold washing solution at 4 °C for 24 h. Cold acetone was then used to remove phosphate crystals and dehydrate (4 °C in fresh acetone overnight). This was replaced by immersion in pure glycol methacrylate (GMA) for 24 h. Samples were then left in cold Technovit infiltration solution (TAAB T220, Berks, UK) overnight at 4 °C. Samples were then set in place in an appropriately sized mould and submersed in Technovit embedding solution (TAAB T220, Berks, UK), the resin surface was covered with mineral oil (Sigma-Aldrich M-3516, Poole, UK) to prevent oxidation and evaporation and placed at -55 °C to infiltrate for 4 days. After this time the incubation temperature was then increased to -20 °C for 2 days to allow polymerisation. Tissue blocks were then sectioned (6  $\mu$ m thick sections) using a polycut microtome and placed onto APTES coated slides.

#### 2.9. Immunohistochemistry

Masked epitopes were exposed by digestion with 0.1% trypsin type III (SigmaT-4665, Poole, UK) in 0.1% CaCl<sub>2</sub> pH 7.8 for 15 min at 37 °C followed by a 5 min wash in PBS. Non-specific binding was then blocked using horse serum (3 drops/10 ml PBS) for 30 min at 37 °C. Primary antibodies, diluted to working concentrations using 1% BSA/PBS, were then incubated on the sections overnight at 4 °C followed by a 5 min

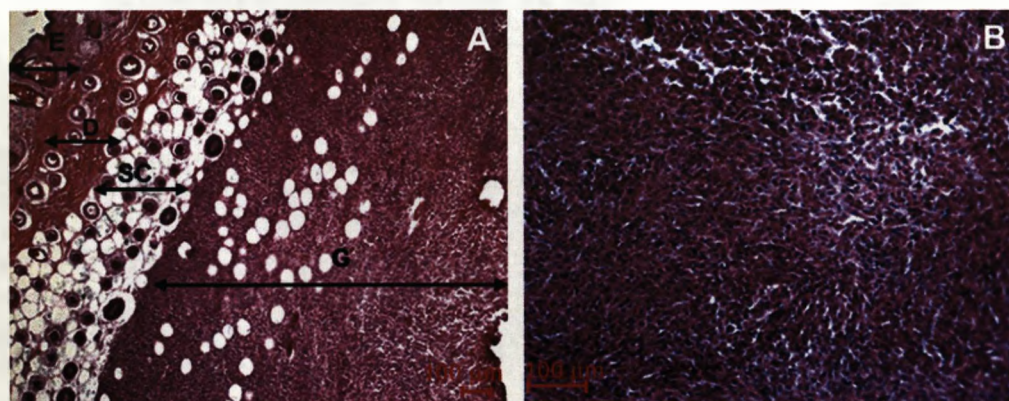


Fig. 4. A. Haematoxylin and eosin staining of explanted section showing location of ectopic tissue formation, E – epidermis, D – dermis, SC – subcutaneous layer, G – gel mass. B. Haematoxylin and eosin staining indicating extensive cellularisation of hydrogel matrix.



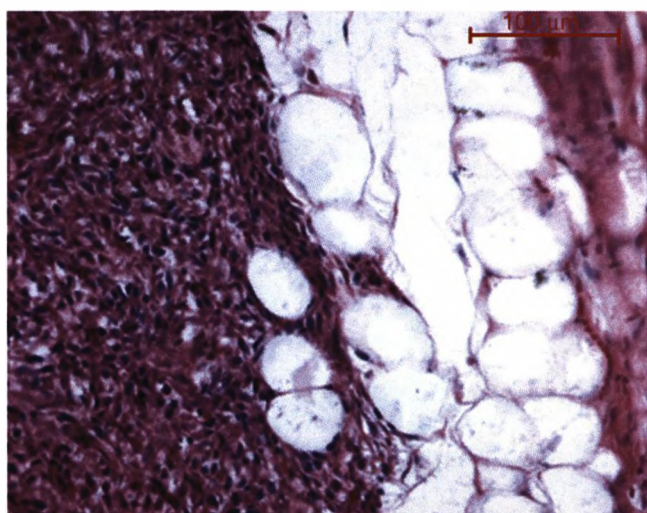


Fig. 5. Haematoxylin and eosin staining of ectopic tissue illustrating the union formed between gel mass and subcutaneous layer.

wash in PBS. Secondary antibodies, diluted using PBS, were incubated on the samples for 60 min at 37 °C. Slides were then washed in PBS and exposed to mouse ABC/AP tertiary antibody kit (Vector laboratories AK-5000, Peterborough, UK) for 30 min at room temperature directly preceded by a further wash in PBS. Slides were then incubated at room temperature with alkaline phosphatase kit in 0.1 M Tris–HCl pH 8.2 followed by two final 5 min washing steps in PBS and distilled water, respectively. Tissue histopathology was conducted on the stained samples using a combination of microscopical techniques: laser scanning confocal; fluorescent and visible light microscopy.

### 3. Results

#### 3.1. In vitro validation of blood plasma derived hydrogel

The combination of the human blood plasma fraction at a concentration of 10% (v/v) in DMEM resulted in the formation of a chemically stable hydrogel at 37 °C. The hydrogel demonstrated the capacity to maintain the proliferation of human articular chondrocytes (HACs) and human dermal fibroblasts (HDFs) *in vitro*

through multiple cell culture passages when cells were surface seeded, impregnated within the gel or seeded under the gel matrix. Cells became distributed throughout the gel in all of the seeding processes (Fig. 1).

When two cell-loaded gel blocks were cast on top of one another, cells demonstrated the capacity to migrate between gel blocks, illustrated using several cell tracking dyes in conjunction with one another to trace cell movement through the gel blocks. It was hypothesised that under gel seeding would provide inherent suitable mechanisms for the phenotypic maintenance of HACs due to hypoxia created as an indirect effect of a reduction in mass transport by the gel matrix which could replicate the hypoxic environment in which these cells are normally located *in vivo* [15]. The presence of glycosaminoglycans was taken to be indicative of a chondrogenic phenotype (Fig. 2). The surface of the gel proved to be a suitable substrate for the growth of MSC, HAC and HDF cells. The bulk volume of the gel reduced during cell culture which was consistent with observations made with more conventional ECM hydrogels due to the tensile forces exerted by the ECM of the cells as they increased in number and proliferated through the matrix of the gel. *In vitro* validation of the capacity of the hydrogel to maintain integrity and proliferation of several human cell lines identified it as a potential candidate for cellular delivery to a defect site by means of a local injection.

#### 3.2. In vivo ectopic tissue model

Immediately post injection the gel mass formed a subcutaneous pocket which was clearly evidenced at 5–7 days by visual examination. Ectopic tissue formation was clearly identified visually at explantation dissection. Ectopic tissue formed attached to the subdermis layer of the skin, with limited adhesion to underlying connective tissues. The ectopic tissues were well vascularised by extensive vascular networks connecting the site of implantation to the peripheral circulation.

In some circumstances this blood supply network was so extensive that it was readily observed to clearly enter the tissue prior to any histopathology, which confirmed the presence of vasculature within the implant (Fig. 3).

Histological examination revealed consistency in the mechanism of formation of ectopic tissue with a cellularised mass formed

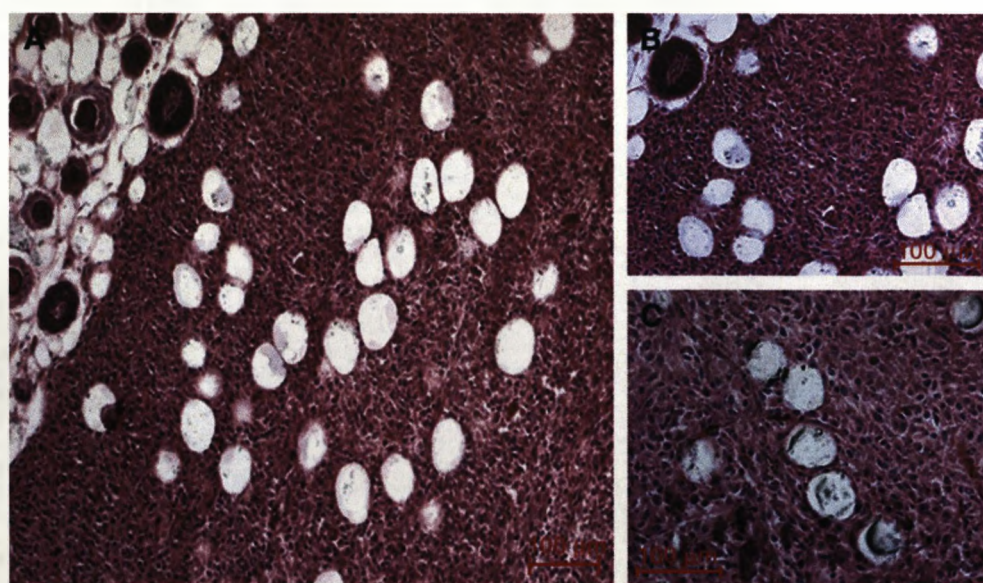
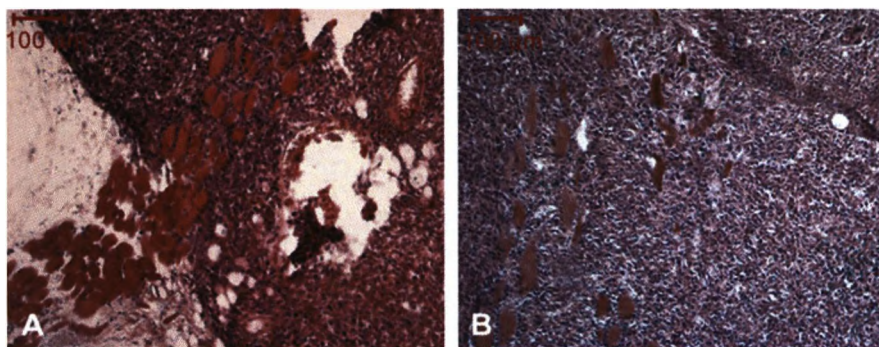


Fig. 6. Haematoxylin and eosin staining of ectopic tissue demonstrating adipocyte infiltration into the tissue. (A. 10×, B. 20×, C. 40×).





**Fig. 7.** Haematoxylin and eosin staining of ectopic tissue showing. A. Entrance of muscle block into the cellularised hydrogel matrix and B. Progression of muscle fibres through the tissue. (A. 10 $\times$ , B. 20 $\times$ ).

below the subcutaneous layer at the site of injection for all implantation sites. The cell-loaded hydrogel matrix formed an extensive cellular tissue with substantial matrix deposition by the cells contained in the implant (Fig. 4). The newly formed tissue integrated intimately with the host tissue (Fig. 5). Tissue demonstrated extensive integration into the host tissue with migration of adipose observed throughout the ectopic tissue, without evidence of fibrous tissue formation and encapsulation (Fig. 6). Ectopic tissue was also demonstrated as host musculature (Fig. 7), in some cases this was as the formation of a completely new muscle block which entered the tissue from the host dermis, penetrated the tissue completely and exited the tissue on the opposite side. Integration of host hair follicles into the neotissue mass was also observed across repeat implants (Fig. 8).

To confirm that the fibroblastic phenotype of the implanted human cells had been maintained throughout the *in vivo* implantation period and to determine the immunoreactivity of the implanted cellularised material, immunohistochemical analyses were conducted utilising the fibroblast specific antibody 5B5, a monoclonal antibody for fibroblast specific D7-Fib (11-fibrau) antigen, these confirmed that the phenotype and also that the speciation of the implanted fibroblasts had been conserved throughout the implantation periods (Fig. 9) (6 weeks post implantation). Explanted tissue was subjected to a larger panel of antibodies as part of the immunohistochemical analysis using

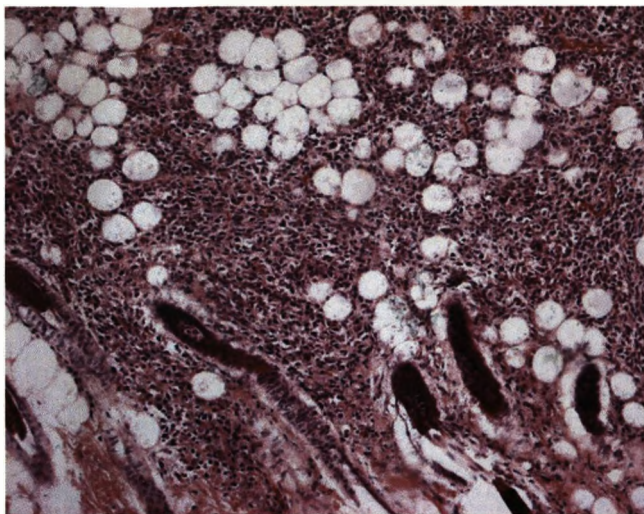


**Fig. 8.** Haematoxylin and eosin staining of new tissue showing host hair follicle infiltration into the cellularised mass.

markers chosen to determine the inflammatory response and immunogenicity of the implant. The tissue was analysed using a panel of antibodies recognising murine macrophage and neutrophil cells in addition to the MHC class II antigen; CD25: a marker of activated T cells; CD68: a marker of activated macrophages; CD5 and CD3T and B cell markers and the dendritic marker CD205 (Fig. 10).

CryoSEM analysis demonstrated the presence of fibrin fibres forming a structural matrix within the tissue. Furthermore, the tissues visualised using cryoSEM confirmed the cellularised nature of the tissue as well as qualifying the intimate organisation of the interaction between the cellular and matrix components of the hydrogel after *in vivo* implantation. Micrographs obtained from tissue explanted after 6 weeks of *in vivo* implantation (Fig. 11) indicated that the fibrin mesh forming the scaffold remained intact and cells integrated within the matrix to form an intimate association with the scaffold. Prolific cellularisation was visualised confirming the observations using histological methods (Fig. 12).

### 3.3. Ectopic bone model

HOBs were used to determine if the scaffold could be used to generate a hard tissue in addition to soft tissues in an ectopic location. In the case of SC implants, no ectopic tissue formation was observed by immunohistochemistry and no osteogenic cells were apparent within the subcutaneous layer around the site of injection. However, tissue formed within a capsule inside the muscle block at the site of IM implantation after a period of 6 weeks. Histological analysis indicated dense highly cellular tissue with cells of differing morphology to those observed in the fibroblastic tissues (Fig. 13).

Further histological analysis using tinctural and immunohistochemistry illustrated negative staining for calcification using Von Kossa; this lack of mineralisation was supported using immunohistochemical staining for the osteogenic extracellular matrix protein osteocalcin which was observed not to be present in these ectopic osteogenic tissues. However, positive staining for the osteogenic master gene core binding factor one (Cbfa1/Runx2) was observed throughout this tissue illustrated (Fig. 14). This evidence further confirmed the capacity of the hydrogel matrix for phenotypic maintenance of the cells through periods of *in vivo* implantation, even though mineralisation was not observed.

## 4. Discussion

The synthesis of an autologous, *in situ*-forming stable hydrogel from a combination of blood plasma and pharmacopeia grade cell culture media has been established. The capacity of the gel to



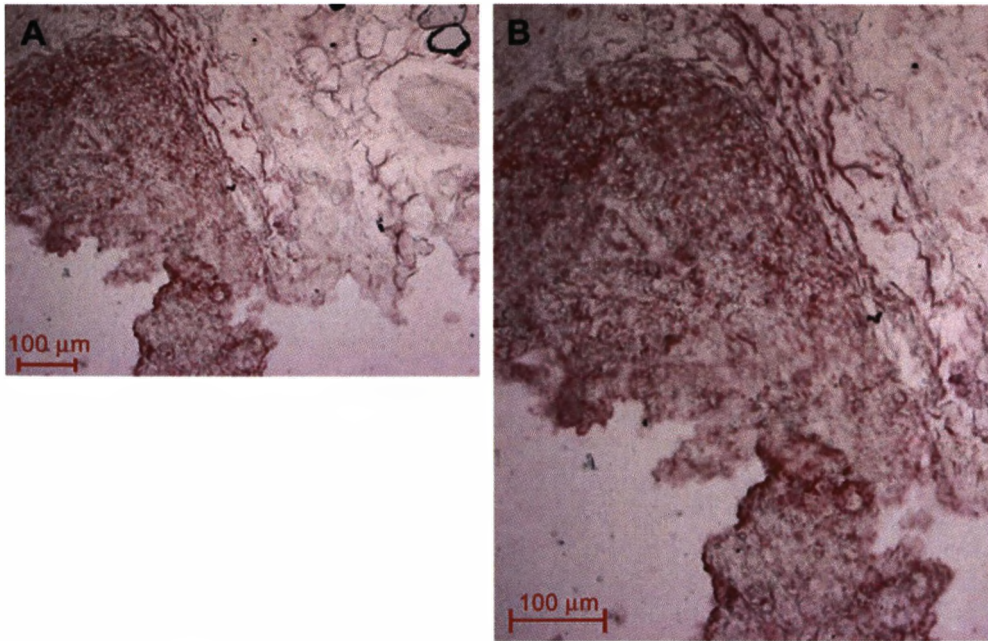


Fig. 9. Immunostaining against human fibroblast specific 5B5 antigen. (A. 10 $\times$ , B. 20 $\times$ ).

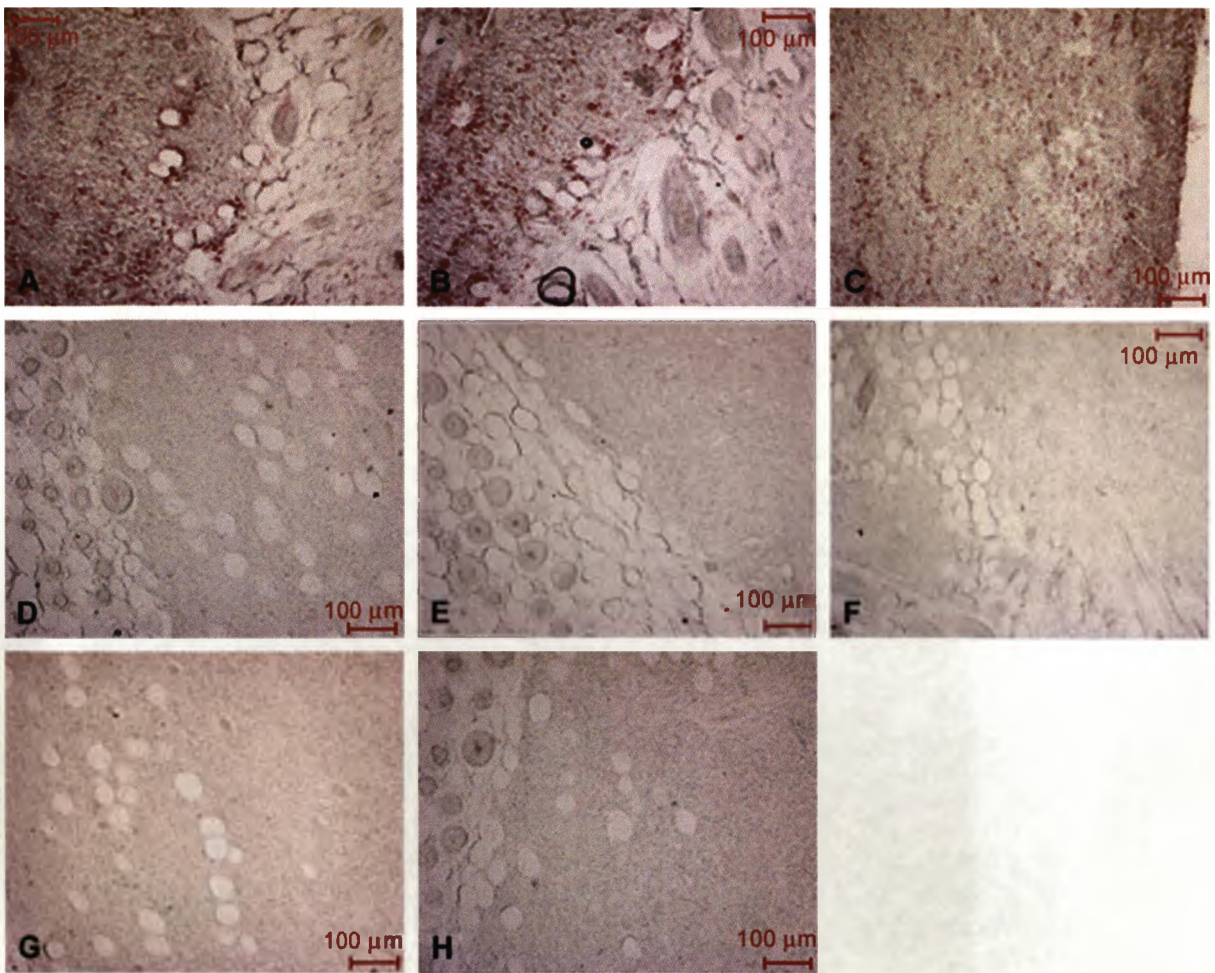


Fig. 10. Immunostaining of ectopic tissue against A. Macrophage cells, B. Neutrophil cells, C. CD68, D. MHC class II, E. CD25, F. CD3, G. CD5 and H. CD205.



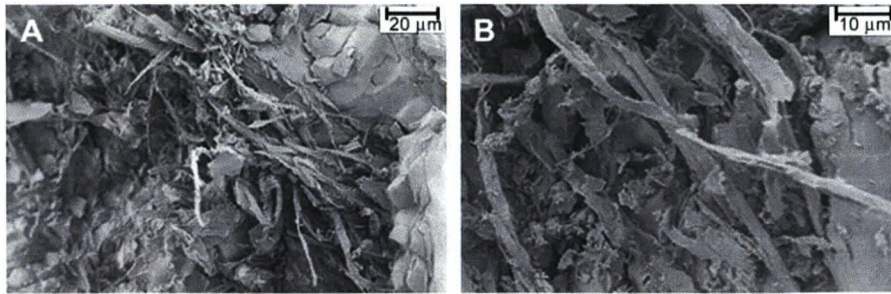


Fig. 11. Scanning electron micrographs detailing fibrin fragments still present in the hydrogel matrix after 6 weeks in culture. (A.  $2.17 \times 10^3 \times$ , B.  $4.67 \times 10^3 \times$ ).

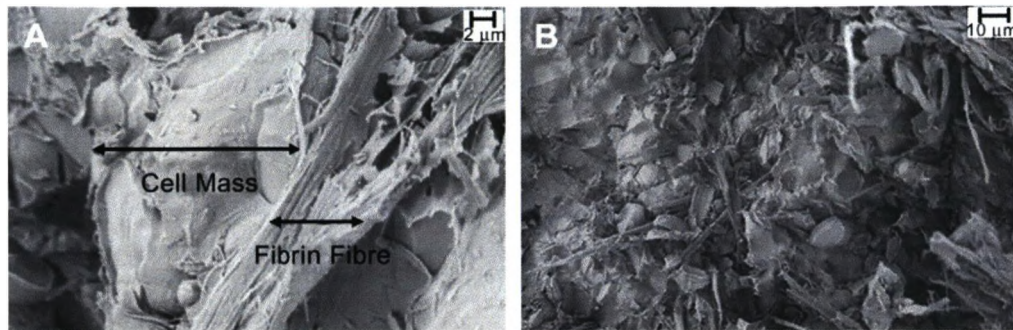


Fig. 12. A. Scanning electron micrographs detailing association of cells with fibrin scaffold. B. Cellularisation within the explanted tissue. (A.  $8.53 \times 10^3 \times$ , B.  $2.30 \times 10^3 \times$ ).

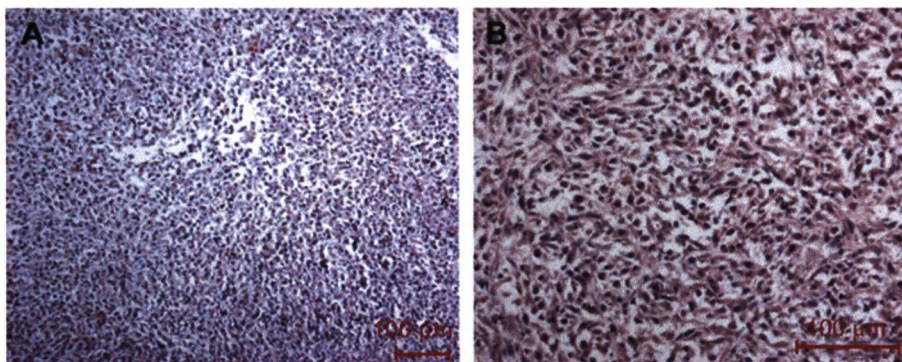


Fig. 13. Haematoxylin and eosin staining of ectopic osteoblastic tissue. (A.  $10 \times$ , B.  $20 \times$ ).

maintain cellular proliferation of HDF, HMSC and HAC cells has been indicated using three distinct seeding methods; under gel, embedded and surface seeded. The cells infiltration throughout the gel could be efficiently tracked using cytoplasmic fluorescent cell tracing dyes and the three seeding methods exhibited varying effects on the different human cells types reflecting the multitude of physiological and mechanical stresses that differ across niches throughout the host in which these cell types are adapted to survive. Optimally, the hydrogel provides a range of mechanical properties depending on the locale in which the cells are seeded thus allowing them to seek a replica physiomechanical environment to their anatomical niche *ex vivo* [16]. HACs seeded under the gel exemplify this point, as the hypoxic environment conferred on the cells by the hydrogel matrix above them, maintained the phenotype of this dynamic cell type prone to rapid de-differentiation when grown under conditions which do not provide them with the correct chemical or mechanical chondrogenic stimuli

[17,18]. The approach provided in this research, presented a suitable means for the routine culture of several cell types whose *in vivo* physiology favours hypoxic growth such as skeletal muscle cells [19], and could provide a means of generating these cells from a multipotent cell source such as mesenchymal or hematopoietic stem cells using physiological rather than chemical stimuli. This provides a patient specific means of overcoming the ethical constraints associated with embryonic stem cells as a donor cell or potentially non-pharmacopeia grade components in the differentiation cocktail [20–22].

The mechanism by which the hydrogel formed allowed simple localised site-specific delivery by means of local injection due to the fluidic nature of the hydrogel components at the time of injection. The only requirement for gelation once blood plasma and cell culture media were combined being the physiological temperature of the body into which the cells were delivered. The gel did not form a mass *in vivo* in the absence of cells, however, in combination



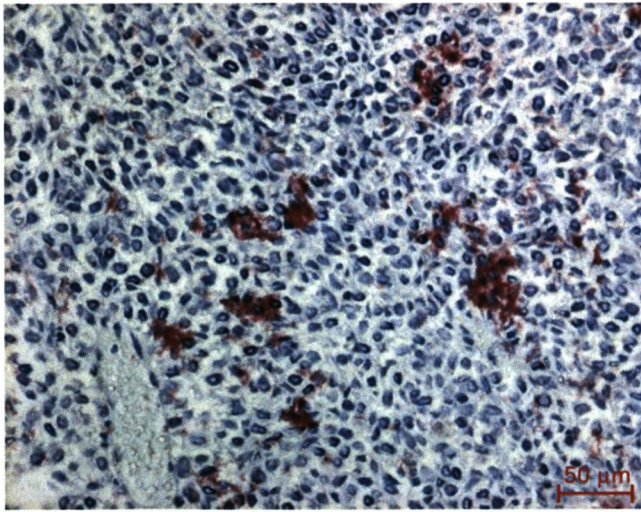


Fig. 14. Immunohistochemical staining of ectopic osteoblastic tissue for the osteogenic master gene product Cbfa1.

with HDFs formed extensive ectopic tissue masses at the site of delivery over periods of as little as 2 weeks implantation using as few as  $1.0 \times 10^5$  cells. The tissue formed was consistently found to be an ectopic subcutaneous tissue mass with excellent vascularisation that could be demonstrated macroscopically encapsulated in a fibrous capsule. Histological analysis of the explanted tissue demonstrated intense host integration with adipocyte infiltration into the neotissue mass was indicated for all implants. Integration with host tissue was further emphasised by the incorporation of host muscle into the ectopic tissue often forming a continuous block through the tissue with clear entry and exit points. Further evidence of excellent host integration was given by observation of hair follicles growing throughout the implants. The human fibroblastic phenotype was maintained throughout the implantation periods, indicating crucial longevity in the implanted cells. The use of immunohistochemistry with an antibody raised against the human D7-Fib (11-fibrau) antigen, a marker of fibroblastic cells [23,24]. The host immune response was minimal with macrophage and neutrophil cell infiltration observed in low numbers. Cell activation or antigen presentation was not recorded in any of these tissues characterised by the negative staining for MHC class II and IL-2 receptor (CD25), indicative of T lymphocyte activation, was also negative. Negative T lymphocyte infiltration was validated by negative staining for the T cell antigen CD5 and T cell receptor subunit CD3 [25–28]. Cryogenic scanning electron microscopy confirmed the direct interaction of the fibrin scaffold with the cells; this fibrin matrix was still intact and therefore functional at 6 week time point. HOBs did not form ectopic tissue when implanted subcutaneously, however, tissue did form when injected intramuscularly, this tissue was easily removable from the host showing little or no adhesion to the surrounding muscle blocks. In a similar manner to the HDF derived tissue this osteoblastic tissue was densely cellular although cell morphology was observably different from the HDF tissue with nuclei appearing less pronounced and extracellular matrix more extensive. These cells demonstrated positive staining for the osteogenic master gene Cbfa1/Runx2 [29], however, did not exhibit any markers of matrix mineralisation suggesting a latent osteogenic cell phenotype or an interesting hypertrophic osteocartilagene intermediate. The expression of this regulatory gene marker implies that an osteogenic phenotype has been maintained throughout the *in vivo* culture period, however, further implant time may be required for functional mineralised bone matrix to be formed.

## 5. Conclusion

Utilisation of blood plasma to produce a physiologically stable hydrogel capable of carrying and supporting cells *in vivo* has provided a significant autologous injectable mechanism for the local delivery and longevity of cells to a defect site. The hydrogel matrix demonstrated the capacity to sustain cell proliferation and phenotype of several human primary cell types both *in vivo* and *in vitro*. The injectable cell-loaded gel demonstrated excellent and consistent integration with host tissues and minimal host immune cell recruitment. The fundamental principles established in this study should lead to a completely patient specific cellular delivery strategy for applications across many cell-based therapies.

## Acknowledgements

These studies were gratefully supported by STEPS, a systems approach to tissue engineering processes and practices; EU grant number FP6-500465.

## Appendix

Figures with essential colour discrimination. Many of the figures in this article are difficult to interpret in black and white. The full colour images can be found in the on-line version, at doi:10.1016/j.biomaterials.2008.09.003.

## References

- [1] Cazeau C, Doursonian L, Touzard C. Use of ceramics of calcium triphosphate in the repair of tibial plateau fractures: a series of 20 cases. *European Journal of Orthopaedic Surgery and Traumatology* 1999;9:171–4.
- [2] Bohner M. Calcium orthophosphates in medicine: from ceramics to calcium phosphate cements. *Injury* 2000;31:37–47.
- [3] Rotunda A, Narins R. Poly-L-lactic acid: a new dimension in soft tissue augmentation. *Dermatologic Therapy* 2006;19:151–8.
- [4] Woo MK, Jun JH, Chen JV, Seo J, Baek HJ, Ryou MH, et al. Nano-fibrous scaffolding promotes osteoblast differentiation and biomineralization. *Biomaterials* 2007;28:343–55.
- [5] Ho MH, Lee JJ, Fan SC, Wang DM, Hou LT, Hsieh HJ, et al. Efficient modification on PLLA by ozone treatment for biomedical applications. *Macromolecular Bioscience* 2007;7:467–74.
- [6] Porter K, Hossain M, Wang M, Radano CP, Baker G, Smith MR, et al. Regulation of osteoblast gene expression and phenotype by polylactide-fatty acid surfaces. *Molecular Biology Reports* 2006;33:1–12.
- [7] Jeon O, Song SJ, Kang SW, Putnam AJ, Kim BS. Enhancement of ectopic bone formation by bone morphogenetic protein-2 released from a heparin-conjugated poly(L-lactic-co-glycolic acid) scaffold. *Biomaterials* 2007;28:2763–71.
- [8] Zhu W, Ding J. Synthesis and characterization of a redox injectable, biodegradable hydrogel. *Journal of Applied Polymer Science* 2006;99:2375–83.
- [9] Xu XD, Wei H, Zhang XZ, Cheng SX, Zuo RX. Fabrication and characterization of a novel composite PNIPAAm hydrogel for controlled drug release. *Journal of Biomedical Materials Research* 2006;81:418–26.
- [10] Ferreira LS, Gerecht S, Fuller J, Shief HF, Vunjak-Novakovic G, Langer R. Bioactive hydrogel scaffolds for controllable vascular differentiation of human embryonic stem cells. *Biomaterials* 2007;28:2706–17.
- [11] Hynd MR, Frampton JP, Dowell-Mesfin N, Turner JN, Shain W. Directed cell growth on protein-functionalized hydrogel surfaces. *Journal of Neuroscience Methods* 2007;162:255–63.
- [12] Wallace DG, Rosenblatt J. Collagen gel systems for sustained delivery and tissue engineering. *Advanced Drug Delivery Reviews* 2003;55:1631–49.
- [13] Wang XY, Kim HJ, Wong C, Vepari C, Matsumoto A, Kaplan DL. Fibrous proteins in tissue engineering. *Materials Today* 2006;9:44–53.
- [14] Nakayama K, Takakuda K, Koyama Y, Itoh S, Wang W, Mukai T, et al. Enhancement of peripheral nerve regeneration using bioabsorbable polymer tubes packed with fibrin gel. *Artificial Organs* 2007;31:500–8.
- [15] Pfander D, Gelse K. Hypoxia and osteoarthritis: how chondrocytes survive hypoxic environments. *Current Opinion in Rheumatology* 2007;19:457–562.
- [16] Ghosh K, Pan Z, Guan E, Ge SR, Liu YJ, Nakamura T, et al. Cell adaptation to a physiologically relevant ECM mimic with different viscoelastic properties. *Biomaterials* 2007;28:671–9.
- [17] Liu G, Kawaguchi H, Ogasawara T, Asawa Y, Kishimoto J, Takahashi T, et al. Optimal combination of soluble factors for tissue engineering of permanent cartilage from cultured human chondrocytes. *Journal of Biological Chemistry* 2007;282:20407–15.

- [18] Takahashi T, Ogasawara T, Asawa Y, Mori Y, Uchinuma E, Takato T, et al. Three-dimensional microenvironments retain chondrocyte phenotypes during proliferation culture. *Tissue Engineering* 2007;13:1583–92.
- [19] Li X, Zhu L, Chen X, Fan M. Effect of hypoxia on the proliferation and differentiation of myoblasts. *Medical Hypothesis* 2007;69:629–36.
- [20] Lennon DP, Edmison JM, Caplan AI. Cultivation of rat marrow-derived mesenchymal stem cells in reduced oxygen tension: effects on in vitro and in vivo osteochondrogenesis. *Journal of Cellular Physiology* 2001;187:345–55.
- [21] Grayson WL, Zhao F, Bunnell B, Ma T. Hypoxia enhances proliferation and tissue formation of human mesenchymal stem cells. *Biochemical and Biophysical Research Communications* 2007;358:948–53.
- [22] Pittenger MF, Mackay AM, Beck SC, Jaiswal RJ, Douglas R, Mosca JD, et al. Multilineage potential of adult human mesenchymal stem cells. *Science* 1999;284:143–7.
- [23] de Moss M, Koevoet WJLM, Jahr H, Versteegen MMA, Heijboer MP, Kops N, et al. Intrinsic differentiation potential of adolescent human tendon tissue: an in-vitro cell differentiation study. *BMC Musculoskeletal Disorders* 2007;8(16).
- [24] van Osch GJVM, van der Veen SW, Marijnissen WJCM, Verhaar JAN. Monoclonal antibody 11-fibrau: a useful marker to characterize chondrocyte differentiation stage. *Biochemical and Biophysical Research Communications* 2001;280:806–12.
- [25] Al-Daccak R, Mooney N, Charron D. MHC class II signaling in antigen-presenting cells. *Current Opinion in Immunology* 2004;16:108–13.
- [26] Ring S, Schaefer SC, Mahnke K, Lehr HA, Enk AH. CD4(+)CD25(+) regulatory T cells suppress contact hypersensitivity reactions by blocking influx of effector T cells into inflamed tissue. *European Journal of Immunology* 2006;36:2981–92.
- [27] Sims GP, Ettinger R, Shirota Y, Yaboro CH, Illei GG, Lipsky PE. Identification and characterization of circulating human transitional B cells. *Blood* 2005;105:4390–8.
- [28] Komata T, Cruikshank WW, Kelso A. Sustained linked stimulation via CD3 and CD4 is required for the IL-4-independent development of IL-4 synthesizing CD4+ T cells. *Immunology and Cell Biology* 2003;81:283–8.
- [29] Tu QS, Zhang J, James L, Dickson J, Tang J, Yang PS, et al. Cbfa1/Runx2-deficiency delays bone wound healing and locally delivered Cbfa1/Runx2 promotes bone repair in animal models. *Wound Repair and Regeneration* 2007;15:404–12.

# APPENDIX 2

Figure and Table Index

## APPENDIX 2

### FIGURE AND TABLE LEGEND INDEX

#### Chapter 1.

- Fig 1.1 Schematic illustrating the origins and differentiation states of mesenchymal stem cells in vivo. [33]* 7
- Fig 1.2 Schematic illustrating the origins and differentiation states of Hematopoietic stem cells in vivo (Kamminga L.M. & De Haan G., 2006,[35])* 9
- Table.1. The various grades of serum free media/media supplements available commercially at time of writing* 16
- Fig.1.3. The molecular structure of the synthetic iron carrier pyridoxal isonicotinoylhydrazone* 18
- Fig.1.4. The molecular structure of the synthetic iron carrier Tropolone* 18
- Fig.1.5. The molecular structure of the synthetic iron carrier Aurintricarboxylic Acid* 18
- Fig.1.6. The role of TGF- $\beta$  in the Smad signalling cascade ([J'Massagué J. & Wotton D, 2000, [264])* 23
- Fig.1.7. Wnt signalling mediated via cAMP (Pourquié O., 2005 [265])* 26

#### Chapter 2.

- Table.2.2. Secondary antibodies used throughout immunohistochemical investigations* 31
- Fig.2.1. Isotype controls carried out in the obtaining of A; Fig. 2.32A, B; Fig. 3.24 and C; 3.25. Non-specific IgG interaction, F-actin & Nuclei* 31
- Table.2.1. Primary antibodies used throughout immunohistochemical investigations* 32
- Fig.2.2. Melt curve analysis of  $\beta$ -actin primer pair amplicon. Flat lines represent no cDNA template controls* 38
- Table.2.3. Parameters of primers used throughout PCR studies* 39



<i>Fig.2.3. Molecular schematic of the reduction of Resazurin to Resorufin which occurs in metabolically active cells</i>	47
<i>Table.2.4. Isotype control antibodies used throughout flow-cytometry investigations</i>	49
<i>Table.2.5. Antibodies used throughout flow-cytometric investigations</i>	50
<i>Fig.2.4. Flow-Cytograms illustrating the reference to non-specific IgG-cell interactions when generating data</i>	49
<i>Fig.2.5. Antigens used throughout flow cytometric analysis of MSC phenotype showing isotype overlay (Shown MSC passage 2, serum free parameters)</i>	51
<i>Fig.2.6. Illustration of the implantation system employed for the delivery of cell loaded hydrogel to a desired in-vivo site</i>	57
<i>Fig.2.7. Full coding sequence of the human AggreCAN transcript provided by the National Centre for Biotechnology Information (<a href="http://www.ncbi.nlm.nih.gov/entrez/viewer.fcgi?val=22209082&amp;from=346&amp;to=2511&amp;view=gbwithparts">http://www.ncbi.nlm.nih.gov/entrez/viewer.fcgi?val=22209082&amp;from=346&amp;to=2511&amp;view=gbwithparts</a>)</i>	62
<i>Fig.2.8. Predicted tertiary structure for a target amplicon within the AggreCAN CDS, generated using European mfold (<a href="http://frontend.bioinfo.rpi.edu/applications/mfold/cgi-bin/dna-form1.cgi">http://frontend.bioinfo.rpi.edu/applications/mfold/cgi-bin/dna-form1.cgi</a>) illustrating primer binding domains.</i>	64
<i>Fig.2.9. Schematic illustrating the dimensions of the filter paper carrier of the platelet poor plasma derived hydrogel during dynamic contact angle studies</i>	65

### **Chapter 3.**

<i>Fig.3.1. Light microscopic observation of methylene blue stained dermal fibroblast cells demonstrating associated fibroblastic morphology in defined basal media with additions of fetal calf serum of 5%</i>	73
<i>Table.3.1. Composition of defined basal media.</i>	74
<i>Table.3.2. Components of serum replacement</i>	75

*Fig.3.2. Stability of human Apo-transferrin in serum free cell culture media quantified using the ELISA method. Error bars represent 1 standard deviation from the mean, n=3* **76**

*Fig.3.3. Comparison of the metabolic activities of human dermal fibroblast cells in a range of serum free and serum containing media formulations using the Alamar blue method. Error bars represent 1 standard deviation from the mean, n=3, \*P<0.05, \*\*P<0.01, \*\*\*P<0.001 compared to serum containing basal DMEM* **78**

*Fig.3.4. Fluorescent microscopic observation of the immunohistochemical staining for the Fibroblast specific D7-Fib antigen and additionally; F-actin and Nucleii after 21 days of serum free culture (positive staining illustrated by arrows)* **79**

*Fig.3.5. Comparison of the metabolic activities of human osteoblast cells in a range of serum free and serum containing media formulations using the Alamar blue method. Error bars represent 1 standard deviation from the mean, n=3, \*P<0.05, \*\*P<0.01, \*\*\*P<0.001 compared to serum containing Osteogenic medium* **80**

*Fig.3.6. Comparison of the metabolic activities of human arterial smooth muscle cells in a range of serum free and serum containing media formulations using the Alamar blue method. Error bars represent 1 standard deviation from the mean, n=3, \*P<0.05, \*\*P<0.01, \*\*\*P<0.001 compared to serum containing commercial medium* **82**

*Fig.3.7. Fluorescent microscopic observation of immunohistochemical staining of arterial smooth muscle cells for the smooth muscle specific  $\alpha$ -smooth muscle actin after 14 days of serum free culture* **83**

*Fig.3.8. Flow cytometric analysis of the presence of  $\alpha$ -smooth muscle actin in populations of arterial smooth muscle cells cultured in serum free and serum containing media formulations. Error bars represent 1 standard deviation from the mean, n=3, \*P<0.05, \*\*P<0.01, \*\*\*P<0.001 compared to serum containing basal medium* **84**

*Fig.3.9. Real time-PCR comparison of the expression of  $\alpha$ -smooth muscle actin in arterial smooth muscle cells cultured in conjunction with serum free media formulations in the presence (SF+Fe) and absence (SF-Fe) of iron after 14 days. Error bars represent 1 standard deviation from the mean, n=6* **85**

*Fig.3.10. Real time-PCR comparison of the expression of Elastin in arterial smooth muscle cells cultured in conjunction with serum free media formulations in the presence (SF+Fe) and absence (SF-Fe) of iron after 14 days. Error bars represent 1 standard deviation from the mean, n=6* **86**

*Fig.3.11. Real time-PCR comparison of the expression of fibrillin-1 in arterial smooth muscle cells cultured in conjunction with serum free media formulations in the presence (SF+Fe) and absence (SF-Fe) of iron after 14 days. Error bars represent 1 standard deviation from the mean, n=6*  
**87**

*Fig.3.12. Real time-PCR comparison of the expression of fibronectin in arterial smooth muscle cells cultured in conjunction with serum free media formulations in the presence (SF+Fe) and absence (SF-Fe) of iron after 14 days. Error bars represent 1 standard deviation from the mean, n=6*  
**88**

*Fig.3.13. Real time-PCR comparison of the expression of Laminin in arterial smooth muscle cells cultured in conjunction with serum free media formulations in the presence (SF+Fe) and absence (SF-Fe) of iron after 14 days. Error bars represent 1 standard deviation from the mean, n=6*  
**89**

*Fig.3.14. Real time-PCR comparison of the expression of smoothelin in arterial smooth muscle cells cultured in conjunction with serum free media formulations in the presence (SF+Fe) and absence (SF-Fe) of iron after 14 days. Error bars represent 1 standard deviation from the mean, n=6*  
**90**

*Fig.3.15. Comparison of the metabolic activities of human bone marrow derived mesenchymal stem cells in a range of serum free and serum containing media formulations using the Alamar blue method. Error bars represent 1 standard deviation from the mean, n=3, \*P<0.05, \*\*P<0.01, \*\*\*P<0.001 compared to Cambrex MSCBM*  
**94**

*Fig.3.16. Light microscopic observation of confluent bone marrow derived mesenchymal stem cells in serum free media containing iron after 14 days of culture*  
**95**

*Fig.3.17. Comparison of a subset of cellular antigens of bone marrow derived mesenchymal stem cells cultured in serum free and serum containing (Cambrex MSCBM) media formulations at confluence, at passage 2, observed using flow cytometry. Error bars represent 1 standard deviation from the mean, n=3, \*P<0.05, \*\*P<0.01, \*\*\*P<0.001*  
**98**

*Fig.3.18. Comparison of a subset of cellular antigens of bone marrow derived mesenchymal stem cells cultured in serum free and serum containing (Cambrex MSCBM) media formulations at confluence, at passage 3, observed using flow cytometry. Error bars represent 1 standard deviation from the mean, n=3, \*P<0.05, \*\*P<0.01, \*\*\*P<0.001*  
**99**

*Fig.3.19. Comparison of a subset of cellular antigens of bone marrow derived mesenchymal stem cells cultured in serum free and serum containing (Cambrex MSCBM) media formulations at confluence, at passage 4, observed using flow cytometry. Error bars represent 1 standard deviation from the mean, n=3, \*P<0.05, \*\*P<0.01, \*\*\*P<0.001* 100

*Fig.3.20. Comparison of a subset of cellular antigens of bone marrow derived mesenchymal stem cells cultured in serum free and serum containing (Cambrex MSCBM) media formulations at confluence, at passage 5, observed using flow cytometry. Error bars represent 1 standard deviation from the mean, n=3, \*P<0.05, \*\*P<0.01, \*\*\*P<0.001* 101

*Fig.3.21. Comparison of a subset of cellular antigens of bone marrow derived mesenchymal stem cells cultured in serum free and serum containing (Cambrex MSCBM) media formulations at confluence, at passage 6, observed using flow cytometry. Error bars represent 1 standard deviation from the mean, n=3, \*P<0.05, \*\*P<0.01, \*\*\*P<0.001* 102

*Fig.3.22. Comparison of a subset of cellular antigens of bone marrow derived mesenchymal stem cells cultured in serum free and serum containing (Cambrex MSCBM) media formulations at confluence, at passage 7, observed using flow cytometry. Error bars represent 1 standard deviation from the mean, n=3, \*P<0.05, \*\*P<0.01, \*\*\*P<0.001* 103

*Table.3.3. Comparison summary of the mean antigenicity of bone marrow derived mesenchymal stem cells in serum free and serum containing media (Cambrex MSCBM) over a number of passages, demonstrated using flow cytometry, \*P<0.05, \*\*P<0.01, \*\*\*P<0.001* 104

*Table.3.4. Comparison of serum containing and serum free media formulations on their capacity to maintain mesenchymal stem cell phenotype by normalisation based on number of statistical significances, \*P<0.05, \*\*P<0.01, \*\*\*P<0.001* 104

*Fig.3.23. Fluorescent microscopic observation of immunohistochemical staining for: A; Nucleostemin, F-Actin, Nuclei. B; STRO-1, F-Actin, Nuclei and C; CD105, Nuclei after 21 days of defined serum free culture (positive staining illustrated by arrows)* 105

*Table.3.5. Composition of defined serum free differentiation media used throughout differentiation assays* 106

*Fig.3.24. fluorescent microscopic observation of immunohistochemical staining of bone marrow derived mesenchymal stem cells for CBFA1/RUNX2, F-Actin and Nuclei after 5 days of defined serum free osteogenic culture (positive staining illustrated by arrows)* 107



Fig.3.25. Flourescent microscopic observation of immunohistochemical staining of bone marrow derived mesenchymal stem cells for *Osteocalcin*, *F-Actin* and *Nuclei* after 21 days of osteogenic culture (positive staining indicated by arrows) **108**

Fig.3.26. Real time-PCR characterisation of a subset of osteogenic genes after 21 days of osteogenic culture of bone marrow derived mesenchymal stem cells. Error bars represent 1 standard deviation from the mean, n=6 **109**

Fig.3.27. Flourescent microscopic observation of immunohistochemical staining of bone marrow derived stem cells after 21 days of chondrogenic culture for *Collagen II*, *F-Actin* and *Nuclei* (positive staining illustrated by arrows) **110**

Fig.3.28. Real time-PCR characterisation of type I and II collagen after 21 days of chondrogenic culture of bone marrow derived mesenchymal stem cells. Error bars represent 1 standard deviation from the mean, n=6 **111**

Fig.3.29. Microscopic observation of Oil Red O and haematoxylin stained bone marrow derived mesenchymal stem cells after 5 days of adipogenic culture (positive staining illustrated by arrows) **112**

Fig.3.30. Microscopic observation of Oil Red O and haematoxylin stained bone marrow derived mesenchymal stem cells after 21 days of adipogenic culture (positive staining illustrated by arrows) **113**

Fig.3.31. Microscopic observation of methylene blue stained dental pulp derived stem cells cultured to confluence under serum free basal conditions **115**

Fig.3.32. Change in the metabolic activity of human dental pulp derived stem cells cultured in conjunction with basal serum free parameters using the Alamar blue method. Error bars represent 1 standard deviation from the mean, n=3 **116**

Fig.3.33. Flourescent microscopic observation of immunohistochemical staining for *A*; *Stro-1*, *Nucleostemin*, *Nuclei*, *B*; *TRA-1-81*, *F-Actin*, *C*; *Sox2*, *F-Actin*, *Nuclei* and *D*; *Oct-4*, *F-Actin*, *Nuclei* after 21 days of defined serum free basal culture (positive staining illustrated by arrows) **117**

Fig.3.34. Comparison of a subset of cellular antigens of dental pulp derived stem cells cultured in serum free and serum containing (Cambrex MSCBM) media formulations at confluence, at passage 4, observed using flow cytometry. Error bars represent 1 standard deviation from the mean, n=3, \*P<0.05, \*\*P<0.01, \*\*\*P<0.001 **118**

*Fig.3.35. Real time-PCR observation of the change in expression of SOX9 relative to basal conditions as a result of subjection to chondrogenic stimuli. Error bars represent 1 standard deviation from the mean, n=6*  
121

*Fig.3.36. Microscopic observation of Alcian blue stained dental pulp derived stem cells after 21 days of defined chondrogenic culture (positive blue staining indicated by arrows)*  
122

*Fig.3.37. Real time-PCR observation of the change in expression of Aggrecan relative to basal conditions as a result of subjection to chondrogenic stimuli. Error bars represent 1 standard deviation from the mean, n=6*  
123

*Fig.3.38. Fluorescent microscopic observation of immunohistochemical staining for Aggrecan in dental pulp derived stem cells during chondrogenic culture after A; 21 days, B; 3 days and C; 5 days (Aggrecan, F-Actin, Nuclei)*  
123

*Fig.3.39. Real time-PCR observation of the change in expression of Collagen II relative to basal conditions as a result of subjection to chondrogenic stimuli. Error bars represent 1 standard deviation from the mean, n=*  
124

*Fig.3.40. Fluorescent microscopic observation of immunohistochemical staining for A; Collagen I, F-Actin, Nuclei and B; Collagen II, F-Actin, Nuclei after 21 days of chondrogenic culture (positive staining illustrated by arrows)*  
125

*Fig.3.41. Real time-PCR observation of the change in expression of Chondroadherin relative to basal conditions as a result of subjection to chondrogenic stimuli. Error bars represent 1 standard deviation from the mean, n=6*  
125

*Fig.3.42. Scanning electron microscopic analysis of dental pulp derived stem cells after 21 days of defined chondrogenic culture (indicated by arrows)*  
126

*Fig.3.43. Real time-PCR observation of the change in expression of CBFA1/RUNX2 relative to basal conditions as a result of subjection to chondrogenic stimuli. Error bars represent 1 standard deviation from the mean, n=6*  
126

*Fig.3.44. Real time-PCR observation of the change in expression of Osteopontin relative to basal conditions as a result of subjection to chondrogenic stimuli. Error bars represent 1 standard deviation from the mean, n=6*  
127

*Fig.3.45. Real time-PCR observation of the change in expression of Osteonectin relative to basal conditions as a result of subjection to chondrogenic stimuli. Error bars represent 1 standard deviation from the mean, n=6* **128**

*Fig.3.46. Real time-PCR observation of the change in expression of CBFA1/RUNX2 relative to basal conditions as a result of subjection to osteogenic stimuli. Error bars represent 1 standard deviation from the mean, n=6* **130**

*Fig.3.47. Fluorescent microscopic observation of immunohistochemical staining for CBFA1/RUNX2, F-Actin and Nuclei after 21 days of osteogenic culture (positive staining indicated by arrows)* **131**

*Fig.3.48. Real time-PCR observation of the change in expression of Osterix relative to basal conditions as a result of subjection to osteogenic stimuli. Error bars represent 1 standard deviation from the mean, n=6* **132**

*Fig.3.49. Real time-PCR observation of the change in expression of Osteopontin relative to basal conditions as a result of subjection to osteogenic stimuli. Error bars represent 1 standard deviation from the mean, n=6* **132**

*Fig.3.50. Real time-PCR observation of the change in expression of Osteonectin relative to basal conditions as a result of subjection to osteogenic stimuli. Error bars represent 1 standard deviation from the mean, n=6* **133**

*Fig.3.51. Fluorescent microscopic observation of immunohistochemical staining for Osteocalcin, F-Actin and Nuclei after 21 days of osteogenic culture (positive staining illustrated by arrow)* **134**

*Fig.3.52. Microscopic observation of Von Kossa stained dental pulp derived stem cells after 21 days of defined osteogenic culture (positive staining illustrated by arrows)* **134**

*Fig.3.53. Real time-PCR observation of the change in expression of SOX9 relative to basal conditions as a result of subjection to osteogenic stimuli. Error bars represent 1 standard deviation from the mean, n=6* **135**

*Fig.3.55. Fluorescent microscopic observation of immunohistochemical staining for Collagen X, F-Actin and Nuclei after 21 days of osteogenic culture (positive staining indicated by arrow)* **136**



*Fig.3.56. Fluorescent microscopic observation of immunohistochemical staining for PPAR-Gamma, and Nuclei after 21 days of adipogenic culture* **139**

*Fig.3.57. Real time-PCR observation of the change in expression of Adiponectin relative to basal conditions as a result of subjection to adipogenic stimuli. Error bars represent 1 standard deviation from the mean, n=6* **139**

*Fig.3.58. Fluorescent microscopic observation of immunohistochemical staining for Adiponectin, F-Actin and Nuclei after 7 days of adipogenic culture (positive staining illustrated by arrows)* **140**

*Fig.3.59. Fluorescent microscopic observation of immunohistochemical staining for Leptin and Nuclei after 21 days of adipogenic culture* **141**

*Fig.3.60. Fluorescent microscopic observation of immunohistochemical staining for Perilipin and Nuclei after 21 days of adipogenic culture* **142**

*Fig.3.61. Microscopic observation of dental pulp derived stem cells under defined adipogenic stimuli subjected to Oil Red O and haematoxylin staining after A; 7 days and B; 14 days (positive staining illustrated by arrows)* **142**

*Fig.3.62. Light microscopic observation of the granularity of dental pulp derived stem cells after 14 days of adipogenic culture due to lipid droplet encapsulation (examples given using arrows)* **143**

*Fig.3.63. Fluorescent microscopic observation of immunohistochemical staining for Nestin, F-Actin and Nuclei after 5 days of neural culture (positive staining illustrated by arrow)* **145**

*Fig.3.64. Real time-PCR observation of the change in expression of Neural Growth Factor relative to basal conditions as a result of subjection to neural stimuli. Error bars represent 1 standard deviation from the mean, n=6* **146**

*Fig.3.65. Fluorescent microscopic observation of immunohistochemical staining for NGF and Nuclei after 14 days of neural culture* **146**

*Fig.3.66. Fluorescent microscopic observation of immunohistochemical staining for Neurofilament, F-Actin and Nuclei after A; 7 days (located both nuclear and cytoplasmic, indicated by arrows), and B; 14 days of neural culture* **148**

*Fig.3.67. Real time-PCR observation of the change in expression of  $\beta$ -III-Tubulin relative to basal conditions as a result of subjection to neural stimuli. Error bars represent 1 standard deviation from the mean, n=6* **149**

- Fig.3.68. Fluorescent microscopic observation of immunohistochemical staining for  $\beta$ -III-Tubulin, F-Actin and Nuclei after 21 days of neural culture (positive staining illustrated by arrows) **149**
- Fig.3.69. Fluorescent microscopic observation of immunohistochemical staining for **A; Synaptophysin**, F-Actin, Nuclei and **B; Synaptic vesicle protein**, F-Actin, Nuclei after 21 days of neural culture (positive staining illustrated by arrows) **150**
- Fig.3.70. Real time-PCR observation of the change in expression of REST relative to basal conditions as a result of subjection to neural stimuli. Error bars represent 1 standard deviation from the mean, n=6 **151**
- Fig.3.71. Real time-PCR observation of the change in expression of Substance P relative to basal conditions as a result of subjection to neural stimuli. Error bars represent 1 standard deviation from the mean, n=6 **152**
- Fig.3.72. Fluorescent microscopic observation of immunohistochemical staining for **Substance P**, F-Actin and Nuclei after 21 days of neural culture **153**
- Fig.3.74. Fluorescent microscopic visualisation of immunohistochemical staining of umbilical cord derived stem cells after 21 days of neural culture for **A; GFAP**, F-Actin, Nuclei, **B; Synaptophysin**, F-Actin, Nuclei, **C; Neurofilament**, F-Actin, Nuclei, **D; Beta-III-Tubulin**, F-Actin, Nuclei, **E; NGF**, F-Actin, Nuclei and **F; Nestin**, F-Actin, Nuclei (positive staining illustrated by arrows) **154**
- Fig.3.73. Light Microscopic observation of neurite morphology of dental pulp derived stem cells after 14 days of culture under defined neural conditions, illustrating neurite processes (arrow) **155**
- Fig.3.75. Quantification of the concentration of human serum albumin in culture media aspirates taken from dental pulp derived stem cells under basal and hepatic culture conditions confirmed using the ELISA method. Error bars represent 1 standard deviation from the mean, n=3, \*P<0.05, \*\*P<0.01, \*\*\*P<0.001 relative to basal media **157**
- Fig.3.76. Fluorescent microscopic observation of immunohistochemical staining for **Serum Albumin**, F-Actin and Nuclei after 21 days of hepatic culture (positive staining illustrated by arrows) **158**
- Fig.3.77. Fluorescent microscopic observation of immunohistochemical staining for  $\alpha$ -fetoprotein, F-Actin and Nuclei after 21 days of hepatic culture (positive staining illustrated by arrows) **159**

*Fig.3.78. Fluorescent microscopic observation of immunohistochemical staining for Cytokeratin 18, F-Actin and Nuclei after 21 days of hepatic culture (positive staining illustrated by arrows)* **160**

*Fig.3.79. Metabolic activity of human dental pulp derived stem cells under defined serum free differentiation conditions using the Alamar blue method. Error bars represent 1 standard deviation from the mean, n=3. No correction for change in cell number was conducted* **162**

#### **Chapter 4.**

*Fig.4.1. Demonstration of role of the necessary components of the dynamic contact angle method for quantification of surface energy* **170**

*Fig.4.2. Advancing contact angles of three test surfaces during immersion into 5% fetal calf serum (v/v) measured using the dynamic contact angle method, n=3* **171**

*Fig.4.3. Comparison of the dynamic contact angle of blood plasma derived hydrogel and plain glass tissue culture substrate across a range of concentrations of fetal calf serum. Error bars represent 1 standard deviation from the mean, n=3, \*P<0.05, \*\*P<0.01, \*\*\*P<0.001 relative to unmodified filter paper; #P<0.05, ##P<0.01, ###P<0.001 hydrogel relative to clean glass* **173**

*Fig.4.5. Light microscopic observation of human articular chondrocytes cultured under platelet poor plasma derived hydrogel for 21 days stained using the Alcian blue method (Positive staining illustrated using arrows)* **176**

*Fig.4.6. Metabolic activity of dental pulp derived stem cells cultured on platelet poor plasma derived hydrogel surface, using the Almar blue method. Error bars represent 1 standard deviation from the mean, n=3* **178**

*Fig.4.7. Light Microscopic comparison of the expansion of dental pulp derived stem cells on Matrigel and platelet poor plasma derived hydrogel* **179**

*Fig.4.8. A. Phase contrast microscopic and B. Macroscopic visualisation of colony forming units formed from Hoechst<sup>dull</sup> isolated dental pulp derived stem cells (colony forming units indicated by arrows)* **181**

*Fig.4.9. Phase contrast microscopic observation of morphological changes of Hoechst<sup>dull</sup> subset of dental pulp derived stem cells cultured on TCP and platelet poor plasma derived hydrogel (example microvascular like assemblies indicated using arrows)* **182**



*Fig.4.10. Phase contrast microscopic observation of the intimacy of organisation between Hoechst<sup>dull</sup> sorted dental pulp stem cells cultured on platelet poor plasma derived hydrogel after 14 days*

**183**

*Fig.4.11. Fluorescent microscopic observation of the cellular intimacy during microvascular assembly using fluorescent cytoplasmic cell tracking*

**183**

*Fig.4.12. Fluorescent microscopic observation of immunohistochemical staining of dental pulp derived stem cells for A; Von Willebrand Factor, Nuclei, B; VE-Cadherin, CD31 and C; CD31 and nuclei after 14 days culture in conjunction with platelet poor plasma derived hydrogel (positive staining illustrated by arrows)*

**185**

*Fig.4.13. Flow-cytometric comparison of the antigenicity of sorted and unsorted dental pulp derived stem cells in conjunction with platelet poor plasma and tissue culture plastic substrate. Error bars represent 1 standard deviation from the mean, n=3, \*P<0.05, \*\*P<0.01, \*\*\*P<0.001 Hoechst dull TCP relative to gel; #P<0.05, ##P<0.01, ###P<0.001 Hoechst bright TCP relative to gel*

**187**

*Fig.4.14. Flow-cytometric comparison of the antigenicity of sorted and unsorted dental pulp derived stem cells in conjunction with platelet poor plasma and tissue culture plastic substrate. Error bars represent 1 standard deviation from the mean, n=3, \*P<0.05, \*\*P<0.01, \*\*\*P<0.001 Hoechst dull TCP relative to gel; #P<0.05, ##P<0.01, ###P<0.001 Hoechst bright TCP relative to gel*

**188**

*Fig.4.15. Comparison of the metabolic activity of Hoechst<sup>dull</sup> selected and heterogeneous populations of dental pulp derived stem cells cultured on blood plasma derived hydrogel matrix using the Almar blue method. Error bars represent 1 standard deviation from the mean, n=3, \*P<0.05, \*\*P<0.01, \*\*\*P<0.001*

**190**

*Fig.4.16. Fluorescent micrographs showing sections taken through the z plane of human articular chondrocyte cells cultured embedded in a platelet poor plasma derived hydrogel block*

**193**

*Fig.4.17. Macroscopic observation of subject post sacrifice indicating visible subcutaneous tissue formation prior to dissection (1:3)*

**196**

*Fig.4.18. Macroscopic visualisation of neotissue formation after 3 weeks as a result of implantation of primary human cells in conjunction with platelet poor plasma derived hydrogel (1:3)*

**196**

- Fig.4.19. Light microscopic analysis of Haematoxylin and Eosin staining of explanted human dermal fibroblast neo tissue after 3 weeks of in-vivo culture (ectopic gel mass indicated by arrow)* **197**
- Fig.4.20. Macroscopic observation of human dermal fibroblast cells after 10 weeks of in-vivo incubation in conjunction with platelet poor plasma derived hydrogel matrix (1:4)* **199**
- Fig.4.21. Macroscopic demonstration of the influence of initial cell number on terminal tissue bulk (1:3)* **201**
- Fig.4.22. Macroscopic comparison of cell seeding number and neotissue bulk at after 6 weeks of in-vivo culture (1:4)* **201**
- Fig.4.23. Macroscopic observation of the vascularisation of a neo-tissue after 6 weeks of in-vivo culture (vasculature indicated using arrows) (1:4)* **202**
- Fig.4.24. Light microscopic observation of Haematoxylin and Eosin stained explanted tissue, demonstrating proximity to host tissue. (E; Epidermis, D; Dermis, SC; Subcutaneous layer and G; Gel mass)* **203**
- Fig.4.25. Light microscopic characterisation of haematoxylin and eosin stained ectopic tissue showing the densely cellular nature of the hydrogel derived tissue mass* **204**
- Fig.4.26. Light microscopic observation of haematoxylin and eosin stained explanted tissue demonstrating the progression of adipose infiltration into the hydrogel derived tissue mass (adipose cells indicated by arrow)* **205**
- Fig.4.27. Microscopic observation of haematoxylin and eosin stained explanted tissue illustrating extensive infiltration of host adipose into the hydrogel derived tissue mass (adipose cells indicated using arrows)* **206**
- Fig.4.28. Microscopic observation of haematoxylin and eosin stained ectopic tissue demonstrating A. complete continuation of a neo-muscle block through the hydrogel derived tissue and B. early infiltration of muscle fibres into the cellular gel mass (muscle fibres indicated by arrows)* **207**
- Fig.4.29. Microscopic observation of haematoxylin and eosin stained ectopic tissues illustrating infiltration of host hair follicles into the hydrogel derived tissue mass. (Hair follicles indicated using arrows)* **207**

- Fig.4.30. Microscopic analysis of hematoxylin and eosin stained ectopic tissue superimosed with circles indicating the infiltration of host microvasculature (microvasculature indicated using arrows)* **208**
- Fig.4.30. Fluorescent microscopic observation of fluorescent in situ hybridisation of explanted tissue with probes targeted against the human Y chromosome* **211**
- Fig.4.32. Confirmation of the human dermal fibroblast origin of the cells in the platelet poor plasma derived neo-tissue. A; immunofluorescent cell tracking dye alone, B; transmitted light alone and C; composite of both immunofluorescent cell tracking and transmitted light images* **213**
- Fig.4.31. Light microscopic visualisation of explanted tissue immunohistochemically stained for the presence of the D7-Fib antigen (positive staining indicated using arrows)* **214**
- Fig.3.33. Real time PCR observation of the human D7-Fib gene in tissues explanted from experimental subjects after 6 weeks of in-vivo culture. Error bars represent 1 standard deviation from the mean, n=6* **216**
- Fig.4.34 Real time PCR observation of the human GAPDH gene in tissues explanted from experimental subjects after 6 weeks of In-vivo culture. Error bars represent 1 standard deviation from the mean, n=6* **217**
- Fig.4.35. Real time PCR observation of the human DNA Topoisomerase-3 gene in tissues explanted from experimental subjects after 6 weeks of in-vivo culture. Error bars represent 1 standard deviation from the mean, n=6* **217**
- Fig.4.36. Light microscopic observation of immunohistochemical identification of the presence of host macrophage cells in explanted neotissue (positive staining illustrated by arrows)* **218**
- Fig.4.37. Light microscopic observation of immunohistochemical identification of the presence of host CD68 positive cells in explanted neotissue (positive staining illustrated using arrows)* **219**
- Fig.4.38. Light microscopic observation of immunohistochemical identification of the presence of host neutrophil cells in explanted neotissue (positive staining illustrated using arrows)* **220**
- Fig.4.39. Light microscopic observation of immunohistochemical confirmation of the absence of host CD205 positive cells in explanted neotissue (neo-tissue area subjected to staining indicated using arrows)* **221**

*Fig.4.40. Light microscopic observation of immunohistochemical confirmation of the absence of host MHCII positive cells in explanted neotissue (neo-tissue area subjected to staining indicated using arrows)* **222**

*Fig.4.41. Electron micrograph of the surface of the ectopic tissue demonstrating the interaction between cells and fibrin meshwork (fibrin scaffold indicated using arrows)* **223**

*Fig.4.42. Electron micrograph confirming the presence of a fibrin meshwork in the neo-tissue after in-vivo culture (fibrin fibres indicated using arrows)* **224**

*Fig.4.43. Electron micrograph demonstrating the interaction between scaffold fibres and cells in the ectopic tissue* **224**

*Fig.4.44. Light microscopic observation of haematoxylin and eosin stained ectopic tissue derived from platelet poor plasma hydrogel in conjunction with human osteoblast cells showing the degree of cellularisation* **226**

*Fig.4.45. Microscopic observation of immunohistochemical recognition of human CBFA1/RUNX2 (positive staining illustrated using arrows)* **227**

*Fig.4.56. Light microscopic observation of Von-Kossa stained ectopic tissue (positive staining illustrated using arrows)* **228**